AD615623

INTERNATIONAL SEMINAR ON THEORETICAL WAVE-RESISTANCE

VOLUME III

DDC
RELEASED
JUN 1 1965
DDC-IRA E

4416-1
COPY 2 OF 3 VEC
HARD COPY $. 7.50
MICROFICHE $. 2.25

Best
Available
Copy

SHIPS OF MINIMUM TOTAL RESISTANCE

Wen-Chin Lin
W. C. Webster
J. V. Wehausen

University of California

In an earlier paper (Webster and Wehausen, 1962), the problem of finding a ship of minimum total resistance with a given after body was treated by a method rather similar to that which will be used below. The chief and most important difference in this paper lies in the computation of the frictional resistance, or to be more precise, the surface area of the hull. In the earlier work this was computed by an approximation which, although apparently consistent with the thin-ship approximation in wave-resistance theory, actually leads to divergent integrals under circumstances in which the area is, in fact, finite. The difficulty is connected with the fact that the condition for the area approximation to be valid is that the slopes f_x and f_z should be small, whereas the corresponding condition for the thin-ship wave-resistance approximation (Michell's integral) is that f/L should be uniformly small; here the hull is represented by $y = f(x,z)$ and L is the length. The approximation for the area which will be used below avoids this difficulty, but at the expense of making the minimization computations considerably more difficult.

A second difference from the earlier paper is that the problem has been somewhat extended. We no longer consider only the problem with given afterbody, but also that in which the whole ship form can be varied. In the later case the displacement and a profile symmetric fore and aft are prescribed. According to well known theorems, the resulting ship of minimum total resistance will be symmetric fore and aft. The computing program has also been so written that the volumetric coefficient can be held constant if this is desired as a side condition in the minimization. However, this side condition is imposed only for the symmetric ship.

FORMULATION OF THE PROBLEM

In order to make the exposition self-contained, some of the preliminary analysis from the paper by Webster and Wehausen (1962) is repeated. The notation is the same except that H instead of T is used to denote the draft.

Representation of the ship

The axes will be taken as shown in Figure 1. The variables have been taken dimensionlessly, lengths in the x-direction being measured by $\ell = 1/2\ L$, those in the transverse direction by $b = 1/2\ B$, and those in the vertical direction by H. However, one should note that for the case of the symmetric ship the length B is not necessarily the beam, but merely

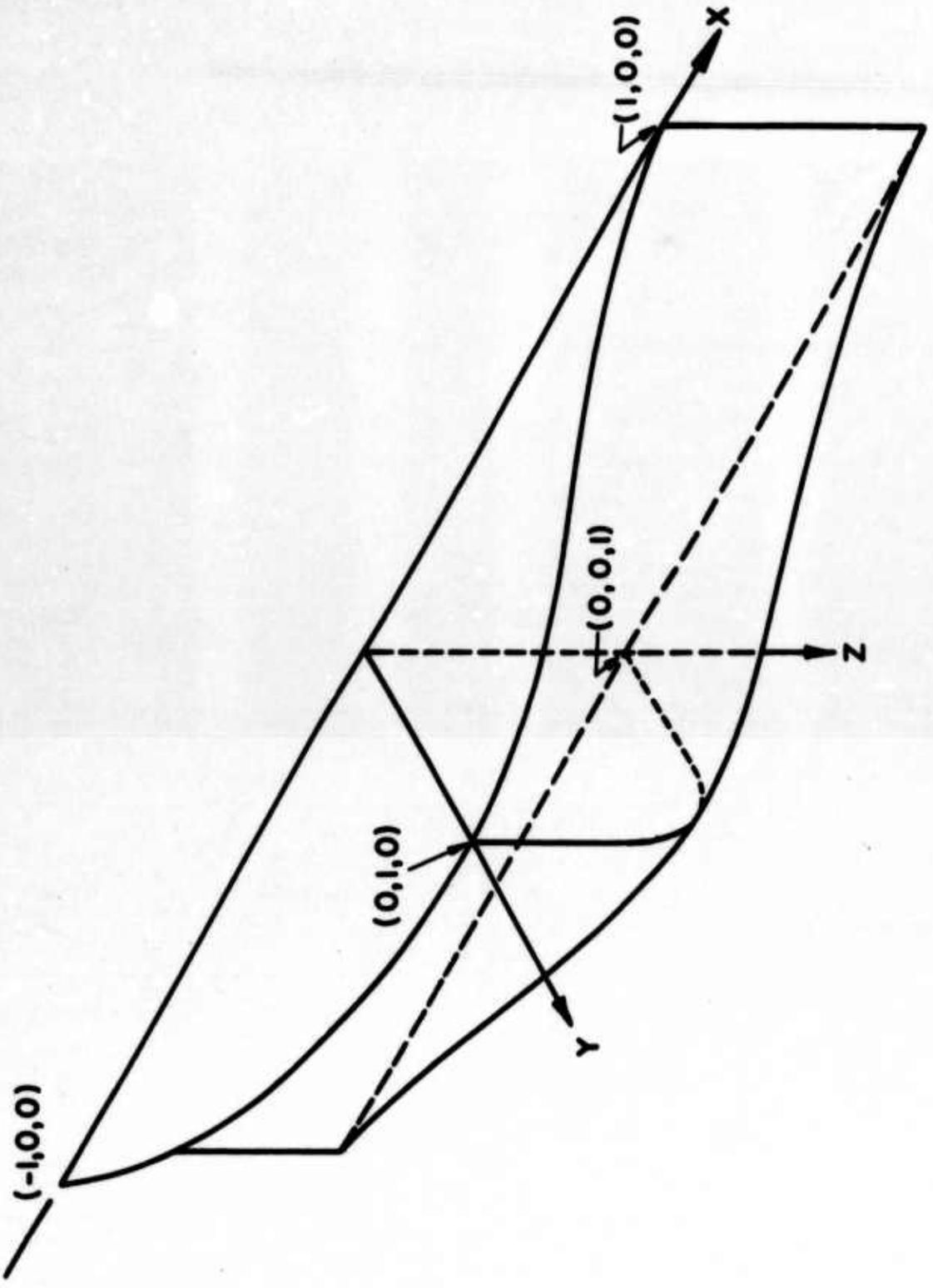


FIGURE 1.

a length scale in the y-direction. The equation of the hull will be denoted by $y = \pm f_a(x,z)$, and that of the forebody by $y = \pm f_b(x,z)$. The volumetric coefficient is given by

$$C_V = \frac{1}{2} \frac{B}{H} \left(\frac{H}{L}\right)^2 \int_{-1}^{1} dx \int_{0}^{1} dz \; f(x,z) \; , \qquad (1)$$

The functions will be approximated by finite Fourier series. As our fundamental set we shall take

$$\left\{ \cos \frac{1}{2} (2m-1) \pi x \cos(2p-1) \pi z \,\middle|\, m,p = 1, 2, \ldots \right\} . \qquad (2)$$

These form a complete set in either $0 \leq x \leq 1$, $0 \leq z \leq 1$ or $-1 \leq x \leq 0$, $0 \leq z \leq 1$ and furthermore also in $-1 \leq x \leq 1$, $0 \leq z \leq 1$ if one wishes to represent only functions symmetric fore and aft. Otherwise one must add to (2) the set

$$\left\{ \sin m\pi x \cos \frac{1}{2} (2p-1) \pi z \,\middle|\, m,p = 1, 2, \ldots \right\} . \qquad (3)$$

The selected fundamental set (2), or (2) and (3), obviously has the property that any finite sum will represent a continuous function vanishing on the edges $x = \pm 1$ and $z = 1$ of the rectangle $|x| \leq 1$, $0 \leq z \leq 1$, in the (x,z)-plane. If the profile of the ship is not this rectangle, and it will not be for the fixed afterbody selected below, one must suppose the hull form to be completed by a piece of the (x,z)-plane. The profile of the forebody of the symmetric ship will be supposed to be the whole appropriate rectangle.

In the case of the fixed afterbody two questions arise. One is that the frictional resistance, i.e. the total area of the hull, will be increased by the added deadwood. This causes, in fact, no difficulty, for since it is fixed it will not enter into the minimization calculations for the forebody. The other is the effect of representing a function vanishing over the deadwood area by a finite Fourier series. This will almost inevitably result in an approximation of the afterbody with negative ordinates in the deadwood region. This may seem a little startling at first, but causes, in fact, no difficulty. There is, however, a difficulty which may arise because of fixing the forebody profile to be a rectangle. If the proper minimum forebody should be a form with a submerged protruding bulb a la Inui, the remaining part of the rectangle will again be filled with deadwood. The difficulty lies in the fact that the frictional resistance of this area will affect its determination in the present calculation.

The series representing the functions $f_a(x,z)$ and $f_b(x,z)$ will be taken as follows:

$$f_a(x,z) = \sum_{m=1}^{M}\sum_{p=1}^{P} a_{mp}\cos\tfrac{1}{2}(2m-1)\,\pi x\cos\tfrac{1}{2}(2p-1)\,\pi z\ ,$$
$$f_b(x,z) = \sum_{m=1}^{M}\sum_{p=1}^{P} b_{mp}\cos\tfrac{1}{2}(2m-1)\,\pi x\cos\tfrac{1}{2}(2p-1)\,\pi z\ . \tag{4}$$

The coefficients a_{mp} are determined from the form of the afterbody and are to be considered as known. The coefficients b_{mp} will be determined by the minimization conditions. For the ship which is symmetric fore and aft the two series are identical and only the second series need be retained. There are certain conditions in the b_{mp} which can be written down immediately. For the case of the fixed afterbody the forebody must fit smoothly onto the afterbody. This requires that the following equations be satisfied:

$$\sum_{m=1}^{M} b_{mp} = \sum_{m=1}^{M} a_{mp}\ ,\quad p = 1, 2, \ldots, P\ . \tag{5}$$

For future reference we note that the volumetric coefficient of the forebody can be obtained in terms of the b_{mp} by substituting the series for $f_b(x,z)$ in (1). This yields

$$C_\nabla = \frac{B}{H}\left(\frac{H}{L}\right)^2\frac{2}{\pi^2}\sum_{m=1}^{M}\sum_{p=1}^{P}\frac{(-1)^{m+p}}{(2m-1)(2p-1)}\,b_{mp}\ . \tag{6}$$

The Wave Resistance

Michell's integral for the wave resistance will be taken in the following dimensionless form:

$$C_M = \frac{R_M}{\rho g B^2 H} = \frac{1}{\pi}\frac{2H}{L}\frac{1}{\gamma_o}\int_{\gamma_o}^{\infty}[C^2 + S^2]\,\frac{\gamma^4}{\sqrt{\gamma^2-\gamma_o^2}}\,d\gamma\ ,$$
$$C + iS\left(\gamma;\ \frac{H}{L\gamma_o}\right) = \int_{-1}^{1}dx\int_{0}^{1}dz\ f(x,z)\ \exp\left[-\frac{2H}{L\gamma_o}\,\gamma^2 z + i\gamma x\right]\ , \tag{7}$$

where R_M denotes the wave resistance and $\gamma_o = gL/2\,u_o^2$, u_o being the ship's speed.

We now introduce the following functions:

$$Cc_m(\gamma) = \int_0^1 \cos\gamma x \cos\frac{1}{2}(2m-1)\pi x dx$$

$$= (-1)^m \frac{2(2m-1)\pi \cos\gamma}{4\gamma^2-(2m-1)^2\pi^2}, \tag{8}$$

$$Sc_m(\gamma) = \int_0^1 \sin\gamma x \cos\frac{1}{2}(2m-1)\pi x dx$$

$$= \frac{4\gamma + (-1)^2\, 2(2m-1)\,\pi \sin\gamma}{4\gamma^2 - (2m-1)^2\,\pi^2},$$

$$E_p\left(\frac{H}{L\gamma_o}, \gamma^2\right) = \int_0^1 \exp-(2H/L\gamma_o)\gamma^2 z \cos\frac{1}{2}(2p-1)\pi z dz$$

$$= \frac{(2H/L\gamma_o)\gamma^2 + (-1)^{p+1}\frac{1}{2}(2p-1)\pi \exp-(2H/L\gamma_o)\gamma^2}{(2H/L\gamma_o)^2\gamma^4 + \frac{1}{4}(2p-1)^2\pi^2},$$

$$B_{mnpq}\left(\frac{H}{L}, \gamma_o\right) = \frac{2H}{\pi L\gamma_o}\int_{\gamma_o}^{\infty}[Cc_mCc_n + Sc_mSc_n]\, EpEq \frac{\gamma^4}{\sqrt{\gamma^2-\gamma_o^2}}\, d\gamma,$$

$$D_{mr.pq}\left(\frac{H}{L}, \gamma_o\right) = \frac{2H}{\pi L\gamma_o}\int_{\gamma_o}^{\infty}[Cc_mCc_n - Sc_mSc_n]\, EpEq \frac{\gamma^4}{\sqrt{\gamma^2-\gamma_o^2}}\, d\gamma.$$

The quantities in (7) may now be expressed in terms of these functions as follows:

$$C + iS = \sum_{m=1}^{M}\sum_{p=1}^{P} a_{mp}[Cc_m - iSc_m]\, Ep + \sum_{n=1}^{M}\sum_{q=1}^{P} b_{nq}[Cc_n + iSc_n]\, Eq, \tag{9}$$

$$C_M = \sum_{m,n=1}^{M}\sum_{p,q=1}^{P}\{a_{mp}a_{nq}B_{mnpq} + b_{mp}b_{nq}B_{mnpq} + 2a_{mp}b_{nq}D_{mnpq}\}.$$

For the ship symmetric fore and aft $a_{mp} = b_{mp}$ and

$$C_M = 2\sum_{m,n=1}^{M}\sum_{p,q=1}^{P} b_{mp}b_{nq}\{B_{mnpq} + D_{mnpq}\}. \tag{10}$$

It is evident from (8) that

$$B_{mnpq} + D_{mnpq} = 2\frac{2H}{\pi L\gamma_o} \int_{\gamma_o}^{\infty} Cc_m Cc_n E_p E_q \frac{\gamma^4}{\sqrt{\gamma^2-\gamma_o^2}}\, d\gamma \ . \qquad (11)$$

The Frictional Resistance

It will be convenient to use for a moment variables with their proper dimensions. The viscous resistance will then be taken as the usual "equivalent flat-plate" resistance, i.e.

$$\begin{aligned} R_V &= \tfrac{1}{2}\rho u_o^2 S C_f(Re) \\ &= \rho u_o^2 C_f(Re) \iint_{S_o} [1+f_x^2+f_z^2]^{\frac{1}{2}}\, dxdz \ , \end{aligned} \qquad (12)$$

where S_o is the area bounded by the profile of the ship at rest, S its wetted surface, Re is the Reynolds number Lu_o/V and C_f the resistance coefficient.

As has been mentioned earlier, the only significant difference between this paper and the earlier paper of Webster and Wehausen (1962) lies in the computation of the area S. In the earlier work the integral in (12) was approximated by

$$\iint_{S_o} (1 + \tfrac{1}{2} f_x^2 + \tfrac{1}{2} f_z^2)\, dxdz \ , \qquad (13)$$

an approximation which overestimates the area. In fact, (13) may become infinite for hull shapes which are perfectly reasonable, for example,

$$f(x,z) = b(1 - \frac{x^2}{\ell^2})\ (1 - \frac{z^2}{H^2})^{\frac{1}{2}} \ .$$

On the other hand, the form of (13) is very convenient for the minimization problem to be considered later, and one would consequently like to retain some of these aspects in another approximation without the same deficiencies. What we shall do is to assume some standard hull, say $y = \pm F(x,z)$, and consider $y = \pm f(x,z)$ as a perturbation of this. The area of the standard hull will be assumed known.

Let us now return to the dimensionless variables. Then (10) may be written in a form parallel to (7):

$$C_V = \frac{R_V}{\rho g B^2 H}$$

$$= \frac{1}{2} C_f \frac{L^2}{B^2} \frac{1}{\gamma_o} \iint_{S_o} [1 + \frac{B^2}{L^2} f_x^2 + \frac{B^2}{4H^2} f_z^2]^{1/2} dxdz , \qquad (14)$$

S_o being now the dimensionless profile. We shall approximate the integral in (14) as follows:

$$\iint_{S_o} [1 + \frac{B^2}{L^2} f_x^2 + \frac{B^2}{4H^2} f_z^2]^{\frac{1}{2}} dxdz \qquad (15)$$

$$= \iint_{S_o} [1 + \frac{B^2}{L^2} F_x^2 + \frac{B^2}{4H^2} F_z^2 + \frac{B^2}{L^2} (f_x^2 - F_x^2) + \frac{B^2}{4H^2} (f_z^2 - F_z^2)]^{\frac{1}{2}} dxdz$$

$$\approx \iint_{S_o} [1 + \frac{B^2}{L^2} F_x^2 + \frac{B^2}{4H^2} F_z^2]^{\frac{1}{2}} dxdz$$

$$+ \frac{1}{2} \iint_{S_o} [1 + \frac{B^2}{L^2} F_x^2 + \frac{B^2}{4H^2} F_z^2]^{-\frac{1}{2}} [\frac{B^2}{L^2} (f_x^2 - F_x^2) + \frac{B^2}{4H^2} (f_z^2 - F_z^2)] dxdz$$

$$= \iint_{S_o} [1 + \frac{B^2}{L^2} F_x^2 + \frac{B^2}{4H^2} F_z^2]^{\frac{1}{2}} dxdz - \frac{1}{2} \iint_{S_o} [1 + \frac{B^2}{L^2} F_x^2 + \frac{B^2}{4H^2} F_z^2]^{-\frac{1}{2}}$$

$$[\frac{B^2}{L^2} F_x^2 + \frac{B^2}{4H^2} F_z^2] dxdz$$

$$+ \frac{1}{2} \iint_{S_o} [1 + \frac{B^2}{L^2} F_x^2 + \frac{B^2}{4H^2} F_z^2]^{-\frac{1}{2}} [\frac{B^2}{L^2} f_x^2 + \frac{B^2}{4H^2} f_z^2] dxdz .$$

The first two integrals, denoted by S_F and A_F, respectively, are fixed as soon as F is decided upon and only the last integral will vary with f. Again the approximation gives an overestimate of the area, and, furthermore, difficulties with the last integral are still possible for

$f(x,z)$ whose behavior in the neighborhood of the submerged part of the profile differs too much from that of the selected function $F(x,z)$. Formula (15) will be the basic of an iteration procedure to be explained later.

It is important to note that in (15) not only H/L but also B/H must be specified as parameters. It was not necessary to fix B/H in the formula for C_M in (7), nor was it necessary in the earlier work when the approximation (13) was used.

Next we compute the part of C_V due to the forebody alone, say C_{Vb}, by substituting (4) in (14) and (15). First, the area of the forebody is given by

$$S_F^+ - A_F^+ + \frac{\pi^2}{8}\frac{B^2}{L^2}\sum_{m,n=1}^{M}\sum_{p,q=1}^{P} b_{mp}b_{nq} \times \tag{16}$$

$$\left\{(2m-1)(2n-1)\iint_{S_o^+}\left[1+\frac{B^2}{L^2}F_x^2+\frac{B^2}{4H^2}F_z^2\right]^{-\frac{1}{2}}\sin\tfrac{1}{2}(2m-1)\pi x\sin\tfrac{1}{2}(2n-1)\pi x\cos\tfrac{1}{2}(2p-1)\pi z\cos(2q-1)\right.$$

$$\pi z\,dx\,dz$$

$$\left.+\frac{L^2}{4H^2}(2p-1)(2q-1)\iint_{S_o^+}\left[1+\frac{B^2}{L^2}F_x^2+\frac{B^2}{4H^2}F_z^2\right]^{-\frac{1}{2}}\cos\tfrac{1}{2}(2m-1)\pi x\cos\tfrac{1}{2}(2n-1)\pi x\sin\tfrac{1}{2}(2p-1)\right.$$

$$\left.\pi z\sin\tfrac{1}{2}(2q-1)\pi z\,dx\,dz\right\}$$

$$= S_F^+ - A_F^+ + \frac{\pi^2}{8}\frac{B^2}{L^2}\sum_{m,n}\sum_{p,q} b_{mp}b_{nq}\,S_{mnpq}\left(\frac{H}{L},\frac{B}{H}\right),$$

where the superior plus signs indicate that the integrals are restricted to the part of the profile spanned by the forebody. It then follows immediately from (14) that

$$C_{Vb} = \frac{1}{2}C_f\frac{L^2}{B^2}(S_F^+ - A_F^+)\frac{1}{\gamma_o} + C_f\frac{\pi^2}{16\gamma_o}\sum_{m,n}\sum_{p,q} b_{mp}b_{nq}\,S_{mnpq}\,. \tag{17}$$

For the afterbody frictional resistance C_{Va} one need only replace the superior plus signs by minus signs and the $\underline{b}$'s by $\underline{a}$'s. However, the value of C_{Va} will not affect the form of the minimizing forebody inasmuch as there is no interaction between fore- and afterbody in this simple model of frictional resistance. For the ship which is symmetric fore and aft it is obvious that one can obtain the total frictional resistance by doubling (17).

Minimization of the Resistance

We now turn to the problem of minimizing the total resistance, as approximated by $R_M + R_V$ subject to certain side conditions. First we note that, if L, B, and H have been fixed, it is equivalent to minimize $C_M + C_V$. The unavoidable side condition[5] has already been introduced, for the ship with the fixed afterbody. For this case it is not in principle necessary to add any further side conditions. For the symmetric ship we must at least add a fixed value of the volumetric coefficient as a side condition. For both, B/H and H/L must be fixed as parameters. However, in the second case the true beam/draft ratio is left free to vary. A further side condition which is obviously important but which cannot be easily included in the problem as formulated below is that the ordinates should be non-negative.

If one introduces the side conditions by means of Lagrange multipliers, the problem reduces to finding a minimum of the following function for the case of the given afterbody:

$$T_a\,(\gamma_o,\ 2H/L;\ b_{mp},\ \lambda_p) = C_M + C_V + 2\sum_{p=1}^{P}\lambda_p\left[\sum_{m=1}^{M} b_{mp} - \sum_{m=1}^{M} a_{mp}\right]. \tag{18}$$

For the ship symmetric fore and aft the appropriate function is

$$T_s\,(\gamma_o,\ H/L;\ b_{mp},\ \mu) = C_M + C_V + 2\mu\left[\sum_{m=1}^{M}\sum_{p=1}^{P}\frac{(-1)^{m+p}}{(2m-1)(2p-1)}\,b_{mp} - \frac{H}{B}\left(\frac{L}{H}\right)^2\frac{\pi^2}{2}\,C_\forall\right]. \tag{18'}$$

In (18) C_M is given by (9) and C_V by C_{Vb} plus the corresponding C_{Va}. In (18') C_M is given by (10) and C_V by twice (17). In either case $C_M + C_V$ consists of a constant plus a quadratic expression in the b_{mp}.

A necessary condition for a minimum of T_a is fulfillment of the following set of linear equations in the unknowns b_{mp}, λ_p:

$$\frac{\partial T_a}{\partial b_{nq}} = 2\sum_{m=1}^{M}\sum_{p=1}^{P}\left[C_f\,\frac{\pi^2}{16\gamma_o}\,S_{mnpq} + B_{mnpq}\right]b_{mp} + 2\left[\sum_{m=1}^{M}\sum_{p=1}^{P} D_{mnpq}a_{mp} + 2\lambda_q\right] = 0,\quad n=1,\ \ldots,\ M;\ q=1,\ \ldots,\ P; \tag{19}$$

$$\frac{\partial T_a}{\partial \lambda_p}\quad 2\left[\sum_{m=1}^{M} b_{mp} - \sum_{m=1}^{M} a_{mp}\right] = 0,\quad p=1,\ \ldots,\ P\ .$$

The analogous equations for the minimum of T_s will not be written out, but are, of course, similar. It is clear from the non-negativeness of the functions C_M and C_V that a solution of (19) will, in fact, yield a minimum of T_a. However, it may (and does) happen that the minimizing hull form has negative ordinates for certain values of the parameters. As has been mentioned earlier, our computational procedure is not adapted to finding a minimum with the inequality $f_b \geq 0$ as a side condition.

In the earlier treatment of Webster and Wehausen (1962) the approximation for the hull area produced a matrix S_{mnpq} whose only non-vanishing elements were the positive main-diagonal terms S_{mmpp}. It is no longer true that all off-diagonal terms vanish, so that one cannot make a definite statement concerning the effect upon the condition of the coefficient matrix in (19) of including the frictional resistance. However, its inclusion does prevent the wild forms from occurring which were obtained earlier when no such restraint was imposed. On the other hand, as was mentioned earlier, its effect is not sufficient to prevent physically unreasonable forms from developing for sufficiently high Froude numbers.

The Computational Procedure

Several different numerical procedures are involved in finding a solution to the problem formulated above, but they are for the most part relatively straightforward. All computations were carried out on the IBM 7090 of the University of California Computer Center. The coefficients B_{mnpq}, D_{mnpq}, S_{mnpq} were computed using Simpson's rule. The singularity at $\gamma = \gamma_o$ in the integrals for B_{mnpq} and D_{mnpq} was handled in the same manner as in the preparation of Weinblum's (1954) tables. The linear Equations (19) were solved using an already available program. In finding the hull area an iterative procedure was used, so that the S_{mnpq} were computed several times for each Froude number. For the problem in the given afterbody, the reflection of this in the midship section was used for the initial choice of F in (15). The associated values of S_{mnpq} were then used to find a solution to (19) and hence a hull shape, say, f_{a1}. The procedure was then repeated, using f_{a1} for F in (15) to find a new hull f_{a2}, and so forth until f_{a4} had been found. Since the difference between f_{a3} and f_{a4} is less than 1%, and between $C_{\forall 3}$ and $C_{\forall 4}$ is less than 0.5%, we conclude that the computation of the area is sufficiently accurate for the purpose at hand. A similar procedure was used for the symmetric ship except that the initial F in (15) was taken as $\cos\frac{1}{2}\pi x \cos\frac{1}{2}\pi z$. The curves for the body plans were also produced by the computer from a special plotting program using the Fourier coefficients b_{mp} as input.

The Fourier series were terminated with $M = P = 6$ as in the earlier paper. As a consequence there is an evident waviness in the lines. As the results show, it would have been a wasted effort to have smoothed out this waviness by increasing P. This was established by a numerical experiment in which $M \times P$ was also taken as 6×1, 6×2, 6×4. This will be discussed later.

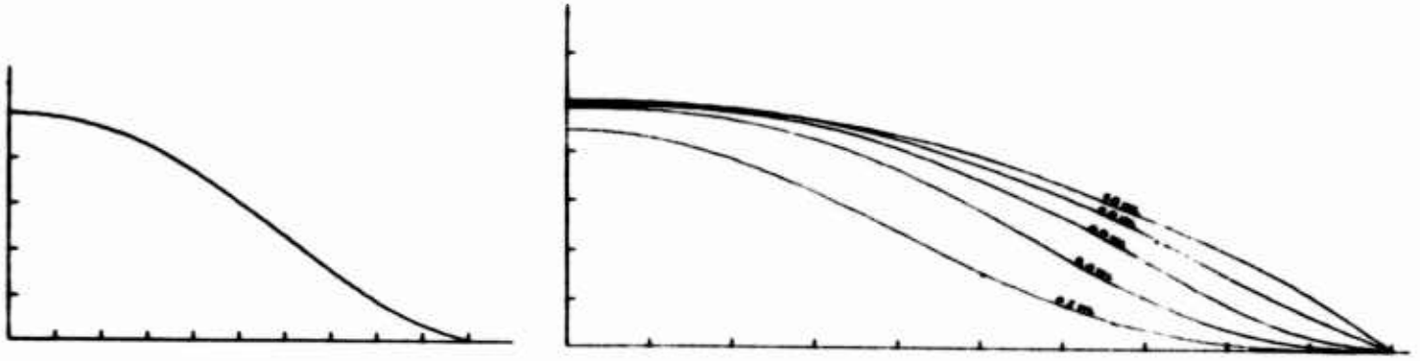
THE OPTIMUM FORMS

Choice of Parameters

The following choices were made for the actual calculations. For the problem with fixed afterbody the same afterbody was used as in the earlier computations of Wehausen, Reichert and Gauthey (1961) and of Webster and Wehausen (1962). Body plans are shown in Figure 2; various geometric form coefficients follow: $C_P = 0.564$, $C_B = 0.508$, $C_\nabla = 2.75 \times 10^{-3}$, $C_\chi = 0.90$. The afterbody was designed to conform as closely as possible to a Taylor Standard Series model of the same prismatic coefficient, but with midship section represented by $y = 1 - z^8$ (because in the first-cited paper a polynomial representation was used). The following further choices were made: $H/L = 0.0437$, $B/H = 3$, $L = 400'$. A specific length had to be chosen because of the inclusion of the frictional resistance. The Schoenherr coefficients plus a roughness allowance 0.0004 were used in computing $C_f(Re)$; in determining Re the viscosity of sea water at 63°F was used.

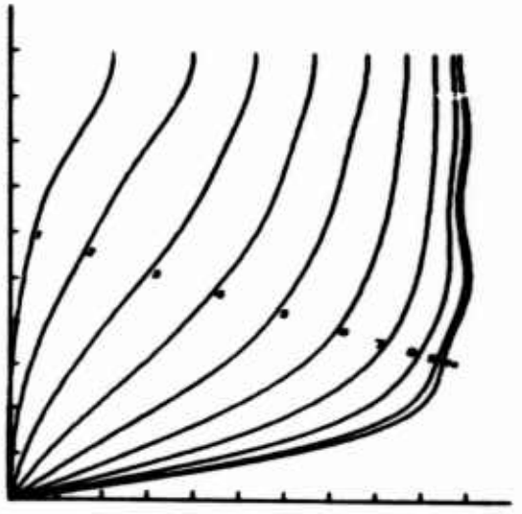
The prismatic coefficient of the afterbody was selected as a suitable one for $\gamma_0 = 4$ ($F_r = 0.354$, $V/L^3 = 1.19$). It is obvious, however, that the afterbody shape should properly be selected for each Froude number. This might reasonably be done by finding the optimum symmetric ship for the given value of γ_0 and then designing an afterbody to conform as closely as possible to this while still avoiding separation and satisfying other requirements.

For the problem of the optimum symmetric ship only the volumetric coefficient among the form parameters was fixed. For $\gamma_0 = 6$ computations were made for $C_\nabla \cdot 10^3 = 1.5$, 3 and 4.5; for all other values of γ_0 the value $C_\nabla \cdot 10^3 = 3$ was used. For the remaining geometrical parameters we chose $H/L = 0.05$, $B/H = 3$ and $L = 400'$. We note again that for this problem B is an arbitrary length scale in the transverse direction and that an optimum value of beam/draft is found for each as a part of the solution.



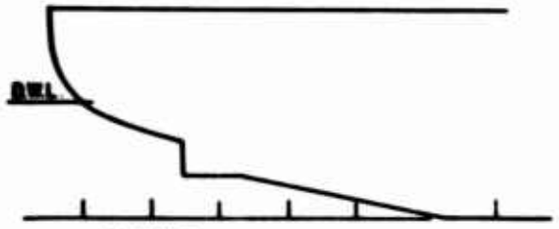
AREA CURVE, WATERLINES AND BODY PLAN FOR AFTERBODY ACTUALLY REPRESENTED BY FOURIER SERIES

$C_B = 0.5105$ $C_p = 0.5680$ $C_x = 0.8987$

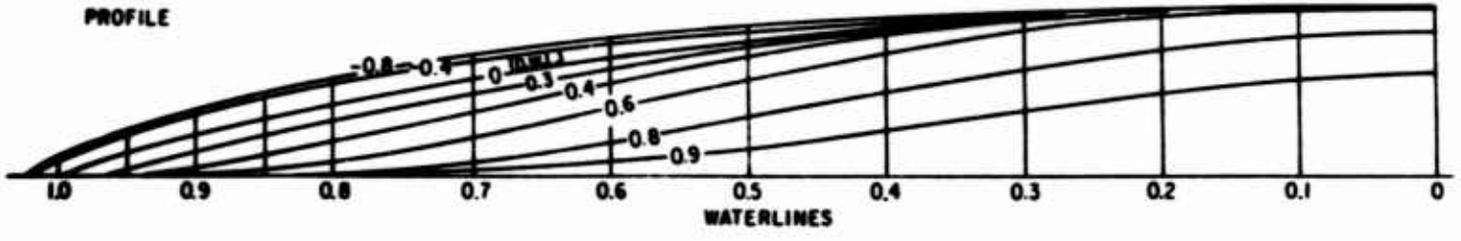


MODEL CHARACTERISTICS

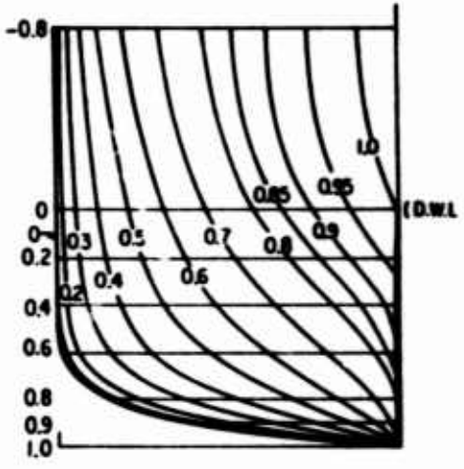
LENGTH - D.W.L.	5.00 FT.
BEAM	7.50 IN.
DRAFT	2.62 IN.
C_B	0.508
C_p	0.564
C_x	0.900



PROFILE



WATERLINES



SECTIONS

FIGURE 2

For the symmetric ship optimum forms were found for integer values of γ_o from 2 to 10, i.e. for Froude numbers between 0.224 and 0.5. Since the forms for $\gamma_o = 2$ and 3 showed negative ordinates of appreciable size at the load water line near the bow and stern, we restricted the computations for the problem with given afterbody to the interval $\gamma_o = 4$ to 9. Since $\gamma_o = 9$ produced negative ordinates, we did not carry the computation to $\gamma_o = 10$. However, inasmuch as we found similarly located negative ordinates for $\gamma_o = 6$ but not for $\gamma_o = 7$, this may have been unduly pessimistic.

The Symmetric Ship

Figures 3 to 11 show section curves, waterlines and the sectional area curve for each integer value of γ_o from 2 to 10. The figures show also the values selected for the parameters, the values of C_M, C_V, C_T for the optimum form as well as the geometric form parameters C_B, C_V, C_P and C_X. However, C_B was computed using the midship section beam, and C_P from the equation $C_P = C_B/C_X$. Hence, for some of the rather outré forms which have developed for $\gamma_o = 2$, 3, and 4 these coefficients have lost their conventional meanings. On Figure 15 are plotted optimum (according to this analysis) values of B/H, C_B, C_P, and C_X as functions of γ_o; in all cases $C_\forall = 0.003$.

For the most part the body plans and graphs speak for themselves, but several points deserve special mention. The enormous bulbs which occur for $\gamma_o = 2$ to 5 would presumably result in a separated flow and thus vitiate the fundamental assumptions of the present analysis. For $\gamma_o = 6$ to 10 the forms are more reasonable in this respect. The size of the bulb decreases to a minimum at $\gamma_o = 7$ and 8 and then slowly increases again. Figure 16 shows C_T and C_V for the optimum ships plotted against γ_o. It is evident that for γ_o between 6 and 10 these forms are indeed "waveless" insofar as the contribution of wave resistance to total resistance is concerned. C_M for these ships is plotted in Figure 17. We note that the resistance coefficient $R/pg\forall$ is related to ours by the equation

$$\frac{R}{pg\forall} = \frac{1}{C_\forall} \left(\frac{B}{H}\right)^2 \left(\frac{H}{L}\right)^3 C \ .$$

The factor is 0.375 for the ship forms discussed above.

The very low values of the wave resistance obtained for these forms raises several questions. It is often assumed that the sectional area curve is of prime importance in determining the wave resistance, and

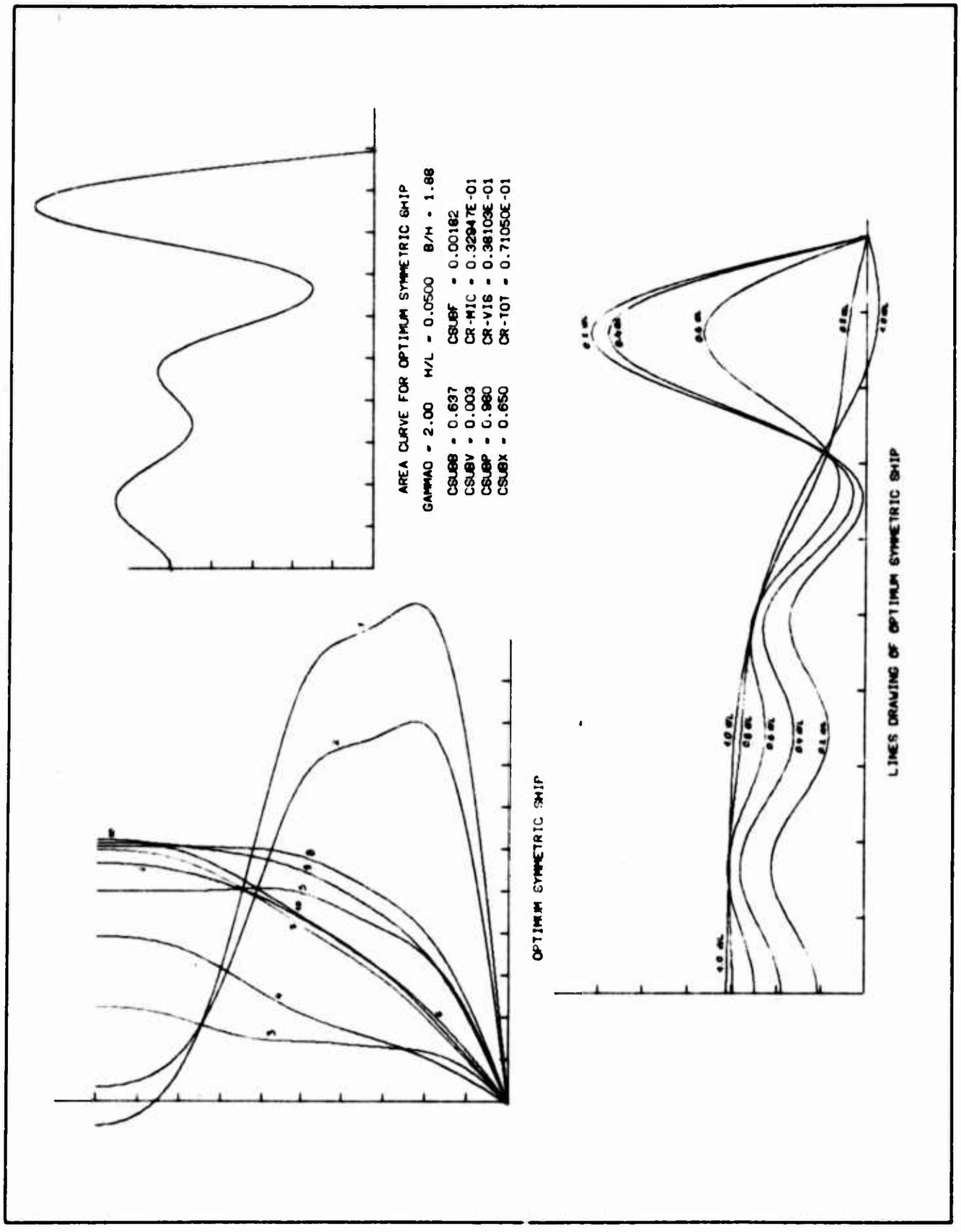

AREA CURVE FOR OPTIMUM SYMMETRIC SHIP
GAMMAO = 2.00 M/L = 0.0500 B/H = 1.88
CSUBB = 0.637 CSUBF = 0.00182
CSUBV = 0.003 CR-MIC = 0.32947E-01
CSUBP = 0.980 CR-VIS = 0.38103E-01
CSUBX = 0.650 CR-TOT = 0.71050E-01
OPTIMUM SYMMETRIC SHIP
LINES DRAWING OF OPTIMUM SYMMETRIC SHIP

FIGURE 3

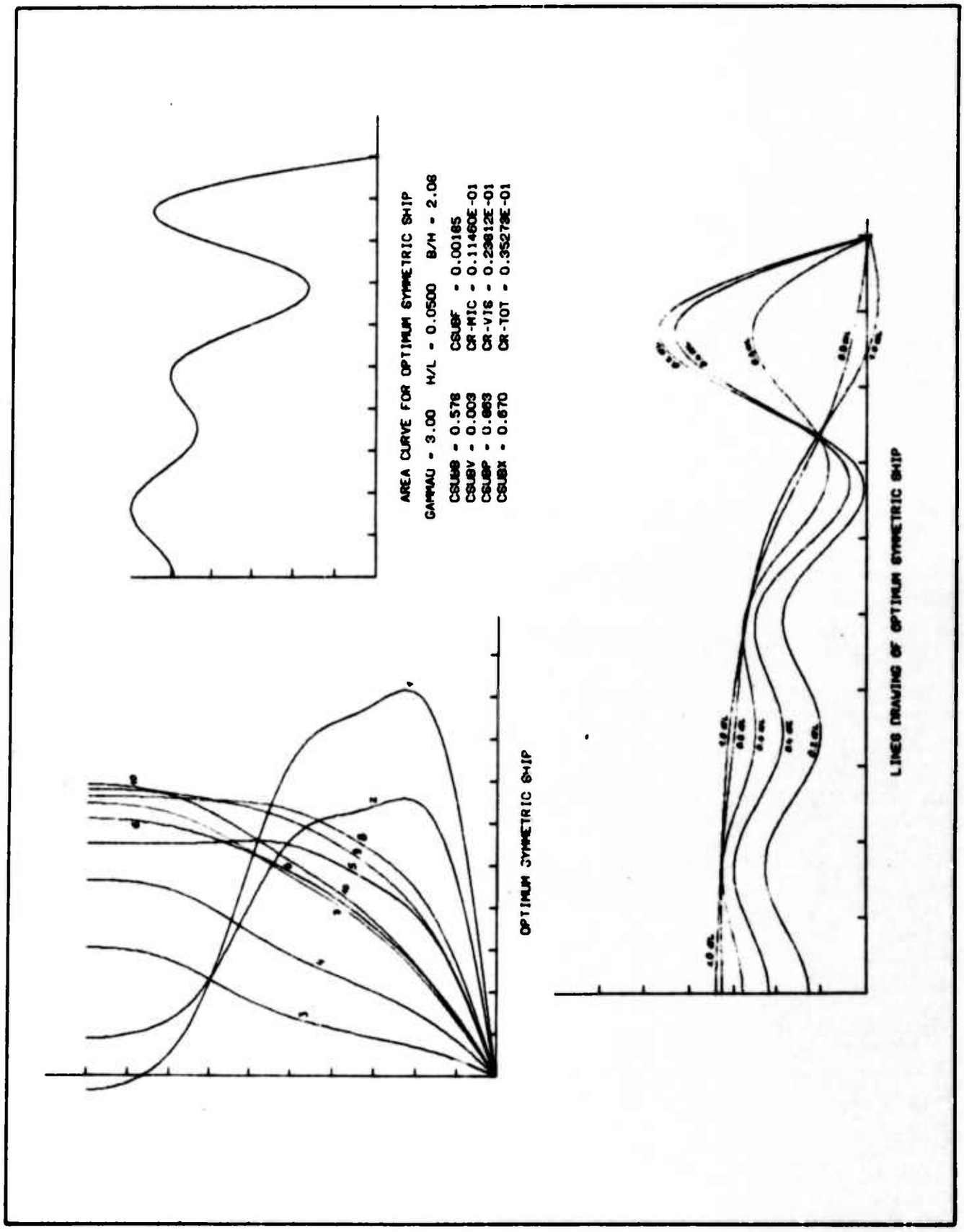

AREA CURVE FOR OPTIMUM SYMMETRIC SHIP
GAMMAU - 3.00 H/L - 0.0500 B/H - 2.08
CSUBB - 0.578 CSUBF - 0.00165
CSUBV - 0.003 CR-MIC - 0.11460E-01
CSUBP - 0.663 CR-VIS - 0.23812E-01
CSUBX - 0.670 CR-TOT - 0.35278E-01
OPTIMUM SYMMETRIC SHIP
LINES DRAWING OF OPTIMUM SYMMETRIC SHIP

FIGURE 4

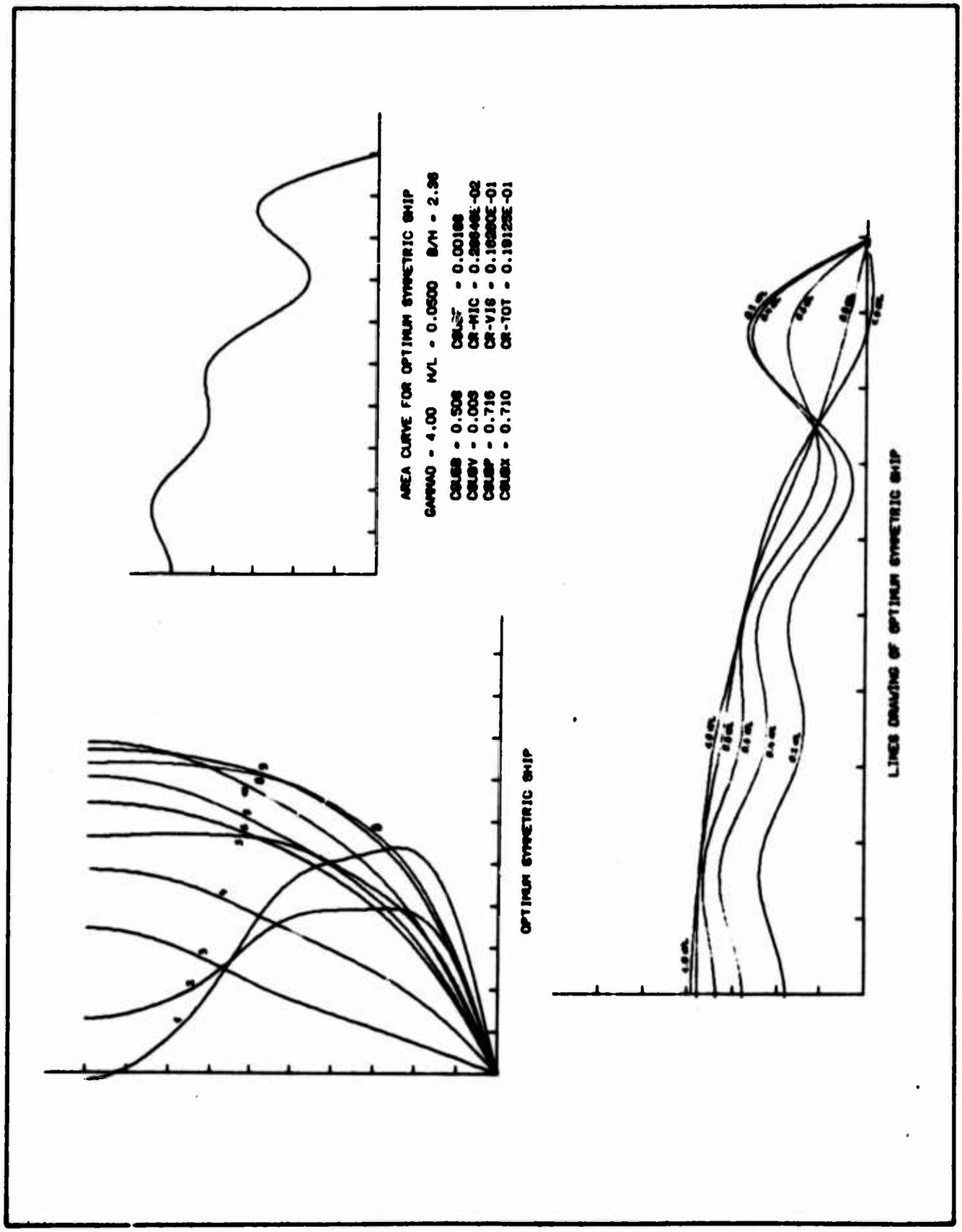

AREA CURVE FOR OPTIMUM SYMMETRIC SHIP
GAMMAO = 4.00 M/L = 0.0500 B/H = 2.36
CBUSB = 0.508 CBUSF = 0.00188
CBUSV = 0.009 CR-MIC = 0.28648E-02
CBUSP = 0.716 CR-VIS = 0.16280E-01
CBUSX = 0.710 CR-TOT = 0.18125E-01
OPTIMUM SYMMETRIC SHIP
LINES DRAWING OF OPTIMUM SYMMETRIC SHIP

FIGURE 5

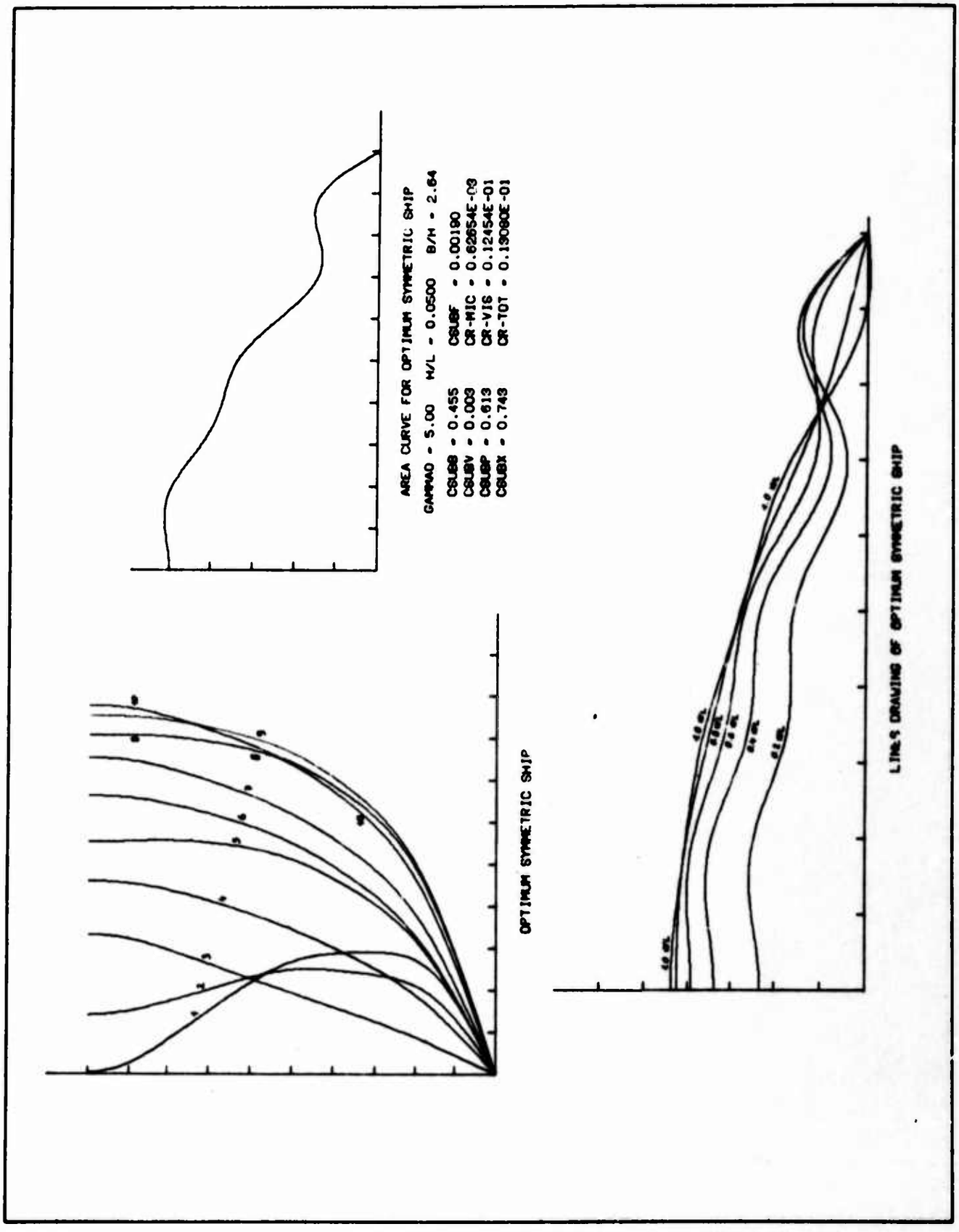

AREA CURVE FOR OPTIMUM SYMMETRIC SHIP
GAMMAO = 5.00 H/L = 0.0500 B/H = 2.64
CSUBB = 0.455 CSUBF = 0.00190
CSUBV = 0.009 CR-MIC = 0.62654E-03
CSUBP = 0.613 CR-VIS = 0.12454E-01
CSUBX = 0.743 CR-TOT = 0.13080E-01
OPTIMUM SYMMETRIC SHIP
LINES DRAWING OF OPTIMUM SYMMETRIC SHIP

FIGURE 6

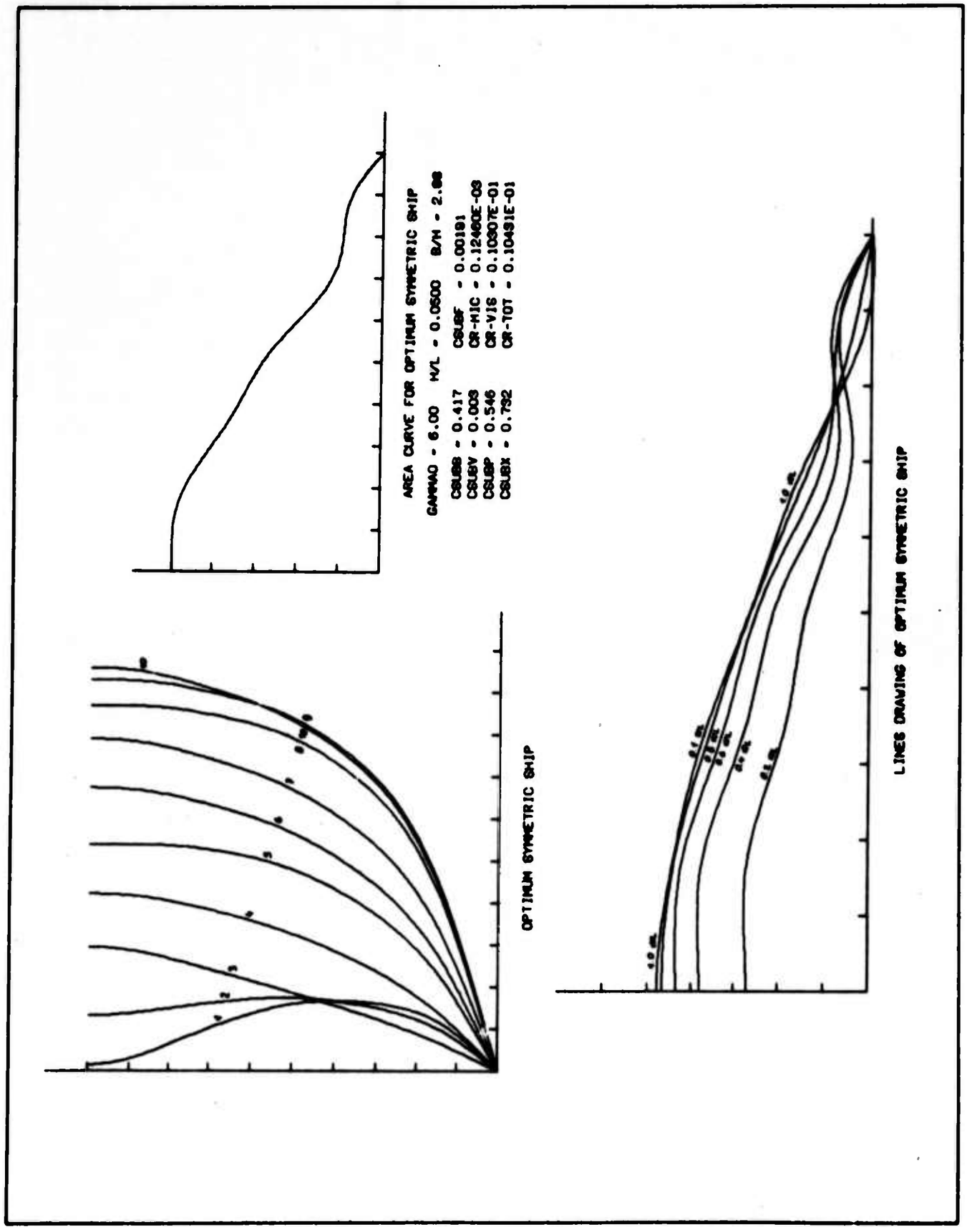

AREA CURVE FOR OPTIMUM SYMMETRIC SHIP
GAMMA0 = 6.00 H/L = 0.0500 B/H = 2.00
CSUBB = 0.417 CSUBF = 0.00191
CSUBV = 0.003 CR-HIC = 0.12460E-03
CSUBP = 0.546 CR-VIS = 0.10307E-01
CSUBX = 0.792 CR-TOT = 0.10431E-01
OPTIMUM SYMMETRIC SHIP
LINES DRAWING OF OPTIMUM SYMMETRIC SHIP

FIGURE 7

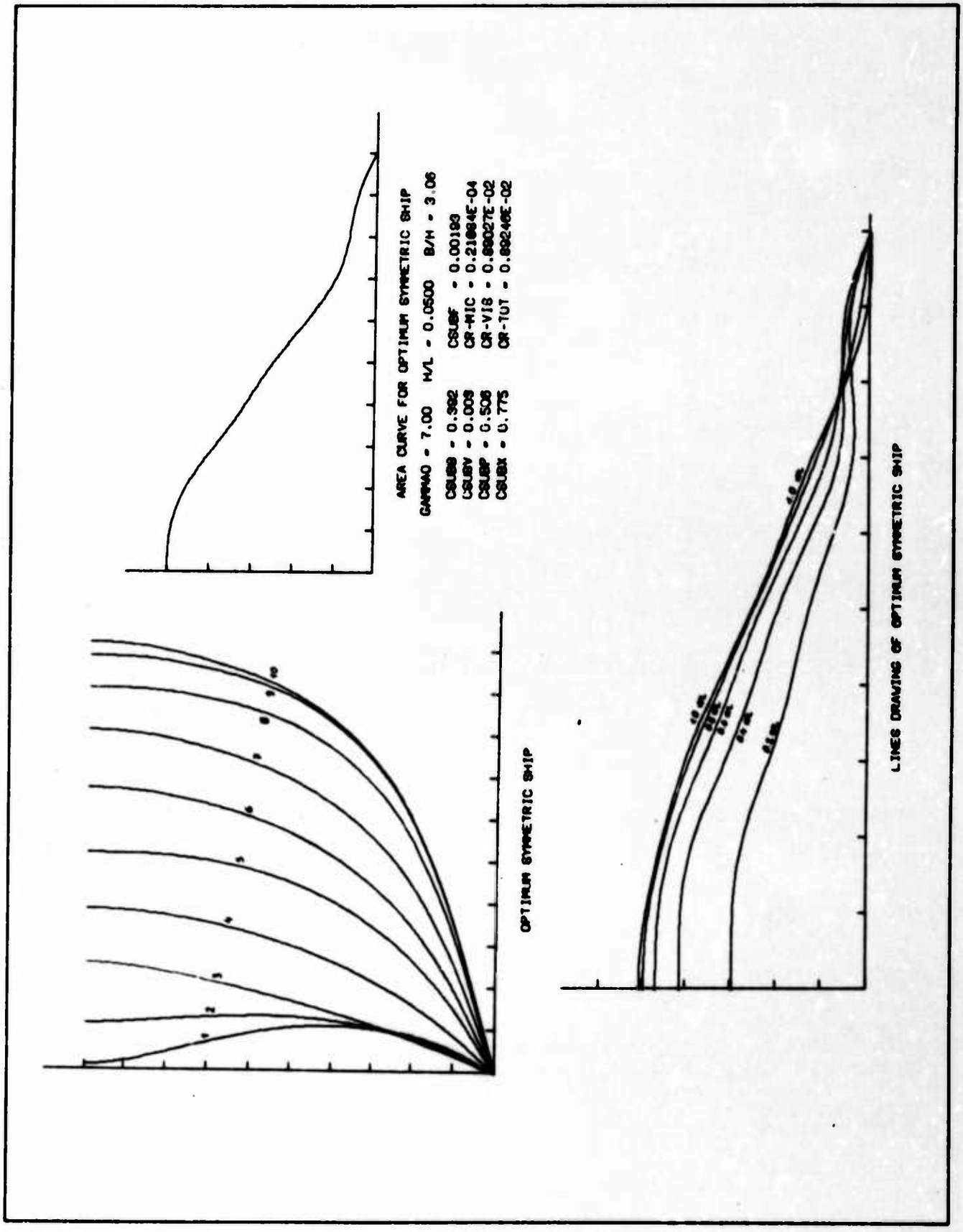

AREA CURVE FOR OPTIMUM SYMMETRIC SHIP
GAMMAO = 7.00 H/L = 0.0500 B/H = 3.06
CSUBB = 0.382 CSUBF = 0.00193
CSUBV = 0.008 CR-MIC = 0.21884E-04
CSUBP = 0.506 CR-VIS = 0.88027E-02
CSUBX = 0.775 CR-TOT = 0.89240E-02
OPTIMUM SYMMETRIC SHIP
LINES DRAWING OF OPTIMUM SYMMETRIC SHIP

FIGURE 8

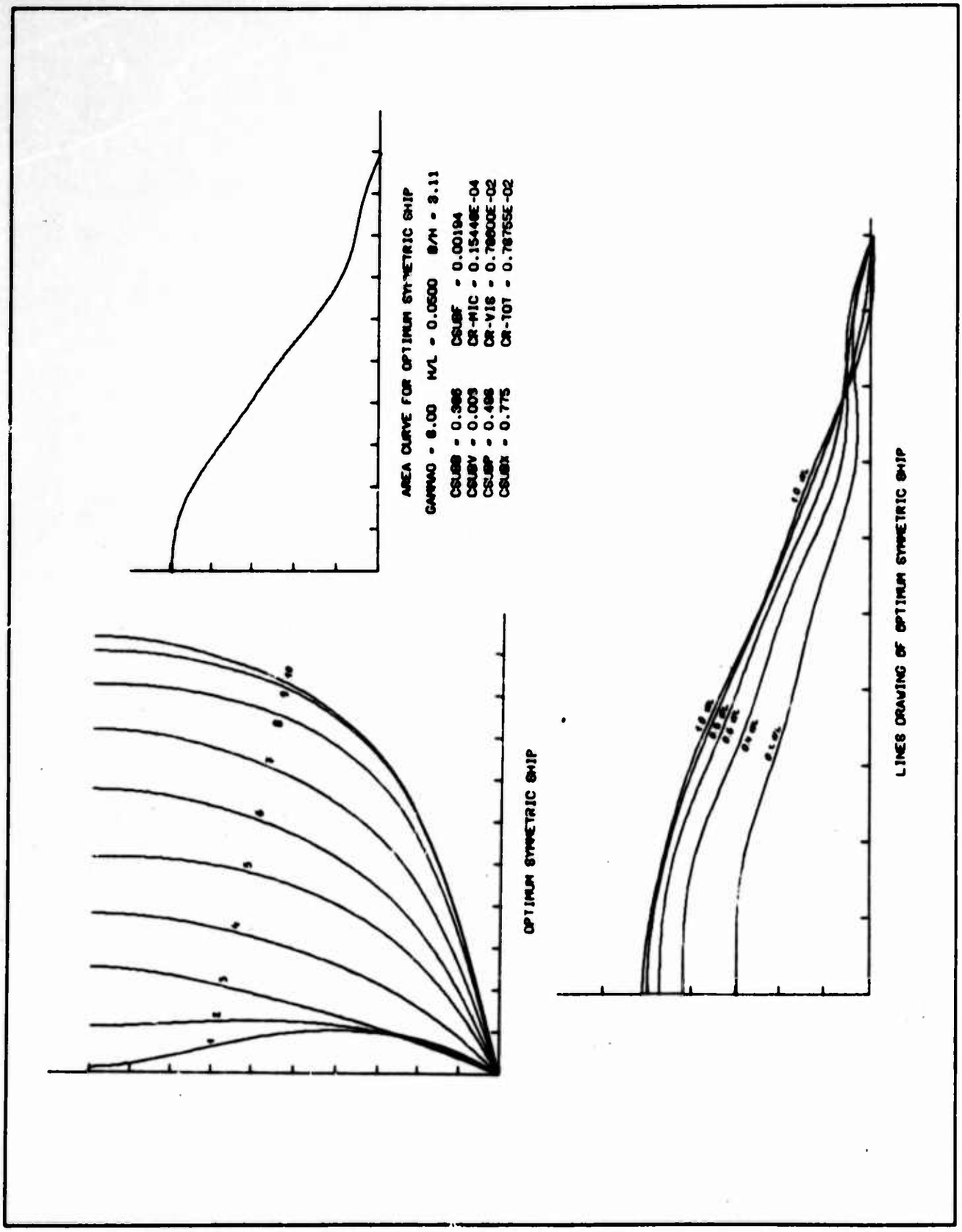

AREA CURVE FOR OPTIMUM SYMMETRIC SHIP
GAMMA0 = 8.00 M/L = 0.0500 B/H = 3.11
CSUBB = 0.386 CSUBF = 0.00194
CSUBV = 0.003 CR-MIC = 0.15448E-04
CSUBP = 0.498 CR-VIS = 0.78600E-02
CSUBX = 0.775 CR-TOT = 0.78755E-02
OPTIMUM SYMMETRIC SHIP
LINES DRAWING OF OPTIMUM SYMMETRIC SHIP

FIGURE 9

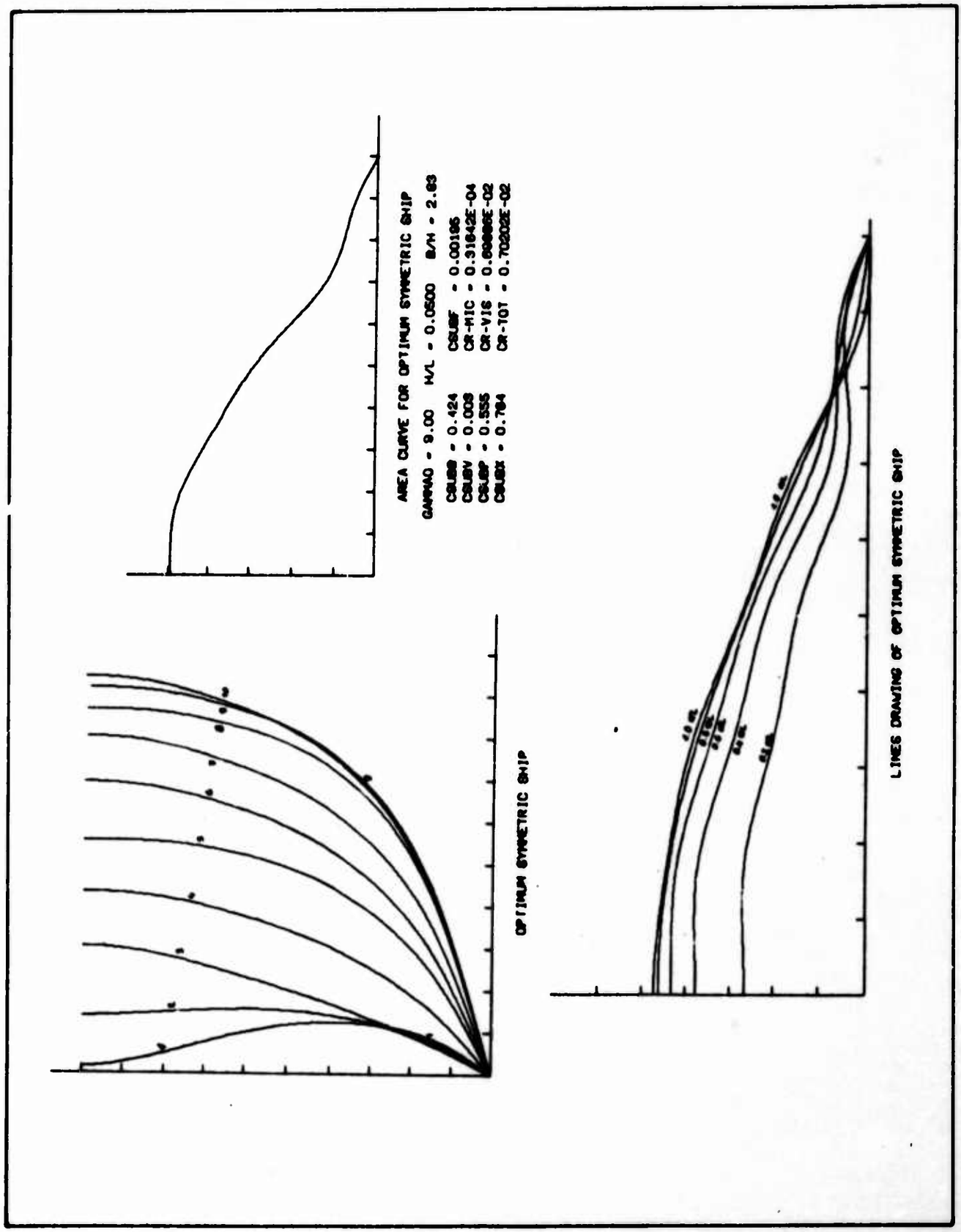

AREA CURVE FOR OPTIMUM SYMMETRIC SHIP
GAMMAO = 9.00 M/L = 0.0500 B/H = 2.83
CSUBB = 0.424 CSUBF = 0.00195
CSUBV = 0.008 CR-FIC = 0.31842E-04
CSUBP = 0.535 CR-VIS = 0.68886E-02
CSUBX = 0.784 CR-TOT = 0.70202E-02
OPTIMUM SYMMETRIC SHIP
LINES DRAWING OF OPTIMUM SYMMETRIC SHIP

FIGURE 10

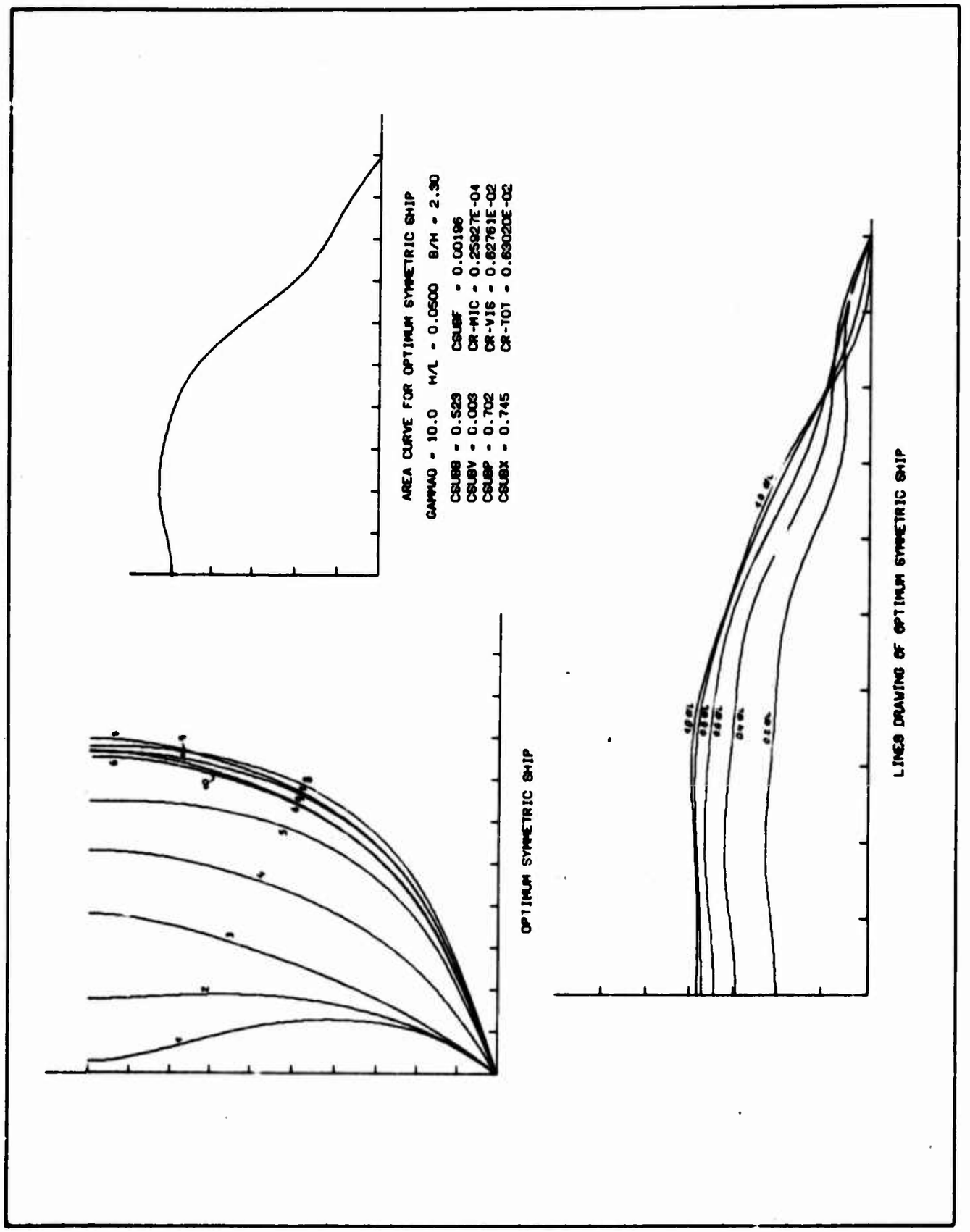

AREA CURVE FOR OPTIMUM SYMMETRIC SHIP
GAMMAO = 10.0 H/L = 0.0500 B/H = 2.30
CSUBB = 0.523 CSUBF = 0.00196
CSUBV = 0.003 CR-MIC = 0.25927E-04
CSUBP = 0.702 CR-VIS = 0.62761E-02
CSUBX = 0.745 CR-TOT = 0.63020E-02
OPTIMUM SYMMETRIC SHIP
LINES DRAWING OF OPTIMUM SYMMETRIC SHIP

FIGURE 11

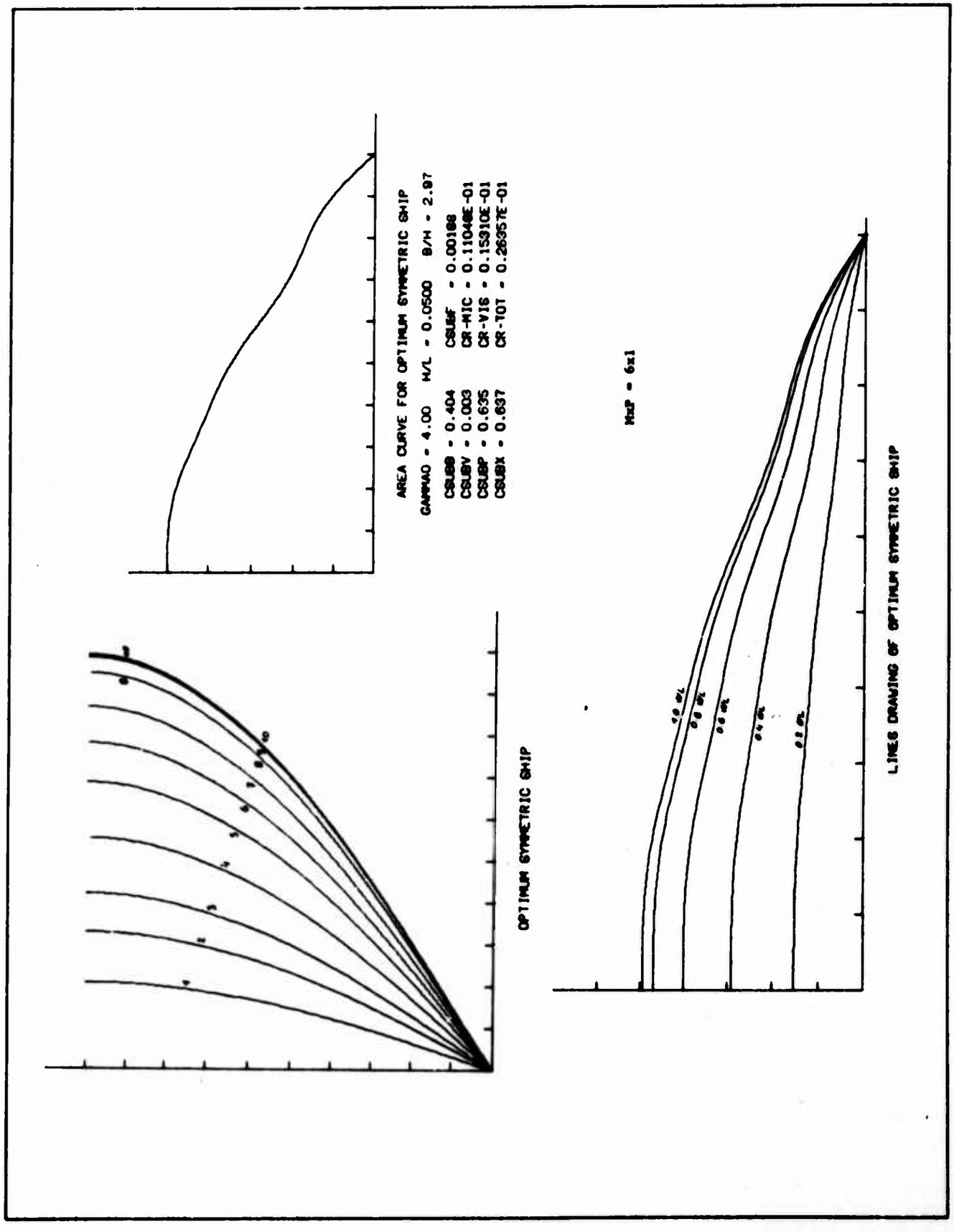

AREA CURVE FOR OPTIMUM SYMMETRIC SHIP
GAMMAO = 4.00 H/L = 0.0500 B/H = 2.97
CSUBB = 0.404 CSUBF = 0.00186
CSUBV = 0.003 CR-MIC = 0.11046E-01
CSUBP = 0.635 CR-VIS = 0.15310E-01
CSUBX = 0.637 CR-TOT = 0.26357E-01
OPTIMUM SYMMETRIC SHIP
MxP = 6x1
LINES DRAWING OF OPTIMUM SYMMETRIC SHIP

FIGURE 12

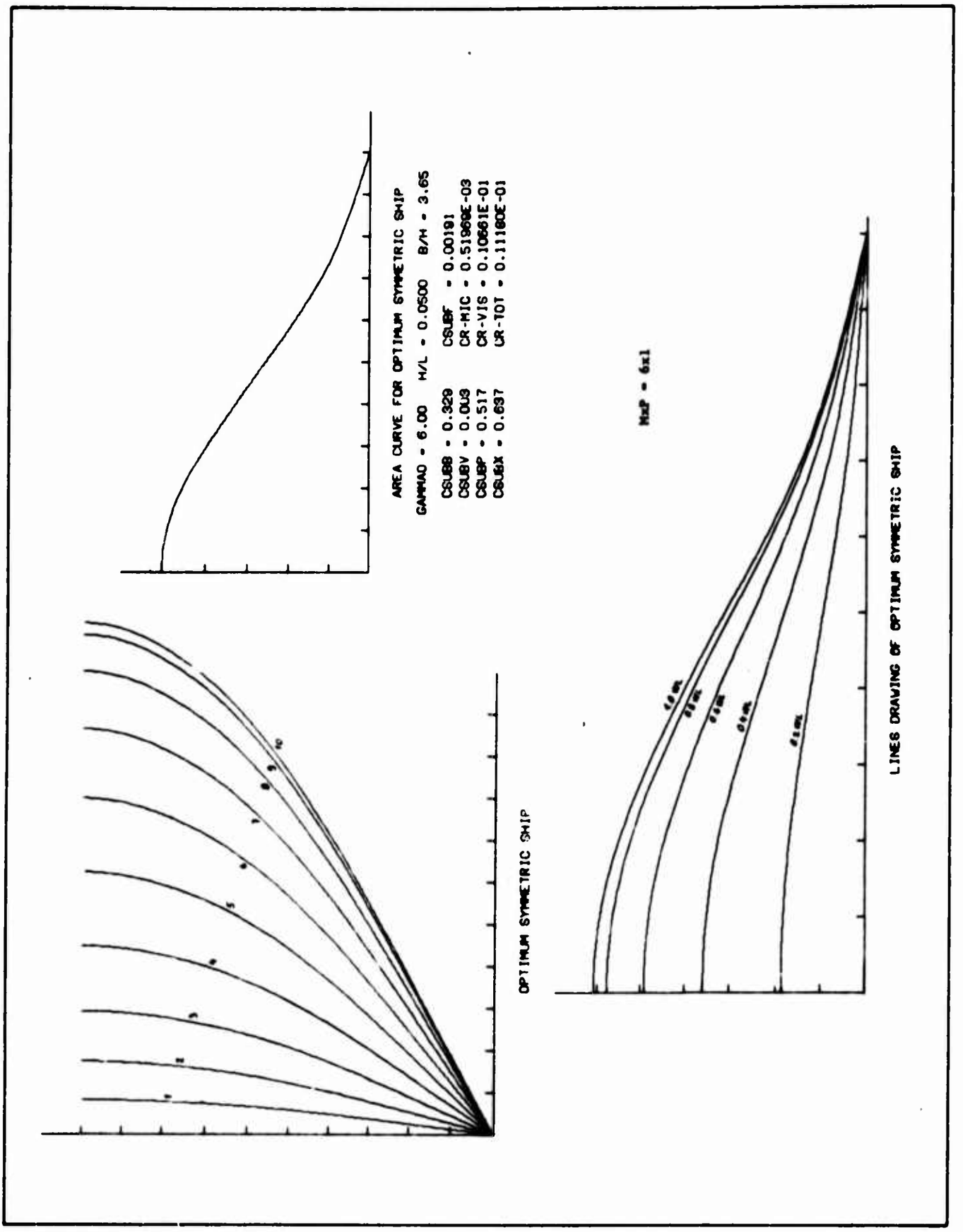

AREA CURVE FOR OPTIMUM SYMMETRIC SHIP
GAMMAO = 6.00 H/L = 0.0500 B/H = 3.65
CSUBB = 0.329 CSUBF = 0.00191
CSUBV = 0.043 CR-MIC = 0.51960E-03
CSUBP = 0.517 CR-VIS = 0.10561E-01
CSUBX = 0.637 CR-TOT = 0.11180E-01
OPTIMUM SYMMETRIC SHIP
MxP = 6x1
LINES DRAWING OF OPTIMUM SYMMETRIC SHIP

FIGURE 13

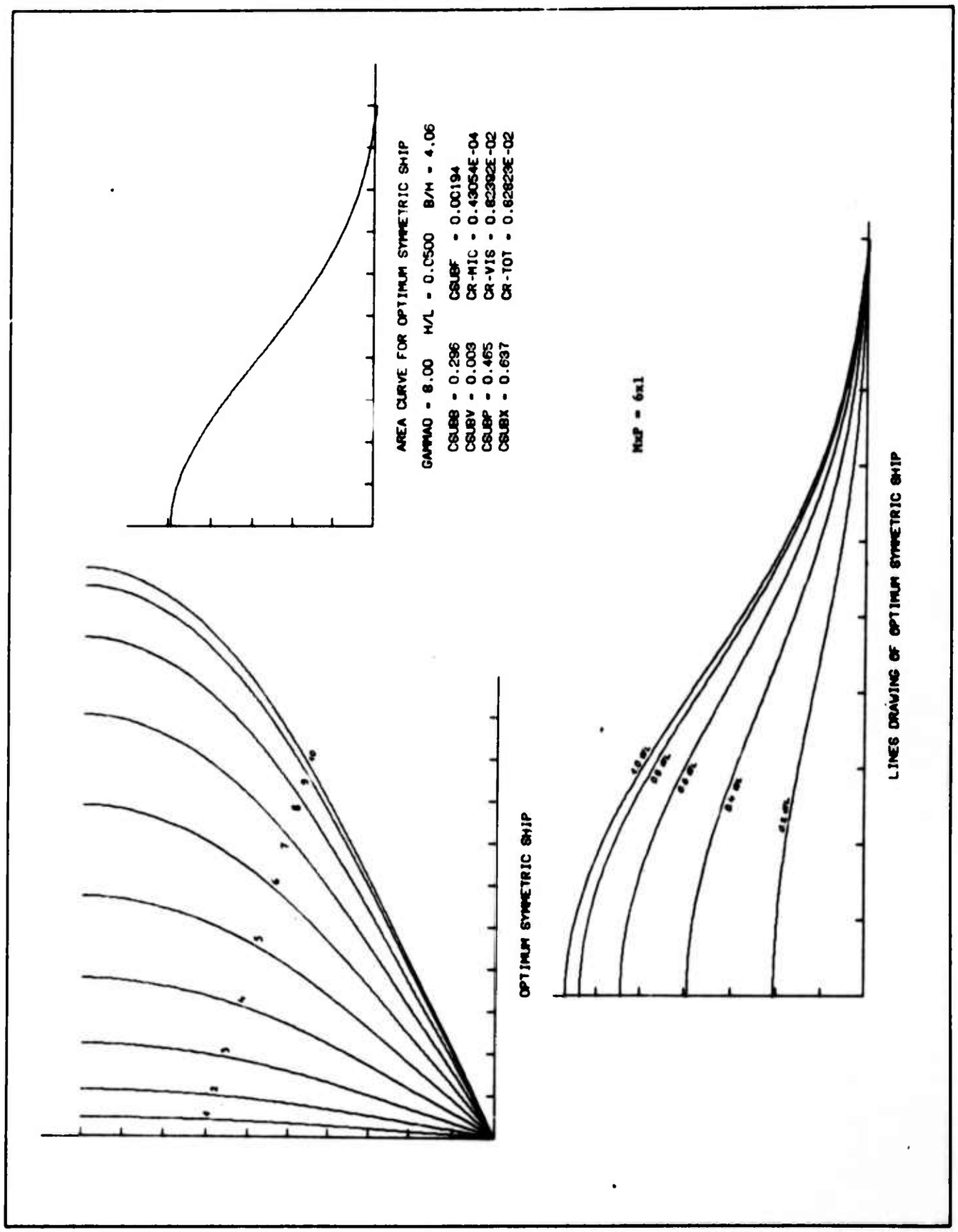

AREA CURVE FOR OPTIMUM SYMMETRIC SHIP
GAMMAO - 8.00 H/L - 0.0500 B/H - 4.06
CSUBB - 0.296 CSUBF - 0.00194
CSUBV - 0.003 CR-MIC - 0.430546-04
CSUBP - 0.465 CR-VIS - 0.823926-02
CSUBX - 0.637 CR-TOT - 0.828236-02
OPTIMUM SYMMETRIC SHIP
MAP - 6x1
LINES DRAWING OF OPTIMUM SYMMETRIC SHIP

FIGURE 14

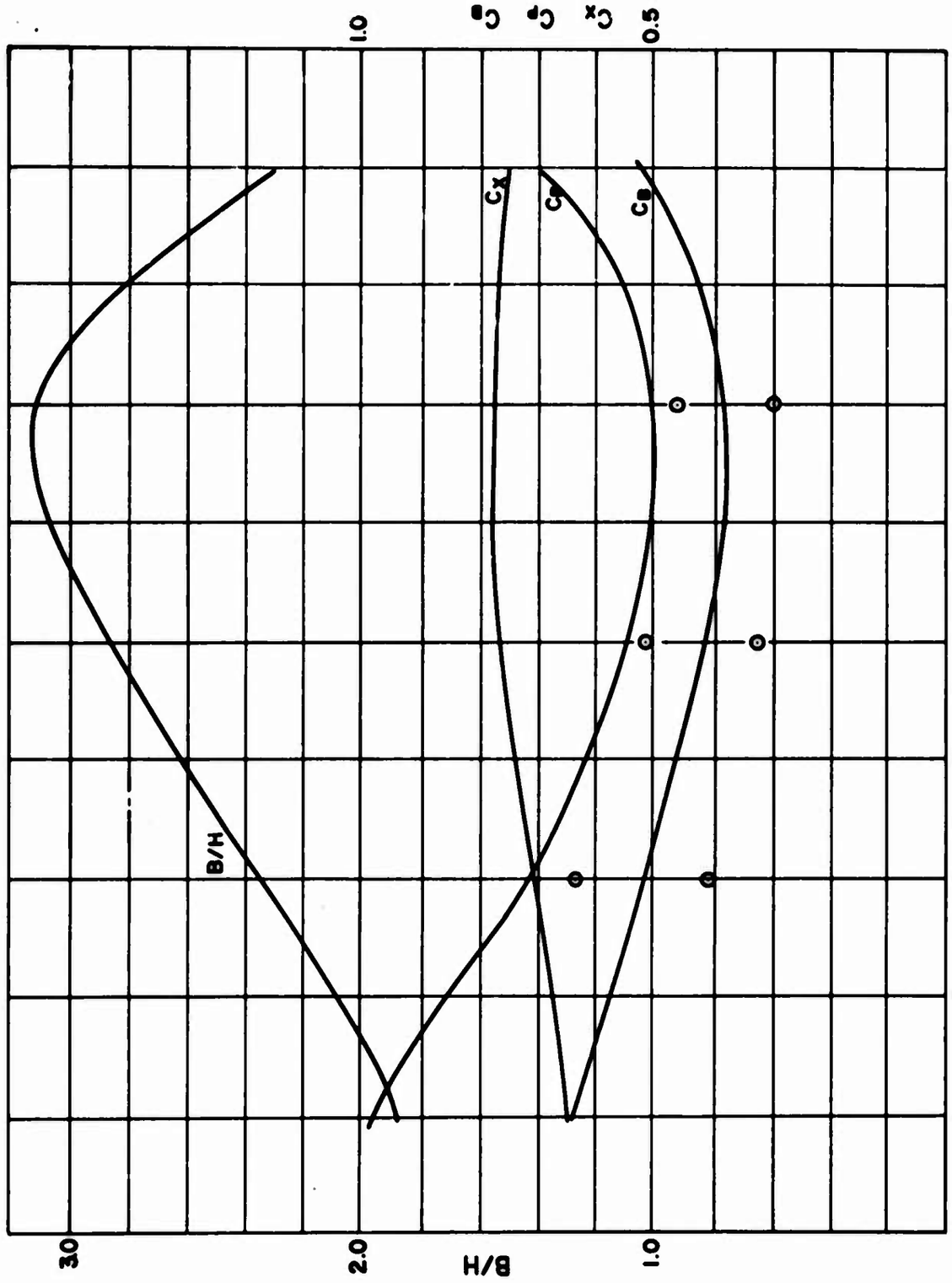


FIGURE 15

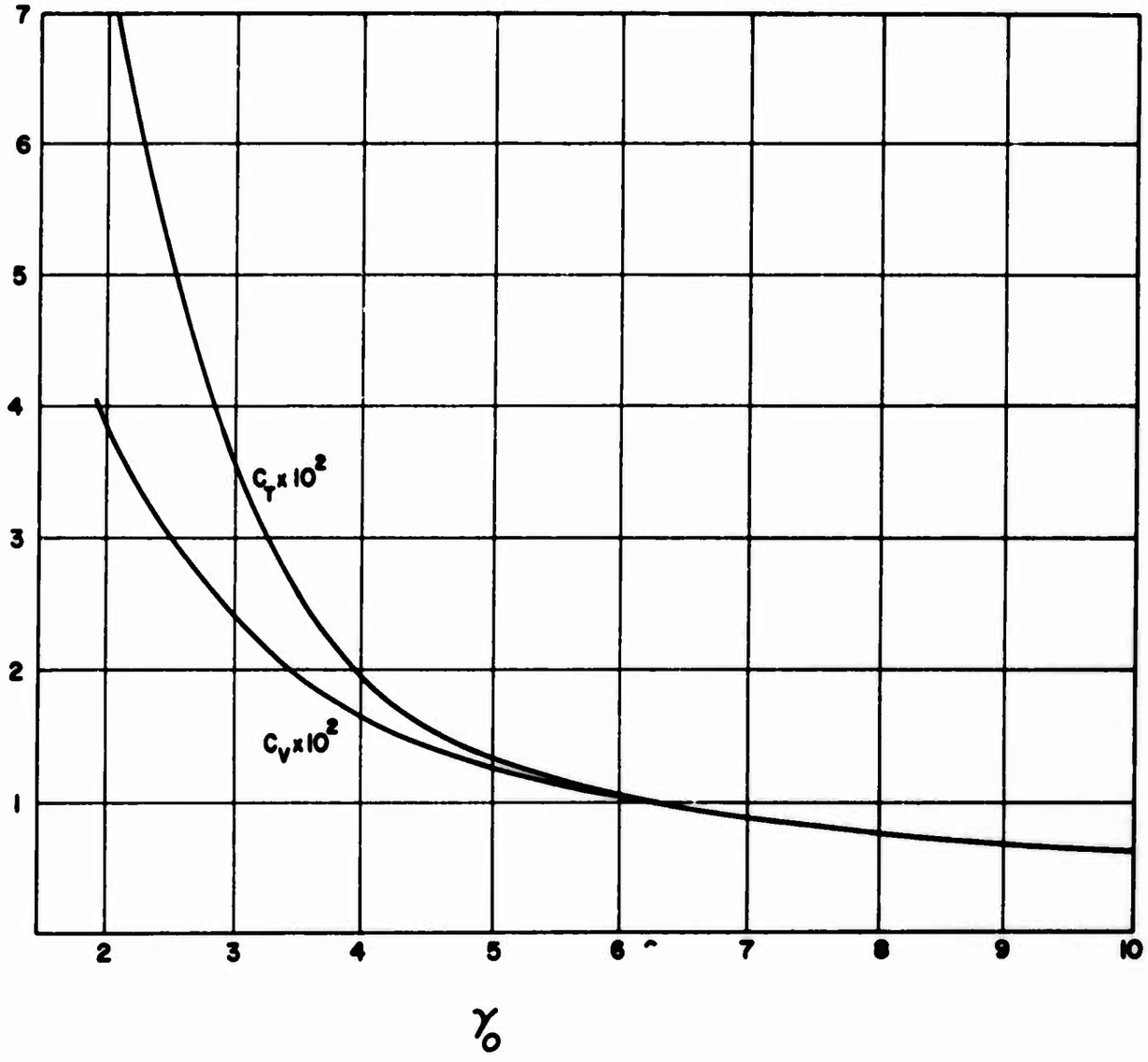


FIGURE 16.

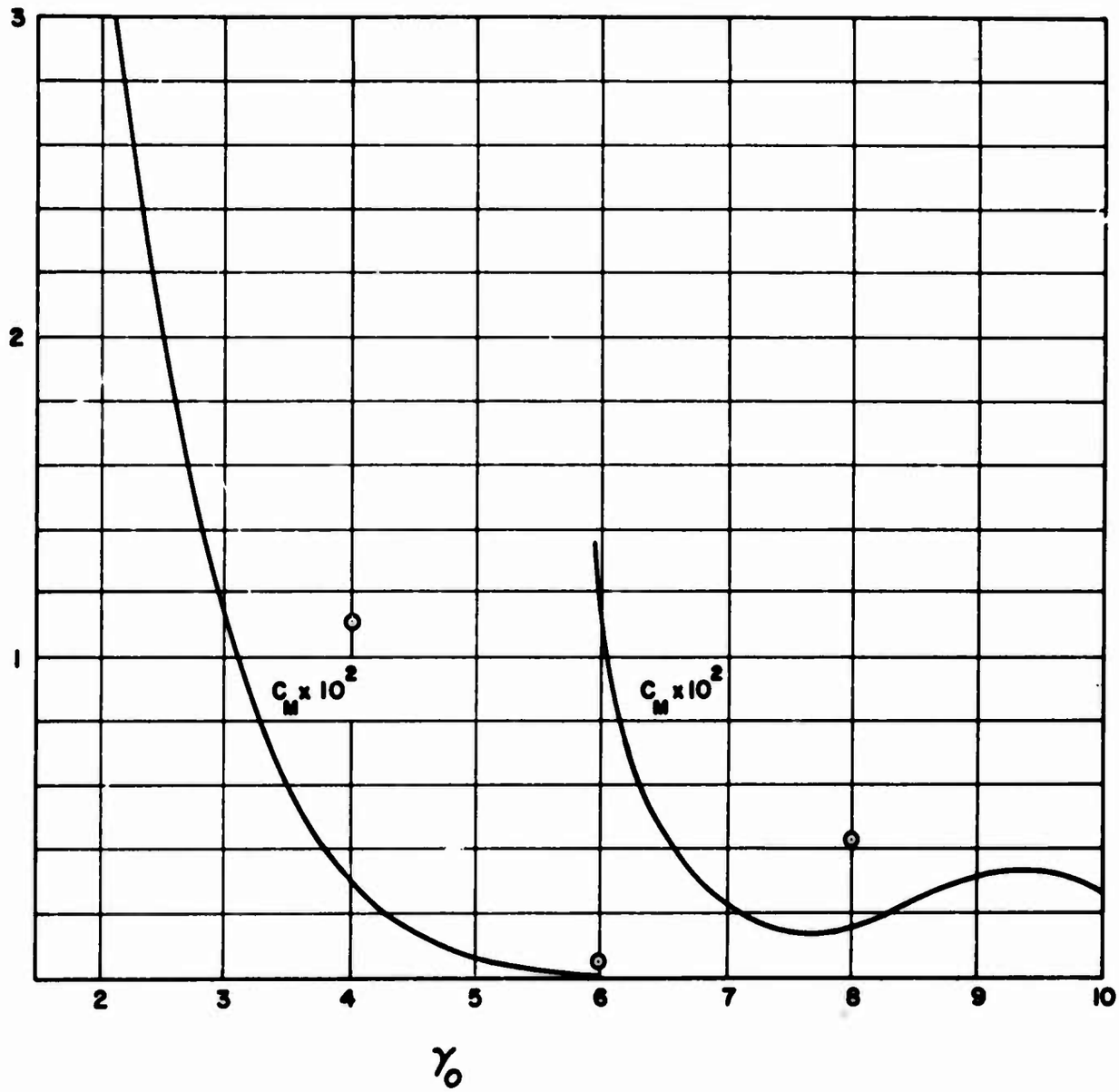


FIGURE 17.

that the distribution in depth is of secondary importance. A computing experiment was made to test this and related conjectures. For $\gamma_o = 4$, 6, and 8 the dimension M x P of the coefficient matrix was taken first as 6 x 1, then as 6 x 2 instead of 6 x 6 as in the other computations. In the 6 x 1 computation all sections are affinely related (cosine curves, in fact) and the only freedom is in the longitudinal distribution. This situation corresponds to that in the papers of Weinblum (e.g. 1957). In the 6 x 2 computation there is a single degree of freedom in the vertical direction which permits variation in vertical distribution along the length. The results were instructive. The frictional resistance varied by only small amounts, less than 5%, whereas the wave resistance was increased by factors of 2.8 to 4.2 in the 6 x 1 computations. On the other hand, in the 6 x 2 computations the wave resistance was already within 15% of that obtained in the 6 x 6 computations. The encircled points on Figures 15 and 17 show results of the 6 x 1 computation. The body plans and sectional-area curves are shown in Figures 12 to 14.

In order to test the effect of restricting the amount of freedom in the longitudinal direction, a computation was made for $\gamma_o = 4$ with a 4 x 4 matrix. The wave resistance of the resulting form was considerably lower than with the 6 x 1 matrix ($C_M = 0.3621 \times 10^{-2}$), but still not as near the 6 x 6 value as with the 6 x 2 matrix. We conclude that longitudinal distribution is, in fact, more important than the vertical providing that at least some provision is allowed for vertical variation with longitudinal position.

For $\gamma_o = 6$ the effect of changing C_∇ was also investigated, the optimum forms for $C_\nabla = 1.5 \times 10^{-3}$ and 4.5×10^{-3} being computed in addition to 3.0×10^{-3}. The forms were very close to being affinely related, with corresponding cordinates being nearly proportional to the values of C_∇. Figure 18 shows graphically the dependence upon C_∇ of several quantities.

It is noteworthy that for all speeds the waterline at the surface is cusped, or practically so. This phenomenon obtains also for the optimum forms with given afterbody.

The Ship with Given Afterbody

The body plans and sectional area curves for the optimum forebodies for $\gamma_o = 4$ to 9 are shown in Figures 19 to 24. Figures 25 and

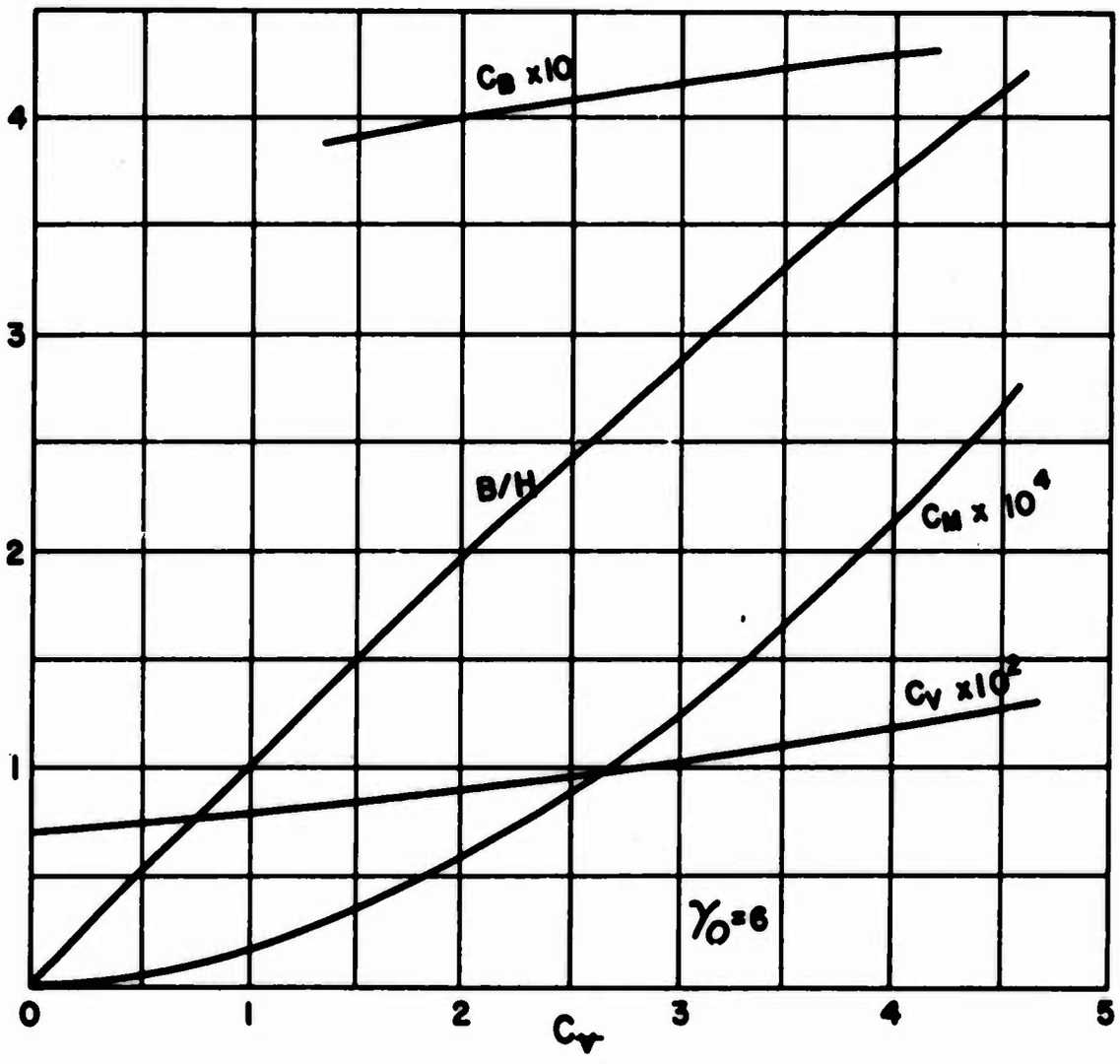


FIGURE 18.

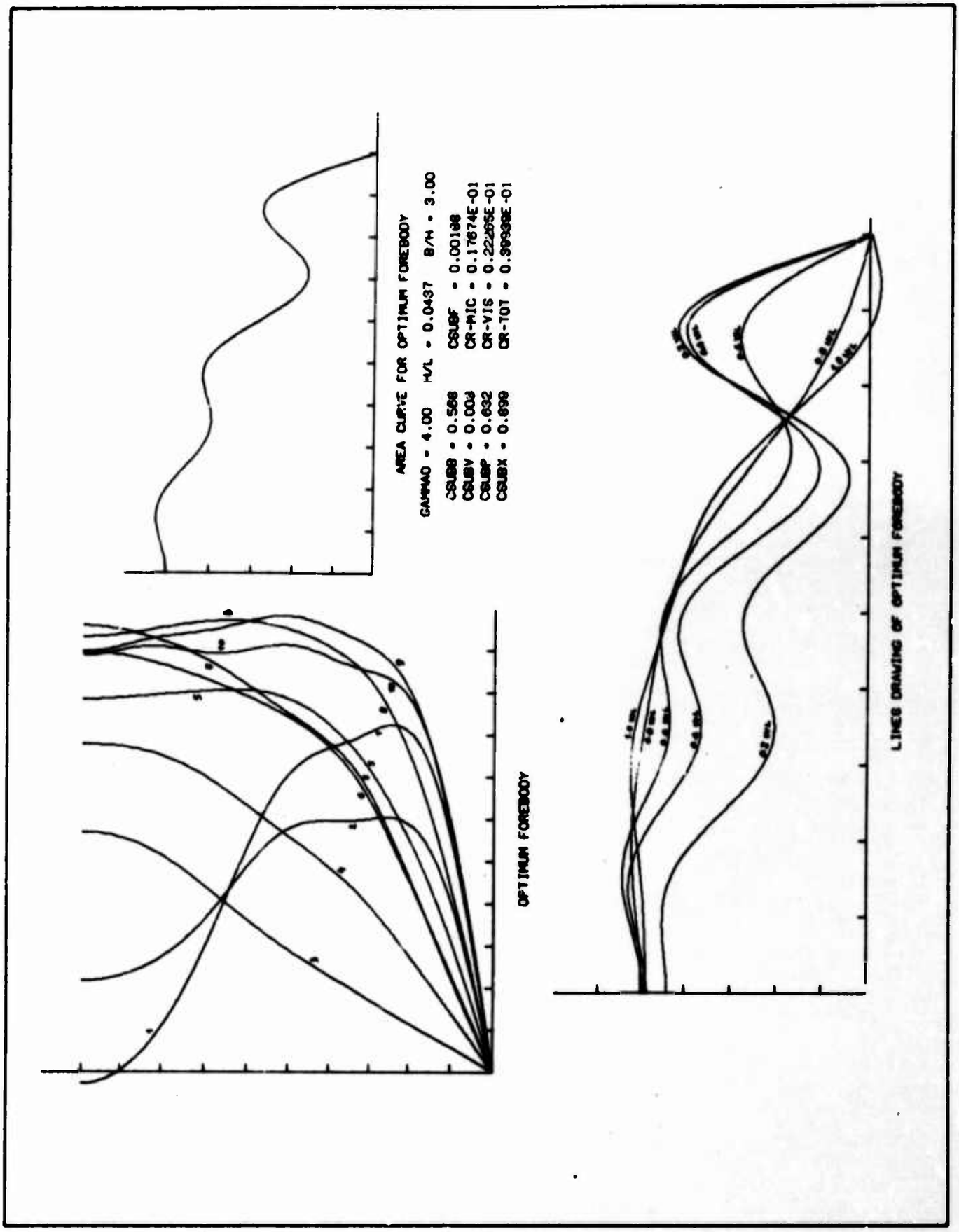

AREA CURVE FOR OPTIMUM FOREBODY
GAMMAO = 4.00 M/L = 0.0437 B/M = 3.00
CSUBB = 0.566 CSUBF = 0.00186
CSUBV = 0.000 CR-MIC = 0.17674E-01
CSUBP = 0.632 CR-VIS = 0.22265E-01
CSUBX = 0.690 CR-TOT = 0.39939E-01
OPTIMUM FOREBODY
LINES DRAWING OF OPTIMUM FOREBODY

FIGURE 19

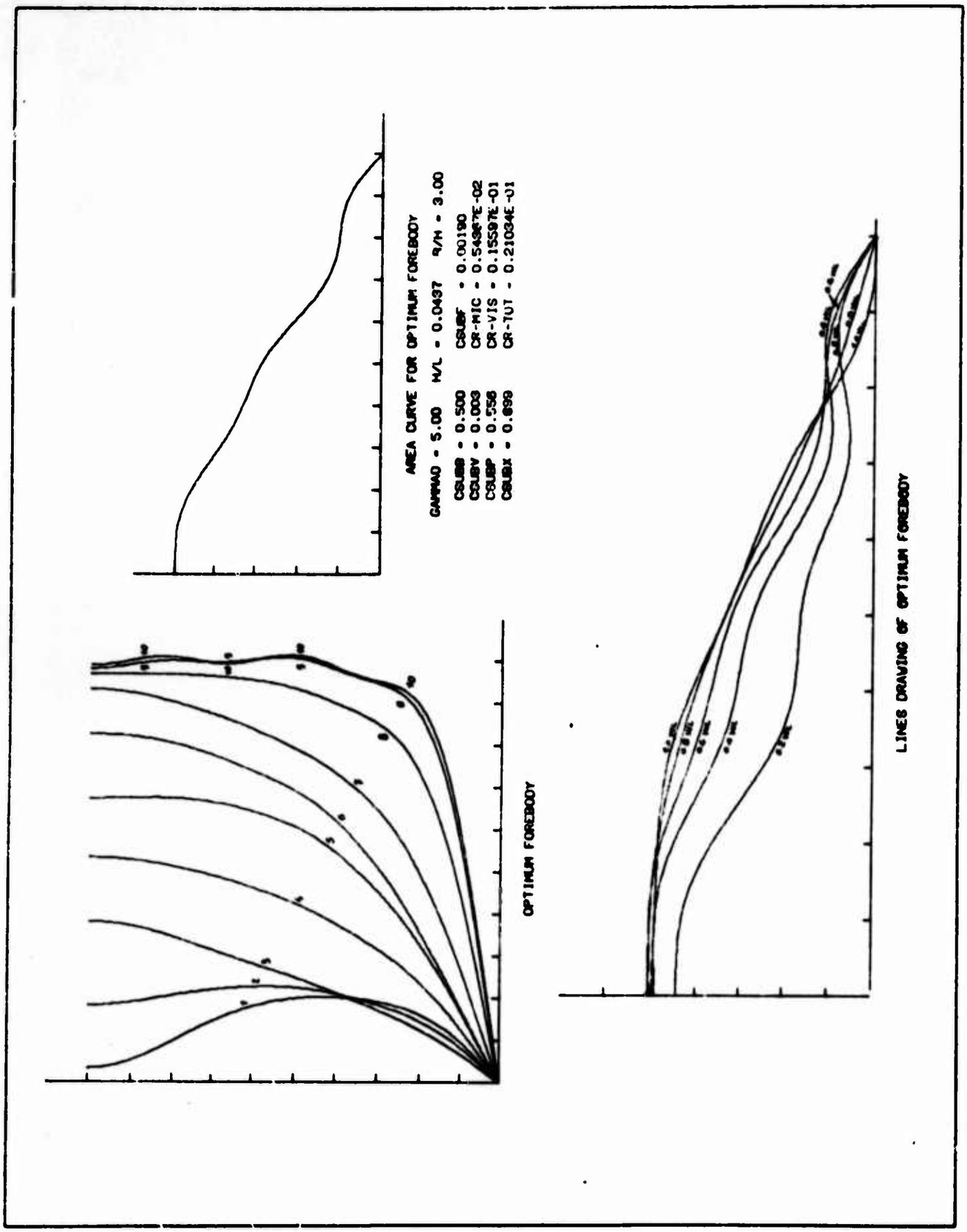

AREA CURVE FOR OPTIMUM FOREBODY
GAMMAO = 5.00 M/L = 0.0497 R/M = 3.00
CSUBB = 0.500 CSUBF = 0.00190
CSUBV = 0.003 CR-MIC = 0.54387E-02
CSUBP = 0.556 CR-VIS = 0.15597E-01
CSUBX = 0.899 CR-TOT = 0.21034E-01
OPTIMUM FOREBODY
LINES DRAWING OF OPTIMUM FOREBODY

FIGURE 20

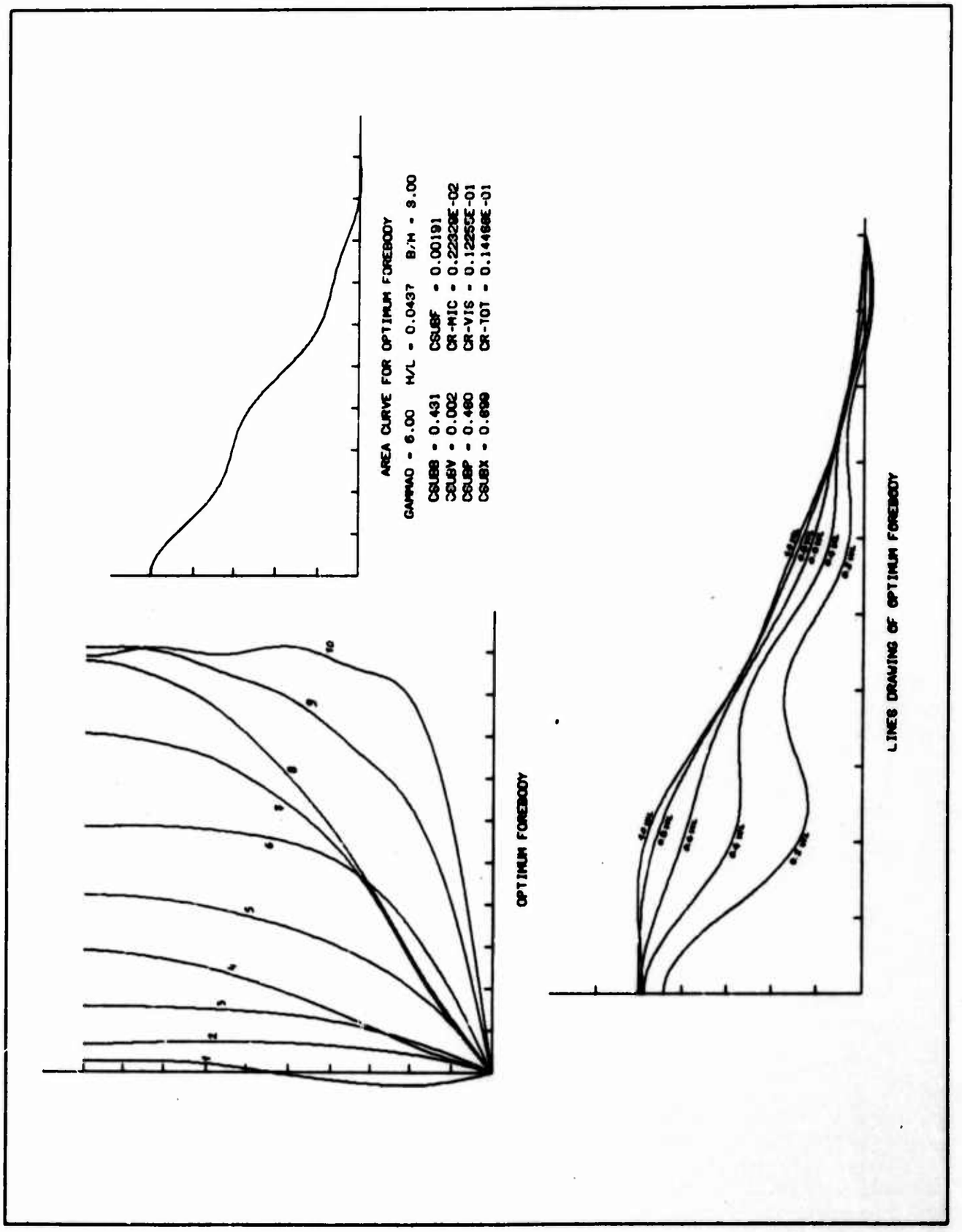

AREA CURVE FOR OPTIMUM FOREBODY
GAMMAO = 6.00 M/L = 0.0437 B/H = 3.00
CSUBB = 0.431 CSUBF = 0.00191
CSUBV = 0.002 CR-MIC = 0.22320E-02
CSUBP = 0.460 CR-VIS = 0.12255E-01
CSUBX = 0.899 CR-TOT = 0.14468E-01
OPTIMUM FOREBODY
LINES DRAWING OF OPTIMUM FOREBODY

FIGURE 21

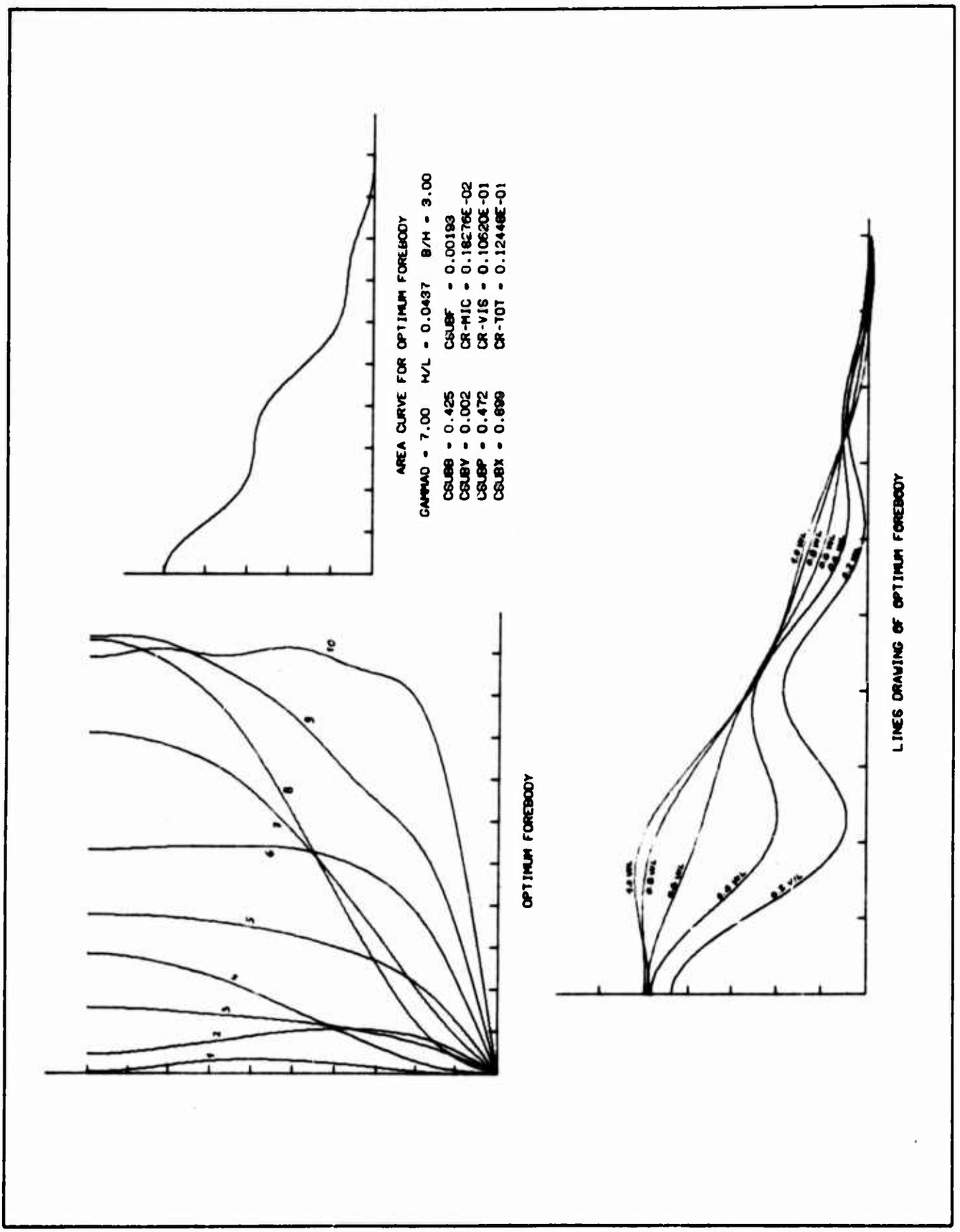

AREA CURVE FOR OPTIMUM FOREBODY
GAMMAD = 7.00 H/L = 0.0437 B/H = 3.00
CSUBB = 0.425 CSUBF = 0.00193
CSUBV = 0.002 CR-MIC = 0.18276E-02
CSUBP = 0.472 CR-VIS = 0.10620E-01
CSUBX = 0.699 CR-TOT = 0.12448E-01
OPTIMUM FOREBODY
LINES DRAWING OF OPTIMUM FOREBODY

FIGURE 22

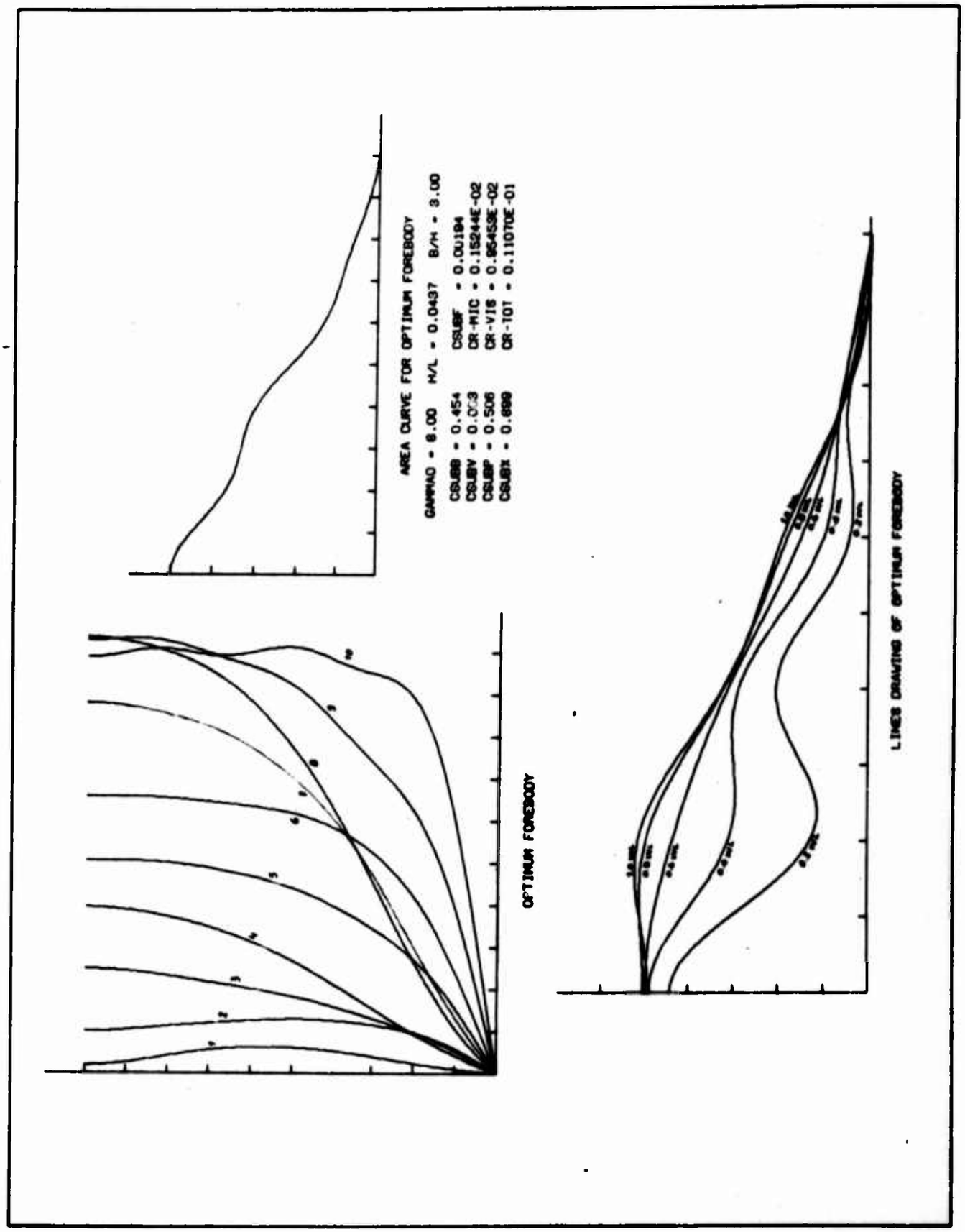

AREA CURVE FOR OPTIMUM FOREBODY
GAMMAO = 8.00 H/L = 0.0437 B/H = 3.00
CSUBB = 0.454 CSUBF = 0.00184
CSUBV = 0.053 CR-WIC = 0.15244E-02
CSUBP = 0.506 CR-VIS = 0.85455E-02
CSUBX = 0.699 CR-TOT = 0.11070E-01
OPTIMUM FOREBODY
LINES DRAWING OF OPTIMUM FOREBODY

FIGURE 23

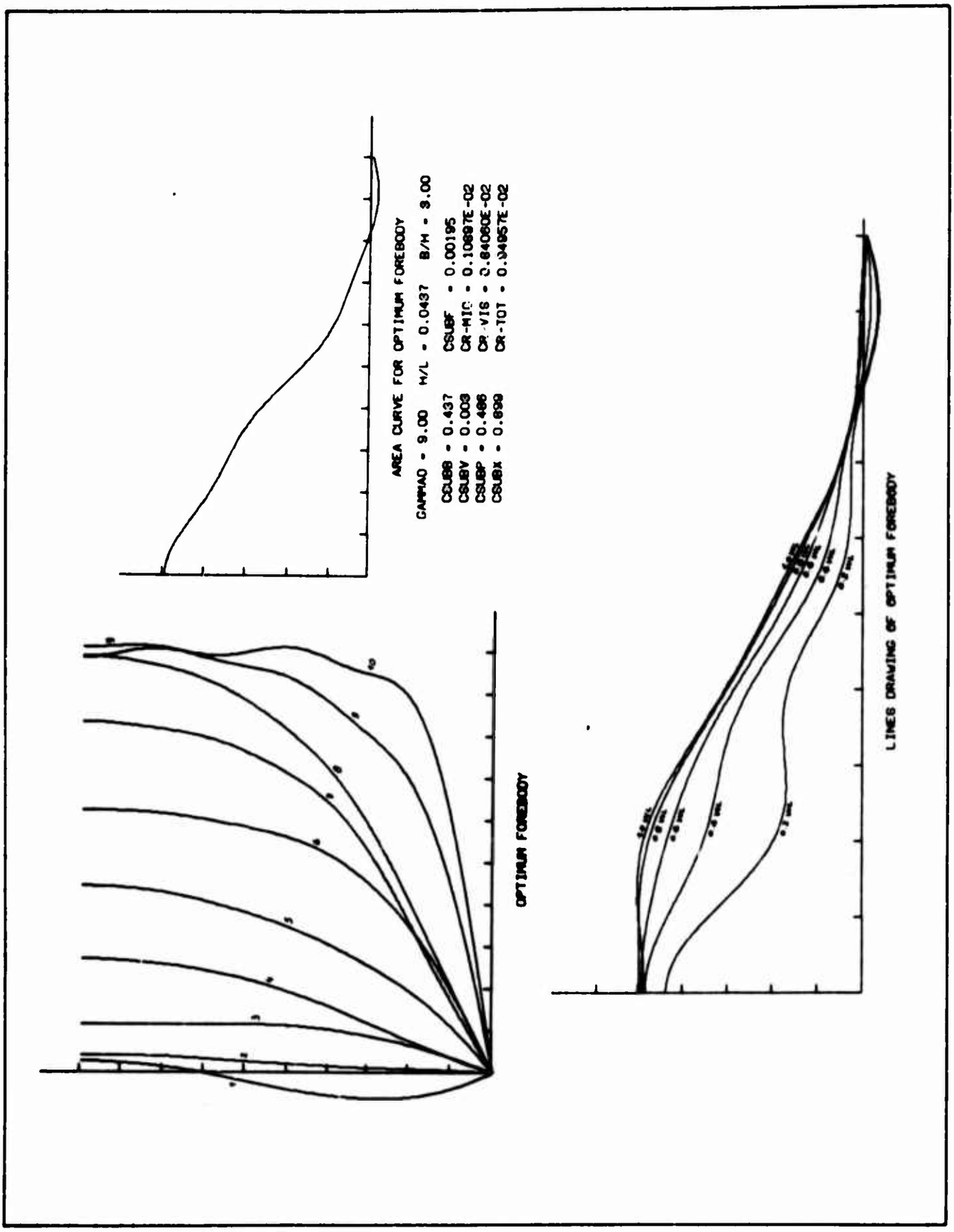

AREA CURVE FOR OPTIMUM FOREBODY
CAPPAO - 9.00 M/L - 0.0437 B/H - 3.00
CSUBB - 0.437 CSUBF - 0.00195
CSUBV - 0.003 CR-MIC - 0.10697E-02
CSUBP - 0.486 CR-VIS - 0.84060E-02
CSUBX - 0.899 CR-TOT - 0.94857E-02
OPTIMUM FOREBODY
LINES DRAWING OF OPTIMUM FOREBODY

FIGURE 24

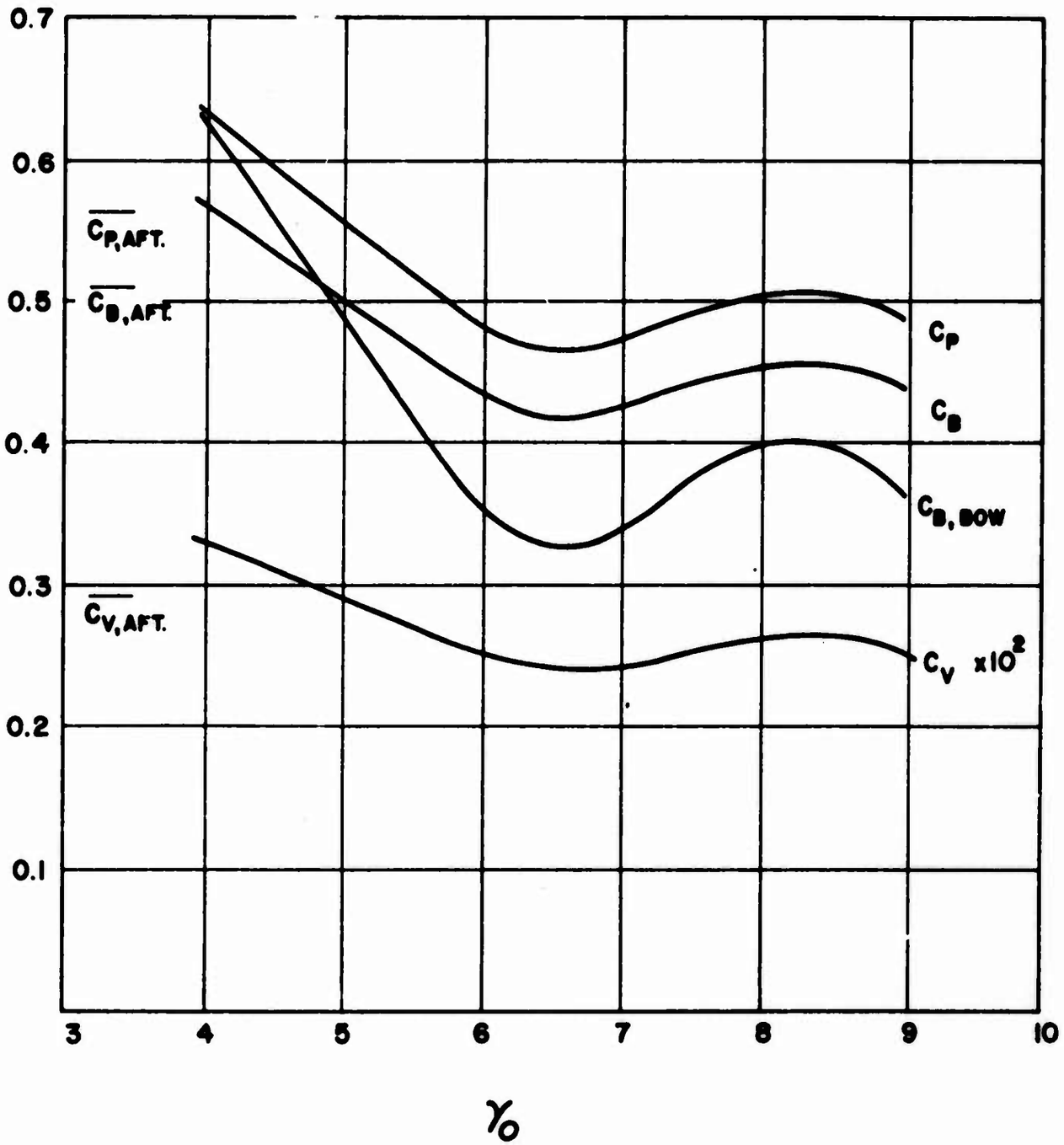

0.7
0.6
0.5
0.4
0.3
0.2
0.1
$\overline{C_{P,AFT.}}$
$\overline{C_{B,AFT.}}$
$\overline{C_{V,AFT.}}$
C_P
C_B
$C_{B,BOW}$
$C_V \times 10^2$
3
4
5
6
7
8
9
10
γ_o

FIGURE 25.

26 are analogues to Figures 15, 16, and 17, respectively, for the symmetric ship. There are, however, certain differences. Here B/H is fixed at 3, but $C_\forall$ can change. Also, since $C_B = C_X C_P = 0.9\, C_P$ and $C_\forall = (B/H)(H/L)^2 C_B = 0.00573 \times C_B$ there is really no more information in the C_P and C_B curves than in the $C_\forall$ curve.

Possibly the most significant information lies in a comparison of the results with those for the symmetric ship. It is evident from a comparison of Figures 16 and 26 that the wave resistance of the optimum ship with given afterbody is an appreciable part of the total resistance in the region $6 \leq \gamma_0 \leq 9$ whereas it was negligible for the symmetric ship. One might feel constrained to be a little cautious here because the volumetric coefficient has decreased. However, inspection of Figure 18 shows that this makes the discrepancy all the more striking. One can only conclude that, on the basis of this criterion, the afterbody is a rather poor one for this speed range. In fact, it compares rather poorly at all speeds with the performance of the symmetric ship.

Concluding Remarks

There is little to add to what has already been said except that experiments appear to be the next appropriate step, at least for the symmetric models with $\gamma_0 \geq 6$. For these an interesting choice confronts one. In order to test the conclusions, should one use the designs for the 400' ship, or should one make new designs for an optimum 5' model?

Finally, we note that it need not be considered surprising if one should be able to make a substantial improvement upon existing ship forms. Empirical methods of investigation operate within a limited scope of variation. Inui has already been very successful with only a few degrees of freedom at his disposal. With thirty-six one should be able to do even better. On the other hand, some further restraints need to be imposed for $\gamma_0 \leq 5$ in order to obtain forms whose behavior will conform to the assumed model of frictional resistance. Unfortunately this will apparently lead to the more difficult numerical problem in which bounds on ordinate and slope are imposed as side conditions.

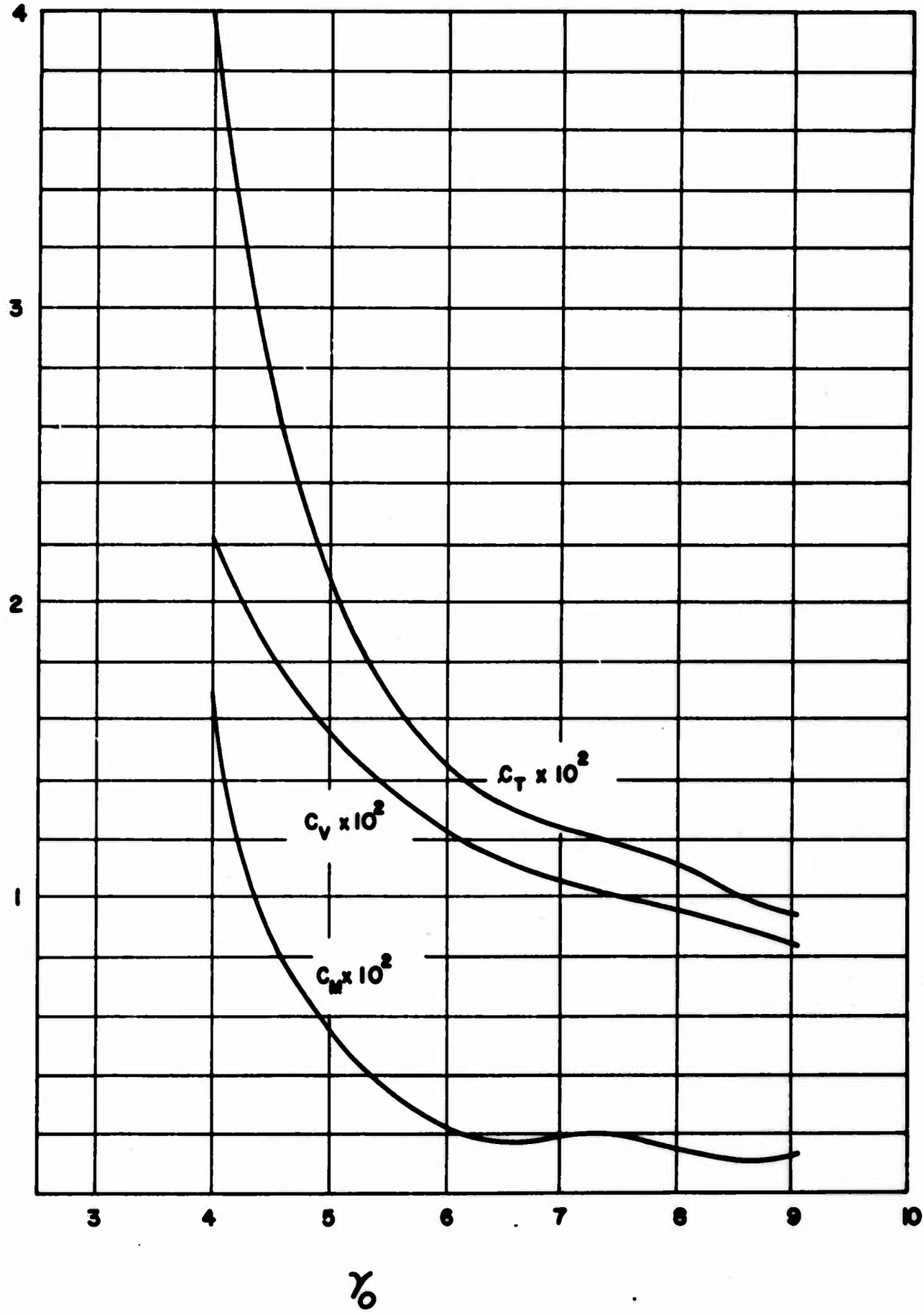


FIGURE 26.

BIBLIOGRAPHY

Webster, W. C. and Wehausen, J. V., "Schiffe geringsten Wallenwiderstandes mit vorgegebenem Hinterschiff," Schiffstechnik 9 (1962), 62-68.

Weinblum, G. P., A Systematic Evaluation of Michell's Integral, David Taylor Model Basin, Report 886 (1954), iii + 43 pp. + 8 figures.

Weinblum, G., Wustrau, D., and Vosers, G., "Schiffe Geringsten Widerstandes," Jahrbuch der Schiffbautchnischen Gesellschaft 51 (1957), 175-204; Erorterung, 205-214.

Wehausen, J. V., Reichert G., and Gauthey, J. R., Ships of Minimum Wave Resistance, Institute of Engineering Research, University of California, Berkeley, Report, Series 82, Issue No. 21 (Oct. 1961) iii + 55 pp.

DISCUSSIONS

by S. W. W. Shor

In this paper the authors have shown how to produce three-dimensional ship-shape forms of very low resistance. Nonetheless, there remains a serious problem in making the results of calculations such as theirs generally useful to practicing naval architects. This is because a practicing naval architect must meet many requirements besides those of low resistance, and it is most unlikely that a form derived solely to solve the resistance problem will immediately solve the other problems too. There is also a communications problem, in that most practicing naval architects are more used to dealing with drawings and tables of offsets than with the constraints one can place on a computer calculation.

Fortunately, a suggestion made by Professor Bessho in one of the papers he presented at this seminar can be extended in such a fashion as to multiply greatly the usefulness of the work of the present authors. He pointed out that if we add some multiple of a source or dipole distribution which has almost zero wave resistance to any other distribution, we add very little resistance. This is because small resistance implies small $|C(f) + iS(f)|$ in the equation

$$R = \int_0^{\pi/2} |C(f) + iS(f)|^2 \cos^3\theta \, d\theta, \qquad (A)$$

where $C(f)$ and $S(f)$ indicate that the functions C and S are functionals of the function f. Since the functionals C and S are linear in f, where the hull is defined by $\eta = f(\xi,\zeta)$, it follows that for any two such functionals f_1 and f_2 we can write

$$C(a_1F_1+a_2f_2)+ iS(a_1f_1+a_2f_2) = a_1[C(f_1)+ iS(f_1)]+ a_2[C(f_2)+ iS(f_2)]. \qquad (B)$$

In consequence, if we have a set of distributions which correspond to ships of very low resistance, then a linear sum of these distributions also corresponds to a ship which has very low resistance. That is, any combination

$$F = a_1f_1 + a_2f_2 + \ldots + a_nf_n \qquad (C)$$

will certainly have low resistance provided that we do not choose a set of coefficients $a_1,a_2,\ldots,a_n$ which are such that $|a_1|+|a_2| + \ldots +|a_n| \gg 1$.

This last requirement is to insure that combinations of hull forms cannot be made which exaggerate the wave-producing qualities of their components. This might occur if small differences between large quantities were permitted.

The practical application of this principle now becomes clear.

(1) the first step is to derive many functions defining hull forms of very small wave-making resistance and tabulate them. The set of such functions is certainly not a complete set, at least under the restrictions placed on Equation (C), for if the set were complete every hull form could be described in terms of the members of this set. Then every hull form would be a form of low wave-making resistance. On the other hand, experience to date seems to indicate that the set is quite a large one. It may well be that we can quickly derive enough forms so that by application of Equation (C) we may find a hull through linear combination which will suit almost any purpose.

(2) Using the library of forms of low resistance complied from results such as those of the present paper, the naval architect takes linear combinations of singularity distributions as in Equation (C) so that he approximately meets the requirements other than resistance of his hull design. Then he calculates the streamlines about this hull by one of the standard methods, and so defines the hull exactly.

(3) If the resulting hull corresponding to the distribution F requires further correction, he does this by a repetition of the process. However, if the corrections are small it will be possible to dispense with the recalculation of the streamlines. That is, if we take the functional $G(F)$ as the set of offsets corresponding to the singularity distribution F, then if the coefficients $b_1, b_2, \ldots, b_n$ are small enough we can write

$$G(F + b_1 f_1 + b_2 f_2 + \ldots + b_n f_n) \approx G(F) + b_1 f_1 + b_2 f_2 + \ldots + b_n f_n . \qquad (D)$$

This means, also, that if a singularity distribution is available whose corresponding streamline pattern has been calculated and defines a hull which nearly meets the requirements of the naval architect, he can proceed directly with Equation (D) and omit entirely the calculation of streamlines mathematically. The problem then reduces to one of adding sets of offsets together.

Since the technique described here permits an infinite number of different hull forms to be derived from the calculation of a finite number

of hull forms of low resistance, I suggest that all forms of low wave-making resistance be compiled as they are calculated so that practical naval architects may make use of them by methods such as are outlined here. It seems reasonable to suppose use of such compilations, rather than direct use of the high-speed computer, micht well become the primary means of application by practicing naval architects of the results developed by theoreticians.

An alternate way of applying work such as that done by Lin, Webster, and Wehausen to the calculation of practical hulls is, of course, the method of steep descent. Any hull which can be described by the functions they have used can be improved unless, of course, it is already an optimum hull within that family of functions. It is sufficient to observe in this respect that Equation (19) of their paper less the last two terms,

$$\frac{\partial Ta}{\partial b_{nq}} = 2 \sum_{m=1}^{M} \sum_{p=1}^{P} \left\{ \left[C_f \frac{\pi^2}{16\gamma_o} S_{mnpq} + B_{mnpq} \right] b_{mp} + D_{mnpq} a_{mp} \right\} , \qquad (E)$$

$$n = 1, \ldots, M; \; q = 1, \ldots, P,$$

defines the gradient of the total resistance. It is only necessary to insure that changes made in a hull by the method of steep descent are orthogonal to the gradients of the quantities to be held constant but as close to the negative of the gradient of the resistance as possible. In consequence, nearly all the work done by the present authors could be adapted easily to finding ways of improving hulls already designed by conventional methods. This might be the fastest method of obtaining application of the theoretical work which they have done.

by Lawrence W. Ward

It is refreshing to see an optimization calculation which treats the total resistance, that is the wave resistance plus something that attempts to include the frictional resistance. In regard to the latter there are two points I would like to raise. First is that the hull wetted surface is not a direct measure of the resistance as we have the strong possibility of separation behind sharp recesses. Perhaps a side condition $f_x \geq -a$ would cause avoidance of some of the more extreme bulb forms. Then we have the idea that it is not necessary to compute the developed surface but rather it is more proper to use the projected wetted surface:

$$S_p = \iint \left[1 + f_z^2 \right]^{1/2} dx \, dz$$

This should be easier and is consistent with the naval architects' ignoring the "secant correction".

AUTHOR'S REPLY

The authors are pleased to see Capt. Shor's two suggestions for putting their method to use in the near future. We had regarded the investigation as being still in a somewhat preliminary stage, as one can see, for example, by the fact that we did not even try to smooth out our lines in order to make them less offensive to the naval architect's eye. However, it was the points mentioned in Capt. Shor's introductory paragraph which actually motivated our formulation of the problem with given afterbody, for this is a simple instance of an a priori constraint, selected for reasons having little to do with wave resistance. Capt. Shor's procedures may, however, be more flexible in use than ours, for they give the possibility of finding an approximate answer, or a direction of improvement, in situations where a formulation and solution of the problem by a method like ours would be too long.

The first method has the disadvantage that it may increase the frictional resistance even though it keeps the wave resistance constant. The method of steep descent can apparently avoid this. Since for most practical Froude numbers the wave resistance of our optimum forms is already much less than the frictional resistance, this may give a significant advantage to the second method. We note that M. G. Krein (see Kostyukov, Theory of ship waves and wave resistance, Liningrad, 1959, p. 180) has suggested using the first method to minimize the frictional resistance while keeping the wave resistance constant. Krein has also given a simple construction for a large class of waveless additions: Let $m(x,z)$ and $n(x,z)$ be two functions defined on S_o for which m_{xx}, n_{xx} and m_z, n_z exist and such that n vanishes on the boundary of S_o; then the hull

$$f + \left[\frac{2H}{L\gamma_o}\frac{\partial^2}{\partial x^2} + \frac{\partial}{\partial z}\right] mn^3$$

has the same (Michell) wave resistance as f itself.

For the practically important problem in which one tries to meet a constraint like

$$0 \leq f(x,z) \leq B \quad , \qquad -C \leq f_x(x,z) \leq D$$

it is not clear to us how either method can be systematically used. We are hopeful of applying quadratic programming techniques to this problem.

Finally we note that Professor Maruo has pointed out in conversation that it is more usual to take the frictional resistance as

$$R_V = \rho u_o^2 C_f(Re) \int\int_{S_o} [1 + f_z^2]^{1/2} \, dx \, dz$$

instead of (12). This could, of course, be handled in the same way as (12).

SOME ASPECTS OF THE PROBLEM OF MINIMUM WAVE-RESISTANCE

Jack Kotik

Technical Research Group, Inc.

SOME ASPECTS OF THE PROBLEM OF MINIMUM WAVE-RESISTANCE

1. Introduction

TRG has been conducting research in wave-resistance for some time. This research is continuing and is expected to lead to practical results in the near future. Some of our more theoretical results are described below, in keeping with the title of this seminar.

2. Minimum Wave-Resistance for Submerged Line Dipole Distributions Having Prescribed Linearized Volume

In the discussion following (see Ref. 1, page 117) I indicated that this mathematical problem, a numerical treatment of which had been discussed by Weinblum (see Ref. 1, page 112) had no solution. No further information was given. Since then additional work has been done,[2,3] and substantial decreases in theoretical wave-resistance have been achieved. Nevertheless the mathematical problem has not been resolved in published work. Bessho[4] has considered the problem, and correctly observes that it has no solution. He claims further that arbitrarily small wave-resistance can be obtained and presents a method for constructing dipole distributions having arbitrarily small wave-resistance and fixed linearized volume. Unfortunately his analysis does not lead to the desired conclusion. In his Equation (1.2.5)

$$G(x) = g^3 \, 0\left[\frac{(gx)^{2N}}{(2N)!}\right] \qquad (1)$$

the 0 is uniform in x but not in N since it depends on the a_{2n} which are solutions of his equations (1.2.4) and hence depend on N. Hence his conclusion following his Equation (1.2.5), "therefore G(x) can be made arbitrarily small by making N arbitrarily large" is not warranted. In view of the interest in this problem displayed by the above-mentioned authors and also by Krein (as quoted briefly in Ref. 5) I present briefly some results obtained by Professor Donald Newman* and myself.

*Yeshiva University, New York, New York.

After normalization the mathematical problem is to find $f(x)$ such that

$$\int_{-1/2}^{1/2} f(x)\,dx = 1 \qquad (2)$$

and

$$C_w = \frac{8F^4}{\pi} \int_1^\infty \frac{\lambda^4}{\sqrt{\lambda^2-1}} e^{-2\lambda^2 F y_o} [I(\lambda F)]^2 \, d\lambda = \text{minimum} \qquad (3)$$

where y_o = dimensionless submergence

$F = gL/c^2$

c = forward speed

and

$$I(\lambda F) = \int_{-1/2}^{1/2} f(x) \cos \lambda F x \, dx \, . \qquad (4)$$

As is well known we can assume $f(x)$ to be even, and we have done so. We can also write

$$C_w = \frac{8F^4}{\pi} \int_{-1/2}^{1/2} \int_{-1/2}^{1/2} f(x)\, f(x')\, K(F|x-x'|)\, dx\, dx' \qquad (5)$$

where

$$K(F|x-x'|) = \int_1^\infty \frac{\lambda^4 e^{-2\lambda^2 F y_o}}{\sqrt{\lambda^2 - 1}} \cos(\lambda F(x-x'))\, d\lambda \, . \qquad (6)$$

It is clear from (3) that for this problem $C_w \geq 0$. We shall take a few lines to prove that for this problem C_w is positive definite ($C_w = 0$ implies $f(x) = 0$ p.p.*) since the question of positive definiteness is presently of some interest. If $C_w = 0$ then from Equation (3) $I = 0$ p.p. for $1 \leq \lambda < \infty$. Now, if $|f(x)|$ is integrable then $I(\lambda F)$ is an entire analytic function and hence vanishes identically. This is possible only if $f(x) = 0$ p.p.

---

* p.p. means almost everywhere. See any book on Lesbesgue theory.

It follows that a necessary and sufficient condition for f(x) to be a solution of the minimum problem is that

$$f(x) = g(x) / \int_{-1/2}^{1/2} g(x)\, dx , \tag{7}$$

with

$$\int_{-1/2}^{1/2} g(x')K(F|x-x'|\, dx' = +1 \quad \text{for} \quad |x| \leq 1/2. \tag{8}$$

Note that if such a g(x) ($\not\equiv$ 0 p.p.) exists its resistance is given, using (5) and (8), by a positive multiple of

$$\int_{-1/2}^{1/2} g(x)\, dx \tag{9}$$

which is thus a positive quantity. However, if $y_o > 0$ and such a g(x) exists (with |g(x)| integrable) then the integral in (8) defines an entire analytic function, and hence (8) holds for all x. However, for large x the integral tends to zero, hence the problem as posed has no solution.

One is led then to ask what is the greatest lower bound of C_w for admissible functions f(x). We have shown that if

$$e > 0 \quad \text{and} \quad \epsilon^2 < \min\, [y_o/(2F\log 3),\ F^{-2}] , \tag{10}$$

and if (for $|x| \leq 1/2$)

$$f_n(x,\epsilon) = 1 + 2(-1)^n n! \sum_{k=1}^{n} \frac{\Gamma([2\pi k\epsilon]^2) \cos 2\pi kx}{\Gamma([2\pi k\epsilon]^2 - n)\Gamma(n+k+1)\Gamma(n-k+1)} \tag{10}$$

then C_w^n (as given by (5)) tends to zero as $n \to \infty$, and (2) is satisfied for all n (≥ 1). Of course the f_n cannot converge to an admissible function, since if they did that function would be a solution of the minimum problem.

The sequence $f_n(x,\epsilon)$ is not intended for use in the design of submerged bodies, but only to help answer a mathematical question about minimum wave resistance. The problem of designing for low wave drag has been treated in the literature, with considerable success.

If we integrate (5) by parts twice with respect to both x and x',assume $f(\pm 1/2) = f'(\pm 1/2) = 0$ and let $y_o \to 0$, and continue to relate f(x) to body shape in the usual linearized way, we get the slender-ship wave resistance formula considered by Vossers, Maruo, Tuck, Ciolkowski and others, some of whom have also discussed the associated minimum problem.

3. Some Slender-Ship Theories of Ship Wave-Resistance

Following the appearance of Vosser's Thesis[6] a number of authors have discussed slender-ship theories of ship wave resistance and motion. A number of papers at the present Symposium deal with this subject. We shall present here a few comments on these theories.

We can identify three slender-ship theories:
(1) NSST (Naive Slender-Ship Theory). The ship is represented by a line distribution of (wave) singularities whose strength is as in an infinite fluid.

(2) MSST (Michell Slender-Ship Theory). This is obtained by letting first the beam, and the draft, tend to zero. The result is the same as if we let first the draft (Hogner) and then the beam tend to zero, as observed Maruo[7] who also derived the result directly.

(3) VSST (Vossers' Slender-Ship Theory). The theory presented by Vossers in Reference 6, but with some of the errors corrected.

For smooth pointed ships all these theories are in agreement with themselves, and predict positive-definite wave resistance. For unpointed (or unsmooth) ships NSST and VSST predict infinite wave-resistance, while MSST predicts finite wave-resistance which becomes negative at high and low Froude numbers. Taylor's Standard Series[8], in which the important parameter t (slope of sectional area curve at its end) is often nonzero, suggests that unpointed ships are important.

Recent studies by Tuck, Joosen and Ciolkowski, to be presented at this seminar, are all in agreement with the theories mentioned above, for smooth pointed ships.

All these theories are based on assumptions which become false at low speed and at high speed. On the basis of some calculations by Peter Thomsen and myself it appears that the range of validity* depends on the ship form and is limited in extent. Additional calculations indicate that D/L and the sectional area curve, which determine the resistance in these theories, are insufficient. This is in accordance with calculations and measurements in the literature. Figure 1 compares MSST, Michell's integral and the first two terms in the expansion of MSST at high Froude number, for a ship having 4th-power waterlines. This figures should be compared with Figure 2, (an elaboration of Figure 1 of Ref. 7) which deals with a ship having 2nd-power waterlines.

We conclude that these theories, in their present form, are not of general value for predicting wave resistance. A fuller discussion will appear in Schiffstechnik.

4. Another Slender-Ship Theory

The trend in recent work has been to emphasize the inadequacies of the Michell-Havelock linearized relation between body shape and singularity distribution. The slender-ship theories discussed above are not a satisfactory alternative. Instead of the Havelock-Michell relation it has been proposed that the direct problem (ship given, find flow) be treated by solving an integral equation purely numerically, as in Reference 9, and the inverse problem (given flow, find ship) be solved purely numerically by integrating the differential equations for streamlines, as in References 10, 11, etc. Although published work on these problems ignores the wave term in the potential, improved calculations are around the corner. While this approach has been and will be fruitful it leads to a certain awkwardness in design problems. All practical design constraints involve ship form and hence a practical treatment of low-drag design problems, if carried out using the ideas mentioned above, requires the solution of the direct or inverse problem at least once and probably several times. This is feasible but not completely satisfying.

Dr. Lurye of TRG and I were lead to consider the analogue, for flow problems, of a slender-body theory under development by us for some other problems. This slender-ship theory has the following properties:

---

*Validity here means a reasonable degree of agreement with experiment or Michell's integral.

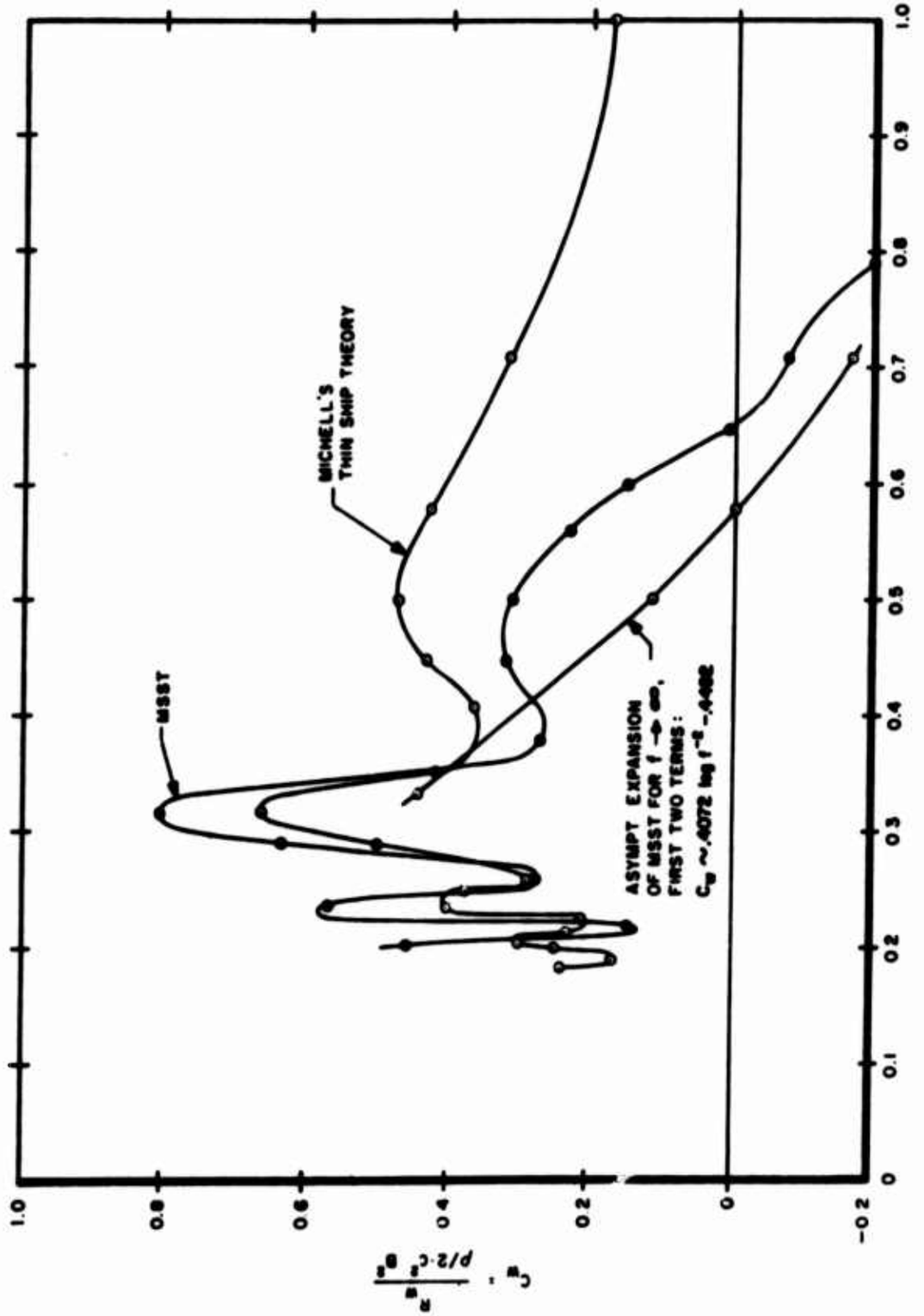


FIGURE 1. WAVE RESISTANCE COEFFICIENTS; HULL: $\frac{D}{L} = 0.05$, $y = \pm B\left[1-(2u)^4\right]$, $u = x/L$

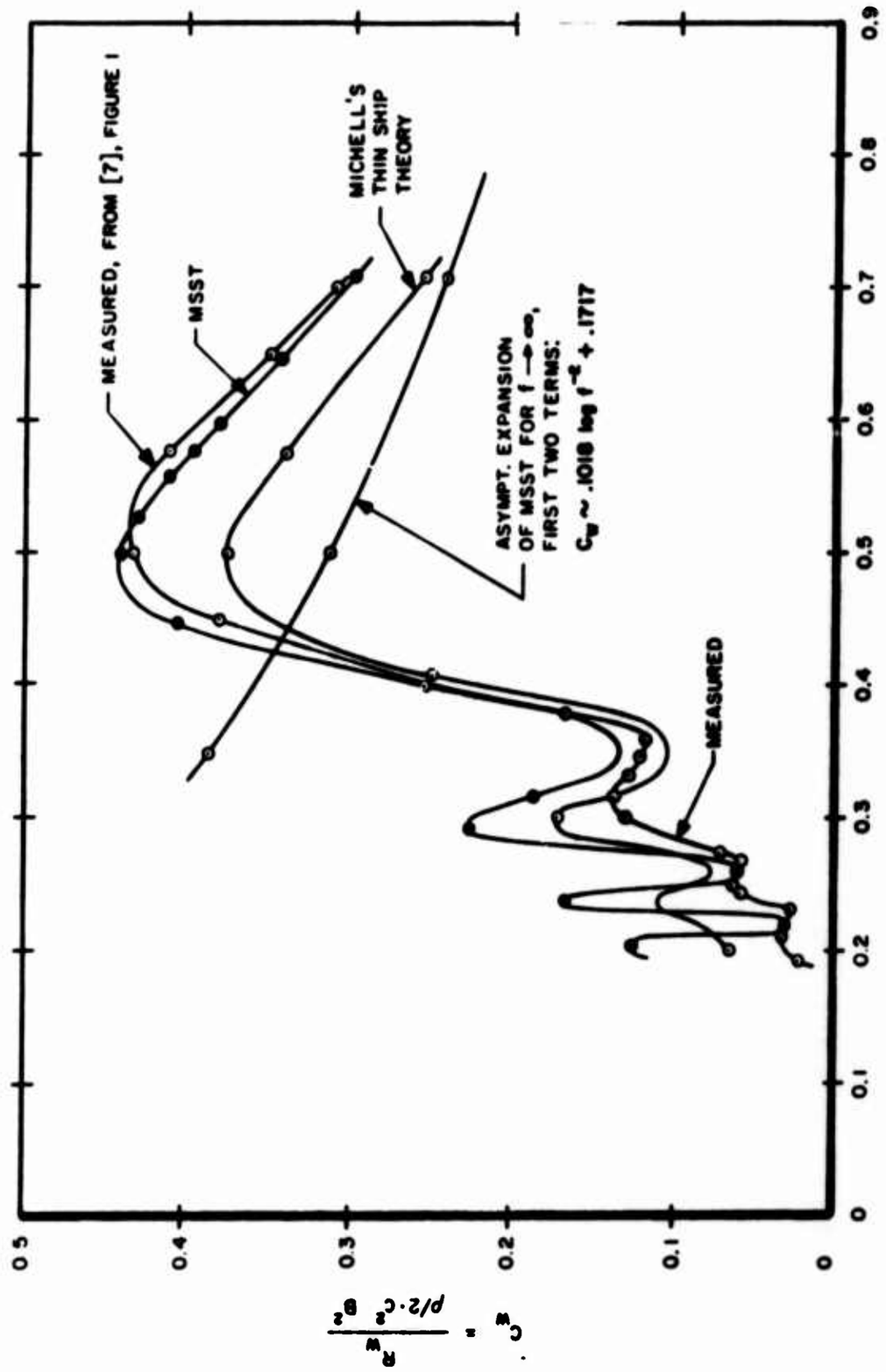


FIGURE 2. WAVE RESISTANCE COEFFICIENTS; HULL: $\frac{D}{L} = 0.05$, $y = \pm B\left[1-(2u)^2\right]$, $u = x/L$

1) The body is replaced by a distribution of singularities* on the body surface, the strength of the distribution at each point on the body being determined by an elementary formula.

2) Considering each singularity to be a wave singularity we get a wave pattern and wave-resistance. The resistance does not depend merely on the sectional area curve, and the resistance is not simply proportional to $(\text{Beam})^4$.

3) The approximate singularity strength is asymptotically exact for slender general ellipsoids in uniform flow, and may be regarded as the first term in a convergent iterative solution of the integral equation for the exact singularity distribution (in uniform flow).

4) Minimum problems formulated within this theory involve the body shape directly, although approximately. While slightly more complicated than Michell's expression the resistance in this theory has prospects of being more accurate.

The same theory (for sources) has already been proposed by Kochin in 1937[12]. Perhaps the relative lack of exploitation of the underlying principle, in any field, as compared with theories involving singularities distributed on a line was due to the relative unattractiveness of the surface integrals. However today's computer techniques make the theory attractive.

The theory is conveniently obtained as follows, at least for smooth bodies. Consider the total potential

$$\Phi(x,y,z) = Ux + \phi(x,y,z) \qquad (4\text{-}1)$$

*Either sources or normal dipoles.

for the uniform flow of an infinite fluid past a slender body. As the slenderness parameter $\epsilon \to 0$, the disturbance potential $\to 0$, even on the body. This is known for general ellipsoids and can be proved for a large class of bodies. We shall use this fact to determine approximately that distribution of normal dipoles on the body surface which will generate the same disturbance potential exterior to the body as does the body itself.

Let $\sigma_D(x,y,z)$ ((x,y,z) on the body surface S) be the exact dipole density. Consider the function $\psi(x,y,z)$ defined as follows:

$$\psi(x,y,z) = \iint_S \sigma_D(x',y',z') \frac{\partial}{\partial n'} \left(\frac{1}{R}\right) dS \qquad (4\text{-}2)$$

where R is the distance from (x,y,z) to the integration point (x',y',z') and $\partial/\partial n'$ is differentiation in the direction of the unit outward normal $\hat{n}(x',y',z')$. ψ is harmonic inside and outside S. From the definition of σ_D, we have

$$\psi_+(x,y,z) = \phi(x,y,z) \qquad (4\text{-}3)$$

where the + means that (x,y,z) is exterior to S. From Equation (4-2) it also follows that $\psi_-(x,y,z)$ is a potential function regular throughout the interior of S.

The jump conditions of potential theory when applied to Equation (4-2) tell us that

$$\sigma_D(x,y,z) = \frac{1}{4\pi} [\psi_+(x,y,z) - \psi_-(x,y,z)] \qquad (x,y,z) \text{ on S} \qquad (4\text{-}4)$$

$$\frac{\partial \psi_-}{\partial n} = \frac{\partial \psi_+}{\partial n} = -U \hat{x} \cdot \hat{n} \qquad (x,y,z) \text{ on S} \qquad (4\text{-}5)$$

where the equality on the far right of Equation (4-5) comes from Equation (4-3) and the kinematic condition on ϕ. ($\hat{x}$ is a unite vector in the positive x direction.)

Equation (4-5) defines a Neumann boundary value problem for the determination of $\psi_-(x,y,z)$ throughout the interior of S. The problem can be solved by inspection to give

$$\psi_-(x,y,z) = -Ux \qquad \text{inside and on S.} \qquad (4\text{-}6)$$

Substituting from Equation (4-6) into Equation (4-4) we get

$$\sigma_D(x,y,z) = \frac{1}{4\pi}[Ux + \psi_+(x,y,z)] = \frac{1}{4\pi}[Ux + 0(x,y,z)] \quad (x,y,z) \text{ on S} \qquad (4\text{-}7)$$

Thus far we have used no slender body approximations and Equation (4-7) is exact. We now introduce the aforementioned result that even on S $\phi \to 0$ as the slenderness parameter $\epsilon \to 0$ to obtain

$$\sigma_D^A(x,y,z) = \frac{1}{4\pi} Ux \qquad (x,y,z) \text{ on S} \qquad (4\text{-}8)$$

This is the desired slender body approximation to the surface density of normal dipoles on a body surface. The distribution represents the body in a uniform flow.

The body can also be represented by a distribution of sources over its surface. It can be shown by an elementary application of Green's theorem that $\sigma_S^A(x,y,z)$, the equivalent slender body approximation to the source density, is given by

$$\sigma_S^A(x,y,z) = \frac{1}{4\pi} U \hat{x} \cdot \hat{n} \qquad (x,y,z) \text{ on S} \qquad (4\text{-}9)$$

This approximation is equivalent to the foregoing one for the dipole distribution in the sense that it generates exactly the same approximate potential outside the body.

In the case of ellipsoids, where the exact potentials are known, one can verify directly that Equations (4-8) and (4-9) are the first non-vanishing terms in the expansions, for small slenderness, of the exact dipole and source densities for ellipsoids.

In order to make a comparison between σ_S and σ_S^A (Equation (4-9)) for a practical form we have utilized numerical values of σ_S for a slightly modified Series 60 hull. The values of σ_S were obtained from Douglas Aircraft via D.T.M.B. and were calculated by methods described in Reference 9. The results appear to be quite accurate. They are presented (in Figure

3) as plots of σ_S and σ_S^A as a function of position on a number of vertical sections of the Series 60 hull. The figures are adapted from Breslin and Eng (this seminar), who presented only σ_S.

The figures reveal a considerable discrepancy between σ_S and σ_S^A. In regions where $\vec{n} \cdot \vec{x}$ is appreciable σ_S and σ_S^A have the same sign, but σ_S is larger in magnitude. In regions where $\vec{n} \cdot \vec{x}$ is small, for instance near the keel and near the waterline amidships, σ_S^A is small. However, if at the same or nearby stations σ_S is large in magnitude then, at the nearby regions where $\vec{n} \cdot \vec{x}$ is small σ_S is moderately large and of opposite sign to the nearby large values of $\vec{n} \cdot \vec{x}$. Qualitatively, it appears that large values of $\vec{n} \cdot \vec{x}$ on a section generate values of σ_S which by themselves would generate a body having $\vec{n} \cdot \vec{x}$ large over that entire section. Hence in order to generate a flat spot in that section we need moderate and opposed values of σ_S. The compensating values of σ_S, described as moderate in magnitude, can become large if the flat spot is small, as in Figure 3e, and one can probably find bodies for which the compensating values of σ_A on a flat spot exceed the predominant values on the portion having appreciable values of $\vec{n} \cdot \vec{x}$. Notice that σ_S^A is a rather better approximation on the average (say over a vertical section) than it is pointwise. Notice also that very near the bow (Figure 2f), where the hull resembles a wedge, σ_S and σ_S^A are almost identical.

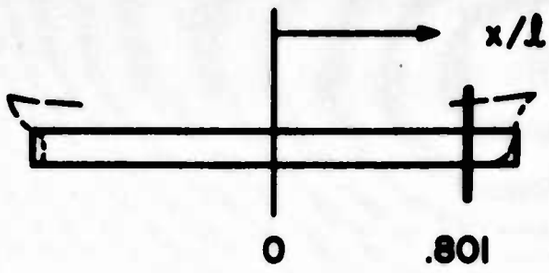
Further comparisons of this type will lead to a better understanding of the relationship between σ_S and σ_S^A.

All the singularity strengths mentioned above are those appropriate to an infinite fluid. This approximation improves with decreasing Froude number, but no published quantitative estimate of the associated error, as regards either the representation of the body or its wave resistance, is known to us. We have begun to study this problem, and also some of the other problems raised by the thoughts leading to Equations (4-8) and (4-9).

5. Zero Wave Resistance

The resistance of a volume distribution σ_s of sources is given (e.g. by Lunde[13]) as

$$R_w = 16\pi K_o^2 \int_1^\infty \frac{\lambda^2 \, d\lambda}{\sqrt{\lambda^2 - 1}} |I + iJ|^2 \qquad (5\text{-}1)$$



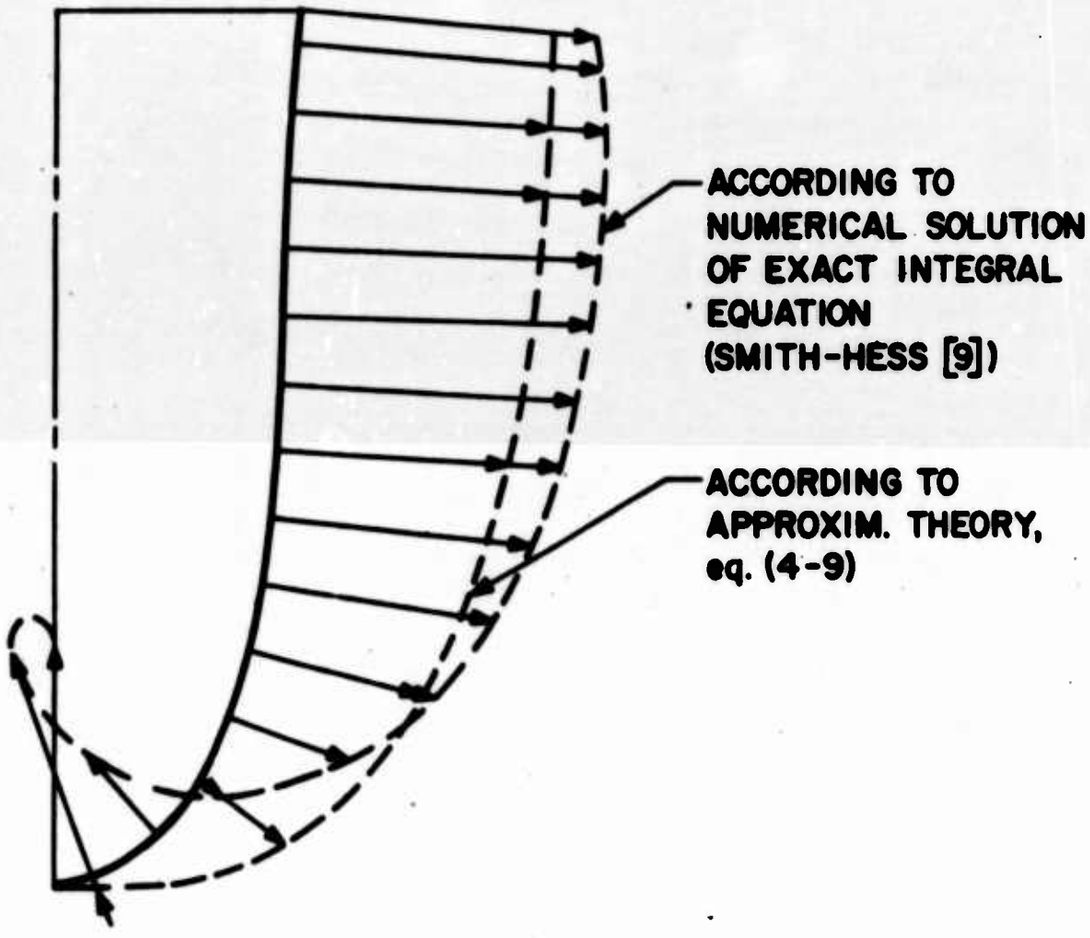


FIGURE 3a. SOURCE STRENGTH DISTRIBUTION AT (X/l) = 0.801

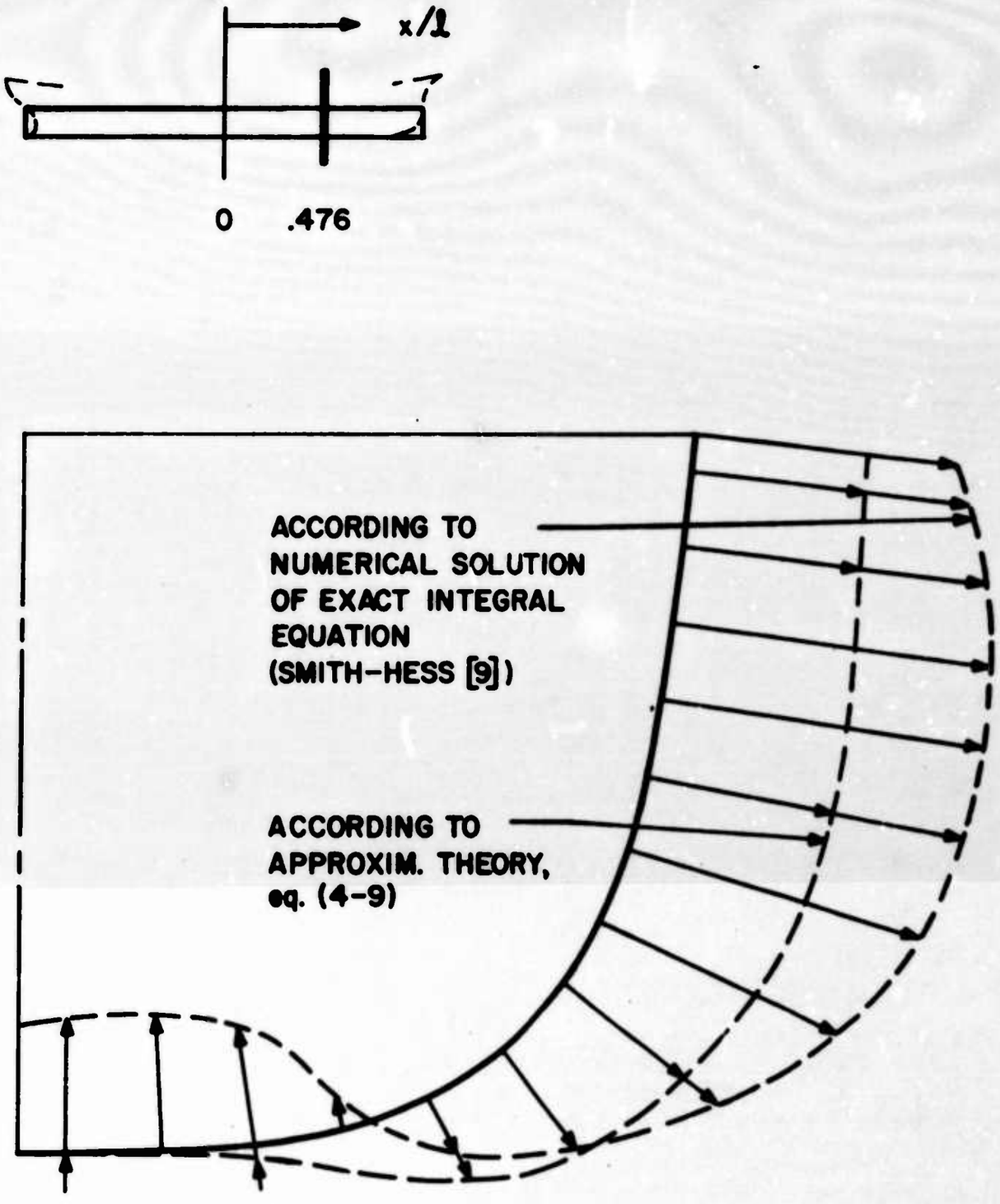
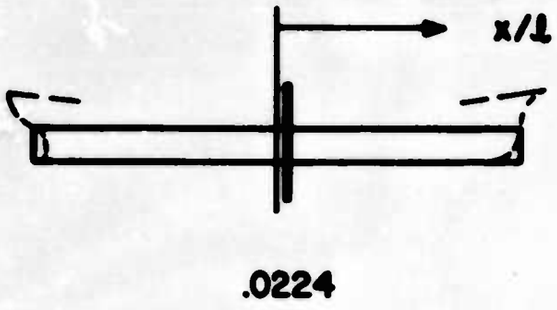


FIGURE 3b. SOURCE STRENGTH DISTRIBUTION AT (X/ℓ) = 0.476



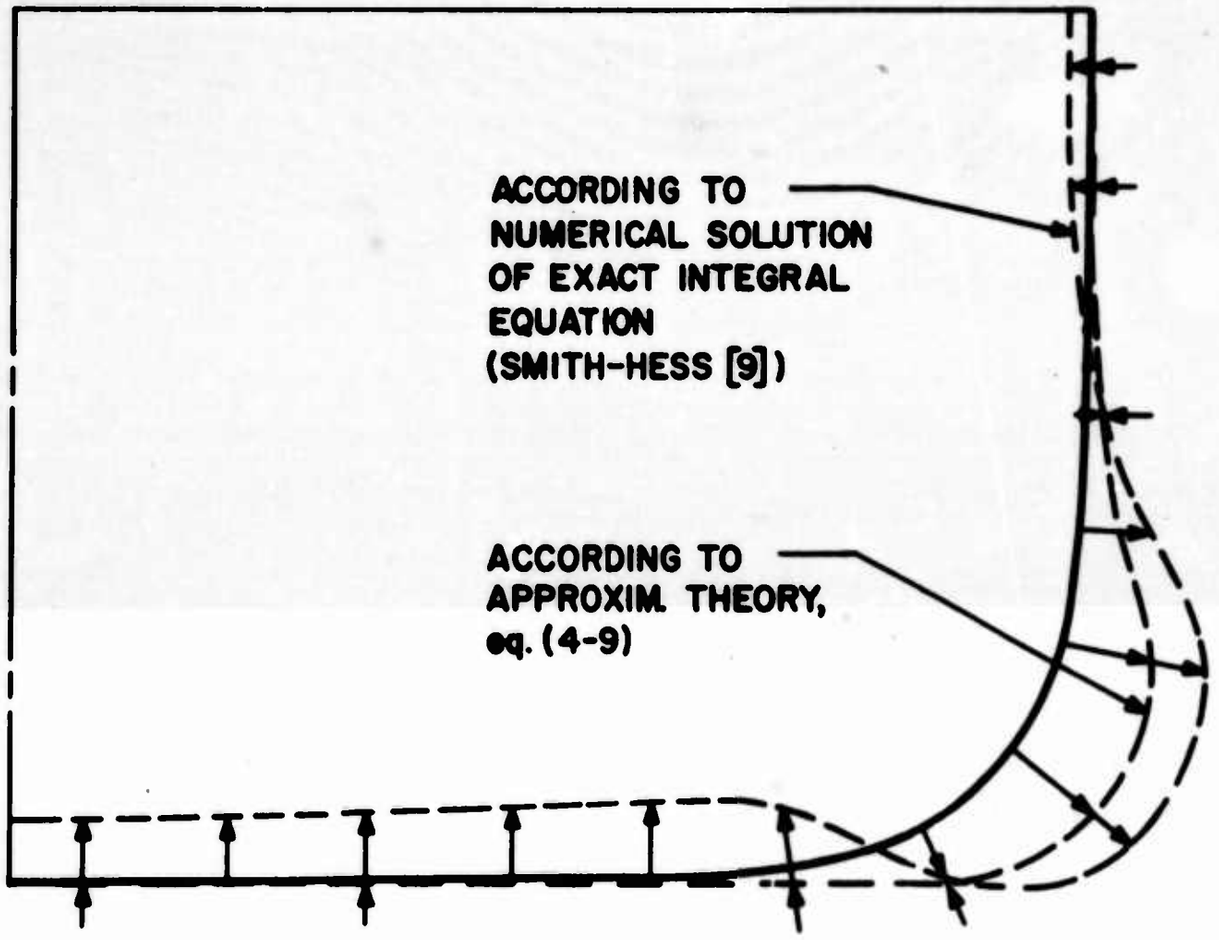
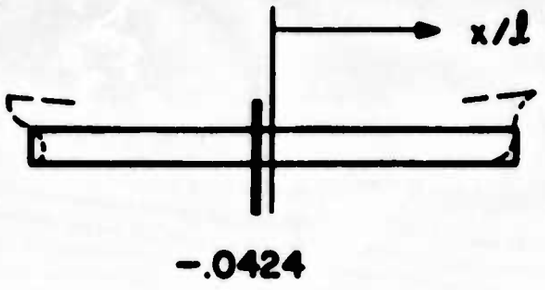


FIGURE 3c. SOURCE STRENGTH DISTRIBUTION AT (X/L) = 0.0224



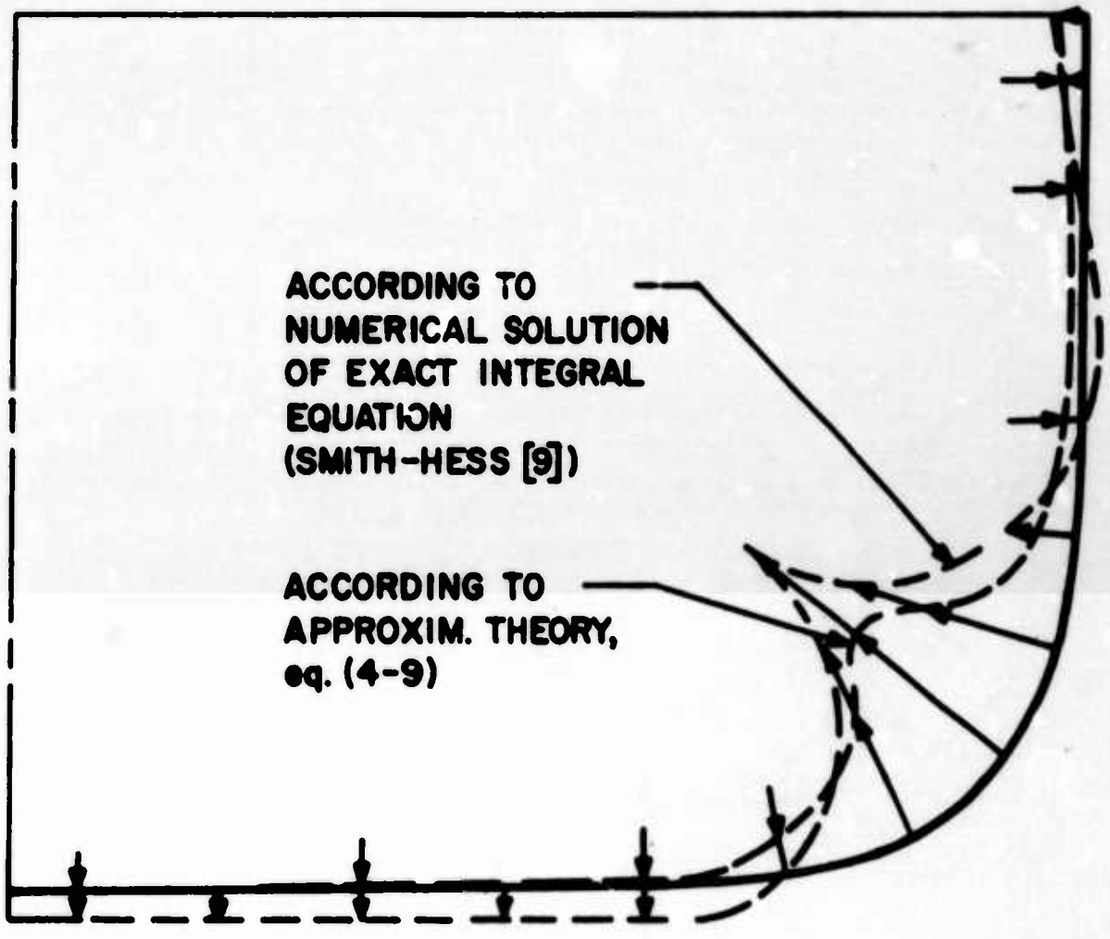
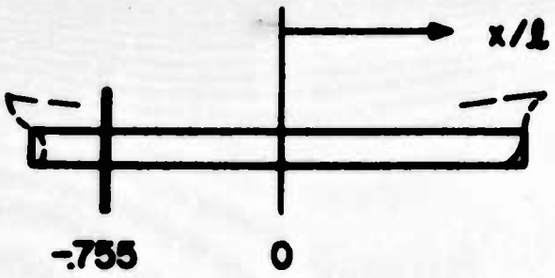


FIGURE 3d. SOURCE STRENGTH DISTRIBUTION AT (X/l) = -.0424



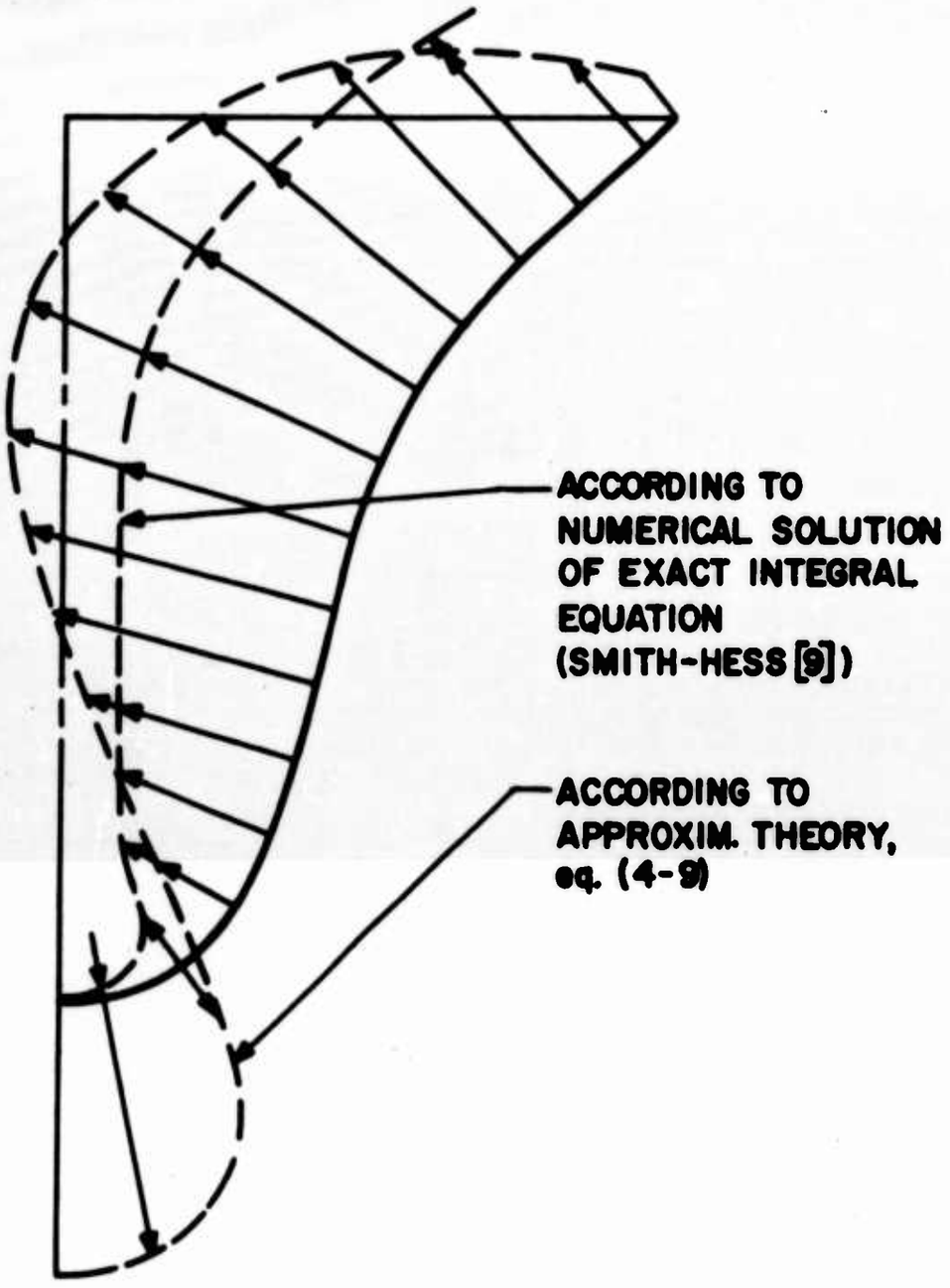
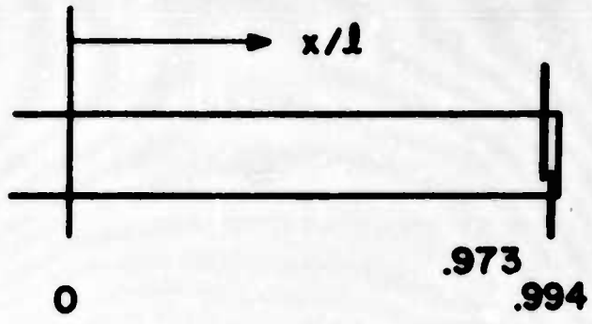


FIGURE 3e. SOURCE STRENGTH DISTRIBUTION AT (X/ℓ) = -.755



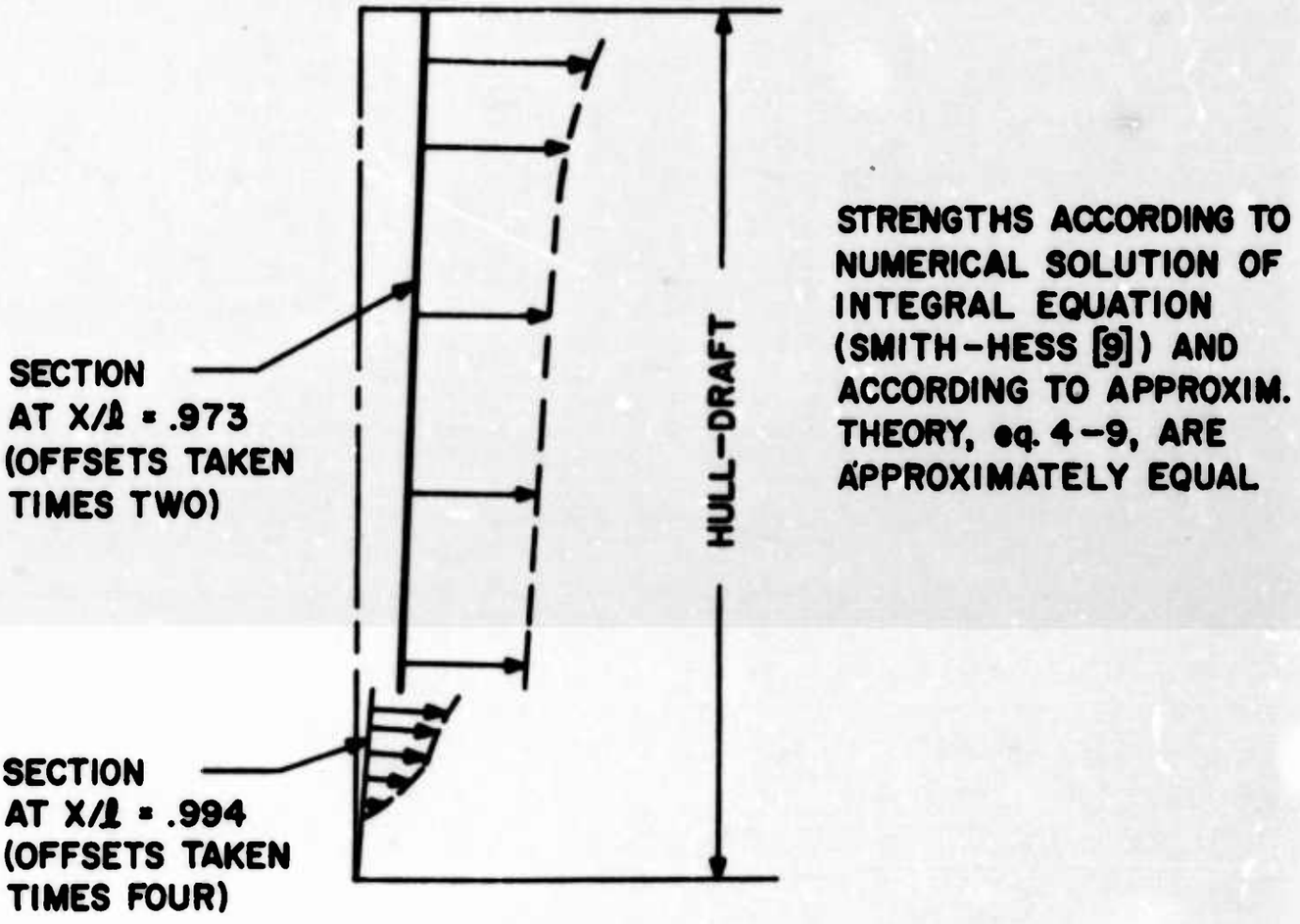


FIGURE 3f. SOURCE STRENGTH DISTRIBUTION
AT (X/ℓ) = .994, (X/ℓ) = .973

where

$$I + iJ = \int\int\int \sigma_s(x,y,z) \exp \qquad (5\text{-}2)$$

$$\{iK_o\lambda x + iK_o\lambda \sqrt{\lambda^2-1}\, y + K_o \lambda^2 z\}\, dxdydz$$

By suitably concentrating σ_s the cases of surface, line and point sources are included, and by introducing linearized relations between source strengths and body shapes R_w can sometimes be interpreted as the approximate wave resistance of some body. It is clear from (5-1) that $R_w = 0$ implies $I + iJ = 0$ p.p. on $1 \leq \lambda < \infty$. It is natural to raise the question of positive definiteness: does $I + iJ = 0$ p.p. for $1 \leq \lambda < \infty$ imply $\sigma_s = 0$? In simple cases (sources on a line segment, simple distributions $\sigma_s = \sigma_s^{(1)}(x)\sigma_s^{(2)}(z)$ on a vertical plane) it is easily shown that R_w is positive definite. In general it is not, so that non-zero distributions can have zero wave-resistance.

It is fascinating to wonder why the question of positive definiteness was not asked and answered many years ago. If Michell had asked himself this question he could surely have answered it. We will devote a few lines to some (essentially equivalent) views of the matter. First, we observe that a function of one variable ($I + iJ$) is controlled by a function of more than one variable (σ_s). This suggests that several functions σ_s may lead to the same $I + iJ$, (which implies zero wave resistance by linearity) but does not show how. Birkoff and Kotik[14] showed explicitly how the wavemaking due to sources on a line can be duplicated by another distribution on a line closer to the free surface. This leads to zero wave resistance if one of such a pair of distributions is changed in sign. They also showed how the heat-conduction equation governs the problem of sources on a vertical plane, and paid special attention to the case in which all the sources are brought to the free surface. However, they paid no attention to positive definiteness or zero wave resistance.

Krein (see Ref. 15) treats the problem and distinguishes between the case in which the dipole distribution is required to be positive (physically-realizable ship in thin-ship theory) and the more general case. He uses the heat-conduction equation to construct a large class of vertical-plane distributions, vanishing outside a finite rectangle, having zero wave-resistance. Krein observes that they must have some negative ordinates (thin-ship theory). Bessho[15] has analyzed the problem in almost the same way and raised the stronger objection that the linearized volume* is always zero. Related but

*For the same subclass, of the class of waveless vertical-plane distributions, considered by Krein.

more special results have been reported by Yim[16], who also addresses himself to practical problems. Captain Shor has considered the problem of rendering a given vertical-plane distribution resistanceless by adding to it a strut-like distribution. The solution of the problem of characterizing the class of waveless volume distributions (vanishing outside a finite region) in a useful way has not yet been reported.

The thermal diffusion process in the vertical plane has an analog in Fourier transform space. Looking at (5-2) let

$$I + iJ\Big|_{o,o} = \int \sigma_s(x,o,o) \exp\{iK_o\lambda x\}\, dx \qquad (5\text{-}3)$$

be the differential contribution of $\sigma_s(x,o,o)$. If that element is now parallel-translated in space its contribution becomes

$$\exp\{iK_o\lambda \sqrt{\lambda^2 - 1}\, y + K_o\lambda^2 z\} \cdot \int \sigma_s(x,o,o)\exp\{iK_o\lambda x\}\, dx \qquad (5\text{-}4)$$

If $y = 0$ this is the exact manifestation of thermal diffusion. Allowing $y \neq o$, the possibility of cancellation appears if the translated distribution is altered to cancel the factor $\exp\{iK\lambda\sqrt{\lambda - 1}\, y + K_o\lambda^2 z\}$, multiplied by -1 and added to the original distribution.

Consider now the question of practical design, the question of ships rather than distributions. We recall the points made by Krein and Bessho, regarding negative linearized ordinates and zero linearized volume for vertical-plane distributions. We note also that Yim's cancellation procedure involves infinitely deep distributions which must be truncated in practice. To consider the problem in its general form, and in Fourier transform space, we note that $I + iJ$, defined by (5-2), is an analytic function* of λ in the plane slit** from -1 to +1 (if $\iiint |\sigma_s|\, dx\, dy\, dz$ is finite) and hence if $I + iJ = 0$ p.p. for $1 \leq \lambda < \infty$ then $I + iJ = 0$ and in particular ($\lambda = 0$) $\iiint \sigma_s = 0$. This is o.k. since it suggests a closed body. However, if we replace λ^2 by λ^4 in the numerator of (5-2) and replace σ_s by σ_D in (5-2) then R_w is the wave-resistance of the distribution of σ_D of x-directed dipoles. Again,

---

* This theme was broached in Section 2 above.

** $I + iJ$ is an entire function of λ if the distribution is symmetric port and starboard

if $\iiint |\sigma_D|\, dx\, dy\, dz$ is finite we have $I + iJ = 0$ and $(\lambda = 0) \iiint \sigma_D = 0$. This is annoying, since for vertical-plane distributions it means that the linearized volume is zero. According to Landweber and Yih[17] the true volume (ignoring free surface) never exceeds the linearized volume ($(2\pi/c)$ times dipole moment), a result valid for general volume distributions. We are thus forced to conclude that if we want to improve our chances of getting bodies we must either accept a positive, but perhaps small, wave-resistance, or else abandon the condition $\iiint |\sigma_s| < \infty$ or $\iiint |\sigma_{D^*}| < \infty$.+

6. Simple Ships of Minimum Wave-Resistance

In the course of conducting the research described in Reference 1, Karp and myself, simultaneously and independently, treated the minimum problem for simple dipole distributions (those described by product functions $f(x)g(z)$) in the same spirit* as strutlike dipole distributions are treated in Reference 1. Strutlike dipole distributions are a special case obtained by taking $g(z) = 1$, $o \leq z < \infty$. Karp and I obtained some analytical results, including a proof that in the limit of high Froude number the optimum $f(x)$ is independent of $g(z)$ and equals the optimum $f(x)$ already found for strutlike dipole distributions.

More recently, TRG's computer group has helped me to treat the problem numerically. Their computer program is of a different character from the one described in Reference 1, in that $f(x)$ is now described by a polynomial

$$f(x) = \frac{1}{\sqrt{(1/4)-x^2}} \sum_{m=o}^{m=N} \sigma_m^{(N)}\, T_{2m}(2x), \qquad (6\text{-}1)$$

(where T_{2m} is the Tchebycheff polynomial of the first kind) rather than by its values at a finite number of points x_i. In checking the present program we made use of strut results, including those presented in Reference 1 and those presented by Maruo[7] and Bessho[4]. Figure 4 shows the minimum wave resistance coefficient vs. Froude Number, as presented

---

+As indicated above the theorem of Landweber and Yih cannot be applied directly to flows having a free surface. Therefore, although $\iiint \sigma_D = o$, we cannot conclude that there are no bodies having zero wave resistance. The existence of such bodies was discussed by Prof. Karp in his talk at this seminar. (Note added August 26, 1963)

*Given $g(z)$ and $\iint fg$, find $f(x)$.

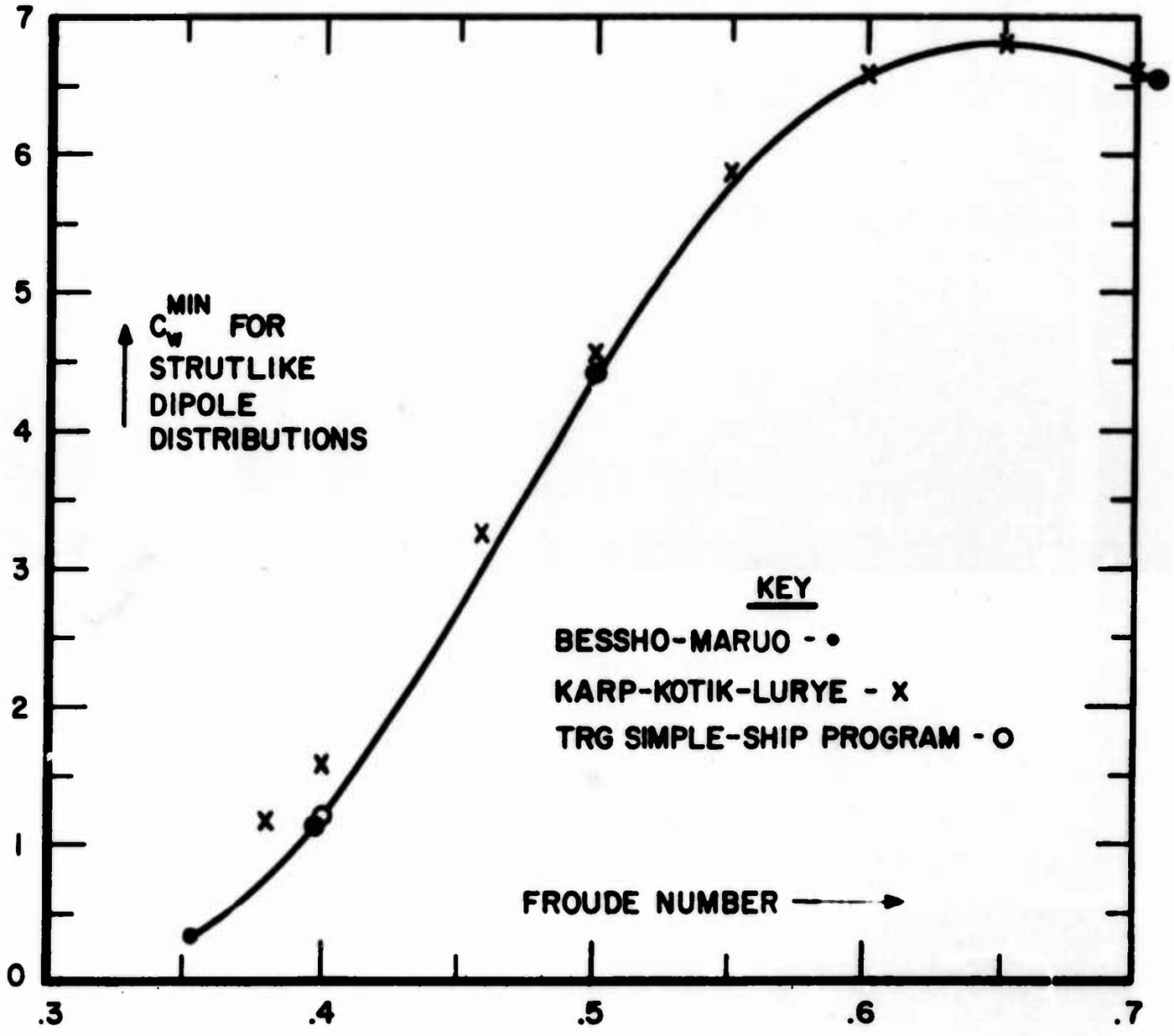

7
6
5
4
3
2
1
0
.3
.4
.5
.6
.7
C_w^{MIN} FOR
STRUTLIKE
DIPOLE
DISTRIBUTIONS
KEY
BESSHO-MARUO - •
KARP-KOTIK-LURYE - X
TRG SIMPLE-SHIP PROGRAM - O
FROUDE NUMBER

FIGURE 4

in Reference 1, in Reference 4 and as found from TRG's new program. The new results are in close agreement with Bessho, whereas the results of Reference 1 begin to deviate at the lower Froude Numbers. The possibility of such a deviation was pointed out in Reference 1. It is due to the increasingly oscillatory character of the kernel and the use of only seven points x_i in the numerical work. The new program allows up to 16 terms in the expansion of f(x), and should give good results at Froude numbers considerably lower than .4. At f = .4 we have the following data:

$$C_w = \begin{matrix} 1.1374 & \text{(TRG)} \\ 1.1384 & \text{(Bessho-Maruo)} \end{matrix}$$

$$2h(x) = 2\sqrt{(1/4-x^2}\, f(x):$$

TABLE 1

x	.0	.25	.5
TRG	1.25648	.86326	.16846
Bessho-Maruo	1.25634	.86307	.16868

We present also our first results for simple ships. We considered a design Froude number of .4, a draft-length ratio of .05 (for the dipole distribution), and the two vertical sections

$$g_1(z) = 1, \quad o \leq z \leq D$$

and

$$g_2(z) = 1 - \left(\frac{z}{D}\right)^4, \quad o \leq z \leq D .$$

In the course of numerical work we also let D/L = .1, .5, 1.0. The resulting optimum f(x) are presented as graphs of $h(x) = \sqrt{(1/4)-x^2}\, f(x)$, in Figure 5. There is a small dependence of the optimum h(x) on D/L and on vertical distribution. The values of the (minimum) wave-resistance coefficient

$$C_w = R_w/\frac{1}{2}\rho c^2 \bar{B}^2 ,$$

where $2\bar{B}LD$ = linearized volume are given in Table 2:

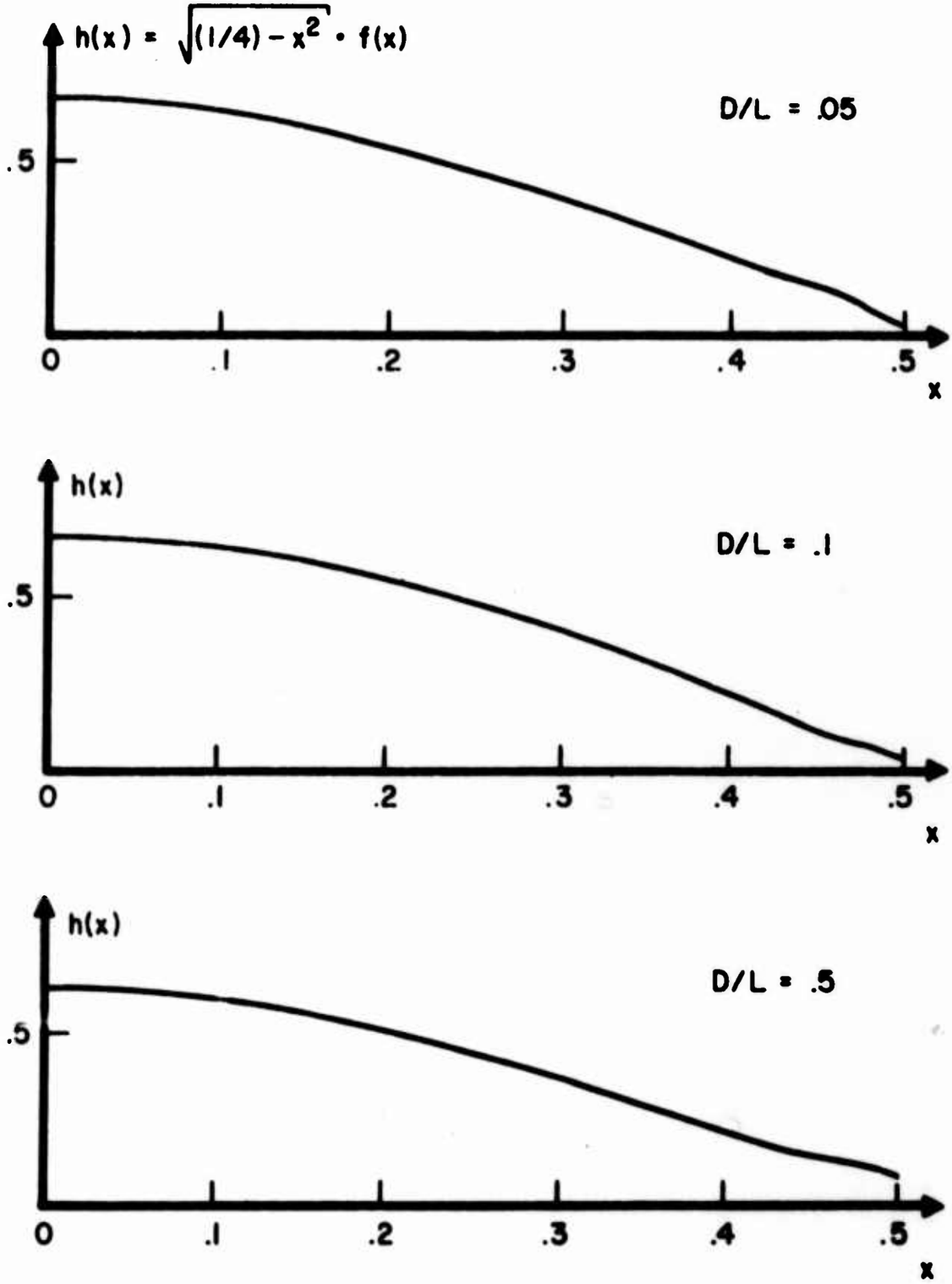


FIGURE 5a. FOURTH-POWER VERTICAL DISTRIBUTION, f = .4, VARIOUS D/L

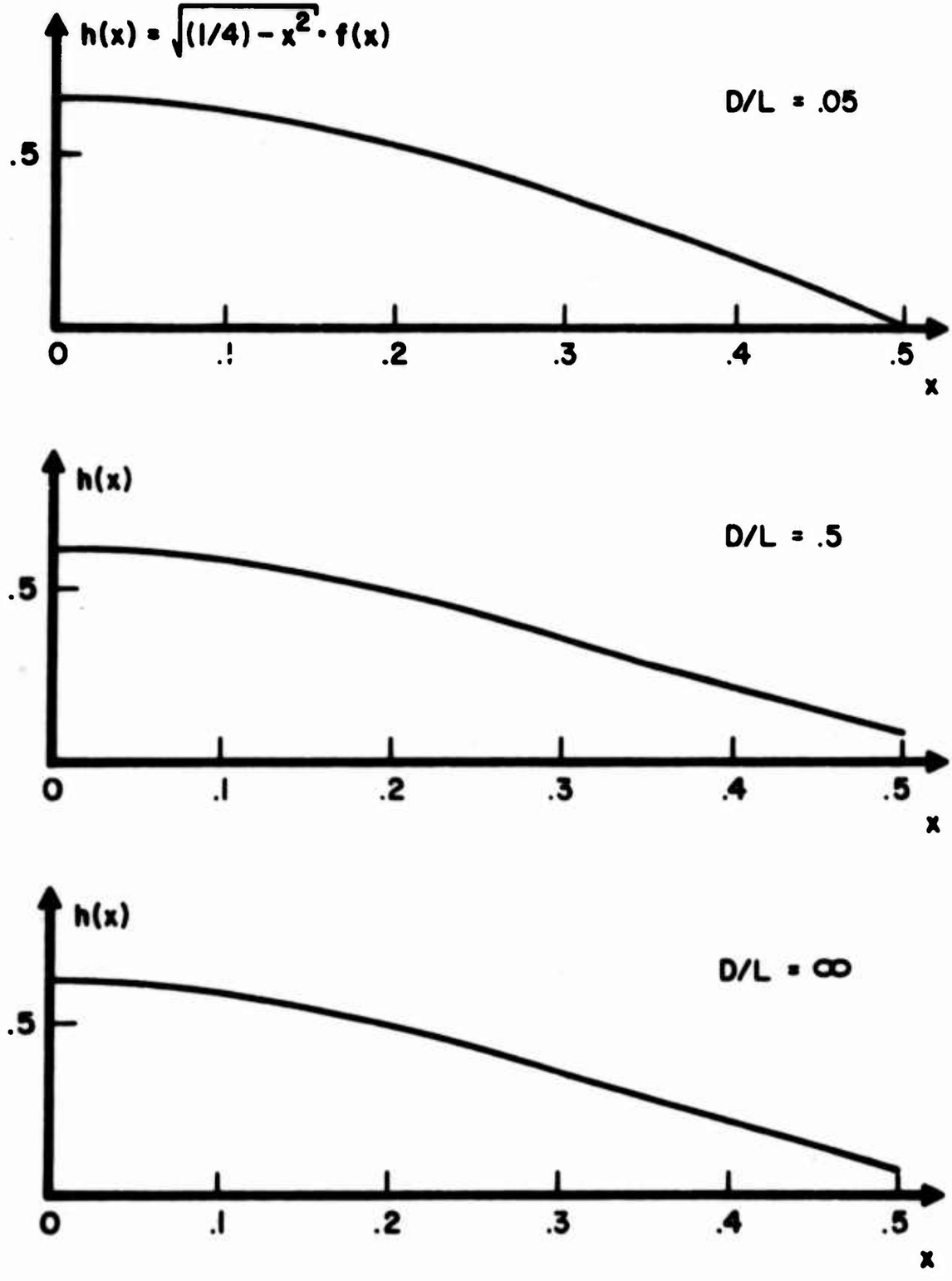


FIGURE 5b. WALL-SIDED VERTICAL DISTRIBUTION, f = .4, VARIOUS D/L

TABLE 2

D/L	$g = g_1(z)$: C_w	$g = g_2(z)$: C_w
.05	.10597	.10867
.1	.32612	.35665
.5	1.1333	1.6357
1.0	1.1954	
∞	1.1979	

As a matter of interest the calculated values of (Maruo's) resistance coefficient for the optimum distribution associated with $g_1(z)$, with D/L = .1, .05 have been compared with the data in Maruo's[18] Figures 5 and 6 respectively, Maruo's models having L/D = 8, 16 respectively, and a 10-th power vertical section. This comparison is conducted in the framework of thin-ship theory, and within the framework of this theory the comparison is for hulls having the same displacement. The fact that Maruo's models have larger D/L by a factor 1.25 is favorable to them, but of course they are not designed for f = .4.

$$\frac{R_W}{(1/2)\rho U^2 L^2} = 1.42 \times 10^{-4} \quad \text{for} \quad D/L = .05$$

$$= 5.39 \times 10^{-4} \quad \text{for} \quad D/L = .1$$

($2\ell = L$).

These points should be plotted on Figures 6 and 5 respectively of Maruo's paper at this seminar.

The ratio of wave-resistance to displacement is given by

$$\frac{R_W}{\rho g V} = \frac{1}{4}\frac{\bar{B}}{D} f^2 C_w \ .$$

Still speaking within thin-ship theory, and using the value $C_w = .10867$ for D/L = .05 and $g = g_2(z)$, and taking $(2\bar{B}/D)$ = (average full beam/draft) = 2, and f = .4 we find

$$\frac{R_W}{\rho g V} = 4.36 \times 10^{-3} \ \text{(lbs/lb)} = 8.72 \ \text{lbs/ton} \ .$$

REFERENCES

1) Karp, S., Kotik, J., and Lurye, J.: "On the Problem of Minimum Wave-Resistance for Struts and Strut-Like Dipole Distributions," Third Symposium on Naval Hydrodynamics, Scheveningen, Netherlands, September, 1960.

2) Sharma, S. D.: "Uber Dipolverteilungen fur Getauchte Rotationskorper Geringsten Wellenwiderstandes," Internationales Symposium uber Schiffstheorie am Institut fer Schiffbau der Universitat Hamburg, 25. bis 27. Januar 1962. Also published in Schiffstechnik, Heft 46, p. 86, April 1962.

3) Eng, King and Hu, Pung N.: "Wave-Resistance Reduction of Near-Surface Bodies," Stevens Institute of Technology, Davidson Laboratory, Report No. R-933, March 1963.

4) Bessho, M.: "On the Problem of the Minimum Wave-Making Resistance of Ships," Memoirs of the Defence Academy, Japan, Vol. II, No. 4, pp. 1-30, January 1963.

5) Kostiukov, A. A.: "Theory of Ship Waves and Wave-Resistance," Leningrad, 1959.

6) Vossers, G.: "Some Applications of the Slender Body Theory in Ship Hydrodynamics," Dissertation paper, Delft, 1962. For the wave-resistance aspect of this paper see Schiffstechnik, Vol. 9, No. 46, pp. 73-78, April 1962.

7) Maruo, H.: "Calculation of the Wave-Resistance of Ships the Draught of Which is as Small as the Beam," Soc. of Nav. Arch., Japan 1962.

8) Gertler, M.: "A Reanalysis of the Original Test Data for the Taylor Standard Series," DTMB Report No. 806 March 1954.

9) Hess, John L., and Smith, A.M.O., "Calculation of Non-Lifting Potential Flow About Arbitrary Three-Dimensional Bodies," Douglas Aircraft Report No. E. S. 40622, March 15, 1962.

10) Thomsen, P. and Eggers, K.: "Zur Berechnung von Umstromungskorpern zu Quell-Senken-Verteilungen," Schiffstechnik, Bd. 7, Heft 38, September 1960.

11) Inui, Takao,: "Wave-Making Resistance of Ships," Transactions of the Society of Naval Architects and Marine Engineers, Vol. 70, pp.283-353, 1962.

12) Kotchin, N. E.: "On the Wave-Making Resistance and Lift of Bodies Submerged in Water," Wave-Resistance Conference, Moscow, 1937.

13) Lunde, J. K.: "On the Linearized Theory of Wave-Resistance for Displacement Ships in Steady and Accelerated Motion," The Society of Naval Architects and Marine Engineers, September 1951.

14) Birkhoff, G., and Kotik, J.: "Some Transformations of Michell's Integral," National Technical University, Athens, Greece, Publication No. 10, 1954.

15) Bessho, M.: "A New Approach to the Problem of Ship Wave," Memoirs of the Defense Academy, Japan, Vol. II, No. 2, April 1962.

16) Yim, B.: "Analysis of the Bulbous Bow on Simple Ships," Hydronautics, Inc., Report No. 117-1, August 1962.

Yim, B.,: "On Ships with Zero Wave Resistance," Hydronautics Inc., Technical Report 117-2, August 1962.

17) Landweber, L. and Yih, C. S.: "Forces, Moments, and Added Masses for Rankine Bodies," J. Fluid Mechanics, 1., p. 319, 1956.

18) Maruo, H.,: This seminar.

ON THE MINIMUM WAVE RESISTANCE OF SHIPS WITH INFINITE DRAFT

Masatoshi Bessho

Defence Academy
Yokosuka, Japan

1. Introduction

The minimum problem of the wave resistance of ships has generally no solution or at least no unique one analytically except special cases.(8)

One of such special cases is of ships with infinite draft represented by draftwise uniform doublet distribution over the vertical center line plane.(7)

In this case, the existence, the uniqueness and characters of the solution were given by Professor Karp and others.(7)

They solved the integral equation numerically, and this was an easy way but difficult to secure a necessary accuracy especially in low speed where the wave resistance becomes very small.

In the other way, the analytical treatment is not only simple too but supplies very many interesting knowledges so far as we have complete tables of necessary functions.

In this paper, the author presents such treatment of the problem with the aid of the text and tables of Mathieu functions which he has been able to use.(4,5)

2. Wave Resistance Formula

Consider the uniform flow with unit velocity flowing from the positive direction of x-axis down to the negative and the doublet of which axis directs to the positive x-axis and distributing draftwise uniformly over the plane $|x| \leqq 1$.

Then, the wave making resistance of this doublet distribution is given as follows.(7,8)

$$R = \rho g^2 \bar{B}^2 / \pi \int_0^{\pi/2} |F(g \sec\theta)|^2 \sec\theta \, d\theta \,, \tag{2.1}$$

with

$$F(p) = \int_{-1}^{1} H(x) \exp(-ipx) \, dx \,, \tag{2.2}$$

where ρ means the water density, g the gravity constant in this unit system and $|F|$ the absolute value of F .

The function $\overline{B}H(x)$ represents the doublet strength except the constant multiplier and equals nearly to the breadth of the ship considered by well-known approximation.

Moreover, $\overline{B}$ stands for the mean breadth, so that the mean value of $H(x)$ should be unit, namely,

$$(1/2)\int_{-1}^{1} H(x)\,dx = 1 \,. \tag{2.3}$$

Changing the order of integration, the formula (2.1) can be written as

$$Cw = 8R/(\rho\overline{B}^2) = 8g^2 \int_{-1}^{1} H(x)\Gamma(x)\,dx \,, \tag{2.4}$$

with

$$\Gamma(x) = -(1/2)\int_{-1}^{1} H(x')Y_o(g|x-x'|)\,dx' \,, \tag{2.5}$$

where Y_o is the Bessel function of the second species.

Taking the variation with respect to $H(x)$ in this formula and neglecting higher order terms, we have

$$\Delta Cw = 16g^2\Gamma(x)[\Delta H(x)\Delta x] \,. \tag{2.6}$$

Namely, the variation of the wave resistance with small deformation of the water plane area is proportional to the function $\Gamma(x)$.

For this property, we name it the influence function following to E. Hogner.(3)

Now, taking the class of functions considered by S. Karp and others, assume the next expansion in series of Mathieu functions, hereafter we follow the notations of McLachlan's text,(4)

$$H(x) = \varphi(\theta)/\sin\theta \,, \quad x = -\cos\theta \,, \tag{2.7}$$

and

$$\varphi(\theta) = \sum_{n=0}^{\infty} a_n ce_n(\theta,q), \quad q = g^2/4 \,. \tag{2.8}$$

Putting this expansion in (2.5) and (2.4), we have

$$\Gamma(x) = \sum_{n=0}^{\infty} \mu_n a_n ce_n(\Theta,q) \ , \tag{2.9}$$

and

$$Cw = 4\pi g^2 \sum_{n=0}^{\infty} \mu_n, q_n^2 \ , \tag{2.10}$$

where

$$\mu_{2n} = -(\pi/2)[A_o^{(2n)}/ce_{2n}(\pi/2,q)]^2 Fey_{2n}(0,q)/ce_{2n}(0,q),$$

$$\mu_{2n+1} = -(\pi/2)[\sqrt{q}A_o^{(2n+1)}/ce'_{2n+1}(\pi/2,q)]^2 Fey_{2n+1}(0,q)/ce_{2n+1}(0,q), \tag{2.11}$$

because of the orthogonality of functions.[4,8]

The form of the right hand side of (2.10) reduces the problem to simple calculation.

Some value of μ_n are shown in Table 1.

3. Minimum Problem I[8]

Firstly, consider the problem to minimize the wave resistance when the ship length, speed and water plane area are given, or in other words Froude number (Fr. = $1/\sqrt{2g}$) and the mean breadth $\overline{B}$ are given.

This means to minimize Cw of (2.4) or (2.10) under the condition (2.3), which is rewritten as follows, putting the expansion (2.7) and (2.8),

$$\sum_{n=0}^{\infty} a_{2n} A_o^{(2n)} = 2/\pi \ , \tag{3.1}$$

Thence, making use of Lagrange's method, we may have the solution as

$$a_{2n} = 2\lambda A_o^{(2n)}/\mu_{2n} = a_{2n}^* \ , \quad a_{2n+1} = 0 \ , \tag{3.2}$$

TABLE 1

	$4q$	1	4	10	16	24	36	50	64	80	100
	ε	1	2	$\sqrt{10}$	4	$\sqrt{24}$	6	$\sqrt{50}$	8	$\sqrt{80}$	10
	Fr.	0.7071	0.5000	0.3976	0.3536	0.3195	0.2887	0.2659	0.2500	0.2364	0.2236
	μ_0	0.644094	0.998125(1)	0.814806(2)	0.132126(2)	0.193168(3)	0.189457(4)	0.202547(5)	0.294995(6)	0.419816(7)	0.478425(8)
	μ_1	1.096150	0.732746	0.194796	0.470898(1)	0.851693(2)	0.992818(3)	0.122314(3)	0.199029(4)	0.313925(5)	0.397238(6)
	μ_2	0.547239	0.686380	0.662995	0.397181	0.138960	0.234523(1)	0.342655(2)	0.624663(3)	0.109448(3)	0.154365(4)
	μ_3	0.344356	0.385909	0.500315	0.582640	0.510346	0.227603	0.547913(1)	0.120592(1)	0.237545(2)	0.373999(3)
	μ_4	0.254270	0.268533	0.306237	0.360255	0.448653	0.495383	0.320119	0.128702	0.344321(1)	0.634796(2)
	μ_5	0.202113	0.208842	0.224475	0.244169	0.279845	0.358126	0.442317	0.402119	0.230739	0.712211(1)
	μ_6	0.167868	0.171617	0.179844	0.189269	0.204374	0.235323	0.290597	0.362817	0.406359	0.305693
	μ_7	-	0.145917	0.150846	0.156245	0.164335	0.179028	0.202103	01235452	0.290416	0.363293
	μ_8	-	0.127026	0.130230	0.133654	0.138613	0.147071	0.159004	0.174202	0.197839	0.241970
	Cvo	6.5518	4.4226	1.1384	0.34299	0.85324(1)	0.14156(1)	0.23083(2)	0.46094(3)	0.87171(4)	0.13191(4)
	Cv1	5.410	14.670	10.849	5.413	2.041	0.5094	0.1154	0.2950(1)	0.6976(2)	1.319(3)
	Cv2	2.790	12.73	23.60	20.36	12.02	4.521	1.441	0.4719	0.1398	0.0330
	δ_o	1.606	1.114	0.7960	0.6827	0.6039	0.5378	0.4910	0.4591	0.4323	0.4074
	m_o	0.7109	0.6358	0.5371	0.4857	0.4401	0.3997	0.3694	0.3480	0.3298	0.3123
Cv	0.5	20.26	53.46	46.35	12.26	1.639	0.6213(1)	0.2905(2)	0.3574(2)	0.2083(2)	0.7188(3)
δ =	0.6	14.43	28.29	14.90	2.038	0.8688(1)	0.1046	0.6263(1)	0.2610(1)	0.8602(2)	0.2134(2)
	0.7	11.24	15.80	3.563	0.3974	0.7623	0.4658	0.1647	0.5553(1)	0.1603(1)	0.3609(2)
	0.8	9.395	9.438	1.142	2.261	2.224	0.9176	0.2758	0.8488(1)	0.2312(1)	0.4970(2)
γ	0.5	-2.217	-1.963	-1.384	-0.7648	-0.3590	-0.1025	0.0204	0.0812	0.1196	0.1462
δ =	0.6	-1.680	-1.369	-0.7638	-0.2885	-0.0114	0.1407	0.2049	0.2331	0.2471	0.2534
	0.7	-1.297	-0.9456	-0.3206	0.0517	0.2374	0.3145	0.3367	0.3416	0.3381	0.3300
	0.8	-1.010	-0.6277	0.0118	0.3069	0.4240	0.4448	0.4356	0.4230	0.4064	0.3874

The numbers (n) in parentheses indicate that the results must be multiplied by 10^{-n}, for example, 0.3441(2) means 0.003441.

TABLE 2

$4q$	1	4	10	16	24	36	50	64	80	100
Fr.	0.7071	0.5000	0.3976	0.3436	0.3195	0.2887	0.2659	0.2500	0.2364	0.2236
a_0	0.89565	0.93186	1.05195	1.13513	1.20958	1.28477	1.34651	1.39366	1.43700	1.48113
a_1	0.61656	0.61952	0.64548	0.74218	0.88398	1.06089	1.22267	1.35534	1.48492	1.62408
a_2	0.09256	0.04368	0.00792	0.00286	0.00141	0.00088	0.00065	0.00052	0.00043	0.00035
a_3	0.63268	0.16586	0.10145	0.04071	0.01451	0.00589	0.00379	0.00310	0.00266	0.00229
a_4	0.00105	0.00268	0.00151	0.00061	0.00017	0.00003	0.00001	0.00000	0.00000	0.00000
a_5	0.00053	0.00595	0.01083	0.00835	0.00436	0.00131	0.00030	0.00008	0.00003	0.00002
a_6	0.00001	0.00003	0.00005	0.00039	0.00002	0.00001	0.00000	0.00000	0.00000	0.00000
a_7	-	0.00006	0.00032	0.00041	0.00034	0.00018	0.00007	0.00003	0.00001	0.00000
b_0	-0.05567	-0.19362	-0.32323	-0.38490	-0.45604	-0.55957	-0.67128	-0.77320	-0.88073	-1.00420
b_2	0.63372	0.59764	0.50740	0.47106	0.50503	0.63798	0.80724	0.96082	1.11919	1.29827
b_4	0.02856	0.12674	0.23008	0.18878	0.09742	0.03211	0.01299	0.00628	0.00669	0.00591
b_6	0.00021	0.00266	0.01692	0.04590	0.02089	0.01157	0.00455	0.00157	0.00047	0.00014
b_8	0.00000	0.00004	0.00006	0.00101	0.00135	0.00116	0.00058	0.00037	0.00016	-

TABLE 3

	$4q$	1	4	10	16	24	36	50	64	80	100
$a_n^{(0)} \times 10^5$	n=0	63662	63662	63661	63662	63661	63662	63663	63662	63662	63662
	2	1387	-24378	-53883	-67762	-78015	-86653	-92584	-96488	-99649	-102496
	4	34	1648	7570	13647	20743	29333	37053	43100	48625	54119
	6	-1	-47	-499	-1327	-2898	-5586	-8853	-12026	-15431	-19321
	8	0	1	19	75	244	665	1367	2250	3344	4843
	10	0	0	0	-3	-13	-54	-146	-290	-519	-884
	12	0	0	0	0	0	3	11	28	60	121
	14	0	0	0	0	0	0	0	-1	-6	-13
	16	0	0	0	0	0	0	0	0	0	1
$a_n^{(1)} \times 10^5$	1	63662	63662	63662	63661	63662	63662	63662	63662	63662	63662
	3	61242	7735	-14585	-37683	-59286	-79624	-94411	-104445	-112736	-120321
	5	-914	-64	2250	7327	15650	28888	43289	56033	68695	82155
	7	6	-1	-128	-632	-1986	-5246	-10308	-16117	-23155	-32057
	9	0	1	4	31	148	575	1506	2910	4994	8175
	11	0	0	0	-1	-8	-43	-150	-360	-748	-1468
	13	0	0	0	0	0	2	11	32	82	195
	15	0	0	0	0	0	0	0	-3	-7	-19
	17	0	0	0	0	0	0	0	0	0	2
$a_n^{(2)} \times 10^5$	0	0	0	0	0	0	-1	-3	1	-1	3
	2	63662	63662	63676	63718	63660	63663	63657	63650	63669	63667
	4	1529	7384	9842	-2338	-25295	-53553	-76853	-95503	-107710	-120977
	6	-26	-102	-153	3496	6060	16883	31896	47462	64645	84522
	8	0	2	-45	-422	-657	-2668	-6893	-12897	-20744	-32294
	10	0	0	3	23	38	252	922	2093	4190	7877
	12	0	0	0	-1	-1	-15	-84	-238	-585	-1338
	14	0	0	0	0	0	1	5	19	60	168
	16	0	0	0	0	0	0	0	-1	-4	-16
	18	0	0	0	0	0	0	0	0	0	1

where λ is Lagrange's constant and determined by (3.1), that is,

$$\lambda = 1/(\pi C_{o,o}), \; C_{o,o} = \sum_{n=o}^{\infty} (A_o^{(2n)})^2/\mu_{2n} \tag{3.3}$$

Putting these values into (2.10), we have

$$Cw = 16g^2\lambda = 16g^2/(\pi C_{o,o}) = Cwo \; . \tag{3.4}$$

Moreover, the influence functions (2.9) becomes

$$\Gamma(x) \; = 2\lambda \cdot \sum_{n=o}^{\infty} A_o^{(2n)} ce_{2n}(\theta,q) = \lambda = Cwo/(16g^2) \; , \tag{3.5}$$

by the expansion of a constant in Mathieu functions.

Secondly, consider the case when the area and the moment or center of floatation of the water plane area are given.

This latter condition is given as, say,

$$(1/4) \int_{-1}^{1} H(x) \; x \; dx = \alpha \; , \tag{3.6}$$

which means that the center of floatation is aft of midship by α times of the ship length, and this determines one more relation between the coefficients other than (3.1), namely,

$$\sum_{n=o}^{\infty} a_{2n+1} A_1^{(2n+1)} = 8 \; \alpha/\pi \; . \tag{3.7}$$

In the same way as the above, we have easily found the following result.

$$a_{2n+1} = 8 \; \alpha \; A_1^{(2n+1)}/(\pi C_{1,1}\mu_{2n+1}) = \alpha \; a^*_{2n+1} \; , \tag{3.8}$$

$$Cw = Cwo + 16 \; \alpha^2 Cw1 \; , \tag{3.9}$$

$$\Gamma(x) = Cwo/(16g^2) + \alpha \; Cw1 \; \cos\theta/(2g^2) \; , \tag{3.10}$$

a_{2n} and Cwo are the same as (3.2) and (3.4) and

$$Cw1 = 16g^2/(\pi \; C_{1,1}) \; , \; C_{1,1} = \sum_{n=o}^{\infty} A_1^{(2n+1)})^2/\mu_{2n+1} \; , \tag{3.11}$$

Thirdly and lastly, let us add to the first problem the condition that the second moment of the area is given arbitrarily.

That is given as

$$(1/8)\int_{-1}^{1} H(x)\, x^2\, dx = m^2$$

$$m^2 = 1/8 + (\pi/32)\sum_{n=0}^{\infty} a_{2n} A_2^{(2n)} \tag{3.12}$$

Then, we find easily the next solution in the same way as the above.

$$a_{2n} = a_{2n}^* + \gamma\, b_{2n}^* \ , \ a_{2n+1} = 0 \ ,$$

$$b_{2n}^* = 2[C_{o,o}\, A_2^{(2n)} - C_{o,2}\, A_o^{(2n)}]/(\pi\, \Delta\, \mu_{2n}) \ , \tag{3.13}$$

$$Cw = Cwo + \gamma^2 Cw2 \ , \tag{3.14}$$

$$\Gamma(x) = Cwo\ (16g^2) - 2\gamma[C_{o,2} - C_{o,o} \cos 2\theta]/(\pi\, \Delta) \tag{3.15}$$

where

$$\Delta = C_{o,o}\, C_{2,2} - C_{o,2}^2 \ ,$$

$$C_{o,2} = \sum_{n=0}^{\infty} A_o^{(2n)} A_2^{(2n)}/\mu_{2n} \ , \ C_{2,2} = \sum_{n=0}^{\infty} (A_2^{(2n)})^2/\mu_{2n} \tag{3.16}$$

$$\gamma = 16(m^2 - m^2) \ , \quad m_o^2 = 1/8 + C_{o,2}/(16 C_{o,o}) \ , \tag{3.17}$$

$$Cw2 = 16g^2 C_{o,o}/(\pi\, \Delta) \ . \tag{3.18}$$

In this place, let us introduce the quantity

$$\delta = 1/H(0) = 1/[\sum_{n=0}^{\infty} a_{2n} ce_{2n}(\pi/2, q)] \ , \tag{3.19}$$

which equals approximately to the usual water plane area coefficient.

In the first problem, this quantity takes the value

$$\delta = \delta_o = \pi C_{o,o}/(2D_o) \ , \ D_o = \sum_{n=0}^{\infty} A_o^{(2n)} ce_{2n}(\pi/2, q)/\mu_{2n} \ , \tag{3.20}$$

and in this case, using the above notations,

$$1/\delta = 1/\delta_o + 2\gamma(C_{o,o}D_2 - C_{o,2}D_o)/(\pi\,\Delta),$$
$$D_2 = \sum_{n=o}^{\infty} A_2^{(2n)} ce_{2n}(\pi/2,q)/\mu_{2n} . \tag{3.21}$$

The quantity m or γ is not familiar than δ, so that the solutions in this case are computed for four given values of δ using this relation.

The numerical values of the above appeared quantities are shown in Table 1 and 2 and Figure 1 to 6, and moreover the expansion coefficients of the solution in Mathieu functions are converted in the ones of trigonometrical functions and shown in Table 3.

Namely, write the solution of the first problem

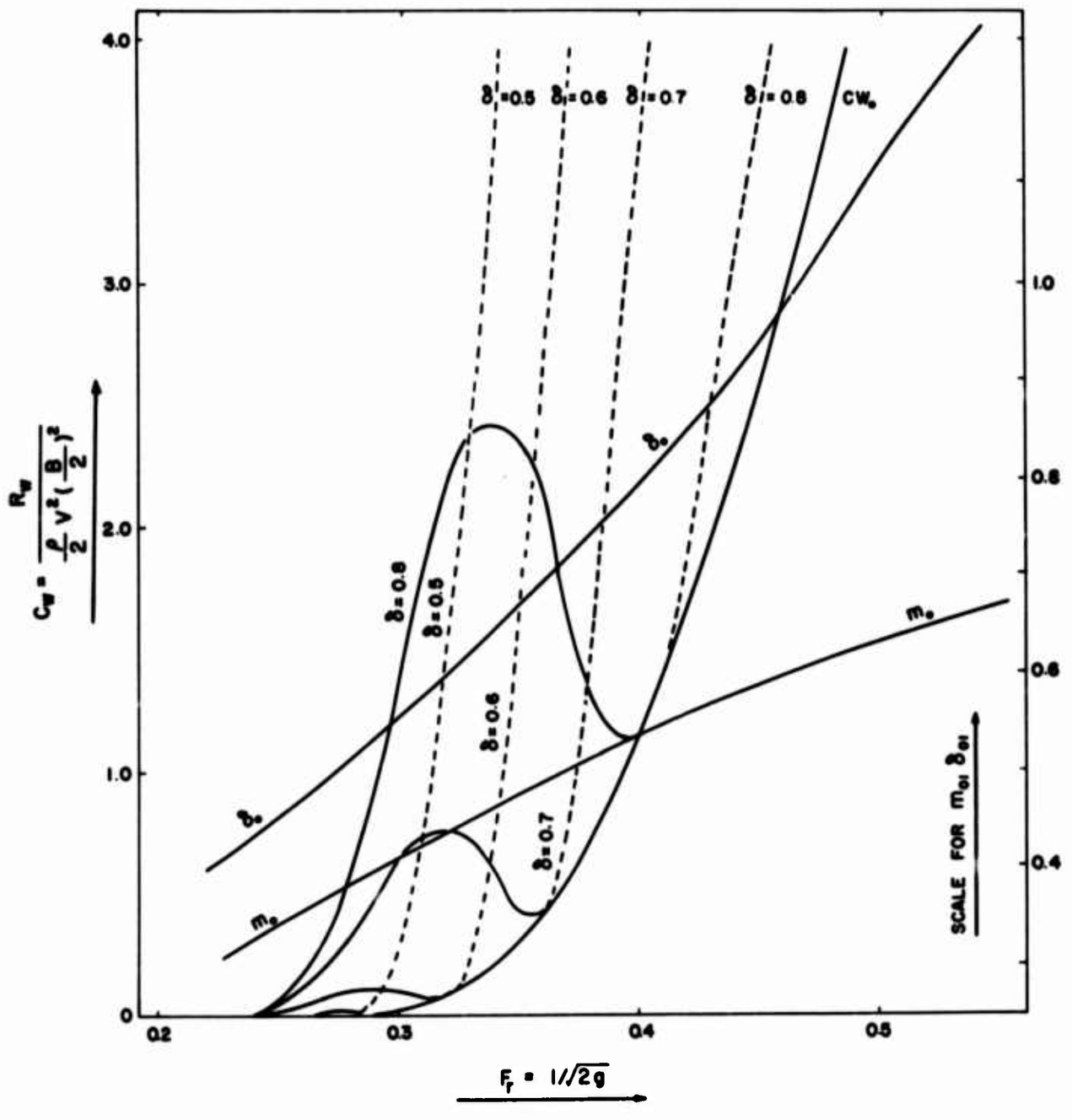
$$Ho(-ccs\theta) = \varphi o(\theta)/sin\theta ,$$
$$\varphi o(\theta) = \sum_{n=o}^{\infty} a_{2n}^{*} ce_{2n}(\theta,q) , \tag{3.22}$$

then we may write by the conversion

$$\varphi o(\theta) = \sum_{m=o}^{\infty} a_{2m}^{(o)} \cos 2m\theta , \quad a_{2m}^{(o)} = \sum_{n=o}^{\infty} a_{2n}^{*} A_{2m}^{(2n)} . \tag{3.23}$$

In the same way, we define the coefficient $a_m^{(1)}$ as follows,

$$H_1(x)\sin\theta = \varphi_1(\theta) = \sum_{n=o}^{\infty} a_{2n+1}^{*} ce_{2n+1}(\theta,q) ,$$
$$\varphi_1(\theta) = \sum_{m=o}^{\infty} a_{2m+1}^{(1)} \cos(2m+1)\theta , \tag{3.24}$$
$$a_{2m+1}^{(1)} = \sum_{n=o}^{\infty} a_{2n+1}^{*} A_{2m+1}^{(2n+1)}$$


$C_W = \frac{R_W}{\frac{\rho}{2} V^2 (\frac{B}{2})^2}$
$F_r = V/\sqrt{2g}$
δ=0.5
δ=0.6
δ=0.7
δ=0.8
CW_0
δ_0
m_0
SCALE FOR m_{01} δ_{01}
4.0
3.0
2.0
1.0
0
0.2
0.3
0.4
0.5
1.0
0.8
0.6
0.4

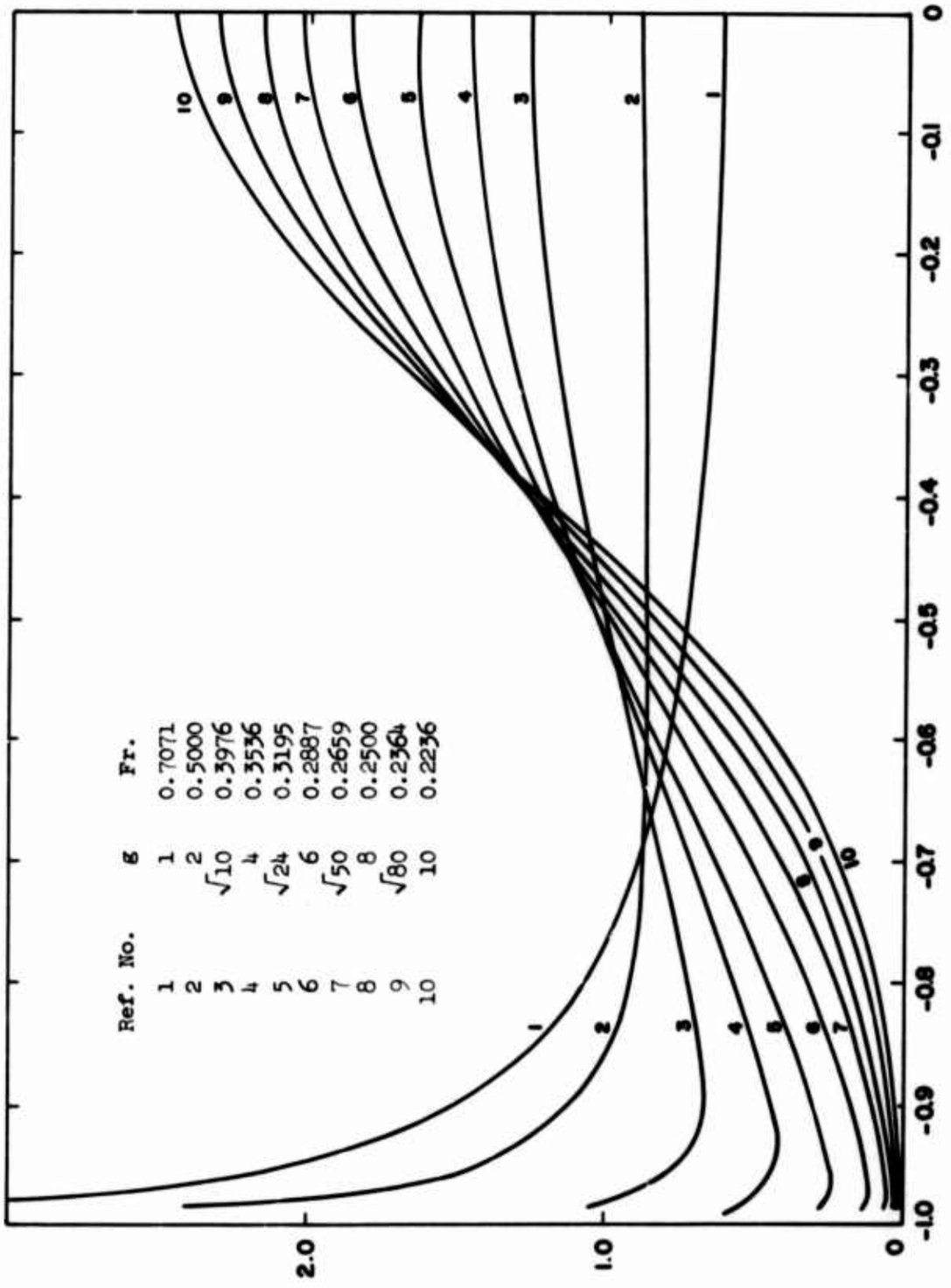

Ref. No. g Fr.
1 1 0.7071
2 2 0.5000
3 √10 0.3976
4 4 0.3536
5 √24 0.3195
6 6 0.2887
7 √50 0.2659
8 8 0.2500
9 √80 0.2364
10 10 0.2236
2.0
1.0
0
-1.0
-0.9
-0.8
-0.7
-0.6
-0.5
-0.4
-0.3
-0.2
-0.1
0
X

Figure 2. $H_o(x)$.

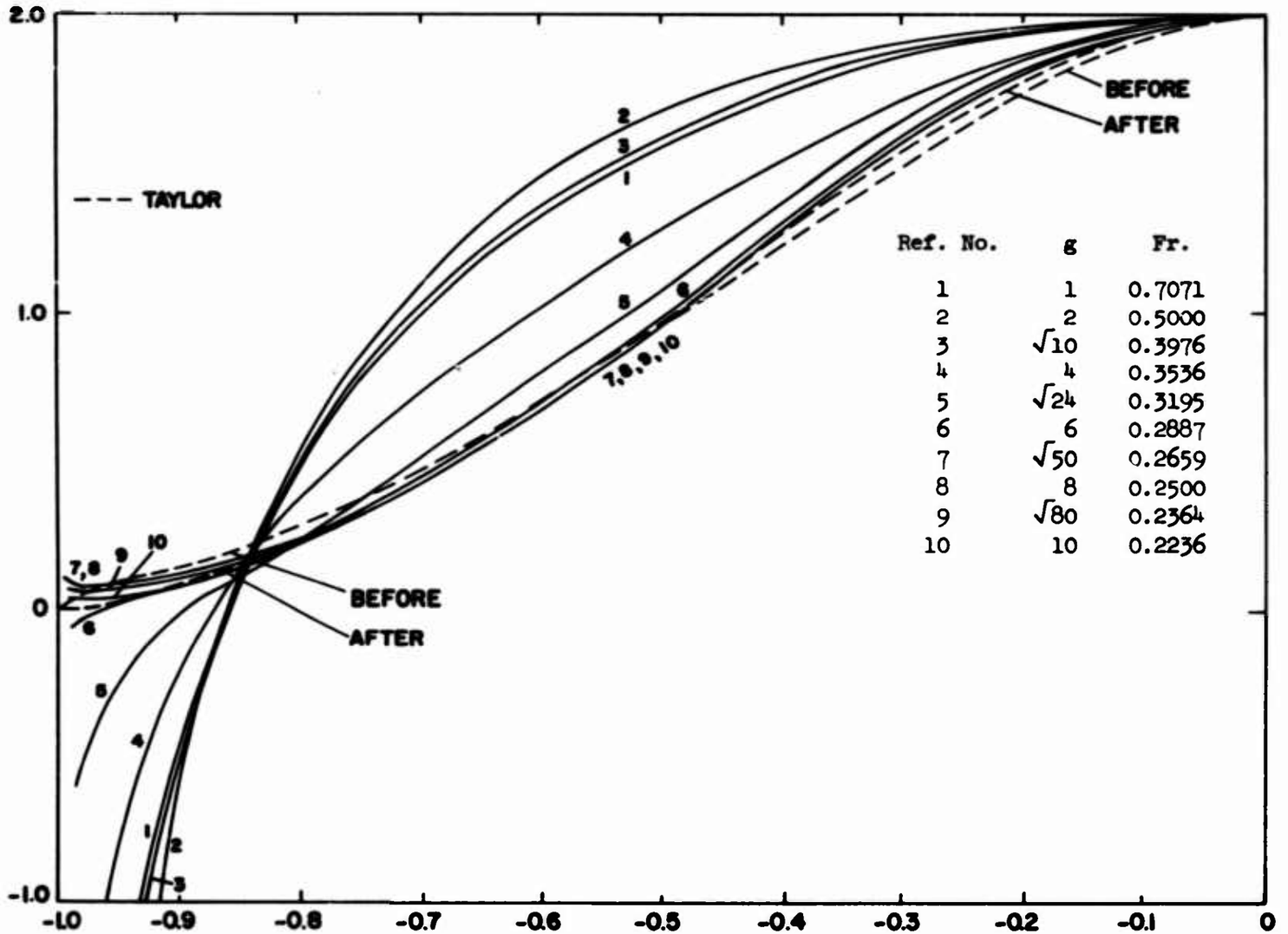


Figure 3. $H_3(x) \cdot \delta = 0.5$

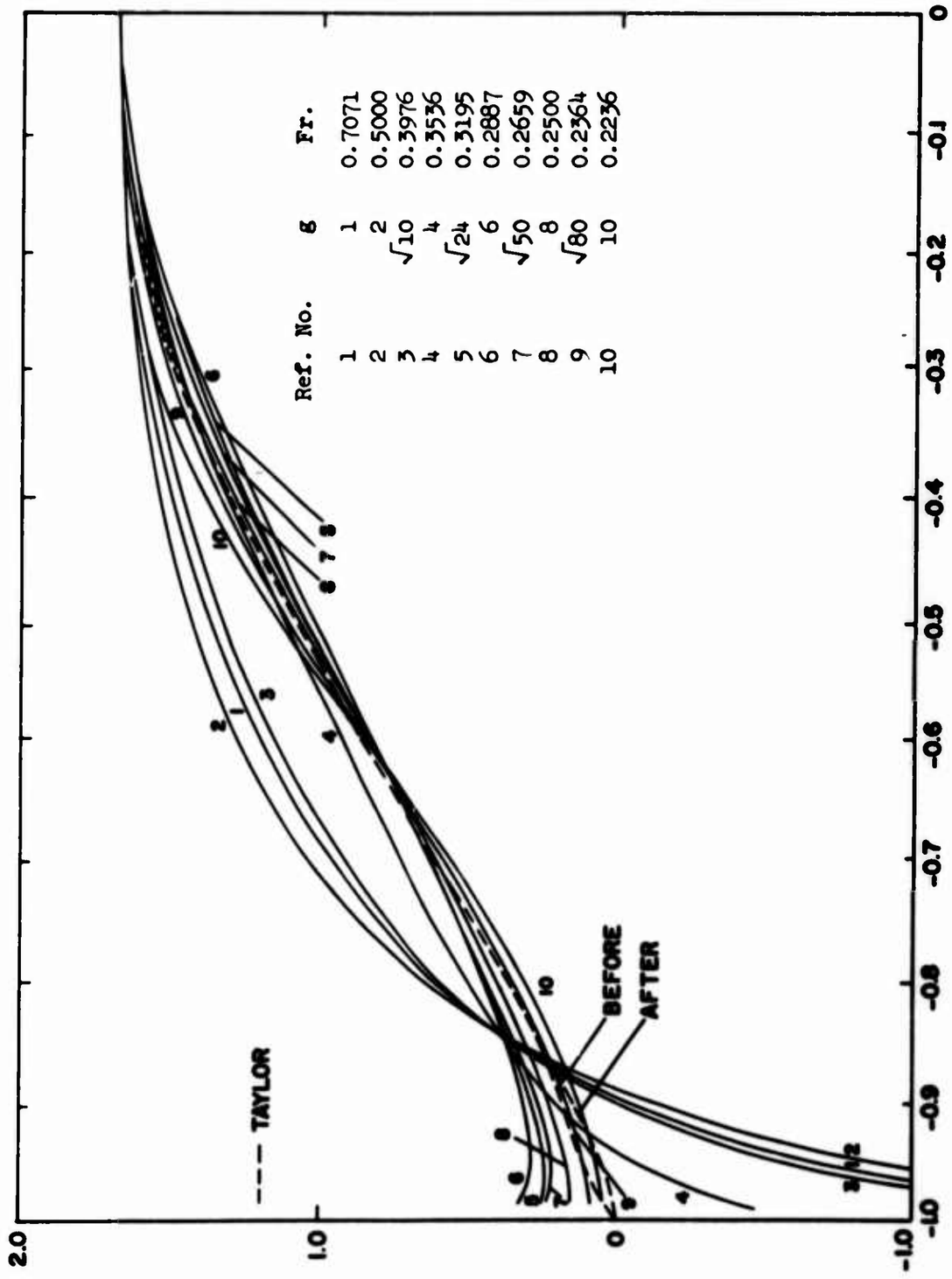


Figure 4. $E_3(x)$, $\delta = 0.6$

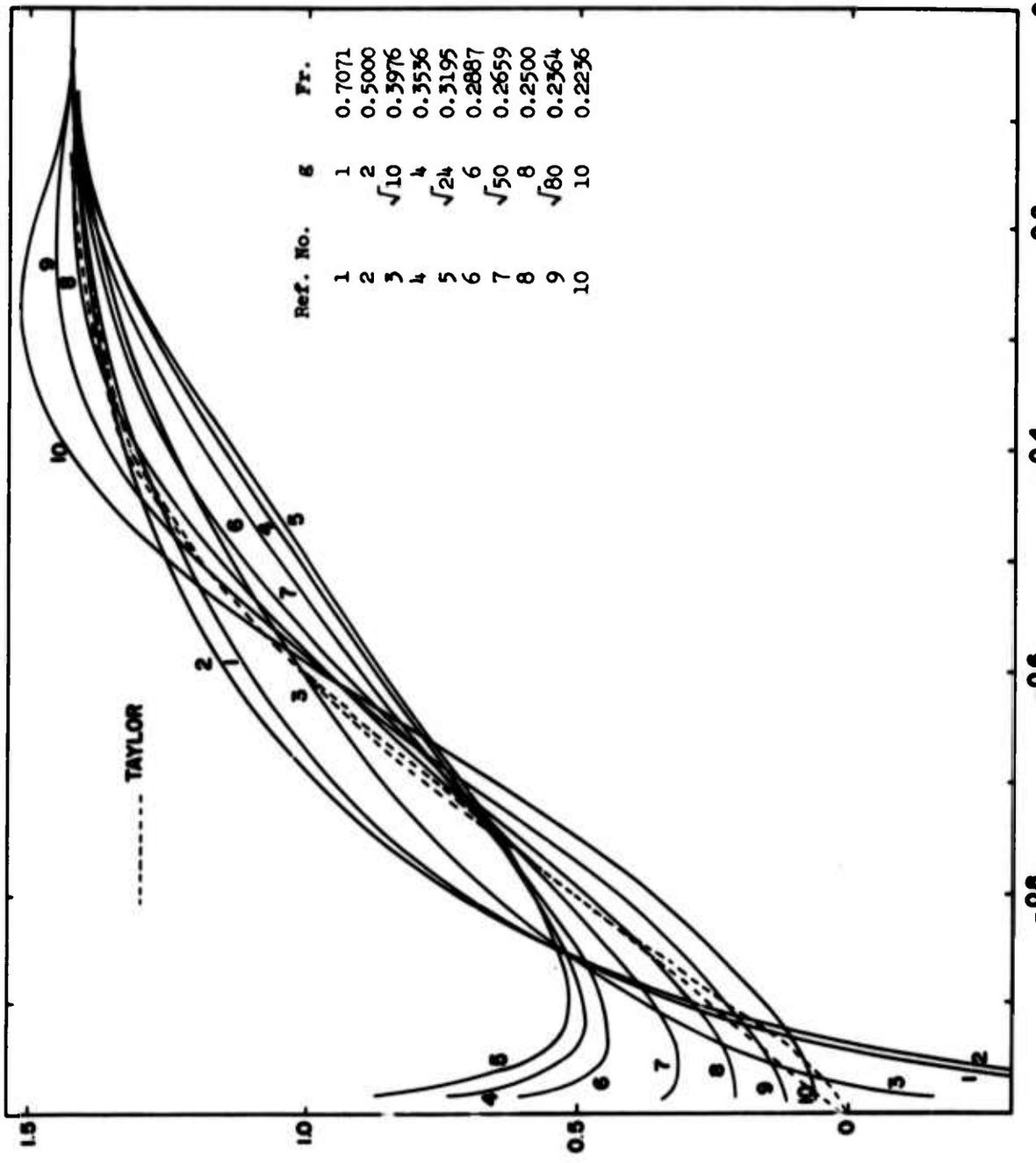


Figure 5. $H_3(x)$, $\delta = 0.7$

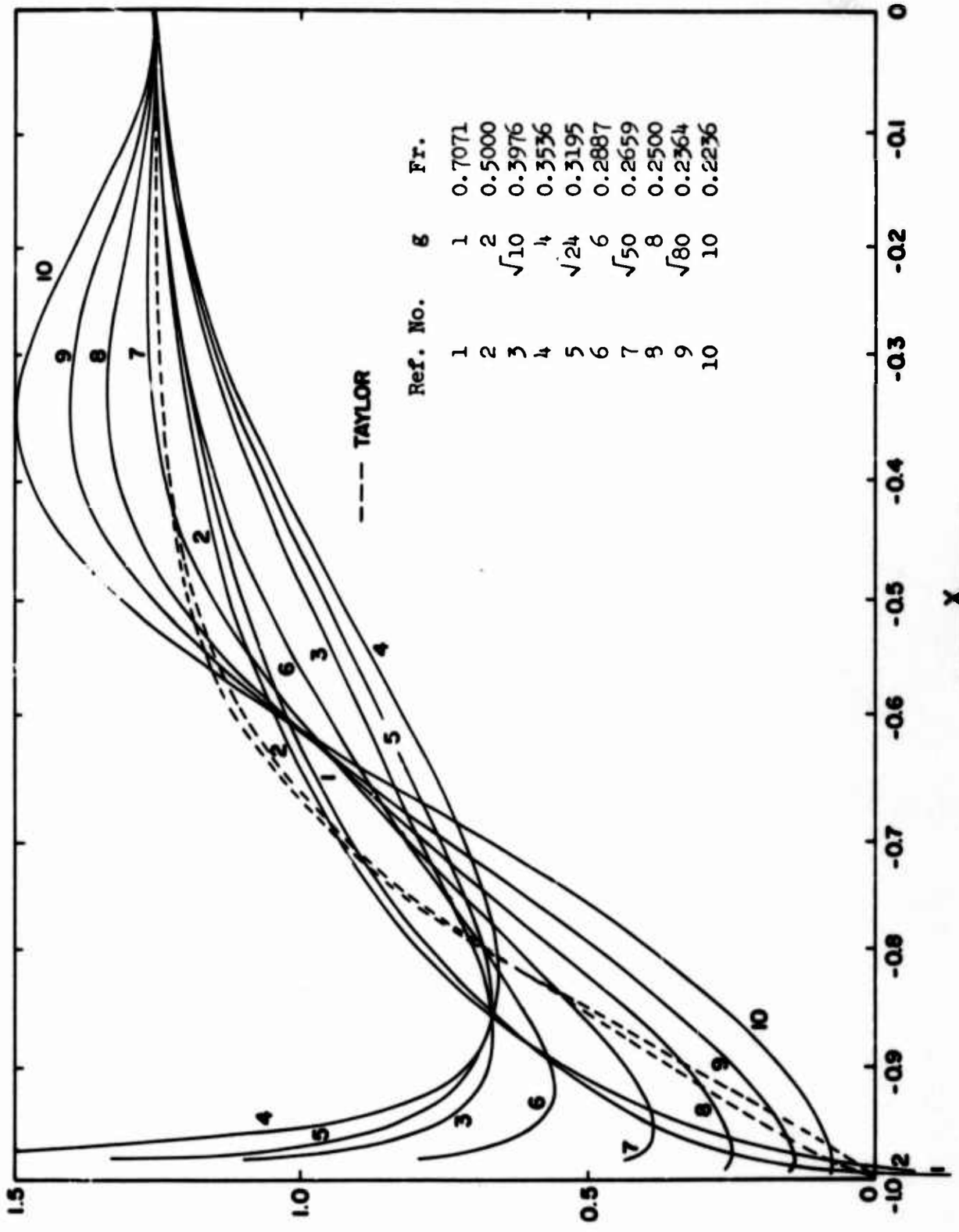


Figure 6. $H_3(x)$, $\delta = 0.8$

$$H_2(x)\sin\Theta = \varphi_2(\Theta) = \sum_{n=0}^{\infty} b^*_{2n} ce_{2n}(\Theta,q) ,$$

$$\varphi_2(\Theta) = \sum_{m=0}^{\infty} a^{(2)}_{2m} \cos 2m\Theta , \qquad (3.25)$$

$$a^{(2)}_{2m} = \sum_{n=0}^{\infty} b^*_{2n} A^{(2n)}_{2m}$$

4. Minimum Problem II[8]

In the preceding paragraph, we do not encounter any theoretical difficulty, but such proposition of the problem is somewhat different from G. Weinblum's.[6]

As widely known, he had considered the problem when the distribution vanished at end points and the area coefficient was given.

It was pointed out by S. Karp and others that this first condition was not adequate analytically.[7]

Here, we will show that the second condition is not adequate too in the same meaning.

The second condition says that $H(0)$ is to be given arbitrarily by (3.19).

By Lagrange's method, introducing two constants, we have the solution

$$a_{2n} = [2\lambda_1 A_0^{(2n)} + \lambda_2 ce_{2n}(\pi/2,q)]/\mu_{2n} . \qquad (4.1)$$

Putting this into (2.9), the influence function in this case becomes

$$\Gamma(x) = \lambda_1 + \lambda_2 \sum_{n=0}^{\infty} ce_{2n}(\pi/2,q) ce_{2n}(\Theta,q) , \qquad (4.2)$$

in which the series of the second term is summed up as the next by interchanging the order of summation and using the relations between Fourier coefficients of Mathieu functions.

$$\sum_{n=0}^{\infty} ce_{2n}(\pi/2,q)ce_{2n}(\theta,q) = \sum_{r=0}^{\infty}\sum_{s=0}^{\infty}\sum_{n=0}^{\infty} (-1)^r A_{2r}^{(2n)} A_{2s}^{(2n)} \cos 2s\theta$$

$$= 1/2 + \sum_{r=0}^{\infty} (-1)^r \cos 2r\theta = (1/2) \lim_{N\to\infty} [\sin(2N+1)(\theta-\pi/2)/\sin(\theta-\pi/2)] , \tag{4.3}$$

This value oscillates the more rapidly as the more N increases, so that we may not find the definite meaning of this problem, that is this problem is not adequate.

As easily seen, we shall meet the same difficulty as in (4.3) when we consider the first condition.

This property of his method may induce an instability of the solution as he wrote.(6)

5. Properties of the Solution

We will notice here some properties especially in low speed, because S. Karp and others gave them in high speed.

One of the most interesting is that the value of μ_n becomes very much smaller by decreasing its order especially in low speed as we see in Table 1.

This means from (2.10) that the lower the order of Mathieu function is, the smaller the wave resistance.

Hence, the optimum distribution consists almost of the first three Mathieu functions as we see in Table 2.

This fact enables next simple asymptotic formulas by making use of asymptotic ones of Mathieu functions, that is,

$$Cwo \fallingdotseq 64g^2 \exp(-2g) , \quad \text{for} \quad g \gg 1 , \tag{5.1}$$

$$\delta_o \fallingdotseq \sqrt{\pi/(2g)} , \tag{5.2}$$

$$m_o^2 \fallingdotseq 1/(4g) , \tag{5.3}$$

$$Cw1 \fallingdotseq 64g^4 \exp(-2g) , \tag{5.4}$$

$$Cw2 \doteqdot 16g^6 \exp(-2g) \ , \tag{5.5}$$

$$\delta = \delta_c/(1 - \gamma g/4) \ , \tag{5.6}$$

These formulas show also more explicitly the above principle in low speed.

Now, the distributions of the first problem without other restriction are shown in Figure 2 and those of the third problem with the given area coefficient in Figure 3 to 6.

In Figure 7 and 8, G. Weinblum's results are shown compared with our results, and notwithstanding that they were computed for the finite draft, they are similar as ours in general but the case when they have a large swan neck. In these cases, our solution has always a negative part, and so it has no practical meaning, but it should be remembered that the area coefficient of the optimum distribution without restriction is always larger than the value in these cases.

In this meaning, the third solutions corresponding to the dotted branch of the resistance curves in Figure 1 have no meaning.

6. Wave Profile

The wave profile of the optimum distribution must have some character different from the ordinary ones.

For this purpose, consider the surface elevation on the x-axis.

It is given as follows in our case.(2)

$$\zeta(x)/\overline{B} = -(g/4) \int_{-1}^{1} H(x')Z[g(x-x')]\, dx' \ , \tag{6.1}$$

with

$$\begin{aligned} Z(u) &= (d/du)[H_0(u) - Y_0(u)] \ , \quad \text{for} \quad u > 0 \ , \\ &= (d/du)[H_0(u) - 3Y_0(u)] \ , \quad \text{for} \quad u < 0 \ , \end{aligned} \tag{6.2}$$

where H_0 means Struve's function.

Now we may write (6.2) as

$$\begin{aligned} Z(u) &= [H_0'(u) - Y_1(u)] + 2Y_1(u) \ , \quad \text{for} \quad u > 0 \\ &= [H_0'(u) + Y_1(u)] + 2Y_1(u) \ , \quad \text{for} \quad u < 0 \end{aligned} \tag{6.3}$$

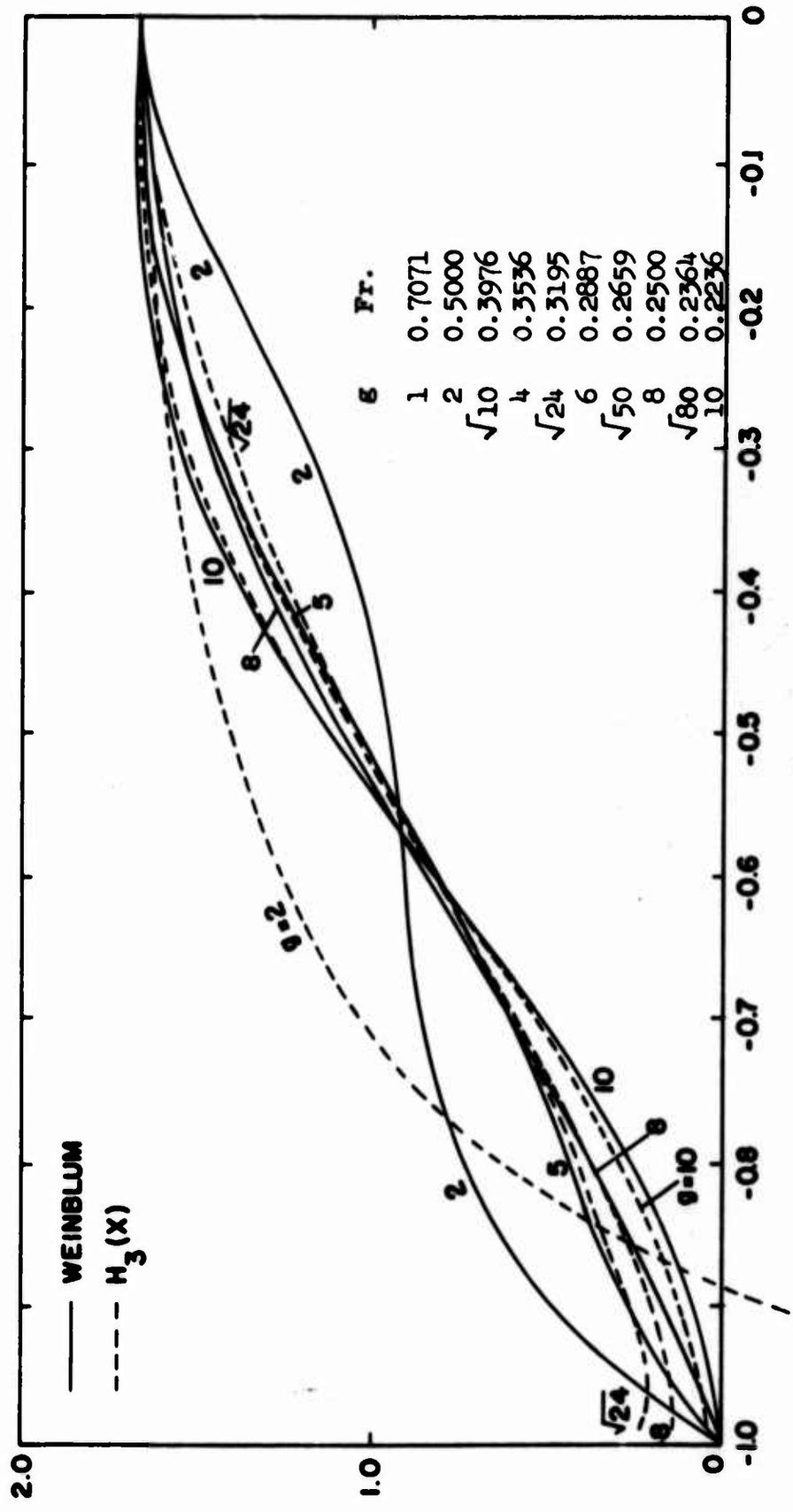


Figure 7. $\eta(x)$, ($\delta = 0.6$).

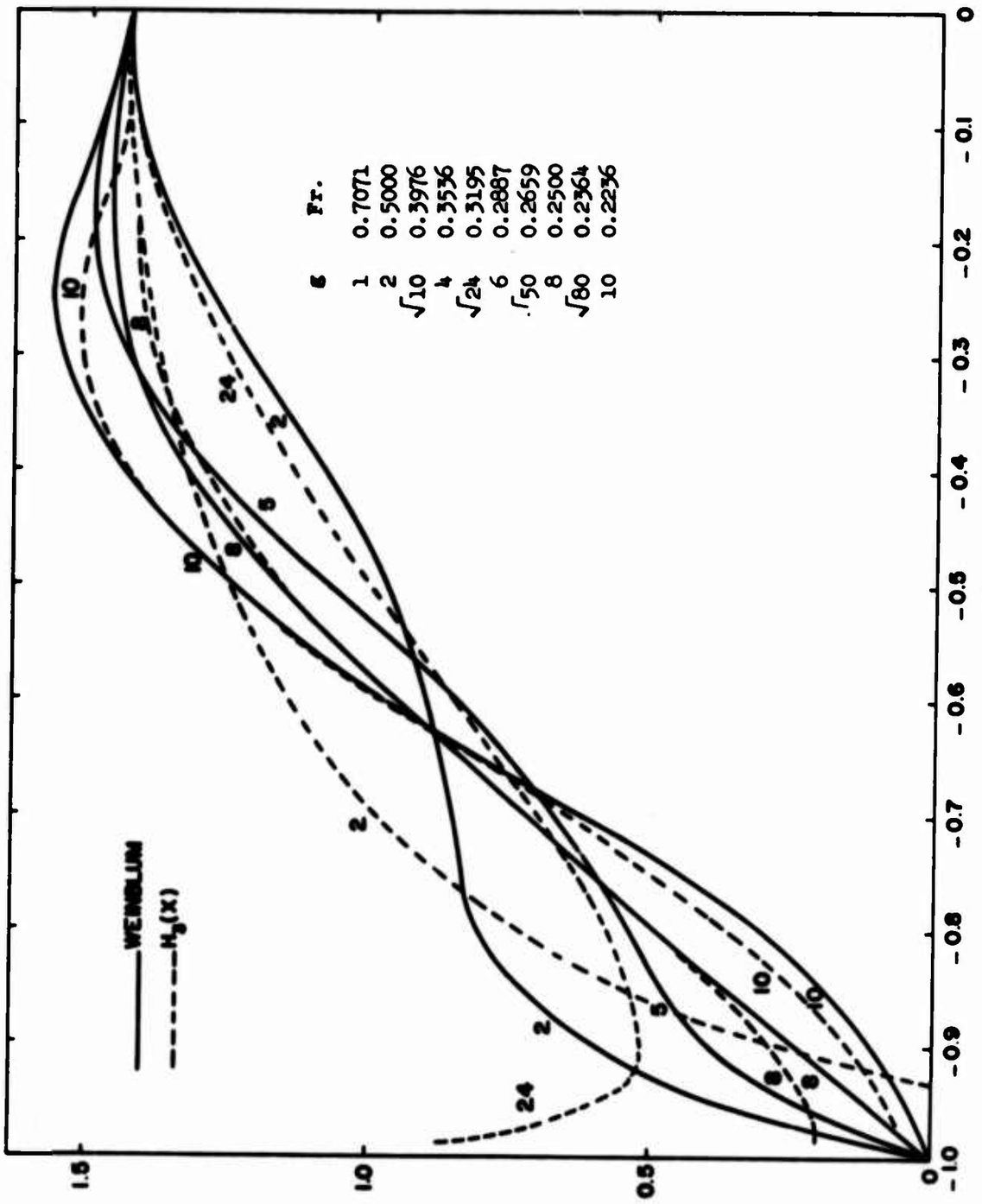


Figure 8. $\eta(x)$, ($\varphi = 0.7$).

In this right hand side, the function in the parentheses is even, but $Y_1(u)$ odd, and both functions tend infinity at $u = 0$ as $1/u$, so that the integral of the even part diverges but the one of the odd part has a definite value in the sense of Cauchy's principal value for $|x| < 1$.

Namely, if we assume the distribution symmetric about the origin, the even part of the surface elevation tends infinity but not for the odd part. That is, remembering (2.5),

$$\text{Odd part of } [\zeta/\bar{B}] = -(g/2) \int_{-1}^{1} H(x')Y_1[g(x-x')]\,dx'$$

$$= -(d/dx)\,\Gamma(x) \ . \qquad (6.4)$$

Hence, this should vanish in the first problem, because the influence function is constant by (3.5), and means that the surface elevation of this optimum distribution should be symmetric about the midship. Inversely, if the surface elevation be symmetric, then the influence function should be constant by (6.4), so that the distribution would be optimum.

In the same way, the odd part of the surface elevation of the third problem is linear by (3.15) but numerically very small in low speed.

Thence, these are the very character to distinguish the optimum distribution.

Lastly, we will give the surface elevation far upper and down stream.

Since we have an asymptotic expansion(1)

$$H_0(u) - Y_0(u) \fallingdotseq 2/(\pi u), \quad \text{for} \quad \gg 1 \ ,$$

putting this into (6.1), we have approximately

$$\zeta(x)/\bar{B} \fallingdotseq [1/(2\pi g x^2)] \int_{-1}^{1} H(x')dx' = 1/(\pi g x^2) \ , \quad \text{for} \quad x \gg 1 \ , \quad (6.5)$$

When x is negative, the elevation consists of the same symmetrical part and the free wave part.

The latter part takes the next form by (6.1) and (6.2),

$$\zeta_f(x)\,\bar{B} = -g \int_{-1}^{1} H(x')Y_1[g(x-x')]dx'$$

$$= -2(d/dx)\,\Gamma(x)\ , \quad \text{for} \quad x < -1\ , \tag{6.6}$$

where the influence function takes a different form from the above in this case when $|x| > 1$.

Namely, for the even distribution, we have

$$\Gamma(x) = -(\pi/2) \sum_{n=0}^{\infty} a_{2n}[A_0^{(2n)}/ce_{2n}(\pi/2,q)]^2\, Fey_{2n}(u,q)\ ,$$

$$\text{for} \quad x = -\cosh u\ , \tag{6.7}$$ [8]

Especially, for the first problem in low speed, this equals nearly to

$$\Gamma(x) \fallingdotseq -(\pi\ 2)a_0^*[A_0^{(0)}\ ce_0(\pi\ 2,q)]\ Fey_0(u,q)$$

$$\fallingdotseq [2\exp(-g)\sqrt{\pi g|x|}]\cos(g|x| + \pi/4)\ , \tag{6.8}$$

so that we have, by differentiation,

$$\zeta_f(x)/\bar{B} = -[4\sqrt{g}\ \exp(-g)/\sqrt{\pi|x|}]\ \sin(g|x| + \pi/4)$$

or

$$-1/2)\sqrt{Cwo/(\pi g|x|)}\ \sin(g|x| + \pi/4)\ , \tag{6.9}$$

7. Conclusion

Summarizing the above results, we may conclude as follows.

i) The minimum problem of the wave making resistance of the doublet distribution which is draftwise uniform and tends infinitely great depth can be solved most easily by making use of Mathieu functions.

ii) The solution of the first problem when the total sum of the doublet or approximately the water plane area is given, the second problem when the center of floatation is also given and the third problem when the second moment of the area is given are solved and shown in tables and figures.

iii) The third problem is solved instead of the one with the restriction for the area coefficient, because the proposition of the problem for this case is not adequate usually.

iv) In low speed, expanding the distribution in Mathieu functions, the lower its order, the smaller the wave resistance becomes, so that the optimum one consists almost of the one of the lowest order.

v) The wave profile along the distribution becomes infinitely large, but it should be symmetric about the midship at the optimum speed in the first problem.

In the last place, the author thanks heartily to Professor Maruo for his kind suggestions and discussions.

Reference

1. G. N. Watson, Theory of Bessel Functions, Cambridge, 1922.

2. T. H. Havelock, Proc. Roy. Soc., A,vol. 108, 1925.

3. E. Hogner, Proc. Roy. Soc., A, vol. 155, 1938.

4. N. W. McLachlan, Theory and Application of Mathieu Functions, Oxford, 1951.

5. N. B. S., Tables Relating to Mathieu Functions, Columbia Univ., 1951.

6. G. Weinblum and others, Jahrb. Schiffbautech, Gessels, Bd. 51, 1957.

7. S. Karp and others, Manuscr. of 3rd Symp. on Naval Hydromech., 1960.

8. M. Bessho, Memos. of Defence Academy, vol. 2, No. 4, Yokosuka, Japan, 1963.

TABLE 1

$4q$	1	4	10	16	24	36	50	64	80	100
s	1	2	$\sqrt{10}$	4	$\sqrt{26}$	6	$\sqrt{80}$	8	$\sqrt{80}$	10
Fr_o	0.7071	0.5000	0.3976	0.3536	0.3195	0.2887	0.2659	0.2500	0.2364	0.2236
μ_0	0.644084	0.998125(1)	0.814806(2)	0.132128(2)	0.198100(3)	0.188457(4)	0.202547(5)	0.294995(6)	0.419816(7)	0.478425(8)
μ_1	1.006180	0.732746	0.194798	0.470899(1)	0.651893(2)	0.992818(3)	0.122314(5)	0.199029(4)	0.313925(5)	0.397258(6)
μ_2	0.547239	0.688380	0.682995	0.897181	0.158880	0.234523(1)	0.342655(2)	0.484663(3)	0.109448(3)	0.154385(4)
μ_3	0.544356	0.995609	0.800515	0.582840	0.510346	0.227803	0.547915(1)	0.120592(1)	0.287545(2)	0.378099(3)
μ_4	0.254270	0.206538	0.206257	0.260255	0.448853	0.695283	0.320119	0.128702	0.344321(1)	0.634796(2)
μ_5	0.202115	0.209842	0.224475	0.244169	0.278845	0.358128	0.442317	0.402119	0.230739	0.712211(1)
μ_6	0.167868	0.171817	0.178044	0.188289	0.204574	0.235223	0.290597	0.382817	0.406359	0.505693
μ_7	-	0.145017	0.150846	0.158245	0.164335	0.178028	0.202105	0.235452	0.290416	0.363295
μ_8	-	0.127088	0.130220	0.138654	0.139615	0.147071	0.159004	0.174202	0.197859	0.241970
ω_0	6.5518	4.4228	1.1284	0.34299	0.85324(1)	0.14156(1)	0.22083(2)	0.46094(3)	0.87171(4)	0.15191(4)
ω_1	5.410	14.670	10.849	5.413	2.041	0.5094	0.1184	0.2960(1)	0.6976(2)	1.519(3)
ω_2	2.780	12.78	23.80	20.36	12.02	4.521	1.441	0.4719	0.1598	0.0330
f_0	1.606	1.114	0.7980	0.6827	0.6039	0.5378	0.4910	0.4591	0.4325	0.4074
m_0	0.7109	0.6358	0.5971	0.4887	0.4401	0.3997	0.3884	0.3480	0.3298	0.3125
C_w 0.5	20.26	53.46	46.36	12.28	1.639	0.6213(1)	0.2905(2)	0.3574(2)	0.2063(2)	0.7188(3)
f_n 0.6	14.45	28.29	14.90	2.028	0.6888(1)	0.1046	0.6283(1)	0.2810(1)	0.8602(2)	0.2134(2)
0.7	11.24	15.80	5.563	0.8974	0.7823	0.4658	0.1657	0.5555(1)	0.1603(1)	0.3809(2)
0.8	9.395	9.458	1.142	2.851	2.284	0.9176	0.2758	0.8488(1)	0.2512(1)	0.4970(2)
0.5	-2.217	-1.983	-1.384	-0.7648	-0.3580	-0.1025	0.0804	0.0812	0.1196	0.1462
γ f_n 0.6	-1.680	-1.309	-0.7638	-0.2886	-0.0114	0.1407	0.2e49	0.2551	0.2471	0.2534
0.7	-1.297	-0.9456	-0.3206	0.0517	0.2374	0.3145	0.3367	0.3416	0.3581	0.3800
0.8	-1.010	-0.6277	0.0118	0.2069	0.4240	0.4448	0.4556	0.4230	0.4064	0.3874

The numbers (n) in parentheses indicate that the results must be multiplied by 10^{-n}, for example 0.3441(2) means 0.003441 .

TABLE 2

$4q$	1	4	10	16	24	36	50	64	80	100
Fr_o	0.7071	0.5000	0.3976	0.3536	0.3195	0.2887	0.2659	0.2500	0.2364	0.2236
a^0_0	0.89565	0.93186	1.05195	1.13513	1.20958	1.28477	1.34651	1.39366	1.43700	1.48115
a^0_1	0.61656	0.61952	0.64546	0.74218	0.88598	1.06089	1.22267	1.35534	1.48492	1.62408
a^0_2	0.09256	0.04868	0.00792	0.00286	0.00141	0.00088	0.00065	0.00052	0.00043	0.00035
a^0_3	0.03268	0.16586	0.10145	0.04071	0.01451	0.00589	0.00379	0.00310	0.00266	0.00229
a^0_4	0.00105	0.00268	0.00151	0.00061	0.00017	0.00003	0.00001	0.00000	0.00000	0.00000
a^0_5	0.00053	0.00595	0.01083	0.00835	0.00436	0.00131	0.00030	0.00008	0.00003	0.00002
a^0_6	0.00001	0.00003	0.00005	0.00039	0.00002	0.00001	0.00000	0.00000	0.00000	0.00000
a^0_7	- -	0.00006	0.00032	0.00041	0.00034	0.00018	0.00007	0.00003	0.00001	0.00000
b^0_0	-0.03567	-0.19362	-0.32323	-0.38490	-0.45604	-0.55957	-0.67128	-0.77320	-0.88073	-0.00426
b^0_2	0.63372	0.59764	00.50740	0.47106	0.50503	0.63798	0.80724	0.93082	1.11919	1.29827
b^0_4	0.02856	0.12674	0.23008	0.18878	0.09742	0.03211	0.01299	0.00828	0.00609	0.00591
b^0_6	0.00021	0.00366	0.01698	0.04590	0.02089	0.01157	0.00455	0.00157	0.00047	0.00014
b^0_8	0.00000	0.00004	0.00006	0.00101	0.00135	0.00116	0.00058	0.00037	0.00016	---

TABLE 3

	$4q$	1	4	10	16	24	36	50	64	80	100
	$m=0$	63662	63662	63661	63662	63661	63662	63663	63662	63662	63662
	2	1587	-24378	-53885	-67762	78015	-86653	-92584	-96488	-99649	-102496
	4	34	1648	7570	13647	20745	29333	37033	43100	48625	54119
	6	- 1	- 47	- 499	- 1327	- 2898	- 5586	- 8853	-12026	-15431	-19321
(o)	8	0	1	19	75	244	665	1367	2230	3344	4843
a_m	10	0	0	0	- 3	- 13	- 54	- 146	- 290	- 519	- 884
	12	0	0	0	0	0	3	11	28	60	121
x10	14	0	0	0	0	0	0	0	- 1	- 6	- 13
	16	0	0	0	0	0	0	0	0	0	1
	1	63662	63662	63662	63661	63662	63662	63662	63662	63662	63662
	3	61242	7785	-14588	-37683	-59286	-79624	-94411	-104445	-112738	-120321
	5	- 914	- 64	2230	7237	15650	28888	43289	56033	68695	82155
	7	6	- 1	- 128	- 652	- 1986	- 5246	-10308	-16117	-23155	-32057
$a_m^{(1)}$	9	0	1	4	31	148	575	1506	2910	4994	8175
	11	0	0	0	- 1	- 8	- 43	- 150	- 360	- 748	- 1468
x10	13	0	0	0	0	0	2	11	32	82	195
	15	0	0	0	0	0	0	0	- 3	- 7	- 19
	17	0	0	0	0	0	0	0	0	0	2
	0	0	0	0	0	0	- 1	- 3	1	- 1	3
	2	63662	63662	63676	63718	63660	63663	63657	63650	63669	63667
	4	1529	7584	9842	- 2338	-25293	-53553	-76853	-93503	-107710	-120977
	6	- 26	- 102	- 153	3496	6080	16883	31896	47462	64645	84522
	8	0	2	- 45	- 422	- 657	- 2668	- 6893	-12897	-20744	-32294
$a_m^{(2)}$	10	0	0	3	25	38	252	922	2093	4190	7877
	12	0	0	0	- 1	- 1	- 15	- 84	- 238	- 595	- 1338
x10	14	0	0	0	0	0	1	5	19	60	168
	16	0	0	0	0	0	0	0	- 1	- 4	- 16
	18	0	0	0	0	0	0	0	0	0	1

EXPERIMENTS ON THEORETICAL SHIP FORMS OF LEAST WAVE RESISTANCE

Hajime Maruo

Davidson Laboratory
Stevens Institute of Technology

EXPERIMENTS ON THEORETICAL SHIP FORMS OF LEAST WAVE RESISTANCE

INTRODUCTION

The problem of finding a ship form which presents the least resistance under conditions imposed by practical requirements has been a goal of ship designers and ship hydrodynamicists. The vast efforts at the experimental towing tanks aims at the fulfillment of this goal. On the other hand, there are attempts to handle the problem from the theoretical point of view, as a consequence of the development of the fluidmechanics. On accepting Froude's hypothesis, that the total resistance of a ship is the sum of its wave resistance and viscous resistance, both components must have close relations with ship forms. The present state of knowledge about viscous flow is not yet sufficient to yield a detailed analysis of the relationship between viscous resistance and the ship form.

On the other hand, a purely analytical discussion is possible for wave resistance, provided the effect of viscosity is neglected and linearization of the equations are permissable. Under these circumstances mathematical methods for minimization of wave resistance have been tried by various researchers since Weinblum published his first attempt.[1] When the wave resistance is given an analytical expression as a functional of the function which gives the equation for the ship's surface, the problem of minimizing it is a purely mathematical problem, i.e., the calculus of variations. There were controversies about the existence of the solution to minimize Michell's integral under a certain side condition which was necessary. Von Kármán[2] and Sretenskii[3] expressed their opinions of denial of the existence of the solution when a ship of constant displacement is considered. Wehausen[4] showed that a solution might exist if some restriction is imposed on the function. Quite recently Karp, Kotik and Lurey[5] showed that a solution does exist for minimizing the strut-like dipole distribution of infinite draft. They have calculated the water line shape of the strut by which the wave resistance is minimized under the condition of a constant sectional area. Their achievement seems to put to end the conflict about the existence of the solution minimizing wave resistance for constant displacement. There is another striking phenomenon when another side condition is introduced, namely, the nonexistence of the solution

for a ship of given breadth. It is attributed to Bessho's finding.[6] Weinblum's calculation[7] concerns the optimum form of a given prismatic coefficient. If the displacement is fixed, constant breadth is implied. Accordingly, a difficulty again appears in the minimization problem.

At any rate, the existence of the solution under the single side condition that the displacement is fixed is certain. The results of Karp and others are derived in a numerical way with the aid of an electronic computor. The solution shows some inaccuracy at Froude numbers lower than 0.4. Accordingly, their results are confined to the higher Froude number range. Unfortunately, the result for higher Froude numbers is not feasible for practical ship forms. Therefore, results for lower Froude numbers are needed. A numerical approach does not appear to be the proper method to obtain a solution at lower Froude number because of the oscillating nature of the Kernel of the integral equation which represents the optimum condition. However, there is an analytical way to solve the integral equation and if one makes use of numerical tables of the necessary functions exact values are determined. It is of great interest to perform the actual measurement of resistance of the form which shows the minimum wave resistance predicted by the theory. Models were tested at the Yokohama University Tank. This is the report of the result.

Determination of the Vertical Strut of Minimum Wave Resistance

It was shown by Kapr and others that Michell's integral in its original form does not serve to determine the optimum form. In place of it, the integral obtained by integration by parts is employed. Take the x-axis as the longitudinal axis of a ship, the y-axis athwartships, and the z-axis draftwise downwards. The coordinates origin is on the load water line, amidships. Consider a thin ship of length 2ℓ, breadth 2b and draft T and let the underwater portion of its surface be expressed by an equation

$$y = \pm f(x,z) \tag{1}$$

The wave resistance given by Michell's integral is

$$R = \frac{4\rho g^2}{\pi U^2} \int_1^\infty \frac{\lambda^2}{\sqrt{\lambda^2 - 1}}\, d\lambda \int_{-\ell}^{\ell}\int_{-\ell}^{\ell}\int_0^T\int_0^T \frac{\partial f(\eta,z)}{\partial x}\,\frac{\partial f(x',z')}{\partial x'} \cos\left\{\frac{g}{U^2}\lambda(x-x')\right\} \times e^{\frac{g}{U^2}\lambda^2(z+z')}\, dxdx'dzdz' \tag{2}$$

If we consider a strut-like ship of uniform water line and infinite draft, the integration with respect to z leads to

$$R = \frac{4\rho U^2}{\pi} \int_1^\infty \frac{d\lambda}{\lambda^2\sqrt{\lambda^2-1}} \int_{-\ell}^{\ell}\int_{-\ell}^{\ell} \frac{df(x)}{dx}\frac{df(x')}{dx'} \cos\left\{\frac{g}{U^2}(x-x')\right\} dxdx' \tag{3}$$

The function f is now a function of x alone. Integrating by parts with x and x' we obtain

$$R = \frac{4\rho g^2}{\pi U^2} \int_1^\infty \frac{d\lambda}{\sqrt{\lambda^2-1}} \int_{-\ell}^{\ell}\int_{-\ell}^{\ell} f(x)f(x')\cos\left\{\frac{g}{U^2}\lambda(x-x')\right\} dxdx' \tag{4}$$

This formula is interpreted as the wave resistance of a dipole distribution whose intensity per unit area is $U\, f(x)/(2\pi)$, with the condition that the function $f(x)$ is zero at both ends is exempted. The condition of constant displacement requires that now the water plane area, A_w, be constant which is given by the equation

$$2\int_{-\ell}^{\ell} f(x)\, dx = A_w = \text{const.} \tag{5}$$

The Eulerian equation which expresses the minimization of Equation (4) under the side condition Equation (5) is

$$\int_1^\infty \frac{d\lambda}{\sqrt{\lambda^2-1}} \int_{-\ell}^{\ell} f(x') \cos\left\{\frac{g}{U^2}\lambda(x-x')\right\} dx' - k = 0 \tag{6}$$

where k is the Lagrangean multiplier. Because of the integral representation for the Bessel function of the second kind

$$Y_o(x) = -\frac{2}{\pi}\int_1^\infty \cos(x\lambda)\, \frac{d\lambda}{\sqrt{\lambda^2-1}} \tag{7}$$

we can write the integral equation, putting $g/U^2 = \kappa$

$$-\frac{\pi}{2}\int_{-\ell}^{\ell} f(x')\, Y_o\{\kappa(x-x')\}\, dx' = k \tag{8}$$

This is a special case of the integral equation of the form

$$\int_{-\ell}^{\ell} \sigma(x') \, Y_o \{\kappa(x-x')\} \, dx' = G(x) \qquad (\ )$$

which was first solved by Dörr.[8] To obtain the solution, we transform the variables by

$$x = -\ell \cos\theta \qquad x' = \ell \cos\theta \qquad (10)$$

and put $\kappa\ell = \kappa_o \qquad \frac{2}{\pi\ell} k = k'$ (11)

If we write the solution in the form

$$f(x) = \frac{A_w}{4\ell} \frac{\sigma(\theta)}{\sin\theta} \qquad (12)$$

the integral Equation (8) becomes

$$-\int_o^{\pi} \sigma(\theta) \, Y_o \{\kappa_o(\cos\theta' - \cos\theta)\} \, d\theta = k' \qquad (13)$$

The eigen-function of the above integral equation is the even Mathieu function of the integral order $ce_n(\theta, q)$ which is a periodic solution of the Mathieu equation

$$\frac{d^2y}{d\theta^2} + (a - 2q \cos 2\theta) \, y = 0 \qquad (14)$$

where $q = 1/4 \, \kappa_o^2$.

If we write the eigenvalue as $1/(2\mu_n)$, the following integral theorem exists.

$$-\int_o^{\pi} Y_o \{\kappa_o(\cos\theta' - \cos\theta)\} \, ce_n(\theta', q) d\theta' = 2\mu_n \, ce_n(\theta, q) \qquad (15)$$

Since the Mathieu functions ce_n form a closed orthogonal system in the interval $0 \leq \theta \leq \pi$, any function can be expanded by them. We have the special case

$$1 = 2 \sum_{n=o}^{\infty} A_o^{(2n)} \, ce_{2n}(\theta, q) \tag{16}$$

It is readily shown that the solution of Equation (13) is symmetric with respect to $\theta = \pi/2$, therefore $\sigma(\theta)$ can be expanded by Mathieu functions of the even order, e.g.

$$\sigma(\theta) = a_o ce_o(\theta) + a_2 ce_2(\theta) + a_4 \, ce_4(\theta) + \ldots. \tag{17}$$

Substituting Equation (17) for $\sigma(\theta)$ in the integrand and Equation (16) for the right-hand side of Equation (13), and making use of Equation (15), comparison of the coefficients of ce_{2n} gives

$$a_{2n} = k' A_o^{(2n)} / \mu_{2n} \tag{18}$$

The coefficient $A_o^{(2n)}$ is the coefficient of the first term of the Fourier expansion of ce_{2n}:

$$ce_{2n}(\theta, q) = A_o^{(2n)} + A_2^{(2n)} \cos 2\theta + A_4^{(2n)} \cos 4\theta + \ldots. \tag{19}$$

The coefficient μ_{2n} was given an explicit expression by Bessho[6] making use of modified Mathieu functions. He also calculated the value of μ_{2n} and gives values of a_{2n}. The coefficients $A_o^{(2n)}$ are obtained from tables.[9] The value of k is determined from relation Equation (5) or

$$\int_o^{\pi} \sigma(\theta) d\theta = 2 \tag{20}$$

The optimum dipole distribution is calculated by Equation (17), but because there is no table available to find the value of ce_n, a trigonometric series (19) is used to calculate the value. The result is shown in Figure 1. At both ends the intensity of the dipole becomes

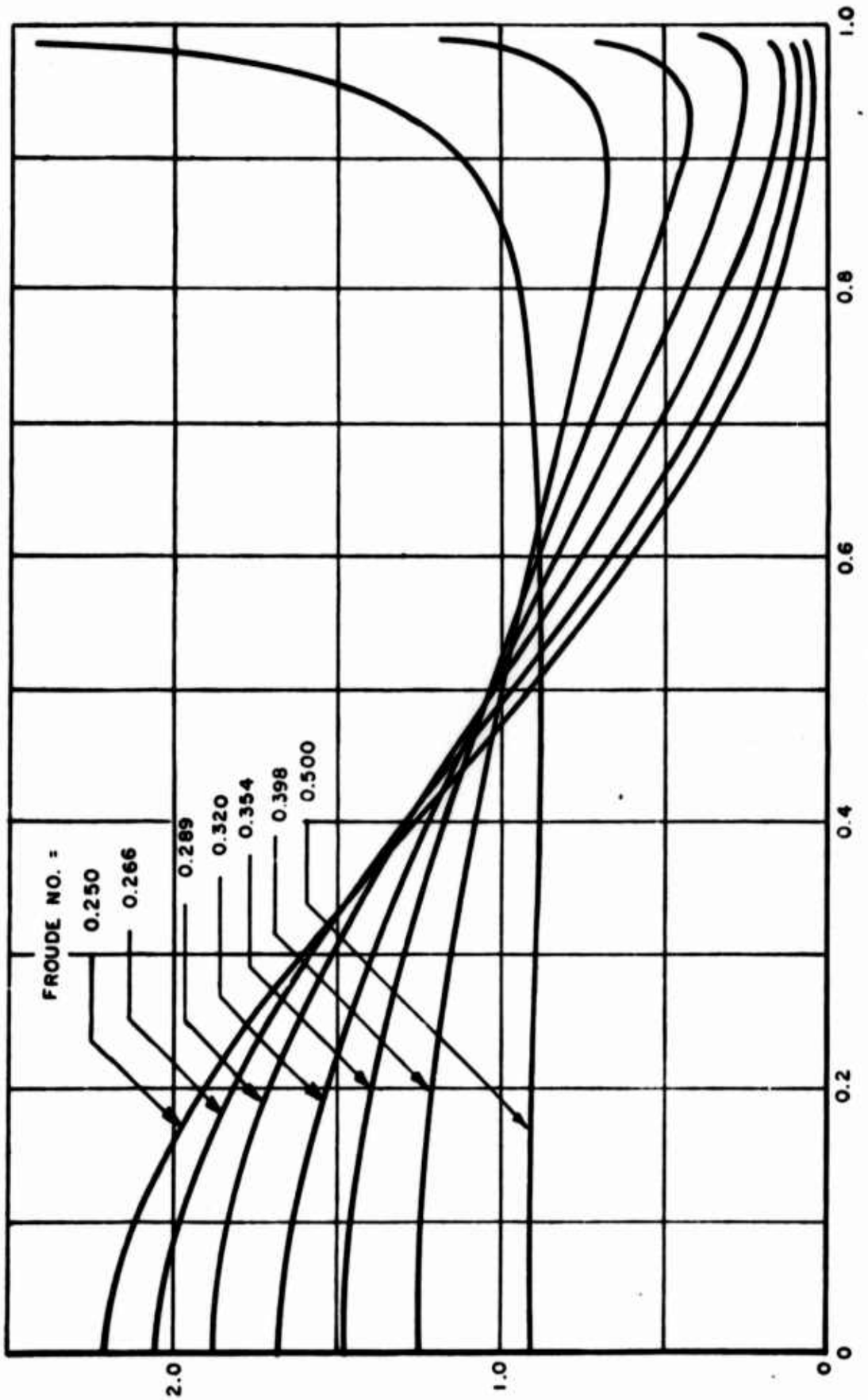


FIGURE I. OPTIMUM DIPOLE DISTRIBUTION FOR A STRUT

infinite, that means the concentration of the singularity. The actual shape of the waterline is obtained by tracing the stream line. We have to remember that the present results issue from linearized theory. Therefore a further step must be made under the restriction of the linearization. As previously shown, the dipole is concentrated at the ends. It is observed that the stream line near the ends is substantially governed by the dipole distribution of the type $\sigma_o/\sin\theta$ where σ_o is the value at $\theta = o$ or π. Therefore, the shape near the ends is determined by the stream line associated with the above dipole distribution. At regions not near the ends, the slope $d f(x)/d\kappa$ is assumed small because of the linearization assumption. The slope of the waterline itself is then given in keeping with Michell's assumption. The shapes in Figure 2 are obtained in this manner. These shapes have the same area which are chosen so as to be

$$A_w/(2\ell)^2 = 0.08$$

The Determination of the Optimum Form of Slender Ships

The results obtained so far are for the case of infinite draft. What is actually needed is the optimum shape for finite or rather small draft. Results may be obtained from Michell's integral with finite draft. However, an analytical method cannot be applied to such a case. With ships of ordinary proportion, the draft is usually less than half the beam. It is doubtful that one can apply the thin ship approximation in this case, there is another approximation that may be fitted to a ship of finite draft; the slender ship approximation. According to the theory of slender ships,[10,11] the wave resistance is equivalent to that obtained from Michell's integral in which the draft tends to zero. Therefore we may expect the ship form that minimizes the wave resistance to be given by slender ship theory. The formula for the slender ship indicates that the wave resistance is determined mainly by the shape of the sectional area curve. Accordingly, we can write the wave resistance in the form

$$R = \frac{1}{2}\rho U^2\kappa^2 \int_{-\ell}^{\ell} dx' \int_{-\ell}^{\ell} \frac{dA(x)}{dx}\,\frac{dA(x')}{dx'} K(x-x')dx' \qquad (21)$$

where $A(x)$ is the area of the cross section at x. In order to give Michell's integral for a wall-sided ship of finite draft, the function K takes the form

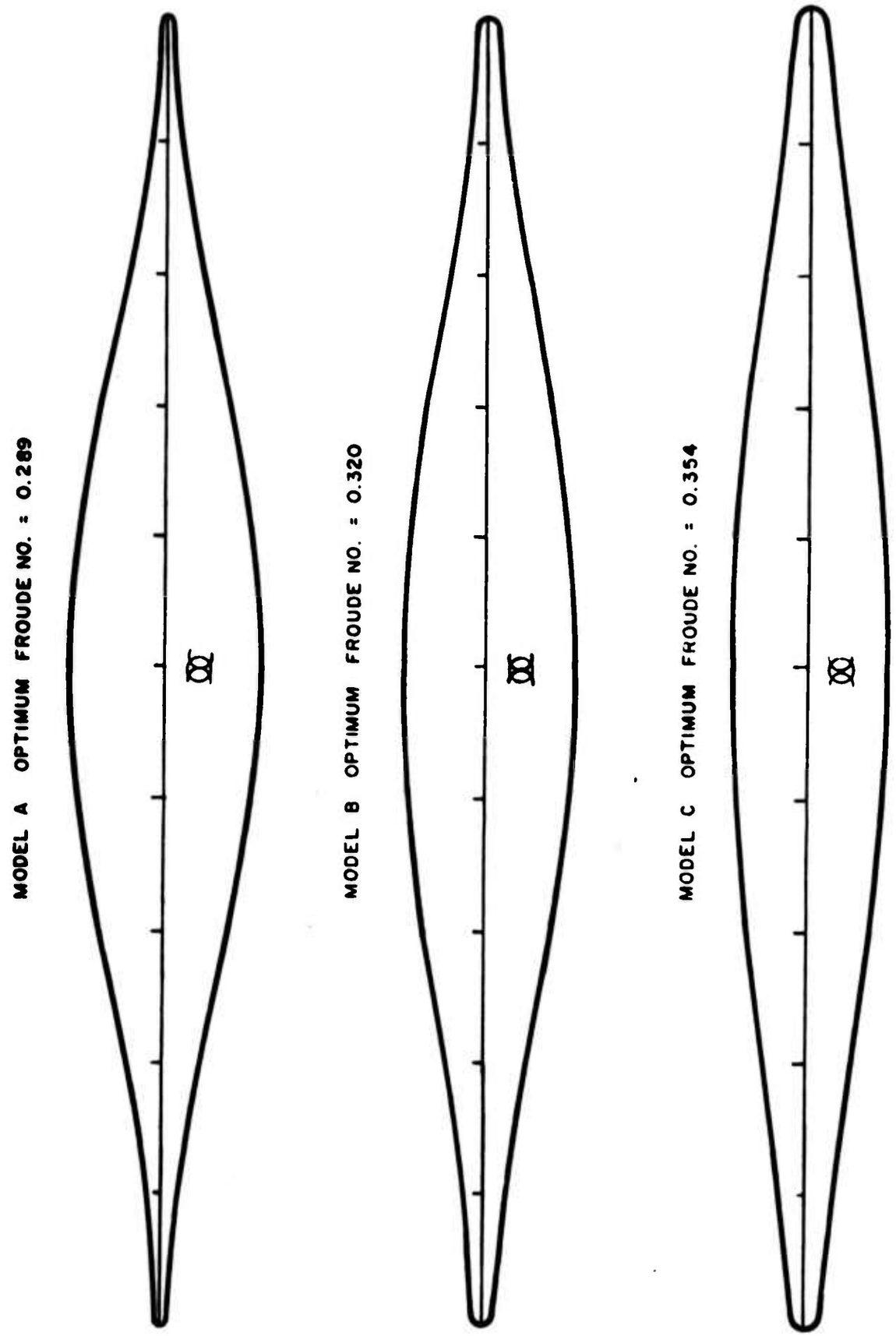


FIGURE 2. WATER LINE OF TESTED MODELS

$$K(x-x') = \frac{2}{\pi(\kappa T)^2} \int (1-e^{-\kappa T\lambda^2})^2 \cos\{\kappa\lambda(x-x')\} \frac{d\lambda}{\lambda^2\sqrt{\lambda^2-1}} \quad (22)$$

Now let us consider the minimization of Equation (21) under the condition of constant displacement, which is given by the equation

$$\int_{-\ell}^{\ell} A(x)dx = -\int_{-\ell}^{\ell} \frac{dA(\kappa)}{dx} xdx = \nabla = \text{const.} \quad (23)$$

where ∇ is the volume of displacement. According to the principle of the calculus of variations, the condition for minimizing Equation (21) under the side condition Equation (23) is expressed by the following equation

$$\kappa^2 \int_{-\ell}^{\ell} \frac{dA(x')}{dx'} K(x-x')d\kappa' + kx = 0 \quad (24)$$

where k is again the Lagrangean multiplier. Note that Michell's integral presents no solution of Equation (24) at all. Integrating Equation (24) twice with respect to κ, and putting

$$K(x) = \frac{d^2L(x)}{dx^2} \quad (25)$$

we obtain

$$\kappa^2 \int \frac{dA(x')}{dx} L(x-x')\,dx' + k_2 + k_1x + \frac{1}{6}kx^3 = 0 \quad (26)$$

where k_1 and k_2 are integration constants. It is obvious that the ship form for minimum wave resistance is symmetric with respect to the midship section, so that $dA(x)/dx$ is an odd function. Since the kernel $L(x-x')$ is symmetric, the terms on the left-hand side of Equation (26) should be odd, which means

$$k_2 = 0$$

Integrating Equation (22) twice and taking the limiting value when the draft tends to zero, we obtain the kernel

$$\kappa^2 L(x) = Y_o(\kappa x) \quad (27)$$

Therefore, we have the integral equation

$$-\int_{-\ell}^{\ell} \frac{dA(x')}{dx'} Y_o \{\kappa(x-x')\}\, dx' = k_1 x + \frac{1}{6} kx^3 \qquad (28)$$

This is another integral equation of the form (9) and can be solved as before. The unknown constant k should be determined by the side condition (23), but there is another unknown k_1. Then k is a function of an arbitrary constant k_1. Now, let us consider the wave resistance at its minimum. If the optimum condition is fulfilled, the relation (24) or

$$\int_{-\ell}^{\ell} \frac{dA(x')}{dx'} K(x-x')dx' = - kx \qquad (29)$$

exists. Substituting in Equation (21) and integrating by parts, we obtain

$$R = \frac{1}{2} \rho U^2 \kappa^2 k\Psi \qquad (30)$$

We can choose the arbitrary constant k_1 so as to make k be zero. Then the wave resistance vanishes in the order of the approximation, i.e., it becomes as small as the higher order in the slender ship approximation.

The solution can be expressed in a dimensionless form like

$$A(x) = \frac{V}{2\ell} S(\xi) \qquad (31)$$

The optimum curve of sectional area obtained in this way is shown in Figure 3. In comparison with Figure 1, there is seen a remarkable difference near the ends. The form of the strut-like ship shows an infinite density of dipole at the ends while the slender ships shows a continuous curve meeting the base line. The concentration of the dipole at the ends will give some dog-bone shaped water lines; especially at high Froude numbers, but this is not the case for slender ships. The coefficient of fineness, the water plane coefficient for the strut-like ships and the prismatic coefficients for slender ships, is the reciprocal of the ordinate at the midship

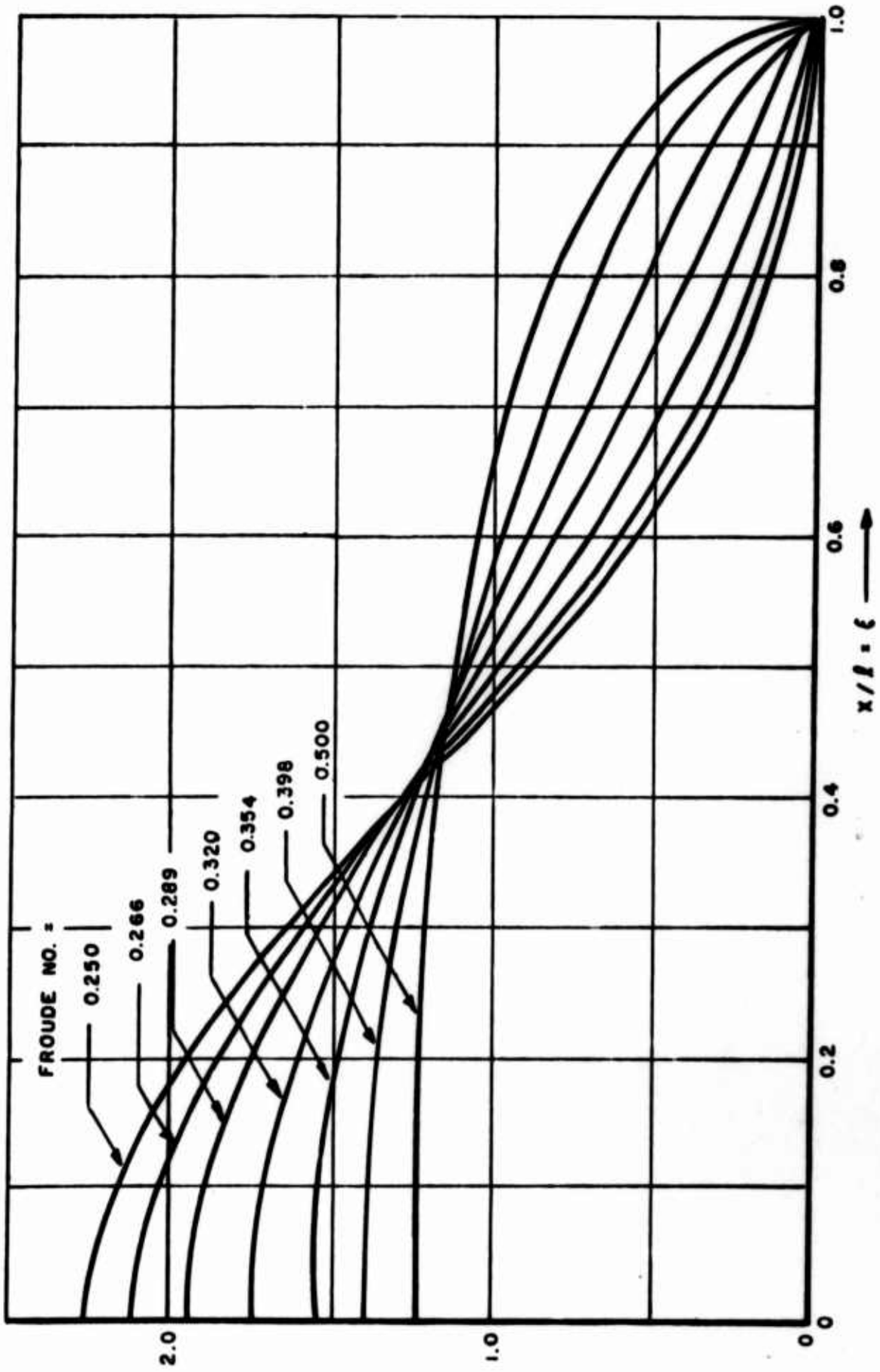


FIGURE 3. OPTIMUM CURVES OF SECTIONAL AREA FOR A SLENDER SHIP

section at x = 0. Figure 4 gives the optimum coefficient of fineness versus the Froude number for both strut-like ships and slender ships.

Resistance Measurement of Optimum Models

The theories given so far are devoted to a strut-like ship of infinite draft and also to a slender ship of small breadth and draft. They are approximations. It is necessary to verify the results by means of experiments. It is impossible to test ship models with infinite draft. At a speed which is not very high, however, the effect of the lower part of the ship model on the wave resistance is comparatively small. Accordingly, the optimum shape determined by the theory for the strut may be compared with measurements for a model whose draft is made as deep as possible. For the result of the theory of the slender ship, the beam draft ratio can be chosen to be an ordinary value. There is a difference between the waterline shape of the optimum strut and the sectional area of the slender ship for the optimum condition at the same Froude number. If we compare the curves at the same coefficient of fineness but to be optimum at different Froude numbers, the difference between them is small if the nose is rounded up as shown in Figure 2 for the case of infinite draft. Accordingly we do not need two sets of models but a set of models in accord with either the curves in Figure 2 or those in Figure 3. Figure 2 depicts the models chosen for the experiments.

Two series of experiments have been carried out, one of which concerns the deep draft case and the other the lesser draft case. There are restrictions as to the size and shape of the model imposed by the facility at the experimental tank. The length of the model should be long enough to secure a turbulent boundary layer, but it is restricted by the dimension of the tank to avoid side-wall effects on the wave resistance as well as a blockage effect. As the models are made of paraffin wax, there is a practical restriction upon the depth of the model imposed by the size of the model cutter. Under these circumstances the length of the models is determined to be 2 meters and the depth to be 0.35 meters. The breadth or the maximum beam is chosen so as to make

$$A_w/(2\ell)^2 = 0.08$$

The shape of water planes are those shown in Figure 2.

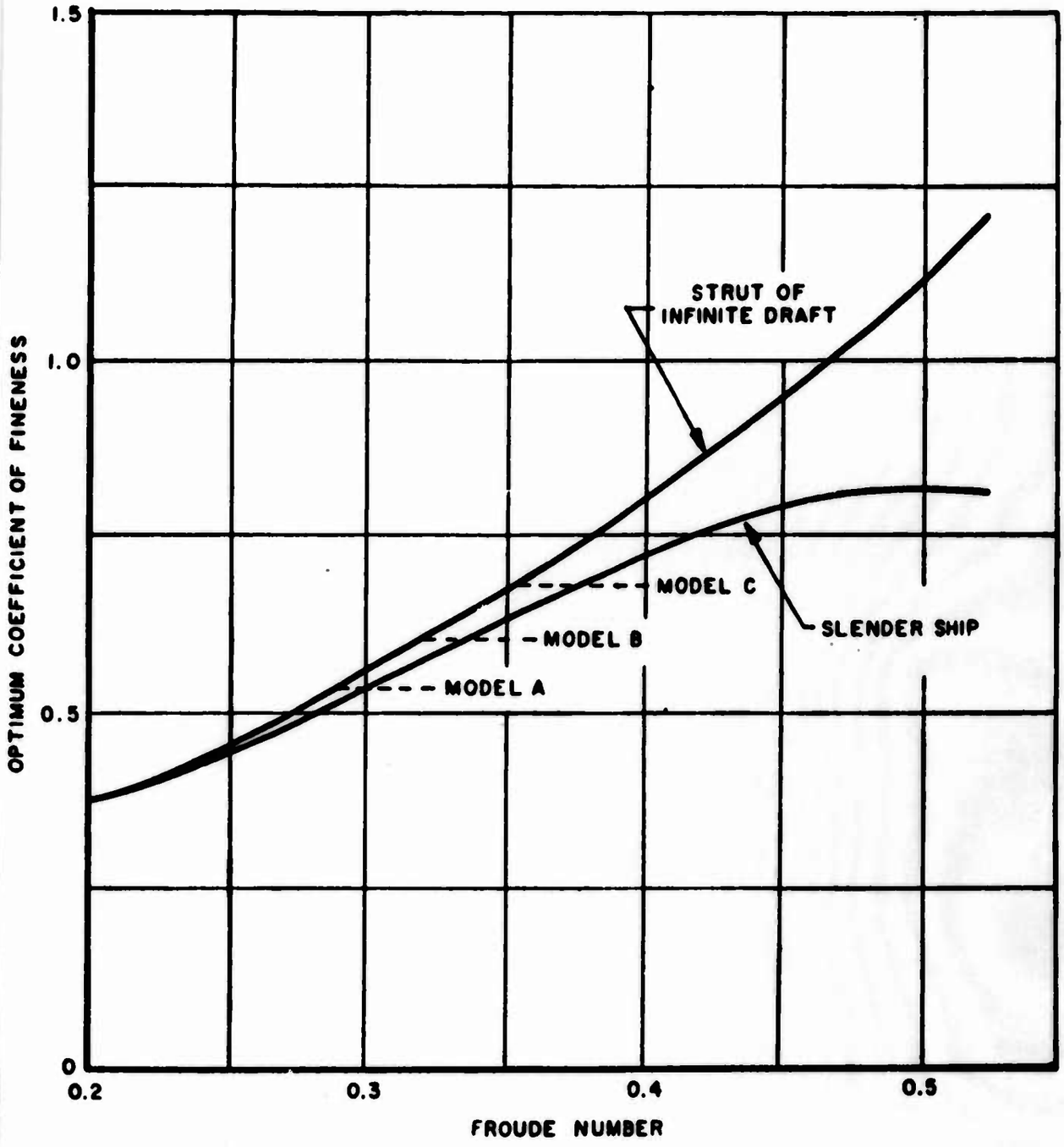


FIGURE 4. OPTIMUM VALUES OF THE COEFFICIENT OF FINENESS FOR STRUTS AND SLENDER SHIPS

The prismatic coefficients of the models tested are 0.537, 0.604 and 0.683, and their optimum Froude numbers are 0.289, 0.320 and 0.354 respectively when the draft is infinite. We call these models A, B and C. The maximum beams of the models are 0.298, 0.265 and 0.234 meters respectively. The draft for the heavy condition is chosen as 0.25 meters so as to secure sufficient freeboard and lateral stability, so that the length draft ratio is 8. The shapes of the frame lines are deduced from the simple equation

$$y = b\,[1 - (z/T)^{10}] \qquad (32)$$

Accordingly, the area coefficient is uniform throughout the cross section and is 0.909. The displacement volume is 0.0727 cubic meters for each model. The draft in the light condition which corresponds to the slender ship is half the deep draft, being 0.125 meters and the displacement volume is 0.0327 cubic meters. As the area coefficient is uniform, the prismatic coefficients are the same as the water plane coefficients. Pins are placed at square station No. 9 1/2 for turbulence stimulation and the total resistance is measured by the usual way.

Discussion of the Results

The skin friction coefficient, determined by the ITTC 1957 Model-Ship Correlation line, is subtracted from the measured total resistance expressed as a dimensionless coefficient to obtain the residuary resistance coefficients which are shown in Figure 5 for the deep draft versus model speed and Froude number. The Froude numbers at which each model shows the minimum wave resistance according to the theory are indicated by vertical lines. They must be the point of contact of the curves with their envelope. In the case of models B and C, the agreement between the theoretically predicted optima and the measured results is fairly good, but in the case of model A, a slight shift to the lower speed is noticed.

The reason for this shift may be explained in the following manner. The length beam ratio of model A is 6.72 and it is difficult to regard it as a thin ship. An effect, then, due to nonlinearity is inevitable. According to the calculation of the streamline of the two-dimensional flow with a dipole distribution in a uniform stream, the dipole strength must be augmented at the middle portion while it must be reduced near the ends, in order to obtain a given water line

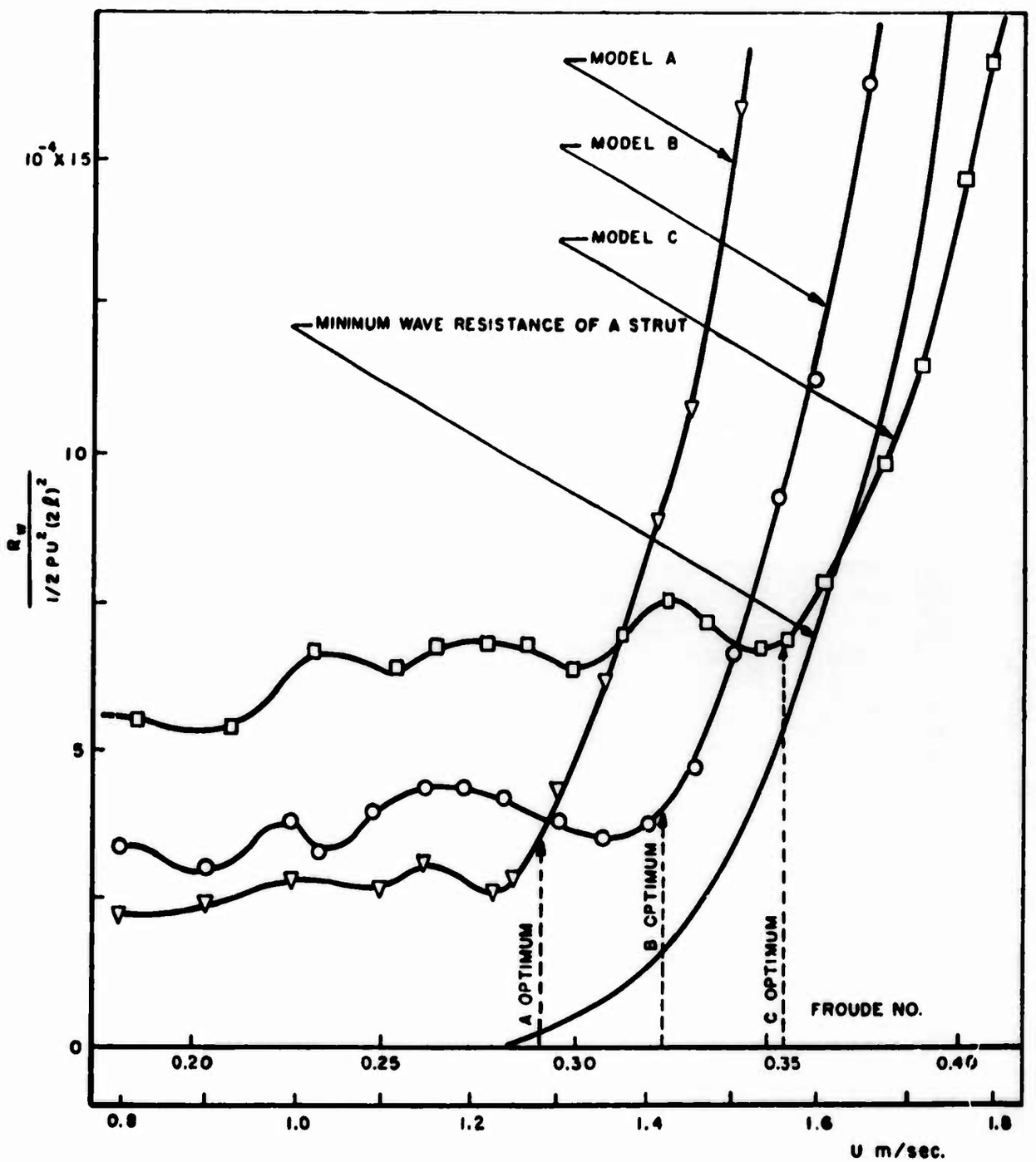


FIGURE 5. MEASURED WAVE RESISTANCE COEFFICIENT AT DEEP DRAFT

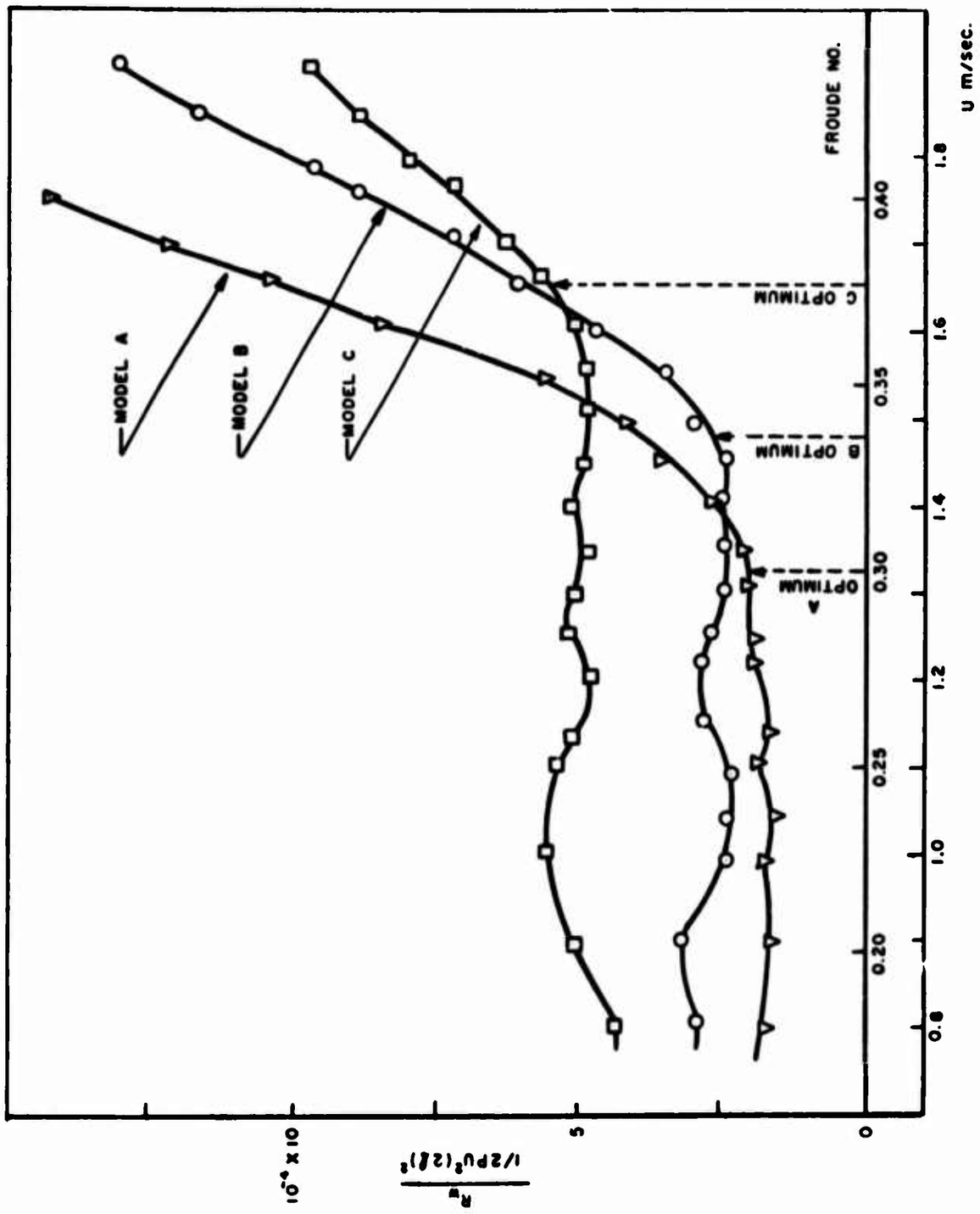


FIGURE 6. MEASURED WAVE RESISTANCE COEFFICIENT AT HALF DRAFT

or streamline form exactly. It is quite possible that the modified dipole distribution presents itself as optimum at a Froude number lower than that predicted by the thin ship theory.

There is a curve of minimum wave resistance shown in Figure 5. As it is determined for infinite draft, agreement with the measurement cannot be expected. The reason that the measured values are higher than the theoretical line seems to be the fact that the residuary resistance still involves an appreciable amount of the viscous resistance. It is difficult to determine the exact amount of the viscous resistance or, being the same thing, the wave resistance. If we tentatively adopt Hughes' method of form factor for the viscous resistance, the wave-resistance coefficient falls under the theoretically given minimum line, especially at high Froude numbers. This is obviously due to the effect of finite draft.

Next, the draft of the models was halved and the resistance is measured. Figure 6 gives the residuary resistance coefficient results. The optimum Froude numbers predicted by the slender ship theory are indicated by vertical lines. Agreement is good throughout the three models. Further improvement will be obtained by subtracting a viscous component from the residuary resistance of model C.

REFERENCES

1. Weinblum, G.: "Schiffe Geringsten Widerstandes," Proc. Third Internat. Congr. Appl. Mech. Stockholm, 1930.

2. Karman, Th. von: "Contributions to the Theory of Wave-Resistance," Proc. Fourth Internat. Congr. Appl. Mech. Cambridge, 1934.

3. Sretenskii, L. N.: "Sur un Probleme de Minumum Dan la Theorie du Navire," C. R. (Dokl) Acad. Sci. URSS (N.S.) 3 1935.

4. Wehausen, J. V.: "Wave Resistance of Thin Ships," Symposium on Naval Hydrodynamics," Washington, D. C. 1956.

5. Karp, S., Kotick, J. and Lurye, J.: "On the Problem of Minimum Wave Resistance for Struts and Strut-Like Dipole Distributions," Third Symp. on Naval Hydromechanics, Wageningen, 1960.

6. Bessho, M.: "On the Problem of the Minimum Wave-Making Resistance of Ships," Memoirs of the Defense Acad. 2-4, 1963.

7. Weinblum, G., Wustrau, D., and Vossers, G.: "Schiffe Geringsten Widerstandes," Jahlbuch, S.T.G. 51, 1957.

8. Dörr, J.: "Zwei Integralgleichungen erster Art, die sich mit Hilfe Mathieuscher Funktionen lösen lassen," Z.A.M.P. 3, 1952.

9. Columbia University, Tables Relating to Mathieu Function, 1951.

10. Vossers, G.: "Some Application of Slender Body Theory to Ship Hydrodynamics," Dissertation Delft, 1962.

11. Maruo, H.' "Calculation of the Wave Resistance of Ships, the Draught of Which is as Small as the Beam," Journal of Zosen Kiokai (Soc. of Naval Arch. of Japan), 112, 1962.

ON SHIPS WITH ZERO AND SMALL WAVE RESISTANCE

B. Yim

Office of Naval Research
Department of the Navy

INTRODUCTION

There are two ways of looking at the merits of a bulb on a ship. One is its effect on the interactions between the waves themselves and the other is its effect on the ship resistance itself as represented by these waves. Recently Inui, Takahei, and Kumano (1960) studied the bulbous bow ship from the former point of view by considering the bulb as a point doublet. They paid special attention to the 180° phase-difference between the bulb wave and the ship bow wave, and tried to make both amplitude functions the same in order to cancel out the wave. Wigley (1936) mentioned this wave phenomenon, but attacked the problem via the wave resistance approach. He derived six rules for the design of a bulb for a ship bow.

This later approach, involving the determination of the wave resistance directly, has been the conventional one used by most investigators. However, this generally leads to many cumbersome mathematical calculations. On the other hand, the method dealing with the interaction between the waves themselves can be simple and leads to a better physical insight. Using this approach, Takahei (1960) studied the "waveless bow" further and Kumano (1960) investigated the "waveless stern." They tried to match up the amplitude function of a doublet, which is a function of the doublet strength and the Froude number, as closely as possible with the amplitude function of a ship. However, it was not very clear how close the doublet distribution could be matched. It will be shown in this report that a doublet distribution whose amplitude function is exactly the same as that of the ship can be found but that it extends along a line from the free surface to infinite depth. With such a doublet distribution at the bow and stern the waves from the bow and stern of the given symmetric ship may be completely canceled and the ideal fluid wave resistance of the ship becomes zero. The semi infinite nature of the extension of the doublet distribution need not be a serious restriction since it will be shown that the effect of discarding that part of the doublet distribution extending from some finite depth to infinity can be made very small.

Further it is shown that a quadrupole distribution at the bow and the stern in addition to the doublet distribution offers practical advantages.

WAVES DUE TO A SHIP AND A BULB

As in the usual analysis, an inviscid, incompresible, and homogeneous fluid in steady flow with a free surface and of infinite depth is considered. The coordinate system O-xyz is right handed with origin on the mean free surface, x positive in the direction of the uniform flow velocity V , and z positive in the upward direction. In this report, except in the sections on two-dimensional streamlines the quantities x , y and other lengths except z are non-dimensionalized with respect to the ship length L ; z is non-dimensionalized with respect to the draft H , and m is non-dimensionalized with respect to V and LH . All equations are expressed in non-dimensional form. All wave height components are assumed to be small and additive.

It is well known that a point source of strength m located at a point $(x_1,0,-z_1)$, where $z_1 > 0$, produces a wave height non-dimensionalized with respect to L at large x given by (see Havelock, 1951),

$$\zeta_s = 8k_o \int_0^{\pi/2} m \exp(-k_o z_1 \sec^2\theta) \sec^3\theta \cos [k_1(x-x_1)\sec\theta] \times \cos (k_1 y \sin\theta \sec^2\theta)\, d\theta \qquad (1)$$

where

$$k_1 = \frac{Lg}{V^2} \quad \text{and} \quad k_o = \frac{Hg}{V^2} \ .$$

Hence, for a line distribution of sources at $y = 0$, $z = -z_1$, $0 \leq x_1 \leq 1$ represented by the series,

$$m(x_1) = \sum_{n=0}^{\infty} a_n x_1^n \qquad (2)$$

the wave height will be

$$\zeta_s = 8k_o \int_0^{\pi/2} \int_0^1 m(x_1) \exp(-k_o z_1 \sec^2\theta) \sec^3\theta \cos\{k_1(x-x_1)\sec\theta\}$$

$$X \cos(k_1 y \sin\theta \sec^2\theta)\, dx_1\, d\theta$$

$$= \frac{8k_o}{k_1^3} \int_0^{\pi/2} \exp(-k_o z_1 \sec^2\theta) \left[\sin(k_1 x \sec\theta) S_1(0) \right.$$

$$- \cos(k_1 x \sec\theta) S_2(0) - \sin\{k_1(x-1)\sec\theta\} S_1(1)$$

$$\left. + \cos\{k_1(x-1)\sec\theta\} S_2(1) \right] \cos(k_1 y \sin\theta \sec^2\theta)\, d\theta \qquad (3)$$

with

$$S_1(a) = \sum_{n=0}^{\infty} \frac{(-1)^n m^{(2n)}(a)}{(k_1 \sec\theta)^{2(n-1)}} \qquad (4)$$

$$S_2(a) = \sum_{n=0}^{\infty} \frac{(-1)^n m^{(2n+1)}(a)}{(k_1 \sec\theta)^{2n-1}} \qquad (5)$$

where

$$m^{(n)}(a) = \left(\frac{\partial^n m(x_1)}{\partial x_1^n} \right)_{x_1 = a}$$

If we put

$$\zeta_s = \zeta_{sB} + \zeta_{ss}$$

where

$$\zeta_{sB} = \frac{8k_o}{k_1^3} \int_0^{\pi/2} \exp(-k_o z_1 \sec^2\theta) [\sin(k_1 x \sec\theta) S_1(0)$$

$$- \cos(k_1 x \sec\theta) S_2(0)] \cos(k_1 y \sin\theta \sec^2\theta)\, d\theta, \qquad (6)$$

$$\zeta_{ss} = \frac{8k_o}{k_1^3} \int_o^{\pi/2} \exp(-k_o z_1 \sec^2\theta) \left[-\sin \{k_1(x-1)\sec\theta\} S_1(1) \right.$$

$$\left. + \cos \{k_1(x-1) \sec\theta\} S_2(1) \right] \cos (k_1 y \sin\theta \sec^2\theta)\, d\theta, \quad (7)$$

then ζ_{sB} can be interpreted as the wave from the bow and ζ_{ss} as the wave from the stern according to the idea of the elementary wave (see Havelock, 1934a). We can see that both ζ_{sB} and ζ_{ss} are, in general composed of sine and cosine elementary waves. Henceforth we will omit the word "elementary" except to avoid ambiguities. In the integrand of ζ_{sB} and ζ_{ss}, the coefficient of $\begin{matrix}\sin \\ \cos\end{matrix} (k_1 x \sec\theta) \cos (k_1 y \sin\theta \sec^2\theta)$ is called an amplitude function.

For a ship of a finite draft, ζ_s has only to be integrated from $z_1 = 0$ to $z_1 = 1$. In this case $S_i(a)$ may be a function of z_1.

We now consider a doublet of strength $-\mu$ nondimensionalized with respect to V and LH^2 located at $x = 0$, $y = 0$, $z = -z_1$. The nondimensional wave height due to this doublet, at large x, is (see Wigley, 1936)

$$\zeta_B = -8k_o^2 \int_o^{\pi/2} \mu \exp(-k_o z_1 \sec^2\theta) \sec^4\theta \sin(k_1 x \sec\theta)$$

$$X \cos (k_1 y \sin\theta \sec^2\theta)\, d\theta \quad (8)$$

where ζ_B is nondimensionalized with respect to L. Note that the sine waves originating from the origin have a negative sign in this case.

CONDITION OF NO WAVE RESISTANCE

We have seen from the previous section that the wave height due to a submerged body or a surface ship may be represented at large x by

$$\zeta = \int_o^{\pi/2} [A_1(\theta) \sin (k_1 x \sec\theta) + A_2(\theta) \cos (k_1 x \sec\theta)]$$

$$X \cos (k_1 y \sin\theta \sec^2\theta)\, d\theta \quad (9)$$

Havelock (1934b) showed that the nondimensionalized wave resistance represented by this wave system is

$$R = 32 \int_0^{\pi/2} \left(A_1^2(\theta) + A_2^2(\theta) \right) \cos^3\theta \, d\theta \qquad (10)$$

where R is related to the wave resistance R_o by $R = \dfrac{R_o}{\frac{\pi}{2}\rho L^2 V^2}$.

The integrand of this wave resistance integral is always positive. Hence, if there exists a ship whose wave resistance is zero, the necessary and sufficient condition for the no wave drag ship is

$$A_1(\theta) \equiv A_2(\theta) \equiv 0 , \qquad (11)$$

(i.e. no wave itself). Of course the trivial solution for this is the case of no singularity or of an infinitely thin frictionless flat plate parallel to the uniform stream, i.e. $\mu = 0$ and $m = 0$. However, there may be a non-trivial solution which makes $A_1(\theta) \equiv A_2(\theta) \equiv 0$ with the proper selection of the singularity distribution. Krein (1955) proved that there does not exist any finite ship whose Michell's resistance (the wave resistance represented by Michell's integral) becomes zero, but he cited a few examples of infinite convoys whose wave resistance is zero. In the next section we will find waveless solutions involving the appropriate combination of a doublet distribution with a source distribution. The basis for these is that while a positive sine wave usually starts from the bow of a ship without a bulb, a negative sine wave starts from a surface point directly above a bulb representable by a point doublet. This has been checked experimentally as well as theoretically by many investigators.

COMBINATION OF DOUBLET AND SOURCE DISTRIBUTION

The problem is therefore, how to find a doublet distribution for a given or otherwise determined proper source distribution in order to make the total wave amplitude function zero; i.e. find the doublet distribution $\mu(x_1,z_1)$ on the longitudinal center plane such that for a given source distribution $m(x_1,z_1)$ on the same plane

$$k_o \int_{-\infty}^{\infty}\int_{-\infty}^{\infty} m(x_1,z_1) \exp(-k_o z_1 \sec^2\theta)\sec^3\theta \cos\left[k_1(x-x_1)\sec\theta\right] dx_1 dz_1$$

$$-k_o^2 \int_{-\infty}^{\infty}\int_{-\infty}^{\infty} \mu(x_1 z_1) \exp(-k_o z_1 \sec^2\theta)\sec^4\theta \sin\left[k_1(x-x_1)\sec\theta\right] dx_1 dz_1 \equiv 0 \qquad (12)$$

Let us consider the simplest case first; vis., a uniform source distribution on the line $0 \leq x_1$, $y_1 = 0$, $z_1 = f$. To a first approximation this represents a semi-infinite paraboloid and is equivalent to the case of $n = 0$ in Equation (2). Then the contribution to the wave from the bow is from Equation (6)

$$\zeta_{sB} = \frac{8k_o}{k_1} \int_o^{\pi/2} a_o \exp(-k_o f_1 \sec^2\theta) \sec^2\theta \sin (k_1 x \sec \theta)$$

$$X \cos (k_1 y \sin \theta \sec^2\theta)\, d\theta \qquad (13)$$

Now this can be matched by a uniform doublet distribution b_o on a vertical line $x = 0$, $y = 0$, $f < z_1 < \infty$. Then the corresponding wave height will be, by an integration of (8) with respect to z_1 from f to ∞ ,

$$\zeta_B = - 8k_o \int_o^{\pi/2} b_o \exp(-k_o f_1 \sec^2\theta) \sec^2\theta \sin (k_1 x \sec \theta)$$

$$X \cos (k_1 y \sin \theta \sec^2\theta)\, d\theta \qquad (14)$$

From Equations (13) and (14) we now see that

$$\zeta = \zeta_{sB} + \zeta_B = 0$$

if

$$b_o = \frac{a_o}{k_1} \quad .$$

Thus according to this result the waves from the point on the surface above the nose of a submerged semi-infinite paraboloid will be completely cancelled by a vertical circular cylinder extending from the nose of the paraboloid to infinite depth. This is the fundamental idea of how the wave amplitude function can be made equal to zero.

Let us now consider a little more general case of Equation (6); e.g., an axially symmetric body. However, the source distribution of Equation (2), which is an ordinary power series, is not the proper one to use for the doublet distribution because this will produce cosine terms, according to Equations (6) and (7) as well as sine terms, while our expression for the waves due to the doublet distribution at

$x = 0$ gives only sine terms. Since there is no easy way to make the amplitude function of the cosine terms $A_2(\theta)$ of Equations (9) and (10) equal to zero by combination with a doublet distribution, one thing to do is to employ source distributions which do not give cosine terms. The other idea is to consider a different singularity distribution which produces cosine waves as well as sine waves to cancel ship waves. This will be discussed later.

With reference to Equations (2), (8), (5), and (6), we note that $m^{(o)}(0) = a_o\ m^{(1)}(0) = 2!a_2$----$m^{(2n)}(0) = (2n)!a_{2n}$ and

$$m^{(1)}(0) = a_1 \ldots\ldots m^{(2n+1)}(0) = (2n+1)!\ a_{2n+1} \qquad (15)$$

i.e., $S_1(0)$ is related to only the even powers of the series (2) while $S_2(0)$ is related to only the odd powers of the series. The amplitude function of the sine terms in Equation (6) is

$$\frac{8k_o}{k_1^3} \quad \exp(-k_o z \sec^2\theta)\ S_1(0)\ ,$$

and that of the cosine terms,

$$\frac{8k_o}{k_1^3} \quad \exp(-k_o z \sec^2\theta)\ S_2(0)\ .$$

We now see that a source distribution given by an even power series does not produce cosine terms. According to Weierstrass' approximation theorem, any continuous curve can be approximated by a polynomial in the domain $0 \leq x \leq 1$. If we consider another curve in $-1 \leq x \leq 0$, symmetric with respect to the first about $x = 0$ the polynomial which represents the whole curve in $-1 \leq x \leq 1$ must be an even power series. Hence we may say any curve in $0 \leq x \leq 1$ can be approximated by a polynomial of even powers in the domain. Equation (2) may therefore be written

$$m(x_1) = \sum_{n=0}^{\infty} a_{2n}\ x_1^{2n}\ . \qquad (16)$$

If we assume that our ship is symmetric about its midsection at $x = 0.5$ then $m(x_1)$ is odd with respect to this point or

$$m(0) = -m(1),\ m'(0) = +m'(1)$$

$$\text{-----} m^{(n)}(0) = (-1)^{n+1} m^{(n)}(1) \tag{17}$$

Since from Equation (16) $m^{(2n+1)}(0) = 0$, from Equation (17) $m^{(2n+1)}(1) = 0$. Hence from Equation (5) $S_2(0) = S_2(1) = 0$.

Similarly from Equations (17) and (4) we can easily see

$$S_1(0) = -S_1(1)$$

Then from Equations (6) and (17), we see that the amplitude functions of ζ_{sB} and ζ_{ss} are exactly the same and both are sine waves.

When the body is not symmetric fore and aft with respect to the midsection, the wave from the stern can be treated separately in a similar manner by changing coordinates. If we take the origin at the stern, and express the source distribution for the body by an even power series, the wave system from the stern can be analyzed in exactly the same way as for the bow.

Therefore the solution to the zero wave drag problem for ζ_{ss} can be treated exactly in the same manner as that for ζ_{sB}.

We now consider only ζ_{sB} of Equation (6) corresponding to the source distribution of Equation (16) along $z_1 = f_1$, $y = 0$,

$$\zeta_{sB} = \frac{8k_o}{k_1^3} \int_0^{\pi/2} \exp(-k_o f_1 \sec^2\theta) \sum_{n=0}^{\infty} \frac{(-1)^n (2n)! a_{2n}}{(k_1 \sec\theta)^{2(n-1)}} \sin(k_1 x \sec\theta)$$

$$X \cos(k_1 y \sin\theta \sec^2\theta)\, d\theta \tag{18}$$

The terms for large n's become very small for the usual range of Froude numbers, and in practice we have only to consider just a few terms of the series given by Equation (16) (see appendix). In order to find the corresponding doublet distribution which cancels the wave height ζ_{sB}, let $\mu(z_1)$ the doublet strength per unit length be expressed as

$$\mu(z_1) = \sum_{n=0}^{\infty} b_n (z_1 - f)^n \equiv \sum_{n=0}^{\infty} b_n \eta^n \tag{19}$$

on the line $x = y = 0$, $f \leq z_1 < \infty$. Thus for $f \leq z_1 \leq f_1$,

$$\zeta_{BF} = -8k_o^2 \int_0^{\pi/2} \int_0^{f_1-f} \sum_{n=0}^{\infty} b_n \eta^n \sec^4\theta \exp[-k_o(\eta+f)\sec^2\theta$$

$$X \sin(k_1 x \sec\theta) \cos(k_1 y \sin\theta \sec^2\theta)\, d\eta\, d\theta$$

$$= -8 \int_0^{\pi/2} \sum_{n=0}^{\infty} \frac{b_n n!}{k_o^{n-1} \sec^{2(n-1)}\theta} [\exp(-k_o f \sec^2\theta) - \exp(-k_o f \sec^2\theta)$$

$$X \sum_{n=0}^{\infty} \frac{k_o^m \sec^{2m}\theta (f_1-f)^m}{m!}] \sin(k_1 x \sec\theta)\cos(k_1 y \sin\theta \sec^2\theta) d\theta \qquad (20a)$$

The value of the second term for $f_1 \to \infty$ vanishes (see Appendix). Thus, for $f_1 \to \infty$,

$$\zeta_B = -8 \int_0^{\pi/2} \exp(-k_o f \sec^2\theta) \sum_{n=0}^{\infty} \frac{n! b_n}{k_o^{n-1} \sec^{2(n-1)}\theta} \sin(k_1 x \sec\theta)$$

$$X \cos(k_1 y \sin\theta \sec^2\theta(d\theta \qquad (20b)$$

If we compare Equations (18) and (20b) we obtain

$$b_n = (-1)^n \frac{(2n)!}{n!} \frac{k_o^n}{k_1^{2n+1}} a_{2n} \qquad (21)$$

as the condition that the regular waves given by Equation (18) be exactly cancelled out by those given by Equation (20b). The doublet distributions (19) located at $x = 0$ and extending from $z_1 = f$ to $z_1 = \infty$ generate a wave system which for an ideal fluid cancels completely the bow wave system due to any given source distribution (Equation (16)). In a similar manner as mentioned before, the stern wave system can be completely eliminated.

For the surface ship, we have only to consider, $m(x_1)$ of Equation (16) as the source strength per unit area on the center plane $y = 0$, for $0 \leq z_1 \leq 1$, $0 \leq x \leq 1$. If we integrate both (18) and (20) with respect to f from $f = 0$ to $f = 1$, we obtain the corresponding amplitude functions

$$A(\theta) \equiv \frac{8k_o}{k_1^3} \int_o^1 \exp(-k_o f \sec^2\theta) \sum_{n=0}^{\infty} \frac{(-1)^n (2n)! a_{2n}}{(k_1 \sec\theta)^{2(n-1)}} \, df \,, \tag{22a}$$

and

$$B(\theta) \equiv 8 \int_o^1 \exp(-k_o f \sec^2\theta) \sum_{n=0}^{\infty} \frac{n! b_n}{k_o^{n-1} \sec^{2(n-1)}\theta} \, df \tag{22b}$$

If Equation (21) holds for all depths f we then get

$$A(\theta) - B(\theta) \equiv 0 \,.$$

Thus for any vertical distribution of sources, Equations (19) and (21) will give the required bow and stern bulb shape to completely cancel the ship waves.

It should be emphasized that the b_n in Equation (22) is no longer exactly the same as that obtained in the expansion of the doublet $\mu(z_1)$ in Equation (19). From Equations (22), (19) and (20) the doublet strength per unit depth is now

$$\mu(z_1) = \int_o^{z_1} \sum_{n=0}^{\infty} b_n (z_1 - \zeta)^n \, d\zeta$$

in the domain $0 \leq z_1 \leq 1$, and (23a)

$$\mu(z_1) = \int_o^1 \sum_{n=0}^{\infty} b_n (z_1 - \zeta)^n \, d\zeta \text{ for } z_1 \geq 1.$$

For the case in which the source strength does not vary with depth

$$b_n = \text{const}$$

and

$$\frac{d\mu(z_1)}{dz_1} = \sum_{n=0}^{\infty} b_n z_1^n$$

or

$$\mu(z_1) = \sum_{n=0}^{\infty} \frac{b_n z_1^{n+1}}{n+1} \quad \text{for } 0 \leq z_1 \leq 1$$

and (23b)

$$\mu(z_1) = \sum_{n=0}^{\infty} \frac{b_n}{n+1} \left[z_1^{n+1} - (z_1 - 1)^{n+1} \right] \quad \text{for } z_1 \geq 1$$

Equations (23b) show that the slope of the doublet distribution along the $x = 0$, $y = 0$ has a discontinuity at $z_1 = 1$. Especially if we consider the one term $n = 0$ (which is an important term for the practical range of Froude numbers (see Appendix)) the bulb shape may be similar to a round pointed pencil.

In summary, we have shown how $A_1(\theta)$ and $A_2(\theta)$ of Equation (9) can be made identically zero. Thus a means of satisfying the necessary and sufficient condition for a zero wave drag ship in an ideal fluid has been obtained. Unfortunately this requires the use of bulbs of infinite draft. In a later section we will consider the effect of cutting off the doublet distribution (or bulb) at some finite depth.

QUADRUPOLE DISTRIBUTIONS

We have represented the ship shape in the preceding by an infinite even power series (16). However, the series may not converge too rapidly, and for the higher Froude numbers, which we may wish to consider, the higher order terms in the series (16), can not be neglected. Suppose we have an arbitrarily specified polynomial of finite terms which represents the source distribution on the center plane (see Weinblum, 1950). Then we have to consider the odd power terms in Equation (2) and thus the cosine wave system occurs as well as the sine wave system in Equation (6) and (7), starting at the bow and the stern. We therefore have to consider some means of cancelling cosine waves.

A point doublet is a one step higher order singularity than a point source; the wave or the flow field due to a doublet is therefore represented by a derivative of that due to a source with respect to the

position of the source (same as the position of the doublet) in the direction of the doublet (see Milne-Thomson). It is well known that a submerged point source produces positive cosine waves (see Equation (1)). Therefore, the negative sine wave can be produced by a negative doublet which produces a closed body in the uniform stream.

Now we consider a one step higher order singularity than a doublet which is called a quadrupole. That is, we consider two doublets of opposite signs, with the magnitude of each strength μ, and the distance between them, a, nondimensionalized with respect to H. Along the same idea of forming a doublet by a source and a sink (see Milne-Thomson 1955), we form a quadrupole by making

$$\lim_{a \to 0} a\mu = \text{finite constant, say, } \lambda \tag{24}$$

which is the strength of the quadrupole. Its waves will be the derivative of the wave height due to a point doublet with respect to the position of the doublet in the direction of the quadrupole, namely cosine waves. The sign of the waves will depend on the sign (direction) of the quadrupole. That is, a point quadrupole with the strength λ_o at $x = 0$, $y = 0$, $z = -z_1$ in the uniform flow V generates the wave height

$$\zeta_q = -8k_o^3 \int_0^{\pi/2} \lambda \exp(-k_o z_1 \sec^2\theta) \sec^5\theta \cos(k_1 x \sec\theta)$$

$$X \cos(k_1 y \sin\theta \sec^2\theta)\, d\theta \tag{25}$$

where $\lambda = \lambda_o/(H^3 L V)$

There are two great features of the quadrupole which will be mentioned in the following sections. One is the same feature which the doublet distribution had with respect to the even power terms of the ship source distribution, but in this case with respect to the odd terms. The other is the composition of a point singularity which produces no wave - say, a no-wave-singularity.

COMBINATION OF QUADRUPOLE AND SOURCE DISTRIBUTIONS

We have mentioned that the odd power terms of the ship source distribution (2) produce cosine waves and that the quadrupole also produces cosine waves. Otherwise, both amplitude functions have similar qualities to those of the even power terms of Expression (2) and for the doublet. Namely, if we consider the odd power terms of Expression (2) say

$$m = a_{2n+1} x_1^{2n+1}, \quad \text{in} \quad \begin{matrix} 0 \le x_1 < 1, \\ 0 \le z_1 \le f, \end{matrix} \tag{26}$$

then the wave due to this source distribution starting from the bow $x = 0$ is from Equation (6)

$$\zeta = -8 \int_0^{\pi/2} a_{2n+1} [1-\exp(-k_o \sec^2\theta)](-1)^n (2n+1)! \; X$$

$$X \; k_1^{-2(n+1)} \cos^{2n+1}\theta \cos(k_1 x \sec\theta) \cos(k_1 y \sin\theta \sec^2\theta) d\theta \tag{27}$$

In exactly similar manner as in matching the doublet distribution to the even power terms of the ship source distribution in order to cancel the bow waves, the corresponding quadrupole distribution may be put as in Equation (23b)

$$\lambda = b_{n+1} \frac{z_1^{n+2}}{n+2} \qquad \text{in } 0 \le z_1 \le 1 \tag{28}$$

$$\lambda = b_{n+1} \frac{[z_1^{n+2} - (z_1-1)^{n+2}]}{n+2} \qquad \text{in } 1 \le z_1 \le \infty \tag{29}$$

then from Equation (25), the wave due to this quadrupole becomes

$$\zeta_q = -8k_1 \int_0^{\pi/2} b_{n+1} \; 1-\exp(-k_o \sec^2\theta) \; (n+1)! \; k_o^{n-1} \; X$$

$$X \cos^{2n+1}\theta \cos(k_1 x \sec\theta) \cos(k_1 y \sin\theta \sec^2\theta) d\theta \tag{30}$$

Hence, if we make

$$b_{n+1} = \frac{(-1)^{n+1} k_o^{n+1} (2n+1)!}{(n+1)! k_1^{2n+3}} \tag{31}$$

the wave due to the odd power term of the source distribution will be completely cancelled. The above argument holds for any integer n. The stern waves due to the terms of odd power in the source distribution can be dealt with exactly in the same manner as those of the bow.

In general, the bow waves have stronger sine components than cosine components, the former depending mostly on the entrance angle of the ship bow. Therefore, the doublet distribution is more important than that of the quadrupole. In fact, this is the reason, which will be shown later, that the combination in practice of optimum distributions of doublets and quadrupoles can produce a closed body, although the quadrupole itself can not.

NO-WAVE-SINGULARITY

By Krein's proof (1955) we know that there exists no singularity distribution which produces a finite closed body and yet produces no wave. However, it would be very useful if we knew of some singularity which by itself may not produce a closed body produced by another singularity distribution when both are combined together, and which in combining produces no additional wave resistance. Krein (1955) first found such a special function $h(x,z)$ which consists of an arbitrary nice function $\phi(x,z)$ of x,z,

$$\frac{\partial^2 \phi}{\partial x^2} + k_o \frac{\partial \phi}{\partial z} \equiv h(x,z) \tag{32}$$

with boundary conditions

$$\phi = \frac{\partial \phi}{\partial x} = 0 \tag{34}$$

on the boundary of the domain of the singularity distribution on the center plane of a ship. He proved that the Michell's wave resistance due to a ship surface $f(x,z)$ is exactly the same as that due to a

ship surface $f(x,z) + h(x,z)$. That is, there are infinitely many ship body forms which have the same resistance and volume.

Here we will see that if we use a point quadrupole in the x direction and a point doublet in the z direction at the same point, the combined singularity will not produce any wave in far downstream. The wave height due to a doublet in the z direction at the point $(0,0,z_1)$ is

$$\zeta_d = 8k_o^2 \int_0^{\pi/2} \mu \exp(-k_o z_1 \sec^2\theta)\sec^5\theta \cos(k_1 x \sec\theta) \, X$$

$$X \cos(k_1 y \sin\theta \sec^2\theta) \, d\theta \qquad (35)$$

Hence if we compare Equation (25) with Equation (35) it will be easily seen that

$$\zeta_d + \zeta_q = 0 \qquad (36)$$

for

$$k_o \lambda = \mu \qquad (37)$$

Since this is a point singularity and it does not produce any wave, it can be distributed in an arbitrary manner anywhere on top of the ship singularity distribution without changing the original ship wave resistance.

In fact, it can be shown that if this no-wave-singularity is distributed continuously, this will be in effect the same as Krein's form. Besides, by differentiating both wave heights ζ_d and ζ_q by the same parameter we may be able to construct innumerable higher order no-wave-singularities. Therefore in this report we will call the aforesaid no-wave-singularity as that of the first order.

BODY STREAMLINE SHAPE DUE TO COMBINATION OF SINGULARITIES IN THE UNIFORM FLOW

Now to utilize the quadrupole in practice we have to investigate the way in which it produces bodies when combined with other singularities in the uniform stream.

To be more general, we may further have to consider the discontinuity (shoulder) in the tangent of the waterlines. Then not only the negative doublet but also the positive doublet at the slope discontinuity may be needed to cancel the negative sine waves.

In the following subsections we will consider body shapes which may be produced by combinations of various singularities which may be utilized in improving ship shapes in order to decrease their wave resistance.

The streamlines produced by the three dimensional singularities in the uniform flow may be obtained by solving the streamline equations

$$\frac{dx}{u} = \frac{dy}{v} = \frac{dz}{w} \tag{38}$$

where

$$u = -\frac{\partial \phi}{\partial x} + V \ , \ v = -\frac{\partial \phi}{\partial y} \ , \ w = -\frac{\partial \phi}{\partial z} \tag{39}$$

represented by distributions of singularities. This could be solved by Runge-Kutta-Gills (Gill, 1951) numerical method. However, the exact form of ϕ due to the singularity under the free surface even under the assumption of the linear boundary conditions is so complicated, that it becomes practically very advantageous to relate the exact shape of the ship to the source distribution, on the assumption of zero Froude number. For example, Inui (1957) used this approximation (double model); he verified the sufficient validity of his method for moderate Froude numbers by comparing theory and his experiments. This method could be used here to find the relation between singularity distributions and ship shapes, as in the case of ships with no-wave singularities and with bulbs made of doublets and quadrupoles. However, considerable insight is gained with much greater simplicity by considering only special simple cases, as the two-dimensional case for instance. Herein we discuss the problem using dimensional quantities unless specified.

Two-Dimensional Doublet and Quadrupole

The complex potential due to a doublet with the strength $-\mu < 0$ and a quadurpole with its strength $\lambda > 0$, with both directions parallel to the x axis, in a uniform flow is

$$w = \phi + i\psi = -Vz - \frac{\mu}{z} + \frac{\lambda}{z^2} \tag{40}$$

where

$$z = x + iy$$

Hence the stream function is

$$\psi = - Vy + \frac{\mu y}{x^2+y^2} - \frac{2\lambda xy}{(x^2+y^2)^2}$$

$$= \frac{-y}{x^2+y^2} \left[V (x^2+y^2) - \mu + \frac{2\lambda x}{x^2+y^2} \right] \qquad (41)$$

If we use polar coordinates

$$x = r \cos \theta, \quad y = r \sin \theta$$

we can easily see that the dividing streamline is

$$y = 0$$

and

$$r^2 = \frac{\mu}{V} - 2 \frac{\lambda}{V} \frac{\cos \theta}{r} \qquad (42)$$

This means that the body is deformed from the sphere

$$r^2 = \frac{\mu}{V} \qquad (43)$$

extending (or shrinking) r by an approximate amount of $\frac{2\lambda}{rV} \cos \theta$ in each direction. In order to have a closed body such that all streamlines inside the surface streamline are wholly contained, the magnitude of λ should not be too large. To obtain the limiting value of λ, we have only to consider the point $\theta = 0$. We put

$$f(r) = r^3 - r \frac{\mu}{V} + \frac{2\lambda}{V} \qquad (44)$$

and notice $f(r) = 2 \frac{\lambda}{V} > 0$ when both $\gamma = 0$ and $\gamma = \sqrt{\frac{\mu}{V}}$. And

$$f'(r) = 0 \text{ at } r = \sqrt{\frac{\mu}{3V}}$$

Hence if

$$f\left(\sqrt{\frac{\mu}{3V}} \right) = - \sqrt{\frac{\mu}{3U}} \left(\frac{2\mu}{3V}\right) + \frac{2\lambda}{V} \leq 0$$

or

$$\frac{\lambda}{V} \leq \left(\frac{\mu}{3V}\right)^{\frac{3}{2}} \tag{45}$$

there exist two roots of $f(r) = 0$ in $0 \leq r \leq \sqrt{\frac{\mu}{U}}$. That is, when λ becomes large from $\lambda = 0$ within the limit of the inequality (45), Equation (44) represents two separate closed streamlines such that one is inside the other (see Figure 5a). If λ becomes larger than $\left(\frac{\mu}{3V}\right)^{3/2}$, the inner streamlines which were inside the inner closed streamline when $\frac{\lambda}{V} < \left(\frac{\mu}{3V}\right)^{3/2}$, pop out and there will be only one closed streamline (see Figure 5b). Therefore λ should satisfy the inequality (45) in order that a meaningful body exist. Figures 6 and 7 show examples of the dividing streamlines. When λ is negative the body form will be reversed along the x axis, and the condition on the magnitude of λ and μ is exactly the same as in the previous case.

A Simple Source and a Doublet in a Uniform Stream

Consider a point doublet with the strength $\mu > 0$ at $z = x + iy = 0$ combined with a point source with its strength $m>o$ at $z = z_o$. Then the complex potential W will be written

$$w = - Vz - m \log (z-z_o) + \frac{\mu}{z} \tag{46}$$

The stream function is

$$\psi = - Vy - m \tan^{-1} \frac{y-y_o}{x-x_o} - \frac{\mu y}{x^2+y^2} \tag{47}$$

By

$$x = r \cos \theta, \quad y = \sin \theta$$

$$\psi = - Vr \sin \theta - m\theta_1 - \frac{\mu \sin \theta}{r} \tag{48}$$

where

$$\theta_1 = \text{arc tan} \left(\frac{y-y_o}{x-x_o} \right)$$

Hence the body streamline is obtained by putting $\psi = -m\pi$. Nondimensionalizing Equation (48) by $Vh \equiv m\pi$

$$\bar{r}^2 \sin \theta + \bar{r} \, (\theta_1/\pi - 1) + \bar{\mu} \sin \theta = 0$$

The streamline due to a source in the uniform flow is well known (see e.g. Milne-Thomson, 1955 p. 199). The combination of source and a positive doublet produces a neck. The strength of the doublet should satisfy

$$\bar{\mu} \equiv \frac{\mu}{Vh^2} < \frac{1}{4} \tag{50}$$

in order for the body streamline to make physical sense. The dividing streamline is plotted in Figure 8 as an example, for a special value of μ .

A SIMPLE SOURCE AND A NO-WAVE-SINGULARITY OF THE FIRST ORDER IN A UNIFORM STREAM

We consider the no-wave-singularity, a quadrupole in the x direction with strength λ and a point doublet in the z direction with the strength μ , both located at the origin, and a point source at z_o in two dimensions. The complex potential due to these singularities is

$$w = \phi \; W \; i\psi = - Vz + i \frac{\mu}{z} + \frac{\lambda}{z^2} - m \log (z-z_o) \tag{51}$$

Hence the stream function is

$$\psi = - Vy + \frac{\mu x}{x^2+y^2} - \frac{2\lambda xy}{(x^2+y^2)^2} - m \tan^{-1} \frac{y-y_o}{x-x_o} \tag{52}$$

Since the no-wave-singularity does not produce any extra fluid, $\psi = - m\pi$ which is the dividing streamline for the half body due to a simple source in the uniform stream will still be the dividing streamline in this case.

If we nondimensionalize ψ by hV where $h = \frac{m\pi}{V}$ is the radius of the half body due to a point source, the dividing streamline can be written as

$$-1 = -\bar{y} - \frac{\theta_1}{\pi} + \frac{\bar{x}\,\bar{\mu}}{(\bar{x}^2+\bar{y}^2)^2} \left[x^{-2} + \left(\bar{y} - \frac{\bar{\lambda}}{\bar{\mu}} \right)^2 - \left(\frac{\bar{\lambda}}{\bar{\mu}}\right)^2 \right] \tag{53}$$

where

$$\bar{y} = y/h, \; \bar{x} = x/h, \; \bar{\mu} = \mu/(Vh^2), \; \bar{\lambda} = \lambda/(Vh^3), \; \theta_1 = \tan \frac{-1y-y_o}{x - x_o} .$$

Although it is very hard to see the exact shape of the dividing streamline without plotting x and y of Equation (53) it may be easy to see just how the original half body streamline is distorted by the no wave singularity. The last term in Equation (53) is positive inside the circle $K\left\{\text{ center at } (0, \frac{\bar{\lambda}}{\bar{\mu}}); \text{ radius, } \frac{\bar{\lambda}}{\bar{\mu}}\right\}$ and $\bar{x} < 0$, and outside the circle K and $\bar{x} > 0$; and negative inside the circle K and $\bar{x} > 0$, and outside K and $\bar{x} < 0$. When $\bar{x}^2+\bar{y}^2 \gg 1$ the distortion of the original dividing streamline is small. The distorted streamline will be of the shape shown in Figure 9. The no-wave-singularity has from Equation (37) the property of

$$\frac{\bar{\lambda}}{\bar{\mu}} = \frac{V^2}{gh} \equiv \frac{1}{k_h} \equiv F_h^{\,2}$$

For $L<6h$ and $F_L>0.3$, $\bar{\lambda}/\bar{\mu} > 0.5$. Hence, for the moderate F_L, the circle K may cut the upper dividing streamline but not the lower one and there are two wiggles in the upper dividing streamline and only one wiggle at lower one as in Figure 9.

FINITE DOUBLET DISTRIBUTION

Submerged Axisymmetric Body with Fore and Aft Symmetry

In order to determine the effect of limiting the doublet distribution to a finite depth we examing the difference between the expressions for ζ_{BF} as given by Equation (20a) with that for ζ_B of Equation (20b).

$$\zeta_R = 8\int_0^{\pi/2} \exp(-k_o f_1 \sec^2\theta) \sum_{n=0}^{\infty} \frac{b_n n!}{k_o^{n-1} \sec^{2(n-1)}\theta} \sum_{m=0}^{n} \frac{k_o^m \sec^{2m}\theta (f_1-f)^m}{m!}$$

$$X \sin(k_1 x \sec\theta)\cos(k_1 y \sin\theta \sec^2\theta)\, d\theta \qquad (54a)$$

This is the uncancelled wave system resulting from cutting off the doublet distribution at depth f_1. Thus instead of each term of the series in $\zeta_B + \zeta_{SB}$ being zero there will be a remainder,

$$\zeta_{Rn} = \int_0^{\pi/2} \exp(-k_o f_1 \sec^2\theta) \frac{b_n n!}{k_o^{n-1} \sec^{2(n-1)}\theta} \sum_{m=0}^{n} \frac{k_o^m \sec^{2m}\theta (f_1-f)^m}{m!}$$

$$X \sin(k_1 x \sec\theta)\cos(k_1 y \sin\theta \sec^2\theta)\, d\theta \qquad (54b)$$

The magnitude of ζ_{Rn} can be easily estimated as

$$\zeta_{Rn} < 8 \exp(-k_o f_1) \frac{b_n n!}{k_o^{n-1}} \sum_{m=0}^{n} \frac{k_o^m (f_1-f)^m}{m!}$$

e.g. $$|\zeta_{Ro}| < 8 \exp(-k_o f_1) \qquad (54c)$$

$$|\zeta_{R1}| < 8 \exp(-k_o f_1 b_1 \{1 + k_o(f_1-f)\} \text{ etc.}$$

For the usual range of Froude numbers, ζ_{Ro} is the dominant term (see Appendix). This decreases exponentially with increasing $k_o f_1$. Although for increasing n, ζ_{Rn} decreases more slowly with increasing $k_o f_1$, its magnitude becomes increasingly smaller than ζ_{Ro}. Therefore, even if the wave amplitude is not completely cancelled out the doublet distribution still has a substantially favorable effect on each term.

Ship with Fore and Aft Symmetry

For a finite draft ship whose source distribution is independent of z, Equations (20), (21) and (22b) give for the wave height at large x due to the infintiely deep doublet distribution alone

$$\zeta_B = -8 \int_0^{\pi/2} (1 - \exp(-k_o \sec^2\theta) \sum_{n=0}^{\infty} \frac{n!\, b_n}{k_o^n \sec^{2n}\theta} \sin(k_1 x \sec\theta)$$

$$\times \cos(k_1 y \sin\theta \sec^2\theta)\, d\theta \qquad (56a)$$

Equation (56a), of course, also represents the negative of the wave system due to the ship bow where b_n is obtained from Equation (21).

If we omit the doublet distribution from the point $z_1 = f_1 > 1$ to $z_1 = \infty$, we obtain the uncancelled wave height due to this by integrating the second term in Equation (20a) with respect to f from 0 to 1.

$$\zeta_R = \sum_{n=0}^{\infty} \zeta_{Rn} = 8 \int_0^{\pi/2} \exp(-k_o f_1 \sec^2\theta) \sum_{n=0}^{\infty} b_n n! \sum_{r=0}^{n} \frac{\{f_1^{r+1} - (f_1-1)^{r+1}\} k_o^{r-n+1}}{(r+1)!\, \sec^{2(n-r-1)}\theta}$$

$$\times \sin(k_1 x \sec\theta) \cos(k_1 y \sin\theta \sec^2\theta)\, d\theta \qquad (56b)$$

This is formally similar to Equation (24a). As in Equations (24b) and (24c), we can write

$$\zeta_{Ro} < 8 \exp(-k_o f_1)\ b_o k_o$$
$$\zeta_{R1} < 8 \exp(-k_o f_1)\ b_1\ \left(1 - \frac{1-2f_1}{2}\right) k_o \qquad (56c)$$

Therefore the same comment about Equation (54a) can be applied to Equation (56a) that is, the uncancelled wave height, ζ_R of Equation (56b) decreases almost exponentially with increasing $k_o f_1$ for the usual range of Froude numbers.

To obtain the approximate correction we may use a perturbation method. We replace b_n by $b_n(1+\epsilon_n)$ in Equations (56a) and (56b). The sum of these two newly formed equations gives the wave height produced by the perturbed doublet distribution of depth f. When we subtract from this the wave system due to the ship bow as given by the negative of Equation (56a) we obtain for each term of the resulting series

$$I_n = -8\, b_n \int_o^{\pi/2} \Big\{ \frac{(1-\exp(-k_o \sec^2\theta))}{k_o^n \sec^{2n}\theta}\, \epsilon_n - (1+\epsilon_n) \frac{\exp(-k_o f_1 \sec^2\theta)}{k_o^n \sec^{2n}\theta}$$
$$\times \sum_{r=0}^{n} \frac{[f_1^{r+1} - (f_1-1)^{r+1}]}{(r+1)!\cos^{2(r+1)}\theta}\, k_o^{r+1} \Big\} \sin(k_1 x \sec\theta)\cos(k_1 y \sin\theta \sec^2\theta)\, d\theta. \qquad (57a)$$

The wave resistance represented by the first term in the wave system I_o (putting $n = 0$ in Equation (57a) except for a constant factor is

$$R(I_o) = \int_o^{\pi/2} \Big\{ \epsilon_o (1 - e^{-k_o \sec^2\theta}) - (1+\epsilon_o) e^{-k_o f_1 \sec^2\theta} k_o \sec^2\theta \Big\}^2 \cos^3\theta\, d\theta\, d\theta$$
$$= \epsilon_o^2 \Big\{ \frac{2}{3} + 2\, e^{-k_o} G_{-2}(k_o) - 4 e^{-k_o/2} G_{-2}\left(\frac{k_o}{2}\right) \Big\} - 2\epsilon_o(1+\epsilon_o)\, k_o$$
$$\times \Big\{ e^{-k_o f_1/2} G_{-1}\left(\frac{k_o f_1}{2}\right) - e^{-(k_o + k_o f_1)/2} G_{-1}\left(\frac{k_o + k_o f_1}{2}\right) \Big\}$$
$$+ k_o^2 (1+\epsilon_o)^2 \frac{e^{-k_o f_1}}{2} K_o(k_o f_1)$$

where

$$\int_0^{\pi/2} \exp(-2k_o \sec^2\theta)\sec^{2n+1}\theta d\theta = \frac{e^{-k_o}}{2n+1} G_n(k_o) \text{ (See Yim 1962a)}$$

$$G_{-1}\left(\frac{k_o f_1}{2}\right) \frac{k_o f_1}{2}\left\{K_1\left(\frac{k_o f_1}{2}\right) - K_o\left(\frac{k_o f_1}{2}\right)\right\}$$

$$G_{-2}(k_o) = \frac{k_o}{3}\left\{ K_1(k_o) + 2 k_o K_o(k_o) - 2k_o K_1(k_o) \right\}$$

$K_o(k_o)$, $K_1(k_o)$ are the modified Bessel functions of the second kind of zeroth and first order respectively. Hence the value of ϵ_o which makes $R(I_o)$ minimum is $\epsilon_o = \frac{-\beta}{2\alpha}$ where

$$\alpha = \frac{2}{3} + 2e^{-k_o} G_{-2}(k_o) - 4 e^{-k_o/2} G_{-2}(k_o/2)$$

$$-2k_o \left\{e^{-k_o f_1/2} G_{-1}(k_o f_1/2) - e^{-(k_o + k_o f_1)/2} G_{-1}\left(\frac{k_o + k_o f_1}{2}\right)\right\} + k_o^2 \frac{e^{-k_o f_1}}{2} K_o(k_o f_1)$$

$$\beta = -2k_o \left\{e^{-k_o f_1/2} G_{-1}(k_o f_1/2) - e^{-k_o + k_o f_1)/2} G_{-1}(k_o + k_o f_1/2) \right\}$$

$$+ k_o^2 e^{-k_o f_1} K_o(k_o f_1).$$

The values of ϵ_o for different Froude numbers and $f_1 = 1$ are given in Table 1. The values of ϵ_n for $n \geq 1$ can be calculated as above. However, since these are not so important in the usual range of Froude number, a rough and easily obtained approximation may be sufficient.

Using the method of stationary phase for $y = 0$

$$I_n = -8\sqrt{\frac{\pi}{2k_1}} \left\{(1-e^{-k_o})/k_o^n \quad \epsilon_n - (1+\epsilon_n)\frac{e^{-k_o f_1}}{k_o^n} \sum_{r=0}^{n} \frac{[f_1^{r+1} - (f_1-1)^{r+1} k_o^{r+1}]}{(r+1)!} \right\}$$

$$X \sin\left(k_1 x + \frac{\pi}{4}\right) . \qquad (57b)$$

If we put $I_n = 0$

TABLE 1

VALUES OF b_n, ϵ_n FOR AN APPROXIMATE SINE SHIP

L/H	F_H	b_o	b_1	b_2	b_3	ϵ_o	ϵ_1	ϵ_2	ϵ_3
16	1.00	0.18750	3.6143-03	4.6448-05	4.4768-07	0.65940	6.8718	32.290	171.71
	1.25	0.29296	8.8241-03	1.7719-04	2.6684-06	0.96717	16.346	111.19	895.72
	1.5	0.42187	1.8298-02	5.2907-04	1.1474-05	1.2008	33.095	313.10	3588.6
	1.75	0.57421	3.3899-02	1.3341-03	3.9379-05	1.3657	60.207	761.61	11815.
24	1.00	0.12500	1.0709-03	6.1166-06	2.6202-08				
	1.25	0.19531	2.6145-03	2.3333-05	1.5617-07				
	1.5	0.28125	5.4215-03	6.9672-05	6.7152-07				
	1.75	0.38281	1.0044-02	1.7569-04	2.3048-06				
	2.00	0.50000	1.7134-02	3.9147-04	6.7076-06				

($3.6143\text{-}03 = 3.6143.10^{-3}$)

(3 X COEFFICIENTS OF SINE SHIP: $a_o = 3.$, $a_2 = -14.804$, $a_4 = 12.176$, $a_6 = -4.0057$)

$$\epsilon_n = \frac{\sum_{m=1}^{n+1} \left[\frac{(f_1 k_o)^m - \{k_o(f_1-1)\}^m}{m!} \right]}{e^{k_o f_1}(1-e^{-k_o}) - \sum_{m=1}^{n+1} \left[\frac{(f_o k_1)^m - \{k_o(f_1-1)\}^m}{m!} \right]} \tag{57c}$$

Equation (57c) is evaluated for $f_1 = 1$ and different Froude numbers, from $n = 1$ to $n = 3$ are shown in Table 1. For $f_1 = 1$,

$$\epsilon_n = \frac{\sum_{m=1}^{n+1} \frac{k_o{}^m}{m!}}{e^{k_o} - 1 - \sum_{m=1}^{n+1} \frac{k_o{}^m}{m!}} \tag{57d}$$

We note that ϵ_n in (57c) is not a function of a_n or b_n but only of f_1, k_o, and n, and is always positive for $f_1 \geq 1$ since the numerator in Equation (57c) is positive, and the denominator in Equation (57c) is larger than that of Equation (57d). The latter is positive due to the fact that

$$1 + \sum_{m=1}^{n+1} \frac{k_o{}^m}{m!}$$

is a partial sum of the series expansion of e^{k_o}. (This is also true for $y \neq 0$ in Equation (57a). Hence if the b_n's are all positive (as for the sine ship treated in the next Section), each horizontal section of the bulb represented by Equations (21) and (23b) in $0 \leq z_1 \leq 1$ will be smaller than any corrected bulb.

Since we determined ϵ_n from the stationary phase at $y = 0$, ϵ_n's $(n \geq 1)$ in Table 1 are overestimated, or rather Equations (21) and (23b) with $b_n(1+\epsilon_n)$ instead of b_n would indicate the upper bound of the size of bulb for minimum wave resistance subject to the conditions of this method.

In order to find the exact optimum doublet distribution on $0 \leq z_1 \leq f$ for the minimization of the wave resistance due to a given ship it is better to attack this problem by a somewhat different approach. That is, we determine the unknown coefficients b_n of the doublet distribution directly by minimizing the wave resistance of a given ship with the bulb (see Yim, 1962b). This is equivalent to the present method provided we obtain ϵ_n by minimizing the wave resistance due to the complete uncancelled wave system directly. ϵ_n is not necessarily always positive, since in this case there are many extra cross product terms. According to Figures 1a and 2a, the exact optimum bulb is thinner near the free surface and thicker near the keel than the one corrected by the method given in this paper.

It should be mentioned here that there is no interaction between the bow and the stern waves for the ideal doublet distribution since in this case the bow and stern waves are separately cancelled out by the bow and stern bulbs respectively. However for the finite doublet lines there exist interactions and the curves of wave resistance versus Froude number have humps and hollows. Therefore the design Froude number of the ship would normally be selected so that it falls at a hollow on the resistance curve. However, since the optimum bulb at the bow or the stern for each Froude number has the effect of smoothing out the resistance curve to a great extent (Yim, 1962a) the unfavorable effect of not falling on a hollow is usually outweighted by the advantage of using an optimum bulb.

CASE OF SINE SHIP

Inui (1960) pointed out that the smaller the Froude number, the greater becomes the importance of the first term in Equation (16). In the practical case we need not take many terms in the series. At moderate ship speeds even one term will be enough since the second term of the series (16) produces wave heights of the order $1/k_1^2 < 0.01$ for $F = .3$ while the first term is considered to be of order 1 (see Appendix). This is natural since it is well known that the first term of the series (16) for the source distribution of the ship is proportional to the angle of entrance of a ship and the angle of entrance has a great influence on the wave resistance.

As an example, the first four terms of the cosine series will be taken for the source distribution in Equation (16). Then the corresponding ship will be a sine ship in the Michell's sense. The coefficients a_n are taken such that the ship half-breadths are nondimensionalized with

respect to the half beam and the stations are measured from the bow and nondimensionalized with respect to the ship length L. The values of a_n, b_n from Equation (21), and ϵ_n from Equation (57c) for different Froude numbers and length-draft ratios are shown in Table 1. The corresponding doublet distributions, Equations (21) and (23b) without perturbation corrections, in $0 \leq z_1 \leq 1$, for different Froude numbers are plotted as the solid curves in Figures 1a and 2a. Also shown in these figures for purpose of comparison, are corresponding curves determined from the exact ship wave resistance minimization theory based on finding directly the optimum doublet distribution for a given ship with a bulb which does not extend below the keel (see Yim, 1962b).

The two dimensional approximate relation of bulb radius r and the strength of doublet μ per unit length of z is $\mu = r^2 V$. This relation, although overestimating the actual radius r, is used as an alternate means of expressing the nondimensional doublet strength in Figures 1a and 2a in order to give some idea of the approximate area distribution of the bulb.

The remarkable reductions of wave resistance due to the bulbs for both cases are shown in Figures 1b and 2b. The bulb sizes near the keel $(z = -1)$ determined from Equation (21) are very much smaller than those shown by the exact method illustrated by the broken curves although near the free surface the former are slightly larger than the latter. The Froude number of least resistance, where the reduction of wave resistance is almost 90 percent, is usually less than the Froude number for which the calculation of the doublet distribution (21) was made. This is due to the fact that we have cut off the infinite ideal doublet distribution at the keel. The figures of doublet distributions (21), uncorrected by perturbations, appear to be almost linear in $0 \geq z \geq -1$. This indicates the importance of the first term $b_0 a_1$ of the series for the doublet distribution (21) or the first term a_0 of the series for the source distribution for a ship in the practical range of Froude numbers, as pointed out earlier and in the Appendix. That is, the equation for the first term in the doublet series $b_0 = a_0/k_1$ is a very simple but very important approximate relation between the ship and the corresponding bulb. It is clear from the equation for the perturbation (57), and Table 1 that the nonlinearity increases when the length of bulb becomes smaller. Hence it may be desirable to increase the magnitude of the doublet strength near the keel or rather extend the doublet distribution below the keel if possible according to the methods indicated in Equation (57). However, according to Figures 1b and 2b the doublet distribution of Equation (21) which gives a much smaller bulb than the exact

optimum one results in a very favorable effect even without the perturbation corrections. Besides even these bulbs are quite large when the Froude number is large. In fact we may expect that the effects of viscosity, cavitation, and other design conditions would ultimately determine the maximum bulb size at these Froude numbers.

CASE OF THE PARABOLIC SHIP

When we consider the source distribution

$$m = c\,(1 - 2x) \quad \text{in} \quad 0 \leq z_1 \leq 1 \tag{58}$$

Michell's linear ship relation

$$m(x) = \frac{1}{2\pi} \frac{\partial y}{\partial x}$$

will indicate that this is a parabolic ship with

$$c = \frac{1}{\pi} \frac{B}{L}$$

where B/L is the beam-length ratio.

Since we have an even power and an odd power term in Equation (58), the bow waves contain both the sine and cosine components. To cancel the sine bow waves we need to put a doublet line of strength from Equation (23b)

$$\frac{\mu}{c} = \frac{z_1}{k_1} \qquad c \leq z_1 \leq 1$$

$$\frac{\mu}{c} = \frac{1}{k_1} \qquad 1 \leq z_1$$

The effect of doublet lines, both the ideal distribution cut off at the keel and the optimum finite distribution has already been demonstrated for a sine ship. In Figures 3a and 3b the optimum finite doublet distribution for the parabolic ship and the corresponding bow wave resistance with and without the doublet distribution are shown (the process of calculation is discussed in Yims paper of 1962b).

To cancel the cosine bow waves we need to superimpose the quadrupole line of the strength from Equations (28) and (29),

$$\frac{\lambda}{c} = \frac{k_o}{k_1^3} z_1^2 \qquad \text{in } 0 \le z_1 \le 1$$

$$\frac{\lambda}{c} = \frac{k_o}{k_1^3} [z_1^2 - (z_1-1)^2] = k_o \frac{(2z_1-1)}{k_1^3} \quad \text{in } 1 \le z_1$$

k_1 is usually larger than 1 and quite large if Froude number is small. k_o is smaller by the factor of the draft length ratio than k_1. Hence inequality (45) would be satisfied for quite a large z_1 for moderate Froude numbers but eventually inequality (45) is violated for z_1 larger than a certain number. However the effect of cutting the line off at a large z_1 may not be serious as was shown for the case of doublet.

The wave resistance due to the cosine bow waves of the parabolic ship with and without the ideal quadrupole line cut off at the keel are shown in Figure 4b. The optimum quadrupole strength and the wave resistance with and without the optimum quadrupole (see Yim 1962b) is also shown in Figures 4a and 4b. Although the effect of the quadrupole line is not as prominent as that of the doublet for the sine wave, even the ideal quadrupole line cut off at keel is shown to be quite favorable for moderate Froude numbers. The wave resistance due to the cosine component of the bow waves even without the bulb as is shown in Figure 4b, is quite small compared to that due to the sine component. However, in practice the cosine components seem to be much larger tha in this theory due to the change of the actual body streamlines caused by boundary layers and wakes.

APPENDIX

Since a_{2n} is the coefficient of a power series which represents the source distribution of a ship, it is usually comparable to the cosine series where $a_{2n} = (-1)^n \pi^{2n}/(2n)!$. It therefore seems reasonable to assume that $(2n)!\, a_{2n} < M\pi^{2n}$, M = finite number, for all n . For usual ships $F^2 = \frac{1}{K_1} < \frac{1}{4}$. Besides the integral

$$C \equiv \int_0^{\pi/2} \cos^{2n-1}\theta d\theta = \frac{2.4.---.2(n-1)}{3.5.---.(2n-1)}$$

is decreasing with increasing n . Hence a typical term in the Equation (18) for the wave height due to the ship can be estimated as

$$\left| \int_0^{\pi/2} e^{-k_o f \sec^2\theta} \frac{(2n)!a_{2n}}{(k_1 \sec\theta)^{2(n-1)}} \sin(k_1 x \sec\theta)\cos(k_1 y \sin\theta\sec^2\theta)d\theta \right|$$

$$< e^{-k_o f} M\pi^2 \int_0^{\pi/2} \frac{\cos^{2(n-1)}\theta}{(k_1/\pi)^{2(n-1)}} d\theta = \frac{\pi^2 MC}{(k_1/\pi)^{2(n-1)}} e^{-k_o f} \qquad (A.1)$$

Since π/k_1 is a small number usually, it is clear how rapidly the integral (A.1) decreases when n increases. Hence in practice we do not need to take many terms of the series in determining the optimum bulb. That is, the magnitude of the corresponding terms for the doublet distribution decrease very rapidly in the usual range of Froude number. Therefore we have only to consider the case of finite n when we consider the limiting case of $z_1 \to \infty$; i.e. the effect of the infinitely long doublet distribution from Equation (20a). For the case of a finite doublet distribution we have

$$\zeta_B = -8 \int_0^{\pi/2} \sum_{n=0}^{\infty} b_n n! \left(\frac{e^{-k_o f \sec^2\theta}}{k_o^{n-1}\sec^{2(n-1)}\theta} e^{-k_o f_1 \sec^2\theta} \right.$$

$$\left. - e^{-k_o f_1 \sec^2\theta} \sum_{r=0}^{n} \frac{(f_1 - f)^{n-r}}{(n-r)!k_o^{r-1}\sec^{2(r-1)}\theta} \right) \sin(k_1 x \sec\theta)$$

$$X \cos(k_1 y \sin\theta \sec^2\theta)\, d\theta$$

Let us denote the terms due to the limit f_1 by R_n. Then for a finite n

$$\lim_{f_1 \to \infty} R_n \to 0$$

because

$$\lim_{f_1 \to \infty} e^{-k_o f} (f_1 - f)^n = 0$$

The argument is the same when the amplitude functions are given by Equation (22).

REFERENCES

Gill, S., "A Process for the Step by Step Integration of Differential Equations in an Automatic Digital Computing Machine," Proc. Cambridge Philos. Soc., Vol. 47, pp 96-108, 1951.

Havelock, T. H., "Wave Patterns and Wave Resistance," T.I.N.A., Vol. 76, pp 430-443, 1934a.

Havelock, T. H., "The Calculation of Wave Resistance," Proc. Roy. Soc. A 144, pp 514-21, 1934b.

Havelock, T. H., "Wave Resistance Theory and its Application to Ship Problems," Trans. SNAME 59, pp 13-24, 1951.

Inui, T., "60th Anniversary Series Vol. 2, The Society of Naval Architects of Japan, 1960.

Inui, T., Takahei, T., and Kumano, M., "Wave Profile Measurements on the Wave-Making Characteristics of the Bulbous Bow," Society of Naval Architecture of Japan, 1960.

Kostchukov, A. A., "Theory of Ship Waves and the Wave Resistance," Leningrad, 1959.

Krein, M. G., Doklady Akademi Nauk SSSR, Vol. 100, No. 3, 1955.

Lamb, H., "Hydrodynamics," Dover Publ, New York, 1945.

Lunde, J. K., "On The Theory of Wave Resistance and Wave Profile," Skipsmodelltankens meddelelse nr. 10, 1952.

Milne-Thomson, L. M., "Theoretical Hydrodynamics," The Macmillan Co. N. Y. 1955.

Takahei, T., "A Study on the Waveless Bow," SNAJ, 1960.

Weinblum, Georg P., "Analysis of Wave Resistance," DTMB Report 710, Sept. 1950.

Wigley, W. C. S., "The Theory of the Bulbous Bow and its Practical Application," Trans. N.E.C.I.E.S., Vol. LII, pp. 65-88, 1936.

Yim, B., "Analysis of the Bulbous Bow on Simple Ships," HYDRONAUTICS, Incorporated Technical Report 117-1, 1962a.

Yim, B., "Minimum Wave Resistance of Bulbous Ships," HYDRONAUTICS, Incorporated Technical Report 117-3, 1962b.

Yim, B., "On Ships with Zero Wave Resistance," HYDRONAUTICS, Incorporated Technical Report 117-2, 1962.

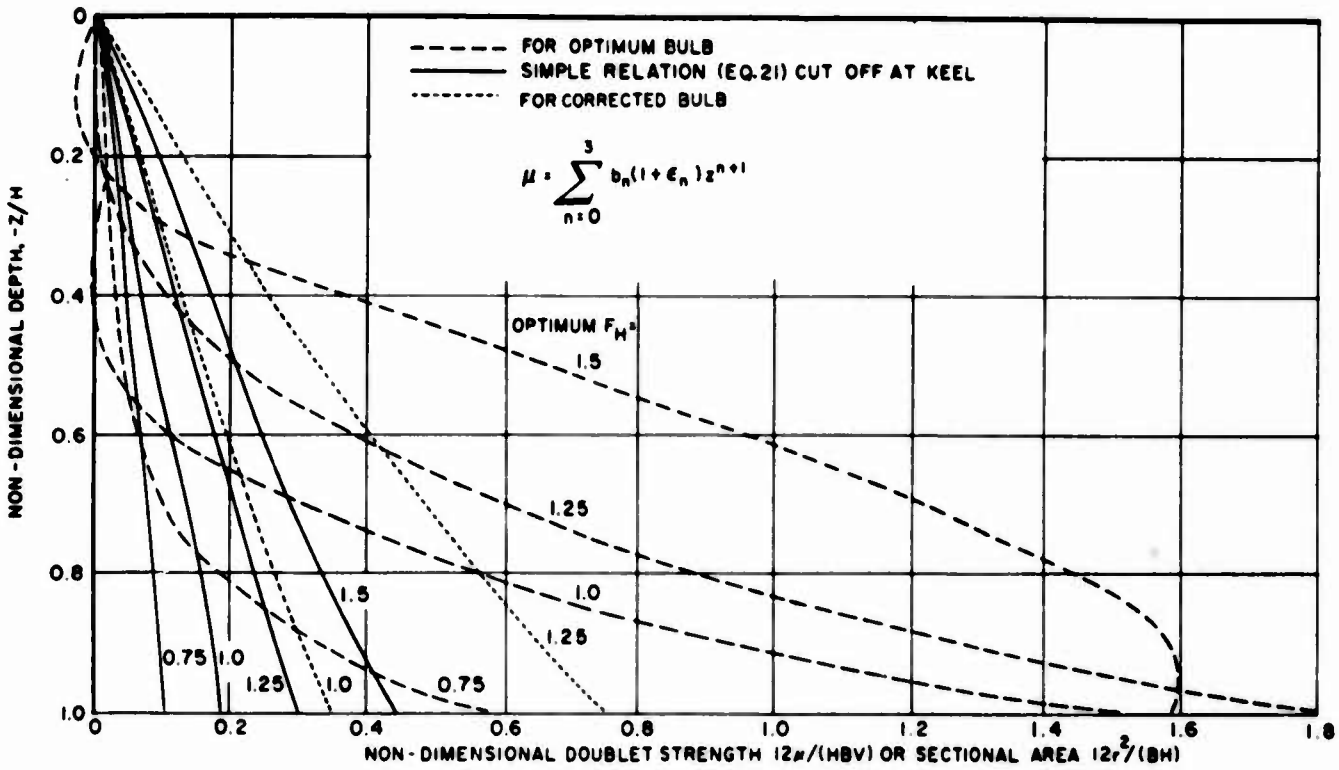


FIGURE Ia DOUBLET DISTRIBUTION FOR SINE SHIP (L/H=16)

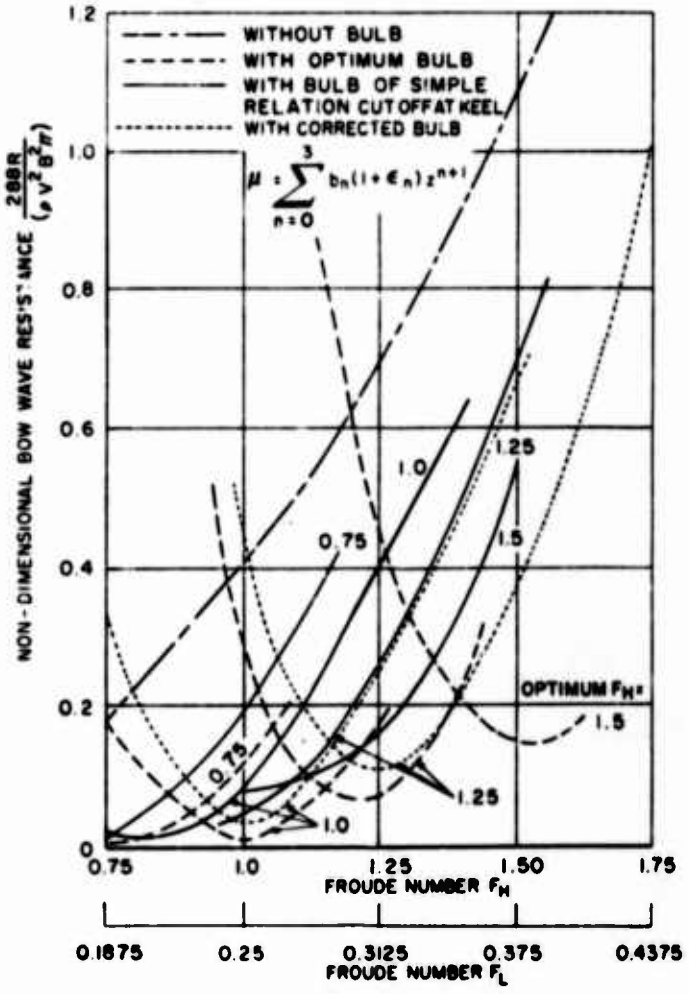


FIGURE Ib- BOW WAVE RESISTANCE OF SINE SHIP
(L/H = 16)

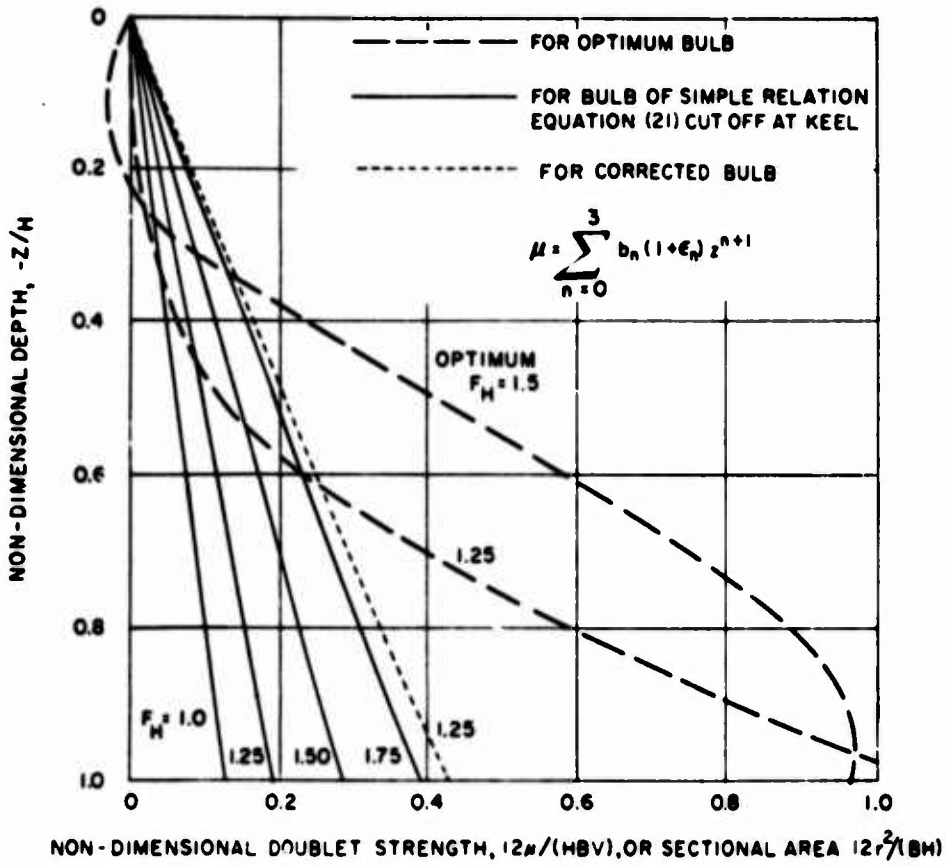


FIGURE 2a - DOUBLET DISTRIBUTION FOR SINE SHIP (L/H = 24)

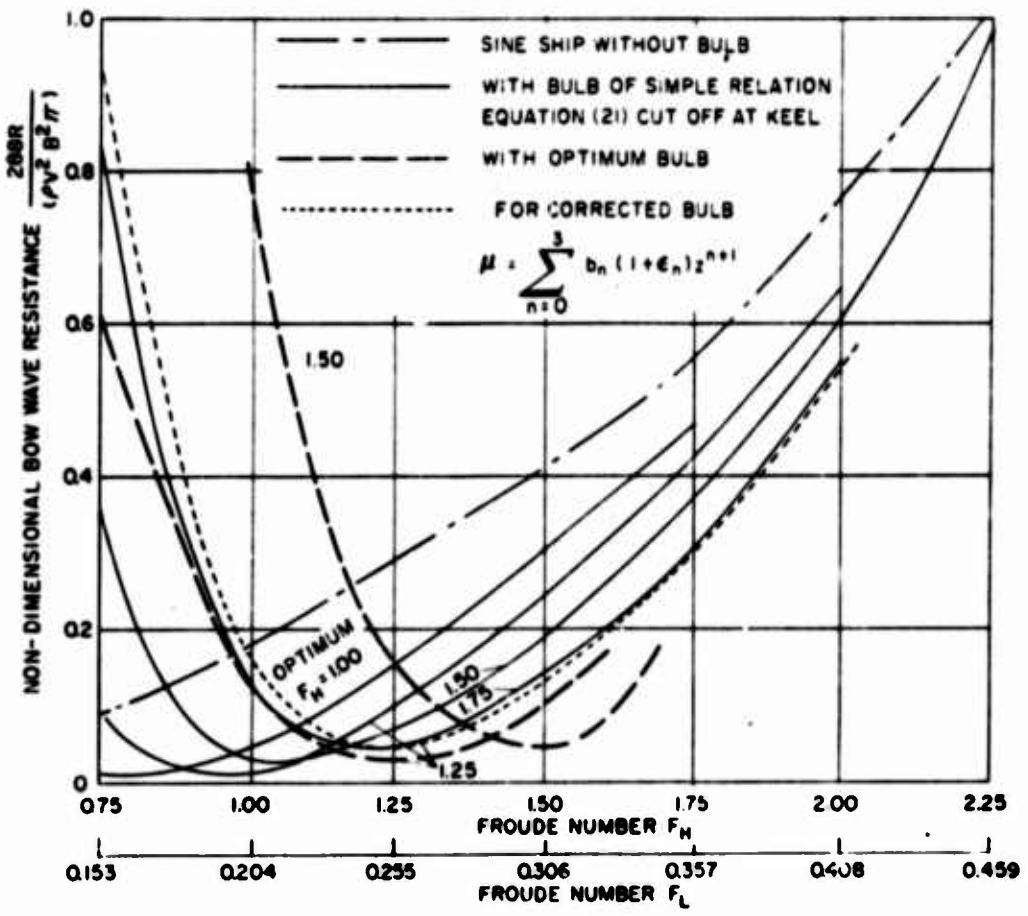


FIGURE 2b - BOW WAVE RESISTANCE OF SINE SHIP ($L/_H$ = 24)

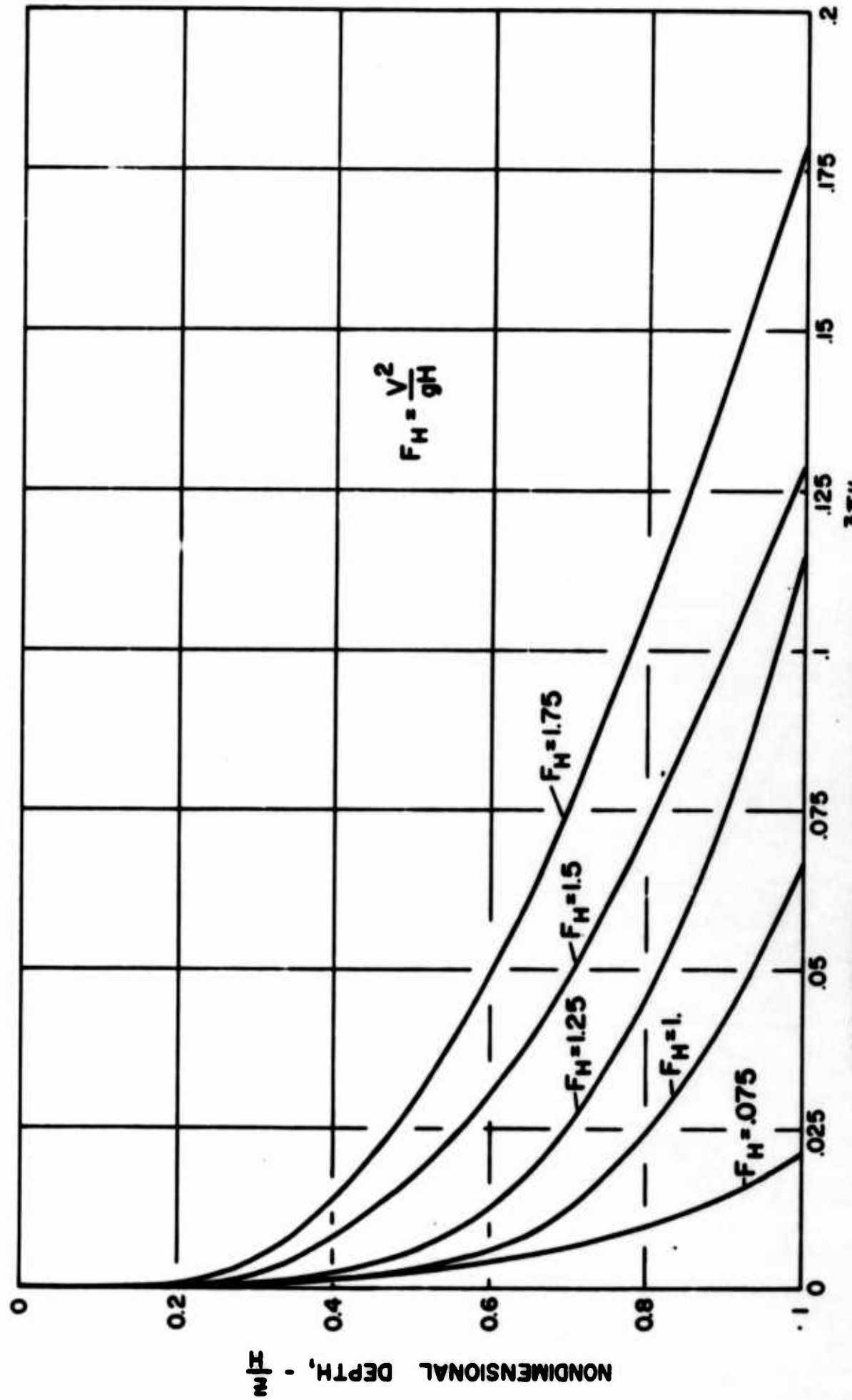


FIGURE 3a DOUBLET DISTRIBUTION FOR A PARABOLIC S

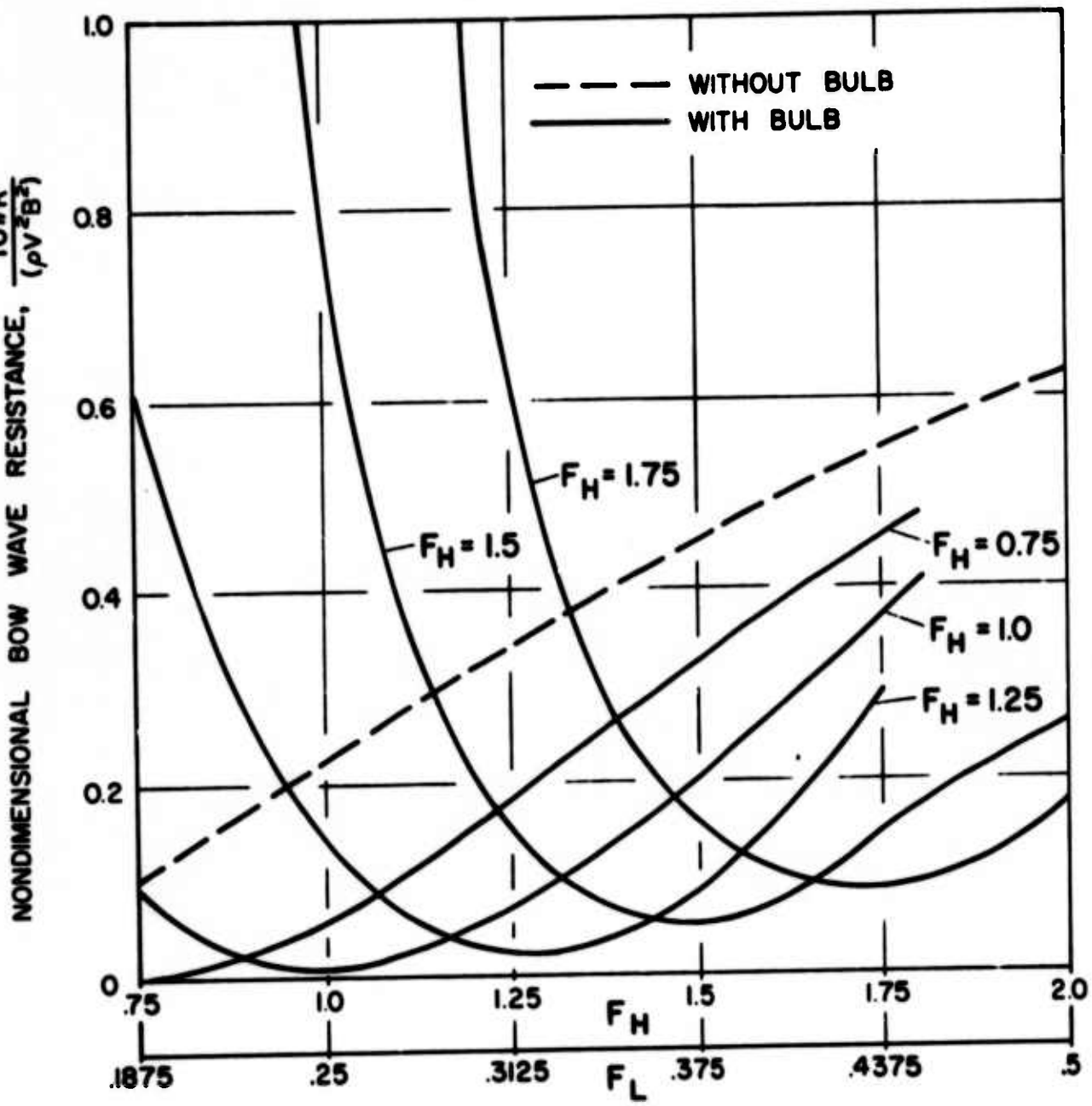


FIGURE 3b BOW WAVE RESISTANCE DUE TO THE EVEN TERM IN THE SOURCE DISTRIBUTION OF A PARABOLIC SHIP $(\frac{L}{H} = 16)$

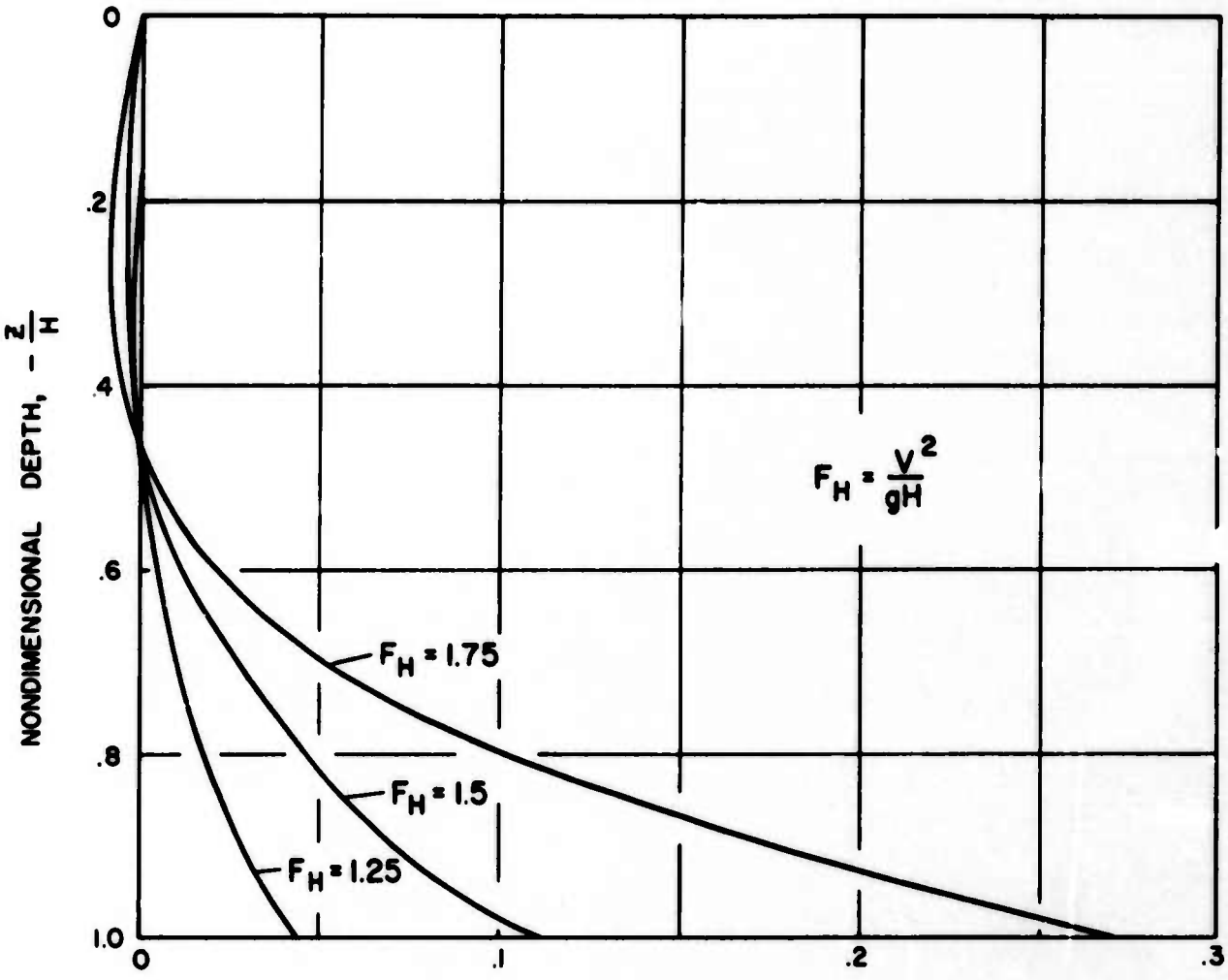


FIGURE 4a QUADRUPOLE DISTRIBUTION FOR A PARABOLIC SHIP, $(\frac{L}{H} = 16)$

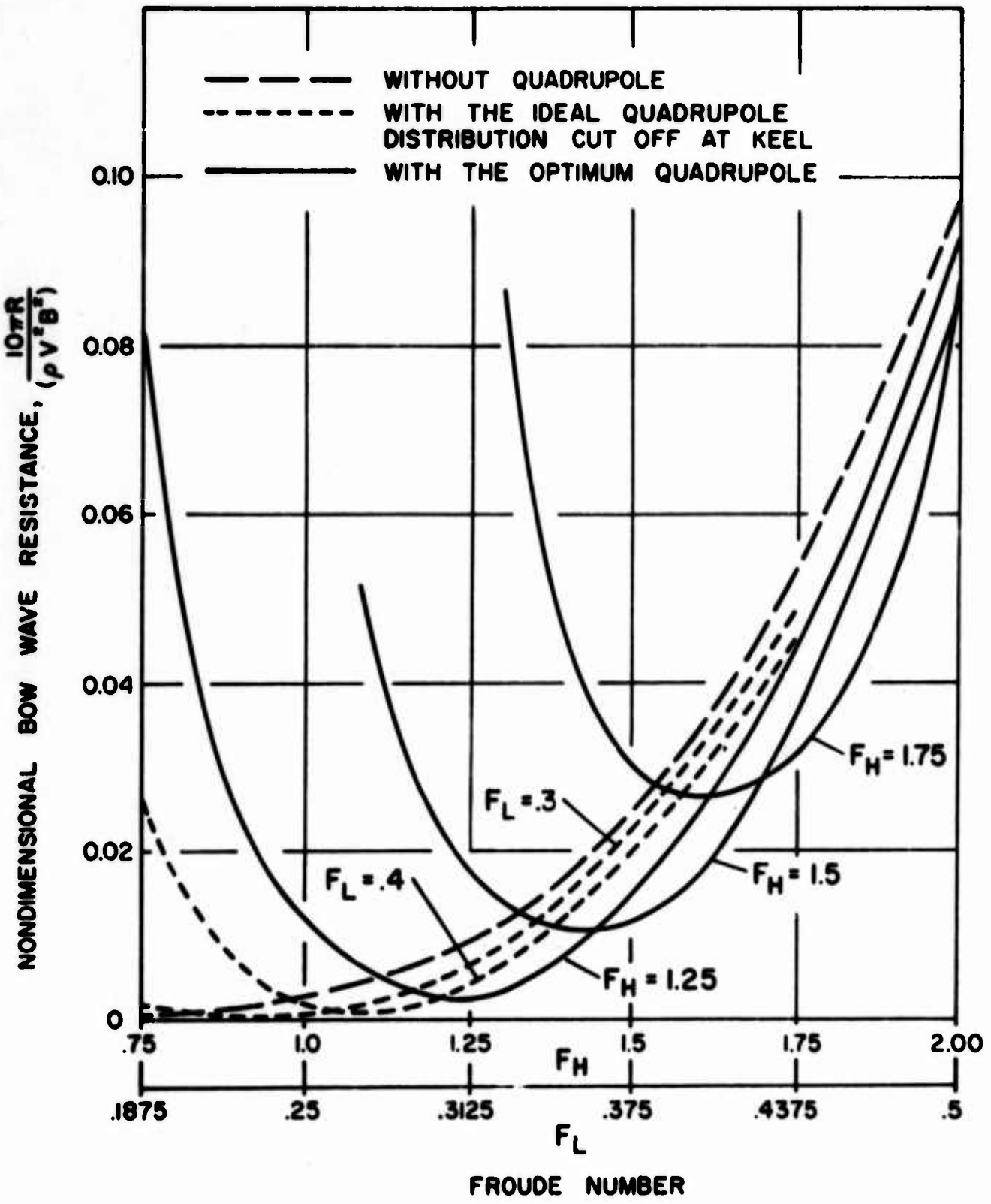
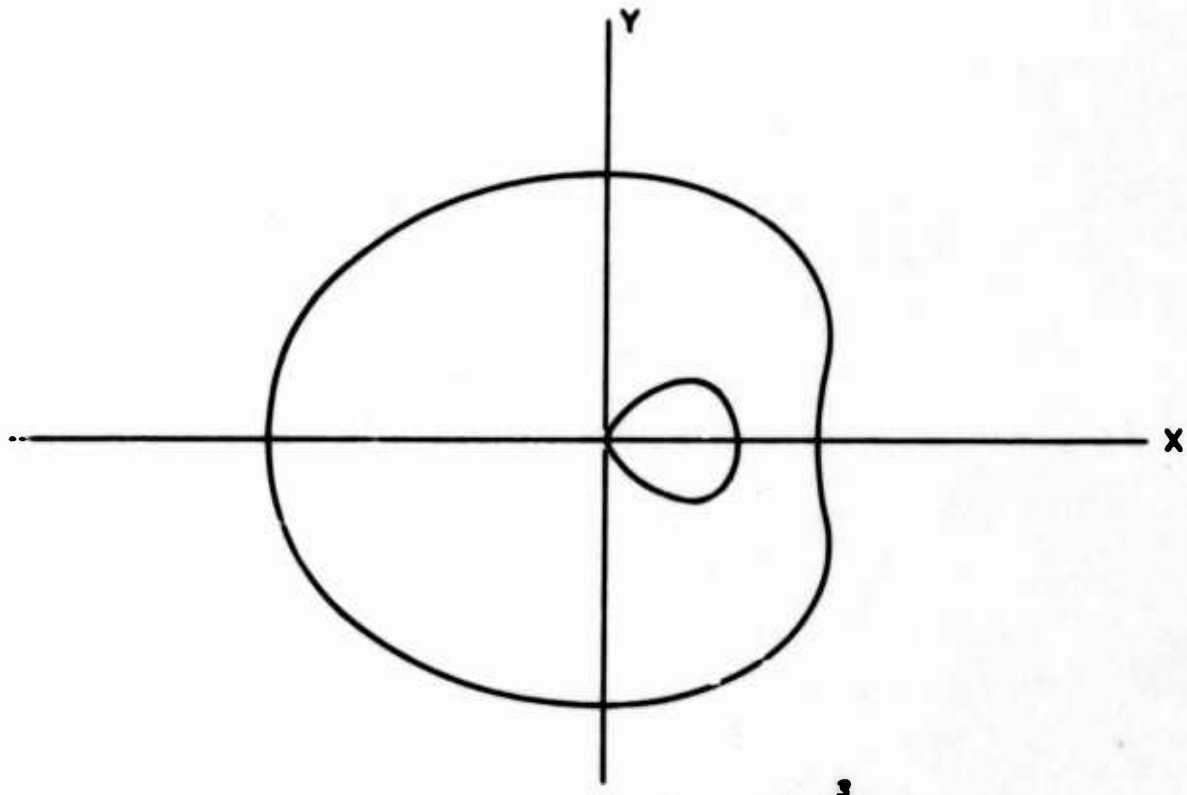
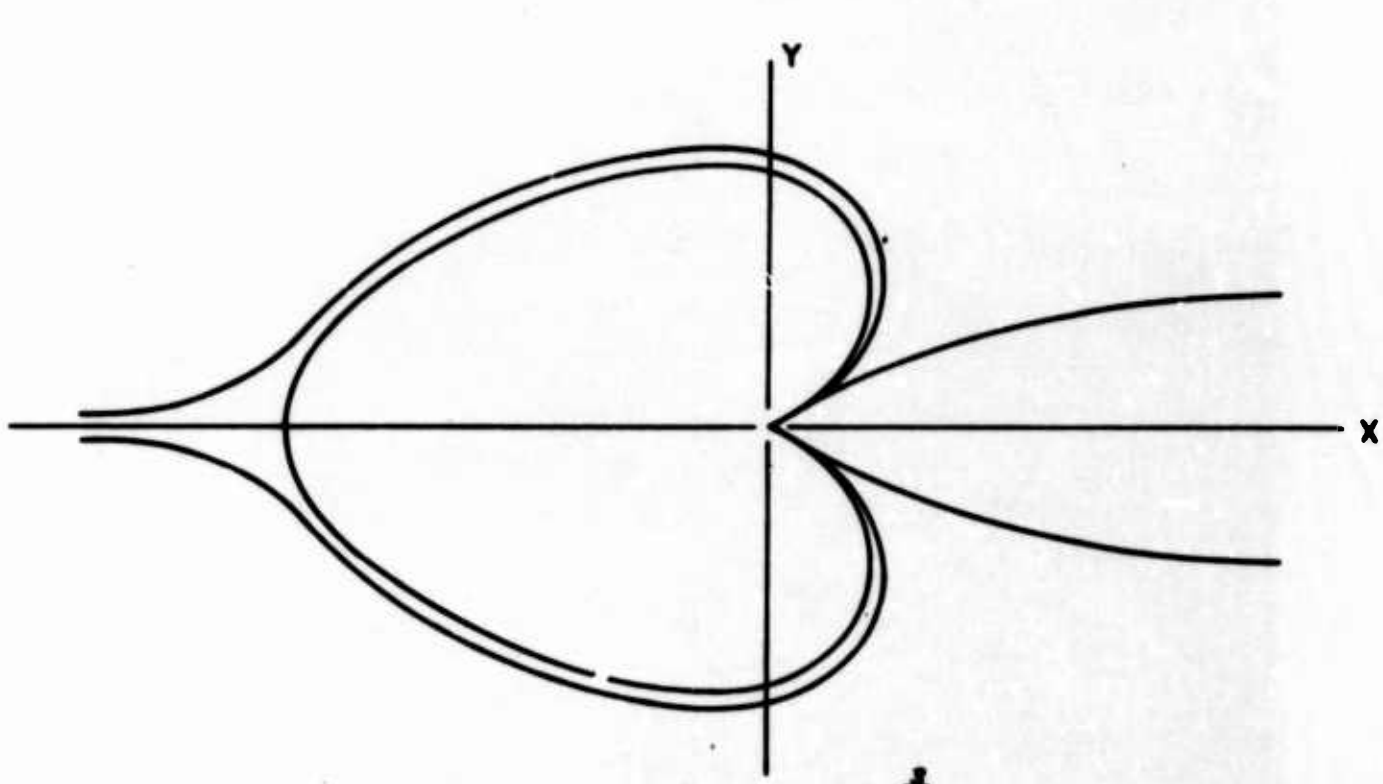


FIGURE 4b BOW WAVE RESISTANCE DUE TO THE ODD TERM IN THE SOURCE DISTRIBUTION OF A PARABOLIC SHIP, $(\frac{L}{H} = 16)$



(a) WHEN $\frac{\lambda}{V} \leq \left(\frac{\mu}{3V}\right)^{\frac{3}{2}}$



(b) WHEN $\frac{\lambda}{V} > \left(\frac{\mu}{3V}\right)^{\frac{3}{2}}$

FIGURE 5 SCHEMATIC DIAGRAM OF DIVIDING STREAMLINES DUE TO A POINT DOUBLET PLUS A POINT QUADRUPOLE AT THE ORIGIN WITH THE DIRECTIONS PARALLEL TO THE AXIS

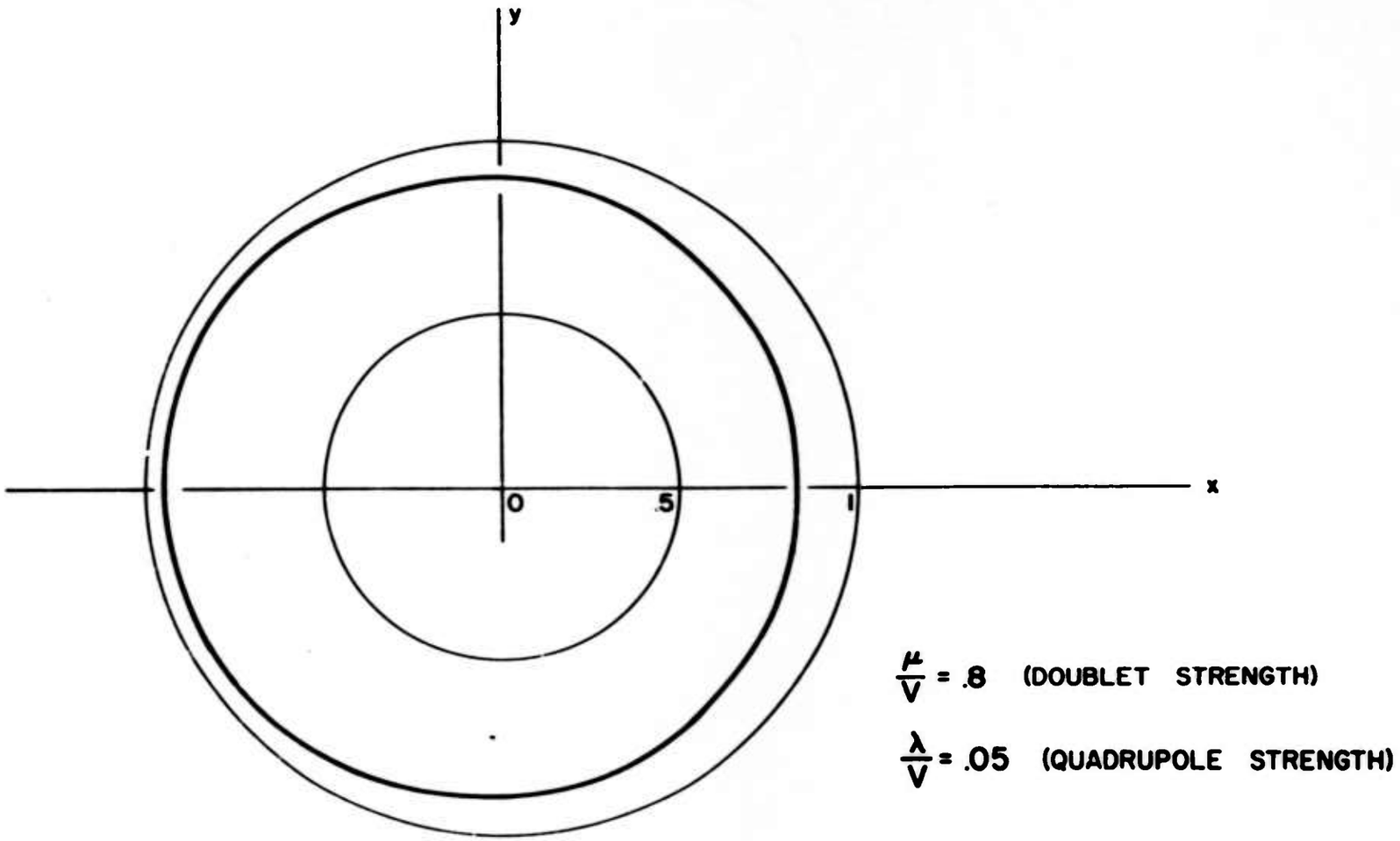


FIGURE 6 TWO DIMENSIONAL DIVIDING STREAMLINE DUE TO A POINT QUADRUPOLE AND A POINT DOUBLET LOCATED AT THE ORIGIN

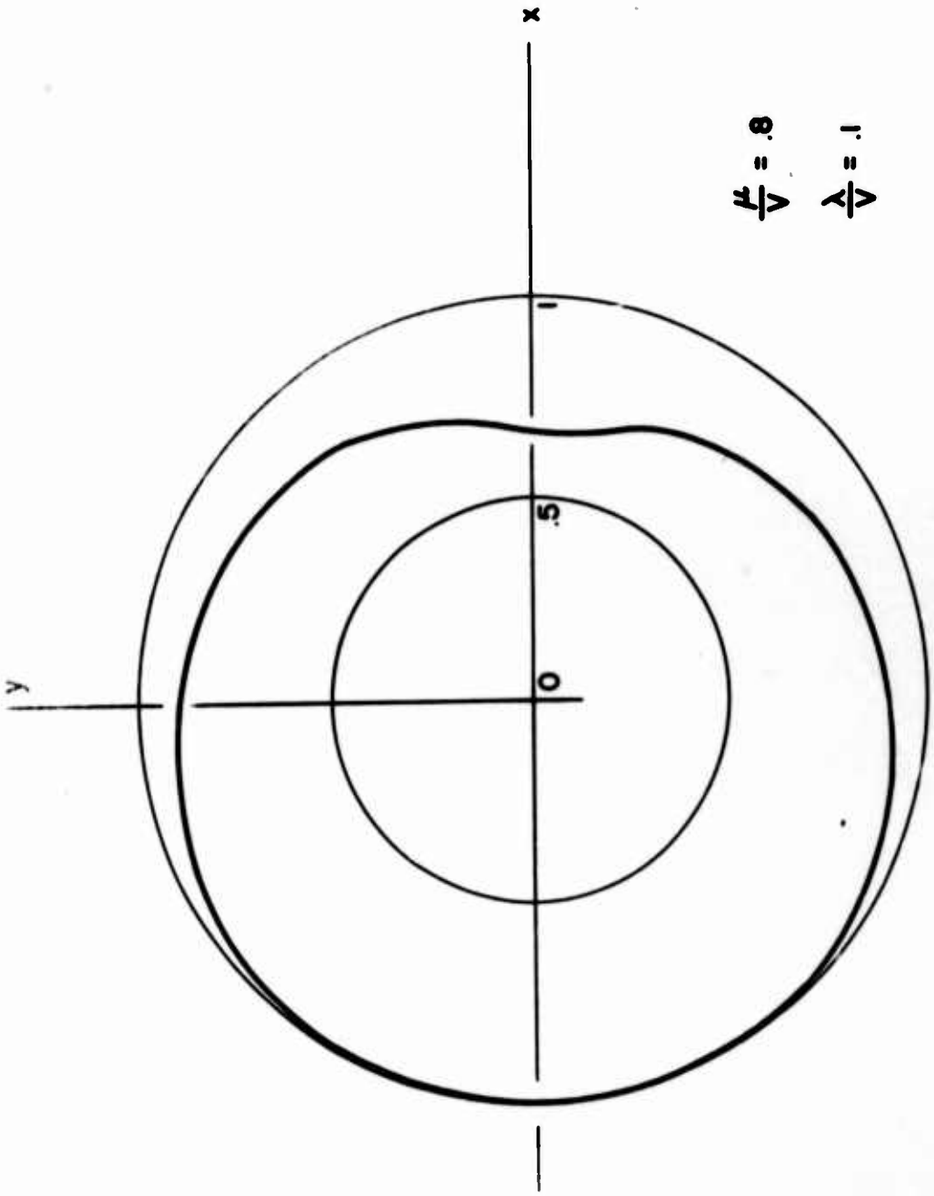
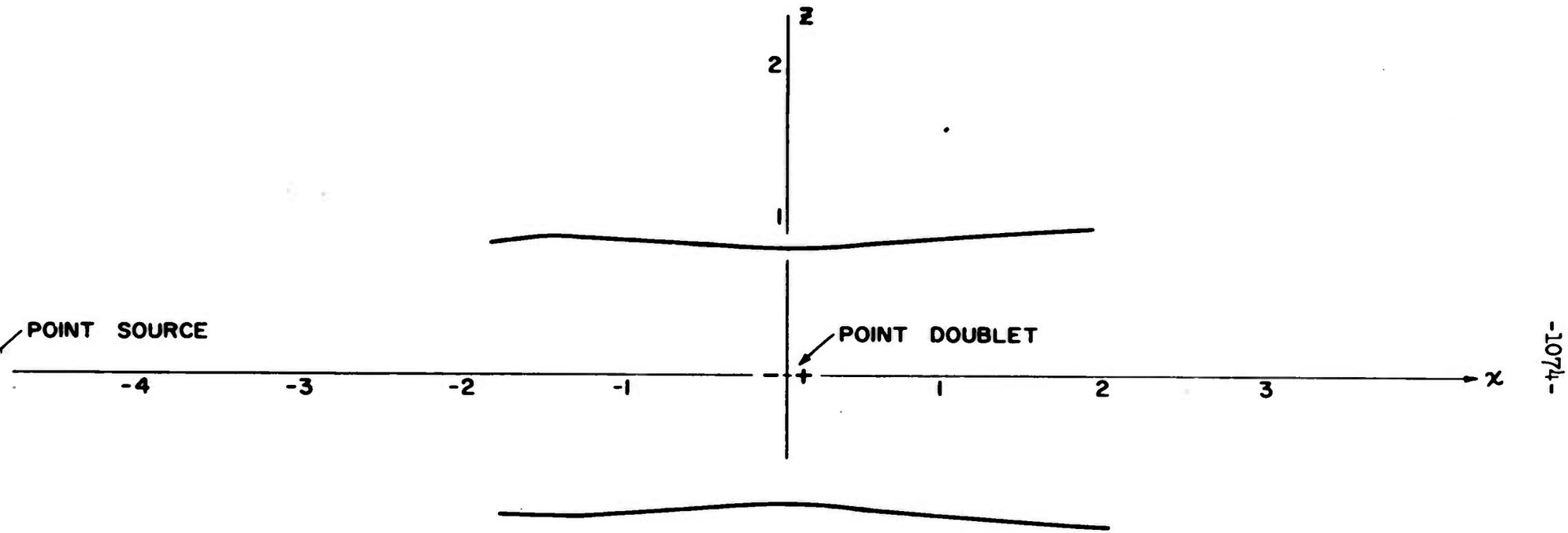


FIGURE 7 TWO DIMENSIONAL DIVIDING STREAMLINE DUE TO A POINT QUADRUPOLE AND A POINT DOUBLET LOCATED AT THE ORIGIN



$\bar{\mu} = .1$ IN Eqn (49)

FIGURE 8 TWO DIMENSIONAL DIVIDING STREAMLINE DUE TO A POINT SOURCE AND A POINT DOUBLET

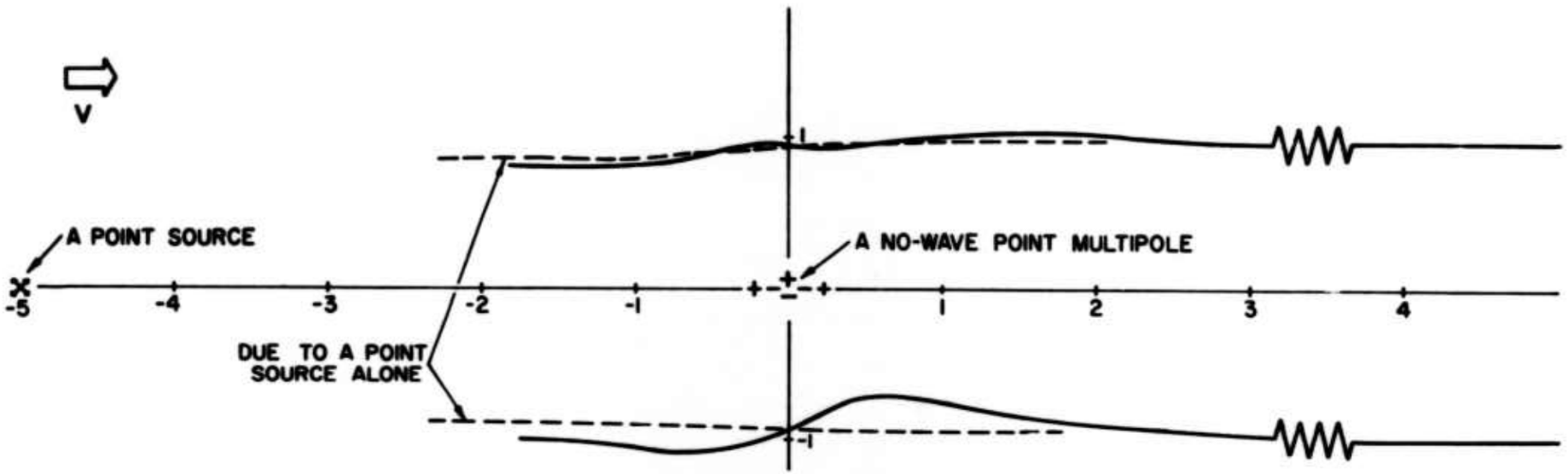


FIGURE 9 TWO DIMENSIONAL DIVIDING STREAMLINE DUE TO A POINT SOURCE AND A NO-WAVE POINT MULTIPOLE

DISCUSSION

by T. Takahei

I have been working on the identical problem these past few years, so that I appreciate Dr. Yim's paper very much. He has not only developed the theory to the extreme extent, but also has introduced newly idea of quadropole and no-wave singularity. I find his work of great personal interest in obtaining more favorite shape to attain wave cancellation conditions.

I would like to make some remarks in regard to the first part of the paper. I have also investigated the possibility of using distributed doublet to obtain a better coincidence between the amplitude functions of the bow wave, $A(\theta)$, and the bulb wave, $B(\theta)$. Plotting $B(\theta)$, for various distribution of doublets, versus θ, I have compared these curves with the curves of $A(\theta)$ versus θ. A quick glance at these figures reveals that the amplitude function of the conical source distribution has in general a better match with the amplitude function of the hull than does that of the single doublet, especially in the region of large θ values. It must be kept in mind, however, that the linearized theory is being used, and that this theory is not very accurate for large values of θ due to the linearization of the free surface conditions. For this reason conclusions reached on the basis of purely mathematical considerations of the linearized theory are not strictly valid. An investigation of the wave steepness in the region of large θ will easily verify this fact (see Figure 7 in the paper at this seminar entitled, "Non-bulbous Hull Forms Derived From Source Distribution on the Vertical Rectangular Plane" by T. Inui).

I am afraid that if the problem of wave cancellation is approached from a mathematical point of view without regard to these facts, the results may lead to the wrong conclusions and will not aid the investigators in revealling the inherent physical character of the problem. This is the reason we emphasize wave observation so much.

Another thing I would like to point out is that due to the weight function $\cos^3\theta$ appearing in the integral for the wave-resistance,

$$R = \pi \rho V^2 \int_0^{\frac{\pi}{2}} [A_F(\theta) - B(\theta)]^2 \cos^3\theta \, d\theta$$

there is no need to take into account too heavily the difference of the amplitude function between the main hull and the single concentrated doublet for large values of θ.

For some time now I have been testing hull forms fitted with bulbs. Some of these bulbs correspond to the cases like Dr. Yim's draftwisely distributed doublet. The top of the bulbs were raised up to the waterline, with the shape of the bulb becoming a kind of cone fitted to the main hull. The test results were disappointing, as we had anticipated the resistance being considerably greater than predicted by theory and especially so in the low speed range The blunt shape of the stem disturbed the water surface sufficiently so that the boundary conditions of the linearized theory were seriously violated, thus producing higher drags than evaluated from that theory. Favorable wave cancellation could and was achieved with the single doublet, or its modifications, however, when the top of the bulb was kept a substantial distance below the water line. For these configurations the linear wave-resistance theory may prove to be valid to a sufficient degree of accuracy.

I would like to describe some of the work completed in Japan so far The major part of our work has been devoted to wave calculations and wave measurements. These have, to a large extent, been neglected in the past because no accurate means of measuring waves were available. In our opinion, waves generated by a ship are directly related to the hull form in contrast to ship wave-resistance, which is the "resultant" effects due to "compound" forces acting on the ship. In this context "resultant" and "compound" mean that the resistance results through an integral process of forces acting against the ship's bulb. For this reason theoretical calculations should be preceeded by experimental determination of wave patterns. Ambiguous factors, such as viscous effects, are also involved in the resistance measurements. It is very difficult to correct for these factors so as to correlate theoretical and experimental resistance results. On the other hand, one is able to completely observe and measure ship waves by means of available methods. Observed waves not only enable us to examine the validity of our theories, but also makes it possible to introduce reasonable corrections and often provides an intuitive insight into the mechanism of the wave-making phenomena.

I believe the above mentioned considerations must be taken fully into account in any evaluation of theoretical predictions, and I would welcome any effort made in regard to the problems concerned

with the ship wave phenomena, through such efforts the development of the field of ship hydrodynamics will proceed in an orderly scientific manner.

I would appreciate it if Dr. Yim would check his theoretical results by experiments inclusive of wave observation.

by H. Maruo

Dr. Yim's paper is truly excellent inspite of its somewhat abstract appearance, because it is not only the refinement of Inui's waveless bulb concept, but it has shown that the ship form of mathematically zero wave resistance can exist. The author has begun with the doublet and proceeds to higher singularity, i.e., quadrapole. In this respect I feel a little regret, that why he does not consider a simpler singularity that is the source. It can be easily proved that the waves generated by a source distribution along a horizontal line which represents a slender ship, can be offset by the waves generated by sources and sinks distributing along vertical lines at both ends. The ship form generated by these singularities is more feasible than Yim's m[illegible]l with vertical doublet distribution. The ship form by the source distribution has a deep (infinite) keel like a yacht. If the vertical keel is cut off at a finite depth, the wave resistance which remains uncancelled is identical to the wave resistance of the main part of the hull when it is submerged at the depth of the bottom of the keel. Experiments about this type of ship model is planned at Yokohama University tank.

by Lawrence W. Ward

I would like to make just one point; in regard to Equation (1) the limits of integration are not correct. I have discussed this point already in connection with Captain Shor's paper. Note:

$$\int_0^{\frac{\pi}{2}} d\theta \quad \text{should be} \quad \frac{1}{2}\int_{-\frac{\pi}{2}}^{\frac{\pi}{2} - \tan^{-1}\left|\frac{y}{x}\right|} d\theta \qquad y>0$$

$$\frac{1}{2}\int_{-\pi/2+\tan^{-1}\left|\frac{y}{x}\right|}^{\pi/2} d\theta \qquad y<0$$

I thank Professor Takahei for his kind compliment and his comment.

(a) As for the large value of $A(\theta)$ in the region of the large θ, I do not think that I have to discuss this point further since Dr. Eggers and Mr. Sharma pointed out and made clear that the large value of the integrand $A(\theta)$ for large θ does not necessarily mean large amplitude of waves. However, I do agree on the fact that we need not be concerned too much with the cancellation of elementary waves in the region of large θ values because of the weight function $\cos^3\theta$ appearing in the integral for the wave-resistance.

(b) As we see in the figures 1a and 2a, the optimum doublet distributions are not like conical distribution. It has a large value near the keel showing that a concentrated doublet near the keel may be a fair approximation to it. However, we notice in the figures 1a and 2a that the ideal doublet distribution cut off at the keel is much smaller in strength than the optimum one for the corresponding Froude number, although it looks like a conical shape. As Dr. Weinblum pointed out in his early paper (1935), the smaller bulb is more effective in the reasonably shallower depth.

I appreciate Professor Maruo's comment. The reason why I dealt with only the doublet and the quadrapole is that, by that way, the cancellation of waves at the bow is independent from that of the stern. Besides, the theory for bow waves is true for stern waves if we do not consider the influence of a propeller and the boundary layer. Yet, it seems to be better to consider the stern bulb including the influence. However, the consideration of source will be very helpful especially in the case when we have to worry about the increase of form drag due to the bow bulb.

In reply to Professor Ward's comment: Equation (1) is the wave height at a large x. At the large distance from the ship singularities the assymptotic behavior of ship waves is well known, and it can be said that the part of integral between $\pi/2$ and $\pi/2 - \tan^{-1}|y/x|$ in Equation (1) is negligible for all y. Therefore, the limit has been taken simply as (1) by Havelock (1951), and Inui (1960), and others as long as they concern the waves at a large x.

CALCULATION OF THE WAVE RESISTANCE OF A SHIP REPRESENTED BY SOURCES DISTRIBUTED OVER THE HULL SURFACE

J. P. Breslin
King Eng

Davidson Laboratory
Stevens Institute of Technology

INTRODUCTION

The purpose of the study reported here was to calculate the wave resistance of a ship represented by a source-sink distribution over its surface. The theoretical analyses of ship wave resistance in the past 65 years have utilized almost entirely representations of the ship by internal singularity distributions, the most common of these being centerline plane distributions employing the thin ship approximation. This yields a very simple relation between the source density, the speed and the local slope of the waterline. While such theoretical studies have been useful in indicating the manner in which many of the hull form parameters affect wave resistance, the thin ship theory has never been applied to a quantitative prediction of ship resistance to the satisfaction of naval architects. While there are certainly several facets of the analysis which leave much to be desired with respect to capturing the effects produced by real fluids, one simple observation that anyone can make is that almost all ships of practical interest are not thin. They are more aptly described as slender in that their length is 5 to 10 times the maximum breadth and, in addition, the breadth of many sections is 2 to 3 times the draft. Ship forms of low longitudinal prismatic coefficient (say less than 0.65) have a combination of thin and slender body characteristics in that their ends, i.e., the entrance and the run portions of their forms, are quite thin. Consequently, it seemed worthwhile to determine the importance of using a mathematical model which more closely represents the geometry of the hull. The opportunity to do this has been provided by the work of Hess and Smith[5] who have calculated the flow about a series 60 hull having a block coefficient of 0.60 using a method which does not depend on thin-ship approximations.

A statement of the problem which must be solved in order to represent a floating ship accurately is first given and followed by a description of the problem solved by Hess and Smith. Formulas for the wave resistance of an ensemble of sources are cited and methods of reducing them to numerical results are discussed. Results of these calculations and those for the thin ship wave resistance and their comparison with the residuary resistance coefficients derived from experiments with a 5-foot model are displayed. A discussion of the probable reasons for the differences obtained between thin ship and surface distributions is followed by hueristic arguments regarding the differences between residuary resistance and computed wave resistance. Finally, recommendations for developing a procedure which may enable practical estimates of ship wave resistance are formulated.

This work has been made possible through the support of the Society of Naval Architects and Marine Engineers under the cognizance of Analytical Wave Relations Panel H-5.

THE BOUNDARY VALUE PROBLEM FOR FLOATING BODIES

Throughout the discussion, the right-hand Cartesian coordinate system (x,y,z) is fixed in the body. The fluid is assumed to be incompressible and inviscid. The motion is taken to be irrotational and hence characterized by a velocity potential Φ which defines the fluid velocity $\vec{q}$ by $\vec{q} = -\nabla\Phi$.

Let us first consider a body moving in an infinite fluid, i.e., without boundaries, at a constant velocity $\vec{V}_\infty$. Its velocity potential Φ must satisfy Laplace's equation in the region C exterior to the body surface S, have a zero normal derivative on S, and approach the free stream potential at infinity.

$$\nabla^2 \Phi = 0 \quad \text{in} \quad C \tag{1}$$

$$\frac{\partial \Phi}{\partial n}\Big|_S = \vec{n} \cdot \nabla\Phi\Big|_S = 0 \tag{2}$$

$$\lim_{|\vec{r}|\to\infty} [\Phi] = -\vec{V}_\infty \cdot \vec{r} \tag{3}$$

where S is the surface of the body
C is the region exterior to S
$\vec{n}$ is the unit outward normal vector at a point on S
$\vec{V}_\infty = \vec{i}V_x + \vec{j}V_y + \vec{k}V_z$
$\vec{r} = \vec{i}x + \vec{j}y + \vec{k}z$

Let φ be the disturbance potential due to the body. Φ can be written as

$$\Phi = -\vec{V}_\infty \cdot \vec{r} + \varphi \tag{4}$$

and φ satisfies

$$\nabla^2 \varphi = 0 \quad \text{in} \quad C \tag{5}$$

$$\frac{\partial \varphi}{\partial n}\Big|_S = \vec{n} \cdot \nabla\varphi\Big|_S = \vec{n} \cdot \vec{V}_\infty\Big|_S \quad \text{on} \quad S \tag{6}$$

$$\lim_{|\vec{r}|\to\infty} [\varphi] = 0 \tag{7}$$

It is known that the potential φ can be represented by continuous source distribution σ on the body surface S, and φ [1] is given as

$$\varphi(x,y,z) = \iint_S \frac{\sigma(q)}{r(P,q)}\, dS \tag{8}$$

where $r(P,q)$ is the distance from the integration point $q(\xi,\eta,\zeta)$ on S to the field point $P(x,y,z)$. φ shown in Equation (8) satisfies Equations (5) and (7) automatically. The distribution of σ must be determined so that φ satisfies the normal derivative condition required by Equation (6). As long as P is not on S, differentiating Equation (8) under the integral sign is permitted.

$$\frac{\partial \varphi}{\partial n} = \iint_S \sigma(q)\, \frac{\partial}{\partial n}\left[\frac{1}{r(P,q)}\right] dS \tag{9}$$

As the field point P approaches the point p on surface S, it is shown in References 1 and 2 that $\partial\varphi/\partial n$ is discontinuous although $\lim_{P\to p} \partial\varphi/2n$ and $\partial\varphi/\partial n\big|_{P=p}$ both exist. In fact, we have

$$\lim_{P\to p} \frac{\partial \varphi}{\partial n} = -2\pi\sigma(p) + \frac{\partial \varphi}{\partial n}\bigg|_{P=p}$$

and, if we define $\partial\varphi/\partial n\big|_S$ as $\lim_{P\to p} \partial\varphi/\partial n$, we have explicitly

$$\frac{\partial \varphi}{\partial n} = -2\pi\sigma(p) + \iint_S \sigma(q)\, \frac{\partial}{\partial n}\left[\frac{1}{r(p,q)}\right] dS \tag{10}$$

Substituting Equation (10) into the boundary condition required by Equation (6), the result is a Fredholm integral equation of the second kind over the surface S.

$$\vec{n}(p) \cdot \vec{V}_\infty = -2\pi\sigma(p) + \iint_S \sigma(q)\, \frac{\partial}{\partial n}\left[\frac{1}{r(p,q)}\right] dS \tag{11}$$

For a floating body, Green's function G is chosen such that G satisfies Laplace's equation in the region C exterior to the body surface S. In addition to satisfying the normal derivative condition on S and approaching to the free stream potential at infinity, G must also satisfy the linearized free surface boundary condition [3]

$$\left(\frac{\partial^2 G}{\partial x^2} + k_o \frac{\partial G}{\partial z}\right)\bigg|_{z=o} = 0 \tag{12}$$

where $k_o = \dfrac{g}{|\vec{V}_\infty|^2}$.

If the body is moving along the positive x-axis at a constant speed U, G(given in Reference (4)) is of the form

$$G(p,q) = \frac{1}{r_1} - \frac{1}{r_2} + H(x,y,z;\ \xi,\ \eta,\ \zeta) \tag{13}$$

where

$$r_1^2 = (x-\xi)^2 + (y-\eta)^2 + (z+\zeta)^2 \tag{14}$$

$$r_2^2 = (x-\xi)^2 + (y-\eta)^2 + (z-\zeta)^2 \tag{15}$$

$$H = \frac{-4k_o}{\pi} R_e \int_0^{\pi/2} \int_{0\rightarrow}^{\infty} \sec^2\theta e^{[k(z+\zeta)+i(x-\xi)\cos\theta]} \frac{\cos[k_o(y-\eta)\sec^2\theta\sin\theta]}{k - k_o\sec^2\theta} dk d\theta \tag{16}$$

$$\vec{V}_\infty = -i\vec{U}$$

and

$$k_o = \frac{g}{|\vec{V}_\infty|^2} = \frac{g}{U^2}\ ,\ \text{the wave number of the motion.}$$

It is shown in Reference 4 that the function H is regular in the lower half plane (i.e., below the free surface) and has the property at vanishing Froude number (infinite wave number)

$$\lim_{k_o\rightarrow\infty}(H) = \frac{2}{r_2} \tag{17}$$

and, at large Froude number,

$$\lim_{k_o\rightarrow 0}(H) = 0 \tag{18}$$

Substituting Equation (13) into (11), the integral equation for surface distribution of a floating body is

$$\vec{n}(p)\cdot\vec{V}_\infty = -2\pi\sigma(p) + \iint_S \sigma(q) \frac{\partial}{\partial n}\left[\frac{1}{r_1(p,q)} - \frac{1}{r_2(p,q)} + H(p,q)\right] dS \tag{19}$$

Within the accuracy of the linearized free surface, the first order approximation of the surface distribution velocity potential is

$$\varphi(P) = \iint_S \sigma(q)\left[\frac{1}{r_1(P,q)} - \frac{1}{r_2(P,q)} + H(P,q)\right] dS \tag{20}$$

where the source distribution σ is determined by Equation (19). Thus, in the presence of the free surface, the source density σ will depend

not only on body geometry but also on the Froude or wave number because of the presence of the function H.

It is obvious that Equation (19) is very difficult to solve, principally because H involves a double integration over wave direction angle and all wave numbers k_o. There is no need to emphasize here the complexities of the problem. Hess and Smith[5] of Douglas Aircraft have solved for the source distribution representing the flow at zero Froude number for a series 60 ship numerically. The integral equation they consider is secured by substituting (17) into (20), namely

$$\vec{n}(p) \cdot \vec{V}_\infty = -2\pi\sigma(p) + \iint_S \sigma(q) \frac{\partial}{\partial n} \left[\frac{1}{r_1(p,q)} + \frac{1}{r_2(p,q)} \right] \quad (21)$$

and, hence, the effect of the presence of the free surface is obtained for small Froude numbers. This corresponds physically to reflecting the ship form in the free surface. Basically, their approach is as follows:

The body surface is approximated by a large number of small plane quadrilateral elements which are formed from the original points defining the body surface. The source density is assumed constant over each of these elements. This assumption reduces the problem of determining the continuous function σ to the problem of determining a finite number of σ (one for each of the planar elements). The contribution of each element to the integral in (21) is obtained by taking the constant but unknown value of σ on that element out of the integral, and then performing the indicated integration of known geometrical quantities over that element. Thus, requiring Equation (21) to hold at one point p gives a linear relation between the unknown values of σ on the plane elements. On each element, one point is selected where Equation (21) is required to hold. This gives a number of linear equations equal to the number of unknown values of σ. Once these are solved, flow velocities may be evaluated at any point by summing the contributions of the plane elements and adding proper components of the onset flow. Thus, the source densities σ's can be obtained by solving this system of simultaneous equations.

The source densities determined in this manner are panel sources, i.e., within an elementary area, the source strength is constant, being uniformly distributed over that area. For the present wave resistance calculations, the panel sources are considered as point sources located at the centroid of the elementary area. There are questions as to the validity of this approach and an investigation has been made. Although no "iron-clad" conclusions can be arrived at from the study, the general

tendencies do show that considering the panels as point sources is sufficiently accurate for the purposes of calculating wave resistance. This is due to the fact that the source panels are all very small compared to the length of the waves generated in the range of Froude numbers of interest.

THE WAVE RESISTANCE OF AN ENSEMBLE OF POINT SOURCES

The wave resistance generated by descrete sources can be calculated from the following expression given in Reference 6 or 7:

$$R = 16\pi\rho k_o^2 U^2 \int_0^{\pi/2} (P_1^2 + P_2^2 + P_3^2 + P_4^2)\sec^3\theta \, d\theta \qquad (22)$$

The functions P_j are, for finite number of point sources, given by the sums

$$P_1 = \sum_i m_i' \cos(x_i k_o \sec\theta)\cos(y_i k_o \sec^2\theta \sin\theta)e^{-k_o z_i \sec^2\theta}$$

$$P_2 = \sum_i m_i' \sin(x_i k_o \sec\theta)\cos(y_i k_o \sec^2\theta \sin\theta)e^{-k_o z_i \sec^2\theta}$$

$$P_3 = \sum_i m_i' \cos(x_i k_o \sec\theta)\sin(y_i k_o \sec^2\theta \sin\theta)e^{-k_o z_i \sec^2\theta}$$

$$P_4 = \sum_i m_i' \sin(x_i k_o \sec\theta)\sin(y_i k_o \sec^2\theta \sin\theta)e^{-k_o z_i \sec^2\theta}$$

where

$m_i' = \sigma_i A_i$, the strength of the source

A_i is the area of the quadrilateral element

(x_i, y_i, z_i) is the selected coordinate of the source point

It is of some interest to observe that the wave resistance can be reduced to a summation involving tabulated functions.

We may write

$$(P_1^2 + P_2^2 + P_3^2 + P_4^2) = \sum_i \sum_j m_i' \, m_i' \cos[k_o(x_i - x_j)\sec\theta]$$

$$\cos[k_o(y_i - y_j)\sec^2\theta \sin\theta]e^{\,k_o(z_i+z_j)\sec^2\theta} \qquad (23)$$

Substituting (23) into (22) and interchanging the order of integration and summation

$$R = 16\pi\rho k_o^2 U^2 \sum \sum m_i' \, m_j' \, r_{ij} \qquad (24)$$

where

$$r_{ij} = \int_0^{\pi/2} \cos(\xi_{ij}\sec\theta)\cos(\eta_{ij}\sec^2\theta \sin\theta)e^{-z_{ij}\sec^2\theta}\sec^3\theta d\theta \tag{25}$$

ξ_{ij} $k_o(x_i-x_j)$, $\eta_{ij} = k_o(y_i-y_j)$ and $\zeta_{ij} = k\,(z_i+z_j)$

By letting $\sec\theta = \cosh\frac{u}{2}$, Equation (25) takes the form

$$r_{ij} = \frac{e^{-\zeta_{ij}}}{4}\int_0^{\infty} \cos(\xi_{ij}\cosh\frac{u}{2})\cos(\eta_{ij}\frac{\sinh u}{2})e^{-\zeta_{ij}\cosh u}(1+\cosh u)du \tag{26}$$

If $i = j$, then $\xi_{ij} = 0$, $\eta_{ij} = 0$ and

$$r_{ii} = \frac{e^{-\zeta_{ii}}}{4}\int_0^{\infty} e^{-\zeta_{ii}\cosh u}(1+\cosh u)du$$

or

$$*r_{ii} = \frac{e^{-\zeta_{ii}}}{4}\,[K_o(\zeta_{ii}) + K_1(\zeta_{ii})] \tag{27}$$

where K_n are the modified Bessel functions of the second kind. There is a series solution for r_{ij}, $i \neq j$.

$$*r_{ij}\ (i\neq j) = \frac{e^{-\zeta_{ij}}}{4\sqrt{\pi}}\sum_{m=o}^{\infty}\sum_{n=o}^{\infty} A_{mn}\xi_{ij}^{2m}\eta_{ij}^{2n}\zeta_{ij}^{-n}\sum_{q=o}^{m+1}\binom{m+1}{q} K_{n+q}(\zeta_{ij}) \tag{28}$$

where

$$A_{mn} = \left(\frac{-1}{2}\right)^{m+n}\frac{\Gamma(n+\frac{1}{2})}{(2m)!(2n)!}$$

$\binom{m+1}{q}$ are the binomial coefficients

---

*See Appendix

Due to the complexity of this solution, however, Equation (28) has little merit for numerical computation. Normalizing the strength of the sources by ℓ^2 and the wave resistance by $\frac{1}{2}\rho U^2 L^2$, expression (24) becomes

$$R' = \frac{R}{\frac{1}{2}\rho U^2 L^2} = 2\pi(k_o L)^2 \sum_i \sum_j m_i m_j r_{ij}$$

where $m_i = \frac{m'}{\ell^2}$ and $L = 2\ell$.

The double series can be thought of as a square matrix with elements $R_{ij} = m_i m_j r_{ij}$. Equation (29) can be written as

$$\frac{R'}{2\pi(k_o L)^2} = (1\ 1 \ldots . 1) \begin{pmatrix} R_{11} & R_{12} \cdots\cdots\cdots & R_{1N} \\ R_{21} & R_{22} \cdots\cdots\cdots & R_{2N} \\ \vdots & \vdots & \vdots \\ R_{N1} & R_{N2} \cdots\cdots\cdots & R_{NN} \end{pmatrix} \begin{pmatrix} 1 \\ 1 \\ \vdots \\ 1 \end{pmatrix} \qquad (30a)$$

or

$$\frac{R'}{2\pi(k_o L)^2} = (m_1\ m_2 \ldots . m_N) \begin{pmatrix} r_{11} & r_{12} \cdots\cdots\cdots & r_{1N} \\ r_{21} & r_{22} & \vdots \\ & & \\ r_{N1} & \cdots\cdots\cdots & r_{NN} \end{pmatrix} \begin{pmatrix} m_1 \\ m_2 \\ \vdots \\ m_N \end{pmatrix} \qquad (30b)$$

Since $r_{ij} = r_{ji}$ as displayed in Equation (25), the square matrices in both (30a) and (30b) are symmetrical matrices. Physically, the diagonal terms are the wave resistance of the individual sources, and the off diagonal terms are the contribution from the interaction between sources. By expressing the wave resistance expression in such form, one can, in principle, observe from computer readouts the contribution to wave resistance from various parts of the body.

STRENGTH DENSITY OF SOURCES DISTRIBUTED ON THE HULL SURFACE AND ON THE CENTER PLANE

Curves of the source densities determined numerically by Hess and Smith[5] for the Series 60, C_B = 0.60 hull are presented in Figures 1a, 1b and 2a through 2e. Also shown in Figures 1a and 1b are the center-plane source densities calculated for the thin ship approximation in which the hull is fitted with a 70-term polymonial presented in Reference 8. It is interesting to note that the surface sources near the water-plane (small z/d) are about twice as strong as the thin ship sources. This is accounted for by the presence of strong sinks needed on the surface to meet the boundary condition in the vicinity of the keel; a comparable sink distribution in forebody (and sources in after-body near the keel) is not present in the thin ship distribution. The hull-surface source distributions shown in Figures 2a through 2e are particularly intriguing displaying rapid changes (as might be expected) at the turn of the bilge. The knowledge of the nature and relative magnitudes of these surface distributions allow us to make qualitative analysis of the results of the resistance calculations.

DESCRIPTION OF MODEL EXPERIMENTS

A model of the Series 60, C_B = 0.60 hull as fitted by polynomials (see Reference 8) was built and towed at Davidson Laboratory. The model has the following principal dimensions:

Length L	5.000 ft.
Beam B	.670 ft.
Draft d	.267 ft.
Wetted Surface S_w	4.233 sq. ft.

It is emphasized that the lines used are those for which Hess and Smith[5] made their calculations. These lines differ in the bow and stern regions from the actual Series 60 lines. The lines used do not contain a propeller aperature and are considerably "thinner" in the stern quarters. It is not believed, however, that these differences would lead to significant effects on wave resistance.

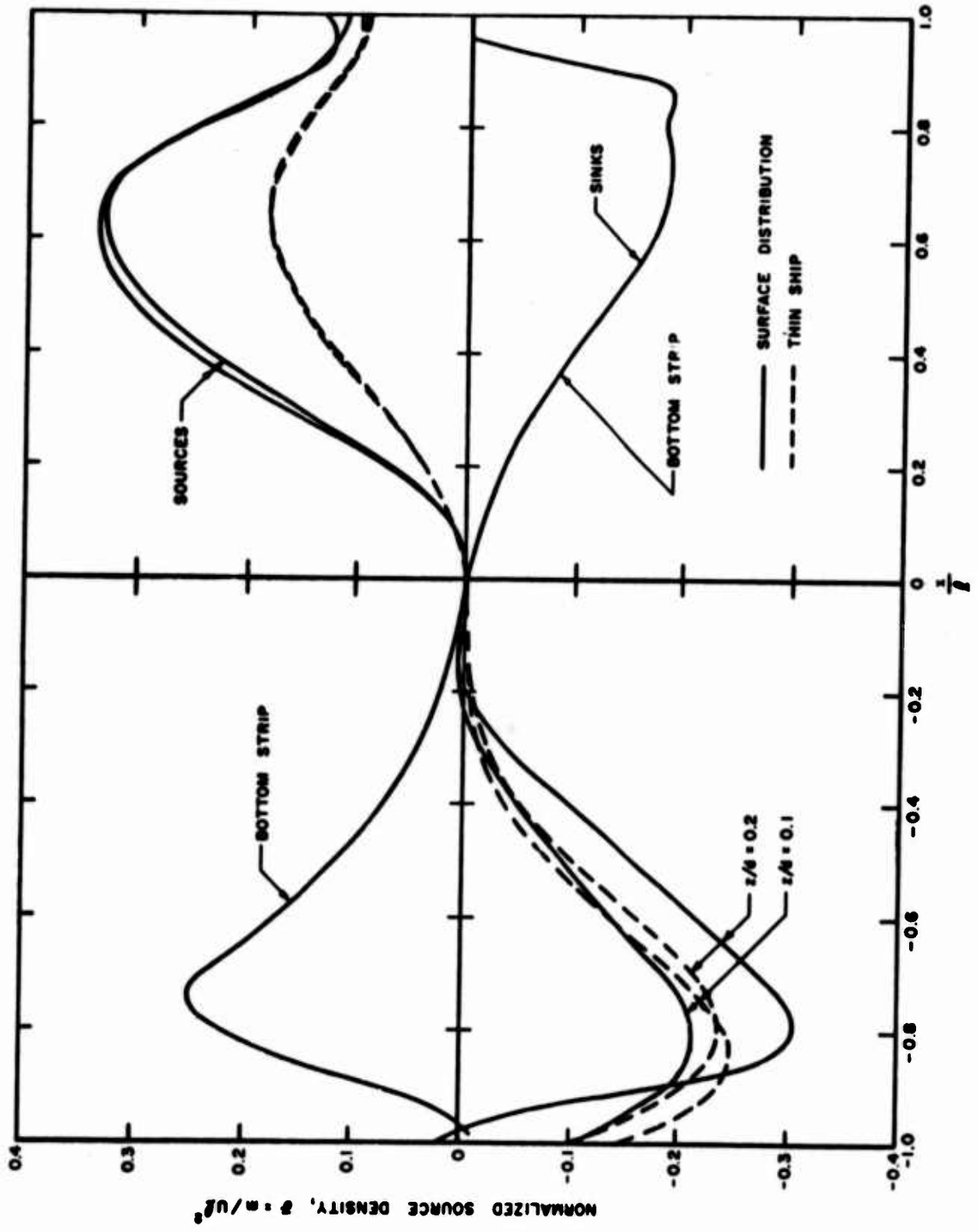


FIGURE 1a. SOURCE DISTRIBUTION AT VARIOUS WATER LINES

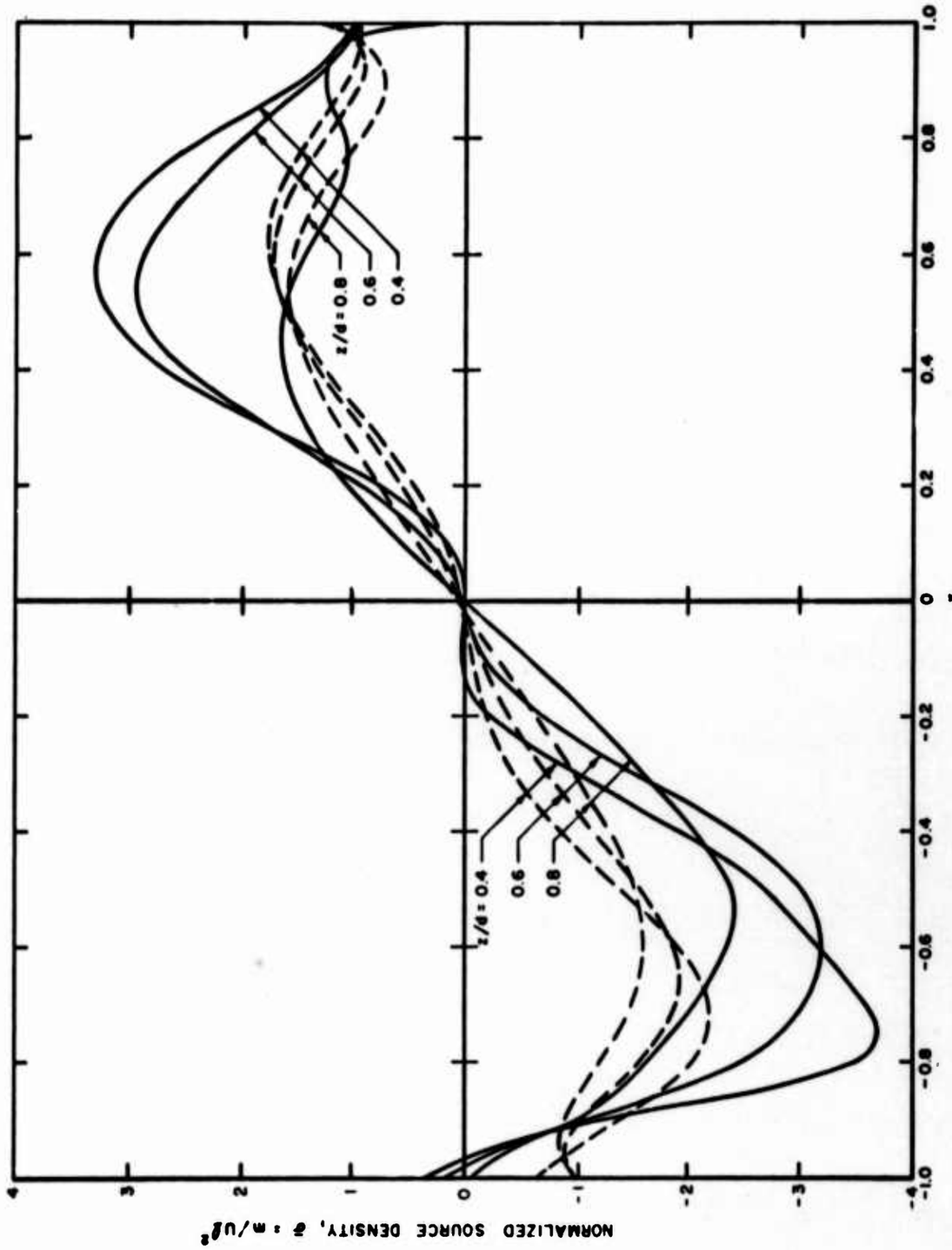


FIGURE Ib. SOURCE DISTRIBUTION AT VARIOUS WATER LINES

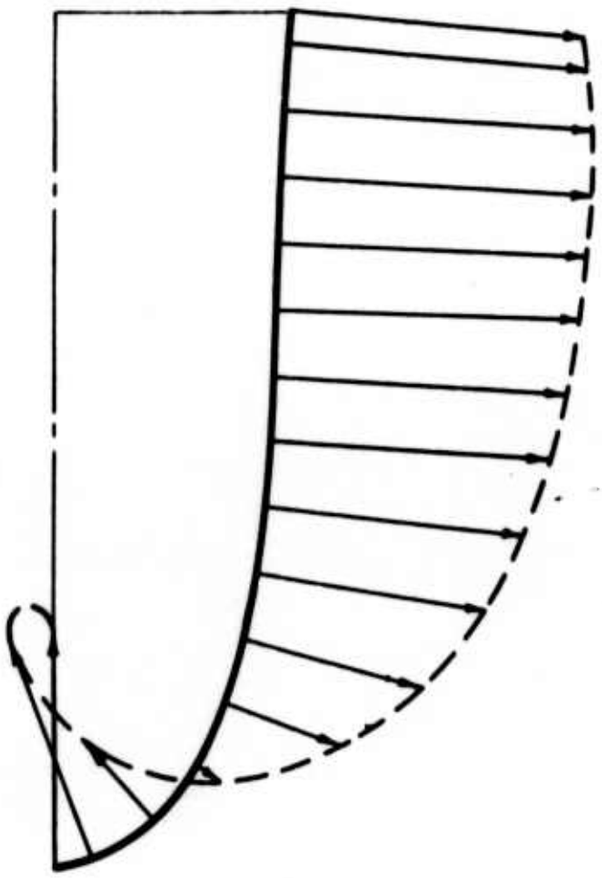


FIGURE 2 a. SOURCE STRENGTH DISTRIBUTION AT $(X/\ell) = 0.801$

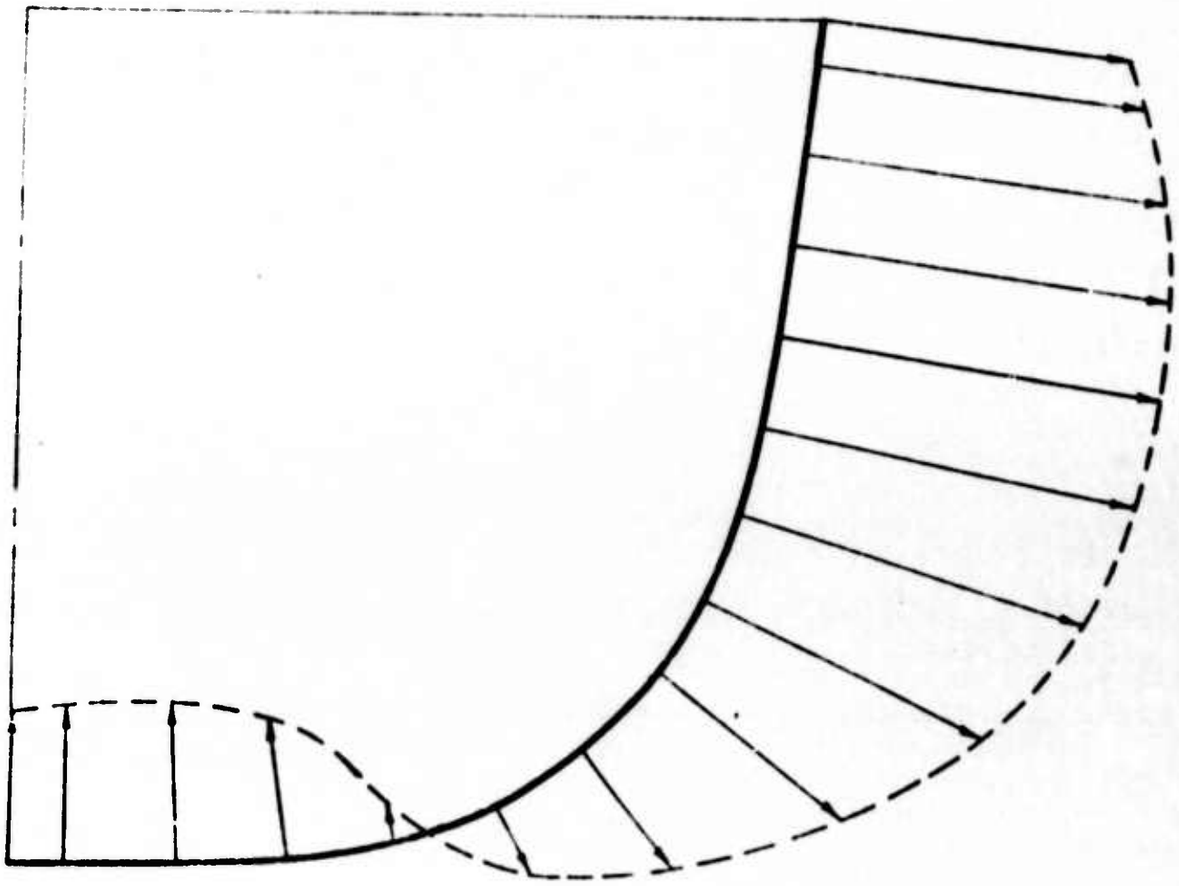


FIGURE 2b. SOURCE STRENGTH DISTRIBUTION AT $(X/\ell)=0.476$

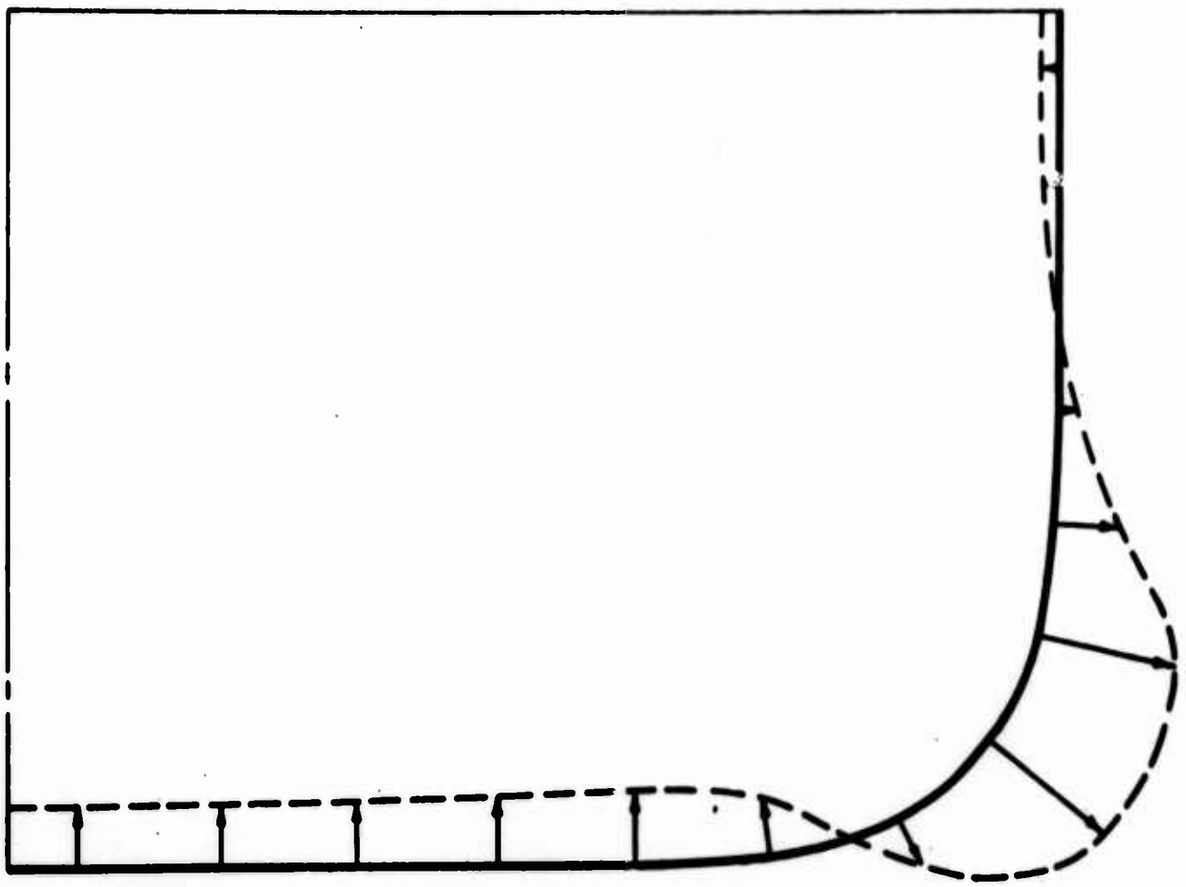


FIGURE 2c. SOURCE STRENGTH DISTRIBUTION AT $(X/\ell)=0.0224$

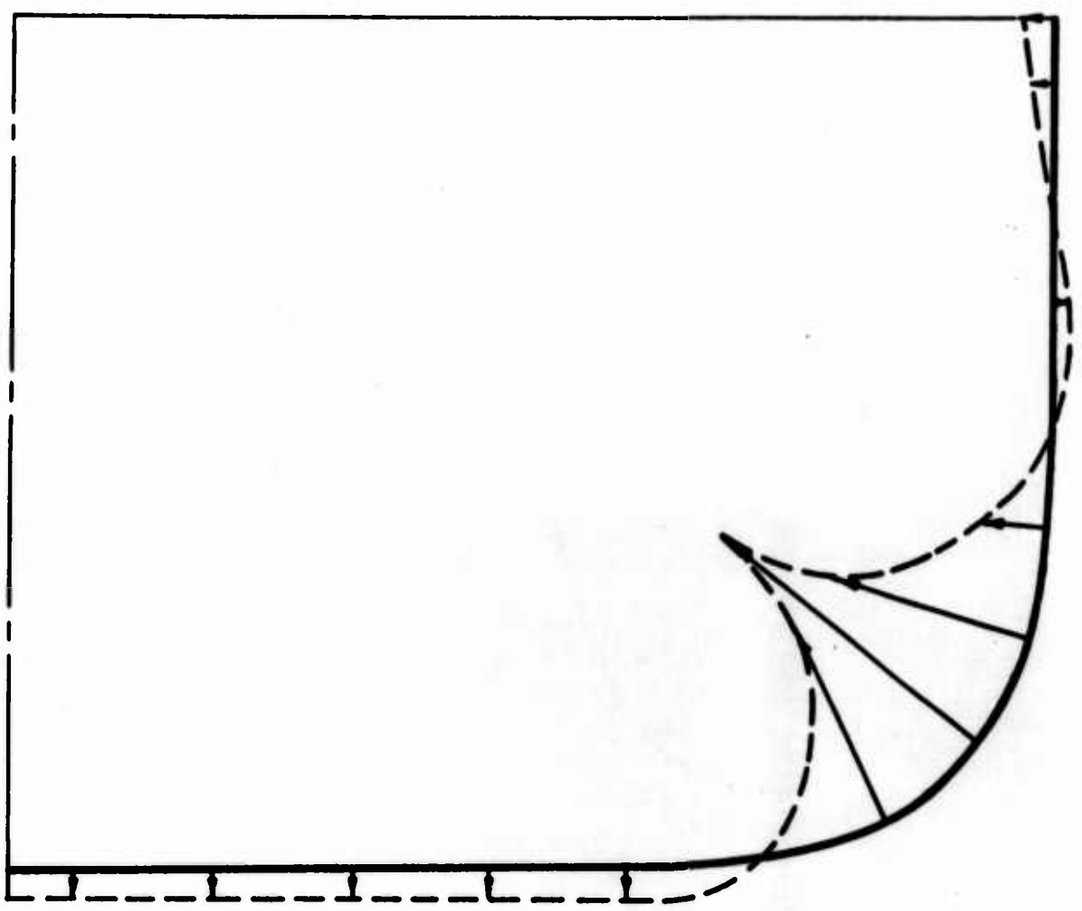


FIGURE 2d. SOURCE STRENGTH DISTRIBUTION AT (X/ℓ)=-0.0424

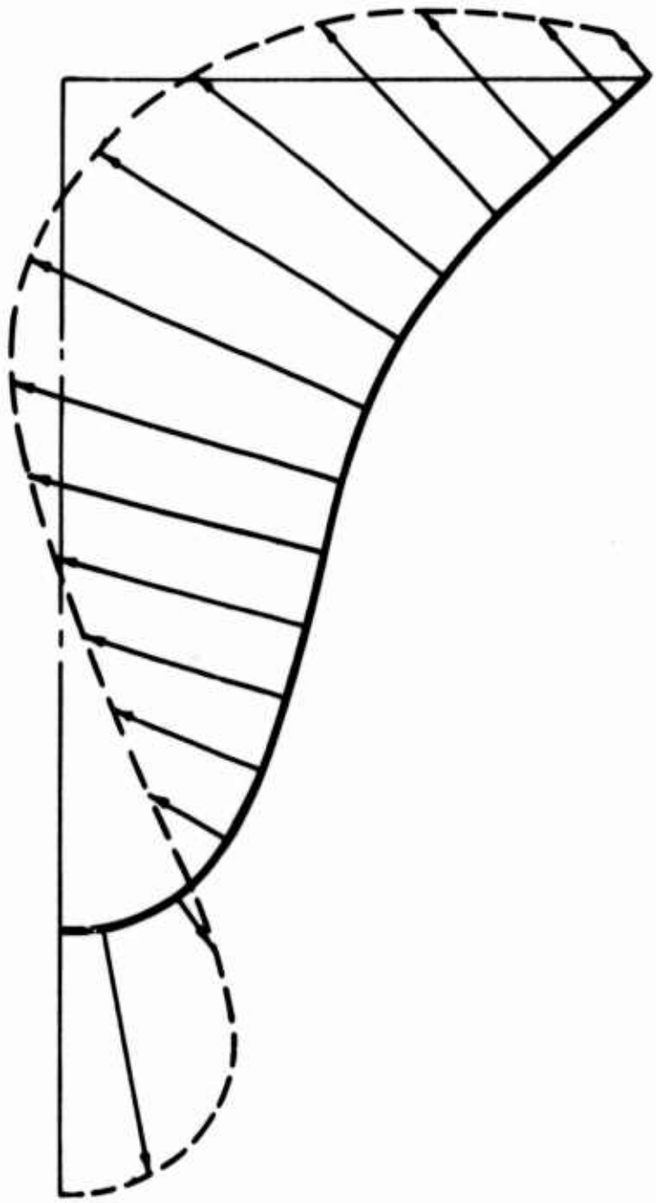


FIGURE 2e. SOURCE STRENGTH DISTRIBUTION AT $(X/\ell) = -0.755$

Towing tests over a wide range of Froude numbers (0.20 to 0.65) were conducted in Tank NO. 3 with the model fixed in heave and trim and also with freedom in heave and trim. Curves of model residuary resistance are given for sake of reference in Figure 3. Curves of residuary resistance coefficient obtained by subtracting the Schoenherr flat plate frictional resistance from the total and dividing the result by $1/2\ \rho L^2U^2$ (where L is the waterline length, the model ends being vertical) are shown in Figure 4. It is seen that the resistance of the model restrained in both heave and trim is less than when unrestrained at higher Froude numbers. This is in keeping with experience, the reason being that the displacement is effectively reduced as a long wave is developed so that the resulting form provides less disturbance to the water.

COMPARISON OF CALCULATED WAVE RESISTANCES AND RESIDUARY RESISTANCE DERIVED FROM EXPERIMENT

In Figure 4, it is seen that the wave resistance computed from surface sources is larger than that from the thin ship sources at all Froude numbers less than 0.53 and the reverse is true at higher numbers. This behavior may be qualitatively explained from the relative magnitudes of the source densities shown in Figures 1 and 2. At low Froude numbers the sources near the surface have a predominant role since those near the keel are attenuated by a function of the form

$$e^{-\frac{2\pi}{\lambda} z}$$

in which the wave length λ and depth to the source element z are of comparable magnitude at low Froude numbers. However, at high Froude numbers the draft becomes small compared to the dominant wave length and the bottom sinks on the hull surface provide sensible interference terms which may account for the reduction in wave resistance below that of the thin ship for $F > 0.53$.

In regard to resistance from model data, it is important to note the excellent agreement between the residuary resistances obtained from the 5-foot Stevens model and the 20-foot model towed under comparable conditions at David Taylor Model Basin. This is typical of the comparisons obtained on normal hull forms from these two towing tanks.

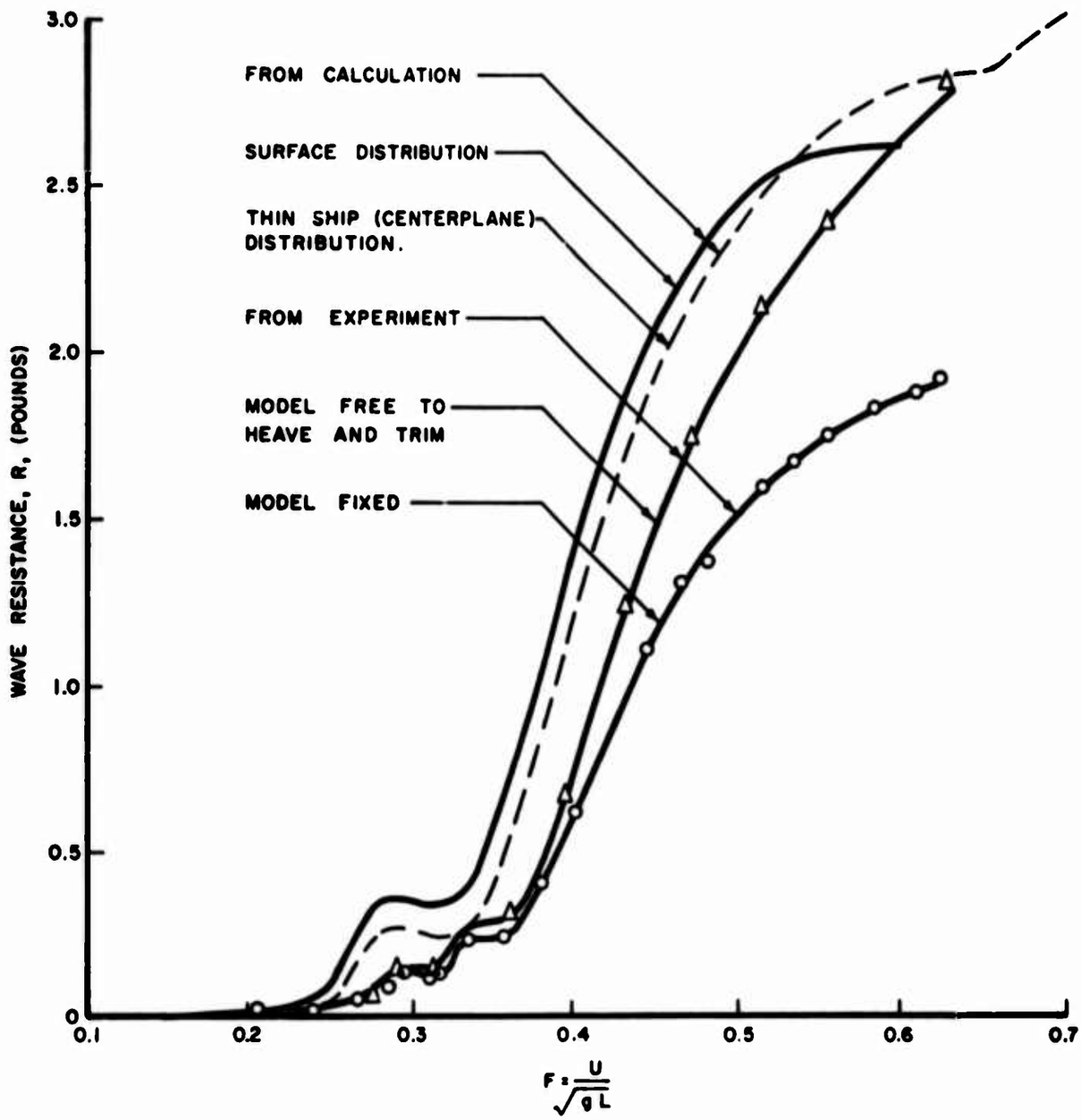


FIGURE 3. MEASURED WAVE RESISTANCE FROM SERIES 60 MODEL VERSUS FROUDE NUMBER. MODEL LENGTH, L, = 5 FEET.

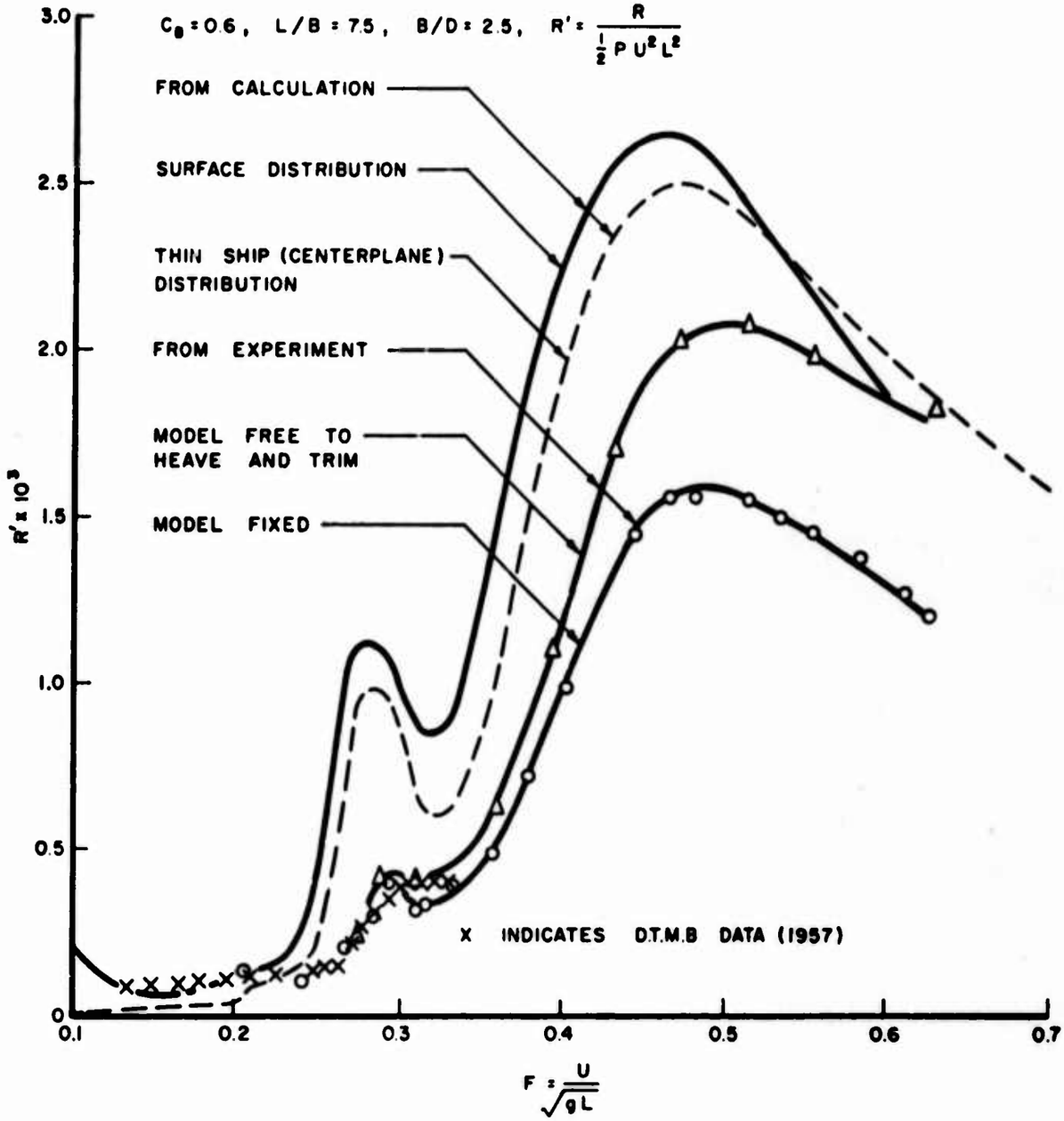


FIGURE 4. WAVE RESISTANCE COEFFICIENT, R_W' OF A SERIES 60 SHIP VERSUS FROUDE NUMBER, F.

Comparison of the theoretical curves of wavemaking resistance with the residuary resistance derived from experiment reveals large differences at all Froude numbers in excess of 0.23. It is believed that these differences may arise from two weaknesses in the theory and from a questionable procedure in the standard reduction of model data. These are:

1) Failure to account for the effect of viscosity on the wave-producing capacity of the stern
2) Failure to account for the effect of the deformed free surface on the hull boundary condition and hence upon the source density
3) The residuary resistance derived in the usual manner from tank tests is not the wave resistance of the model.

Many observers of model tests have noted the fact that the stern waves generated by a model are much less pronounced than those generated by the bow. But the present theory makes use of a potential function which provides a disturbance pressure distribution achieving full stagnation pressures both at the bow and the stern. Pressure distributions obtained from wind tunnel, water tunnel and towing tanks always reveal a significant reduction in pressure in the trailing edge region of all bodies, even those that are thin due to the action of viscosity. It would, therefore, seem much more reasonable to modify in a rational fashion the source strength in the disturbance potential and, hence, the free surface Green's function to allow for this softening effect of viscosity on the stern pressures and thus provide much smaller stern waves in the mathematical model.

A quick demonstration of the pronounced influence of stern lines on the humps and hollows exhibited by the usual representations at low Froude number is afforded by Figure 5. Here it may be seen that the wave resistance of a thin strut with parabolic water lines is modified in the direction of experimental behavior by providing a cusped after-body thereby reducing the disturbance pressure coefficient at the trailing edge from 1.0 to 0.086. The humps and hollows at low Froude number are strongly attenuated and the resistance decreased.

Sir Thomas Havelock[12] has shown in greater detail the important effects obtained by modifying the stern lines to account for the gross action of viscosity in the generation of wave drag by the extreme stern shape. In this connection, Inui has advocated a procedure to correcting model resistance data to account for the attenuated stern waves and a shift in phase between the theoretical and observed wave profile. However, application of his correction curves to this case of the Series 60 does not yield

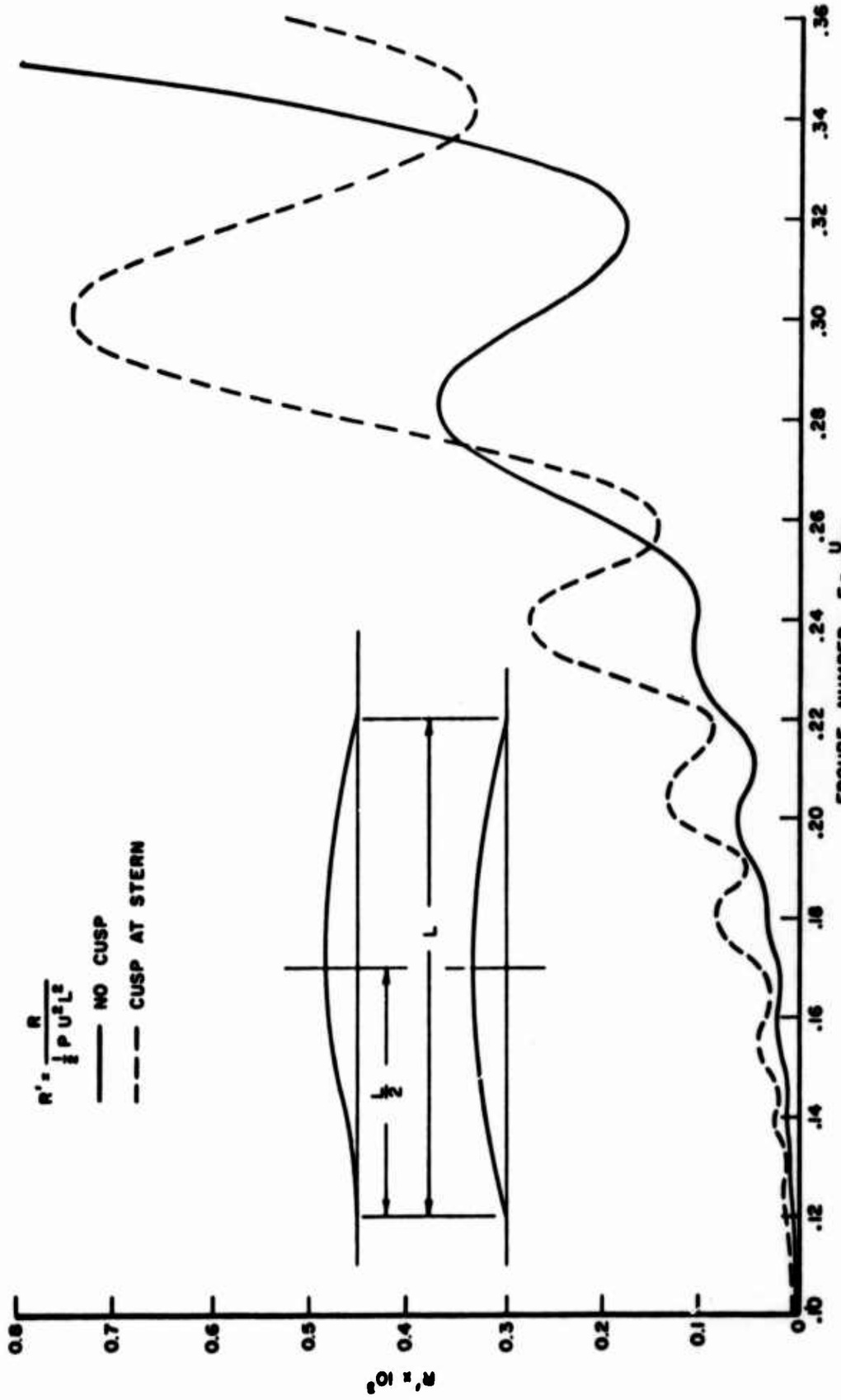


FIGURE 5. COEFFICIENT OF WAVE RESISTANCE OF INFINATE STRUT

any noticeable correction to the theory. It seems safe to say that no entirely rational procedure has yet been devised to correct the theoretical wave resistance calculation. A proposal for a new procedure will be given later.

The fact that the existence of waves generated by the first order mathematical model is ignored in regard to the determination of the source density from the hull boundary condition is considered to be an important omission in the presently employed scheme. This omission must certainly become important as $F \rightarrow 0.50$ and may be important at Froude numbers much lower than this. Inclusion of the effect of the function H in Equation (19) at each F appears to be dependent upon developing a computer program which can economically compute the double integral (k- and θ integrals) upon which H depends. It would seem feasible to devise a less accurate representation of the hull by use of fewer singularities in order to investigate the importance of the image contribution to the boundary conditions at all Froude numbers of interest.

Almost all model tank experimenters agree that the residuary resistance (as usually calculated by subtracting out some flat plate friction) is not the wave resistance of the hull. Thus, in addition to wave drag, the residuary resistance also contains the viscous pressure drag, the skin friction arising from three-dimensional form effects and spray drag at large speeds. Several efforts have recently been made to isolate wave resistance by measuring the waves at some distance astern and also by making a multi-tube wake survey well abaft of a model. The results of these studies are stimulating but, until they have been scrutinized in detail and applied more widely, it does not seem possible to draw a well-founded conclusion. It is the authors' opinion that wind tunnel experiments with a reflected model can be effective in isolating the skin friction and viscous form drag of ship hulls.

CONCLUSIONS AND RECOMMENDATIONS

The calculation of wave resistance from a mathematical model made up of sources distributed over the surface which accurately meet the boundary condition as $F \rightarrow 0$ shows that a larger resistance is secured than from the corresponding thin ship method for all Froude numbers of practical interest. However, this improved representation of the hull does not yield better agreement with residuary resistance derived from model tests except at exceedingly low Froude numbers.

It is recommended that steps be taken to remove the lack of realism in the mathematical model with respect to the wave-generating characteristics of the stern. This might be done by measuring the pressure distribution in the stern region and into the wake of a reflecting model in a wind tunnel at the same Reynolds number achieved in the towing tank. The drag of the lower half model could also be secured while in the tunnel. One may then calculate a source-sink distribution which would meet the kinematic condition on the fore part--say forward two-thirds of the length and would also satisfy the pressure variation over the latter third length and into the wake. This would require solving a mixed boundary value problem analogous to cavity flows except that the pressure varies as determined from the measurements in lieu of being constant as in the cavity region. The model can then be towed in a tank and the wind tunnel drag subtracted from the total to leave the wave resistance plus the free surface effect on the viscous drag (which should be small). The wave resistance predicted from the source distribution (determined in the manner described) above can then be compared to difference to towing tank and wind tunnel data to check the validity of the procedure. It would be best to attempt this procedure on a strut ship first since a method exists for solving the integral equation for the source density required to meet both kinematic and pressure conditions in two dimensions.

REFERENCES

1. Sternberg, W. and Smith, T., "The Theory of Potential and Spherical Harmonics," University of Toronto Press, 1961.

2. Kellogg, O. D., "Foundation of Potential Theory," Dover Edition, 1953.

3. Stoker, J. J., "Water Waves," Interscience Publication, 1957.

4. Peters, A. S. and Stoker, J. J., "The Motion of a Ship, as a Floating Rigid Body, in a Seaway," Communications on Pure and Applied Mathematics, Volume X, No. 3, August 1957.

5. Hess, J. L. and Smith, A. M. O., "Calculation of Non-Lifting Potential Flow About Arbitrary Three-Dimensional Bodies," Douglas Aircraft Report No. E. S. 40622, March, 1962.

6. Lunde, J. K., "On the Theory of Wave Resistance and Wave Profile," Skipsmodelltankens Meddelelse NR. 10, April 1952.

7. Lunde, J. K., "On the Linearized Theory of Wave Resistance for Displacement Ships in Steady and Accelerated Motion," Trans. SNAME, Vol. 59, 1952, pp. 25-76.

8. Gerritsma, J., Kerwin, J. E., Newman, J. N., "Polymonial Representation and Damping of Series 60 Hull Forms," International Shipbuilding Progress, Vol. 9, No. 95, July 1962.

9. Birkhoff, G., Korvin-Kroukovsky, B. V., Kotik, J., "Theory of the Wave Resistance of Ships - Part 1: The Significance of Michell's Integral," SNAME, November 1954.

10. Watson, G. N., "Theory of Bessel Functions," Second Edition, 1952.

11. McLachlan, N. W., "Bessel Functions for Engineers," Oxford University Press, 1941.

12. Havelock, T. H., "Calculation Illustrating the Effect of Boundary Layer on Wave Resistance," Transactions of the Inst. of Naval Architects, March 1948.

APPENDIX

Evaluate the integral of the form

$$r_{ij} = \frac{e^{-z_{ij}}}{4} \int_0^\infty \cos(x_{ij}\cosh\frac{u}{2})\cos(y_{ij}\frac{\sinh u}{2})e^{-z_{ij}\cos hu}(1+\cosh u)du \tag{1}$$

where

$$x_{ij} = k_o(\xi_i - \xi_j)$$

$$y_{ij} = k_o(\eta_i - \eta_j)$$

$$z_{ij} = \frac{k_o}{2}(\zeta_i + \zeta_j)$$

If $i = j$, then $x_{ii} = 0$, $y_{ii} = 0$ and $z_{ii} = k_o\zeta_i$. Hence

$$r_{ii} = \frac{e^{-z_{ii}}}{4} \int_0^\infty e^{-z_{ii}\cosh u}(1+\cosh u)du \tag{2}$$

From Reference 10, p. 181, Equation (2) is represented by modified Bessel functions of the second kind

$$r_{ij} = \frac{1}{4} e^{-z_{ii}}[k_o(z_{ii}) + k_1(z_{ii})] \tag{3}$$

If $i \neq j$, expand the cosine function in Equation (1) into Maclaurin's series

$$\cos(x_{ij}\cosh\frac{u}{2}) = \sum_{m=0}^{\infty} \frac{(-1)^m}{2^m(2m)!} x_{ij}^{2m}(1+\cosh u)^m \tag{4}$$

$$\cos(y_{ij}\frac{\sinh u}{2}) = \sum_{m=0}^{\infty} \frac{(-1)^n}{2^{2n}(2n)!} y_{ij}^{2n}(\sinh u)^{2n} \tag{5}$$

Upon substituting Equations (4) and (5) into (1) and interchanging the order of summation and integration, the expression r_{ij} for $i \neq j$ becomes

$$r_{ij} = \frac{1}{4} e^{-z_{ij}} \sum_{m=0}^{\infty}\sum_{n=0}^{\infty} \frac{(-1)^{m+n} x_{ij}^{2m} y_{ij}^{2n}}{(2m)!(2n)!2^{(m+2n)}} \int_0^\infty e^{-z_{ij}\cosh u}(1+\cosh u)^{(m+1)}\sinh^{2n} du \tag{6}$$

From Reference 11, p. 165, Equation (126) is given as

$$\int_0^\infty e^{-z\,\cosh u} \sinh^{2n} u\, du = \frac{2^n}{\sqrt{\pi}}\,\Gamma(n+\tfrac{1}{2})\; z^{-n} K_n(z) \qquad (7)$$

By successively differentiating Equation (7) under the integral sign with respect to z and using the relationship

$$K_{n+1}(z) = \frac{n}{z}\,K_n(z) - K_n'(z)$$

a recursion formula can be obtained

$$\int_0^\infty e^{-z\,\cosh u} \cosh^{q} u\, \sinh^{2n} u\, du = \frac{2^n}{\sqrt{\pi}}\,\Gamma(n+\tfrac{1}{2}) z^{-n}\, K_{n+q}(z) \qquad (8)$$

Upon expanding $(1 + \cosh u)^{m+1}$ and applying Equation (8), the integral in (6) becomes

$$\int_0^\infty e^{-z_{ij}\cosh u}(1+\cosh u)^{m+1}\sinh^{2n} u\, du = \frac{2^n}{\sqrt{\pi}}\,\Gamma(n+\tfrac{1}{2}) z_{ij}^{-n} \sum_{q=0}^{m+1} \binom{m+1}{q} K_{n+q}(z_{ij}) \qquad (9)$$

where $\binom{m+1}{q}$ is the binomial coefficient.

Denoting

$$A_{mn} = \frac{(-1)^{m+n}}{2^{m+n}}\,\frac{\Gamma(n+\frac{1}{2})}{(2m)!\,(2n)!}$$

$$r_{ij} = \frac{e^{-z_{ij}}}{A\sqrt{\pi}} \sum_{m=0}^{\infty}\sum_{n=0}^{\infty} A_{mn}\, x_{ij}^{2m}\, y_{ij}^{2n}\, z_{ij}^{-n} \sum_{q=0}^{m+1} \binom{m+1}{q} K_{n+q}(z_{ij}) \qquad (10)$$

ON THE RELATIONS BETWEEN A PRACTICAL SHIP-HULL FORM AND AN ATTEMPTED SINGULARITY DISTRIBUTION

Nobutatsuo Yokoyama

Fishing Boat Laboratory
Fisheries Agency of Japan

ON THE RELATION BETWEEN PRACTICAL SHIP'S HULL FORM AND AN ATTEMPTED SINGULARITY DISTRIBUTION

ABSTRACT

A simulation of ship body is attempted in this paper with linear singularity distributions on some stratified horizontal lines in the center plane. For the first step an algebraic power series is applied to this method, and could not entirely succed in obtaining analytical aspect on the relation between the form of ship hull and distribution. This simple method, however, appears to be promising if the resulting fluctuation of solution is removed by means of mathematically smoothed function for approximated distribution and increase of boundary points widely covering the hull surface to the practical extent. For the local examination this method is still applicable by spreading boundary points around a focused part.

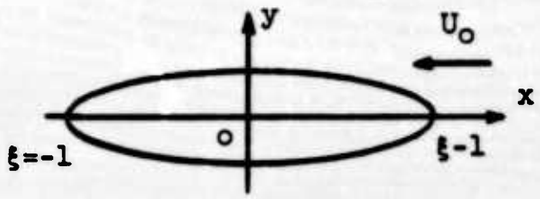
Contents

1. Introduction
2. Outline of the Method
3. Induced Velocity Term Integrals
4. Coefficients for Singularities Distribution
5. Stream on the Hull Surface
6. Numerical Evaluation
7. Conclusion

gave a useful contribution and suggested the superiority of Chebyshev polynomials. In this paper the use is made of familiar power series simply because it is easy for integrals of potential series and the purpose is in an investigation over the possibility of this method, and improvements are left aside. In the evaluation of wave resistance care should be taken for a use of derivatives of thus obtained density distribution.

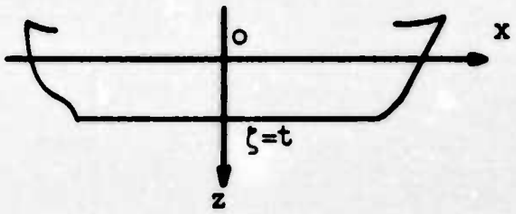
2. OUTLINE OF THE METHOD

A ship body represented with $y = f(x,z)$ $[-1 \leq x \leq 1, -t \leq z \leq t]$ is assumed to be placed in the uniform flow - U_o, and to produce a velocity field which has the same potential as a certain density distribution of sink and source



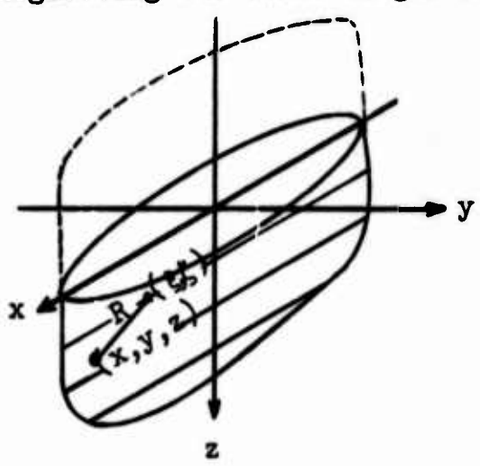
$$mU_o = U_o m(\xi, \zeta)$$

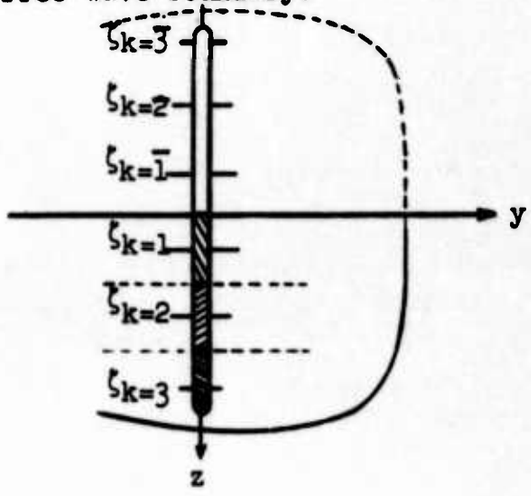
where (ξ, ζ) is coordinate of a point on the center line plane, that is, generally closed surface covering singularities inside of the hull surface. Assume that R denotes the distance from a point $(\xi, 0, \zeta)$ on the source surface to a point (x,y,z) in the field outside of the hull, and the velocity potential at that point becomes



$$\phi = U_o x + \frac{U_o}{4\pi} \int_{-T}^{t} \int_{-1}^{1} \frac{m}{R} \, d\xi d\zeta \qquad (1)$$

considering the mirror image distribution against a rigid water surface, but neglecting the other images to the free wave boundary.





The boundary condition, therefore, should be considered on the closed hull surface as follows:

$$\left(-\frac{\partial f}{\partial x}, 1, -\frac{\partial f}{\partial z}\right) \cdot \left(-\frac{\partial \phi}{\partial x}, -\frac{\partial \phi}{\partial y}, -\frac{\partial \phi}{\partial z}\right) = 0 \qquad (2)$$

that is,

$$U_o \frac{\partial f}{\partial x} + \frac{U_o}{4\pi}\left(\frac{\partial f}{\partial x}\frac{\partial}{\partial x} - \frac{\partial}{\partial y} + \frac{\partial f}{\partial z}\frac{\partial}{\partial z}\right)\int_{-t}^{t}\int_{-1}^{1} \frac{m}{R}\, d\xi d\zeta = 0 \qquad (3)$$

as a closed surface,

$$\int_{-t}^{t}\int_{-1}^{1} m d\xi d\zeta = 0 \qquad (4)$$

In the investigation of hydrodynamical aspect longitudinal distribution has been studied for a long time on the two dimensional problem and and it becomes very familiar and important to us. For convenience of calculation and acceptable understanding $m(\xi, \zeta)$ is longitudinally replaced with continuous conventional type of functions and vertically treated as several distributions on appropriate discrete layers for lengthwise function on the layer k,

$$m(\xi) = \sum_{r=o}^{n} a_r F_r(\xi)$$

$$= \sum_{r=o}^{n} a_r \xi^r \qquad (5)$$

assuming $F_r(\xi) = \xi^r$,
and for vertical discrete division layer k is decided with Chebyshev ordinate rule,

$$m(\xi, \zeta) = \frac{t}{N} \sum_{k} \sum_{r} a_{kT} F_r(\xi) \qquad (6)$$

Thus the integral Equation (3) is resolved to a group of relevant simultaneous equation with (n+1)k unknowns. In Equation (3) $\partial f/\partial x$ and $\partial f/\partial z$ had better to be graphically picked up from the body diagram in practice except for analytic models.

3. INDUCED VELOCITY TERM INTEGRALS

To obtain induced velocity components in Equation (3) the following form of integral term becomes necessary

$$A = \int \frac{F_r(\xi)}{R^3} \, d\xi$$

when $F_r(\xi) = \xi^r$,

$$A_k = \int_o^1 \frac{\xi^r}{R_k^3} \, d\xi \qquad (7)$$

$$R_k = \sqrt{(x-\xi)^2 + y^2 + (z-\zeta_k)^2} \qquad [-1 \le \xi \le 1, \; -t \le \zeta \le t]$$

In the above integration when $(x-\xi), y, (z-\zeta) \to 0$, the integrand reaches the highest peak and for the numerical computation, therefore, it is better to divide into two ranges at the peak since the coordinate (ξ, ζ) of the special point can easily be found; and otherwise, these could be analytically integrated as shown in Appendix 1. The vertical division by Chevyshev rule is also shown in Appendix 2.

4. COEFFICIENTS FOR SINGULARITIES DISTRIBUTION

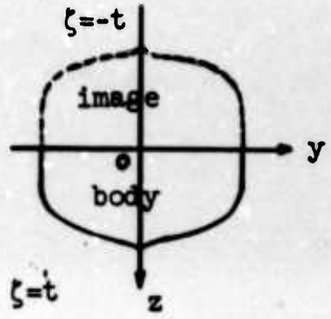
The boundary condition Equation (3) is rewritten as follows:

$$-\left(f_x \frac{\partial}{\partial x} \; \frac{\partial}{\partial y} + f_z \frac{\partial}{\partial z}\right) \int_{-t}^{t} \int_{-1}^{1} \frac{m}{R} \, d\xi d\zeta = 4\pi f_x$$

Double integral in the above equation can be reduced to the sum of every layer's value.

$$\int_{-t}^{t} \int_{-1}^{1} = \int_{-t}^{o} \left[\int_{-1}^{o} + \int_{o}^{1} \right] + \int_{o}^{t} \left[\int_{-1}^{o} + \int_{o}^{1} \right] = \frac{t}{N} \left[\Sigma \int \text{Image} + \Sigma \int \text{Body} \right]$$

where N is the number of Chebyshev's depthwise division both in the body and the symmetrical image.



The simultaneous equations are finally resulted in as

$$\frac{4\pi N}{t} f_x = \sum_{k=1}^{N} \Bigg[\underbrace{\int_0^1 [\{f_x x - y + (z-\zeta_k) f_z\} - f_x \xi] \frac{m_k}{R_k^3} d\xi}_{\text{(body)}} + \underbrace{\int_0^1 [\{f_x x - y + (z+|\zeta_k|) \quad f_x\} - f_x \xi] \frac{m_k}{\bar{R}_k^3} d\xi}_{\text{(image) (fore)}} - \int_0^1 [\{ \quad " \quad \} + f_x |\xi|] \frac{\bar{m}_k}{R_k^3} d\xi - \underbrace{\int_0^1 [\{f_x x - y + (z+|\zeta_k|) \quad f_x\} f_x |\xi|] \frac{\bar{m}_k}{\bar{R}_k^3} d\xi}_{\text{(aft.)}} \Bigg] \tag{8}$$

fore distrb. aft. distrb.

$$m_k = \sum_{r=0}^{n} a_{kr} \xi^r \qquad \bar{m}_k = \sum_{r=0}^{n} \bar{a}_{kr} |\xi|^r \tag{9}$$

The form of practical computation is like the following and here bar on a letter means notation for afterbody from midship that is ranged in $\xi = -1 \sim 0$, and another bar on a suffix shows a corresponding value in the image.

$$\sum_{k=1}^{N} \left[\sum_{r=0}^{n} (C_{\bar{k}\bar{r}} + C_{kr}) a_{kr} - \sum_{r=0}^{n} (\bar{C}_{\bar{k}\bar{r}} + \bar{C}_{kr}) \bar{a}_{kr} \right] = \frac{4\pi N}{t} f_x$$

$$C_{kr} = B_k A_{kr} - f_x A_{k(r+1)} \qquad B_k = f_x x - y + (z-\zeta_k) f_z$$

$$C_{\bar{k}\bar{r}} = B_{\bar{k}} A_{\bar{k}\bar{r}} - f_x A_{\bar{k}(\overline{r+1})} \qquad B_{\bar{k}} = f_x x - y + (z+|\zeta_{\bar{k}}|) f_z$$

$$\bar{C}_{kr} = B_k \bar{A}_{kr} + f_x A_{k(r+1)} \qquad \frac{R_k}{R_{\bar{k}}} = \sqrt{(x-\xi)^2 + y^2 + \frac{(z-\zeta_k)^2}{(z+|\zeta_{\bar{k}}|)^2}}$$

$$C_{\bar{k}\bar{r}} = B_{\bar{k}} A_{\bar{k}\bar{r}} + f_x A_{\bar{k}(\overline{r+1})} \qquad \frac{\bar{R}_k}{R_{\bar{k}}} = \sqrt{(x+|\xi|)^2 + y^2 + \quad "}$$

5. STREAM ON THE HULL SURFACE

The velocity distribution on hull surface can be easily obtained as induced velocity components by the body placed in uniform infinite flow without free surface.

$$\frac{u}{U_o} = -\frac{1}{4\pi}\frac{\partial}{\partial x}\int\int\frac{m}{R}\,d\xi d\zeta - 1 = \frac{1}{4\pi}\int\int\frac{x-\xi}{R^3}\,m d\xi d\zeta - 1$$

$$\frac{v}{U_o} = -\frac{1}{4\pi}\frac{\partial}{\partial y}\int\int\frac{m}{R}\,d\xi d\zeta = \frac{1}{4\pi}\int\int\frac{y}{R^3}\,m d\xi d\zeta$$

$$\frac{w}{U_o} = -\frac{1}{4\pi}\frac{\partial}{\partial z}\int\int\frac{m}{R}\,d\xi d\zeta = \frac{1}{4\pi}\int\int\frac{z-\zeta}{R^3}\,m d\xi d\zeta \ .$$

In the form of computation,

$$\frac{u}{U_o} = \frac{t}{4\pi N}\left[X\sum_{k=1}^{N}(S_{Fk} - S_{Ak}) - \sum_{k=1}^{N}(S'_{Fk} + S'_{Ak})\right] - 1$$

$$\frac{v}{U_o} = \frac{t}{4\pi N}\cdot Y\sum_{k=1}^{N}(S_{Fk} - S_{Ak})$$

$$\frac{w}{U_o} = \frac{t}{4\pi N}\left[Z\sum_{k=1}^{N}(S_{Fk} - S_{Ak}) - \sum_{k=1}^{N}(S''_{Fk} - S''_{Ak})\right]$$

$$S_{Fk} = \sum_{r=o}^{n}(A_{kr} + A_{\overline{kr}})a_{kr} \qquad \bar{S}_{Ak} = \sum_{r=o}^{n}(\bar{A}_{kr} + \bar{A}_{kr})\bar{a}_{kr}$$

$$S'_{Fk} = \sum_{r=o}^{n}(A_{k(r+1)} + A_{\overline{k(r+1)}})a_{kr} \qquad S'_{Ak} = \sum_{r=o}^{n}(\bar{A}_{k(r+1)} + \bar{A}_{\overline{k(r+1)}})\bar{a}$$

$$S''_{Fk} = \zeta_k\sum_{r=o}^{n}(A_{kr} - A_{\overline{kr}})a_{kr} \qquad S''_{Ak} = \zeta_k\sum_{r=o}^{n}(\bar{A}_{kr} - \bar{A}_{kr})\bar{a}_{kr}$$

Thus obtained velocity (u,v,w) lies in the tangential plane to the surface $y = f(x,z)$, namely

$$(x,y,z) : (f_x, -1, f_z) = 0$$

hence

$$\frac{u}{v} f_x + \frac{w}{v} f_z = 1 \qquad (11)$$

This relation is used as a verification of the calculation.

The condition (4) as a closed surface is also used for the check, but it should be added to the before mentioned simultaneous equation group, since the accuracy of the solution could not be expected enough to satisfy the closed condition.

$$\int_{-t}^{t}\int_{-1}^{1} m\,d\xi d\zeta = \int_{o}^{t}\left(\int_{o}^{1} m - \int_{o}^{1} \bar{m}\right) d\xi d\zeta = 0$$

$$\sum_{k=1}^{N}\sum_{n=o}^{n} \frac{1}{r+1}\,(a_{kr} - \bar{a}_{kr}) = 0 \qquad (12)$$

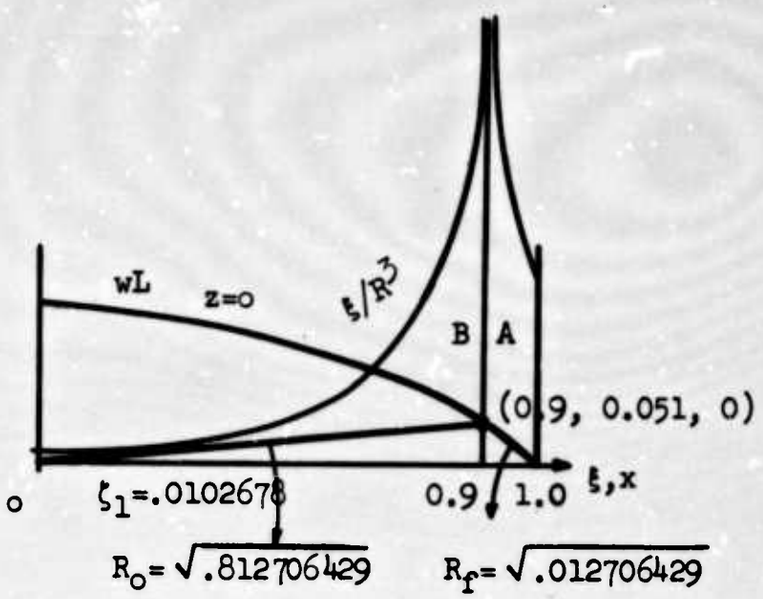
6. NUMERICAL EVALUATION

Induced Term Integral

When the term (7) is calculated with three different methods for a surface point (0.9, 0.051, 0) of the model M-44 on a stratum $\zeta_1 = .0102\ 6728$ as an example with peaked integrand, the difference of results becomes as follows:

Analytical solution	$A_{10} = A_{10} =$	696.6499	(C %)
Gauss 10 ordinates	$=$	598.3921	(- 14 %)
Simpson's 2nd rule	$=$	1037.9155	(+ 49 %)

As such peaked integrand always appears at $\xi = x$ on any given stratum ζ_x integral range can be divided into two, A and B, and thus the accuracy of numerical integration comes in the restriction of calculation



rule. The above evaluation in such a way becomes as follows:

Gauss 10 ordinates $A_{10} = A_{10} = 694.3853$ (- 0.33 %)

Simpson's 2nd rule $= 659.3567$ (- 5.36 %)

A numerical example of A_{kr} for M-44 is presented in Figure 1 for $k = 1, 4$, $r = 0, 1, 2, 3, 5$ with respect to $z = 0$ water line and $z = 0.120$ (draft/half length of ship).

From this diagram it is realized that the system of Equation (8) consists of one group of large A and another group of very small A at the fore and aft end of extremely narrow water line, and this fact suggests that care should be taken for the significant figures of every numeral, especially considering multiplication and subtraction.

Evaluated Distribution

This method is tried on two models, S-202 derived from the known distribution of 0.8ξ and M-44 whose fore body has approximate distribution of $1.36 \sin(\pi\xi/2)$ and after body is conventionally practical. As an easy trail algebraic power series are assumed for the undetermined distribution (5). Figure 2 is a computed result about S-202 for two kinds of 9 surface points illustrated in the diagram, and Figure 3 is a result for 36 points on the surface of M-44. A certain part of the result appears to be near the true phase and the other is unsatisfactory. An impudently smoothed mean

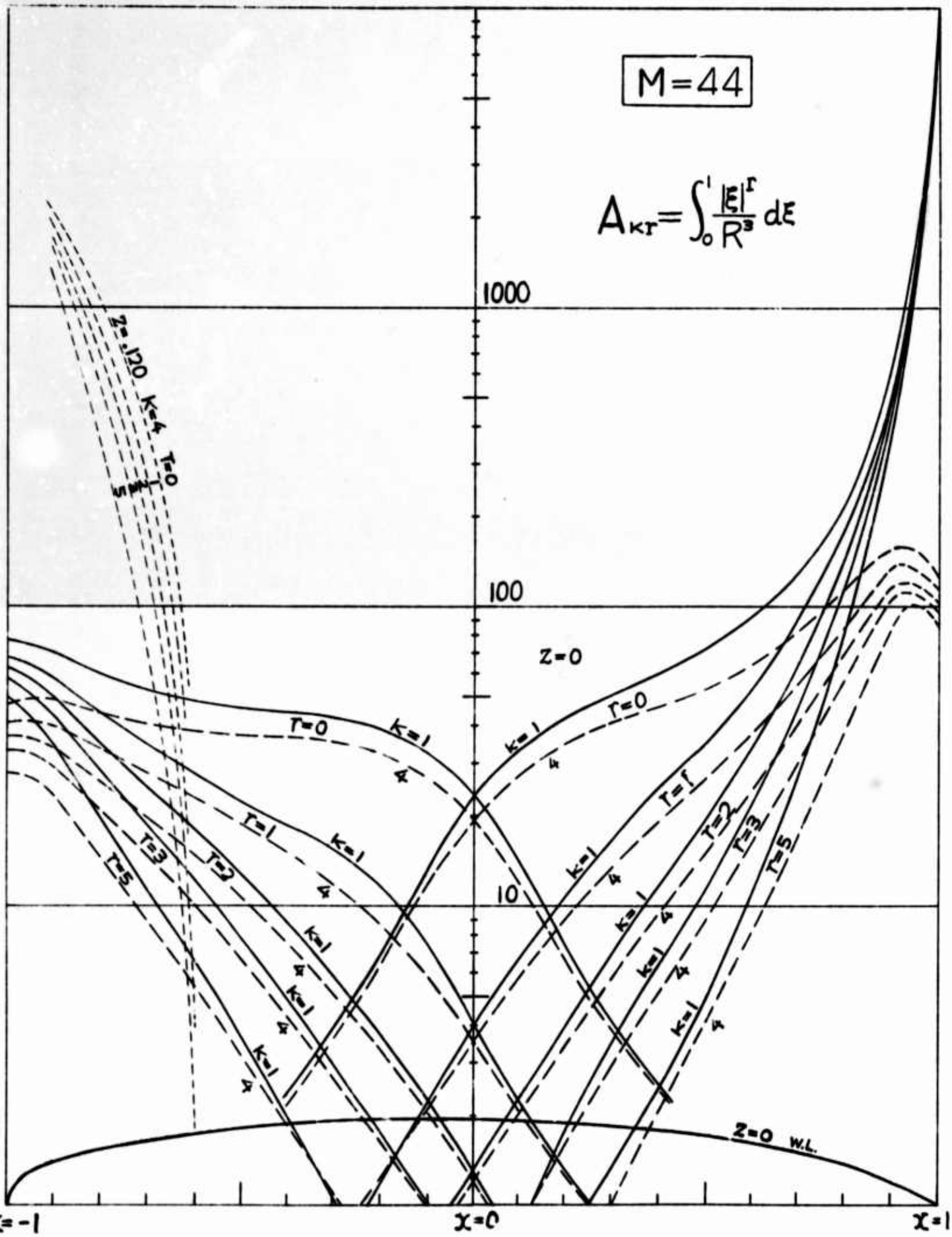

M=44
$A_{kr}=\int_0^1 \frac{|\xi|^r}{R^3}\,d\xi$
1000
100
10
Z=0
Z=0 W.L.
Z=-.120 K=4 r=0 1 2 3 5
r=0 k=1 4
r=1 k=1 4
r=2 k=1 4
r=3 k=1 4
r=5 k=1 4
X=-1
X=0
X=1

Figure 1

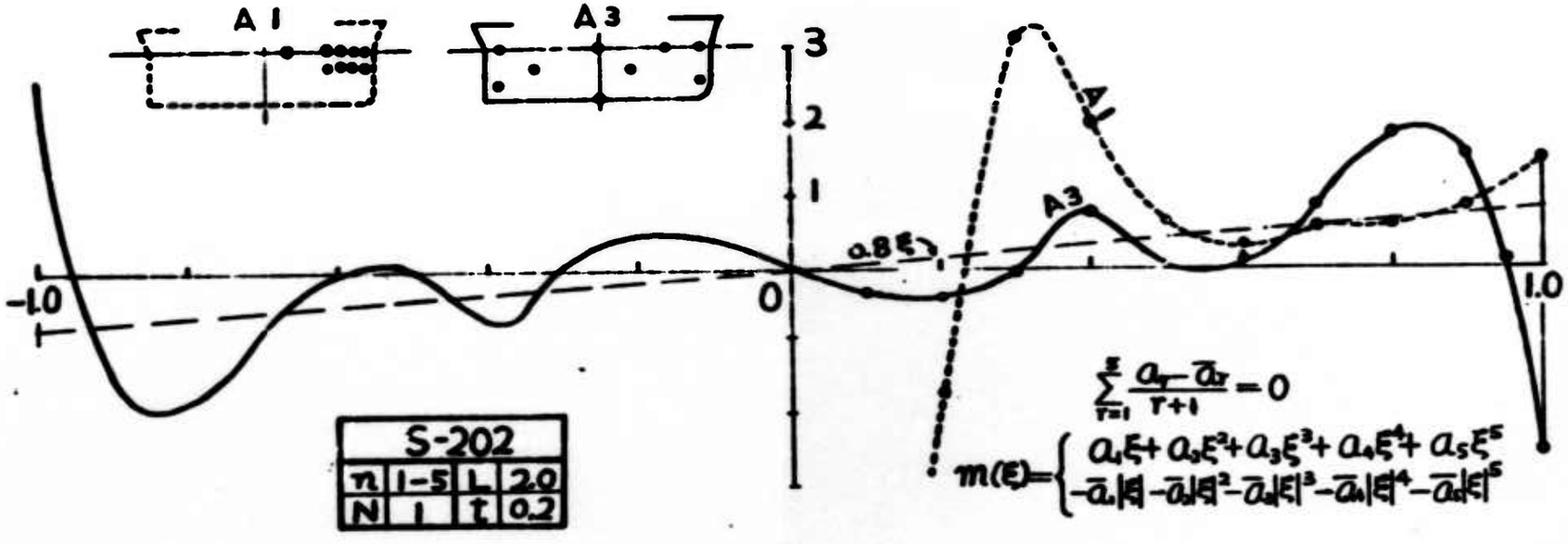

A1
A3
3
2
1
-1.0
0
1.0
0.8ξ
A1
A3
S-202
n 1-5 L 2.0
N 1 t 0.2
$\sum_{r=1}^{s} \frac{a_r - \bar{a}_r}{r+1} = 0$
$m(\xi) = \begin{cases} a_1\xi + a_2\xi^2 + a_3\xi^3 + a_4\xi^4 + a_5\xi^5 \\ -\bar{a}_1|\xi| - \bar{a}_2|\xi|^2 - \bar{a}_3|\xi|^3 - \bar{a}_4|\xi|^4 - \bar{a}_5|\xi|^5 \end{cases}$

Figure 2

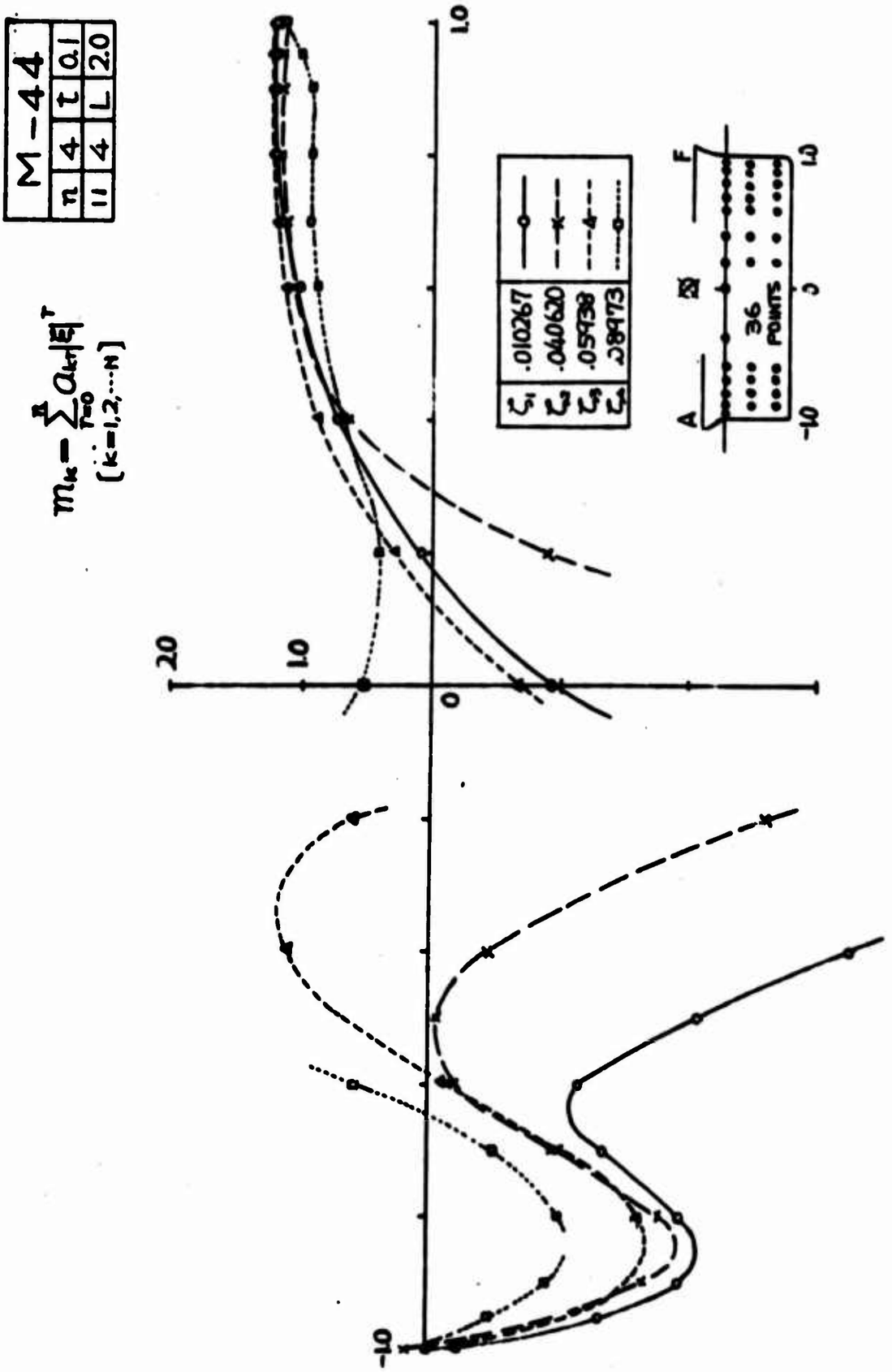

M-44
n 4 t 0.1
11 4 L 2.0
$m_k = \sum_{n=0}^{n} a_{kn} |E|^n$
(k=1,2,...N)
2.0
1.0
0
-1.0
1.0
0
-1.0
ζ_1 .010267
ζ_2 .040620
ζ_3 .09138
ζ_4 .28973
A
F
36 POINTS

Figure 3

of these results might not be said untrue, but the reason remains to be closely examined and eliminated as well as possible.

One of the possible reasons for the wavy fluctuation is expectedly in the way of mathematical approximation to a function for the discrete surface points with unavoidable errors. Another effective reason is the extraordinary change of the 'kernel' in the integral Equation (3); that is, the boundary condition on a surface point is greatly affected by the nearest source and hardly influenced even by a strong source in the far distance. For this reason it possibly results in an erroneous estimation to determine a part of source density mostly by the far away boundary condition, because large differences among R^{-3}'s very often reach magnitudes of three to five figures. This may be a possible explanation for the difference between A1 and A3 in Figure 2 and the wide fluctuation on the after body in Figure 3.

The first cause can be removed by means of mathematical treatment with least square or minimax approximation and the second may require a great number of calculation on a fine mesh of net covering surface and trial corrections. These complete computation could be performed by a computer of large capacity and specially high speed which can solve system of equations for more than 100 unknowns.

7. CONCLUSION

It is still possible to obtain rather reliable quantities on the same points as the boundary conditions are satisfied, which do not contain any higher differentials of the distribution than the condition (but may have integrations of it). For instance the velocity components on the surface is calculated for some points along the waterline z = 0 of S-202 as follows:

x	.95	.6	0	-.4	-.9
u/U_o	-0.6401320	-1.167479	-1.212021	-1.170944	-0.6508040
v/U_o	0.0533882	0.0941225	0.000000	-0.0597086	-0.0460179
w/U_o	0.0000000	0.0000000	0.000000	0.000000	0.0000000

The first purpose to simulate ship form with singularity could not succeed in giving an analytical concept about the relation between them. The further attempt, however, to utilize Chevyshev

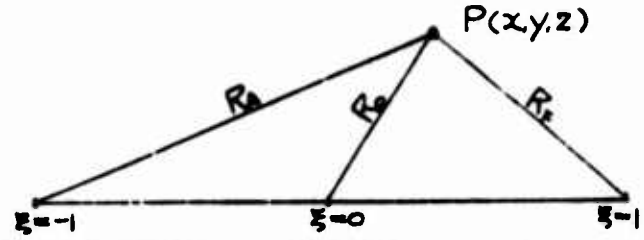
polynomials for Equation (5) and to adopt more extensive conditions covering the ship surface appears to be promising, though it may consume laborious effect of computers. However hard it may be, theoretical developments should proceed to make hydrodynamics not only applied on the practice of ship design but also lead the tank test experiment for a possible close cooperation.

REFERENCES

1. Hess, J. L., and Smith, A. M. O.: "Calculation of Non-Lifting Potential Flow About Arbitrary Three-Dimensional Bodies," Report No. E.S. 40622, Douglas Aircraft Co., 1962.

2. Martin, D. W.: "Polynomial Representation of Some Ship Section Area Curves and the Calculation of the Associated Wave Resistance," Quart. Journ. Mech. and Applied Math., Vol. XIV, Pt. 1, 1961.

Appendix 1



R, $\bar{R}$ $= \sqrt{(x \mp |\xi|)^2 + y^2 + (z-\zeta)^2}$ $\qquad \rho^2 = y^2 + (z-\zeta)^2$

$R_0 = \sqrt{x^2 + y^2 + (z-\zeta)^2}$

$R_F = \sqrt{(x-1)^2 + y^2 + (z-\zeta)^2}$

$R_A = \sqrt{(x+1)^2 + y^2 + (z-\zeta)^2}$

$$A_{K0} = \int_0^1 d\xi / R_K^3 = \frac{1}{\rho_K^2}\left[\frac{x}{R_{K0}} - \frac{x-1}{R_{KF}}\right] \; ; \; \bar{A}_{K0} = \int_{-1}^0 d\xi / R_K^3 = \frac{1}{\rho_K^2}\left[\frac{x+1}{R_{KA}} - \frac{x}{R_{K0}}\right]$$

$$A_{K1} = \int_0^1 \xi\, d\xi / R_K^3 = x A_{K0} + \left[\frac{1}{R_{K0}} - \frac{1}{R_{KF}}\right] \; ; \; \bar{A}_{K1} = \int_{-1}^0 \xi\, d\xi / R_K^3 = x \bar{A}_{K0} + \left[\frac{1}{R_{KA}} - \frac{1}{R_{K0}}\right]$$

$$A_{K2} = \int_0^1 \xi^2 d\xi / R_K^3 = x^2 A_{K0} - 2x A_{K1} - \left[\frac{x}{R_{K0}} - \frac{x-1}{R_{KF}} - \ln\left(\frac{x + R_{K0}}{x-1+R_{KF}}\right)\right]$$

$$\bar{A}_{K2} = \int_{-1}^0 \xi^2 d\xi / R_K^3 = x^2 \bar{A}_{K0} - 2x \bar{A}_{K1} - \left[\frac{x+1}{R_{KA}} - \frac{x}{R_{K0}} - \ln\left(\frac{x+1+R_{KA}}{x+R_{K0}}\right)\right]$$

$$A_{K3} = \int_0^1 \xi^3 d\xi / R_K^3 = x^3 A_{K0} - 3x^2 A_{K1} + 3x A_{K2} - \left[R_{K0} - R_{KF} + \rho_K^2\left(\frac{1}{R_{K0}} - \frac{1}{R_{KF}}\right)\right]$$

$$\bar{A}_{K3} = \int_{-1}^0 \xi^3 d\xi / R_K^3 = x^3 \bar{A}_{K0} - 3x^2 \bar{A}_{K1} + 3x \bar{A}_{K2} - \left[R_{KA} - R_{K0} + \rho_K^2\left(\frac{1}{R_{KA}} - \frac{1}{R_{K0}}\right)\right]$$

$$A_{K4} = \int_0^1 \xi^4 d\xi / R_K^3 = x^4 A_{K0} - 4x^3 A_{K1} + 6x^2 A_{K2} - 4x A_{K3} + \left[\frac{1}{2}\{x R_{K0} - (x-1) R_{KF}\} + \rho_K^2\left(\frac{x}{R_{K0}} - \frac{x-1}{R_{KF}}\right) - \frac{3}{2}\rho_K^2 \ln\left(\frac{x + R_{K0}}{x-1+R_{KF}}\right)\right]$$

$$\bar{A}_{K4} = \int_{-1}^0 \xi^4 d\xi / R_K^3 = x^4 \bar{A}_{K0} - 4x^3 \bar{A}_{K1} + 6x^2 \bar{A}_{K2} - 4x \bar{A}_{K3} + \left[\frac{1}{2}\{(x+1) R_{KA} - x R_{K0}\} + \rho_K^2\left(\frac{x+1}{R_{KA}} - \frac{x}{R_{K0}}\right) - \frac{3}{2}\rho_K^2 \ln\left(\frac{x+1+R_{K0}}{x+R_{K0}}\right)\right]$$

$$A_{K5} = \int_0^1 \xi^5 d\xi / R_K^3 = x^5 A_{K0} - 5x^4 A_{K1} + 10x^3 A_{K2} - 10x^2 A_{K3} + 5x A_{K4} - \left[\frac{1}{3}(R_{K0}^3 - R_{KF}^3) - 2\rho_K^2 (R_{K0} - R_{KF}) - \rho_K^4\left(\frac{1}{R_{K0}} - \frac{1}{R_{KF}}\right)\right]$$

$$\bar{A}_{K5} = \int_{-1}^0 \xi^5 d\xi / R_K^3 = x^5 \bar{A}_{K0} - 5x^4 \bar{A}_{K1} + 10x^3 \bar{A}_{K2} - 10x^2 \bar{A}_{K3} + 5x \bar{A}_{K4} - \left[\frac{1}{3}(R_{KA}^3 - R_{K0}^3) - 2\rho_K^2 (R_{KA} - R_{K0}) - \rho_K^4\left(\frac{1}{R_{KA}} - \frac{1}{R_{K0}}\right)\right]$$

$$A_{K6} = \int_0^1 \xi^6 d\xi / R_K^3 = x^6 A_{K0} - 6x^5 A_{K1} + 15x^4 A_{K2} - 20x^3 A_{K3} + 15x^2 A_{K4} - 6x A_{K5} + \left[\frac{1}{4}\left\{\frac{x^5}{R_{K0}} - \frac{(x-1)^5}{R_{KF}}\right\} - \frac{5}{8}\rho_K^2\left\{\frac{x^3}{R_{K0}} - \frac{(x-1)^3}{R_{KF}}\right\} - \frac{15}{8}\rho_K^4\left\{\frac{x}{R_{K0}} - \frac{x-1}{R_{KF}}\right\} + \frac{15}{8}\rho_K^5 \ln\left(\frac{x + R_{K0}}{x-1+R_{KF}}\right)\right]$$

$$\bar{A}_{K6} = \int_{-1}^0 \xi^6 d\xi / R_K^3 = x^6 \bar{A}_{K0} - 6x^5 \bar{A}_{K1} + 15x^4 \bar{A}_{K2} - 20x^3 \bar{A}_{K3} + 15x^2 \bar{A}_{K4} - 6x \bar{A}_{K5} + \left[\frac{1}{4}\left\{\frac{(x+1)^5}{R_{KA}} - \frac{x^5}{R_{K0}}\right\} - \frac{5}{8}\rho_K^2\left\{\frac{(x+1)^3}{R_{KA}} - \frac{x^3}{R_{K0}}\right\} - \frac{15}{8}\rho_K^4\left\{\frac{x+1}{R_{KA}} - \frac{x}{R_{K0}}\right\} + \frac{15}{8}\rho_K^5 \ln\left(\frac{x+1+R_{KA}}{x+R_{K0}}\right)\right]$$

$$A_{K7} = \int_0^1 \xi^7 d\xi / R_K^3 = x^7 A_{K0} - 7x^6 A_{K1} + 21x^5 A_{K2} - 35x^4 A_{K3} + 35x^3 A_{K4} - 21x^2 A_{K5} + 7x A_{K6} - \left[\frac{1}{5}(R_{K0}^5 - R_{KF}^5) - \rho_K^2 (R_{K0}^3 - R_{KF}^3) + 3\rho_K^4 (R_{K0} - R_{KF}) + \rho_K^6\left(\frac{1}{R_{K0}} - \frac{1}{R_{KF}}\right)\right]$$

$$\bar{A}_{K7} = \int_{-1}^0 \xi^7 d\xi / R_K^3 = x^7 \bar{A}_{K0} - 7x^6 \bar{A}_{K1} + 21x^5 \bar{A}_{K2} - 35x^4 \bar{A}_{K3} + 35x^3 \bar{A}_{K4} - 21x^2 \bar{A}_{K5} + 7x \bar{A}_{K6} - \left[\frac{1}{5}(R_{KA}^5 - R_{K0}^5) - \rho_K^2 (R_{KA}^3 - R_{K0}^3) + 3\rho_K^4 (R_{KA} - R_{K0}) + \rho_K^6\left(\frac{1}{R_{KA}} - \frac{1}{R_{K0}}\right)\right]$$

APPENDIX 2

CHEVYSHEV ORDINATES

N	2	3	4	5
$\frac{\zeta_1}{t}$	$\frac{1}{2} - \frac{1}{2\sqrt{3}}$ 0.5 - 0.28867513	$\frac{1}{2} - \frac{1}{2\sqrt{2}}$ 0.5 - 0.35355339	$\frac{1}{2} - \sqrt{\frac{1}{6}\left(\frac{1}{2} + \frac{1}{\sqrt{5}}\right)}$ 0.5 - 0.39732724	$\frac{1}{2} - \sqrt{\frac{5}{48} + \frac{\sqrt{11}}{48}}$ 0.5 - 0.41624874
$\frac{\zeta_2}{t}$	$\frac{1}{2} + \frac{1}{2\sqrt{3}}$ 0.5 + 0.28867513	$\frac{1}{2}$ 0.5	$\frac{1}{2} - \sqrt{\frac{1}{6}\left(\frac{1}{2} - \frac{1}{\sqrt{5}}\right)}$ 0.5 - 0.09379624	$\frac{1}{2} - \sqrt{\frac{5}{48} - \frac{\sqrt{11}}{48}}$ 0.5 - 0.18727072
$\frac{\zeta_3}{t}$		$\frac{1}{2} + \frac{1}{2\sqrt{2}}$ 0.5 + 0.35355339	$\frac{1}{2} + \sqrt{\frac{1}{6}\left(\frac{1}{2} - \frac{1}{\sqrt{5}}\right)}$ 0.5 + 0.09379624	$\frac{1}{2}$ 0.5
$\frac{\zeta_4}{t}$			$\frac{1}{2} + \sqrt{\frac{1}{6}\left(\frac{1}{2} + \frac{1}{\sqrt{5}}\right)}$ 0.5 + 0.39732724	$\frac{1}{2} + \sqrt{\frac{5}{48} - \frac{\sqrt{11}}{48}}$ 0.5 + 0.18727072
$\frac{\zeta_5}{t}$				$\frac{1}{2} + \sqrt{\frac{5}{48} + \frac{\sqrt{11}}{48}}$ 0.5 + 0.41624874

FISHING BOAT OF THE WAVELESS HULL FORM

Nobutatsu Yokoyama

Fishing Boat Laboratory
Fisheries Agency of Japan

FISHING BOAT OF THE WAVELESS HULL FORM

1. Introduction

There would be found some apparent differences as shown in Table 1 and Figure 1 in the proportion of speed, displacement and power to the ship length between fishing boats in Japan smaller than 70 m. and average larger cargo liners. These statistical results since 1950 may be interpreted as there have been no other ways than increasing the power of the engine and any results of hydrodynamical efforts have not been considered to improve hull shape in preventing the expected speed loss resulting from the increase of ship-displacement by increasing C_b to leave L unchanged on account of the ruled restriction for LBD or GT. Consequently the effect of full C_b on the wave resistance must be necessity appear on the results of tank test in Figure 2 which has been conducted by the Fishing Boat Laboratory, Fisheries Agency, with the Japanese fishing boat models built for these ten years. Considering that in Figure 1 most operating speed at sea comes between $V/\sqrt{Lg} = 0.25$ and 0.35 it is evident in Figure 2 that most full ships have a peculiar tende :y to climb up the hump of the wave resistance and, that is, they have to waste excess power of some extent which might be saved by a hydrodynamical improvement for the hull form. There may possibly be two methods of the improvement; viz. the one of reducing wave-resistance with a hull-shape transformation or of an escape from making wave by submerging under water or being dynamically lifted above; and the other of actively cancelling the formation of ship wave by a counteracting body specially designed on the 'waveless-hull form' theory.

The facinating theory has been established by Prof. Inui (1960)[1] based on his exact calculation of wavemaking resistance and careful analysis of the experiment, and it has predicted possibility of the existence of a real 'waveless-hull form'. For the bow wave and the stern wave respectively Takahei[2] and Kumano[3] (1960) have proved the precise coincidence between the theory and the experiment conducted with two theoretically calculated models. And in 1961 an actual sea test was undertaken by these investigators with 80 m. passenger boat. "Kurenai Maru" and its waveless aspect was successfully filmed from a helicopter. In applying this fundamental theorem, however, to practical fishing boat design not only some more details should be explored, but the substantial difference should also be recognized from the existing design of bulbous bow. The author points out in this paper an important recognization that the bulb would not always become a means of

TABLE 1

RATIOS FOR GENERAL BOATS

	GT	L/B	$\nabla f/(0.1L)^3$	$V^*/\sqrt{Lg}$	HP/GT	C_b
passenger boat	126	4.17	9.0	.362	2.54	.521
chemical tanker	146	4.66	13.1	.252	0.82	.705
oil tanker	199	5.59	11.2	.278	1.41	.771
do.	290	5.52	11.4	.268	1.38	.740
cargo boat	499	5.70	9.9	.270	1.60	.722
fish carrier	1391	6.35	7.7	.250	1.12	.687
oil tander	2262	6.44	8.0	.187	0.88	.753
ferry boat	4982	6.37	7.1	.203	0.67	.772
cargo boat	9548	7.41	5.7	.235	1.18	.699
do.	14302	7.39	5.9	.203	0.84	.730
oil tanker	28972	6.99	6.2	.193	0.61	.809
do.	31109	6.69	6.4	.180	0.51	.809

GT: gross tonnage, L/B: ratio of L_{pp} to molded breadth, ∇f: displacement of fully loaded ship, $L = L_{pp}$: length between perpendiculars, V^*: service speed, HP: rated horse power, C_b: blook coefficient for full-load condition.

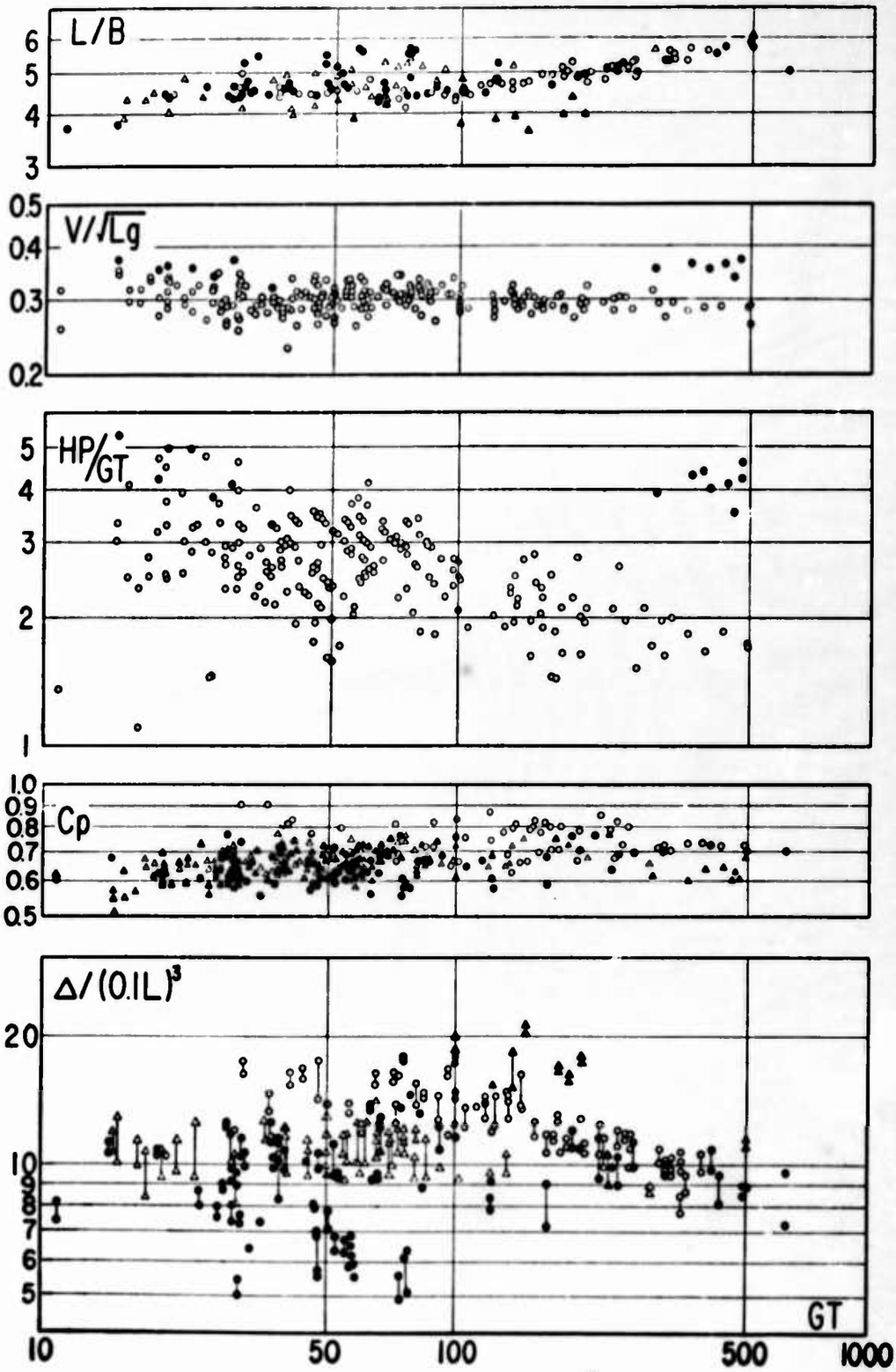


Figure 1. In the ratios of L/B, C_p, $\nabla/(0.1L)^3$: ● fisheries inspection boat, bonito-tuna long line boat, ▲ trawler, ▲ the other fishing boats: in the ratios of $V/\sqrt{Lg}$, HP/GT: ● fisheries inspection boat, ○ the other fishing boats. V: trial speed.

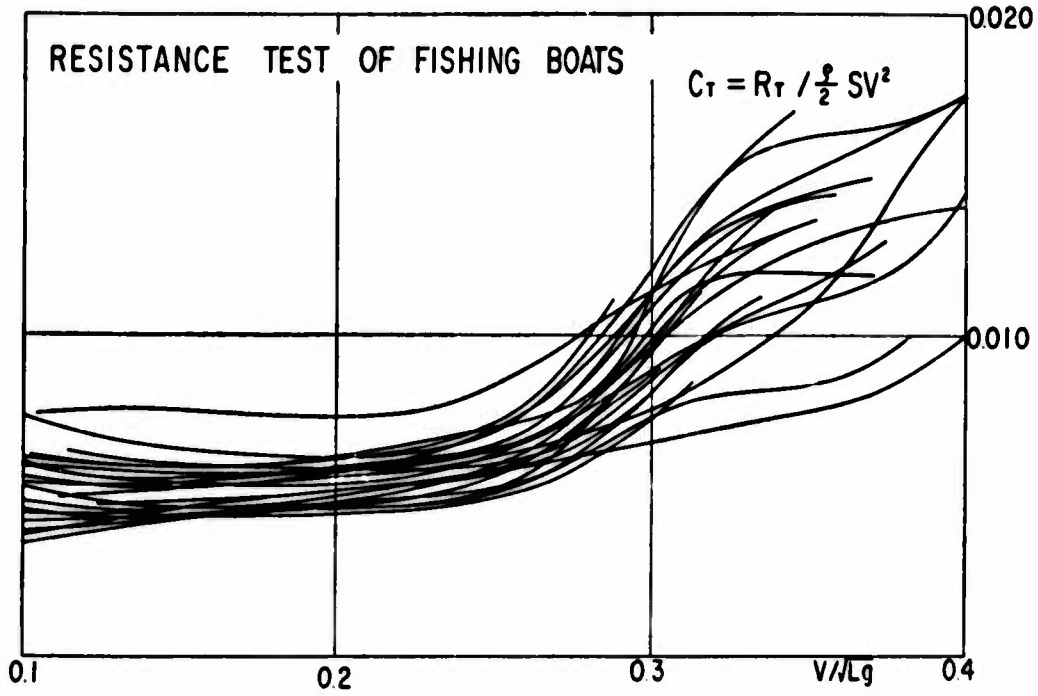

RESISTANCE TEST OF FISHING BOATS
$C_T = R_T / \frac{\rho}{2} SV^2$
0.020
0.010
0.1
0.2
0.3
V/√Lg
0.4

Fig. 2.

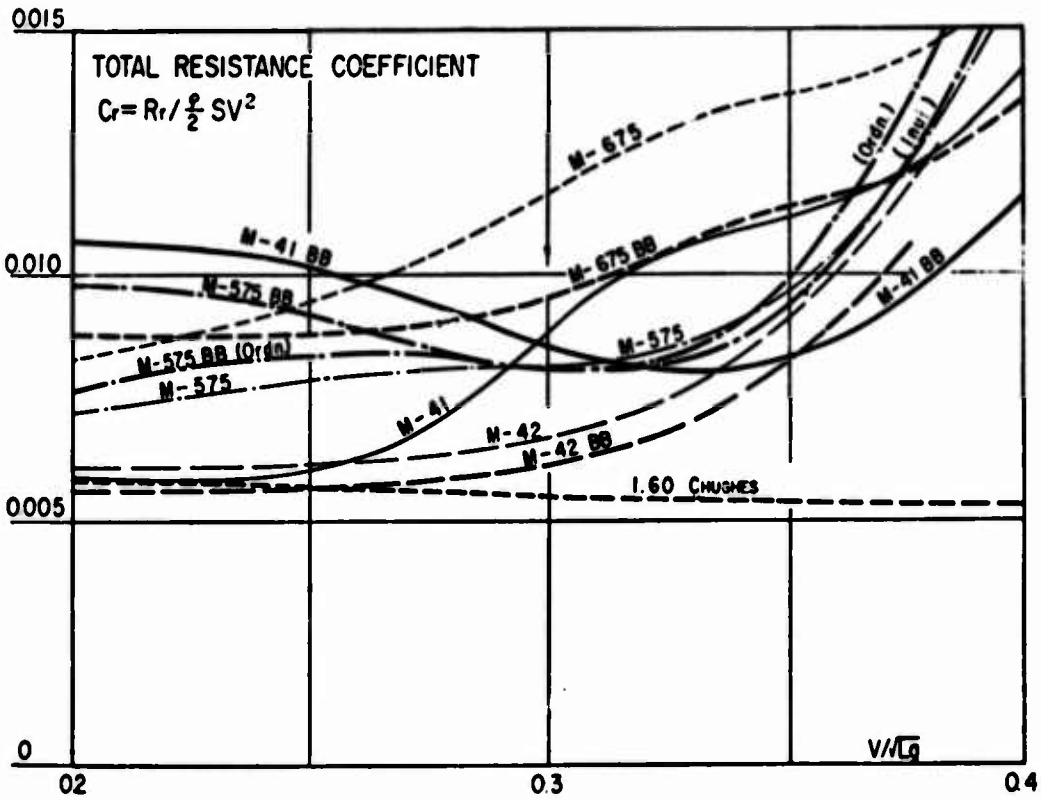

0015
TOTAL RESISTANCE COEFFICIENT
$C_r = R_r / \frac{\rho}{2} SV^2$
M-675
(Ordin.)
(Lewis)
M-41 BB
M-675 BB
0.010
M-575 BB
M-575
M-575 BB (Ordin)
M-575
M-41
M-42
M-42 BB
1.60 CHUGHES
0005
0
V/√Lg
02
0.3
0.4

Fig. 3.

reducing the wave-making resistance of any kind of ships, but only when combined with a specific form of hull which should be designed on an entirely new stand-point it will work as an effective wave eraser at an intended speed.

The present paper gives first exemplified experiments with models of existing fishing boats either on the usual bulbous bow design or on the "waveless theory" and shows the former a chance example of increasing resistance and the latter in somewhat effective but incomplete waveless condition. A close analysis of the waves generated from every part of the existing hull proves the situation resulted from unfavorable wave component for the counteraction. The author contributed to give some information of potential use to practical design on thorough investigations about the wave counteraction with a mathematical model, the dimensions of which are quite similar to the average fishing boat, and presented another favorable test results for a practical waveless trawler model of new fashion by making the best possible use of these results.

2. Bulb for Existing Boats

Generally the ship waves are composed of the local disturbances at bow and stern, and the free waves discharged behind the ship. The former is quite free from the wave resistance since they are longitudinally symmetrical in ideal fluid, but the latter has much the most complicated effect on it. The elevation of the free waves ζ_{ws} of ships for practical use is expressed in general form as:

$$\zeta_{ws} \sim \Sigma \int_{-\pi/2}^{\pi/2} A_1\, V, m_1, T\ ,\ \theta \sin(V, x + \delta_1, y, \theta) d\theta \qquad (1)$$

In case that the ship is possibly represented by an equivalent source distribution m, ξ, ζ, the above amplitude function A_1 in (1) may become

$$A_1 = \frac{g \sec\theta}{\pi V^3} \int_{-T_1}^{0} \exp\left(\frac{g}{V^2} \zeta \sec^2\theta\right) \int_{\xi_1} m_1(\xi, \zeta)\, d\xi d\zeta \qquad (2)$$

Similarly the free wave elevation of the bulb may be expressed as follows:

$$\zeta_{WB} \sim \int_{-\pi/2}^{\pi/2} B(V,M,f,0)\ \sin(V,x+\epsilon,y,0)\ d\theta \qquad (3)$$

The wave amplitude function of counteracted wave C and the transfer of the resultant profile δ are consequently obtained as

$$\left.\begin{aligned} C^2 &= [\sum_i (A_i \cos\delta'_i) + B\cos\epsilon']^2 + [\sum_i (A_i \sin\delta'_i) + B\sin\epsilon']^2 \\ \delta' &= \tan^{-1}[\{\Sigma (A_i \sin\delta'_i) + B\sin\epsilon'\}/\{\Sigma(A_i\cos\delta'_i) + B\cos\epsilon'\}] \end{aligned}\right\}$$

$$\delta' = (V,\delta,\theta) \qquad \epsilon' = (V,\epsilon,\theta) \qquad (4)$$

where V denotes ship speed; m_i and M: strength of equivalent source and doublet; T_i and f: draft and depth of m_i and M; (x,y,θ): coordinate of a considering point in the fluid surface and direction from m_i or M; A_i and B: amplitude function of ship waves and bulb. Then the resulting wave resistance, therefore, will be represented by

$$R_W = \pi\rho V^2 \int_0^{\pi/2} C^2 \cos^3\theta d\theta \qquad (5)$$

When the stern wave can be put aside, the condition necessary for the least wave resistance is obviously $C \to$ min., and this will be realized when

$$\left.\begin{aligned} B &= -A_{bow}, \qquad \delta_{bow} = \epsilon \\ A_{i\,\text{except bow \& stern}} &\to 0 \end{aligned}\right\} \qquad (6)$$

The composition of the summation $\sum_i$ in (1) or the component amplitude A_i in (2) has much important influence on the effectiveness of waveless counteraction as shown explicit in the following experiments (a) and (b), and it entirely depends upon the shape of ship's lines - not only the coefficients, C_p, C_m, C_w, but also the form of waterlines and bow-buttock lines, even if the case of having the same coefficients.

(a) Ineffective Example: A bulbous bow model, M-575BB, Table II and III, of usual design heretofore in use was prepared by means of being transformed from the ordinary model, M-575, by shifting 10% of the original ship's volume to the bulb inside the stem to keep the displacement unchanged, which has low prismatic coefficient, 0.575 and gives excellently low resistance between $V/\sqrt{Lg} = 0.25$ and

Table II: particulars of the models

	model of existing small trawler				model of 'waveless hull' form	
	European		Japanese			
	M-575	M-675	M-41	M-42	M-43	M-44
L_{pp} (m)	2.000	2.000	1.963	1.963	2.000	2.000
B mld (m)	0.544	0.502	0.388	0.424	0.410	0.410
T fore (m)	0.160	0.145	0.142	0.155	0.100	0.100
T_m (m)	0.200	0.185	0.168	0.183	0.267	0.240
B/L	0.272	0.251	0.198	0.215	0.205	0.205
T_f/L	0.0800	0.0725	0.0724	0.0790	0.0500	0.0500
T_m/L	0.1000	0.0825	0.0856	0.0932	0.1335	0.1200
∇ (m^3)	0.09920	0.09920	0.07663	0.07663	0.10867	0.10773
S (m^2)	1.2364	1.1904	1.0806	1.1466	1.1337	1.3150
A (m^2)	0.0863	0.0735	0.0603	0.0697	0.0841	0.0818
$\nabla/(0.1L)^3$	12.40	12.40	10.13	10.13	13.58	13.47
A/LT_f	0.270	0.253	0.216	0.229	0.421	0.409

L: length, B: breadth, T: draft, ∇: volume-displacement, S: wetted surface area, A: midship section area.

Table III: particulars of the bulbs

	$\Delta\nabla$ (m^3)	ΔS (m^2)	A_b/A_m	a_0/L	b/L	f/L
BB (M-575)	0	0.0044	0.100	0.020	−0.025	0.055
BB (M-675)	0.00393	0.0905	0.209_3	0.035	0.015	0.044_8
BB (M-41)	0.00307	0.1007	0.290_4	0.038	0.038	0.047_8
BB (M-42)	0.00228	0.0596	0.122	0.025	0.023_5	0.052
BB1 (M-43)	0.00485～0.01207	0.0994～0.2443	0.373_5	0.050	0.010～0.125	0.050～0.125
BB2 (do.)	0.00452	0.1181	0.269_9	0.042_5	0.042_5	0.075
BB3 (do.)	0.00275	0.0936	$0\ 193_7$	0.036	0.036	0.075
BB (M-44)	0.00736	0.1609	0.171_8	0.037	0.037_5	0.062_5

BB: bow bulb, $\Delta\nabla$: volume of bulb, ΔS: surface area of bulb, A_b: max. sectional area of bulb, A_m: midship area, a_0: radius of estimated bulb sphere, b: distance of bulb center from FP, (forward: possitive), f: immersion of bulb center, L: length between perpendiculars.

0.30 according to the comparative resistance test programmed by Traung[4] (1957), FAO, UN, and carried out by the author[5] (1958). Contrary to the initial anticipation of reducing resistance the towing test with the model showed a noticeable increase, for instance shown in Figure 3. By an analysis of shipside profiles of the resultant wave like an example in Figure 4, it is clearly realized that the fact was introduced by wrong counteraction between the bow wave and the relatively mislocated bulb. Besides this model a large extruded bulb was fitted for a comparison outside the stem of M-575 and M-42 Table II and III keeping their draft as same as the original, both of which are much the finer models - C_p of the latter is likewise 0.580 - than the ordinarily built ships nowadays and showed good results in towing and also in self-propelled test as mentioned before. The towing results in Figure 3, however, are not so appreciable as expected. Such ineffectiveness as those must be brought by some influential wave components of parasitic sources distributed in both hulls which have been modified forced to have quite low prismatic.

(b) Incomplete Example: For the study of further effect on existing fishing boats of full fore- and aft-body, M-675 and M-41, Table II and III, whose C_p are 0.675 and 0.633 are submitted to the test coupled with a phase-adjusted bulb after the shipside wave examined. The test result in Figure 3 indicates a preferable reduction at $V/\sqrt{Lg} = 0.30 \sim 0.35$ and that may be resulted in on account of the cancellation of the bow wave which represents the major component of the whole wave generated by the rather simple-formed hull. The more carefully, however, the water surface is observed, still the more unoverlookable waves could be found remain and not partially cancelled waves are left. This phenomenon may be comprehended to depend upon its incomplete waveless form of main hull.

The facts, (a) and (b), instruct us nothing but the importance of the development for a peculiar hull not having parasitic sources and of the investigation of the effect of bulb location.

3. The Effect of Bulb

A comprehensible frame-work for the effect of bulb on the resultant wave resistance could be given by the following ratio of amplitude function,

$$\left(\frac{C}{A}\right)^2 = \left(1 - \frac{B}{A}\right)^2 + 2[1 - \cos(K_o b \sec\theta)]\frac{B}{A} \qquad (7)$$

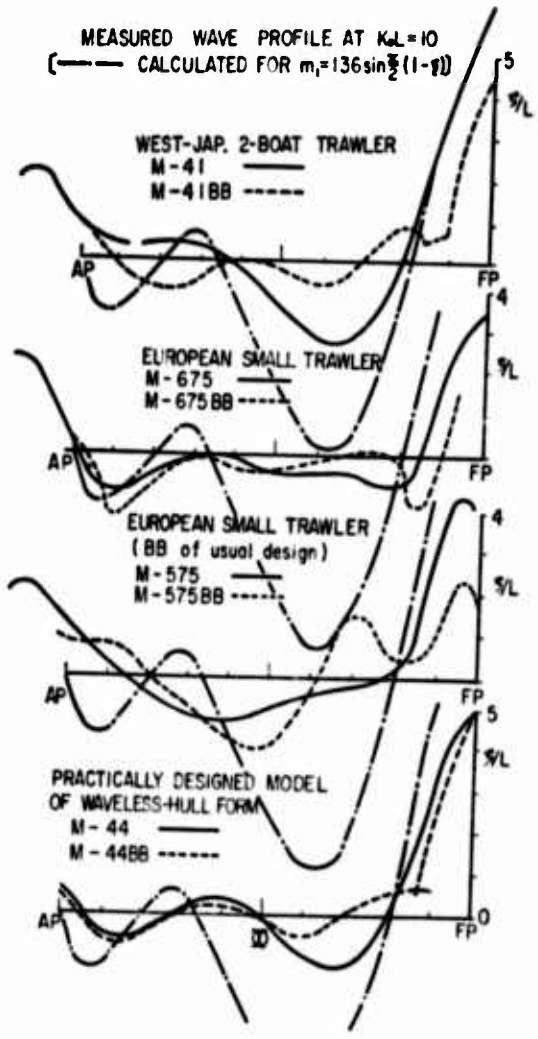


Fig. 4.

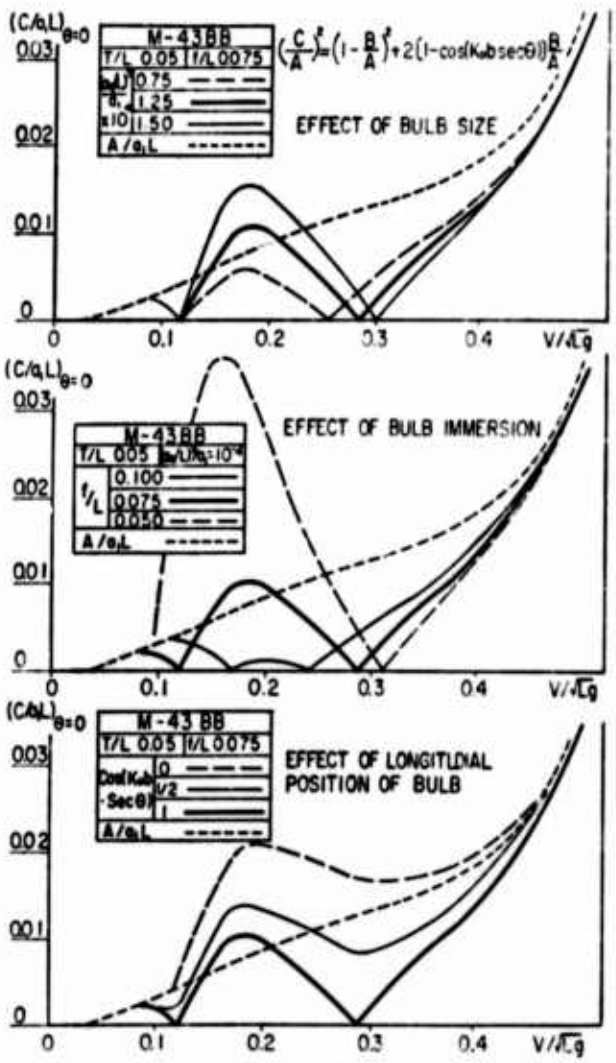


Fig. 5.

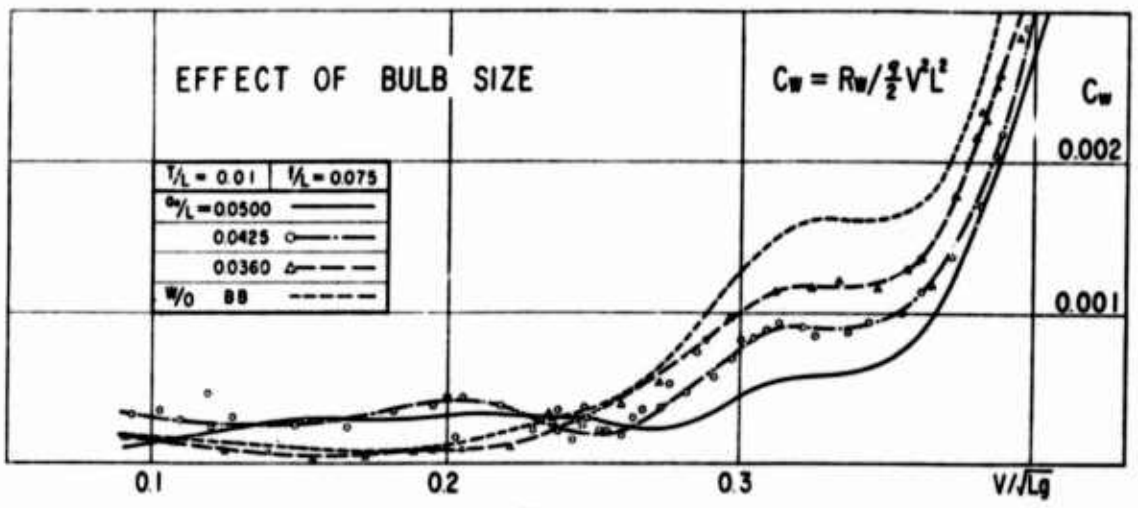


Fig. 6.

where b means the distance between each location of the wave source for A and B. The effect of bulb size and locations will be analogized by the illustration of Figure 5 in the form of parameters, $(a_o/L)^3/a_1$, f/L, $\cos(K_o b)$, when $\theta = 0$ for the simplification, where $K_o = g/V^2$, and a_o means the radius of the spherical bulb. The truer resistance may be expressed by superposing on these curves the other effects of θ, fundamental terms of the other component waves and one another's interfering terms which should disappear right at the complete waveless points generally found at certain two Froude numbers. From the above illustration it would be understood that the complete waveless state could be realized only when $b = 0$ and in the incomplete counteraction there might be even a case of resistance increasing.

These calculated aspects are precisely proved in Figures 6, 7, and 8 by the experiments with a mathematical model M-43 whose lines are obtained along the streamlines of flow produced by the distributed source and sink $V \cdot m(\xi, \zeta)$ as follows in the uniform stream V without free surface:

$$m(\xi, \zeta) = m_1(\xi) \cdot m_2(\zeta); \quad -1 \leq \xi \leq 1; \quad -t \leq \zeta \leq t$$

$$m_1(\xi) = a \sin(\pi\xi/2); \quad a_1 = 1.36$$

$$m_2(\zeta) = 1; \qquad\qquad t = 0.05 \qquad\qquad (8)$$

and the dimension of M-43 is given in Tables II and III. In the above experiment the wave resistances are deduced by reducing the form drag from the resultant according to the Hughes method assuming the form factor $k = 0.60$ all alike, because of the indeterminate phase of the total resistance at low speed on account of the interaction. The turbulence of the model surface is stimulated by a row of plate studs placed on the station of 9.5 and the turbulent separation is maintained by stimulators of the same kind arranged on the bulb at $a_o/2$ abaft the front end.

The calculation of the free wave produced by the source distribution (8) shows that the bow and stern waves should be created exactly at FP. and AP. In reality, however, the distribution for M-43 near the water surface should be modified in the approximation of second order at best to satisfy the condition of ship surface especially under the perturbation of free wave, and in consequence the generating point of bow or stern wave may possibly be shifted by the modification as far as the following distance afore FP. or abaft AP. assuming F^n-0 when $n \geq 6$:

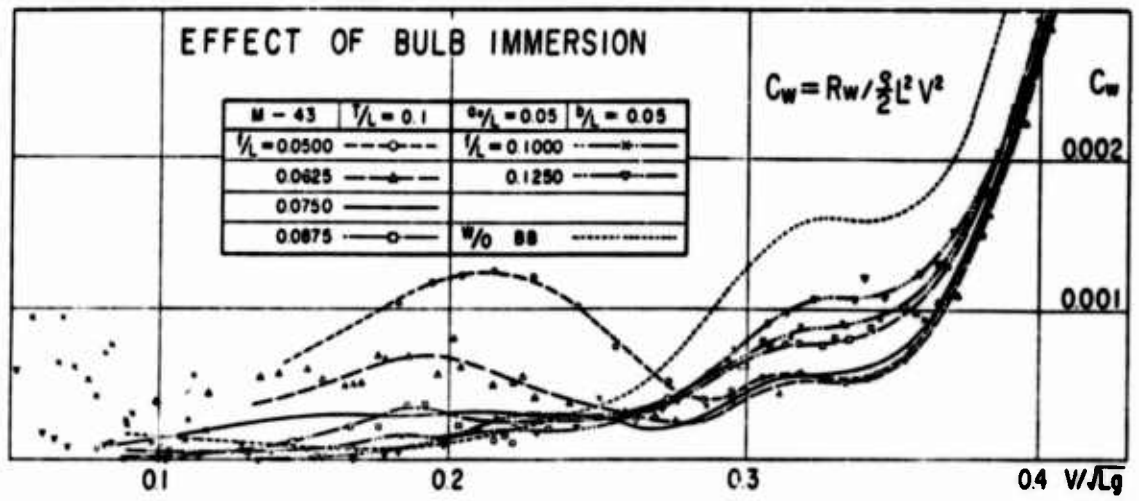

EFFECT OF BULB IMMERSION
M - 43
$^T/_L$ = 0.1
$^{C_b}/_L$ = 0.05
$^b/_L$ = 0.05
$^T/_L$ = 0.0500
0.0625
0.0750
0.0875
$^T/_L$ = 0.1000
0.1250
W/O BB
$C_W = R_W / \frac{\rho}{2} L^2 V^2$
C_W
0.002
0.001
0.1
0.2
0.3
0.4
$V/\sqrt{Lg}$

Fig. 7.

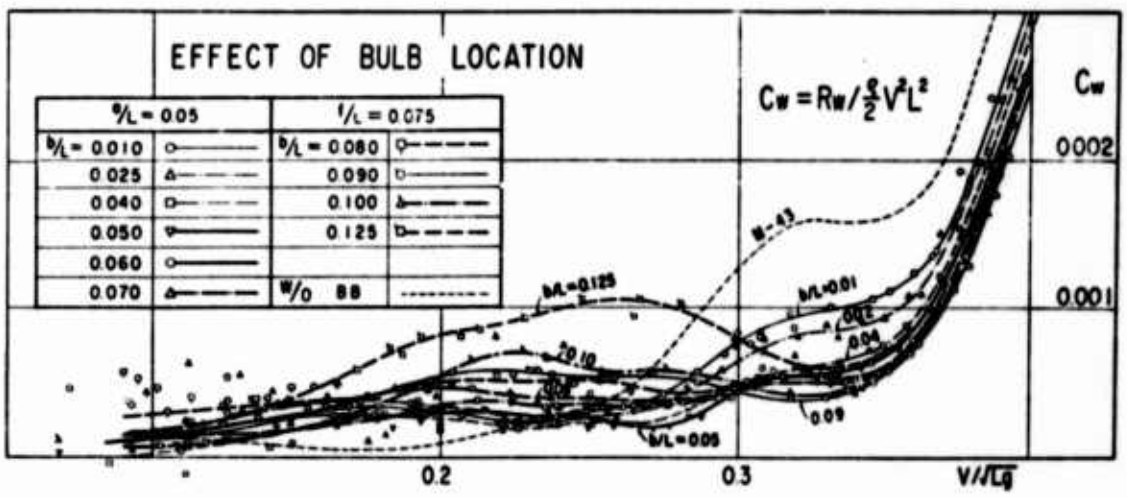

EFFECT OF BULB LOCATION
$^{C_b}/_L$ = 0.05
$^T/_L$ = 0.075
$^b/_L$ = 0.010
0.025
0.040
0.050
0.060
0.070
$^b/_L$ = 0.080
0.090
0.100
0.125
W/O BB
$C_W = R_W / \frac{\rho}{2} V^2 L^2$
C_W
0.002
0.001
M=43
$^b/_L$=0.125
$^b/_L$=0.01
0.10
0.09
$^b/_L$=0.005
0.2
0.3
$V/\sqrt{Lg}$

Fig. 8.

$$\frac{b}{L} \sim \frac{1}{K_oL} \tan^{-1}\left(-\frac{\partial\zeta}{\partial x}\right)_{x=o}, \quad K_oL = 1/F^2 \tag{9}$$

where b = shift of the wave profile, ζ = elevation of the wave surface. Such tendency as above mentioned is also confirmed by the experiment, in which the center of bulb comes to project as far as 5% of L from FP. at a waveless point, $V/\sqrt{Lg} = 0.270$.

The size of the bulb should be decided both by the amplitude function of the main hull and of the bulb in (3), where the latter could be practically replaced by a doublet, especially in spherical bulb. For the model M-43 with U-frame line

$$\left.\frac{A}{L}\right|_U \sim \frac{a_1}{\pi} K_oL \frac{[1 - \exp(-K_oT \sec^2\theta)]\sec^2\theta}{(K_oL \sec\theta)^2 - \pi^2} \tag{10}$$

and samely for the V-frame model, $m_2(\zeta) = 1 + \zeta/t$

$$\left.\frac{A}{L}\right|_V \sim \frac{a_1}{\pi} \frac{L}{T} \frac{K_oT \sec^2\theta - 1 + \exp(-K_oT \sec^2\theta)}{(K_oL \sec\theta)^2 - \pi^2}$$

These could be generalized in the following form applying the Michell's assumption for thin ships -

$$u \frac{\partial y}{\partial x} = w \frac{\partial y}{\partial z} \to 0, \qquad v = -V \frac{\partial y}{\partial z} \quad -$$

to the fore end of the model $a_1 \sim 2\alpha$, where V·m means flow volume per unit time and area; α half angle at the entrance of water-line; (u, v, w) a flow velocity; (x, y, z) a point on the surface of ship; V the ship speed; $F = V/\sqrt{Lg} = 1/\sqrt{K_oL}$:

$$A/L \sim (2\alpha/\pi) \quad (F, T/L, \theta) \tag{11}$$

And the amplitude function of a spherical bulb, the draft of whose center is $\zeta = -f$,

$$\frac{B}{L} \sim -2\left(\frac{a_o}{L}\right)^3 (K_oL)^2 \sec^4\theta \exp(-K_of \sec^2\theta) \tag{12}$$

in general

$$\sim -\left(\frac{a_o}{L}\right)^3 \mathcal{B}(F, f/L, \theta) \qquad (13)$$

Since at complete waveless point B/A = 1 and b = 0 in (7).

$$B_* = \frac{(a_o/L)^3}{2\alpha/\pi} = \frac{\mathcal{J}(F, T/L, \theta)}{\mathcal{B}(F, f/L, \theta)} \qquad (14)$$

Figure 9 is the example of B_*/π for M-43 of U-frame, to which (10) and (12) are applicable. From the illustration at F = 0.275, f/L = 0.100

$$a_o/L = \sqrt[3]{a_1 B^*/\pi} = 0.05 \quad \text{for } 2\alpha \sim a_1 = 1.36$$

and this coincides with the experiment.

4. Waveless Trawler Model for Practical Use

Through the foregoing investigation it would be recognized that the effectiveness of the bulb at a designed speed depends upon the lines of the main hull having no parasitic wave except the bow and stern (paragraph 2) and upon the size and location of the bulb relative to the bow or stern wave (paragraph 3). Under these considerations a practical trawler model, M-44BB, was derived after some complementary exploring with M-43 about an effect of flat bottom and of finer entrance etc. The fore-body of M-44 in Figure 10 is almost the same as M-43 except a slightly flat bottom and a little finer entrance, and the aft-body is lifted flat upwards to have satisfactory reserve buoyancy for trawling and to avoid the separation of flow. The point a full deliberation should be placed on is that these transformation for practical boat has to be be tried to maintain the characteristics of the bow wave of M-43 as well as possible which is effectively able to be cancelled with a bow-bulb and not to increase the stern and the other parasitic waves. As shown by the result in Figure 11, M-44BB would possibly be regarded as a fairly successful paractical model of waveless hull form counting on its considerable reduction of resistance. If allowed to hope for more, the bulb should be made somewhat larger to meet a little higher waveless speed and located a little forward to

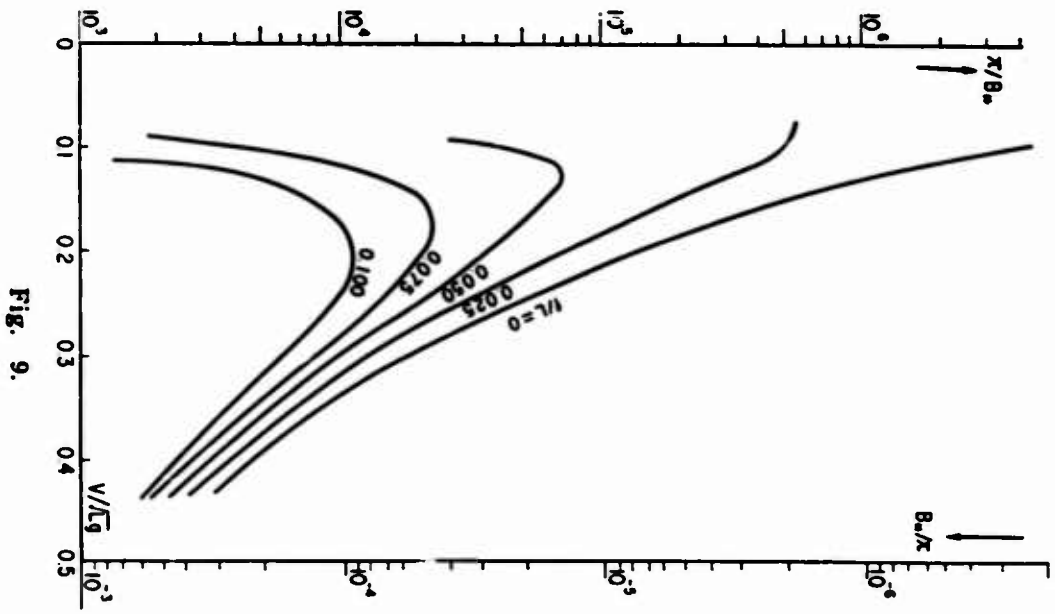


Fig. 9.

Principal Dimmension Ratios for M-44

L_{oA}/L_{WL}	1.17
L_{pp}/L_{WL}	1.00
B_m/L_{WL}	0.21
d_m/L_{WL}	0.12
$\nabla/(0.1L_{WL})^3$	13.446
Ordinate Apart/L_{WL}	0.10
Water Line Apart/L_{WL}	0.03
Bow & Buttock Line Apart/L	0.03

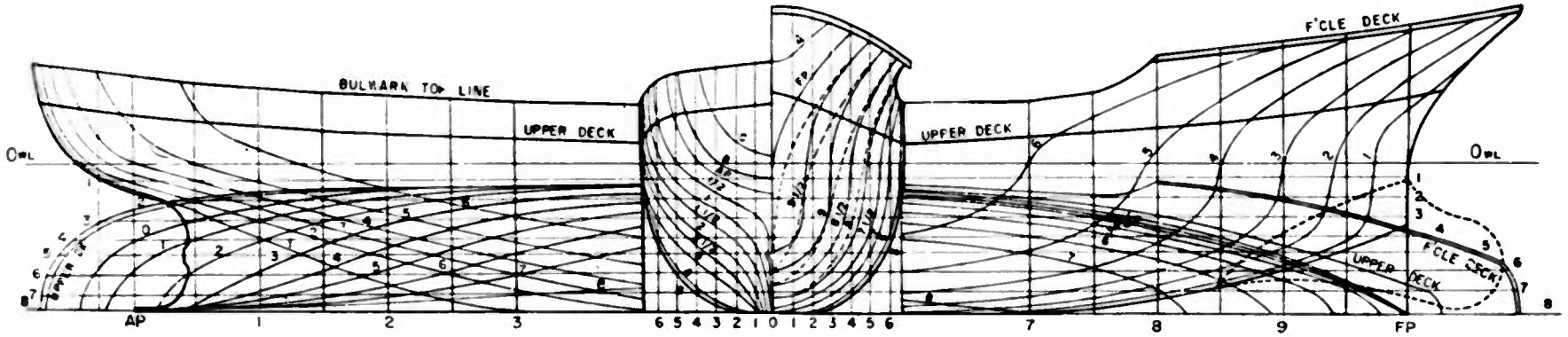


Fig. 10.

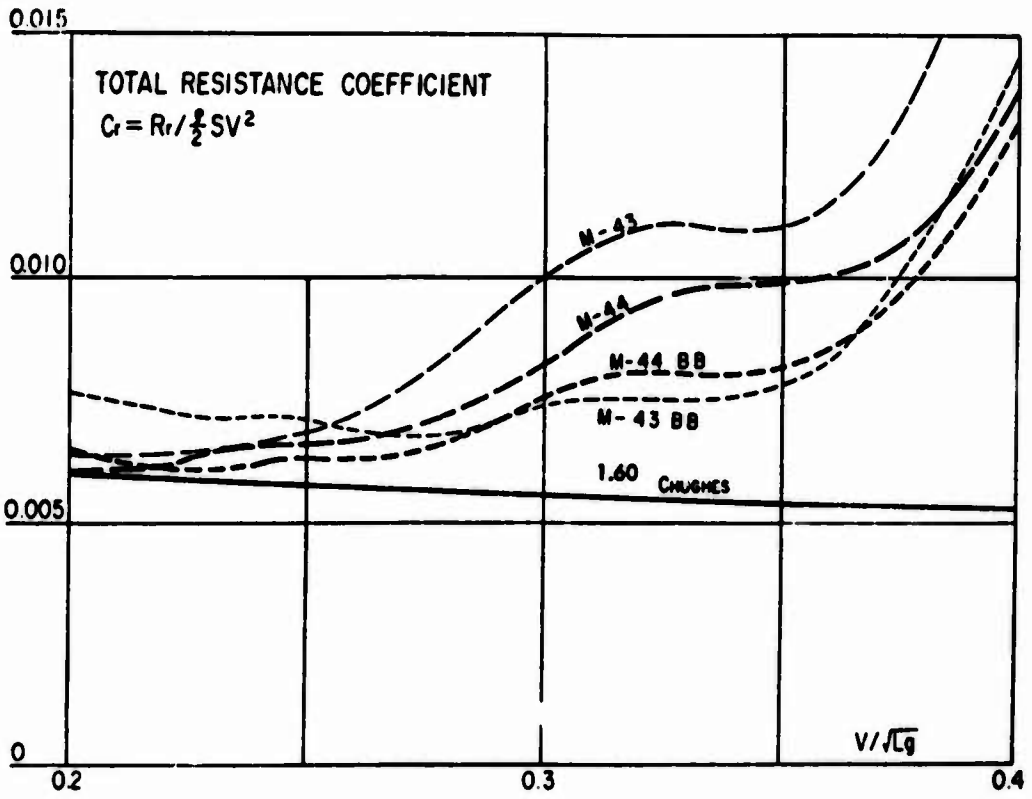


Fig. 11.

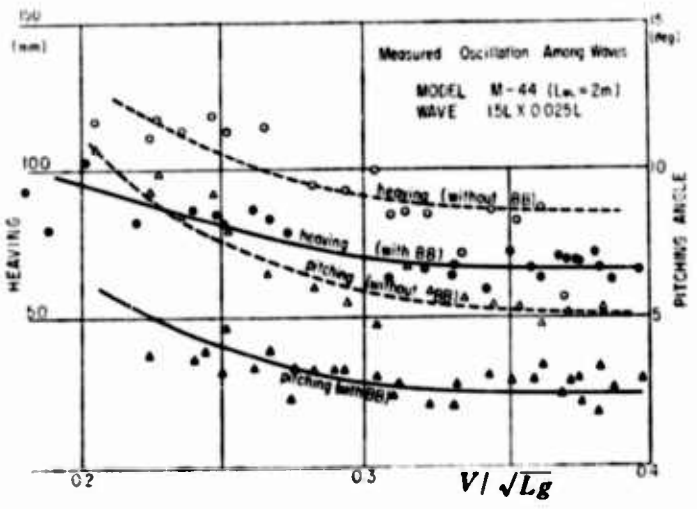


Fig. 12.

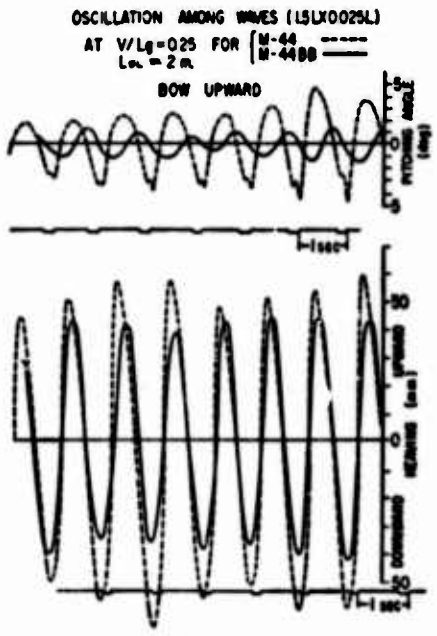


Fig. 13.

complete waveless effect if not work against practical maneuvering operation, or, otherwise, a more hollow fore-body should be investigated.

Propulsive factors are compared between the self-propulsion tests with 2-m. model of M-44 and M-44BB fitted with the stock propeller of 0.145 m. in diameter and 0.087 m. in pitch. According to the result in Table IV 10% gain in hull efficiency at $V/\sqrt{Lg} = 0.30$ is brought about by 7% increase of wake which may be resulted in on account of the diminution of negative wave wake.

A comparative wave test with the same models having 0.25L radius of gyration are carried out in the wave of 1.5L long and L/40 high and the period of free pitching is 1.17 sec. for M-44 and 1.27 sec. for M-44BB. The gain of 12.3% in the thrust deduction for M-44BB may come from a reduction of motion by the restricting effect of bulb as shown later in Figure 12. The cause of much the same PC for both models contrary to the considerable difference in hull efficiency lies in the fall of relative rotative efficiency for M-44BB which is inflicted by an increase of relative motion between wave and the model as a result of the restricting effect by the bulb.

The motion among waves is considerably holded by the bulb as recorded in Figure 12 and Figure 13. The pitching amplitude is reduced to half of the model without the bulb and the heaving amplitude is improved to 80% of that. By the action of the bulb the phase of pitching proceeds about 90 deg. ahead of the heaving that gives a visual impression of favorable control over the bow motion.

5. Conclusion

The most important conclusions drawn from the preceding investigation may be summarized as follows:

(1) The main hull should be a waveless hull form having no parasitic waves. If not attainable practically, the lines should be made as simple and natural as possible.

(2) The location of bulb has a priority order of selection for the waveless effect.

(3) The size of bulb depends on the waveless speed but it should not introduce an increase of the form drag.

(4) The effect of bulb on propulsion is more favorable than expected.

(5) The performance among waves may also be much improved.

(6) The foregoing results may give hopeful suggestions except fears for maneuvering, anchoring and some operations, but there is a promising practicability if hollow waveless lines are cultivated to bring back the bulb towards FP.

REFERENCES

(1) Inui, Takahei, Kumano: "Tank Test of the Wave-Making Effect by Bulbous Bow," ZKK 108.

(2) Takahei: "Study on Waveless Bow," ZKK 108 and 109.

(3) Kumano: "Study on Waveless Stern," ZKK 108 and 109.

(4) Traung: "The Prismatic Coefficient," Fishing Boats of the World II, 1958.

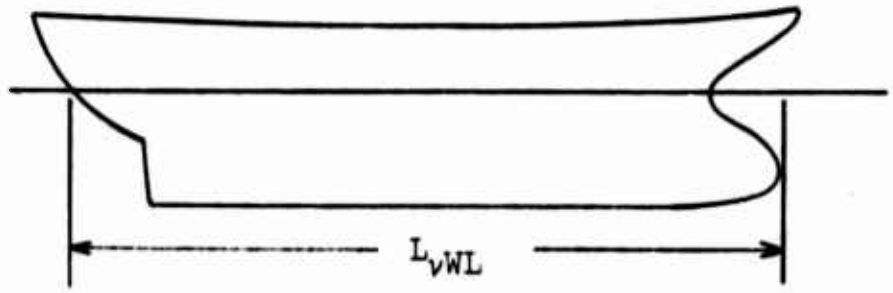
(5) Yokoyama, Kobayashi: "Resistance Test of European Wodden Trawlers," Technical Report of Fishing Boat No. 13, 1959.

(Abr, ZKK: Journal of "ZOSEN KIOKAI", The Society of Naval Architects of Japan).

DISCUSSIONS

by Lawrence Ward

I think we need a new definition of length when dealing with extreme bulb forms and propose an "underwaterline" length L_{vWL} as follows:



This I believe would be more fair when comparing bulb forms to non-bulb forms.

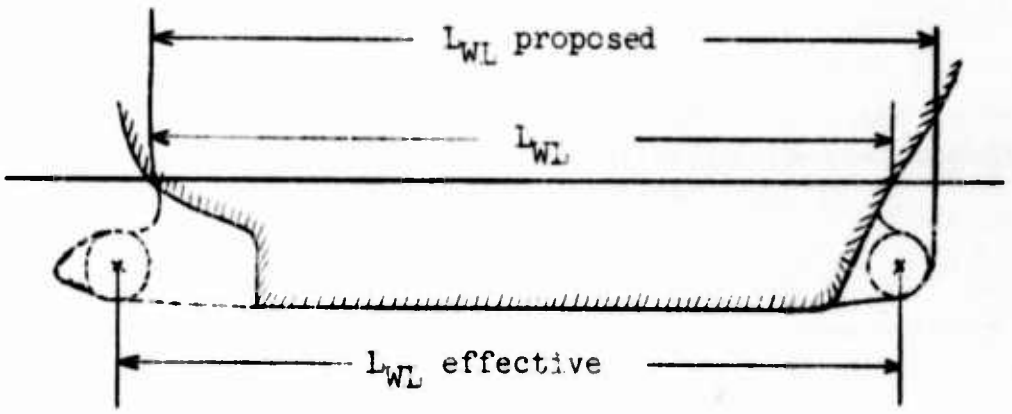
by Dr. Gadd

I would like to ask Mr. Yokomama if he is convinced that the use of large bulbs is the best way of achieving low resistance.

At the National Physical Laboratory, Mr. Doust has performed a statistical analysis of trawler model-test results, in terms of geometrical characteristics such as angle of entrance, block coefficient ets. He is able to select optimum combinations of these parameters to meet any specified design limitations and yet to give least resistance. His best forms having the same major shape characteristics as Mr. Yokoyama's have much lower wave resistances, though they have no Bulbs at all. This raises the whole question as to how valuable wave theory in its present form may be for design, as compared with more empirical approaches, and I would welcome Mr. Yokoyama's comments on this.

AUTHOR'S REPLY

As a theoretical result a special definition of length may not be necessary for the ship with a bulb however extremely protruded from the fore perpendicular, because the size and position of a bulb should be determined with the wave produced by the hull without the bulb, whose Froude number is based on the normal water-line length. Exactly speaking, however, the effective generating point of usual hull-wave is placed a little forward from the real bow end on account of the perturbation effect of the free surface or some other effects. A strict definition, therefore, may be that the (effective) length should be the distance from the (effective) center of the bow-bulb to that of the stern-bulb which is also usually a little afterward from the waterline-end even if without stern-bulb, and all the existing surface ship without bulb can not be the exception of such definition. Practically there may, therefore, be no need for the new definition for the wave-resistance, but the proposed length may possibly be worth for maneuvering, longitudinal motion or construction.



The use of bulb with a waveless hull could be one attempt for achieving low resistance at a fixed speed, and the size of bulb, large or small, depends only upon the amplitude of the hull-wave resulted from a hull-shape and a designed speed, but it may not be the best way upto now. If there could exist an 'ideal' ship, she might be resistanceless at any speed and must have an excellent performance in any weather condition. Mathematical, intuitive and empirical -- all researches must naturally be on the way to such an 'ideal' ship. Mathematically the hull of the minimum resistance could be pursued by means of variational calculus. The waveless theory may be intuitionally developed on the idea of the cancellation of a hull-wave with a bulb-wave. And empirical efforts have been made to exploit an ideal form since the Taylor's series. These general aspects may be predictable from Bessho's mathematical analysis about the minimum resistance, whose identical solution seems not generally to exist except under some restricted conditions.

On the other hand for the ship design there are many practical requests for the ship form not only on the point of wave resistance, but also of the other ship performances, and many combined effects must be harmonized on the superior design. It should be, therefore, noticed that Doust's analysis can statistically reveal every effect of the practical factors on the model resistance, and it will much contribute to the pursuit of the minimum resistance, when it could give some possible suggestions about influential factors on the variational method or the intuitive attempt. Generally speaking, three ways of the pursuit -- mathematical, intuitive and empirical -- should be parallelly proceeded or those limit of the application should be clarified in order to realize the 'ideal' ship.

For the waveless design, there must be many possible combinations, -- e.g. a large bulb and a ship of rather high wave (at a high speed), a small bulb and a special low-wave-hull, bulbless hull, or special derivation based on the Yim's zero wave theory. The models, M-43 and M-44, are a kind of the waveless attempt for a fishing boat requested for a wider deck and a heavy displacement for ship length, and their hulls which are obtained from a co-sinusoidal source distribution, produce rather high waves easily cancelled by a large-bulb-wave at a high Froude number. The approximately waveless design can be an attempt to realize an ideal condition at a fixed speed, but it may not be so ideal that there might be unfaborable defects on the other speed range or on the other performance for the practice. The Bessho's analysis suggests there can exist many shapes which have the same wave resistance and it is so hopefull that more faborable hulls of the lowest resistance could be discovered theoretically or empirically. The Doust's analysis is, therefore, very helpfull for the less-wave design, especially bulbless or with a small bulb, and its result may be waited for with full expectation among the theoretical group.

A HIGH-SPEED CARGO LINER DESIGN BASED UPON THE "WITH-BULB" WAVELESS CONCEPT

Reiji Tsunoda
Kyoshi Kasahara
Katsuyoshi Takekuma

Yokohama Shipyard & Engine Works
Mitsubishi Nippon Heavy-Industries, Ltd.

A HIGH-SPEED CARGO LINER DESIGN BASED UPON THE "WITH-BULB" WAVELESS CONCEPT

INTRODUCTION

The work to be reported here is not a theoretical one but an application example of already established "with-bulb" waveless concept, so the authors would at first like to mention the circumstances and necessity which lead them to the application of "with-bulb" waveless concept for high-speed cargo liner designs.

Referring to the situations which surrounded the Japanese shipyards a few years ago, most of the shipyards suffered from excessive competitions to get work in hands among themselves or against overseas shipyards, as a results of which they had to make more effort than before to design any better ship from economical point of view. A part of the effort has naturally been directed to find out a hull form of better performance, but the only tool for that object was conventional model series tests, from accumulation of which shipyard engineers could manage to pick up the optimum hull form under given design requirements. However, the tool had its own deficiencies as have been at times pointed out by Professor Inui, the largest of which was that there was no leading theory connecting hull forms and their experimental results, and the engineers had to connect them by imaginations.

The authors' company had also accumulated a large amount of model test results and had some kinds of optimum hull forms of good propulsive performance, and there seemed to be left little possibility of improving those optimum hull forms by further accumulation of conventional model test results. The need to seek for better hull forms (especially of high-speed cargo liners) were getting more serious to the contrary. (Refer to N. P. on page 4.)

Looking at naval architectural field in our country and abroad, many excellent papers dealing with ship's propulsive performance had been published by that time, but they were only too theoretical, suggesting little for shipyard engineers in general how to apply the theory for practical ship designs with satisfactory results.

Apart from these naval architectural circumstances in general, important and basic frameworks of "with-bulb" waveless forms had been

constructed in Japan, mainly by the staffs of the Experimental Tank of the University of Tokyo, with many series of model tests which brought about fruitful results (for example, Reference 1) for the researchers in general, enough to confirm the validity of the fundamental theory used. However, most of those models were purely of theoretical forms, or slightly modified ones at most, and there remained a small gap to be bridged over to adapt "with-bulb" waveless forms to actual ship designs.

Considering these situations stated above, the authors started last year to apply the "with-bulb" waveless form theory to the design of a sort of high-speed cargo liners, while examining problems in all phases inherent in the large bulbous bow ships. These types of ships seemed to be advantageous to adopt the hull forms mentioned above by reason that they had to sail usually at rather high speed as commercial vessels, and that their hull forms were necessarily fine enough not to make shoulder waves which disturb full application of the theory. On applying these hull forms to actual ships, many problems had to be investigated and settled, namely general arrangement, outfitting of fore body, strength and construction of bulb part together with its connection to main hull, ship's manoeuvrability, propulsive performance in waves, etc. In this initial development work, stress was laid on acquiring better resistance and propulsion characteristics in still water and examining rough water performance, but other items mentioned above were also studied to be integrated into actual ship designs. Some optimum designs being obtained under given design conditions and with above-mentioned problems settled, they were model tested of their propulsive performances and the results were analyzed.

The authors will briefly report a part of our development work, mainly concerning the initial design of hull forms and model tests results.

An example of the efforts made during these thirty years is shown in Figure 12. A sudden jump of the admiralty coefficient (C_{adm}) which has taken place from 1962 Ship "A" to 1963 Ships "B" and "C" is remarkable. The authors feel honored that their efforts as well as the valuable basic researches exerted at The University of Tokyo Experimental Tank has motivated this epoch-making technical revolution.

1. HULL FORM DESIGN

1.1 Design Conditions and Requirements

Full load was chosen as designed loading condition. Basic requirements imposed on the authors' designs at this load were as follows.

Displacement		=	about 17,800 ton
Mt. of inertia of waterplane	I	=	about 63,200 m^4 *
draft moulded	d	$\leqq$	9.00 m
designed speed		=	about 20 knots (Fn = 0.2673 or Kol = 14)

Note: *Corresponds to GM = 0 at full load arrival condition.

1.2 Main Hull Form Design

On this stage it is first necessary to find out source distributions corresponding to hull forms in compliance with design requirements. For instance the first ship was determined to be 145 m in length between perpendiculars, 21.4 m in breadth moulded (or Bm/Lpp = 0.1476) - breadth being considerably dependent on Lpp and I-, and 9 m in draft. Then the problem reduces to deciding the form of source distribution function and its constants either by trial and error method or interpolating the coefficients using definite integrations of some sort of source distribution moment functions and end value of source distribution. The chosen source distribution should have proper characteristics (as for weighed amplitude functions, or phase shift functions, or midship wave generation), and of course be less wave-making itself.

Source distribution function adopted was of uniform source strength draftwise over the distributed range, and was to be expressed as follows:

$$m(\xi, \zeta) = a_1\xi \mp a_2\xi^2 \quad \begin{pmatrix} -1 \le \xi \le 0 \\ 0 \le \xi \le 1 \end{pmatrix} \qquad (1)$$

$$T/L = 0.04 \qquad -T/L \le \zeta \le 0$$

The coordinate system (ξ, ζ) may be interpreted as ξ for longitudinal direction (+ sign forward) and ζ for vertical direction (+ sign upward), with their origin at the middle point of assumed theoretical hull form length, on the center line of load waterplane. Both ξ and ζ are made dimensionless through dividing actual length by $l = L/2$ (half of theoretical hull form length). T is the depth of source distribution below load waterline.

The next steps are to calculate the corresponding hull forms by stream-line integration, then to cut the curved, calculated bottom at the depth corresponding to designed draft with proper fairing around bilge part, and thus to obtain "practical" fore half body. Finally a conventional aft body having good propulsive characteristics is to be connected to the fore half body, again followed by due fairing about the connected section to get final main hull form which meets displacement requirement, and also longitudinal center of buoyancy requirement if possible.

Through the process described above, the authors got three main hulls, namely the first ship (2.5 m model named M. No. 196), the second ship (do. M. No. 198), and the third ship (do. M. No. 205). Their particulars are listed in Table 1, and their load waterline curves with corresponding source distribution patterns are shown in Figure 1.

Referring to the features of these main hull forms, the first ship was rather restricted in length and beam. To satisfy stability (I) requirement under those particulars full waterplane form had to be adopted, which resulted in a parallel part of about 15% Lpp in aft body. The adoption of parallel part seems to have caused disturbing aft shoulder waves which directly relate to wave-making resistance increase as explained later.

Breadth of the second ship was, taking the result of the first ship into consideration, increased a little enough to have sufficient moment of inertia of waterplane without parallel part which might cause aft shoulder waves. Both two ships had their centers of buoyancy fairly fore compared with the conventional hull form of the

TABLE 1

PARTICULARS OF MODELS

MODEL (SHIP)	M. No. 196 (1)	M. No. 198 (2)	M. No. 205 (3)	MODEL "A"
Lpp in m	2.5 (145.0)	2.5 (145.0)	2.5 (150.0)	6.0 (150.0)
L wl in m	2.564 (148.7)	2.564 (148.7)	2.558 (153.5)	6.1595 (153.988)
Bm in m	0.369 (21.4)	0.3868 (22.4)	0.3750 (22.5)	0.8334 (20.5)
dm in m	0.1555 (9.0)	0.1555 (9.0)	0.1475 (8.5)	0.3627 (9.05)
∇f (Main Hull)	0.08825 (17649)	0.08898 (17799)	0.07959 (17621)	1.13595 (18193)
∇f (With-Bulb)	0.09004 (18008)	0.09060 (18119)	0.08125 (18018)	
l.c.b. (Main Hull)	1.73 % Lpp	1.154 % Lpp	2.53 % Lpp	abt. 1.48 % Lpp
l.c.b. (With-Bulb)	0.70 % Lpp	0.27 % Lpp	1.58 % Lpp	
Cb (Main Hull)	0.614	0.592	0.576	0.626 (non-bulbous)
Cb (With-Bulb)	0.629	0.605	0.586	
Cp (With-Bulb)	0.652	0.648	0.623	0.641 (non-bulbous)
Source Coefficient				
a_1	3.3612	3.6840	3.466	
a_2	3.1612	3.4840	3.366	

Note: 1. l.c.b's are all abaft the midship.

2. ∇f denotes volume of displacement in m^3 for models and displacement in ton for ships.

3. Particulars of 6 m models are omitted as they are less important.

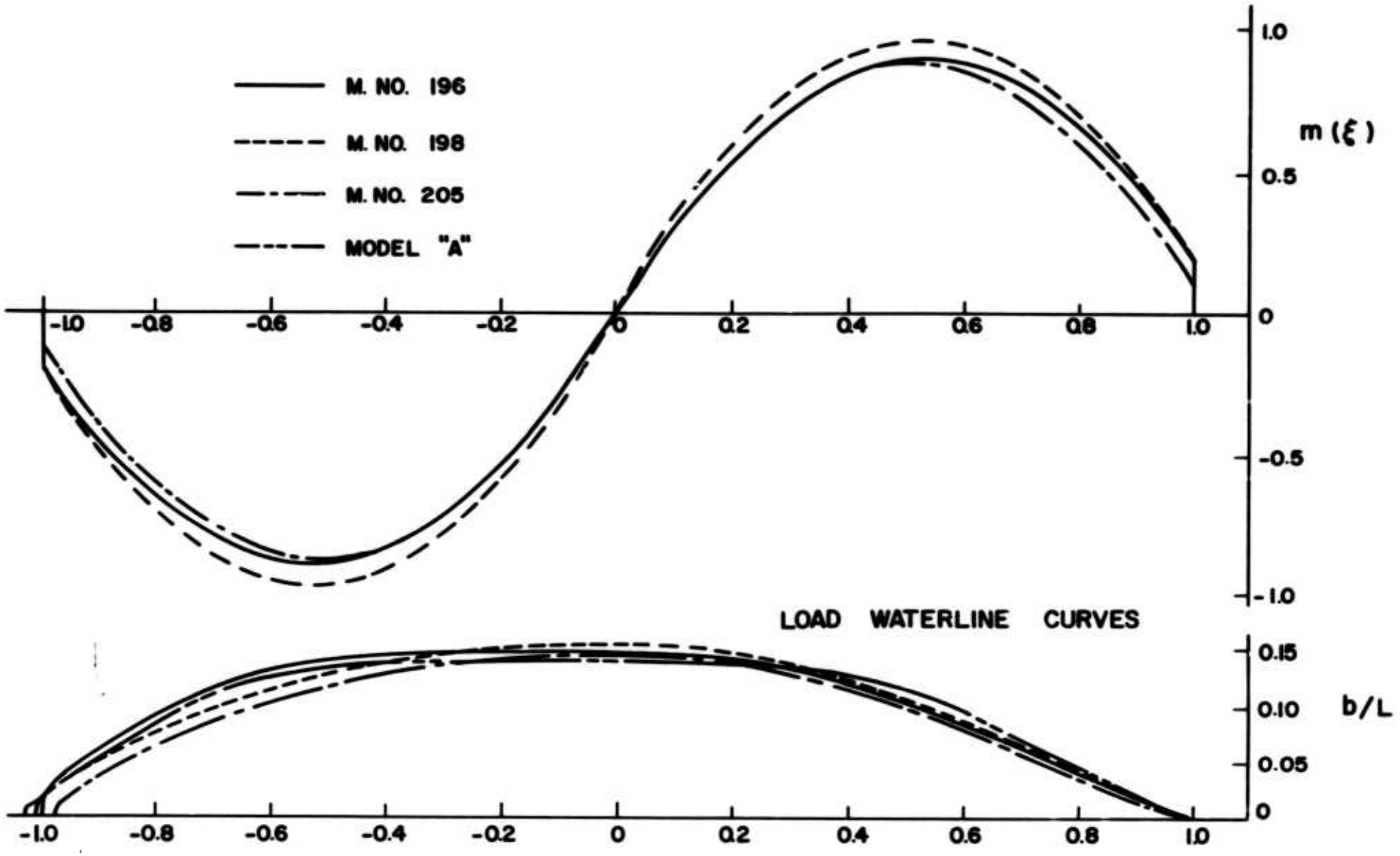

SOURCE DISTRIBUTION CURVES
M. NO. 196
M. NO. 198
M. NO. 205
MODEL "A"
m (ξ)
1.0
0.5
0
-0.5
-1.0
-1.0
-0.8
-0.6
-0.4
-0.2
0
0.2
0.4
0.6
0.8
1.0
LOAD WATERLINE CURVES
b/L
0.15
0.10
0.05
0

Figure 1.

same type, due to bulb and U-form theoretical framelines of fore half body, hence their general arrangements had to be changed to semi-aft bridge type.

The third ship was designed with particulars less different from conventional ones, namely with Lpp = 150 m and Bm = 22.5 m. At the same time caution has been payed as much as possible to improve deficiencies of the former designs that optimum bulbs to those hull forms were rather large, that waves due to cutting off the bottom together with waves from source discontinuities at midship might affect resistance characteristics and that centers of buoyancy were apt to shift forward. As for aft half body, features of the second ship hull form were reserved to the utmost with its length kept unchanged, hence the maximum section of the whole hull form came a little abaft the middle of it. Additionally, modifications of theoretical framelines about bilge part were carefully dealt with, to make minimum and gradual deviations inside the theoretical framelines. Better results were fortunately obtained as shown later.

1.3 Bow Bulb Design

As there seem to be so much variations of loading conditions with cargo liners under discussions, it is a natural need to restrict bulb size within allowable limit. Also, from outfitting and maneuvring point of view projection of bulb should generally be as little as possible. The investigations of available data on the assumed route of the designed ships indicated that the lower limit of displacement at sea might sufficiently be designated by 75% full displacement, and the limitation on size and immersion of bulbs not to stir water surface heavily were determined based on this loading condition. Design points of bulbs were decided at full load condition and Fn = 0.2673 (or KoL = 14), the same as those of main hull. Various series of bulbs were designed, calculated of their characteristics and tested, and finally chosen "optimum" bulbs in all respects are listed in Table 2.

Weighed amplitude functions for those bulbs together with those for main hulls are shown in Figure 2.

On connecting bulbs to main hull, care has been taken not to make excessive deformations of original shapes through fairing process, and not to ignore necessary modifications to prevent from unwanted separations of flow behind bulb on the other hand.

TABLE 2

PARTICULARS OF BULBS

MODEL	M. No. 196	M. No. 198	M. No. 205
Bulb	B-3	A-2	H-4
a/L in %	2.5	2.4	2.0
f/d in %	74.0	65.0	57.0
h/L in %	-0.5	-1.0	-1.0

Note: a = radius of bulb

f = immersion of bulb center below load waterline

d = draft moulded

h = projection of bulb center from fore end of model

L = 2ℓ

ℓ = length of theoretical half body

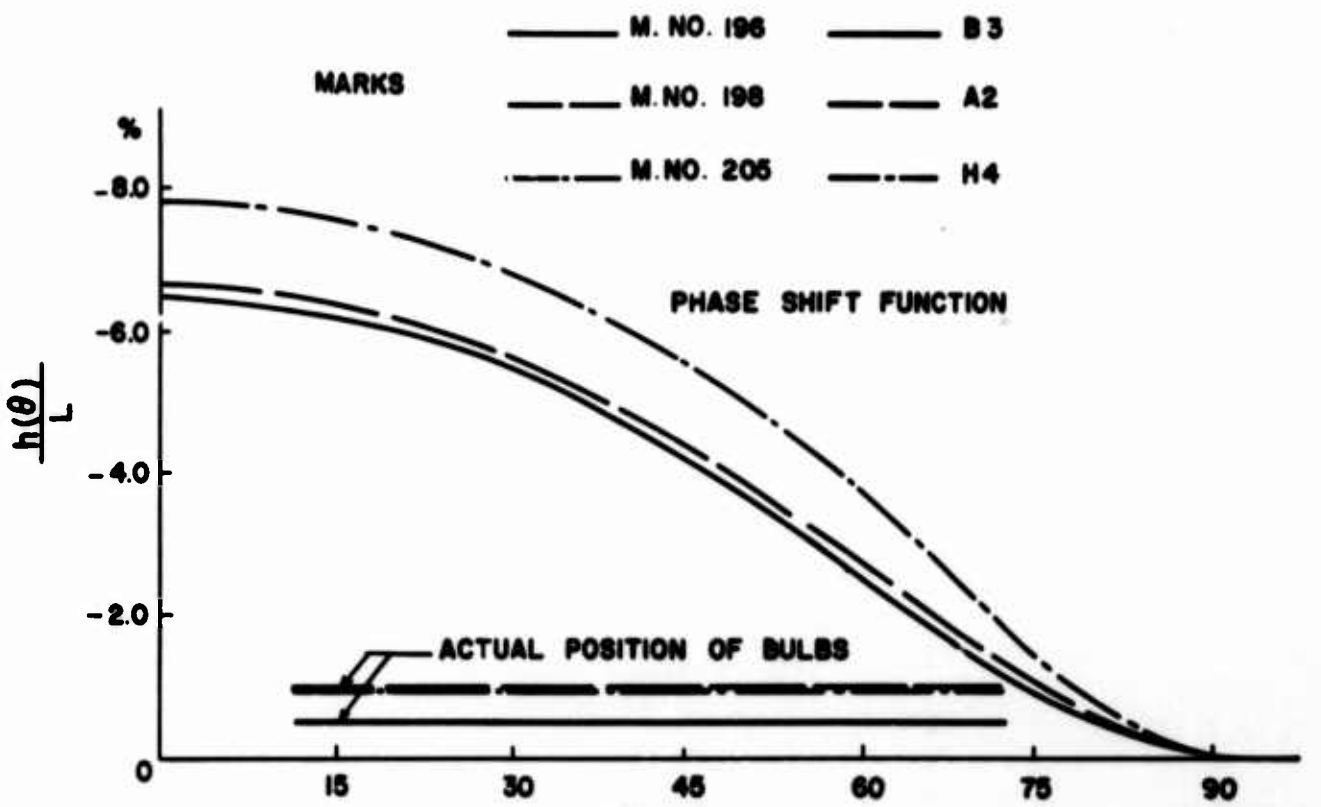


Figure 2a. Characteristics of Source Distribution and Bulb at Fn = 0.267.

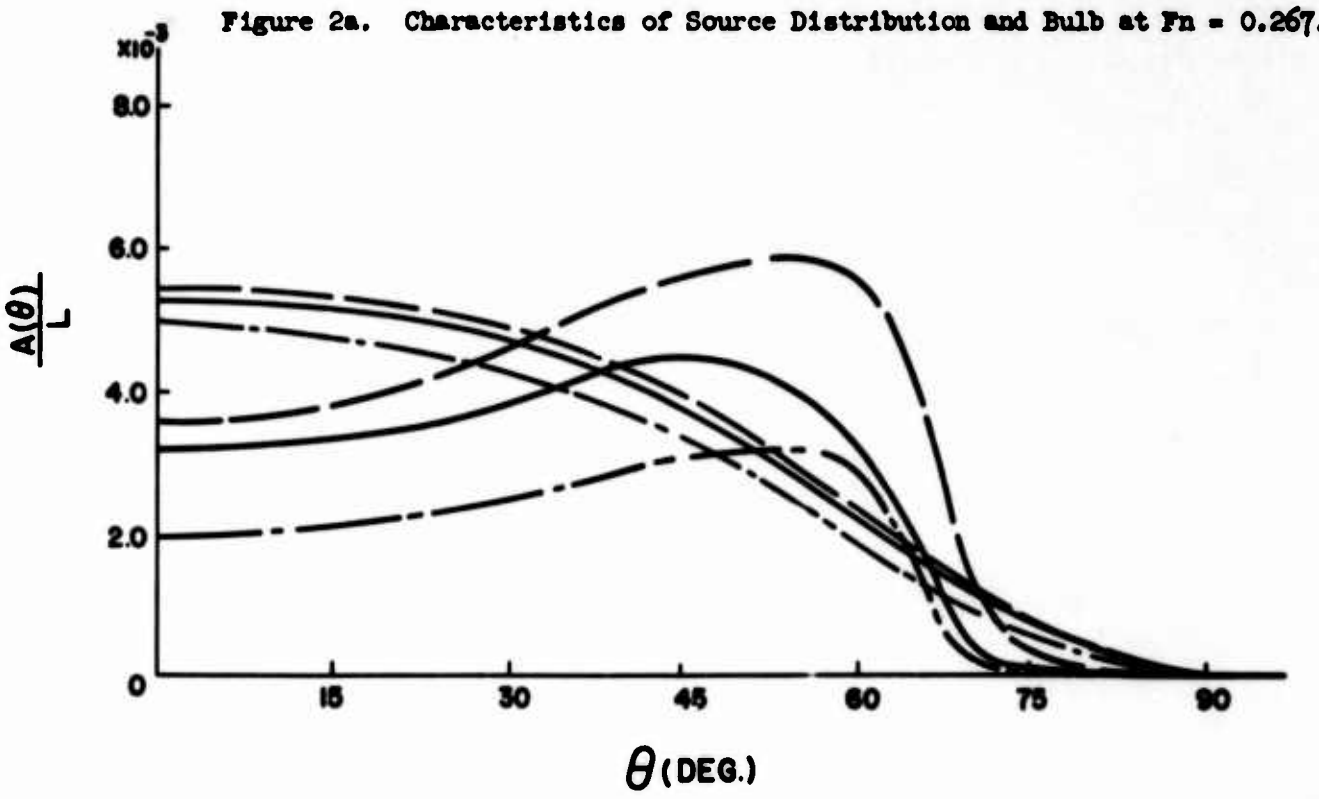


Figure 2b. Weighed Amplitude Function

2. TEST CONDITIONS AND METHOD OF ANALYSIS

The resistance tests of 2.5 m models were carried out at the Experimental Tank of the University of Tokyo. The large-scale resistance and self-propulsion tests with 6 m models were carried out at Mejiro No. 1 Tank of Ship Research Institute.

Loading conditions at which models were tested are shown in Table 3.

Turbulence stimulations were as follows.

2.5 m model (without bilge keel)

Main Hull (without bulb):
one row studs at station No. 9 1/2.

With-Bulb:
one row studs at a quarter of diameter of bulb from the fore end of bulb.

6 m model (with bilge keel of about Lpp/3 in length)

one row studs at station No. 9 1/2.

Particulars of propeller used at self-propulsion test are as shown in Table 4.

Experimental results were analyzed in the following way. The wave-making resistance coefficient "Cw" of 2.5 m model was obtained using Hughes' friction line, the form factor K being estimated by measuring the resistance of main hull (without bulb) form at low speed. This K value was used for the analysis of with-bulb form, too.

$$Ct = Rt/\tfrac{1}{2}\rho V^2 L^2_{wl}$$

$$Cfo = 0.066/(\log Rn-2.03)^2 \times S/L^2_{wl} \qquad (2)$$

$$Cf = (1 + K) \times Cfo$$

$$Cw = Ct-Cf$$

TABLE 3

KIND (TESTS CARRIED OUT

MODEL		M. No. 196		M. No. 198		M. No. 205	
Kind of Test	Loading Condition	2.5 m Model	6 m Model	2.5 m Model	6 m Model	2.5 m Model	6 m Model
Resistance	Full Load	*	*	*	*	*	*
	93% ∇ f	*	*	*	*		
	75% "		*	*	*	*	*
Self-Propulsion	Full Load		*		*		*
	93% ∇ f		*		*		*
	75% "		*		*		*

Note: 1. ∇ f denotes displacement at full load condition.

2. In case of M. No. 196 and M. No. 205, tests of 6 m main hull (without bulb) forms were omitted.

3. All the tests in this paper were carried out with 0% trim.

4. *Denotes the experiment carried out.

5. As for Model "A", both Resistance and Self-Propulsion Tests were carried out with 6 m models, at loading conditions of Full, 76.8% Full, 50% Full, and 20% Full Load.

TABLE 4

PARTICULARS OF PROPELLER USED AT SELF-PROPULSION TEST (6 m MODEL)

Diameter	0.250 m (0.250)	Max. Blade-Width Ratio	0.311 (0.226)
Pitch Ratio	0.800 (0.800)	Mean Blade-Width Ratio	0.263 (0.192)
Exp. A. Ratio	0.550 (0.500)	Angle of Rake	$10^{\circ}00$ ($10^{\circ}00$)
Boss Ratio	0.180 (0.180)	Section	Aerofoil (")
Blade-Thick. Ratio	0.050 (0.050)	Number of Blades	4 (5)

Note: Numerals in the parentheses are of the propeller used for Model "A".

where

Ct = total resistance coefficient

Cfo = Hughes' friction line at K = 0

Cf = frictional resistance coefficient

Rt = total resistance

ρ = density of water

v = speed

Rn = Reynold's number

s = wetted surface area

Lwl = load waterline length at full load condition.

As concerns 6 m models, Froude's formula was used for the calculation of both residual resistance coefficients and friction correction at self-propulsion test. However, the wave-making resistance coefficient Cw was also calculated using the same method as for 2.5 m models. The analysis of propulsive performance was based on thrust.

At the time of resistance tests of 2.5 m models at full load condition, the wave profiles were photographed at the appointed speeds.

Additionally, apart from wave profiles, wave patterns were photographed in 35 mm stereo-slides and large-size stereographs at the following speeds, namely, Fn = 0.236, 0.250, 0.267, and 0.289.

3. EXPERIMENTAL RESULTS IN STILL WATER

3.1 Observation of Wave Profiles

Referring to Figures 3a to 3d, the authors will first discuss the difference among three main hull forms, M. No. 196, M. No. 198, and M. No. 205.

M. No. 196 produced large aft shoulder waves at full load condition because of its parallel part in aft body. M. No. 198, though without a parallel part, produced them a little. The reason why they produced aft shoulder waves may be attributed to the effect of discontinuities of derivatives at midships in source distribution functions and the flattened bottoms. And bow wave of M. No. 198 was higher than that of M. No. 196, because the latter source strength must be increased to get higher beam/length ratio with constant mo, the fore end strength of source distribution.

The waves of M. No. 205 were simpler and lower than those of the formers, and it seemed that its aft shoulder waves were hardly recognized.

In case of with-bulb forms, the above-mentioned relative phenomena were again noticed for three models. The cancelling effect of bulbs on bow waves is observed sufficient.

3.2 Observation of Wave Patterns by Stereographs

(Relating Figures are Figures 4a to 4d)

The above-mentioned phenomena, namely the generation of aft shoulder waves and bulbs' cancelling effect, etc., were more clearly seen through the observation of wave patterns by stereographs.

As concerns main hull forms, the appearances of wave patterns near the model M. No. 196 were considerably complex, while those of M. No. 198 were simpler than the former, and those of M. No. 205 were the simplest of all.

In case of with-bulb forms, the above-mentioned phenomena were also observed, and waves of M. No. 205 were lower than those of the formers.

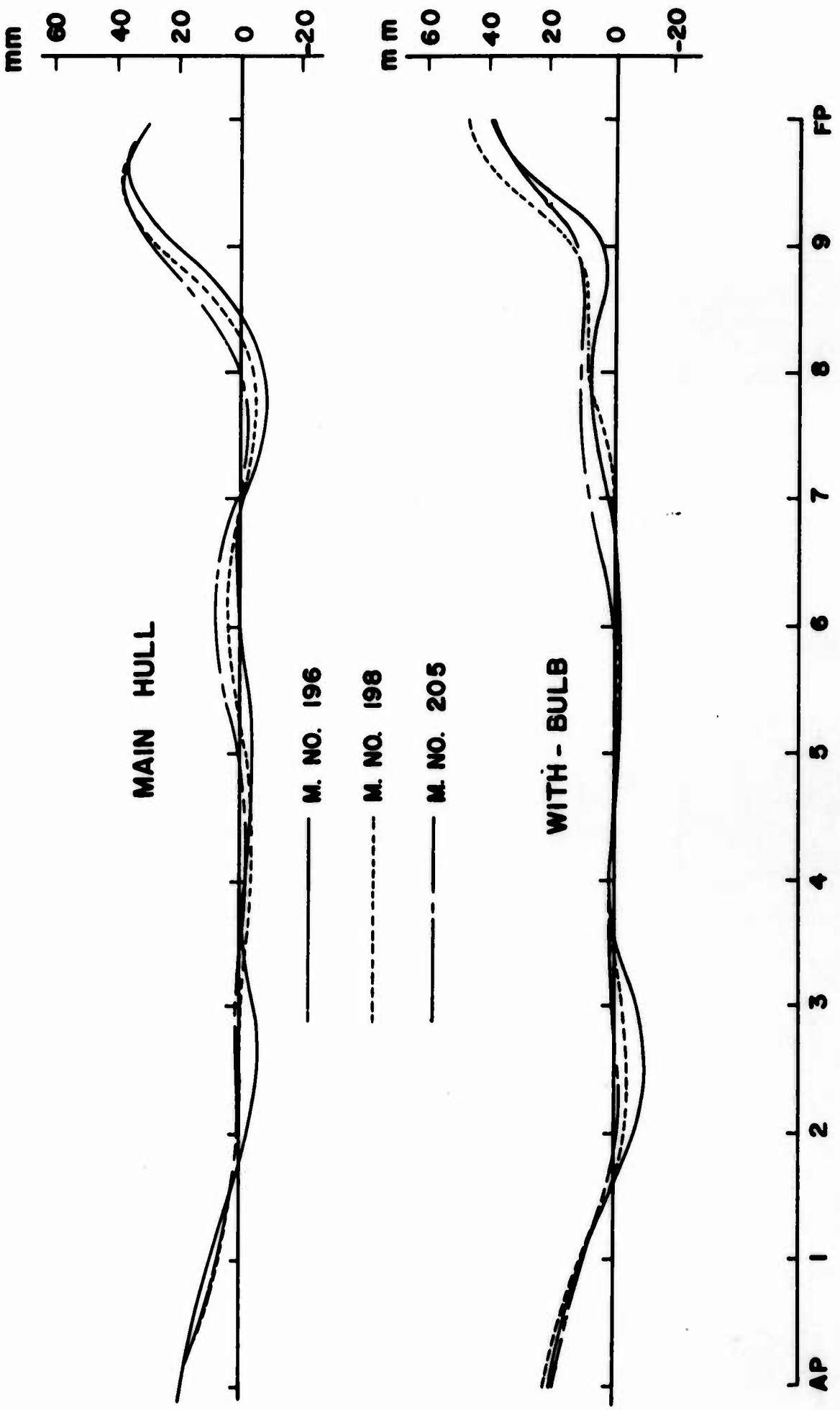


Figure 3a. Wave Profiles, Full Load Condition, Fn = 0.236.

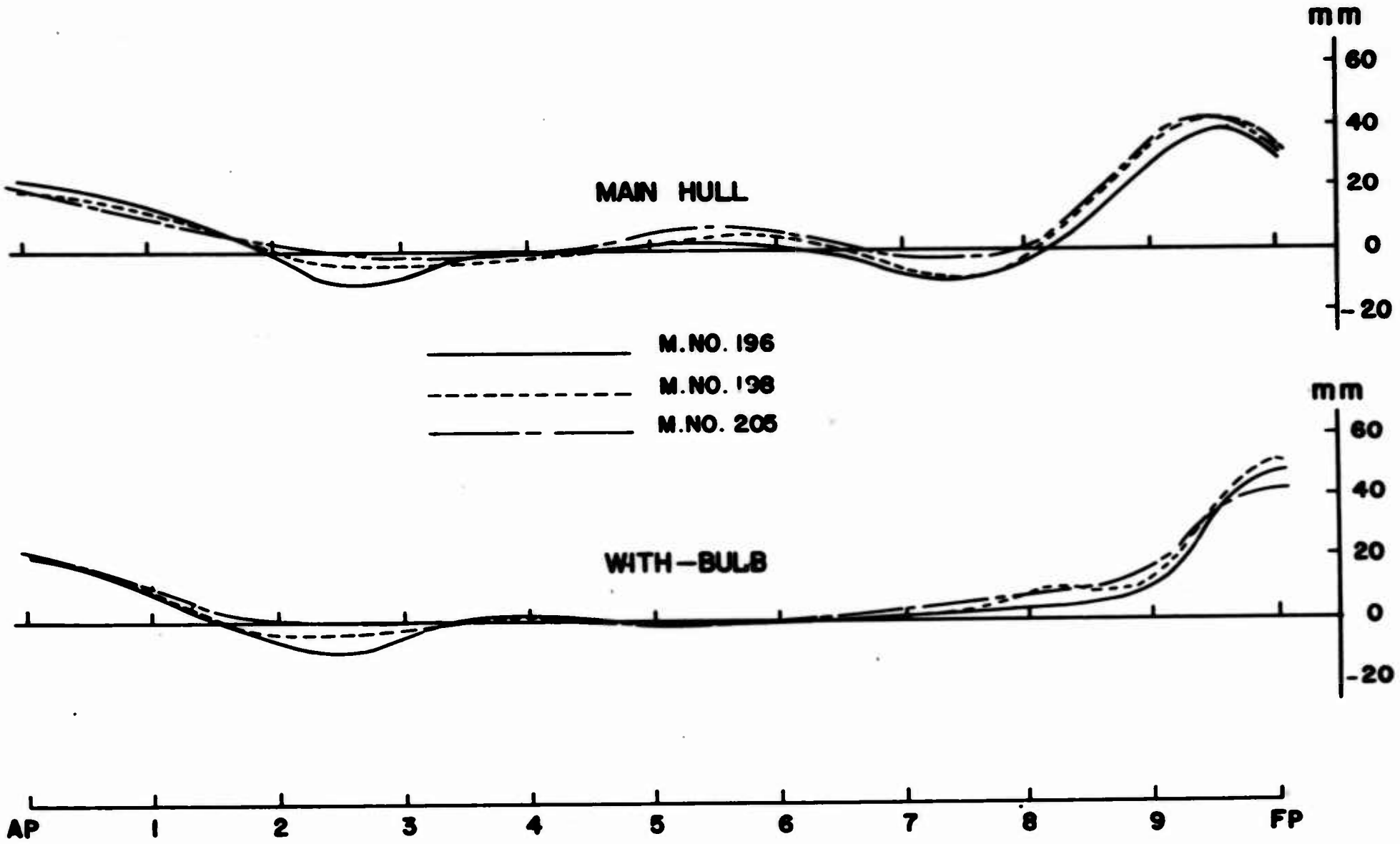


Figure 5b. Wave Profiles, Full Load Condition, Fn = 0.250.

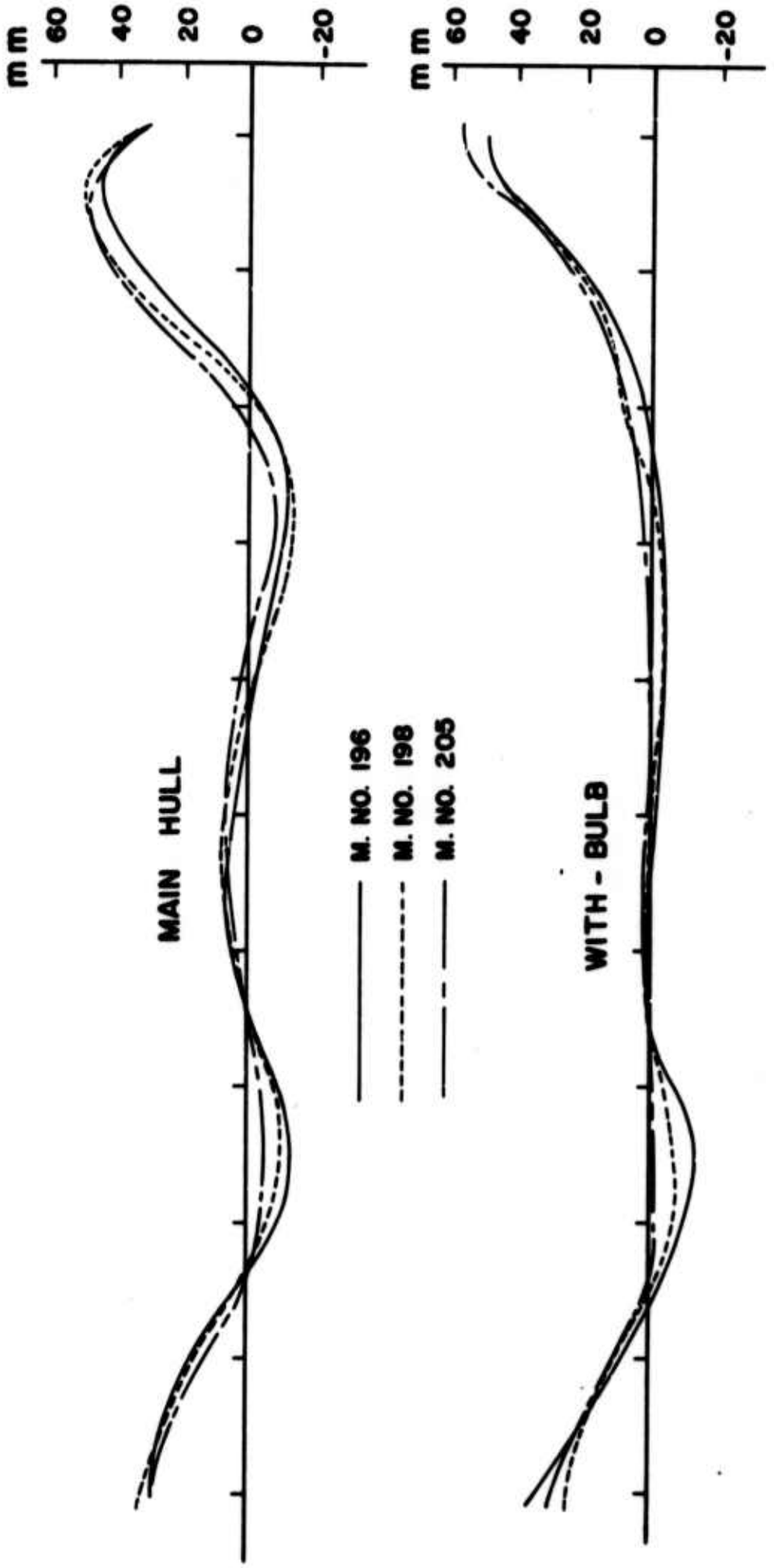


Figure 3c. Wave Profiles, Full Load Condition, Fn = 0.267 (designed speed).

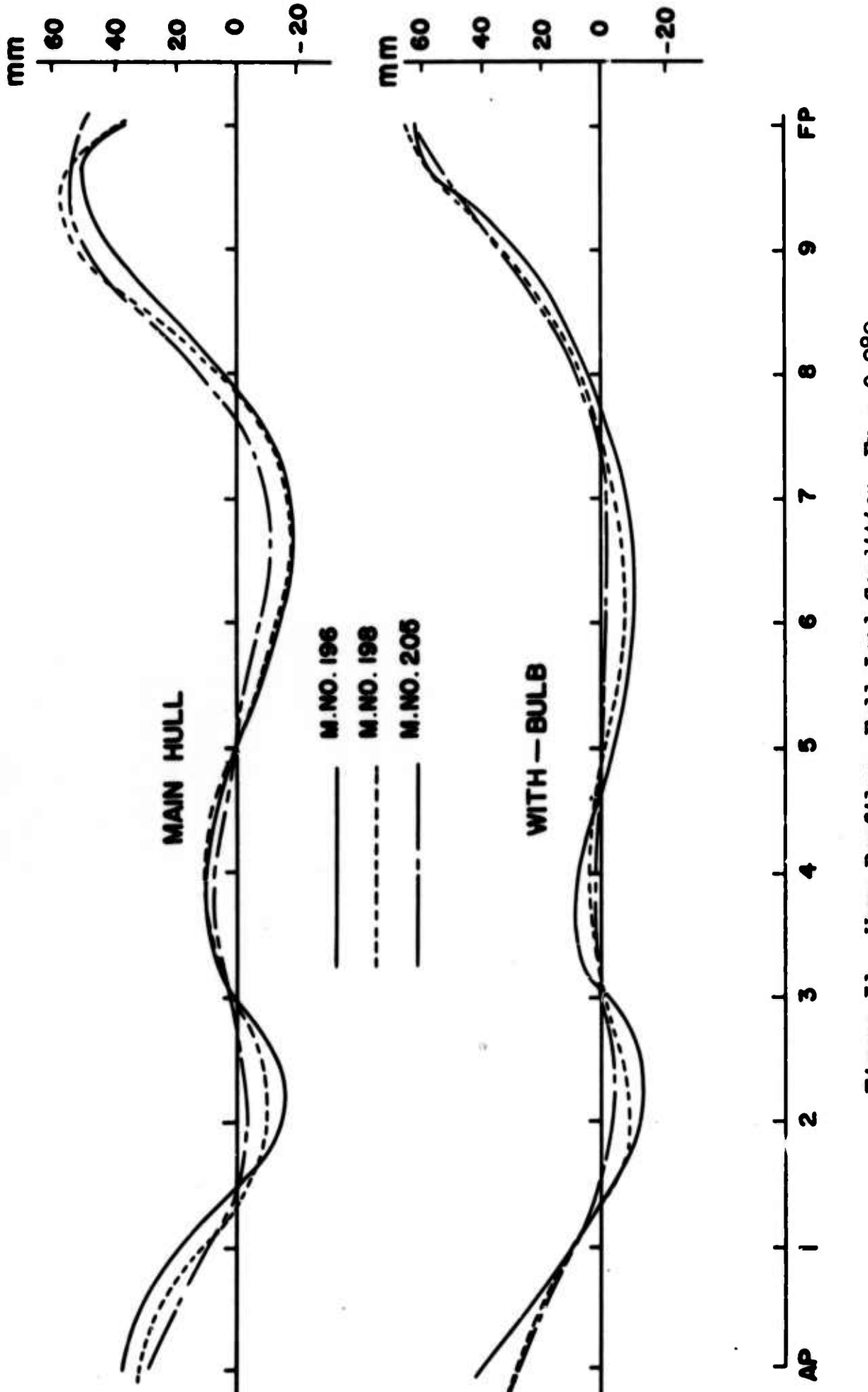
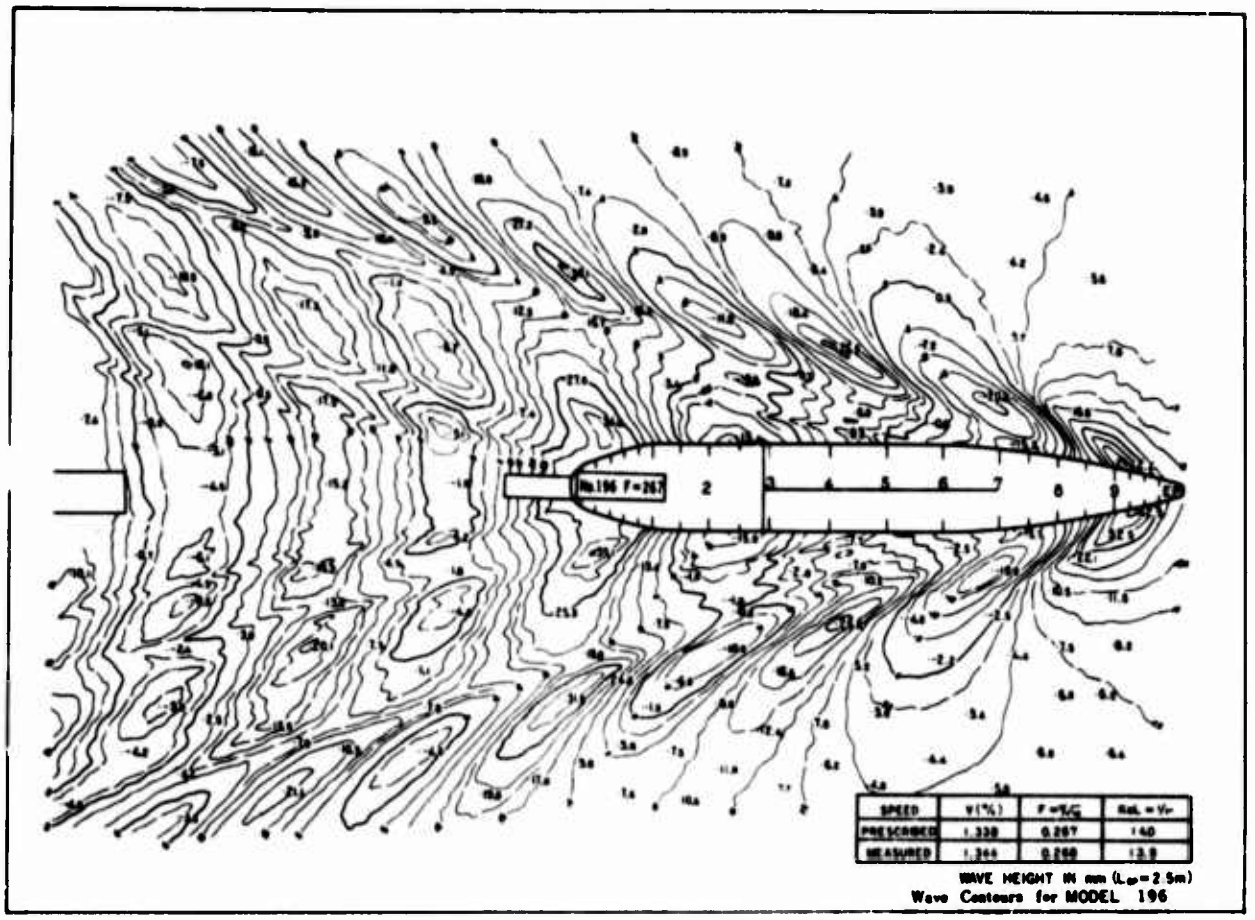


Figure 3d. Wave Profiles, Full Load Condition, Fn = 0.289.





Fig. 4a. Wave Patterns of M.No. 196 (Without Bulb), upper, and M.No. 196B-3 (With Bulb), lower.



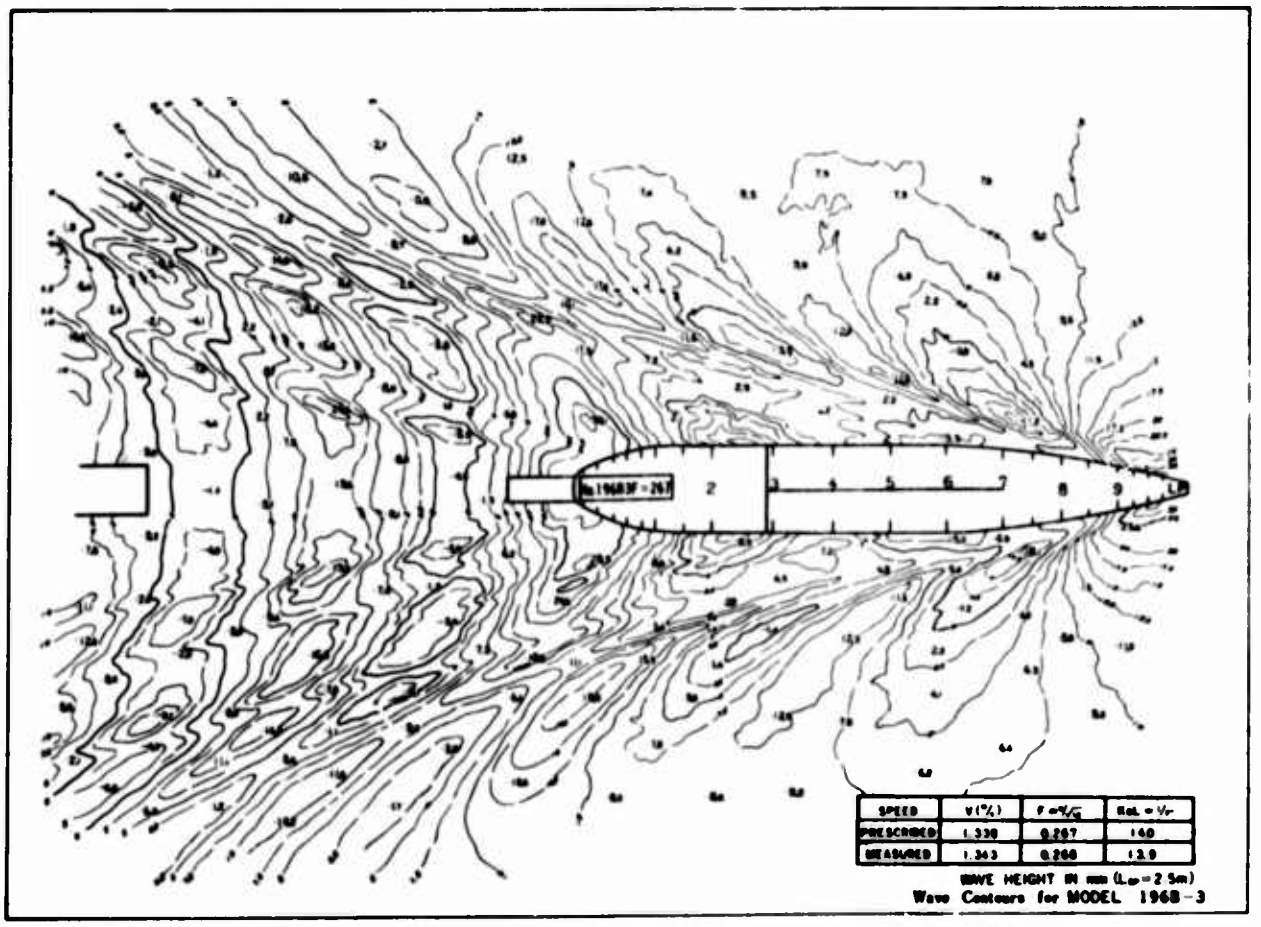


Fig. 4b. Wave-Contours of M.No. 196 (without bulb), upper, and M. No. 196B-3 (with bulb), lower.

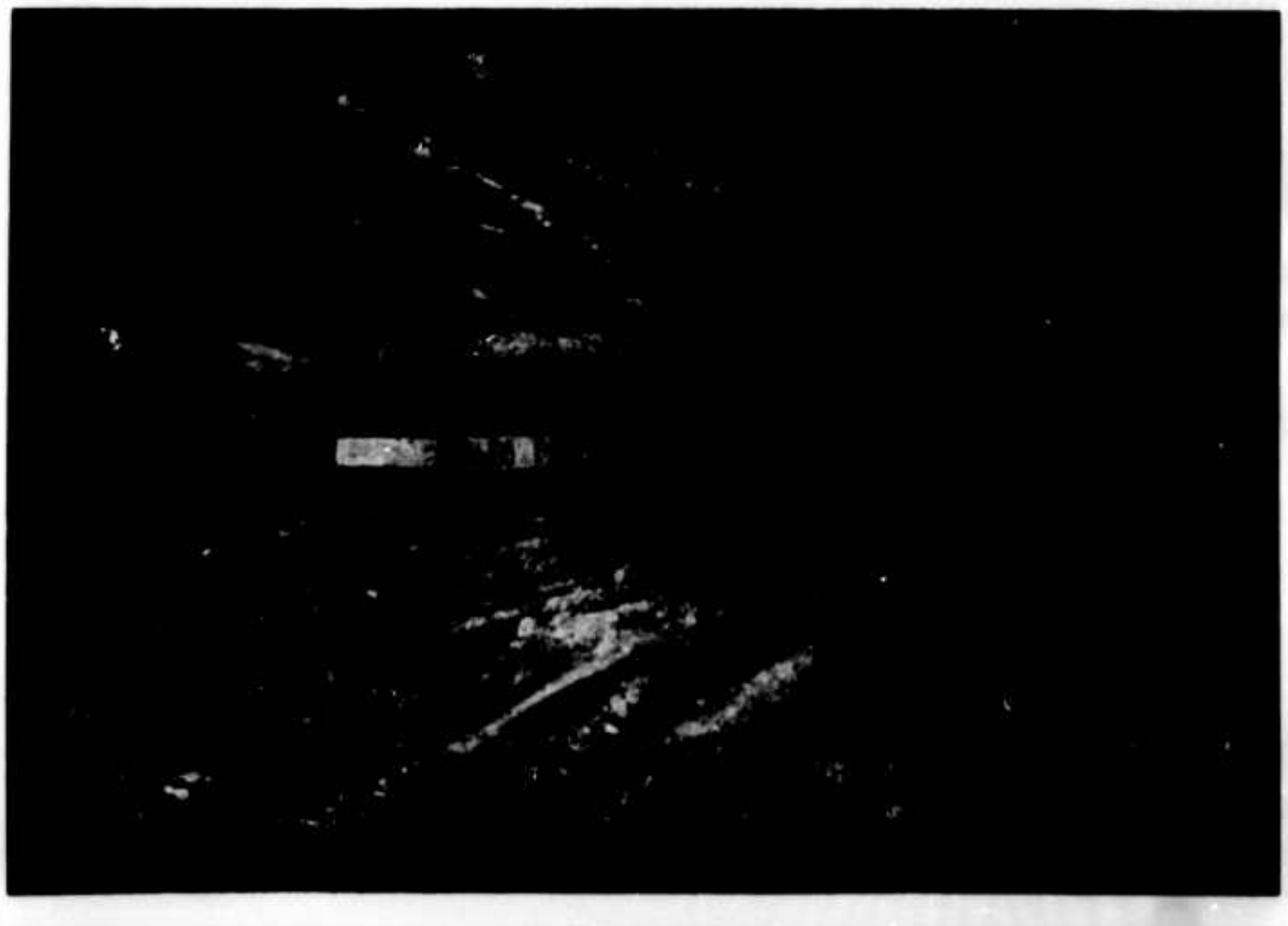
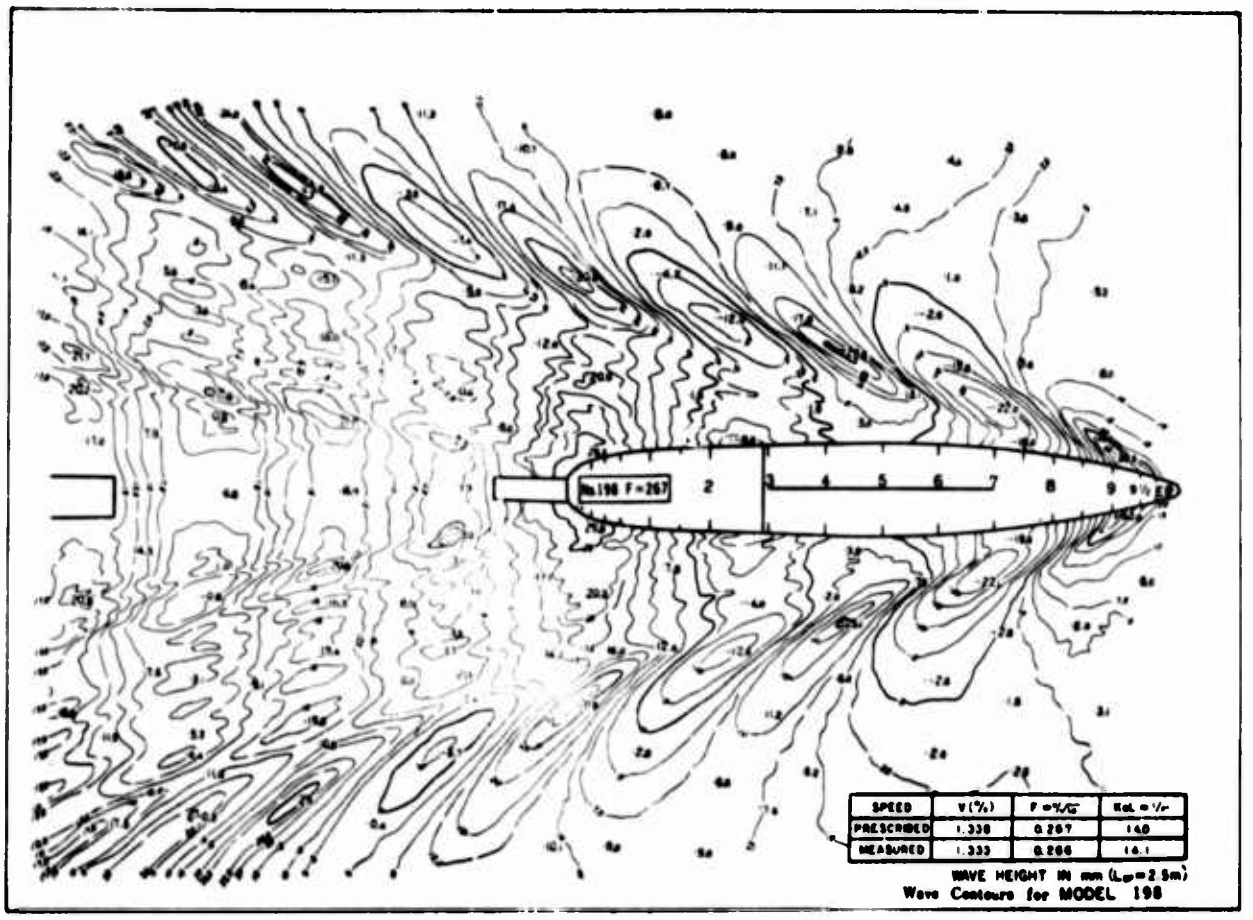


Fig. 4c. Wave Patterns of M.No. 198 (without bulb), upper, and M.No. 198A-2 (with bulb), lower.



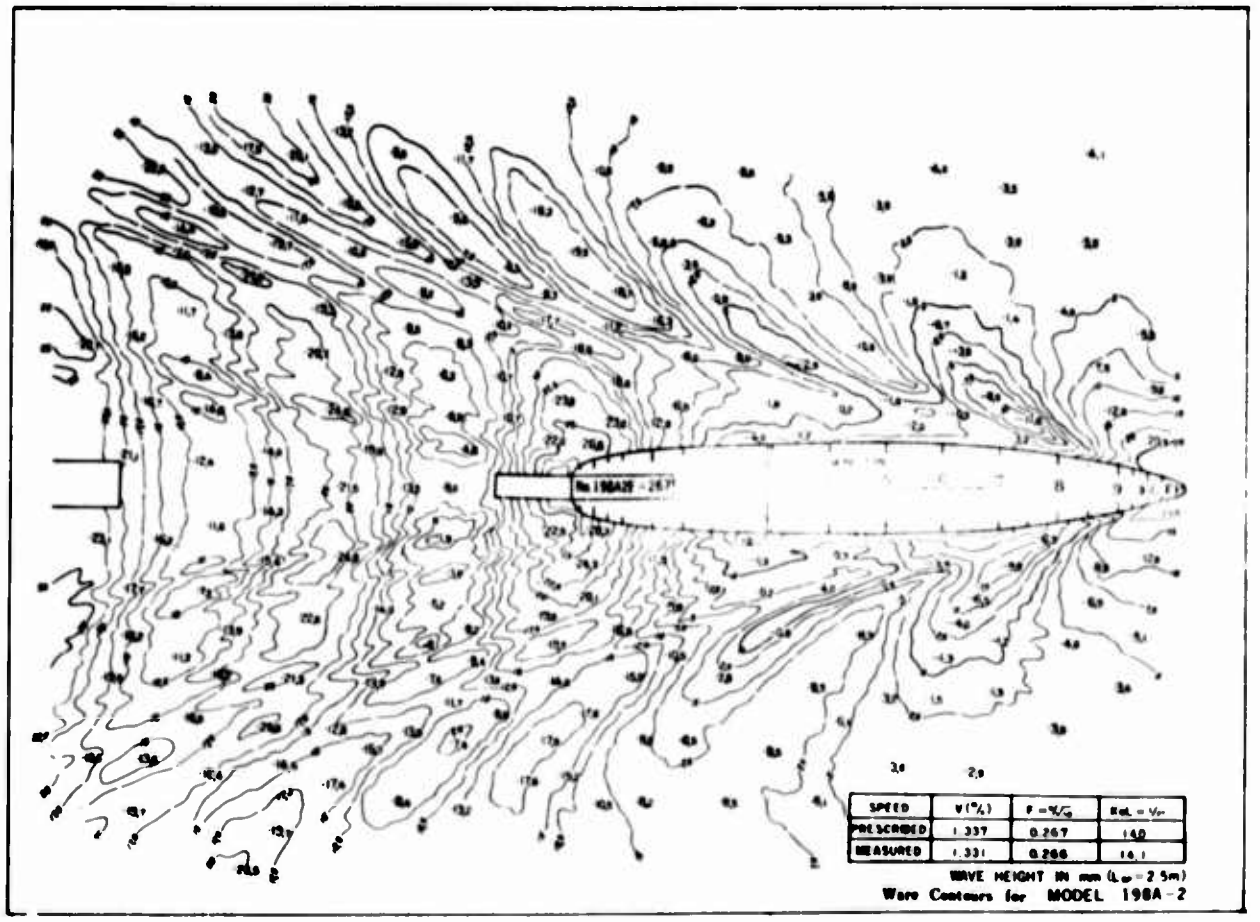


Fig. 4d. Wave-Contours of M.No. 198 (without bulb), upper, and M.No. 198A-2 (with bulb), lower.

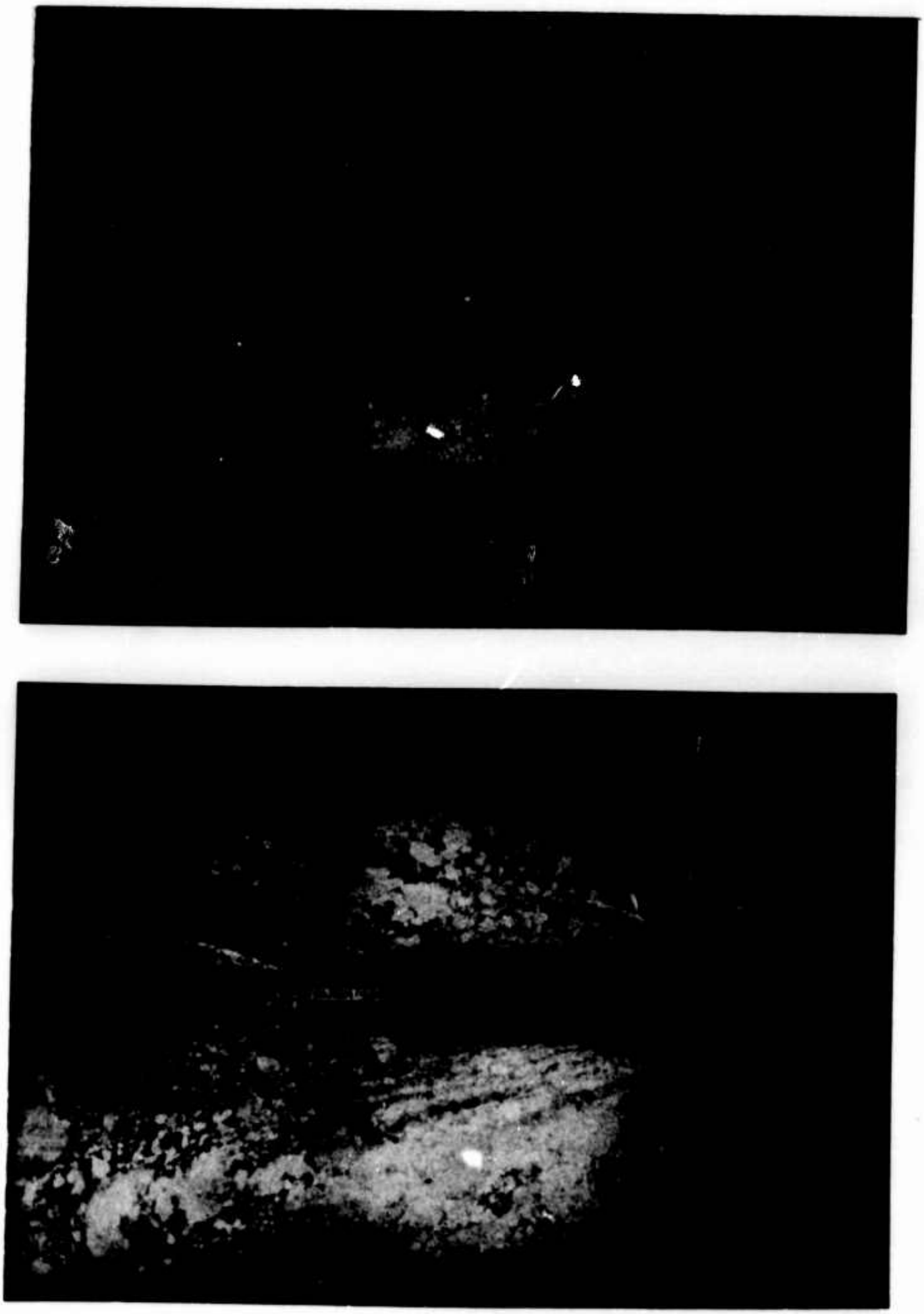
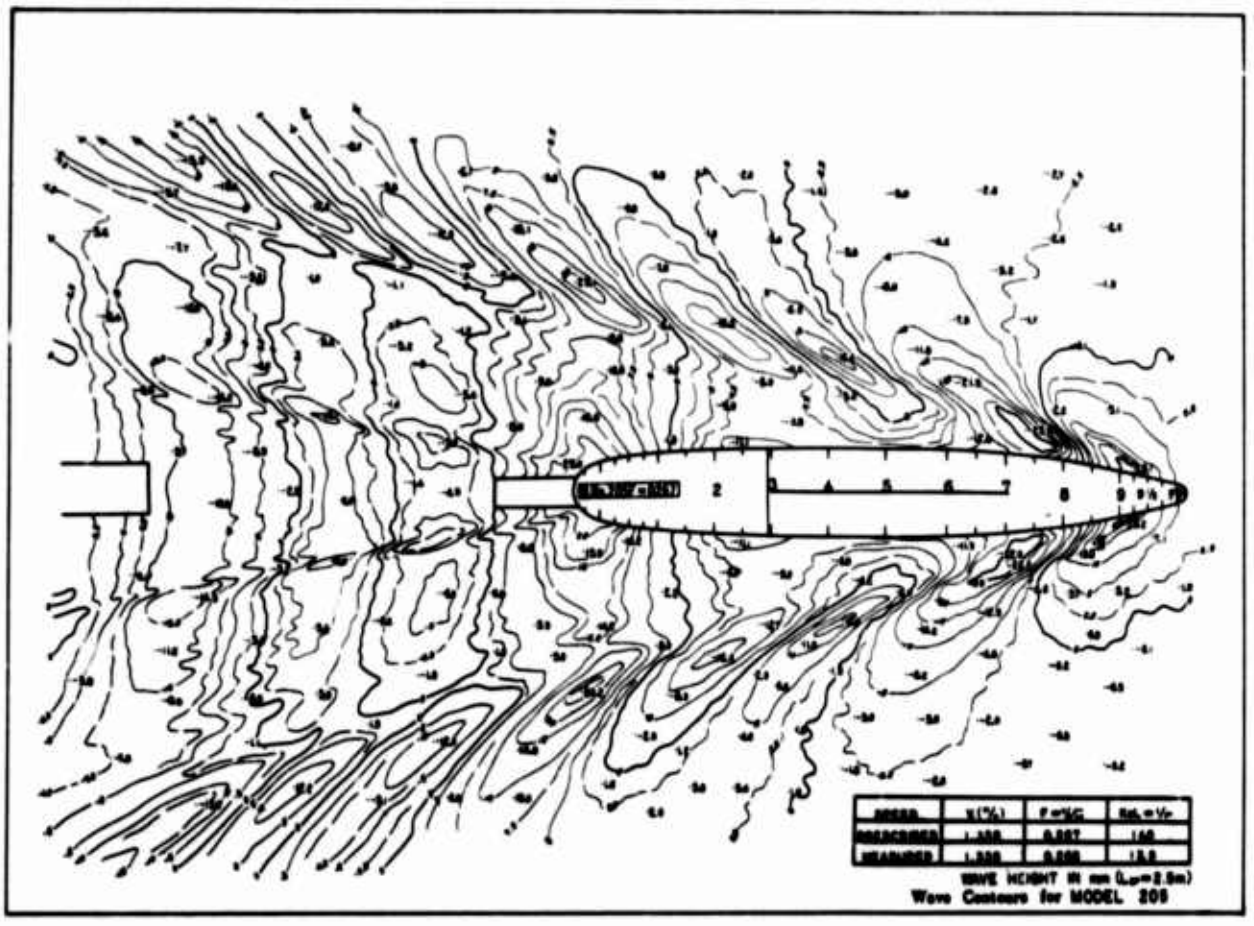


Fig. 4e. Wave Patterns of M.No. 205 (without bulb), upper, and M.No. 205H-4 (with bulb), lower.



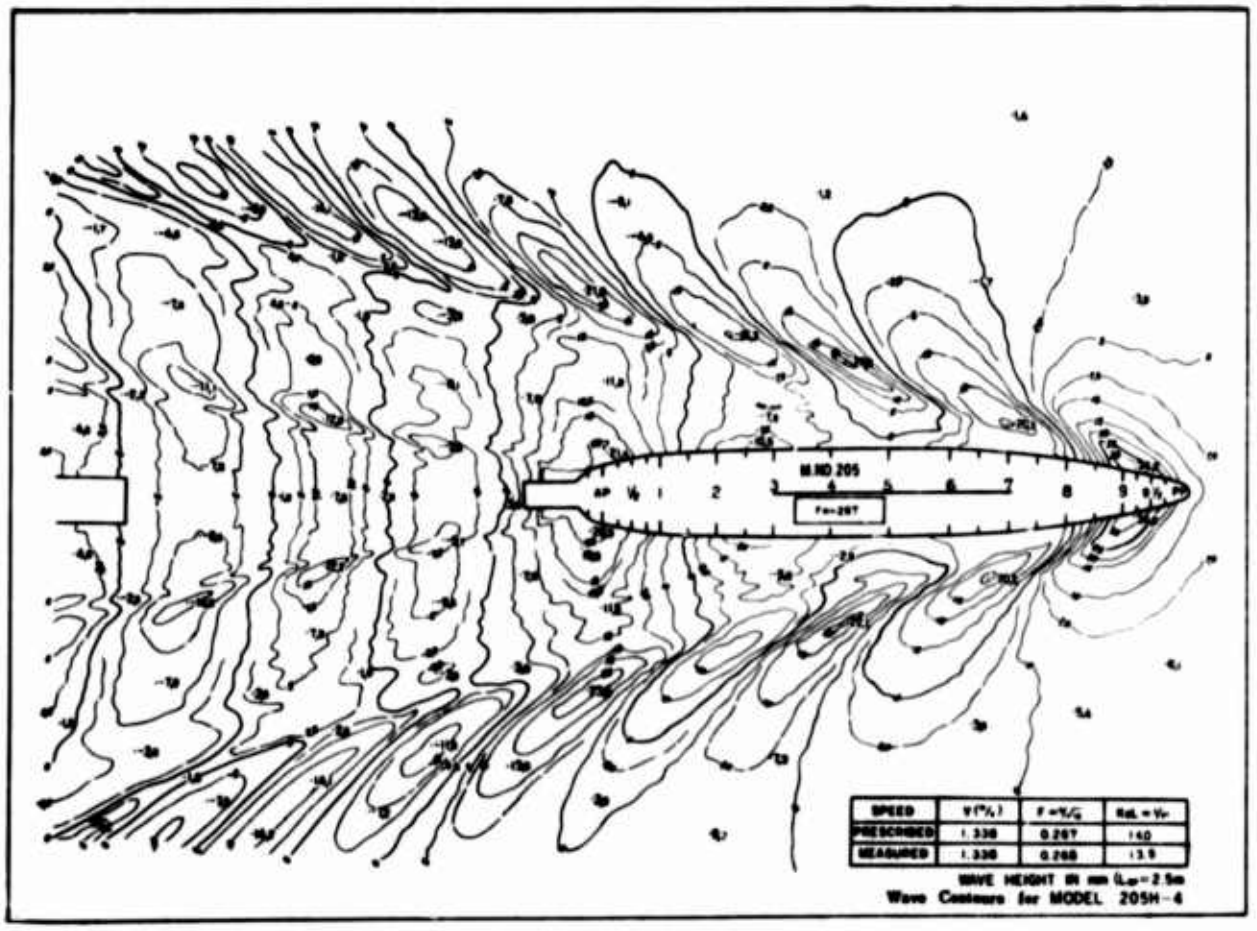


Fig. 4f. Wave-Contours of M. No. 205 (without bulb), upper, and M.No. 205H-4 (with bulb), lower.

From these observations of both wave profiles and wave patterns, M. No. 205 may be interpreted as the most promising of all with respect to wave-making characteristics, in its main hull form case and with-bulb case.

3.3 Results of Resistance Tests

Reference should be made to Figures 5a to 5c, 6a to 6c, and 7a to 7c.

The value of form factor K was decided to be 0.27 for the whole models through the process described in Chapter 2. K values for 6 m models, also analyzed for reference, proved to be a little higher (probably due to fitting of bilge keels).

On comparing curves of wave-making resistance coefficient Cw of main hulls of 2.5 m and 6 m models, there seemed to be little difference between them at full load condition as well as at 75% full displacement condition enough to be discussed together, so the authors will hereafter use the results of 2.5 m model tests representatively.

At full load condition, differences among Cw curves of the three ships well correspond to those among the observed wave characteristics as to be explained below.

At first, in Cw curve of M. No. 196 there occurs an apparent hollow part from Fn = 0.24 to 0.25, probably due to its long parallel part. As concerns M. No. 198, the amount of Cw is larger than that of M. No. 196, though the tendency of its Cw curve is rather simple and monotonous. As concerns M. No. 205, the amount of Cw is the smallest of all.

In case of the with-bulb forms, the cancelling effect of bulb is seen over a wide range of Froude Numbers. The amount of Cw decrease due to bulb fitting at full load condition, designed speed are:

M. No. 196	36%
M. No. 198	40%
M. No. 205	42%

Calculation of the effective horsepowers (EHP) of assumed actual ships using the above-mentioned Cw curves give probable EHP

Model	M.No. 196	M.No. 196+B3	M.No. 198	M.No. 198+ A2	M.No. 205	M.No. 205+B4	Model "A"
L wl ^{m}	2.564	2.564	2.564	2.564	2.558	2.558	6.1595
Volume$^{m^3}$	0.08825	0.09004	0.08898	0.09060	0.07959	0.08125	1.13595
Wetted S$^{m^2}$	1.2492	1.2935	1.2542	1.2958	1.1558	1.1910	7.06099
Draft FP^{m}	0.1555	0.1555	0.1555	0.1555	0.1475	0.1475	0.3627
Draft	0.1555	0.1555	0.1555	0.1555	0.1475	0.1475	0.3627
Draft AP^{m}	0.1555	0.1555	0.1555	0.1555	0.1475	0.1475	0.3627
Trim %	0	0	0	0	0	0	0
Water Temp.	20.7°C	23.4°C	25.2°C	21.8°C	11.0°C	9.19°C	20.0°C
Marks							

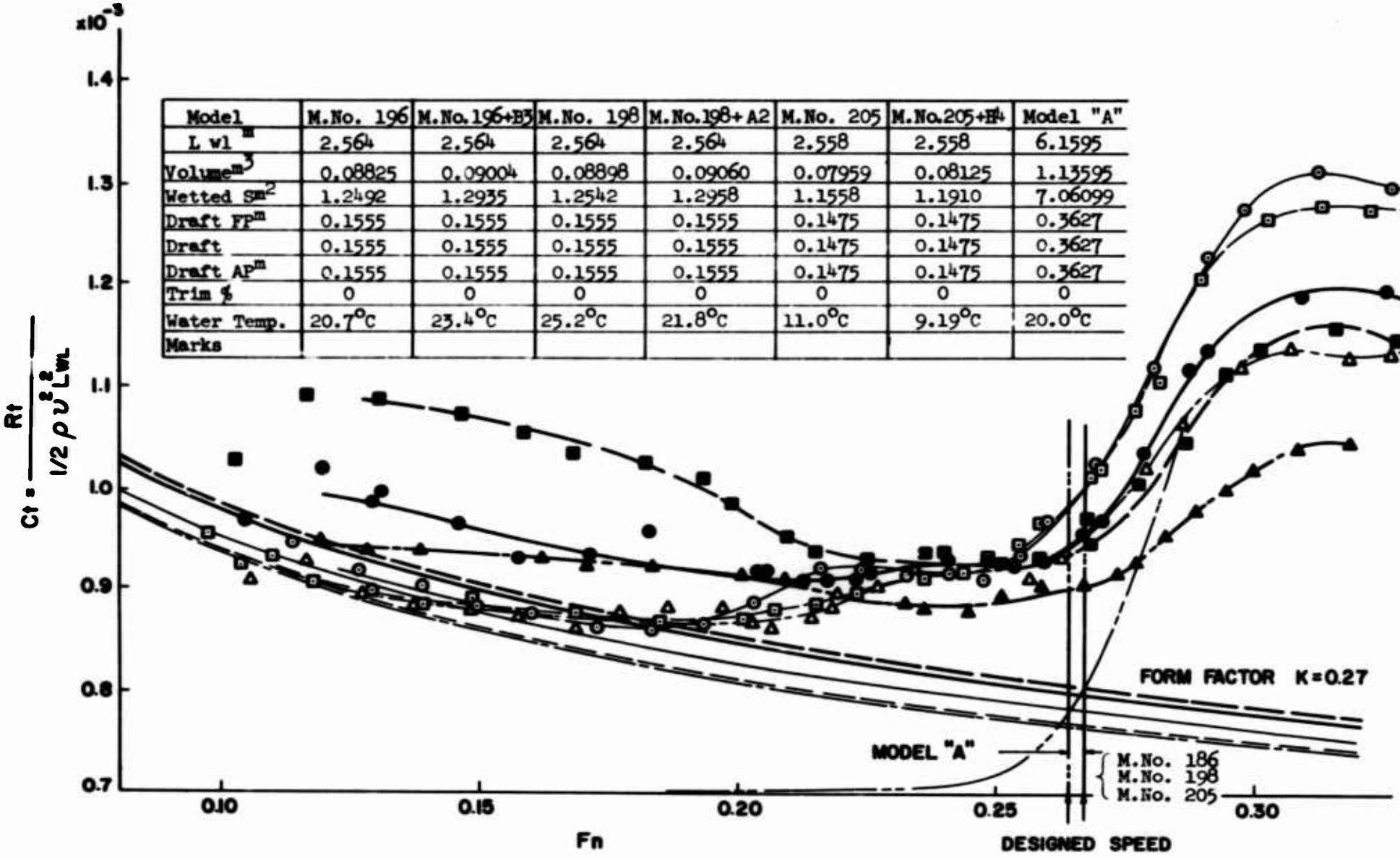
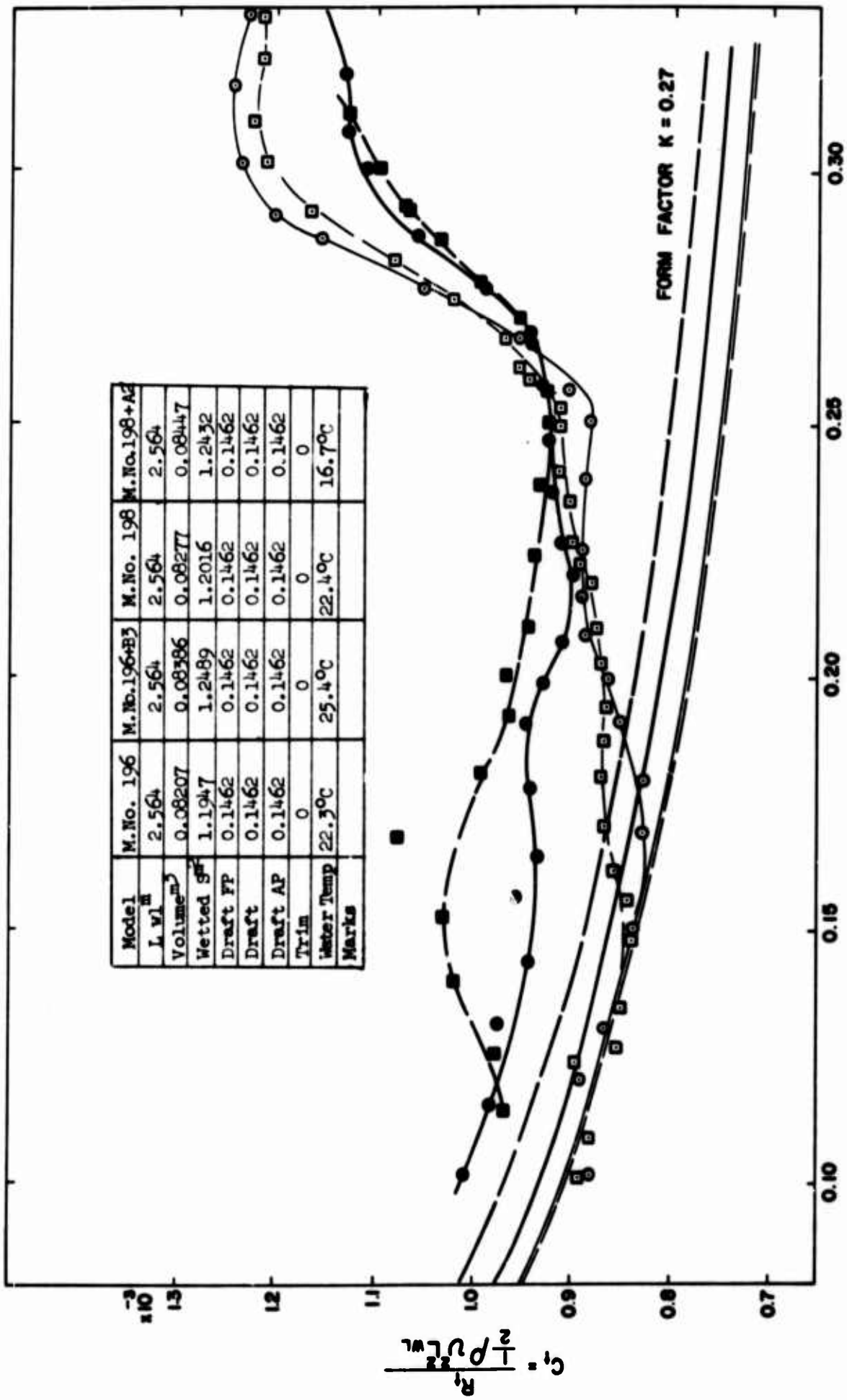
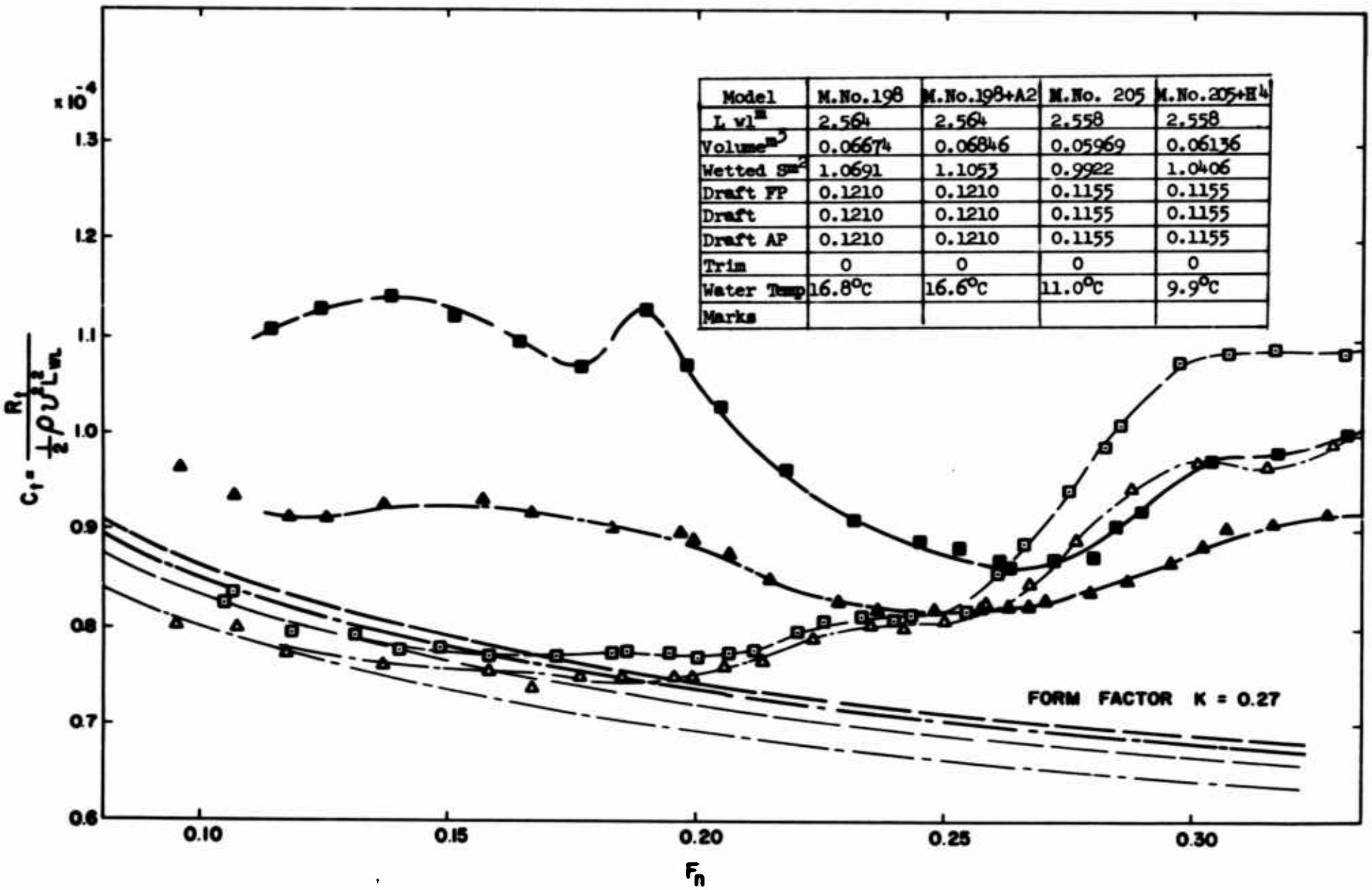


Figure 5a. Total Resistance Coefficient, Full Load Condition.



Model	M.No. 196	M.No.196+B3	M.No.198	M.No.198+A2
L.wl m	2.564	2.564	2.564	2.564
Volume m^3	0.08207	0.08386	0.08277	0.08447
Wetted S^{m^2}	1.1947	1.2489	1.2016	1.2432
Draft FP	0.1462	0.1462	0.1462	0.1462
Draft	0.1462	0.1462	0.1462	0.1462
Draft AP	0.1462	0.1462	0.1462	0.1462
Trim	0	0	0	0
Water Temp	22.3°C	25.4°C	22.4°C	16.7°C
Marks				

Figure 5b. Total Resistance Coefficient, 93% Full Displacement Condition.



Model	M.No.198	M.No.198+A2	M.No. 205	M.No.205+H4
L wl m	2.564	2.564	2.558	2.558
Volume m^3	0.06674	0.06846	0.05969	0.06136
Wetted S m^2	1.0691	1.1053	0.9922	1.0406
Draft FP	0.1210	0.1210	0.1155	0.1155
Draft	0.1210	0.1210	0.1155	0.1155
Draft AP	0.1210	0.1210	0.1155	0.1155
Trim	0	0	0	0
Water Temp	16.8°C	16.6°C	11.0°C	9.9°C
Marks				

Figure 5c. Total Resistance Coefficient, 75% Full Displacement Condition.

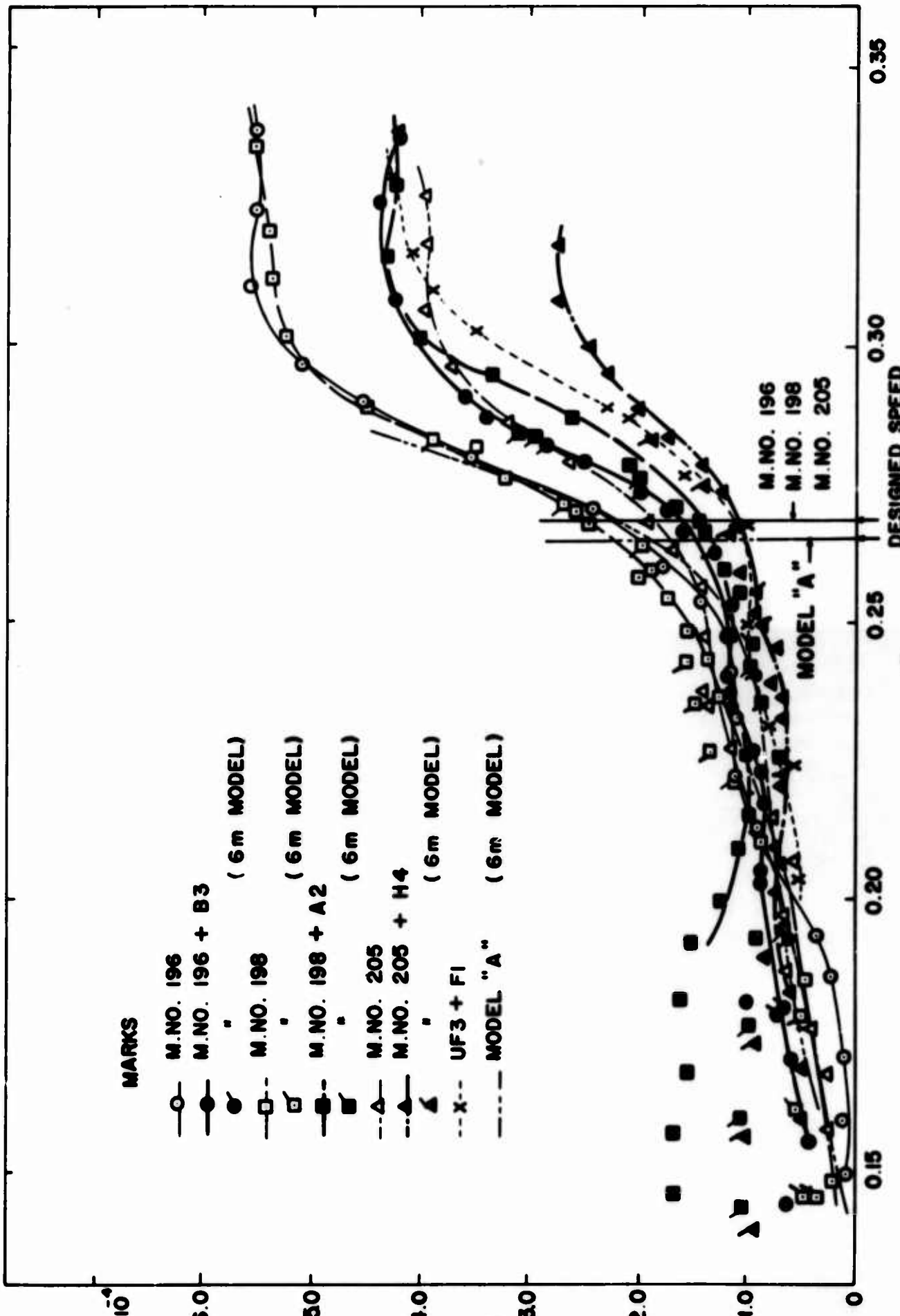


Figure 6a. Wave-Making Resistance Coefficient, Full Load Condition.

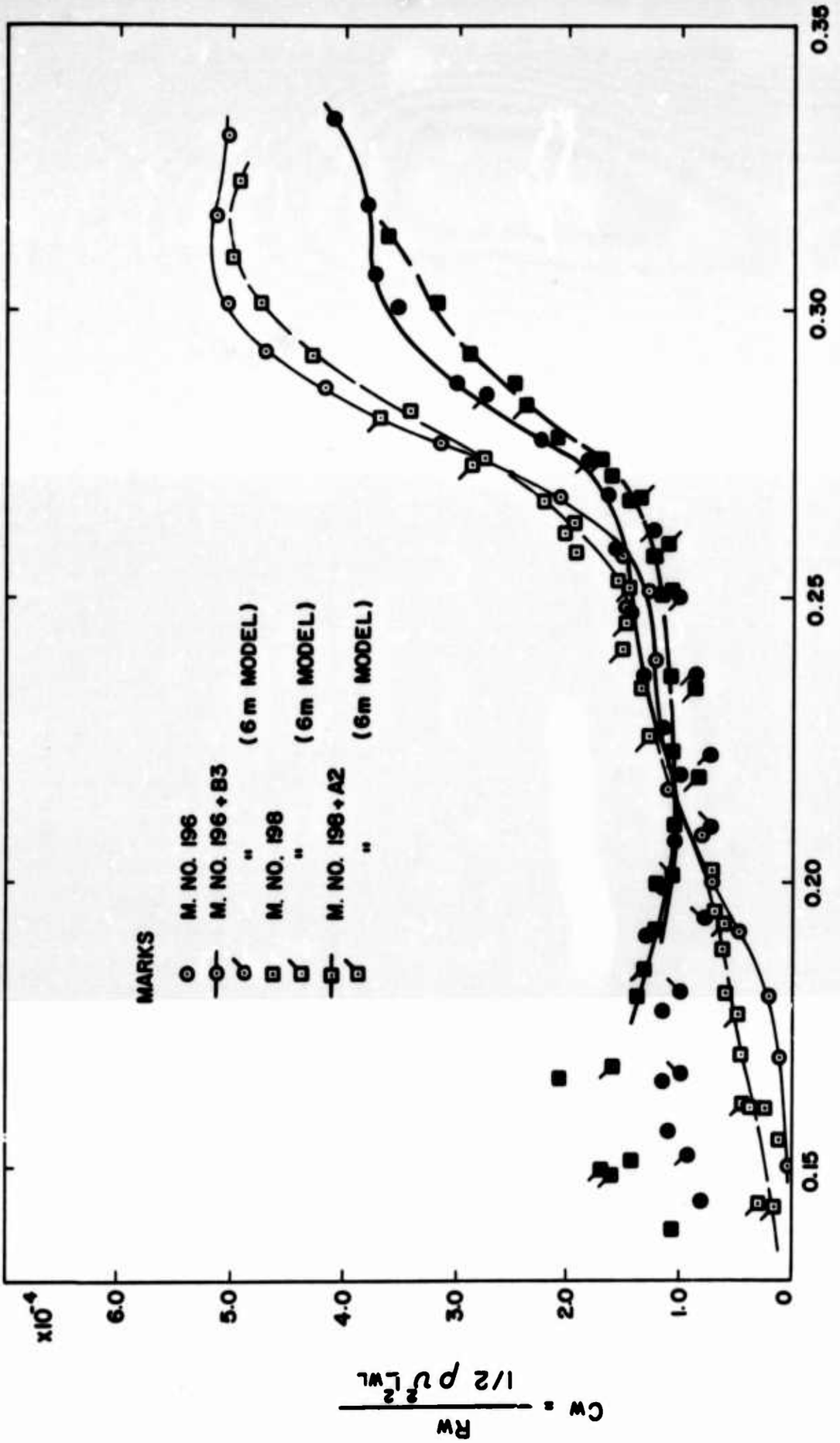


Figure 6b. Wave-Making Resistance Coefficient, 93% Full Displacement Condition.

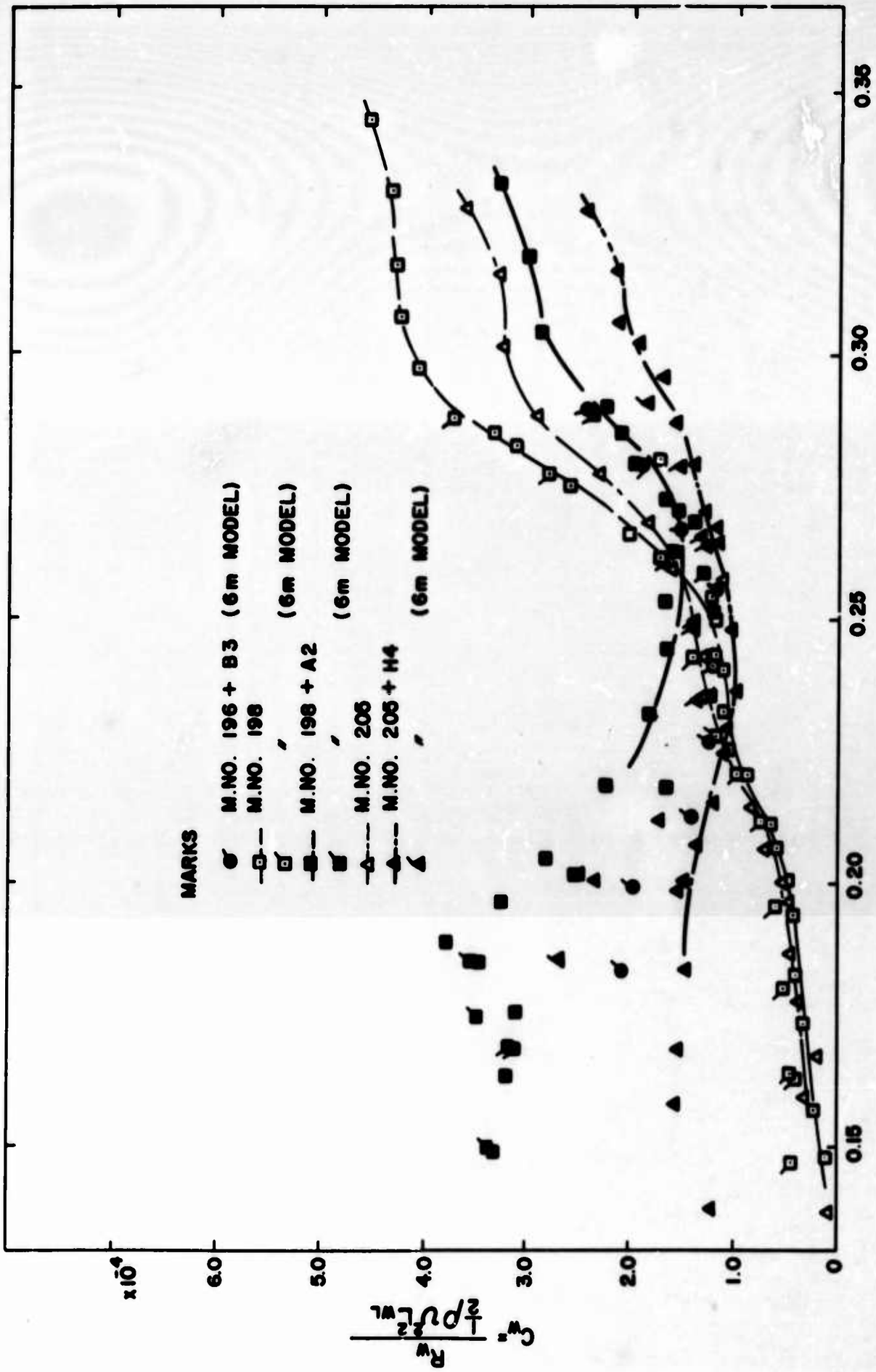


Figure 6c. Wave-Making Resistance Coefficient, 75% Full Displacement Condition.

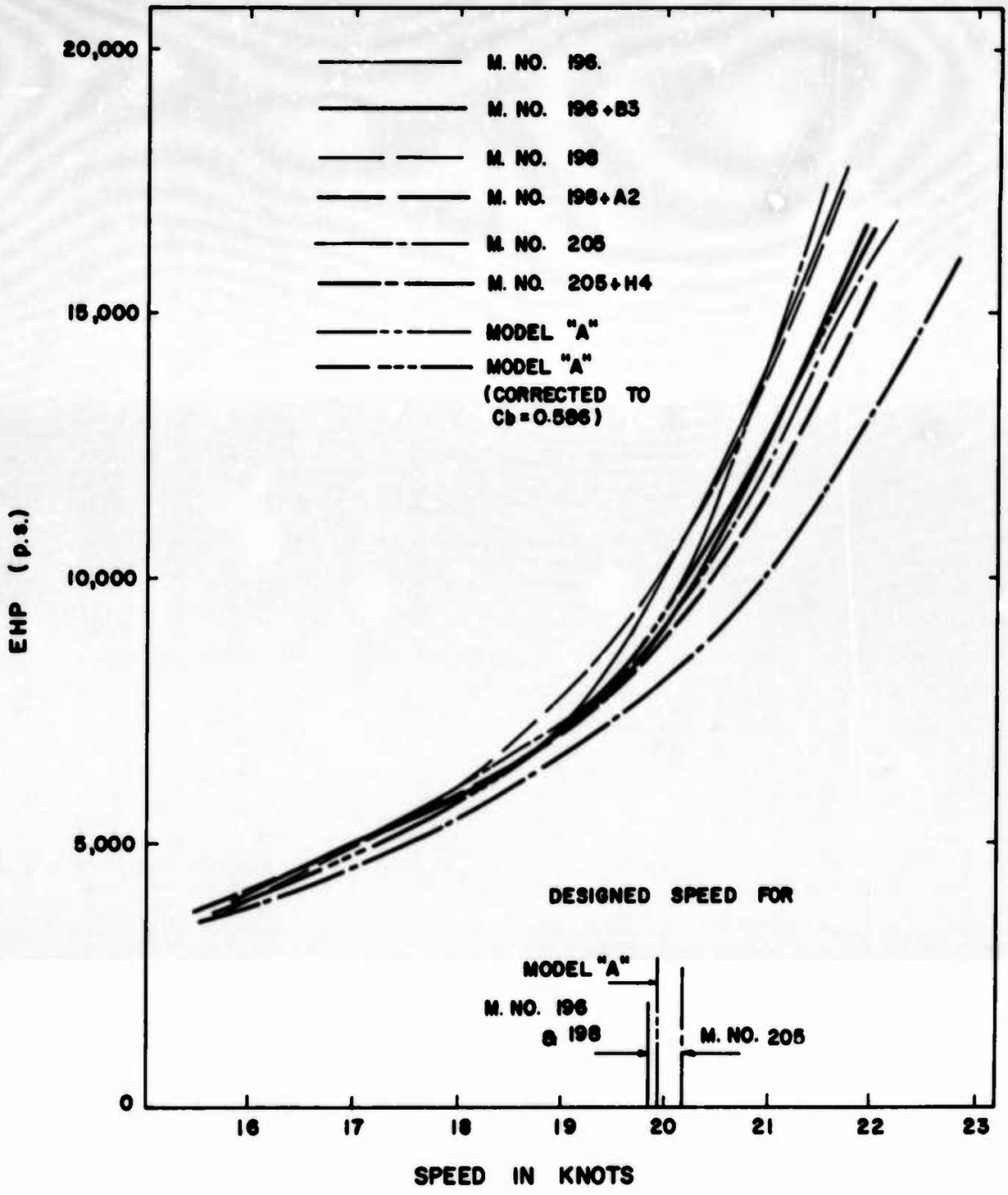


Figure 7a. EHP Curves, Full Load Condition.

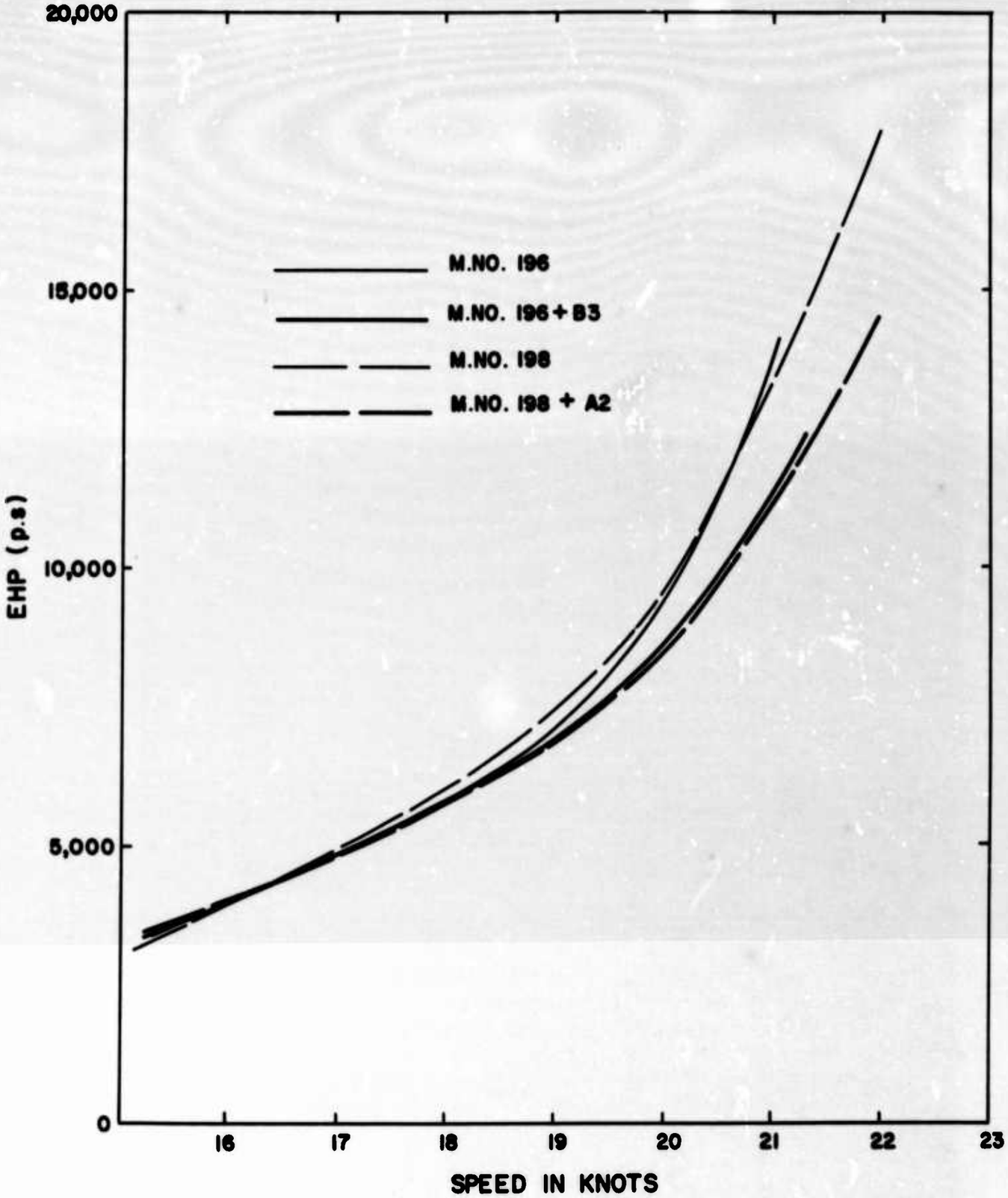


Figure 7b. EHP Curves, 93% Displacement Condition.

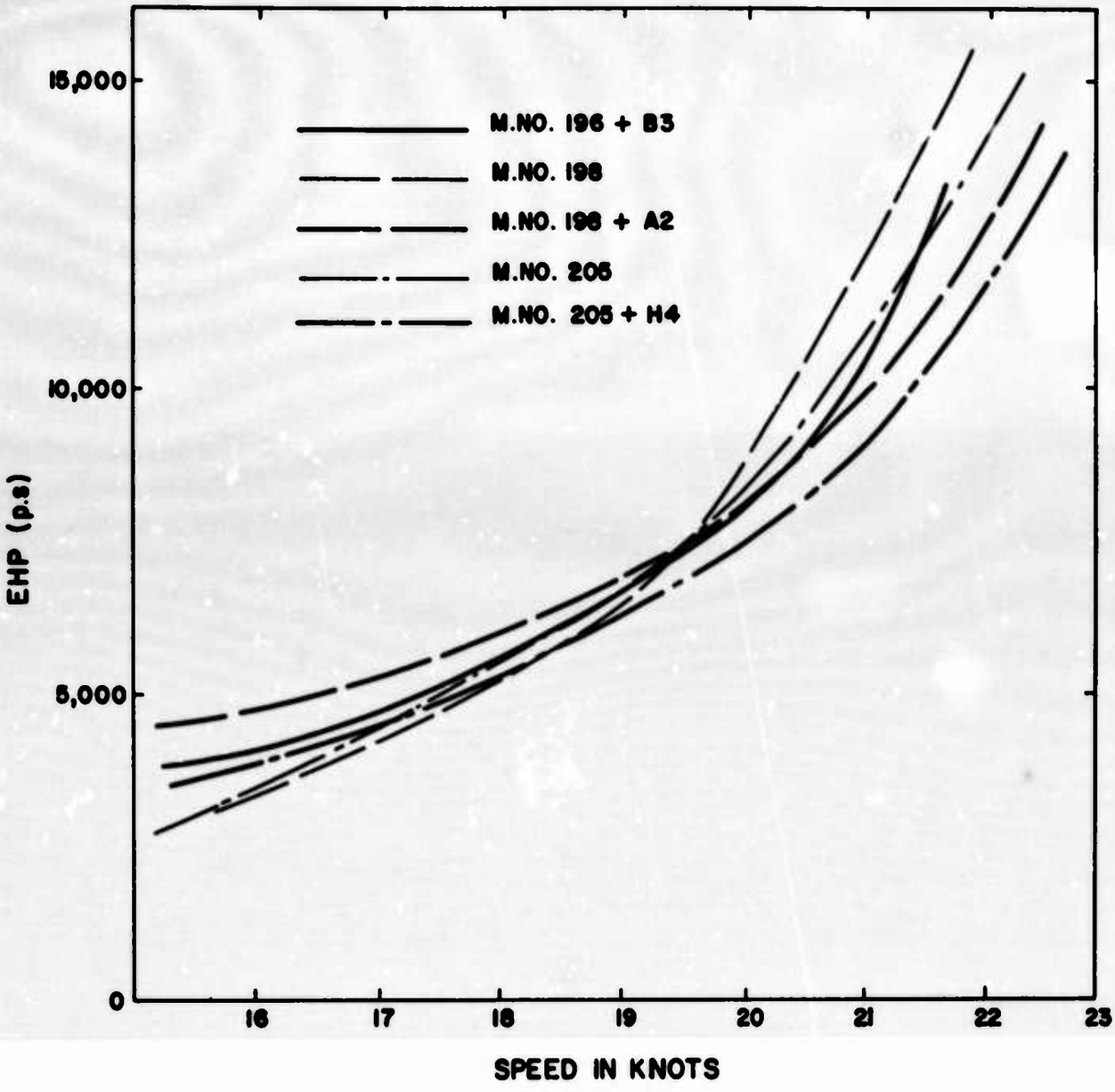


Figure 7c. EHP Curves, 75% Displacement Condition.

decrease at the corresponding condition as follows. EHPs were derived through Hughes' method, with roughness allowance ΔCf assumed to be 0.2×10^{-3}.

M. No. 196	10%
M. No. 198	13%
M. No. 205	13%

The same tendencies could be pointed out from the calculated results at 93% full displacement condition (numerical comparisons of Cws and EHPs are omitted).

As for the results at 75% full displacement condition where bulbs are close to water surface, the cancelling effect of bulbs seems to remain, but when compared with the without-bulb case the performance gets worse over wider ranges of Froude Numbers than at the above loading conditions. Besides, differences among the three ships are also recognized. The EHP decrease to be expected at designed speed are as follows:

M. No. 198	7%
M. No. 205	11%

3.4 Results of Self-Propulsion Tests

Reference should be made to Figures 8a to 8c.

The authors will first quote the case of M. No. 198 to show the difference between main hull form and with-bulb form, and then compare the results of three ships in their with-bulb cases. Effect of loading condition is also considered.

a) Difference of Self-Propulsion Factors between Main Hull Form and With-Bulb in the Case of M. No. 198.

1-w (w being wake fraction) As for with-bulb form 1-w decreases by about 3% at full load and 93% full displacement conditions compared with that of main hull form, which suggests a little improvement of propulsive performance through bulb fitting.

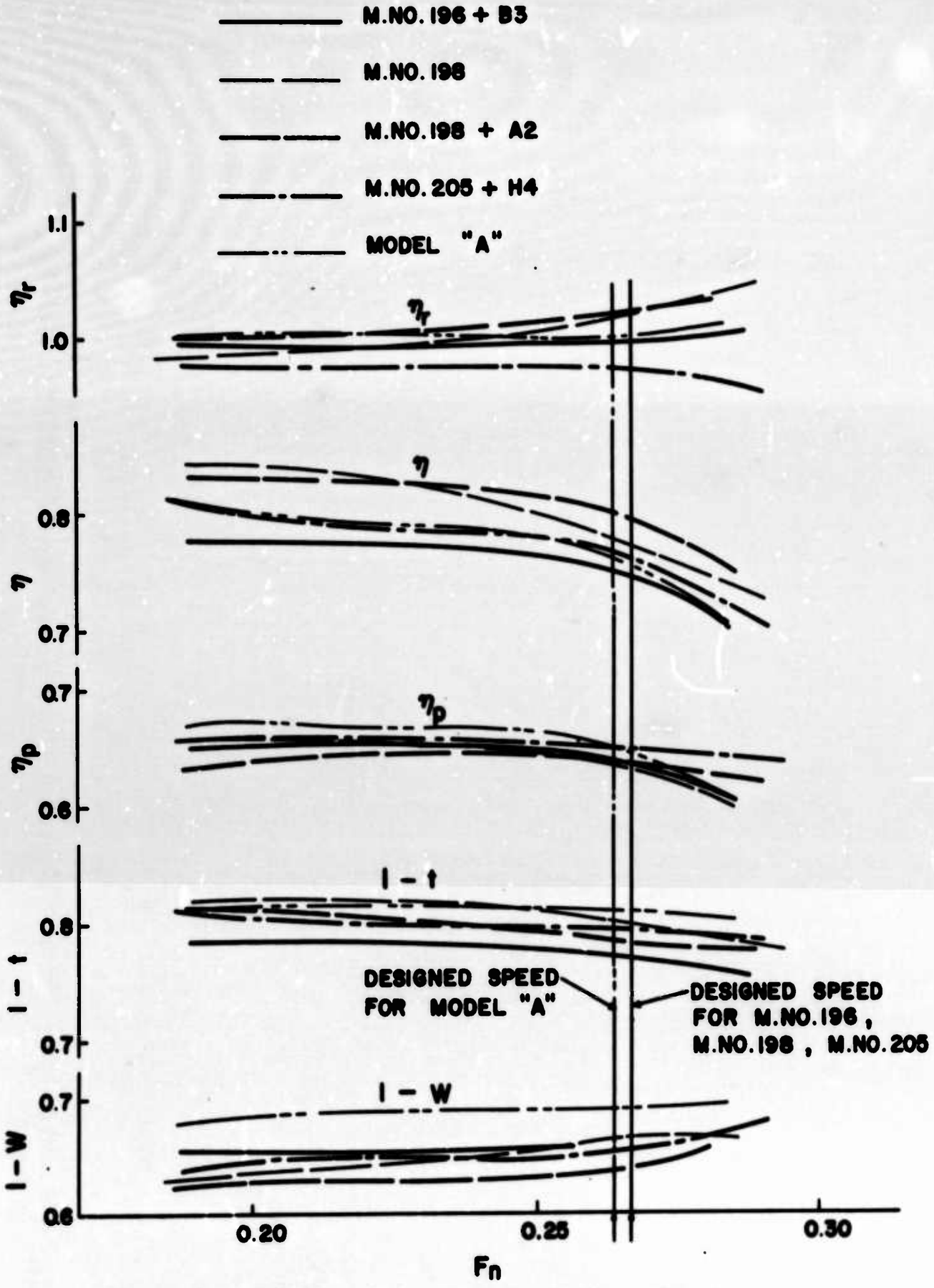


Figure 8a. Self-Propulsion Factors, Full Load Condition.

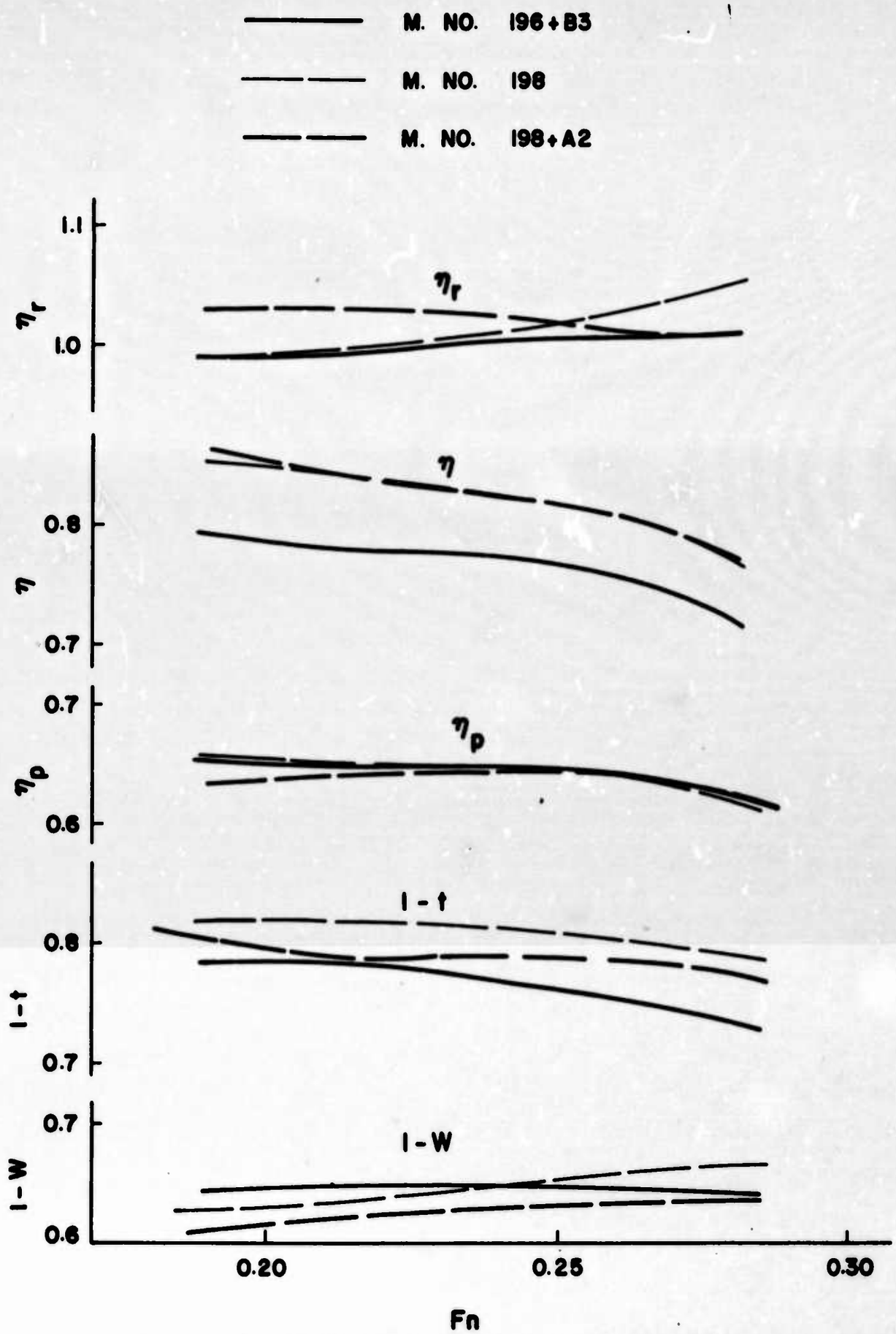


Figure 8b. Self-Propulsion Factors, 93% Displacement Condition.

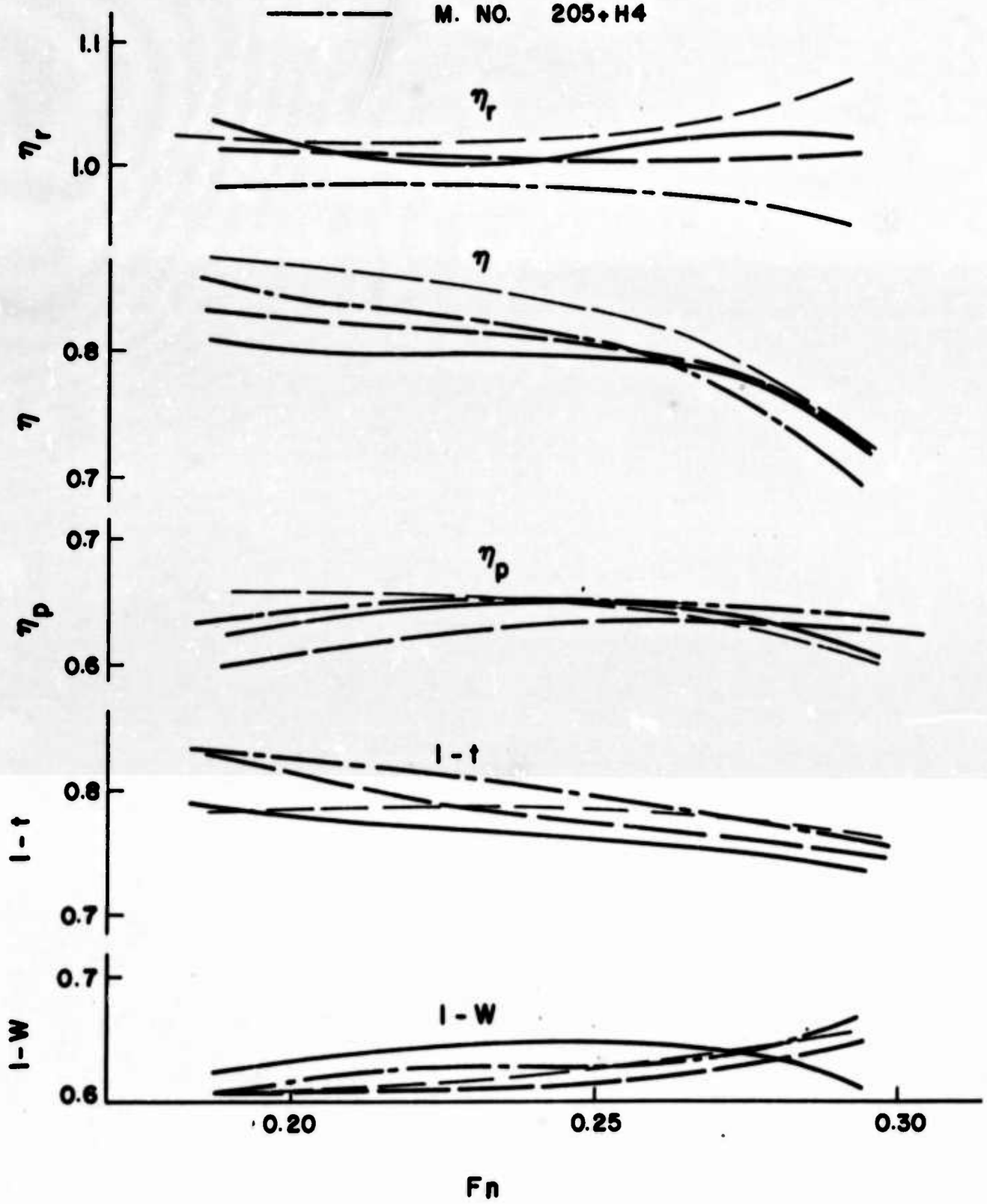


Figure 8c. Self-Propulsion Factors, 75% Displacement Condition.

1-t (t being thrust deduction)
1-t decreases by about 2 to 3% in high speed range of full load and 93% full displacement condition through bulb fitting, which indicates a fall of propulsive performance.

η_r (relative rotative efficiency)
At full load and 93% full displacement conditions, η_r of with-bulb form is lower than that of main hull form in the high speed range, and the tendency are remarkable at 75% full displacement condition.

η (propulsive coefficient)

At full load and 93% full displacement conditions, η of with-bulb form is slightly higher than that of main hull, integrating 1-w improvement and 1-t decrease in the relation $((1-t/1-w) \times \eta_r \times \eta_p)$ (η_p being propeller efficiency), but the order of superiority changes at 75% full displacement condition.

b) Comparison of Self-Propulsion Factors of Three With-Bulb Hull Forms at Full Load Condition

1-w the values of M. No. 196 and 205 are nearly equal, but the value of M. No. 198 is lower than those of the formers.

1-t the values of M. No. 198 and 205 are nearly equal, but the value of M. No. 196 is lower than those of the formers.

η_r of three ships, the value of M. No. 198 is the highest and that of M. No. 205 is the lowest.

η of three ships, η of M. No. 198 is the highest and that of M. No. 196 is the lowest.

These descriptions are to be equally applied to the case of 75% full displacement condition, except that η_r of M. No. 196 approaches and exceeds that of M. No. 198 in higher speed range.

General conclusions would hardly be derived as to the self-propulsion factors from the limited numbers and conditions of models,

but M. No. 198 seems to be most superior of all in its with-bulb case as well as in main hull form case.

c) Comparison of DHP Curves of With-Bulb Case

DHP curves derived from EHPs in 3.3 and self-propulsion factors of 6 m models are shown in Figures 9a to 9c for reference, which may serve as a rough basis for comparison of overall performance.

From these curves at full load condition, M. No. 205 seems to have best propulsive performance of all with M. No. 198 a little inferior to it and M. No. 196 worst of all. The discrepancy becomes larger as the ship's speed exceeds 20 knots. At 75% full displacement condition, M. No. 205 is most superior only in the speed range higher than 19 knots, under which speed its superiority is exceeded by M. No. 198.

The tendency stated above may indicate that the best resistance performance of M. No. 205 is rather cancelled by its lower value of propulsive coefficient η (or more precisely, relative rotative efficiency η_r). The values of η_r of M. No. 205 are a little suspicious however, when compared with other data of similar aft body model, and further clarification of the reason might be necessary.

3.5 Comparison with a Conventional Ship

From practical designing point of view, comparisons of overall propulsive performance of with-bulb ships (described throughout Chapters 1 to 3) with that of a conventional ship is of great interest. The authors chose as an example a conventional ship (hereafter named Model "A"), recently designed under almost the same requirements as for the with-bulb ships and made some comparative calculations.

Model "A" has one of optimum hull forms developed through model series tests, and meets the following basic requirements at full load condition.

Displacement = about 18,170 ton

Mt. of inertia of waterplane I = about 69,660 m^4 *

Note: * Corresponds to GM = 0 at full load arrival condition.

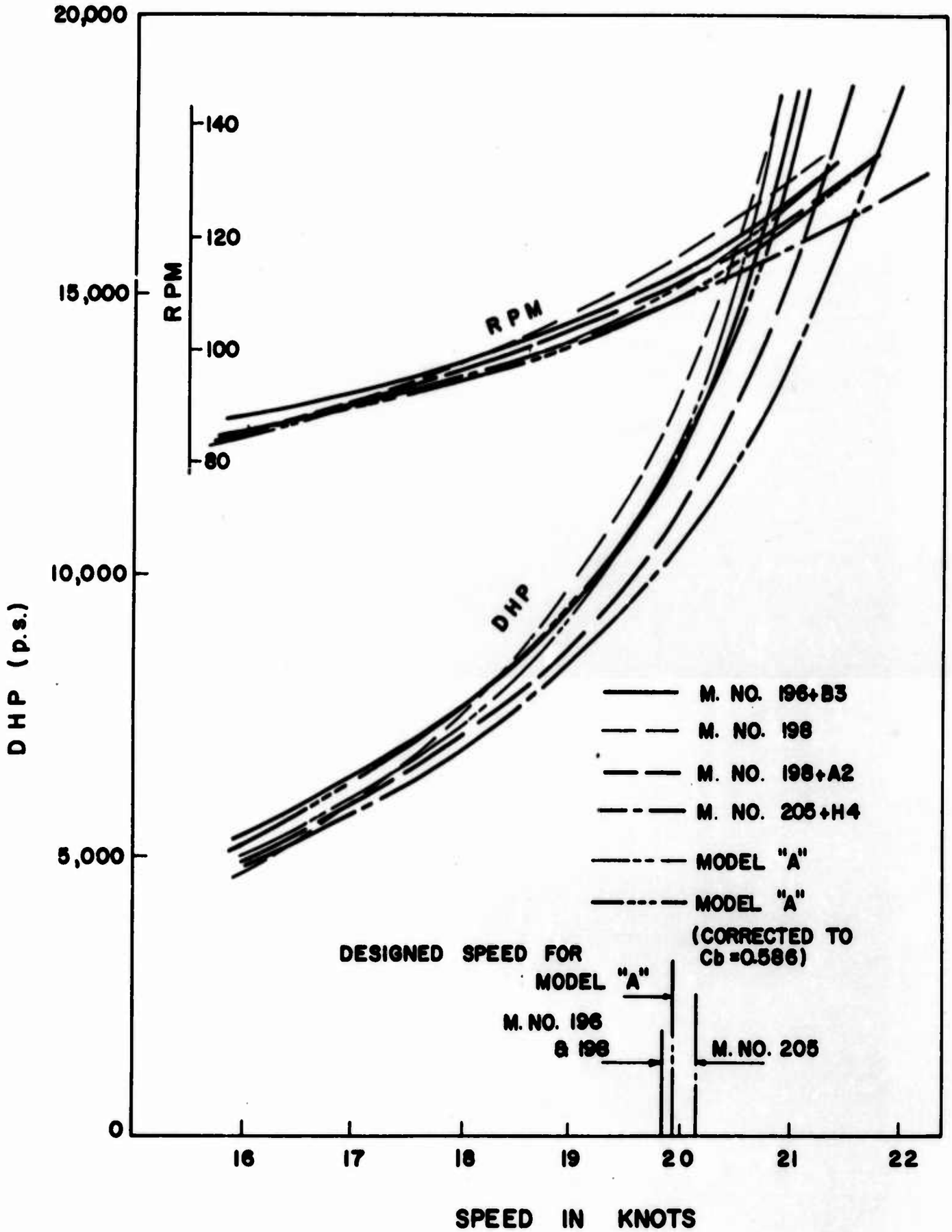


Figure 9a. DHP and RPM Curves, Full Load Condition.

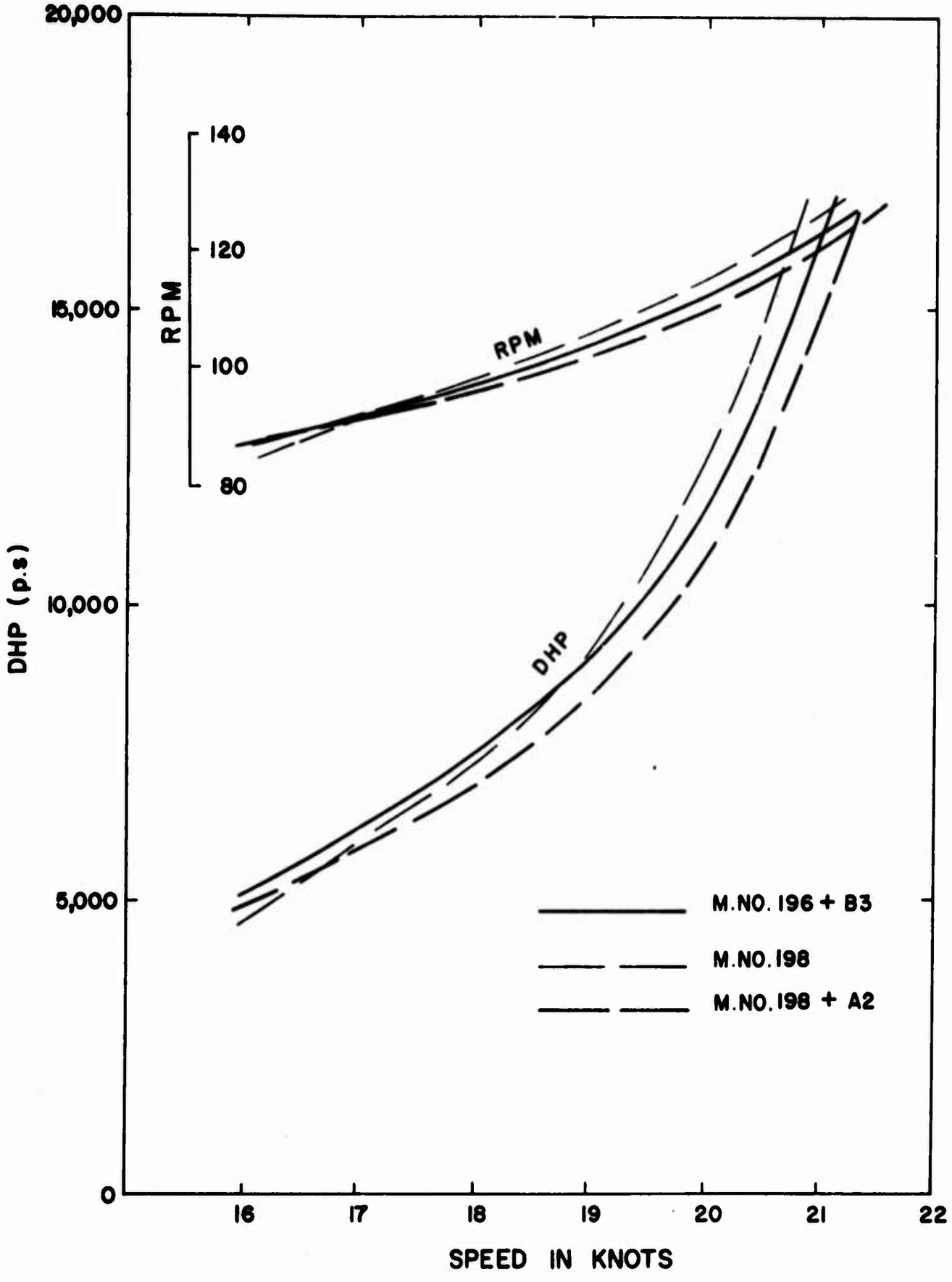


Figure 9b. DHP and RPM Curves, 93% Displacement Condition.

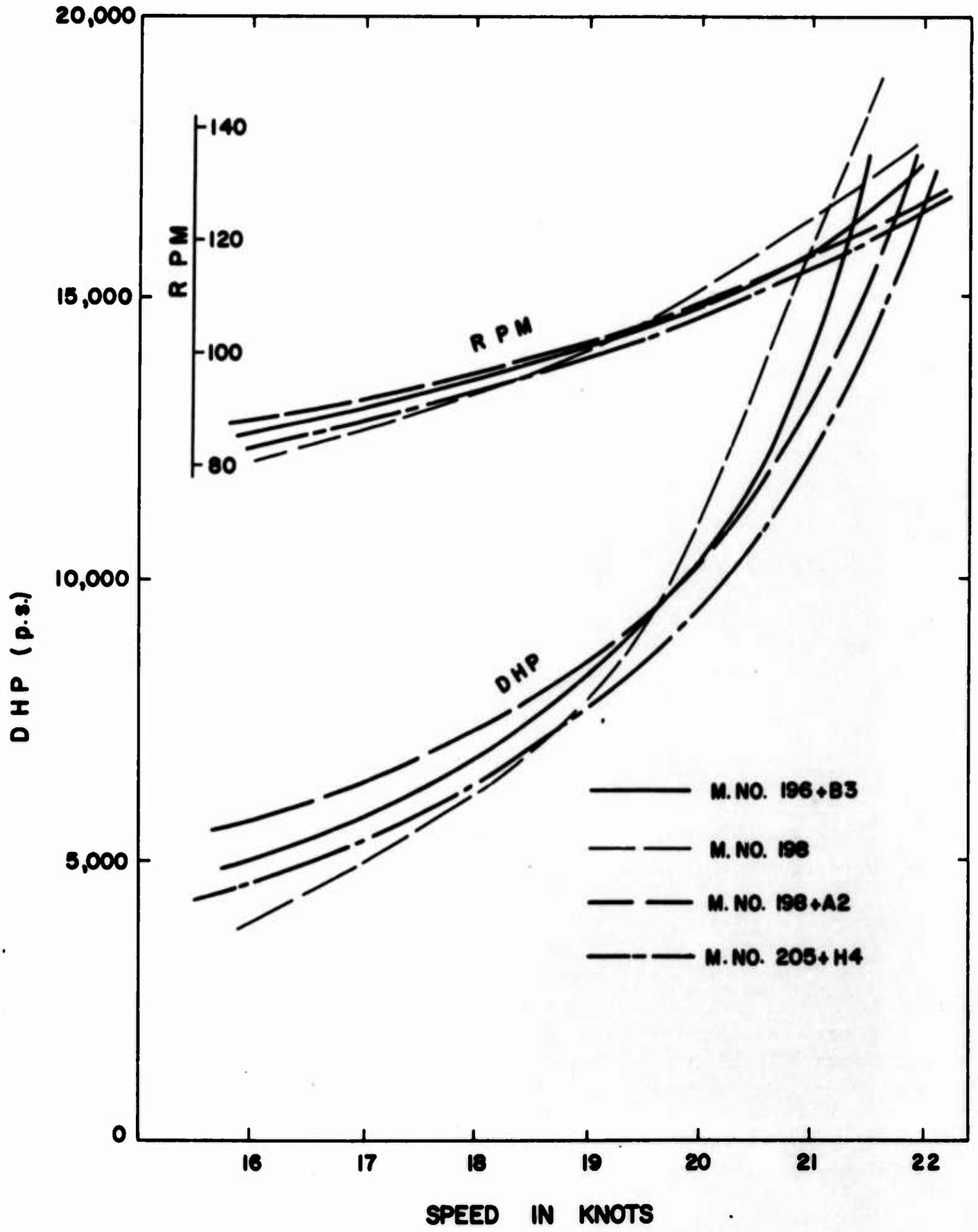


Figure 9c. DHP and RPM Curves, 75% Displacement Condition.

Draft moulded d = 9.05 m

Designed speed = 19.7 knots (Fn = 0.2608)

Particulars of Model "A" are listed in Table 1, and its waterline curve is shown in Figure 1.

Resistance and Self-Propulsion Tests had been carried out of its 6 m model, in the same manner as of other 6 m models (concerning the way of experiment and method of analysis), at full and 6 loading conditions.

Because other loading conditions do not correspond to 93% and 75% full displacement, experimental and analyzed results of Model "A" only at full load condition are added to Figure 5a, 6a, 7a, 8a, 9a and 10a.

Curves of EHP and DHP of Model "A" (corrected to Cb = 0.586) are also estimated using other series tests results and added to the figures, in order to facilitate a direct comparison of Model "A" with M. No. 205 + H4.

In all power curves superiority of M. No. 205 + H4 is clear over the whole speed range, and it shows, when compared at 19.8 knots (about the designed speed) of full load condition, such low horse powers as listed below.

	EHP	DHP	η
M. No. 196 + B3	8,600 P.S.	11,500 P.S.	.748
M. No. 198 + A2	8,470 P.S.	10,720 P.S.	.790
M. No. 205 + H4	7,750 P.S.	10,070 P.S.	.770
Model "A"	8,880 P.S.	11,650 P.S.	.762
Model "A"	8,880 P.S.	11,500 P.S.	.772

(Corrected to Cb = 0.586)

Thus DHP decreases of 1,430 P.S. (12.4%) will be expected by M. No. 205 + H4 compared with the conventional ship Model "A" (corrected to Cb = 0.586). Differences of propulsive efficiencies seem small in this case.

Practical estimation of overall performance of these ships should be done on the BHP curves with suitable propellers designed and other empirical factors adopted respectively, and Appendix 1 (with Figures 13a and 13b (later added))will be of some use to realize the superiority of "with-bulb" waveless hullforms (especially M. No. 205 + H4) in overall performance.

Name		Speed at $\frac{0.85}{1.15}$ MCR
Model "A"	17500^{PS} x 115^{RPM}	20.22 Knots
M. No. 196 + B3	13500 x 118	19.33
M. No. 198 + A2		19.49
M. No. 205 + H4		20.23

As to the power reduction at 19.8 knots, BHP decrease of 2,150 p.s. (18.7%) will be expected with M. No. 205 + H4 compared with the conventional Model "A".

4. EXPERIMENTAL RESULTS IN WAVES

Reference should be made to Figures 10a, 10b, and 11.

Before still water tests described in Chapter 2 were carried out, self-propulsion tests in regular waves were conducted to acquire the general information of the performance of with-bulb hull forms in waves, attaching in turn two types of bulbs to a conventional hull form, and recording thrust and motions in regular waves at the Experimental Tank of the University of Tokyo. Using the response amplitude operators derived from above-stated records and thrust measurement at self-propulsion test in still water, various performances in actual seaway where these ships are bound to sail and under several weather conditions were further estimated. Model motions in regular waves were also filmed by 16 mm movie camera.

The outline of experiment is as follows.

Principal Dimensions

Model	Lpp x Bm x d	= 2.5m x 0.3571m x 0.1488m
(in Full Scale	do.	= 150m x 21.43m x 8.930m)

Propeller

Diameter	0.100 m
Pitch Ratio	0.80
Exp. Area Ratio	0.50
No. of Blades	4

Bulbs

B1 (projected)	a/Lpp = 2.0%, f/d = 76%, H/Lpp = 2.5%
B2 (not projected)	a/Lpp = do., f/d = do., H/Lpp = -2.5%

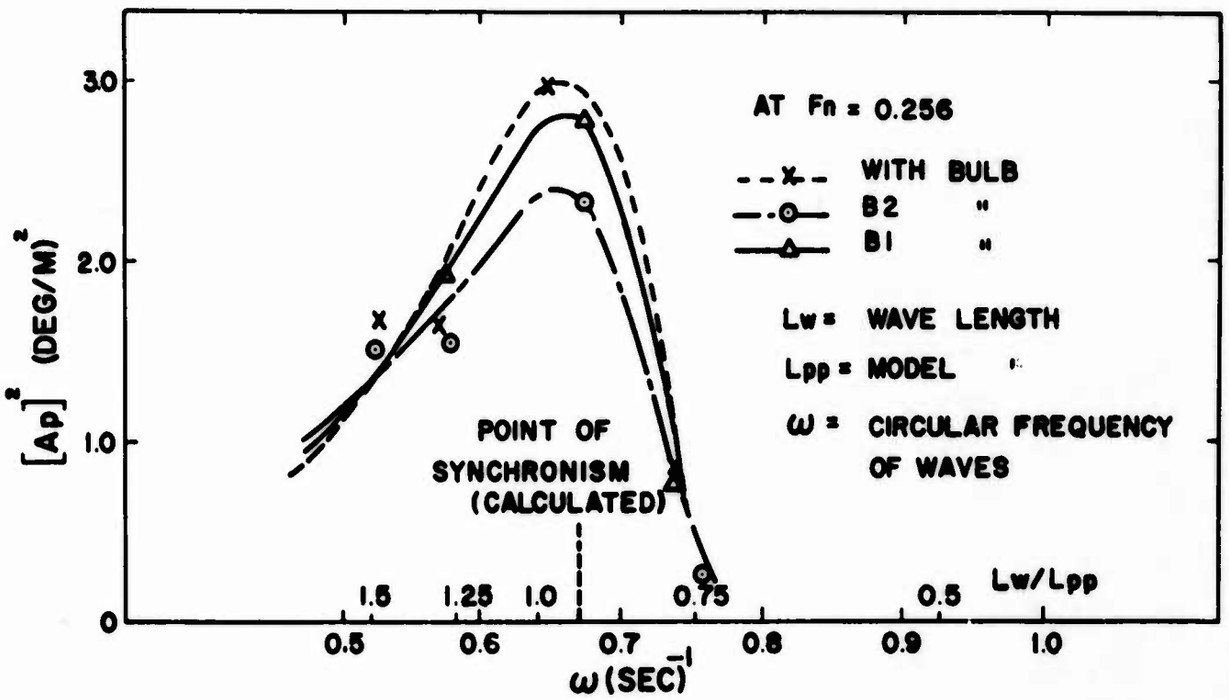


Figure 10a. Response Amplitude Operator of Pitch.

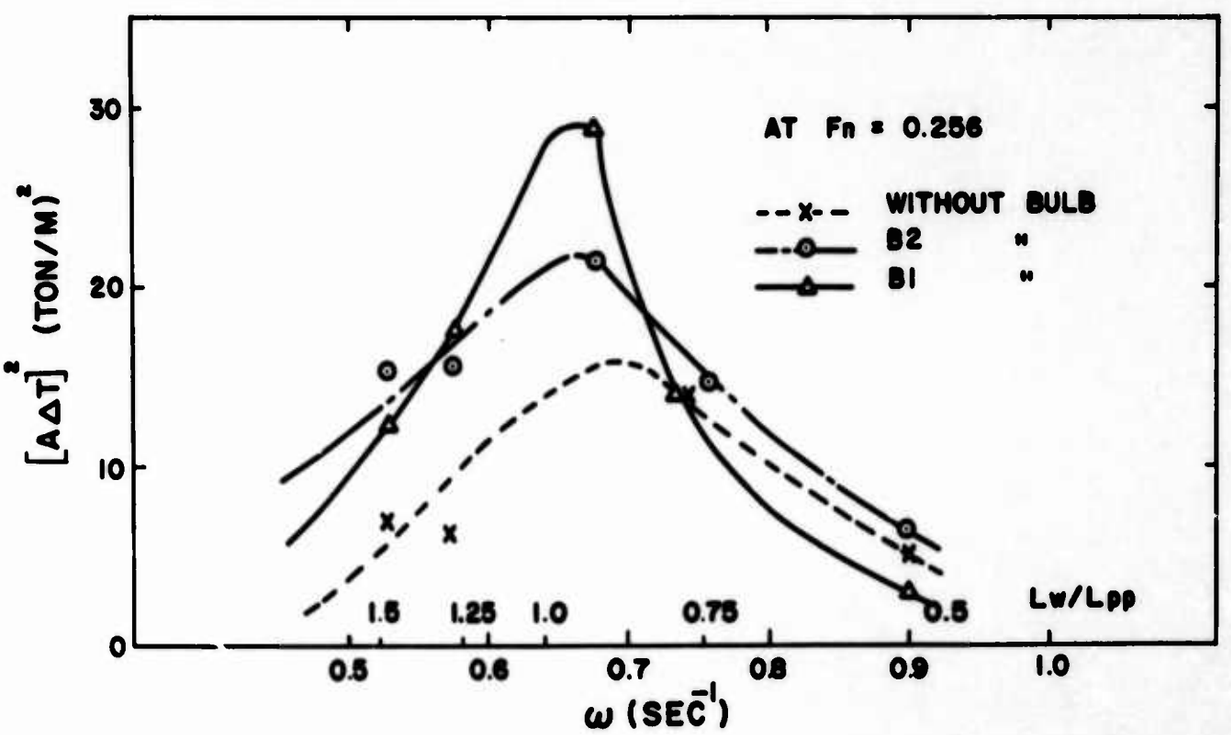


Figure 10b. Response Amplitude Operator of Thrust Increase.

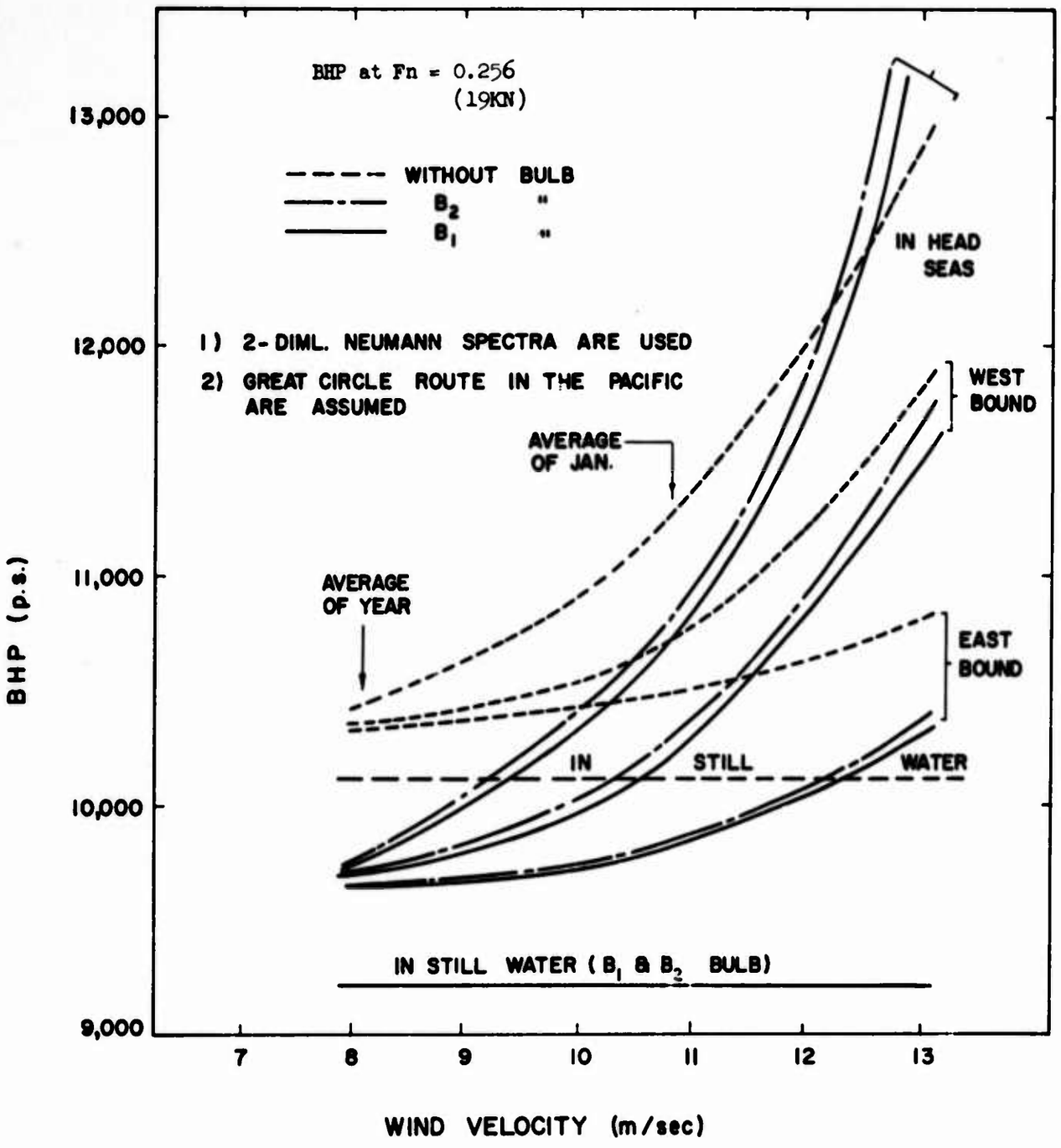


Figure 11. Comparison of BHPs in a Seaway.

where a is radius of bulb
f is immersion of bulb center below waterplane at full load condition
h is the projection of bulb center ahead of the fore end of main hull.

Designed Loading Condition

Full Load Condition

Designed Speed

Fn = 0.256 (19 Kn in full scale)

Waves

Wave Height = 0.05 m
Wave Length/Lpp = 0.75, 1.0, 1.25, 1.50

Radius of Gyration

Main Hull 25% Lpp
With-Bulb Form 26% Lpp

The results of this experiment are summarized as follows:

The previous expectation was verified that motions (mainly pitch) of with-bulb forms got decreased, while thrust increase in waves became larger than those of main hull forms, especially in longer waves. The tendency was more remarkable with B1 bulb forms, as was also expected.

The amount of power increase of with-bulb forms, estimated using response amplitude operators of thrust increase derived and statistical treatment considering various possible weather conditions over the route, little differed from that of main hull (without bulb) forms, probably owing to the dominant wave components of shorter length in the wave spectra used. In considerable rough seas where longer waves predominate, the power increase of with-bulb forms would be so large as not to be compensated by their superior performances in still water.

5. CONCLUSION

From the experimental results heretofore described, the followings could be summarized.

1) Resistance and propulsion performances of "with-bulb" forms are satisfactory about designed loading conditions and in higher speed range including designed points, but gradually get worse as the conditions are off the designed loading condition or designed speed. Attentions should also be payed to self-propulsion factors as not to decrease overall propulsive performance.

2) According to the features of "with-bulb" forms mentioned in 1), they seem to be much suitable for passenger boats or tankers, whose loading conditions are little changed through their voyages.

3) General tendencies are confirmed that bulb fitting is favorable as regards ship motions, while it is unfavorable for thrust increase in waves. However, it is concluded that motions and power increase of with-bulb forms in seaway are little different from those of conventional forms, unless sea and weather conditions are extraordinarily violent.

4) Through the conclusions stated in 1) to 3), the authors are sure of the possibility that various "with-bulb" high speed cargo liners satisfying design requirements and having better resistance and propulsion performances, and having not inferior characteristics in all practical respects compared with conventional form ships can be designed.

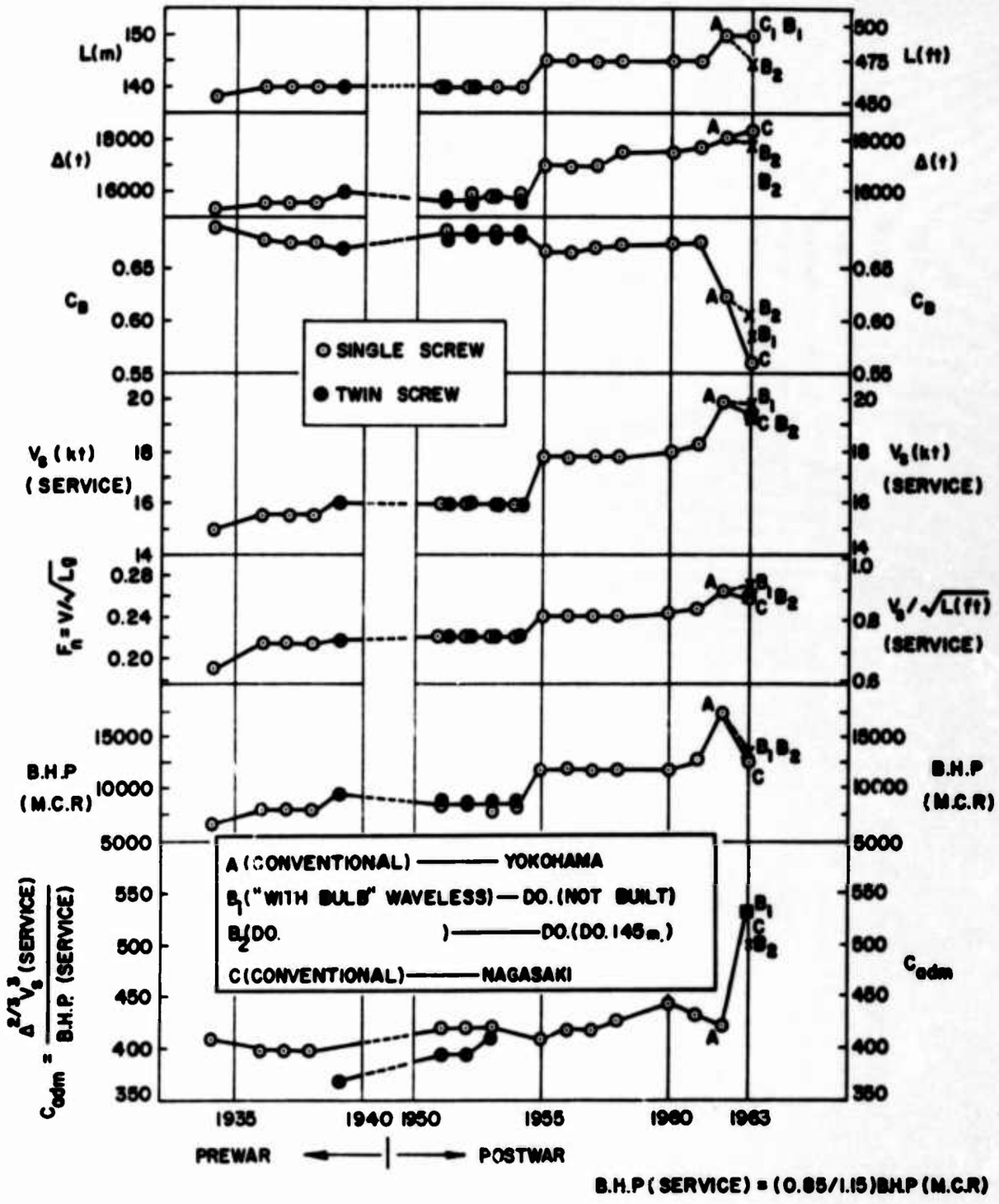


Figure 12. Trends in Propulsive Performances of NYK Cargo Liner, Japan, 1934-1963.

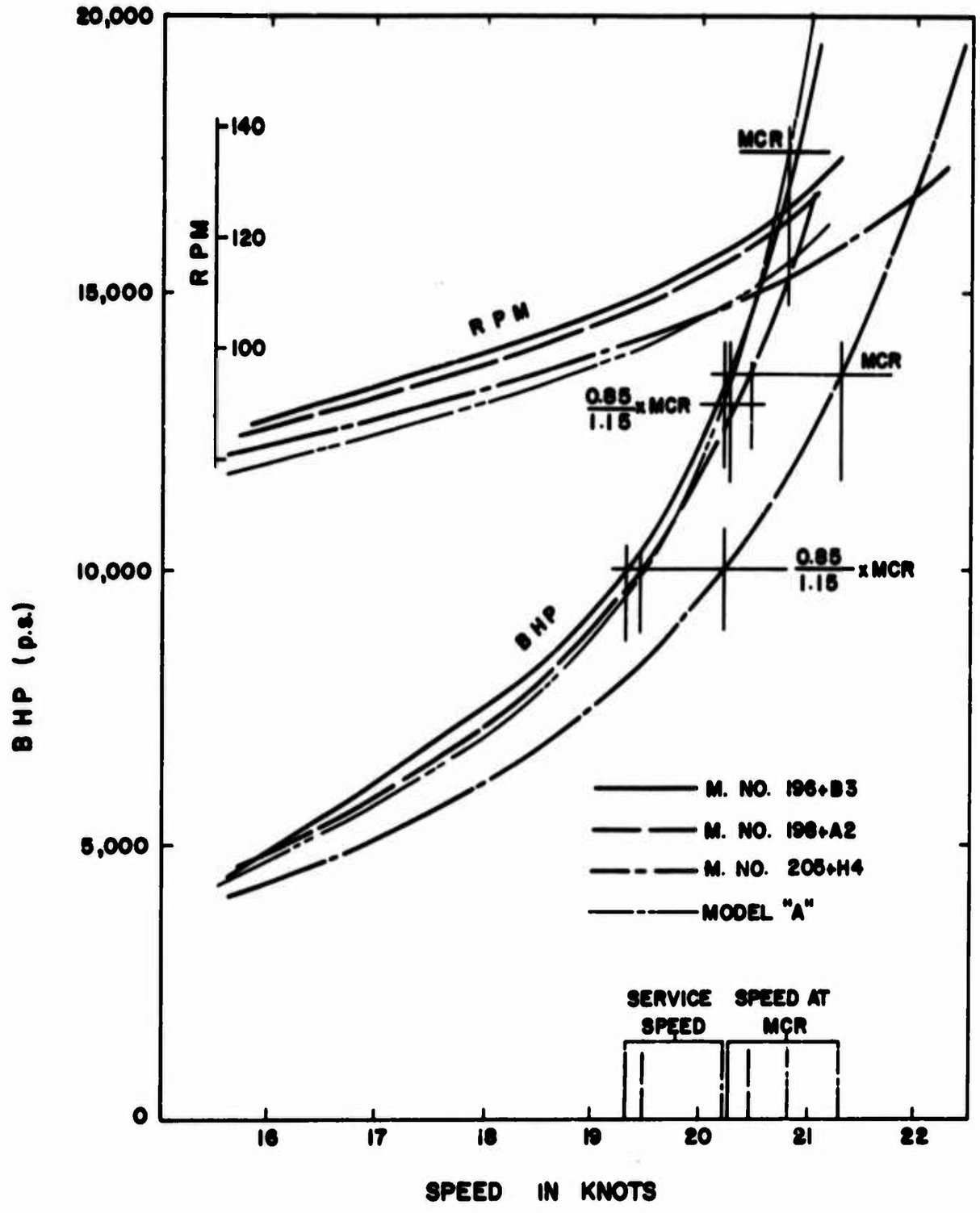


Figure 13a. BHP and RPM Curves, Full Load Condition.

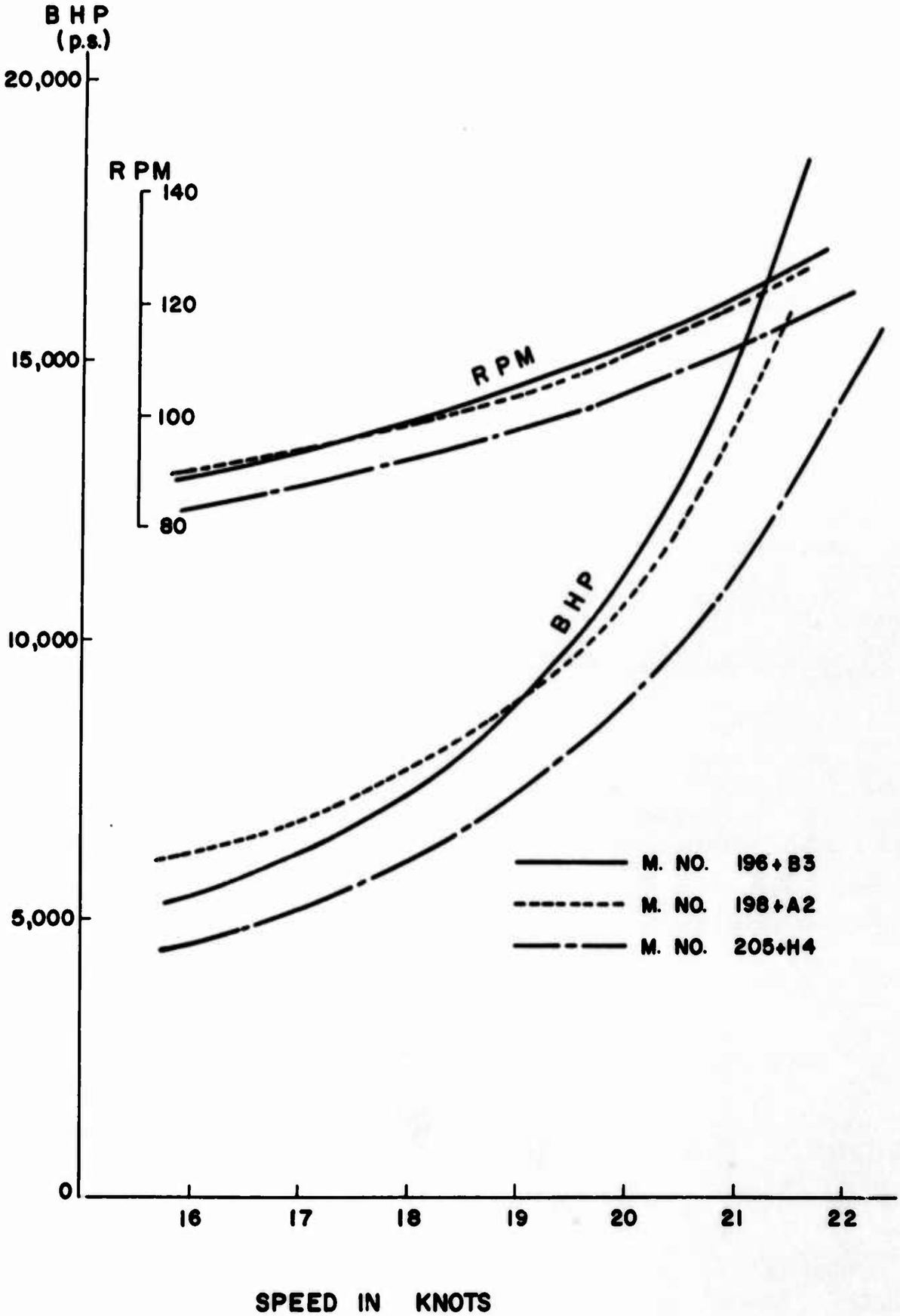


Figure 13b. BHP and RPM Curves, RPM 75% Displacement Condition.

ACKNOWLEDGMENTS

The authors would like to express their cordial gratitude to those who have helped and cooperated with them throughout to promote the work.

Professor Inui, the inventor of "with-bulb" waveless concept, has assisted them with theoretical advices and eagerly lead them to acquire better results model by model. The authors could never imagine getting the fruitful results reported in this paper without him. Assistant Professor Tagori and other staffs of the Experimental Tank of the University of Tokyo have helped the authors with minute execution of large amounts of experiments and advice as to the experiments. Pioneering work of Mr. Kajitani and Mr. Ikehata (Ref. 1) gave the greatest support for the authors during the work.

The whole experiment of 6 m models were owing to Dr. Tsuchida (Head of Powering Div., Ship Research Institute), Dr. Yokoo (Head of Ship Propulsion Div., do.) and the staffs of Mejiro Tank of S.R.T.

This paper is a part of research work in the author's comany, hence final and deepest gratitude is to the superiors of the company who have permitted presentation of the paper, to Vice Manager, Yamagata (Hull Designing Dept.) and to all the staffs of Planning Section, Hull Designing Dept., who gave the authors consistent encouragement and effective aids as to the basic design of these ships.

REFERENCES

1. M. Ikehata and H. Kajitani,

   "Ship Hull Form Design Method Based Upon the Waveless Form Theory" Thesis for Master's degree at the University of Tokyo, March 1962.

2. T. Inui

   "Wave-Making Resistance of Ships" SNAME Vol. 70., 1962.

3. Other papers listed in Appendix 3 of paper 2) above.

Appendix 1

Assumptions Made and Particulars of Propellers Roughly Designed for Prediction of BHP Curves

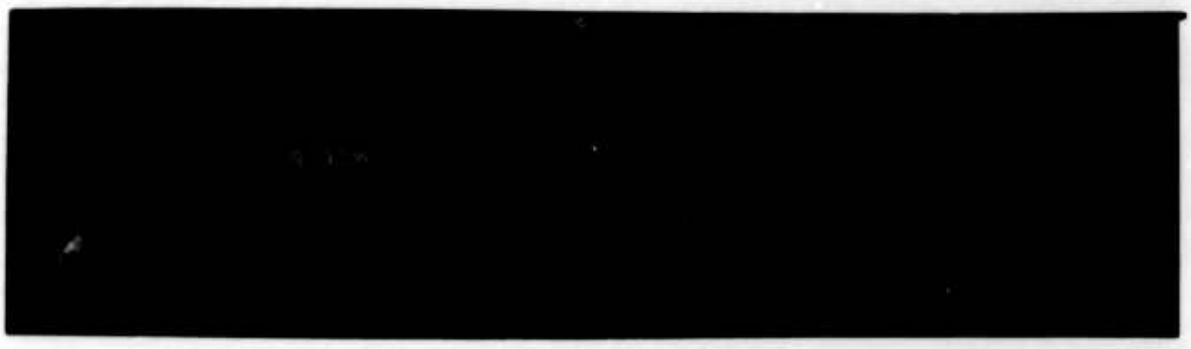
MODEL No. (SHIP)	196 + B3 (1)	198 + A2 (2)	205 + H4 (3)	MODEL "A"
EHP Cal.	by Hughes' Method			
ΔCf	$-.05 \times 10^{-3}$		$-.13 \times 10^{-3}$	
Self-Prop. Factors	as referred to Figs. 8a and 8c			
1-Ws/1-Wm	1.08		1.10	
Transmission Eff.	0.95			
Main Engine (MCR)	$13,500^{PS} \times 118^{RPM}$			$17,500^{PS} \times 115^{RPM}$
Propellers				
Diameter	6.05	6.10	6.05	6.23
Pitch Ratio	0.861	0.85	0.91	0.91
Ex. A. Ratio	0.55			0.50
Section	Aerofoil			
Number of Blades	4			5
Used Chart	MAU (Standard Series of S.R.I.)			

APPENDIX 2

MODELS OF WAVELESS FORMS WITH BULB







AN APPLICATION OF THE WAVELESS THEORY TO THE DESIGN OF A DESTROYER FORM

Seiji Takezawa

The Ship Model Basin Laboratory
Japan Defence Academy

AN APPLICATION OF THE WAVELESS THEORY TO THE DESIGN OF A DESTROYER FORM

ABSTRACT

The design problem concerning a large sonar dome for modern destroyers is studied from the "With Bulb" waveless concept. Theoretical prediction about the possible attainable amount of reduction in wave resistance -- 50 percent at $F_n = 0.30$ and 30 percent at $F_n = 0.40$ -- is satisfactorily ascertained by the resistance tests on two 8 meter destroyer models, both of practical forms. Twenty large bulbs, which were designed so as to be substitutable for the conventional sonar domes, were tested; first, of a basic, simple, spherical type; second, of a more practical dome type.

The problem is then attacked, not only from the standpoint of resistance but also with all ship hydrodynamical design considerations in mind, i.e., the self-propulsion test both in still water and in regular tank waves, the sea-keeping qualities prediction for the actual complicated sea states, and also the radio-controlled self-propulsion maneuvering test.

From these wide ranged researches, the practicability of the "waveless" sonar dome is successfully ascertained.

I. INTRODUCTION

Recently, modern destroyers have a tendency to be equipped with a large sonar dome. As that dome becomes larger, its size cannot be ignored in comparison with the main hull. Then, considering the increase of the ship resistance due to the dome, the conventional shape and location of bottom sonars is definitely unfavorable.

The starting point of this investigation exists in the discovery that a bulbous bow is able to contain the large sonar transducer. Although a bow bulb designed for this purpose is larger than the ordinary bulbous bow, the bulb that is obtained by the application of Professor Inui's "waveless theory" is also quite large. Therefore the theoretical basis for this investigation is founded on the "waveless theory."

This investigation treats the case where the large sonar dome is to be equipped to a certain main hull. From an ideal wave-interference viewpoint of the waveless theory, this case is the so-called "incomplete" wave-interference problem. However, the main scope of this study was restricted to this case for practical design reasons. The tested forms of bow bulb can be divided into two types. The first type is similar to the sphere, where it is easy to apply the theory. The second type is similar to the bottom sonar dome, in which case it is readily able to enclose the ordinary sonar transducer. Moreover the vertical position of the bulb is so selected to fulfill the requirement for the sonar itself.

The results obtained in this study were originally published in Japan, 1962, 1962, by the author[1,2]. It has been proved that the bow sonar dome has superior resistance characteristics in comparison with the bottom dome. In this paper, which includes test results on two kinds of new domes, M.59- 9 and M.59- 10, the theoretical treatments on the wave-making resistance of the destroyer with the large bow dome are particularly discussed. The performances in irregular waves and in turning motion are also briefly described.

The experiments in this paper were carried out at the Ship Model Basin of Japan Defence Agency, Meguro, Tokyo, from August 1960 to March 1963.

II. ESTIMATION OF WAVE RESISTANCE FOR A DESTROYER FORM WITH A LARGE BOW BULB

2.1 Reduction Ratio of Wave-Making Resistance Due to a Large Bow Bulb

Two basic hull forms, M.No. 59 and M.No. 60, which are not mathematical at all, but are completely practical, are treated. The following procedure of analysis was adopted. By making use of the measured wave-making resistance of the basic hull, the reduction in wave resistance due to the addition of a large bulb is calculated, not the absolute values of the wave-making resistance of the hull form fitted with the large bulb. By this procedure, we may be able to keep the errors as small as possible due to the incomplete mathematical treatment of the main hull form. Furthermore, the calculations can be much simplified. Wave-cancellations generally consist of two controlling factors, the phase as well as the amplitude of a set of the free wave systems, main hull wave and bulb wave. However, we will only consider here a single controlling factor, the amplitude relationship, by assuming that the "inverse phase" relationship is completely satisfied in all cases. In accordance to this, all bulbs treated in this paper are located in the nearly constant shiplengthwise position with their center position, i.e., 0.03L forward of F.P., which is considered as approximately the optimum position for a bulb.

With a very fine hull form which has no parallel middle body, it may be possible to consider the whole free wave system consisting of the bow and stern waves only, without any shoulder waves. In these cases, a ratio of the fundamental term of wave-making resistance of the main hull with the bulb to that term of the main hull only, that is the reduction ratio of the fundamental term (Ω), will be given in the following Equation (1).

$$\Omega \equiv \frac{R'_{W-B}}{R'_W} = \frac{\int_0^{\pi/2} \{A_F(\theta) - B(\theta)\}^2 \cdot \cos^3\theta \cdot d\theta}{\int_0^{\pi/2} \{A_F(\theta)\}^2 \cdot \cos^3\theta \cdot d\theta} + \frac{\beta^2}{1+\beta} \qquad (1)$$

R'_W : Fundamental term of wave-making resistance of the main hull itself.

R'_{W-B} : Fundamental term of wave-making resistance of the main hull with a bulb.

And the reduction ratio of the interference term of wave-making resistance (ψ) are given, as follows:

$$\psi \equiv \frac{R''_{W-B}}{R''_{W}} = \left| \frac{A_F(\theta) - B(\theta)}{A_F(\theta)} \right|_{\theta=0} \qquad (2)$$

R''_W : Interference term of the wave-making resistance of the main hull itself.

R''_{W-B} : Interference term of the wave-making resistance of the hull with a bulb.

Hereupon

$$R_W = R'_W + R''_W , \qquad R_{W-B} = R'_{W-B} + R''_{W-B}$$

R_W, R_{W-B} : Total wave-making resistance

$$C_W = \frac{C_W}{1/2\ \rho L^2 V^2}$$

$$= C'_W + C''_W = \frac{R'_W}{1/2\ \rho L^2 V^2} + \frac{R''_W}{1/2\ \rho L^2 V^2}$$

$$C_{W-B} = C'_{W-B} + C''_{W-B}$$

Therefore

$$\Omega = \frac{C'_{W-B}}{C'_W} , \quad \psi = \frac{C''_{W-B}}{C''_W}$$

The definitions of the symbols are the same as those in Reference 3.

$A_F(\theta)$: Amplitude function of the bow wave of the main hull.

$B(\theta)$: Amplitude function of the bulb.

: Viscosity correction factor of the stern wave height.

On the other hand, the measured results of the wave-making resistance of the main hull being known, the fundamental terms and the interference terms on the main hull can be estimated by the use of the measured total wave-making resistance curves. Accordingly, when Ω is able to be calculated from Equation (1), the fundamental term of the hull form with the bulb is obtained by multiplying the fundamental term of the main hull by that Ω. Similarly, the interference term of the hull form with a bulb is calculated from the measured interference term of the basic hull and the estimated ψ from Equation (2). Then, by adding them, the total wave-making resistances are obtained.

This method has been already discussed by Professor Takahei, but according to this method both of Ω and ψ cannot be calculated, unless the $A_F(\theta)$ are found. The mathematical representation of the main hull form is required, as is a suitable expression for $B(\theta)$.

2.2 Mathematical Approximation to the Basic Hulls

As the basic hulls treated in this paper are asymmetric shiplengthwise and are of special forms cutting down at the stern, it is difficult to represent the hull forms by a complete mathematical formula. On the other hand, the scope of this study is sufficiently satisfied by a consideration of the correlation between the bulb and the basic hull, so we do not need a strict mathematical representation of the hull form, which would ordinarily be necessary for an analysis of the absolute value of C_W. Therefore, we will select a simple method leading up to the first assumption

In spite of considering the ship form to be two-dimensional, and referring to the prismatic curve, the basic hull form is asymmetric shiplengthwise. But, we will try to compare with a certain asymmetric hull form, that is the cosine-hull form designed by Professor Takahei[3,4].

The cosine-hull form is defined by the following equations:

$$m(\xi,\zeta) = m_1(\xi') \cdot m_2(\zeta') \qquad (3)$$

$$2\xi/L = \xi', \quad 2\zeta'/L = \zeta'$$

$$m_1(\xi') = a \cdot \sin\left(\frac{\pi}{2}\sqrt{1-\xi'}\right)$$
$$\xi' = 0(\text{F.P.}) \sim 2(\text{A.P.}) \qquad (4)$$

$$m_2(\zeta') = 1, \quad (\text{U - type distribution})$$
$$\zeta' = -t \sim 0, \quad \text{where } t = 2T/L \quad (T = \text{draft}) \qquad (5)$$

As the basic hull of this study is one of a V-frame line, the following Equation (6) replaces Equation (5).

$$m_2(\zeta') = 1 + \zeta'/t \quad (\text{for V-frame line})$$
$$\zeta' = -t \sim 0, \quad \text{where } t = 2T/L, \ (T: \text{draft}) \qquad (6)$$

The hull form using $a_1 = 0.4$ and $t = 0.1$ in Equations (3) (4), and (5) was named C-101 by Professor Takahei. Comparing with C-101 and the basic hull in this report (M.59- ⓪, M.60- ⓪) on the sectional area, Figure 1 is obtained. Table 1 shows these particulars. From this data we can understand that M.59- ⓪, M.60- ⓪ do not belong to separate groups, considering the type of the frame line. Hereafter we will adopt M.60- ⓪ as the basic hull form. The following equation is obtained by considering the ratio of the fundamental term of wave-making resistance for M.60- ⓪ (C_w - M60) to that for C-101 (C'_w - C101). However considering β as the only viscosity correction factor, it is assumed that the value of β for the equivalent hull form of M.60- ⓪ is the same value for C-101.

$$\frac{C'_{w\text{-M60}}}{C'_{w\text{-C101}}} = \frac{\int_0^{\pi/2} \{A_{M60}(\theta)\}^2 \cdot \cos^3\theta \cdot d\theta}{\int_0^{\pi/2} \{A_{C101}(\theta)\}^2 \cdot \cos^3\theta \cdot d\theta} \qquad (7)$$

$A_{M60}(\theta)$: Amplitude function of bow wave on M.60- ⓪.

$A_{C101}(\theta)$: Amplitude function of bow wave on C-101.

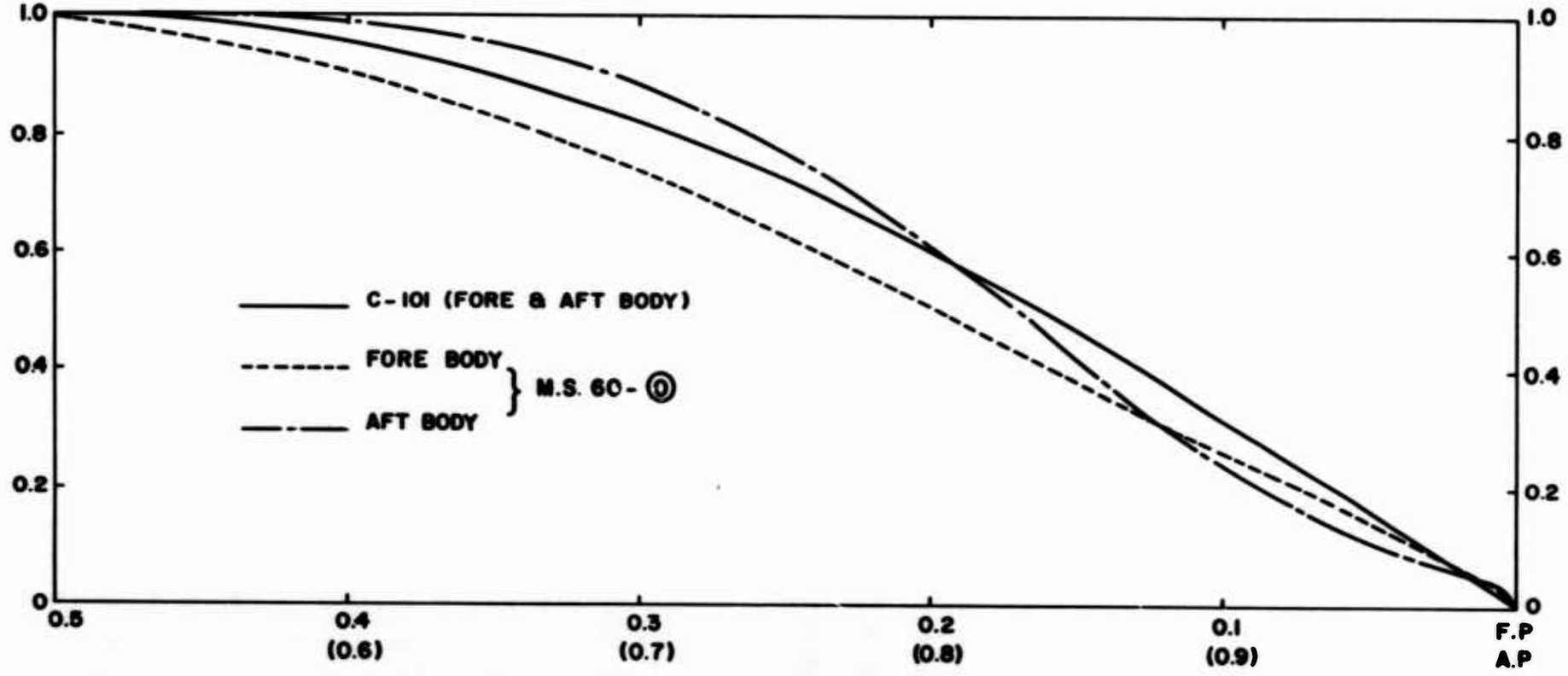


Figure 1

SECTIONAL AREA CURVE

TABLE 1

	M.No. 60	C-101	C-201
T/L	0.0314	0.03	0.03
B/L	0.116	0.0904	0.1208
$\nabla/(L\text{-}1/10)^3$	1.872	3.968	5.968

TABLE 2

F_n	0.50	0.41	0.35	0.29	0.20
k_0L	4	6	8	12	25
α_{M60}	0.646	0.573	0.595	0.564	0.593

TABLE 3

F_n	0.50	0.45	0.41	0.35	0.29	0.25	0.20	0.14
k_0L	4	5	6	8	12	16	25	50
β	0.862	0.860	0.855	0.847	0.837	0.830	0.746	0.595
$1+\beta^2$	1.743	1.739	1.731	1.717	1.701	1.689	1.557	1.354

$$\frac{A_{M60}(\theta)}{L} = \frac{a_{M60}}{\pi K_0 L} \cdot \frac{1 - \dfrac{U(K_0T_2, \theta) \cdot \cos^2\theta}{K_0T_2}}{1 - \left(\dfrac{\pi}{K_0L} \cdot \cos\theta\right)^2} \qquad (8)$$

where $T_2/L = 0.0314$

$$\frac{A_{C101}(\theta)}{L} = \frac{a_{C101}}{\pi K_0 L} \cdot \frac{U(K_0T_1, \theta)}{1 - \left(\dfrac{\pi}{K_0L} \cdot \cos\theta\right)^2} \qquad (9)$$

where $a_{C101} = 0.4$, $T_1/L = 0.05$

$K_0 = g/V^2$, $K_0L = 1/F^2$

L: ship length, V: ship speed

F: Froude number

herein, $U(K_0T, \theta) = 1 - \exp.(-K_0T \cdot \sec^2\theta)$

Regarding Equation (7), from the experiments both the denominator and the numerator of the left side have been determined already, and the denominator of the right side is calculated by the formula (9). The only unknown quantity in the numerator of the right-hand side is a_{M60}, which is determined by Equation (8), a_{M60} can be calculated by Equations (7), (8), and (9).

According to above mentioned method a_{M60} can be estimated without use of β, but the value of β being known a_{M60} can be looked for from Equations (10) and (8).

$$C_{w\text{-}M60} = 2\pi(1 + \beta^2) \int_0^{\pi/2} \left\{\frac{A_{M60}(\theta)}{L}\right\}^2 \cdot \cos^3\theta \cdot d\theta \qquad (10)$$

Table 2 has been obtained by the former method. The results show that the approximate mathematical representation of M.60- 0, is nearly equal to the case in which is $a_1 = 0.6$ in Equation (4) and $T/L = 0.0314$ in Equation (6). Calculating the wave-making resistance of the mathematical hull form defined by $a_1 = 0.6$ and Equations (3), (4), and (6), the results are compared with the measured results of M.60- 0 in Figure 2. However, the values of β to be equal to C-101 are assumed, those values being given in Table 3.

Figure 2 shows that the correlation between the measured and estimated values is good except for the speed range over the Froude number of 0.45.

2.3 Mathematical Approximation to the Bow Bulb

The generating wave of the spherical bulb is equal to the generating wave of an advancing point doublet as confirmed in References (3) and (5). Accordingly, the amplitude function of the spherical bulb, $B(\theta)$, is given by the following equation.

$$\frac{B(\theta)}{L} = -2\left(\frac{a_o}{L}\right)^3 \cdot (K_o L)^2 \cdot \sec^4\theta \cdot \exp(-K_o f \sec^2\theta) \quad (11)$$

f : depth of spherical bulb center.

a_o : radius of spherical bulb.

L : ship length.

The bulb being a complete sphere, the amplitude function is simply calculated by the above equation. As a large number of the bulbs treated in this study are not of the simple spherical shape, some assumptions are required to decide f and a_o. It is assumed that the equivalent sphere for obtaining the effect of the bulb is the maximum inside osculating sphere of the bulb form, referring to the resistance tests results corresponding with the bulb forms. Therefore in this study f and a_o in Equation (11) are decided by the maximum inside osculating spheres (see Figure 3). Particulars of these bulbs are shown in Table 4. The reason for assuming the above is the fact that the main object of the present paper does not lie in the absolute value, but in the difference between the two cases with and without bulb. If the section of bulb is not a circle,

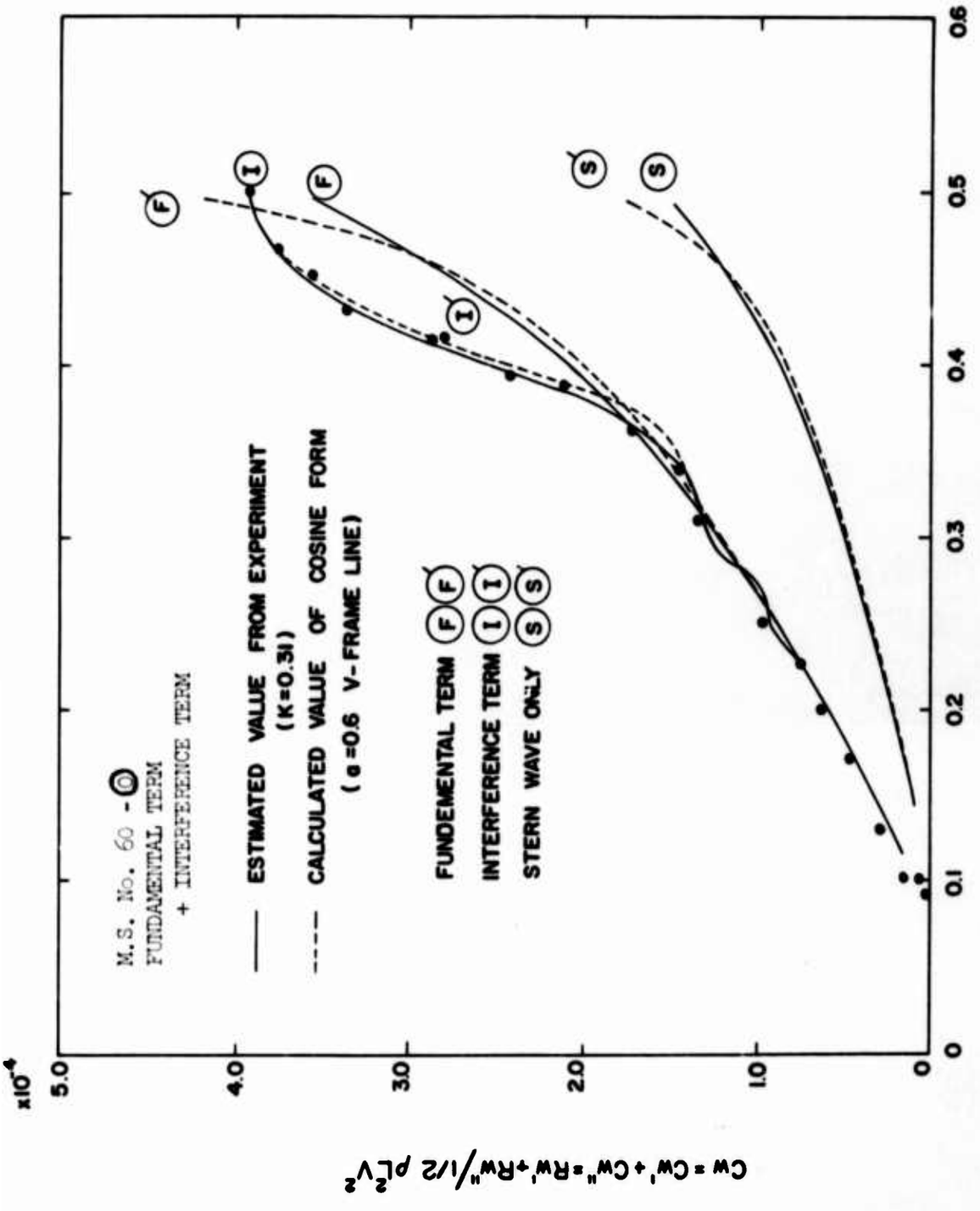

M.S. No. 60 - ⓪
FUNDAMENTAL TERM
+ INTERFERENCE TERM
—— ESTIMATED VALUE FROM EXPERIMENT (K=0.31)
---- CALCULATED VALUE OF COSINE FORM (a=0.6 V-FRAME LINE)
FUNDEMENTAL TERM (F)(F)
INTERFERENCE TERM (I)(I)
STERN WAVE ONLY (S)(S)
x10⁻⁴
5.0
4.0
3.0
2.0
1.0
0
0.1
0.2
0.3
0.4
0.5
0.6
Cw = Cw' + Cw'' = Rw' + Rw'' / 1/2 ρL²V²
Fn = V/√Lg

Figure 2

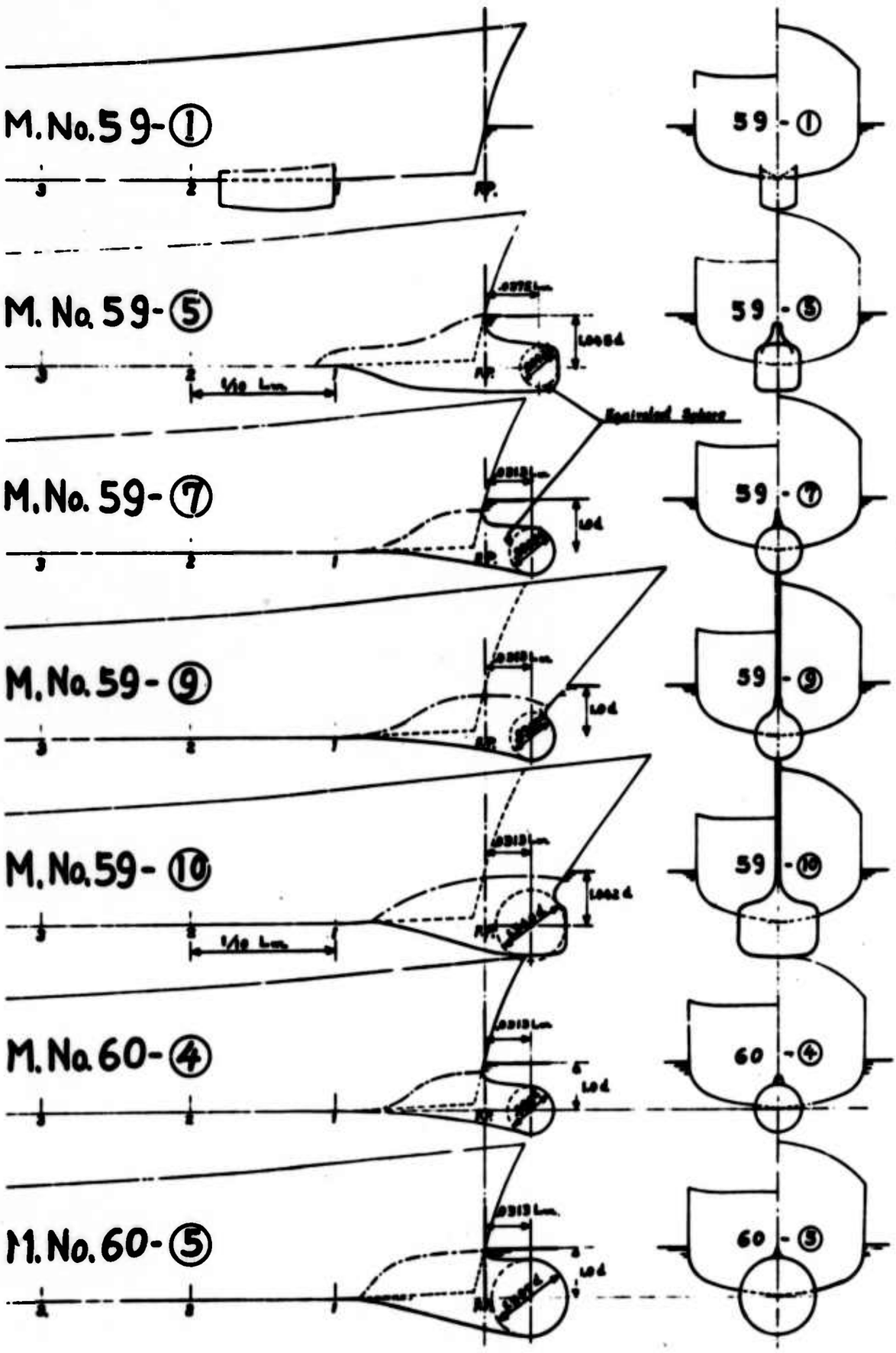


Figure 3. Profiles and Front Views.

it is better the equivalent sphere be decided on the basis of the sectional curve of the bulb (Figure 4). In M.59- 10 the values estimated by that method are adopted. The correlations between the equivalent spheres and the forms of the fairing parts after the main parts of bulbs will vary with each case, but that method may be adapted in almost all cases, except for a very long fairing part.

As the bulbs in this study are nearly similar, the ship-lengthwise position of the bulb center will be nearly constant, that is about 3% of load waterline length - forward of the F.P. This position is the nearly optimum one deduced from previous experiments. In this study the position is fixed on 3% of LWL by requirements based on practical design considerations. It is supposed as before mentioned that the phases of the generating waves of these bulbs are the inverse phases of the bow waves.

2.4 Comparisons Between Measured and Estimated Results

2.4.1 Wave-Making Resistance

Considering M.59- 0 to be of the same form as M.60- 0 as a rough approximation, $A_F(\theta)$ of M.59- 0 and M.60- 0 in Equations (1) and (2) are calculated by the assumption that a_{M60} in Equation (8) is equal to 0.6. $B(\theta)$ is calculated by Equation (11), using the value of bulb depth and radius indicated in Figure 3. From such procedure the wave-making resistance of the hull form with a bulb is estimated from Equations (1) and (2). Figures 5 and 6 show the comparisons between the calculated values and the measured values. The estimated values of the ordinary speed range give the good results except for M.59- 10 and M.60- 5, which is the very large bulb. Generally speaking, at high speeds the estimated values are larger than the measured ones. On the very large bulbs the accuracy of estimation is not good because of their serious eddy-making. Another cause for the discrepancy in the very large bulbs is the assumption that the phases of the bulb waves are exactly equal to the inverse phases of the bow waves.

2.4.2 Effective Horsepower

Figure 7 shows EHP as obtained from Figures 5 and 6. The results show that M.60- 4, M-59- 7, 9, the spherical bulbs, give the quantitative coincidence. Since there are large inaccuracies on

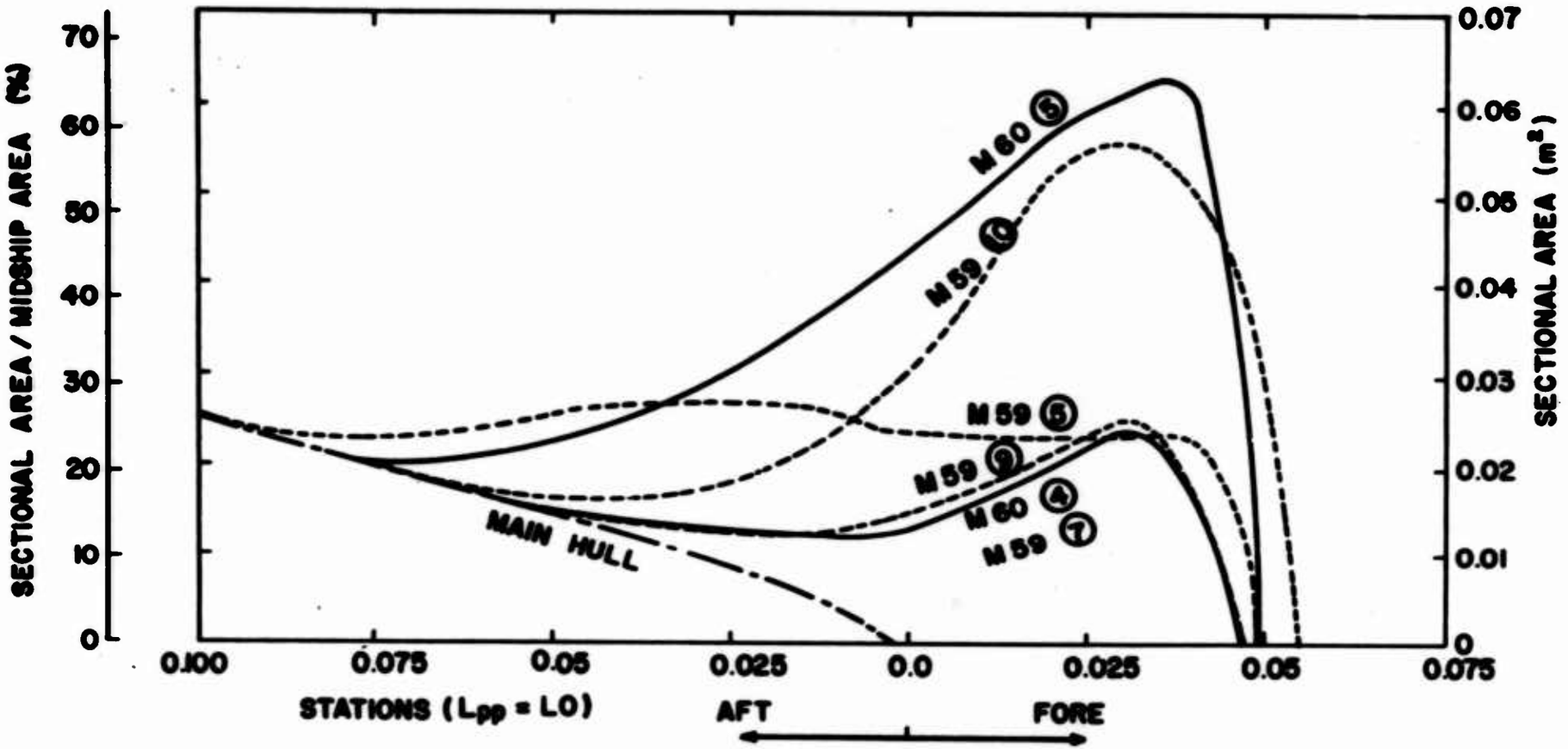


Figure 4.
Sectional Area Curve (Bulb Only).

$$C_W = C_W' + C_W'' = R_W / 1/2\,\rho\, L^2 V^2$$

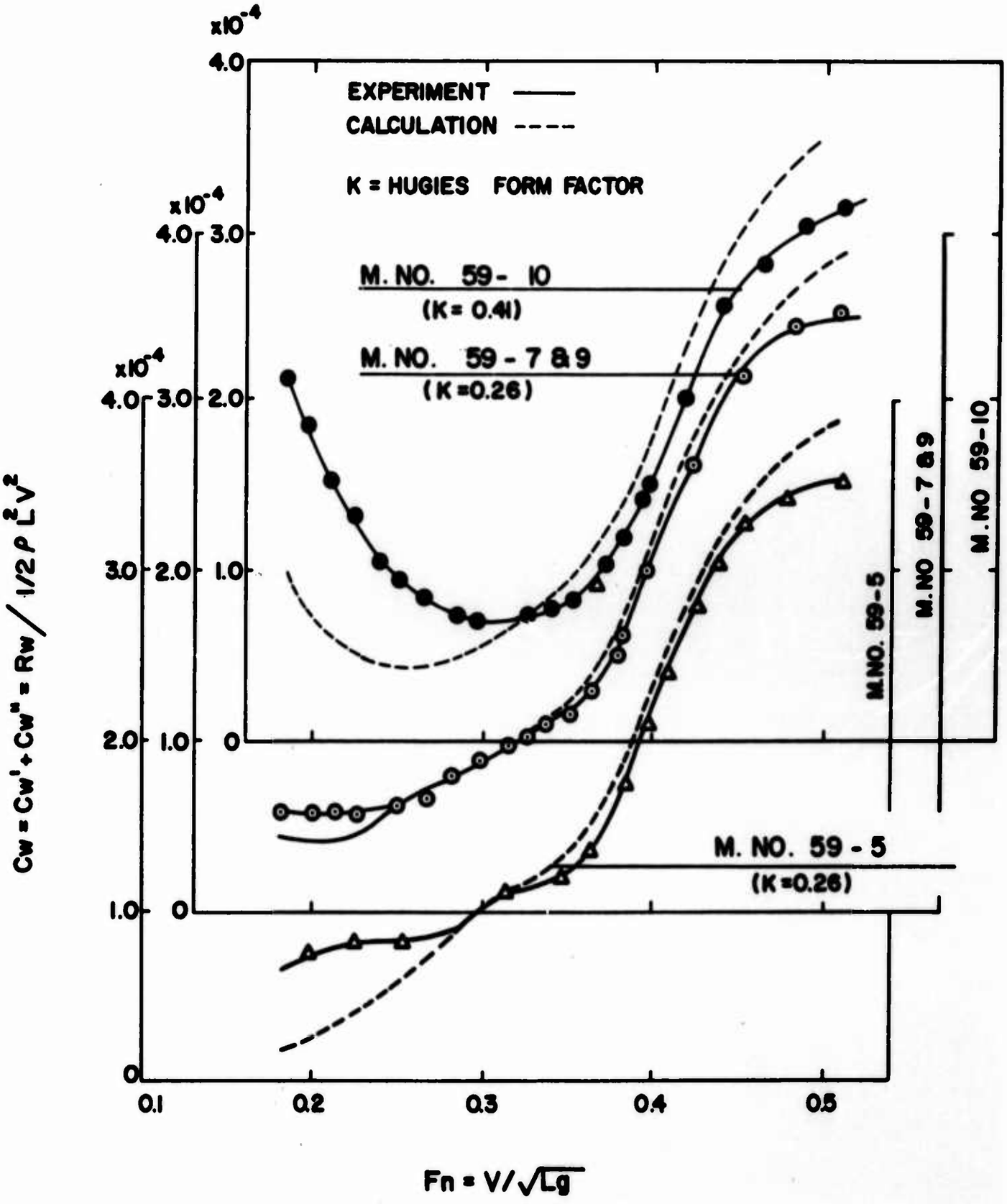


Figure 5

M. S. No. 59 - (5), (7), (9), (10).
Comparisons Between Experiments
and Calculations.

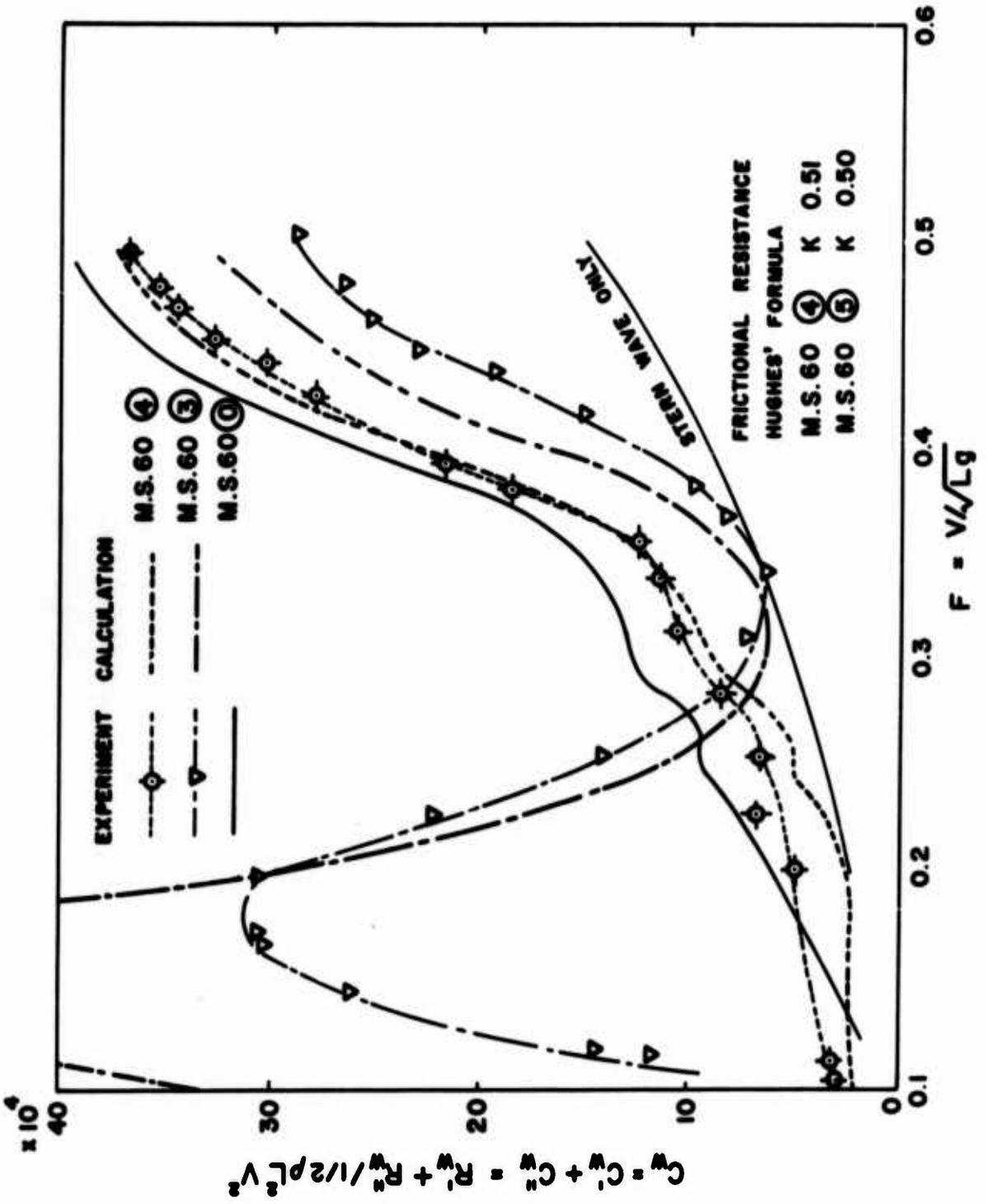


Figure 6
M. S. No. 60 - 4, 5.
Comparisons Between Experiments
and Calculations

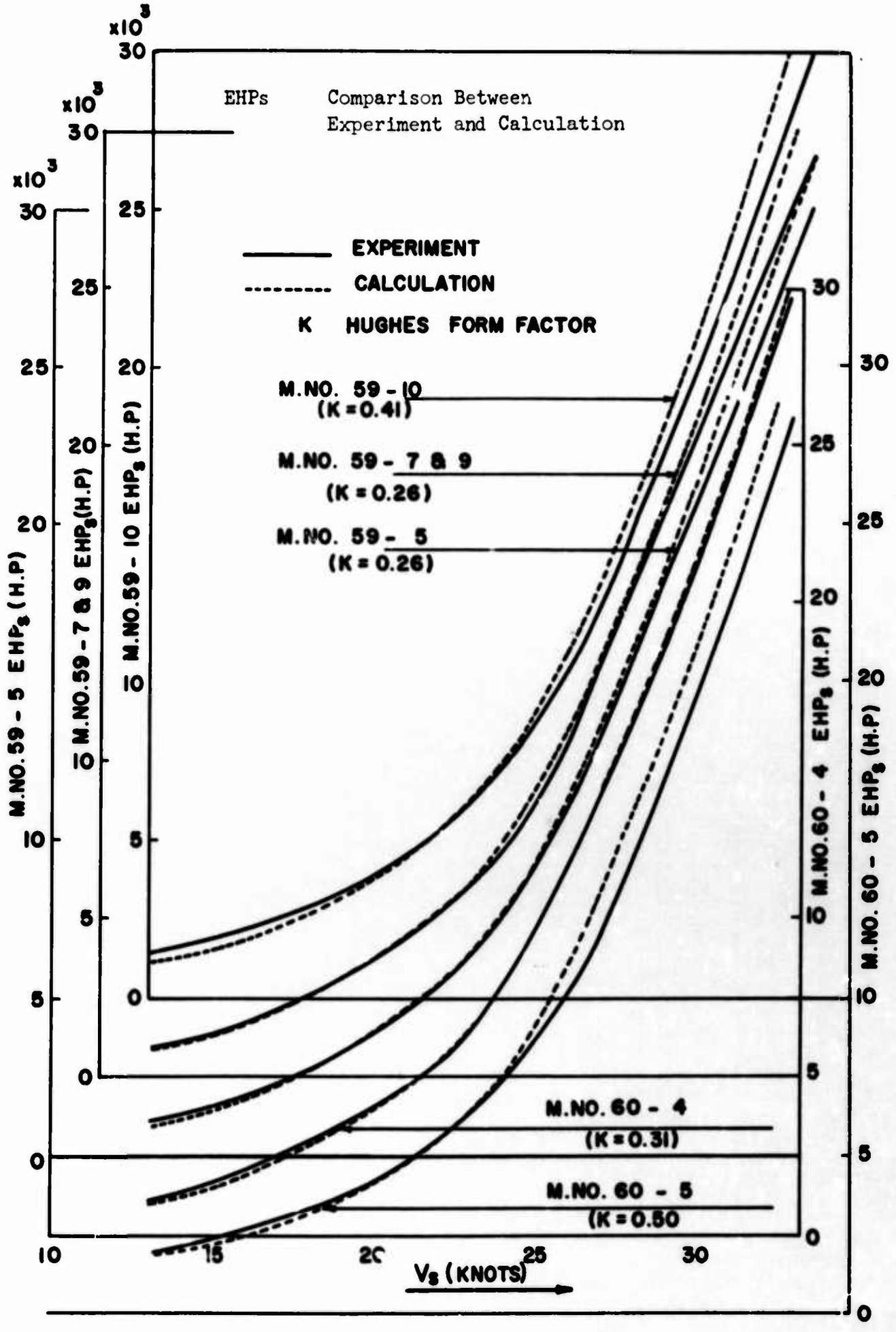

EHPs Comparison Between
Experiment and Calculation
EXPERIMENT
CALCULATION
K HUGHES FORM FACTOR
M.NO. 59 - 10
(K = 0.41)
M.NO. 59 - 7 & 9
(K = 0.26)
M.NO. 59 - 5
(K = 0.26)
M.NO. 60 - 4
(K = 0.31)
M.NO. 60 - 5
(K = 0.50
M.NO.59 - 5 EHPs (H.P)
10 M.NO.59 - 7 & 9 EHPs (H.P)
10 M.NO.59 - 10 EHPs (H.P)
10 M.NO.60 - 4 EHPs (H.P)
10 M.NO.60 - 5 EHPs (H.P)
Vs (KNOTS)

Figure 7

TABLE 4

PRINCIPAL PARTICULARS OF BULBS

Model		L_{WL} (m)	L_{OA} in Water (m)	∇ (cm^3)	$\Delta\nabla$ (cm^3)	$\nabla+\Delta\nabla$ (cm^3)	$\Delta\nabla/\nabla$ (o/o)	$\Delta\nabla/\nabla+\Delta\nabla$ (o/o)	S (m^2)	ΔS (m^2)	$S+\Delta S$ (m^2)	$\Delta S/S$ (o/o)	$\Delta S/S+\Delta S$ (o/o)	Position of bulb center from F.P. & of L_{WL}	$\frac{\nabla+\Delta\nabla}{(L_{WL})^3}10^3$	$\frac{Ab_{max}}{A_{max}}$ (%)
M.No.59	⓪	8.00	8.0025	958,330	0	958,330	0	0	8.0883	0	8.0883	0	0	-	1.872	-
	①	8.00	8.0025	"	12,410	971,240	1.347	1.329	"	.2026	8.2909	2.505	2.444	Aft 13.25	1.897	16.955
	⑤	8.00	8.4025	"	35,830	994,160	3.739	3.604	"	.4964	8.3847	6.137	5.782	Fore 3.75	1.942	24.946
	⑦	8.00	8.3775	"	18,050	976,380	1.884	1.849	"	.3518	8.4401	4.350	4.168	Fore 3.13	1.907	25.732
	⑨	8.452 (8.00)	8.3775	"	18,850	977,180	1.967	1.929	"	.4284	8.5167	5.297	5.030	Fore 3.13	1.909	26.762
	⑩	8.447 (8.00)	8.4375	"	48,830	1,007,160	5.095	4.848	"	.6669	8.7552	8.245	7.617	Fore 3.13	1.967	58.340
M.No.60	⓪	8.00	8.0025	958,330	0	958,330	0	0	8.3033	0	8.3033	0	0	0	1.872	0
	④	8.00	8.3775	"	17,950	976,280	1.893	1.839	"	.3503	8.8036	4.218	3.979	Fore 3.13	1.907	25.639
	⑤	8.00	8.4525	"	60,070	1,018,400	6.268	5.898	"	.7362	9.0395	8.866	8.144	3.13	1.989	65.637

Principal Particulars of Main Hulls	M.No.59	M.No.60
	draft = 26.86 Cm (even)	draft = 25.05 Cm(even)
	L_{WL}/B = 9.25 B/d = 3.22 L_{WL}/d = 29.79	L_{WL}/B = 8.63 B/d = 3.70 L_{WL}/d = 31.94
	C_b = .511 C_p = 620 C = .824 C_w = .765	C_b = .511 C_p = .620 C = .824 C_w = 765
	d/L = .0335 B/L = .108	d/L = .0314 B/L = .116

∇ : Dispt. of Main Hull, with Appendage
$\Delta\nabla$: Increase of Dispt. by Bulb
$\nabla+\Delta\nabla$: Total Dispt with Bulb

S : Wetted Surface Area, with Appendage
ΔS : Increase of W.S.A. by Bulb
$S + \Delta S$: Total W.S.A. with Bulb

Pos. of Bulb Ctr: Pos. of Max. Sec. Area of Bulb
$A_{b\ max}$: Max. Sec. Area of Bulb
A_{max} : Max. Sec. Area of Main Hull
L_{OA} in Water : Max. Length under Water Sur.

M.60- 5 , M.59- 10 the very large bulbs, these estimated values can not be used for practical purposes. But in place of the quantitative viewpoint, we can try to compare the estimated curves with each other. This comparison well explains the qualitative characteristics of each bulb.

2.4.3 Design Speed of Bulbs

The maximum cancellation effect of bulb appears theoretically at a certain speed, that is, the design speed. Assuming that the cancellation is predominately in the transverse elementary wave ($\theta = 0^{\circ}$ 35° 16'), the design speeds are estimated as in Figure 8. Meanwhile from Figure 6 the "measured" design speed, that is the speed giving the minimum wave-making resistance will be obtained. These "measured" design speeds are $F_n = 0.34$ for M.60- 5 and $F_n = 0.20$ for M.60- 4 , respectively. The estimated design speed of M.60- 4 nearly coincides with the "measured" one, on the contrary M.60- 5 is not coincident. Therefore it can be seen that the assumptions mentioned above can be used for large bulbs, but cannot be adopted for extremely large bulbs. In very large bulbs the actual values of design speed can be obtained by multiplying the estimated values by about 1.2.

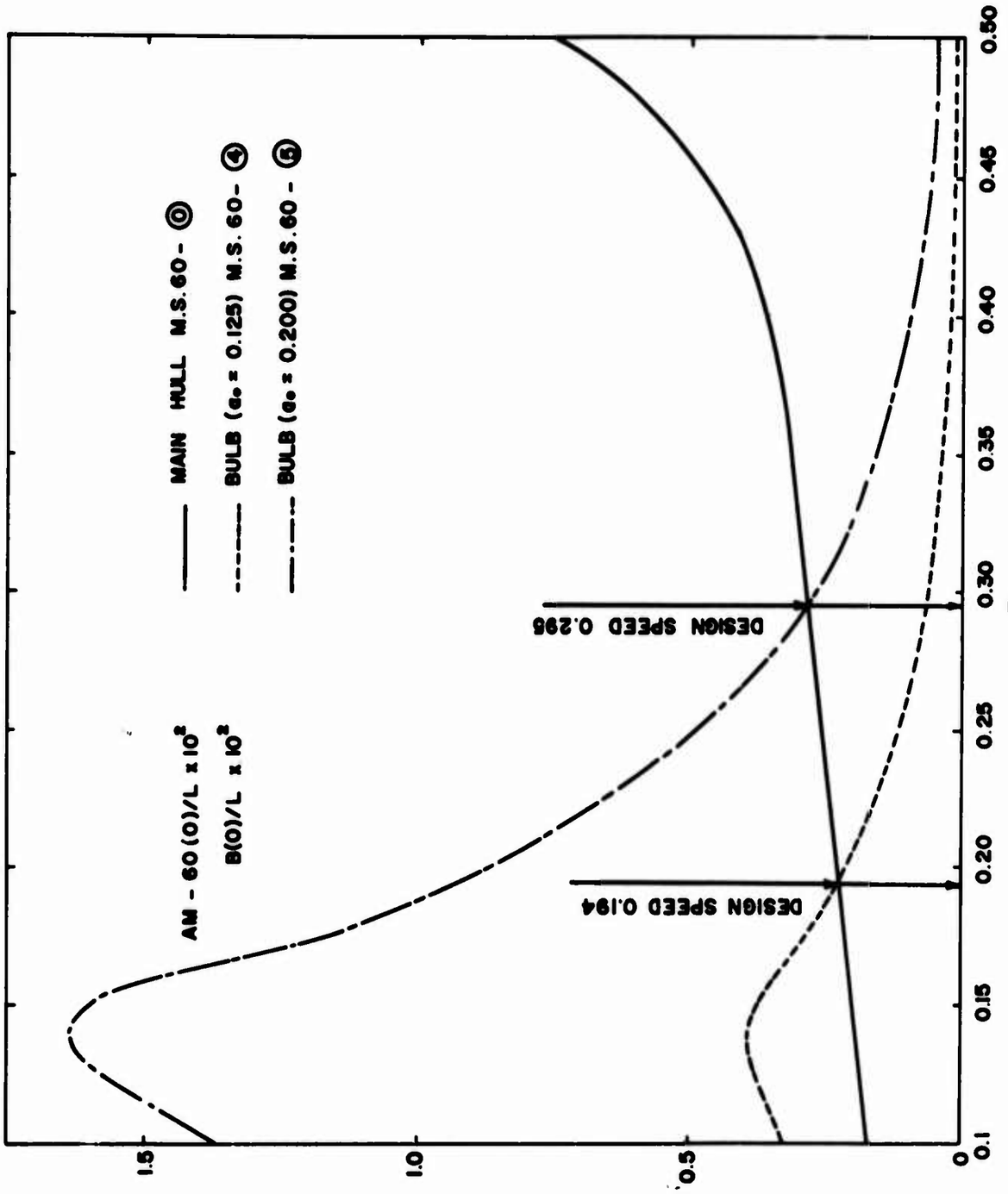

MAIN HULL M.S.60- ⓪
BULB (a_o = 0.125) M.S.60- ④
BULB (a_o = 0.200) M.S.60 - ⑤
AM - 60(0)/L x 10^2
B(0)/L x 10^2
DESIGN SPEED 0.194
DESIGN SPEED 0.295
1.5
1.0
0.5
0
0.1
0.15
0.20
0.25
0.30
0.35
0.40
0.45
0.50
F_n

Figure 8

III. GENERAL DESIGN CONSIDERATIONS ON A DESTROYER FORM WITH A LARGE BOW SONAR DOME

3.1 Performance in Still Water

Generally speaking, it has been ascertained, in the preceding chapter, that the performance with bulb is superior to that without bulb, in spite of the fact that a precise prediction of the effect of a bulb could not be made because of the practical basic hull presently adopted. There are many proofs of this in Appendices (B), (C) and related Reference 1.

Bow bulbs equipped with the sonar transducers therein are divided into two classes, that is the large bulb corresponding to the usual sonar transducer and the extremely large bulb corresponding to the unordinarily large transducer. In this study, the extremely large bulbs are M.59- 10 and M.60- 5, the large bulbs are all the others. The large bulbs give good performances over an almost whole range of ship speeds. While in the extremely large bulbs the speed range which shows good performances is not so wide compared with the former. Further, their benefits in resistance are not superior to the former at all. To increase the performance of the extremely large bulbs beyond that achieved in this study will be difficult without reforming the basic hull itself.

In comparison with the conventional equipment of sonar domes like M.59- 1, however, both the large and the extremely large bulbs shown in this paper are practicable enough from the standpoint of improvement of performance in still water.

3.2 Performance in Waves

The performance of destroyers in waves is important for two reasons. The one is that the destroyer must maintain high speeds even in rough seas, the other is that equipment must be kept operational even in rough seas. The former relates to the ship motions and speed decreases in heavy seas, and the latter relates to the exposure of the bow bottom, because the sonar performance is of particular interest in this study. This study treats only the performance in head seas as being the severest condition, but the general trends in all directions of waves will also be obtained.

The performances in head seas with bulb and without bulb are shown in Appendices (D) and (E). The results generally show that in ship motions the hull with a large bulb is better than the basic hull, and in propulsive performances the former is slightly inferior to the latter. For the destroyer, which is navigating in rough seas, it has been generally accepted that her critical navigating speed is determined not by the propulsive power of the plant, but by the limit of the maximum endurable ship motions. Therefore it can be said that the performance of a destroyer with a large bulb is superior to that of a destroyer without a large bulb. In this study rolling is not considered since large bulbs do not have a great influence on rolling.

The exposure of the ship's bottom seriously impairs the sonar operation. This, the position of the sonar on the bottom would seem to be of great importance. But roughly speaking, it is assumed that differences of the detecting ability between bow sonars and bottom sonars do not exist, because in conditions exposing the bow dome air bubbles in the bottom layer as well as the bottom exposure have a bad influence upon the bottom sonars. In still water it is believed that the capability of a bow sonar is usually superior to that of bottom sonars, because the bow sonar is further away from the origin of hull noises, and the air mixture layer about the bow dome is less than along the ship bottom.

3.3 Maneuverability

Except for a very unusual hull form, it is scarcely possible that the maneuverability of destroyers will come into question, because the steering characteristics of destroyers are easy controllable by slight changes of rudder area or skeg area, which do not seriously influence other ship performances. That this is true also for a destroyer with a large bow bulb is shown by the results of steady turning model tests described in Appendix (F).

As regards the huge bow bulbs, it is interesting that a positive effect on the emergency stop can be expected due to the large resistance at very low speed.

IV. CONCLUSION

The author has attempted a very practical application of the waveless theory to the conventional destroyer form. The approximation on the decrement of resistance due to a large bow bulb for a certain basic hull of a practical form is given in the first half of this paper. This method can be applied to define the bulb size in the initial stages of design in these cases.

In the latter half of this paper, the practicability of the destroyer with the large bow bulb is generally considered according to the results obtained from various model tests. Generally speaking, the destroyer with the large bulb has been ascertained in this paper to be practical, considering the obtained improvement on the performances in still water and waves. From the practical standpoint, the problems of construction, docking and anchorage will come into question, so that the details of form and construction must be considered further. But the type as M.59- (5), (7) will give a near practical solution. On the extremely large bulb the data shown in this paper is not enough to appraise. It is believed that the extremely large bulb as M.59- (10), M.60- (5) is too excessive in its size, the bulb being out of proportion with the main hull and the decrement of resistance being less than expected. Moreover refining the form, building the bow and fulfilling the demand based on practical use becomes difficult. Therefore it would be much better if a new basic hull matched to such extremely large bow domes would be designed or if the size of the sonar transducer would be reduced while mai taining the same sonar ability.

REFERENCES

(1)* S. Takezawa: "A Study on the Large Bulbous Bow of a High Speed Displacement Ship--Part I: Resistance in Still Water," Journal of Soc. N.A., Japan, Vol. 110, 1961.

(2)* S. Takezawa: "A Study on the Large Bulbous Bow of a High Speed Displacement Ship--Part II: Performance in Waves," Journal of Soc. N.A., Japan, Vol. 111, 1962.

(3)* T. Takahei: "A Study on the Waveless Bow, (Part I)," Journal of Soc. N.A., Japan, Vol. 108, 1960.

(4)* T. Takahei: "Calculations of Ship Hull Forms with Electronic Digital Computers," Reports of College of Engineering, Ibaraki University, Vol. 8, 1960.

(5)* T. Inui: "Profile Measurements on the Wave-Making Characteristics of the Bulbous Bow," Journal of Soc. N.A., Japan, Vol. 108, 1960.

(6) S. Takezawa: "Ship Motions in Average Sea States (Part I)," prepared for the fall meeting of The Soc. of Nav. Arch., Japan, November 1963.

(7) S. Takezawa: "On the Relations Between Wind Wave Scale and Ship Motions," Unpublished Report of the Technical Research and Development Institute, Japan Defense Agency, 1963.

(8) S. Takezawa: "Steady Turning Model Tests on DD-Hull," Unpublished Report of the Technical Research and Development Institute, Japan Defense Agency, 1962.

N.B.:- References denoted by (*) were translated into English by the University of Michigan.

APPENDIX A

PREMISE ON THE DESIGN OF SONAR DOME

The bow bulbs herein discussed being considered as bow sonar domes, the following design conditions are given from a viewpoint of the acoustics.

1) The bulb must be large enough to be equipped with a certain sonar transducer.

2) The draftwise location of the bulb center must be as deep as nearly equal to or slightly deeper than the fore draft of the main hull.

3) The sonar transducer being a vertical cylinder, it is better that the bulb has a wall side or vertical semi-cylindrical side in the fore part.

4) The bottom of the bulb should not be very deep because of the difficulty in docking.

5) The after part of the bulb must be refined in its form so as to avoid the dome noise.

The bulb form must be designed from the viewpoint of the ship hydrodynamics, keeping in mind the premises mentioned above. M.50- (1) shows the ordinary method of the sonar fitting. M.59- (5) shows the conventional sonar dome attached to the bow. M.50- (10) is a form to be equipped with an extremely large transducer at the bow, and a vertical fin that has almost no displacement is attached for reasons of strength and seaworthiness. The other forms are spherical bulbs, both for the purpose of decreasing resistance and for theoretical research. In general, these bulbs are very large in comparison with conventional bulbous bows, maximum sectional area is as small as 1/4 to 1/2 of the bulbs in this discussion.

APPENDIX B

RESISTANCE AND EHP IN STILL WATER

The models used are of wood, 8 meters in length between perpendiculars including all appendages. The results of the resistance tests are shown as the residual resistance coefficient, Cr, in Figures A-1 and A-2. Frictional resistance was calculated by the Hughes' formula, and the form factor K is assumed to be 0.26 for M.No. 59 and to be 0.28 for M.No. 60. Residual resistance, R_r, is represented as follows

$$C_r = \frac{R_r}{\frac{1}{2}\rho L^2 V^2} = C_t - C_f = \frac{R_t}{\frac{1}{2}\rho L^2 V^2} - \frac{S}{L^2}(1+K) \quad \frac{0.066}{(\log_{10} R_w - 2.03)^2}$$

R_t : total resistance

S : wetted surface area

R_n : Reynolds number.

In these calculations it is assumed that L is constant, that is 8.00 m. in all models including M.59- (9), (10).

The effective horsepower was calculated on the basis of a ship length of 115 m., again in terms of the length between perpendiculars.

EHP calculated from Figures A-1 and A-2 is shown in Figure A-3, assuming the following roughness correction, ΔC_f .

$$\Delta C_f = \Delta R_f / \frac{1}{2}\rho S V^2 = 0.00035$$

The general trend of the test results are shown as follows:

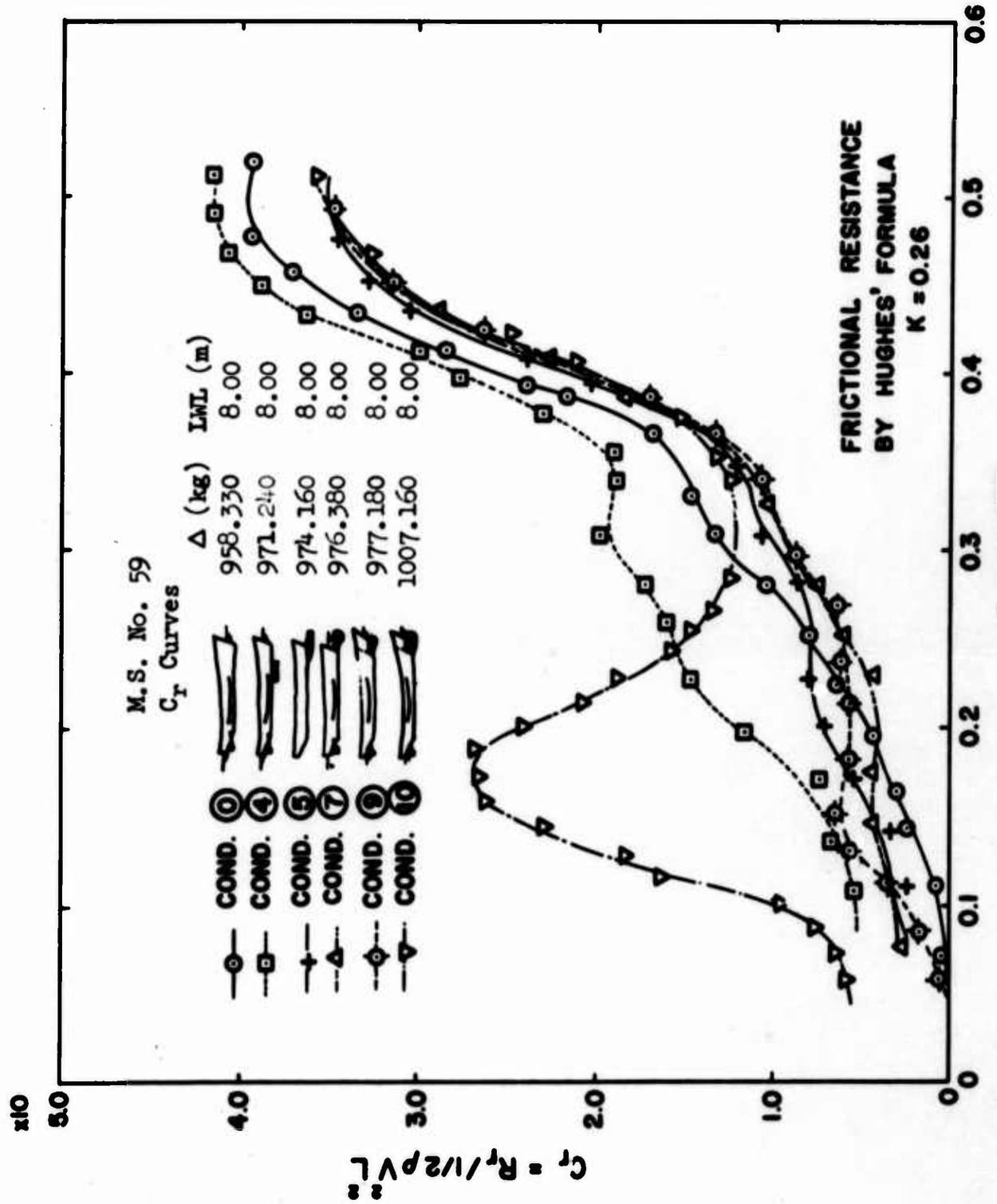

M.S. No. 59
C_r Curves
Δ (kg) LWL (m)
COND. ⓪ 958.330 8.00
COND. ④ 971.240 8.00
COND. ⑤ 974.160 8.00
COND. ⑦ 976.380 8.00
COND. ⑨ 977.180 8.00
COND. ⑩ 1007.160 8.00
FRICTIONAL RESISTANCE
BY HUGHES' FORMULA
K = 0.26
$C_r = R_r / 1/2 \rho V^2 L^2$
x10
5.0
4.0
3.0
2.0
1.0
0
0.1
0.2
0.3
0.4
0.5
0.6
$F = V/\sqrt{Lg}$

Figure A-1

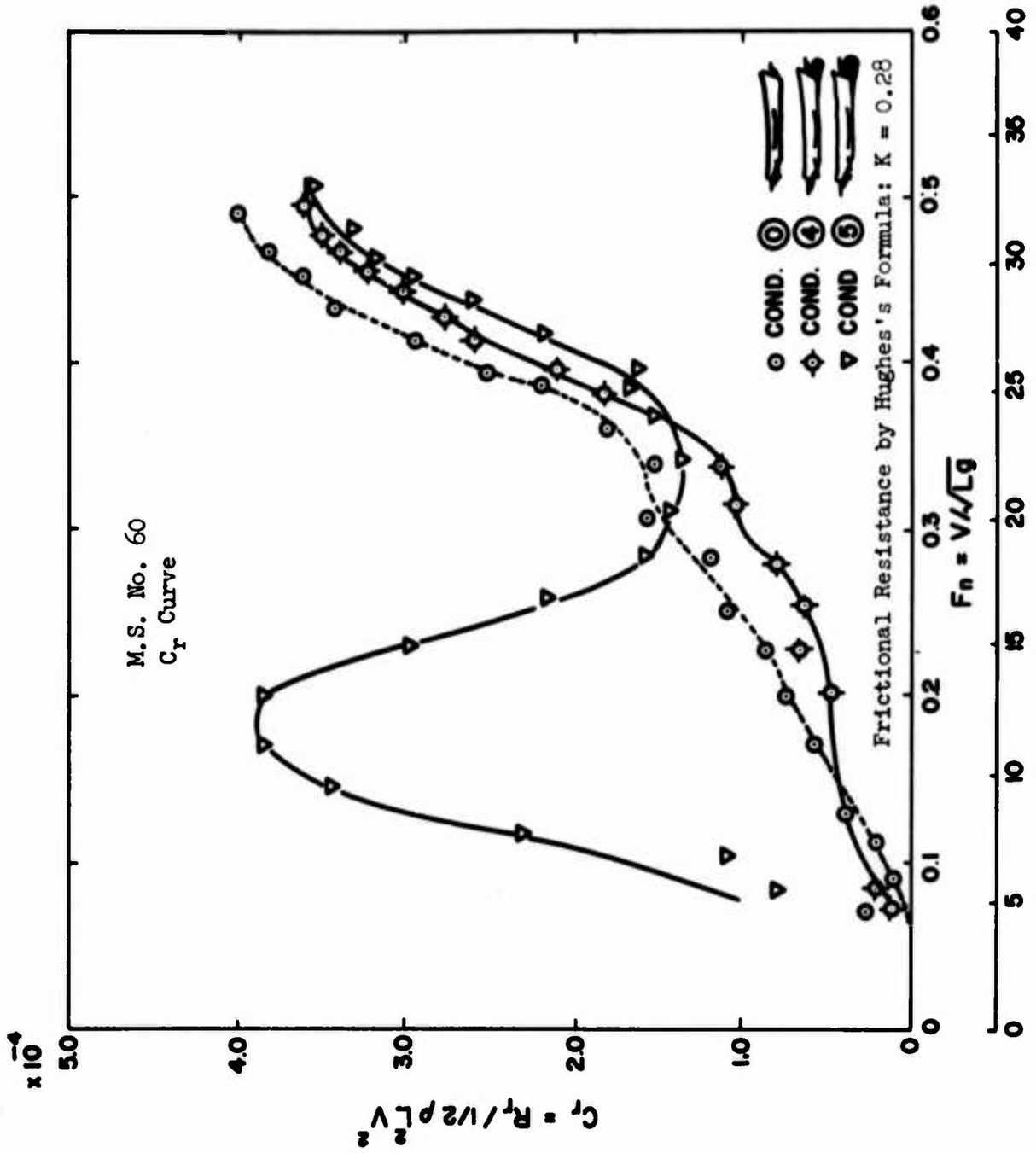

M.S. No. 60
C_r Curve
Frictional Resistance by Hughes's Formula: K = 0.28
COND. ⓪
COND. ④
COND ⑤
$C_r = R_r / 1/2 \rho L^2 V^2$
x 10⁻³
Fn = V/√Lg
Vs (KNOTS)

Figure A-2

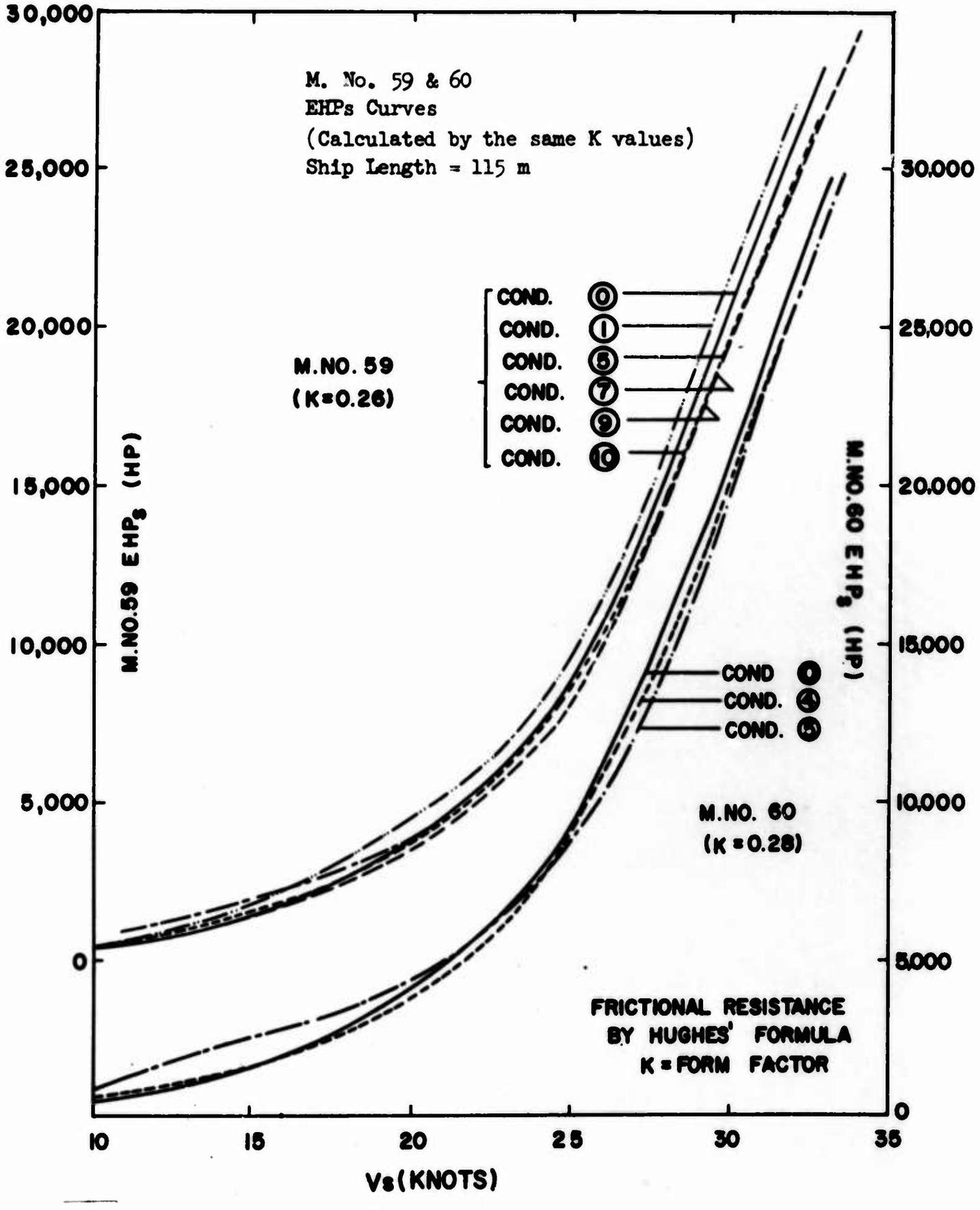

M. No. 59 & 60
EHPs Curves
(Calculated by the same K values)
Ship Length = 115 m
M.NO. 59
(K=0.26)
COND. 0
COND. 1
COND. 5
COND. 7
COND. 9
COND. 10
M.NO.59 EHPs (HP)
M.NO.60 EHPs (HP)
COND 0
COND. 4
COND. 5
M.NO. 60
(K = 0.28)
FRICTIONAL RESISTANCE
BY HUGHES' FORMULA
K = FORM FACTOR
30,000
25,000
20,000
15,000
10,000
5,000
0
10
15
20
25
30
35
Vs(KNOTS)

Figure A-3

1) The performances of the hulls with large bow bulbs are generally better than that of the basic hull alone, in spite of the increase of displacement.

2) The extremely large bulbs give performances not so well as previously expected especially in the high speed ranges. It is considered that the form resistance increase due to the eddy-making is cancelling partly the wave resistance decrease.

3) At the cruising speed of this type of ships, that is 18 kts - 20 kts, the hull forms with large bow bulbs are superior to the basic hull alone over whole speed range, except in the case of the extremely large bulbs (M.59- 10 , M.60- 5.)

4) Between the two cases, with and without large bulbs, about 7% in EHP decrease or about 0.5 kts in speed increase are obtained. Moreover, in comparison with the existing method of fitting a sonar dome, that is M.59- (1) , the maximum speed increase at the same power amounts to about 1.7 kts, because of a fairly large resistance augmentation due to the existing sonar dome.

5) It appears that the basic form of bulb is not always required to be a sphere, as shown in a comparison between M.59- 10 and M.60- 5) or between M.59- (5) and M.59- (7).

6) The attachment of a detector like M.59- (9) has little or no influence on the hydrodynamic characteristics. Therefore such a form is recommended as one of the practical bow forms.

The author's published paper related to the problem in this Appendix B: Reference 1.

APPENDIX C

DHP IN STILL WATER

The results of the self-propulsion tests in still water are shown in Figures A-4 and A-5. The tests were carried out using the same propeller. The skin friction correction based on the Froude's formula is adopted. The models used are the same models as the resistance tests (8 meter wooden models).

In general, some slight differences of the self-propulsion factors are found between the basic hull and the hull fitting with a large bulb, but comparing the DHP tests with the aforementioned EHP tests, the trends are quite similar with each other. Therefore it is concluded that the hull form to be superior in towing condition holds the superiority under self-propelled conditions.

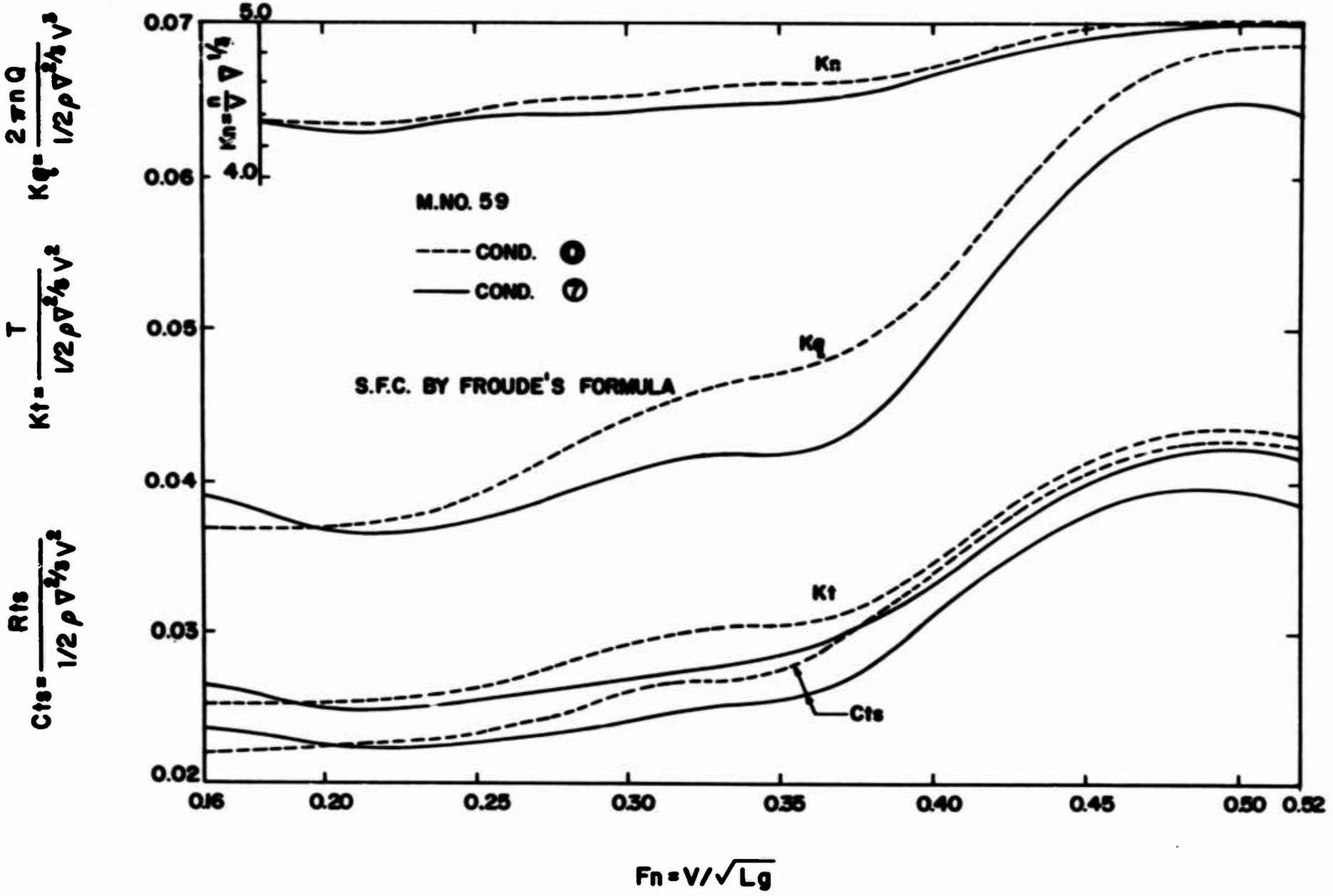

$Kq = \frac{2\pi nQ}{1/2\rho\nabla^{2/3}V^3}$
$Kt = \frac{T}{1/2\rho\nabla^{2/3}V^2}$
$Cts = \frac{Rts}{1/2\rho\nabla^{2/3}V^2}$
$Kn = \frac{n}{\sqrt{\nabla}}\nabla^{1/3}$
5.0
4.0
0.07
0.06
0.05
0.04
0.03
0.02
Kn
Kq
Kt
Cts
M.NO. 59
COND. ④
COND. ⑦
S.F.C. BY FROUDE'S FORMULA
0.16
0.20
0.25
0.30
0.35
0.40
0.45
0.50
0.52
$Fn = V/\sqrt{Lg}$

Figure A-4

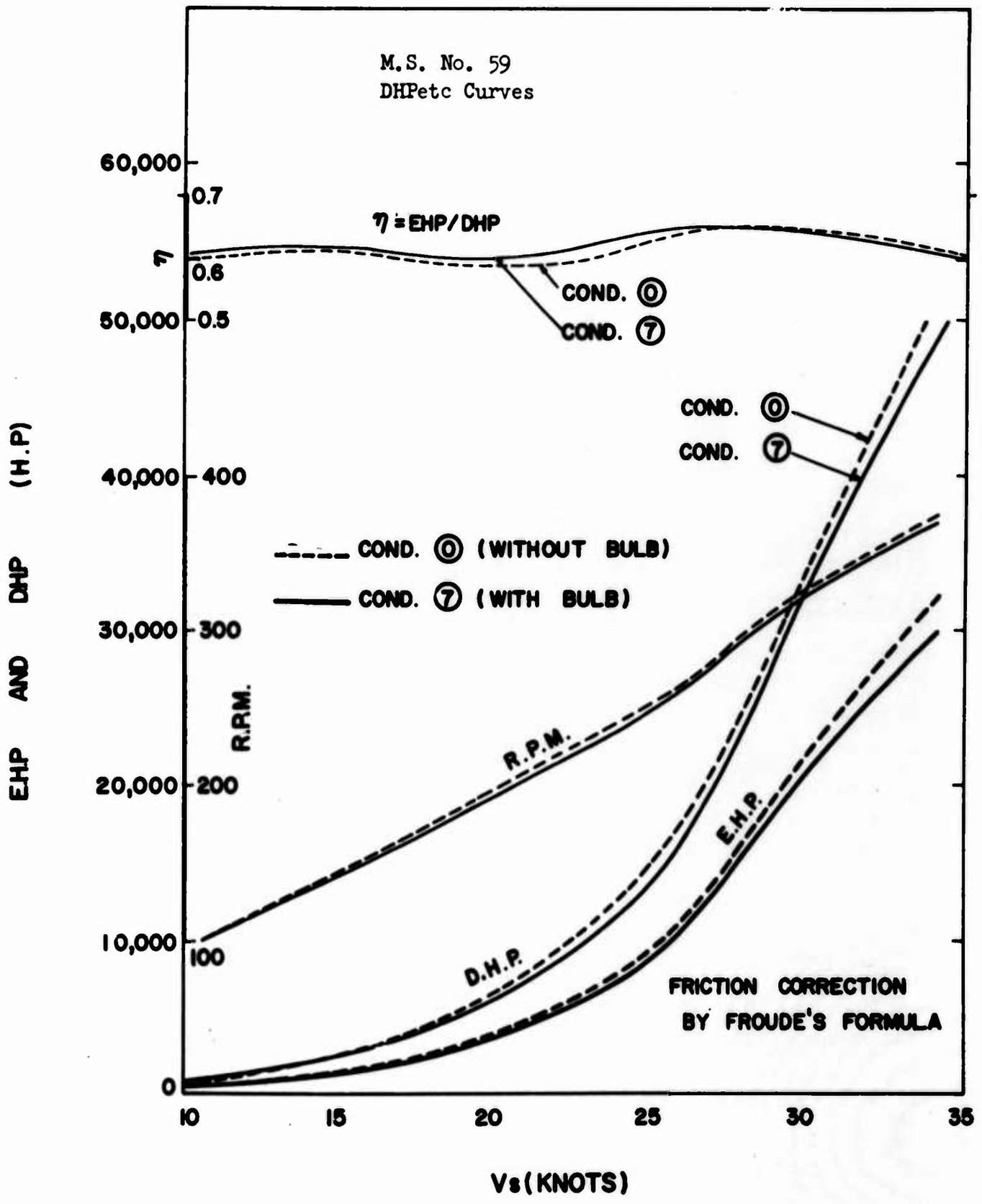

M.S. No. 59
DHPetc Curves
60,000
0.7
η = EHP/DHP
η
0.6
50,000
0.5
COND. ⓪
COND. ⑦
COND. ⓪
COND. ⑦
40,000
400
COND. ⓪ (WITHOUT BULB)
COND. ⑦ (WITH BULB)
30,000
300
R.P.M.
R.P.M.
20,000
200
E.H.P.
D.H.P.
10,000
100
FRICTION CORRECTION
BY FROUDE'S FORMULA
0
10
15
20
25
30
35
EHP AND DHP (H.P)
Vs(KNOTS)

Figure A-5

APPENDIX D

SHIP MOTIONS IN WAVES

The self-propulsion tests in regular head seas were carried out on the four kinds of models, that is three series models without bulbs (M.58, M.59, M.60) and a model with a large bow bulb (M.59-7). These models were 8.00 meter wooden models, and the longitudinal radius of gyration in air was adjusted to 2.0 meters in all models.

The transfer functions of ship motions or the response amplitude operators were obtained from the experiments mentioned above. Then the motions of ships, whose length between perpendiculars is 115 meters, in irregular waves were estimated from those transfer functions and the well-known Neumann's wave spectrum. The assumed wave spectrum, corresponding to the average actual sea state, was decided by the following method. In the first place, the author investigated the relationship between wind velocity and mean wave height in average sea states. Next, he tried to substitute the assumed partially developed Naumann wave spectrum for the average relations between wind velocities and mean wave heights. Hereupon, the significant wave heights of the assumed wave spectra are equal to the mean wave heights of actual average sea states. Moreover, he calculated the ship motions in that assumed spectrum by the usually adopted method, that is E. V. Lewis' method. It is assumed that the values calculated by this method are equivalent to the ship motions in actual average sea.

Pitchings in irregular waves corresponding both to the partially developed average sea states and to the nearly fully developed Neumann waves are shown in Figures A-6 and A-7, respectively. Similarly, bow vertical accelerations are given in Figures A-8 and A-9. The x-axis in these figures can be converted into mean wave heights in average seas. Moreover, the relationship between the mean wave heights and pitching or bow acceleration is shown in Figure A-10. Assuming certain critical values of ship motions against pitching and bow acceleration, the upper limits of the navigable mean wave heights are obtained as shown in this figure.

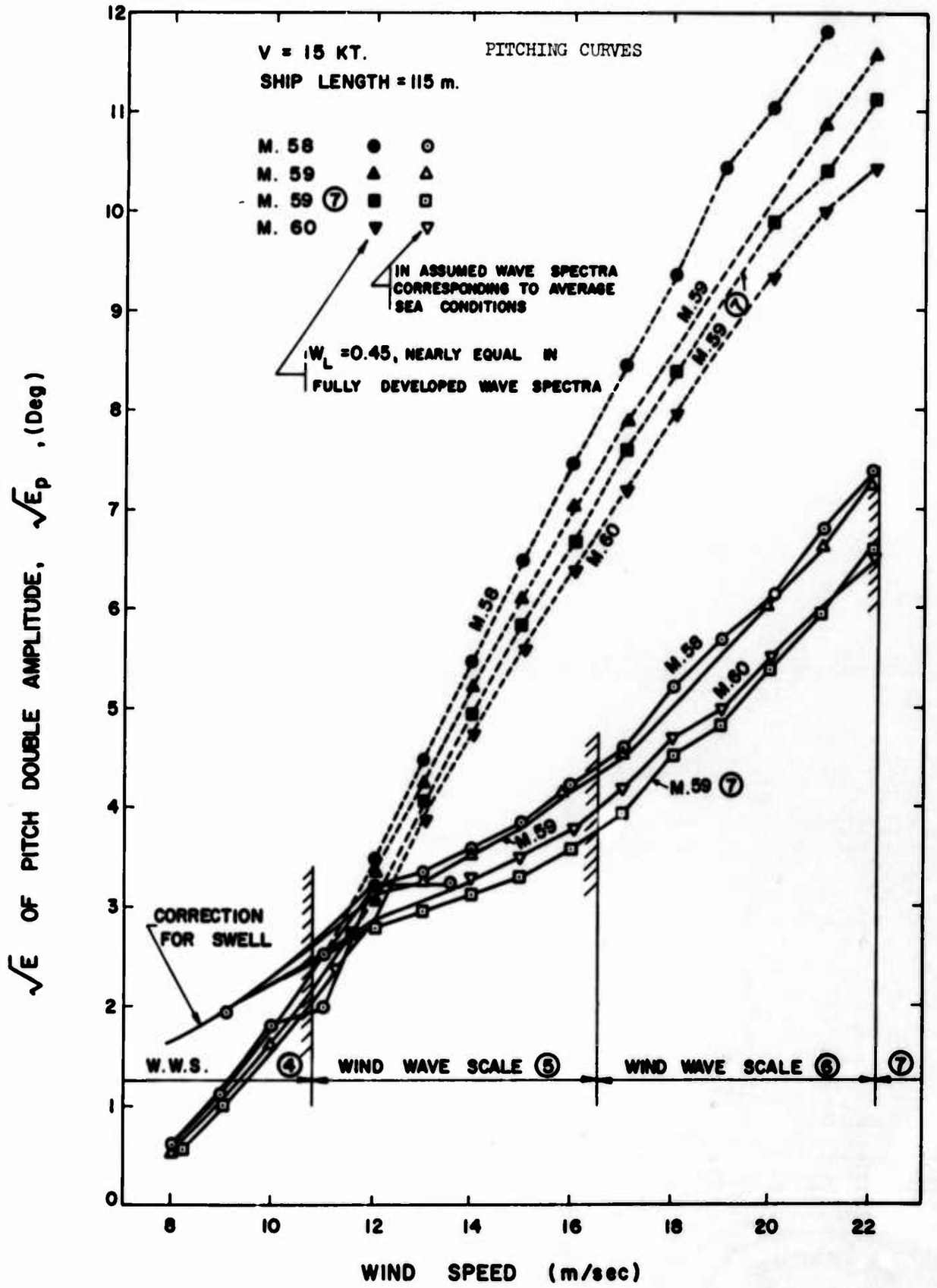

V = 15 KT.
SHIP LENGTH = 115 m.
PITCHING CURVES
M. 58
M. 59
M. 59 ⑦
M. 60
IN ASSUMED WAVE SPECTRA CORRESPONDING TO AVERAGE SEA CONDITIONS
W_L =0.45, NEARLY EQUAL IN FULLY DEVELOPED WAVE SPECTRA
CORRECTION FOR SWELL
W.W.S.
④
WIND WAVE SCALE ⑤
WIND WAVE SCALE ⑥
⑦
$\sqrt{E}$ OF PITCH DOUBLE AMPLITUDE, $\sqrt{E_p}$, (Deg)
WIND SPEED (m/sec)

Figure A-6

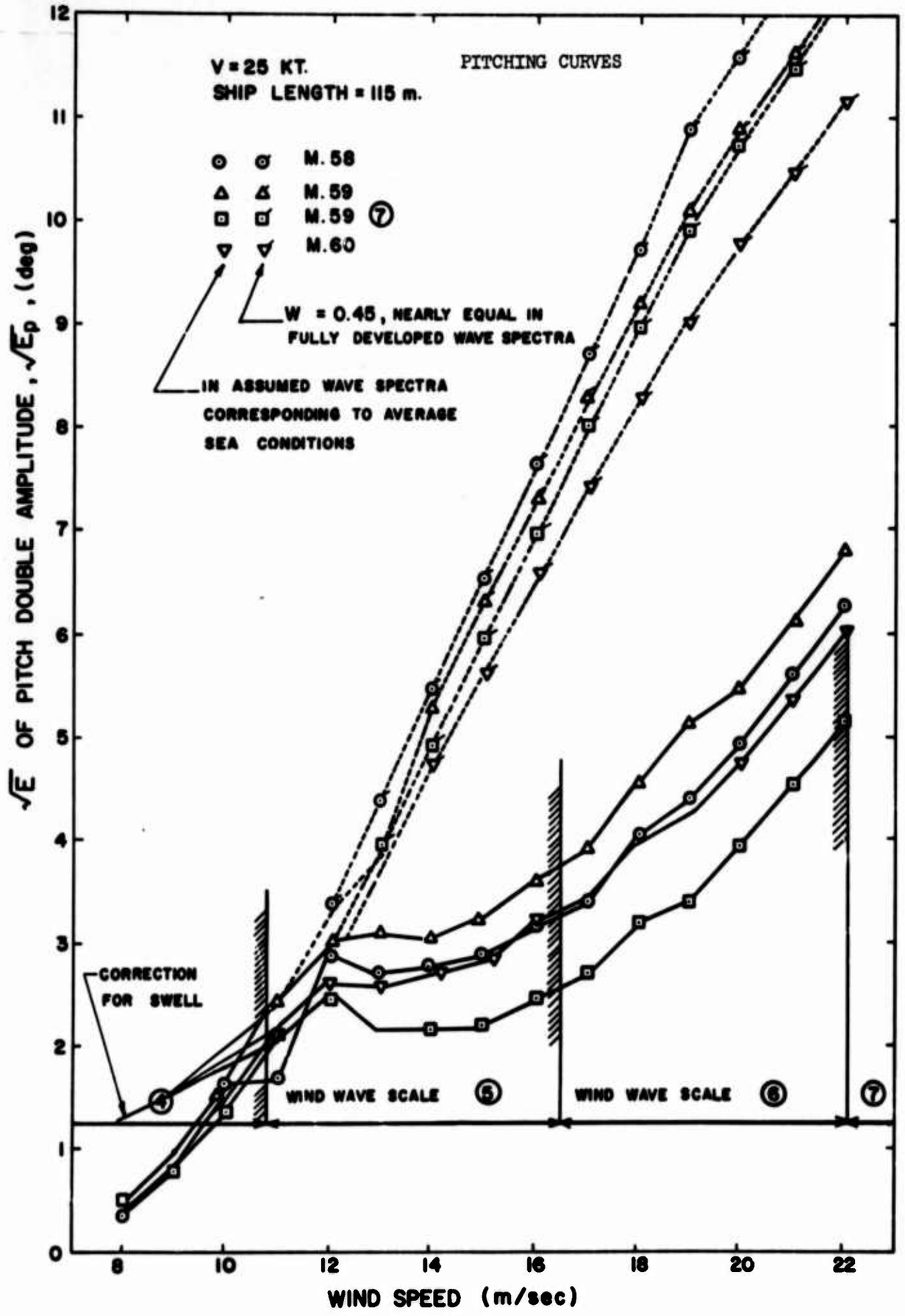

V = 25 KT.
SHIP LENGTH = 115 m.
PITCHING CURVES
M. 58
M. 59
M. 59 ⑦
M. 60
W = 0.45, NEARLY EQUAL IN FULLY DEVELOPED WAVE SPECTRA
IN ASSUMED WAVE SPECTRA CORRESPONDING TO AVERAGE SEA CONDITIONS
CORRECTION FOR SWELL
WIND WAVE SCALE ⑤
WIND WAVE SCALE ⑥
⑦
√E OF PITCH DOUBLE AMPLITUDE, √Ep, (deg)
WIND SPEED (m/sec)
0
1
2
3
4
5
6
7
8
9
10
11
12
8
10
12
14
16
18
20
22

Figure A-7

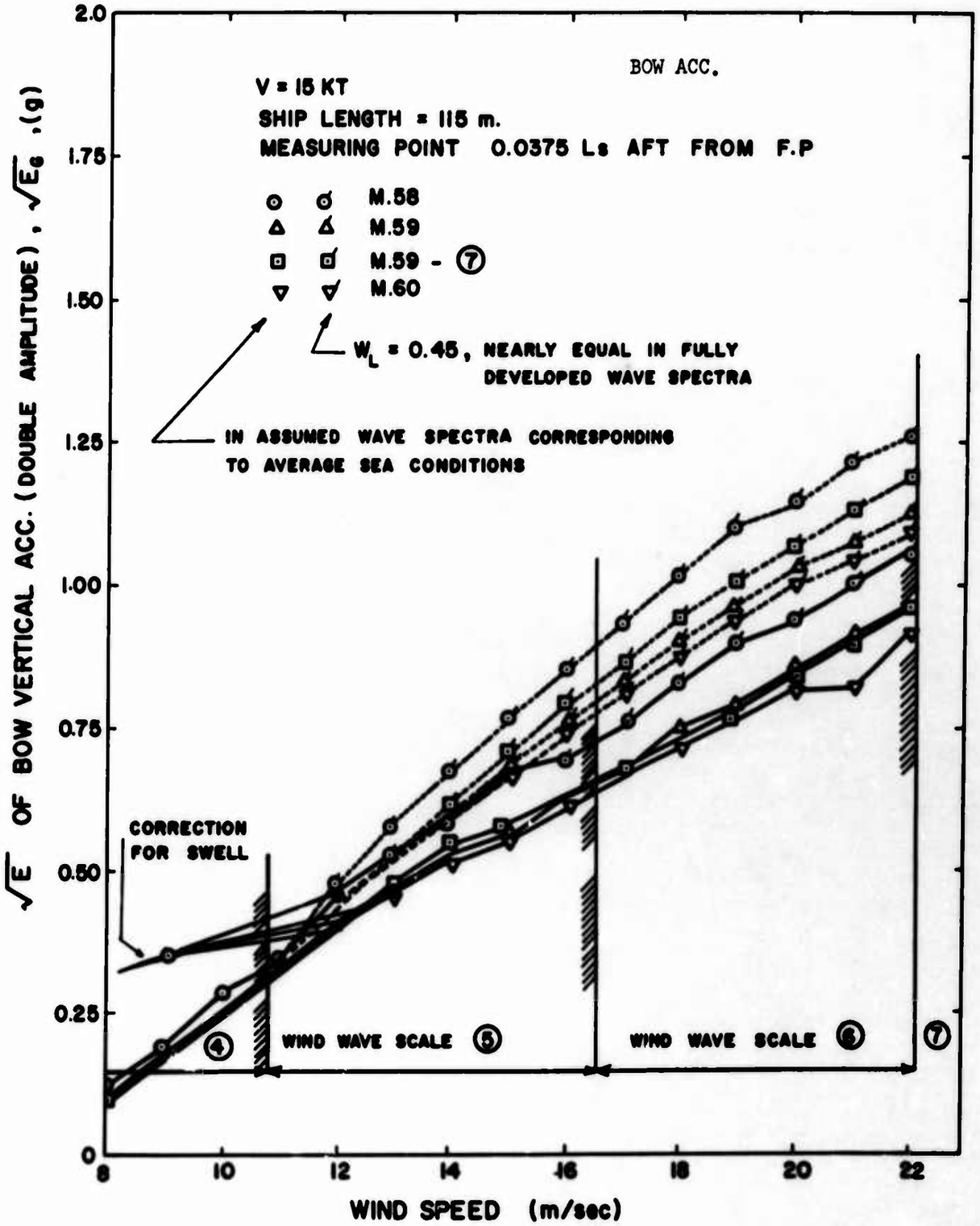

BOW ACC.
V = 15 KT
SHIP LENGTH = 115 m.
MEASURING POINT 0.0375 Ls AFT FROM F.P
M.58
M.59
M.59 - ⑦
M.60
W_L = 0.45, NEARLY EQUAL IN FULLY DEVELOPED WAVE SPECTRA
IN ASSUMED WAVE SPECTRA CORRESPONDING TO AVERAGE SEA CONDITIONS
CORRECTION FOR SWELL
④
WIND WAVE SCALE ⑤
WIND WAVE SCALE ⑥
⑦
$\sqrt{E}$ OF BOW VERTICAL ACC. (DOUBLE AMPLITUDE), $\sqrt{E_6}$, (g)
WIND SPEED (m/sec)
2.0
1.75
1.50
1.25
1.00
0.75
0.50
0.25
0
8
10
12
14
16
18
20
22

Figure A-8

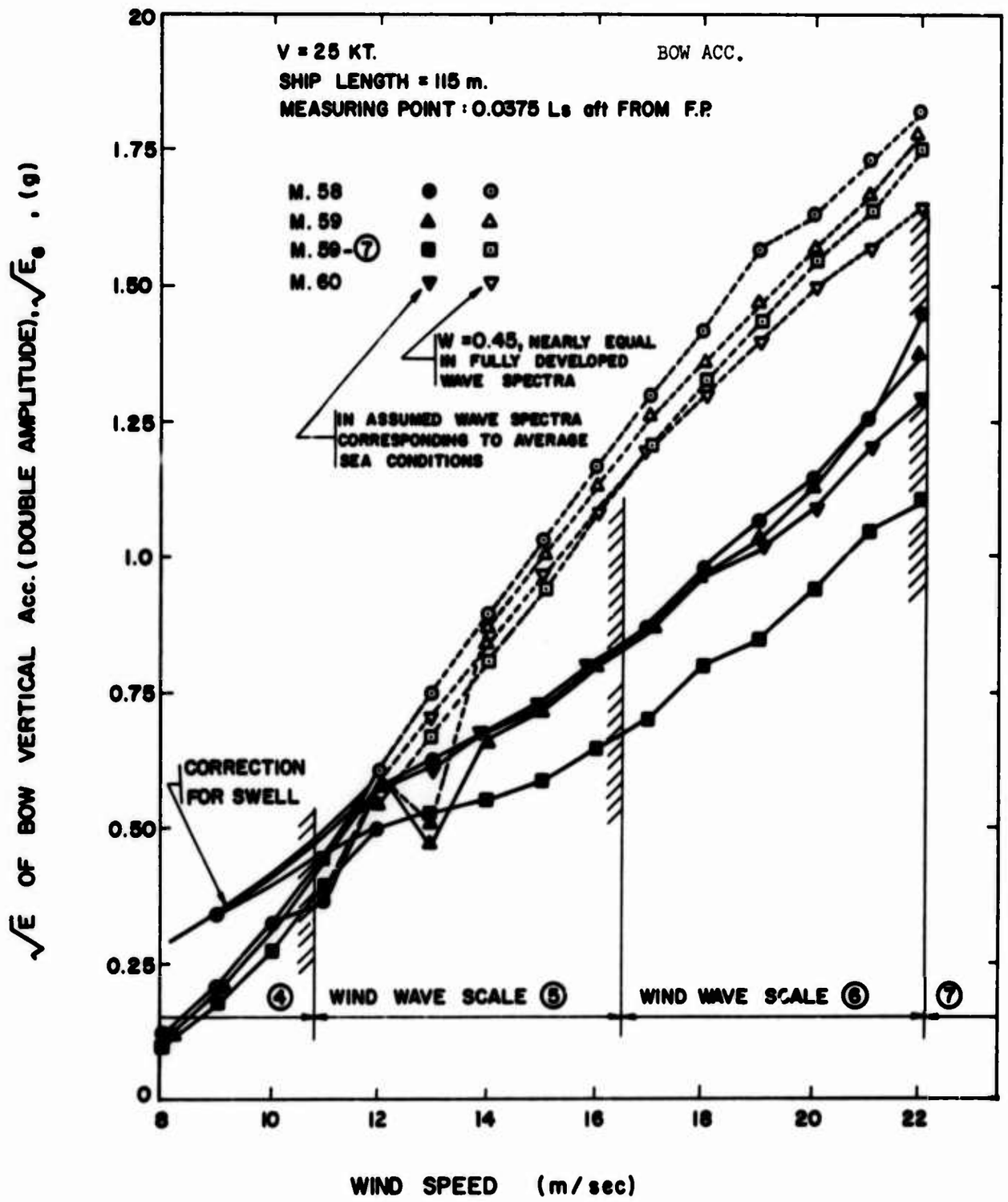

V = 25 KT.
BOW ACC.
SHIP LENGTH = 115 m.
MEASURING POINT : 0.0375 Ls aft FROM F.P.
M. 58
M. 59
M. 59-⑦
M. 60
W =0.45, NEARLY EQUAL IN FULLY DEVELOPED WAVE SPECTRA
IN ASSUMED WAVE SPECTRA CORRESPONDING TO AVERAGE SEA CONDITIONS
CORRECTION FOR SWELL
④ WIND WAVE SCALE ⑤
WIND WAVE SCALE ⑥
⑦
√E OF BOW VERTICAL Acc. (DOUBLE AMPLITUDE), √E₀ , (g)
WIND SPEED (m/sec)
0
0.25
0.50
0.75
1.0
1.25
1.50
1.75
20
8
10
12
14
16
18
20
22

Figure A-9

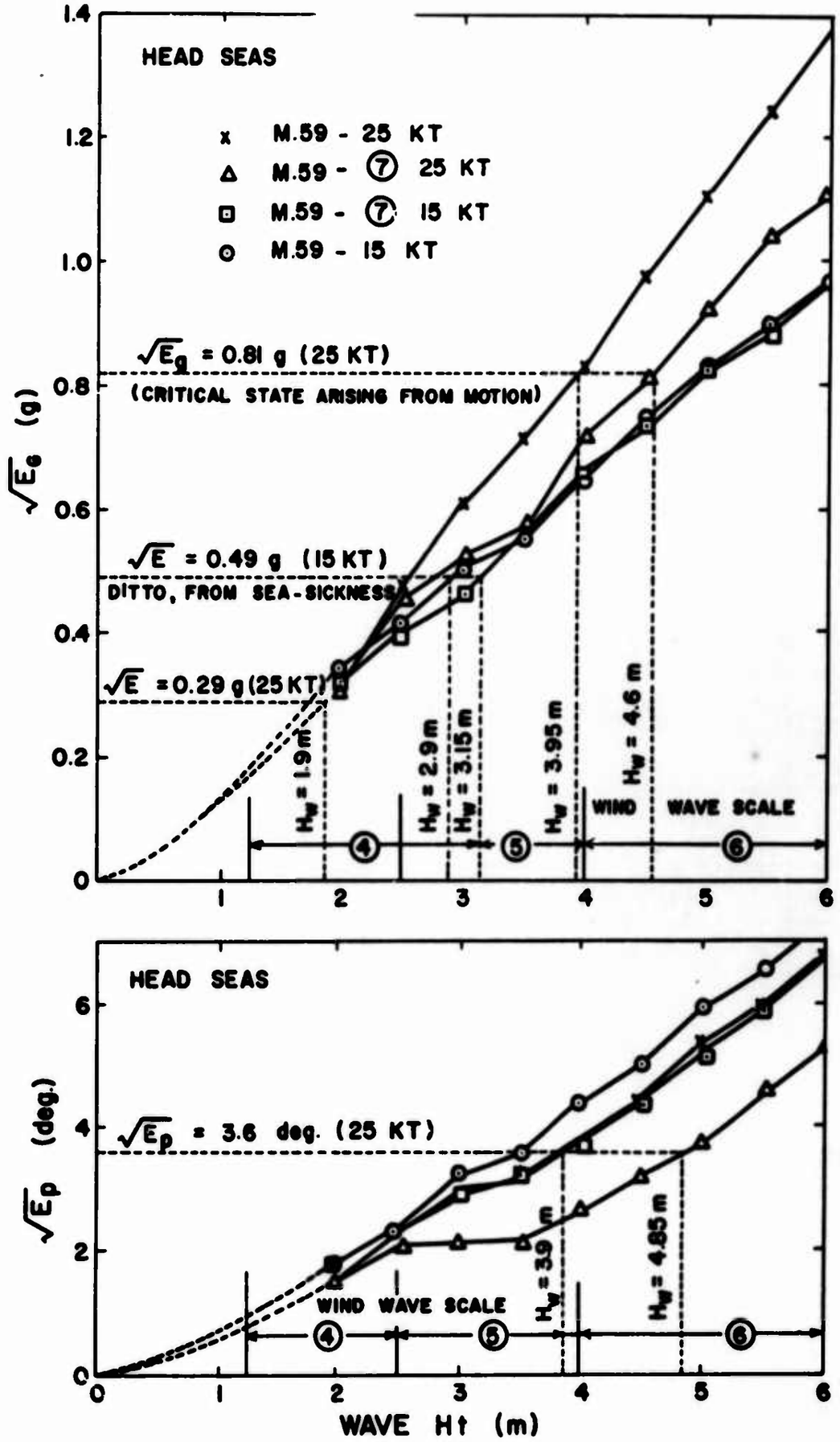

HEAD SEAS
x M.59 - 25 KT
△ M.59 - ⑦ 25 KT
⊡ M.59 - ⑦ 15 KT
⊙ M.59 - 15 KT
√Eg = 0.81 g (25 KT)
(CRITICAL STATE ARISING FROM MOTION)
√E = 0.49 g (15 KT)
DITTO, FROM SEA-SICKNESS
√E = 0.29 g (25 KT)
Hw = 1.9 m
Hw = 2.9 m
Hw = 3.15 m
Hw = 3.95 m
Hw = 4.6 m
WIND WAVE SCALE
④
⑤
⑥
√Eθ (g)
HEAD SEAS
√Ep = 3.6 deg. (25 KT)
Hw = 3.9 m
Hw = 4.85 m
WIND WAVE SCALE
√Ep (deg.)
WAVE Ht (m)

Figure A-10

The results show that the large bow bulb evidently has the effect of moderating ship motions. For instance, the upper limit of the navigable wave heights of M.59-7 is higher by about 1 meter than that of M.59 in pitching in the case of a ship speed of 25 knots (see Figure A-10). But, in long waves as in the fully developed Neumann waves at high wind velocity that effect is somewhat decreased (see Figures A-6 and A-9).

The author's published paper related to the problem in this Appendix D: Reference 6.

APPENDIX E

SPEED DECREASE IN WAVES

The thrust increase in irregular waves is obtained by the Maruo, Tasaki and Taniguchi's method. Figures A-11 and A-12 show the thrust increase in the partially developed average sea states and in the nearly fully developed Neumann waves. These values are calculated by the same wave spectrum that is used in Appendix D. Then considering the wind resistances, the speed decreases in those irregular waves are estimated as shown in Figures A-13 and A-14.

In this paper, the speed decrease in waves indicates the differences between speed A and B, where A is the ship speed in still water, while B is the speed which is maintainable in the actual sea states at the same powering rate.

Generally, it is shown that the thrust increase and speed decrease of the ship with a large bulb navigating in rough seas are larger than that of the basic hull alone, and that trend is especially remarkable in the nearly fully developed sea states, or in long waves. Meanwhile, considering the cases to be held a certain power in waves as well as in still water, the supportable ship speed of the hull with a large bulb in waves is not greatly different compared with that of the basic hull alone, especially in short waves or in average sea states. Because the needed power of the hull with a large bulb in still water is generally less than that of the basic hull, the total power of the hull with a bulb in waves is nearly equal to that without a bulb, in spite of the fact that the increase in power due to waves is rather large.(2)

The author's published paper related to the problem in this Appendix E: Reference 7.

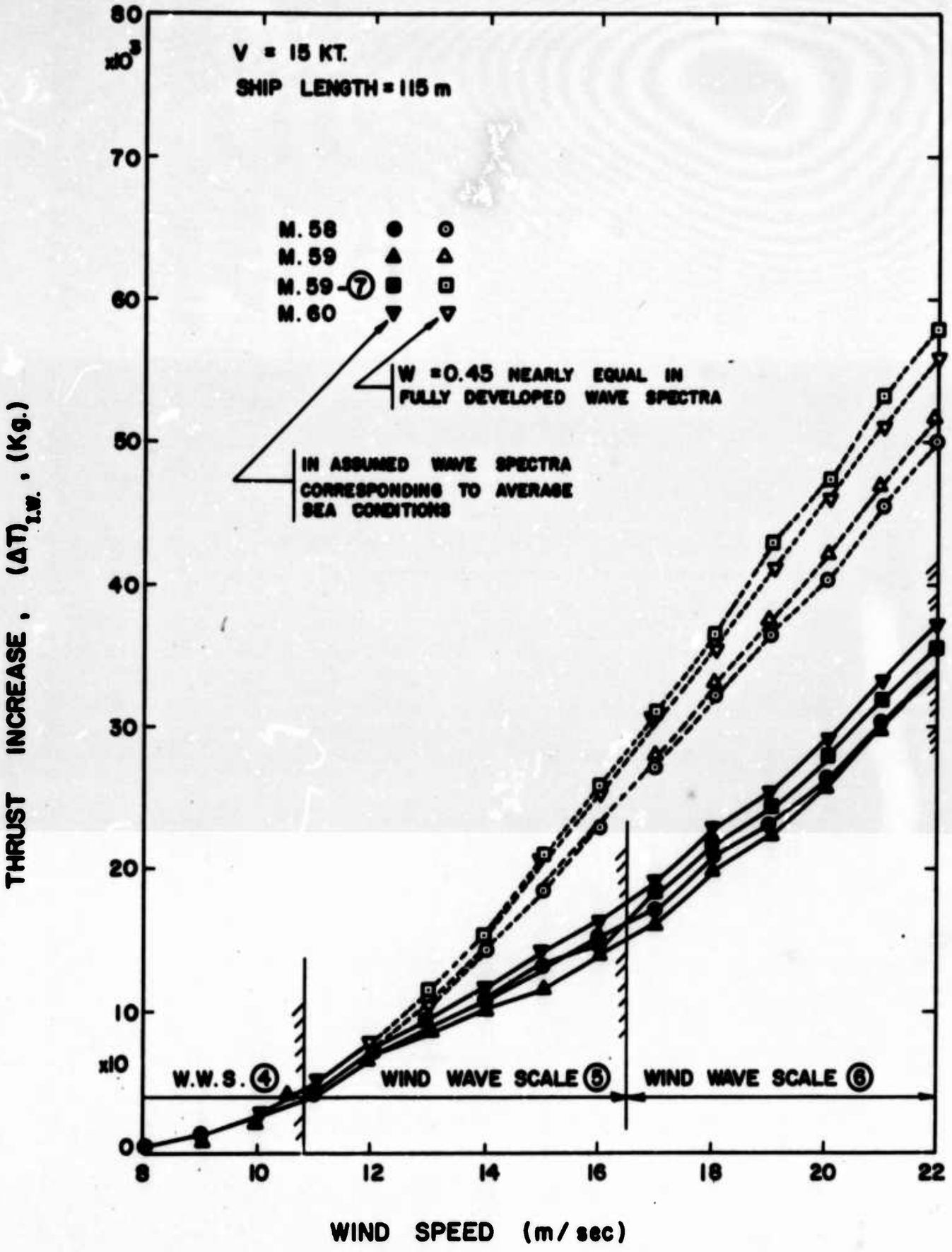


Figure A-11. Thrust Increase.

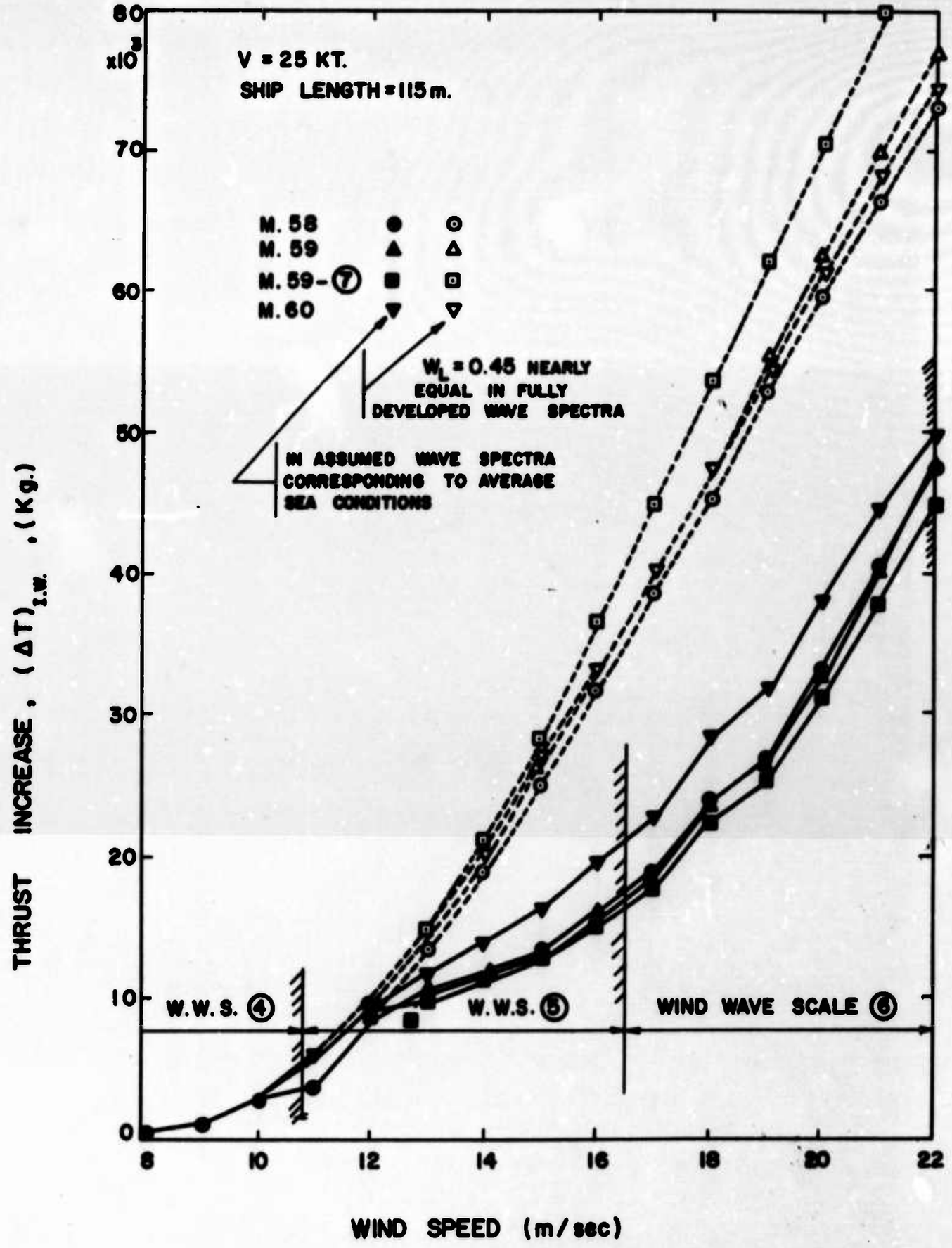


Figure A-12. Thrust Increase.

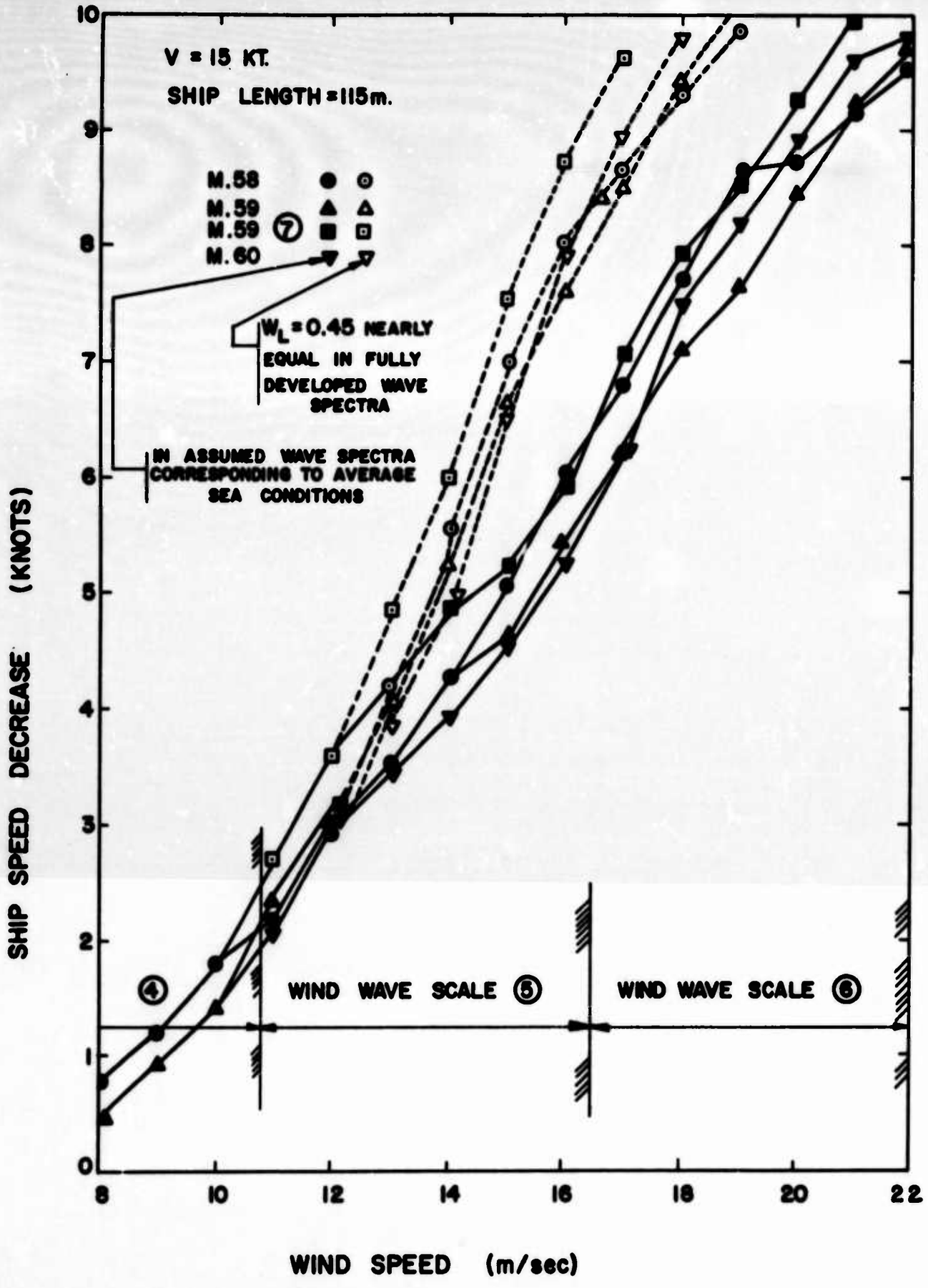


Figure A-13. Speed Decrease
(based on Waves and Winds)

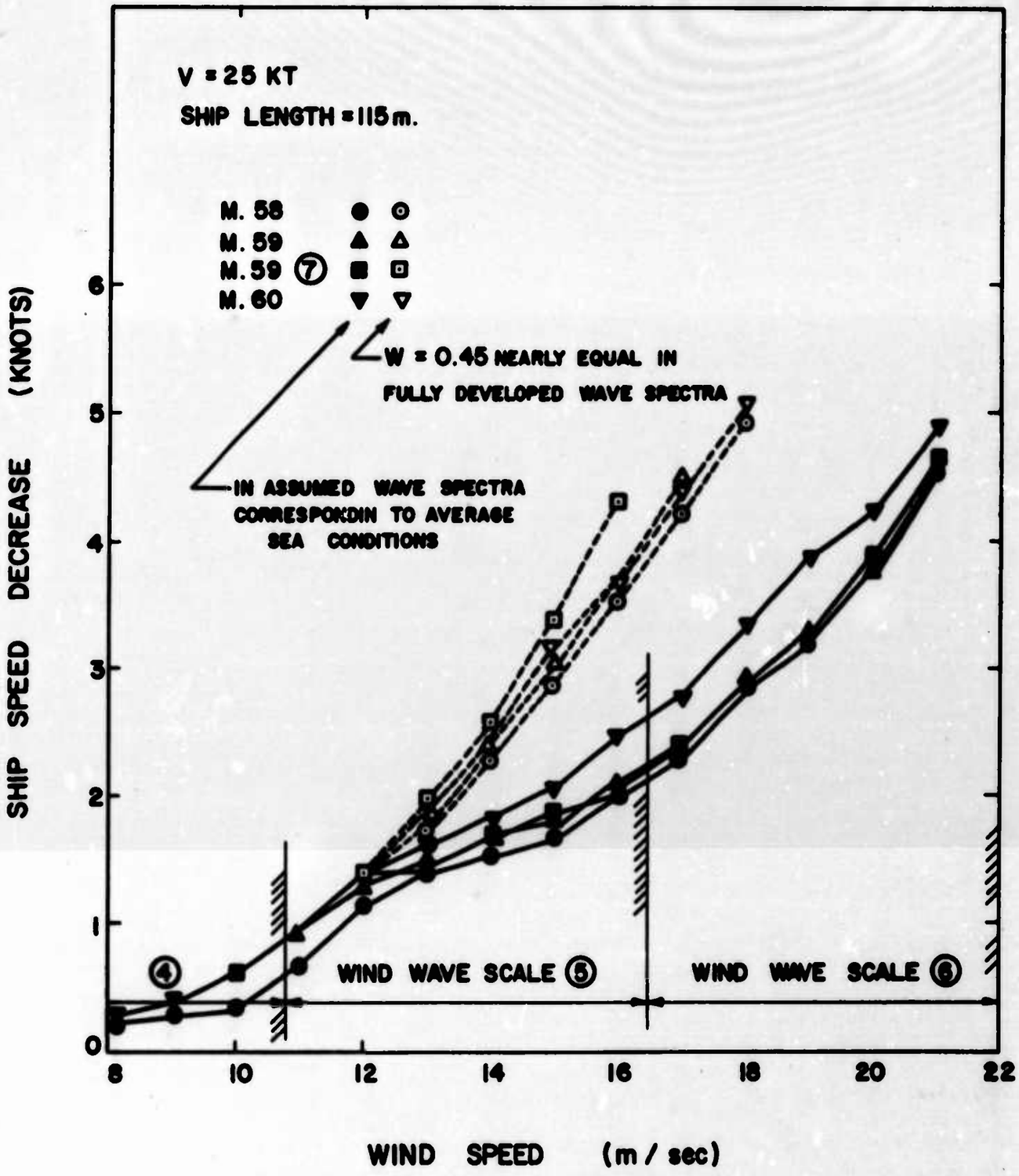


Figure A-14. Speed Decrease
(based on Waves and Winds)

APPENDIX F

TURNING CIRCLE

The author carried out the self-propulsion tests by radio controlled 8 meter models with and without a large bulb, for the study of turning circle as well as for the investigation of the wave pattern.

The results of steady turning tests are shown in Figure A-15. The larger either the turning radius ratio L/R or the non-dimensional turning angular velocity, the better the maneuverability. Actually, the points farther from the origin of Figure A-15 indicate good performances, departing from the well-known two-dimentional relationship more and more. In these tests the same twin-rudders and twin-propellers are used in each model.

The data in this figure should not be used quantitatively without making appropriate corrections to take into consideration the different characteristics of the propulsive units of ship and model.

The author's unpublished report related to the problem in this Appendix F: Reference 8, where a 16 mm. cine-film (colored) is available.

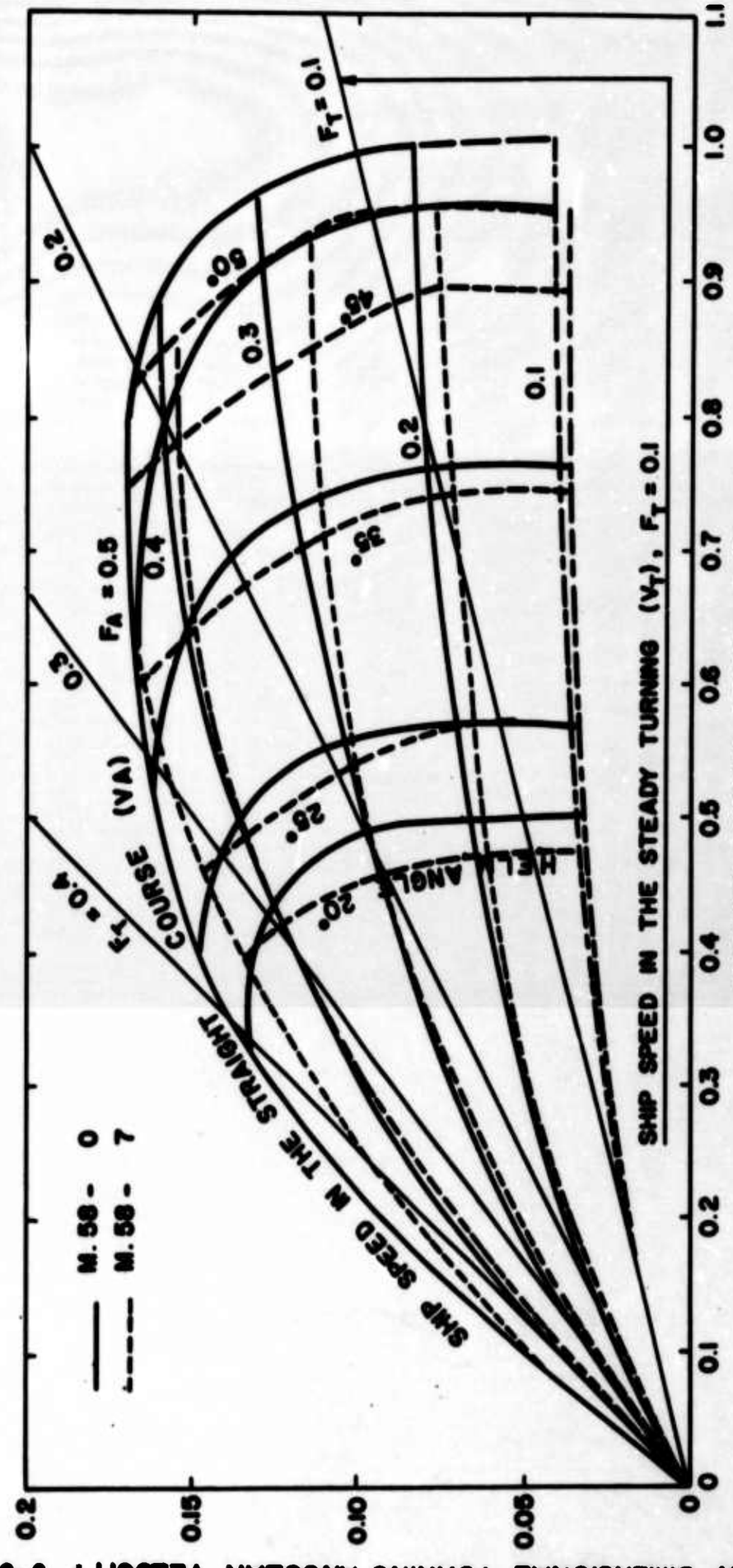

NON DIMENSIONAL TURNING ANGULAR VELOCITY $\dot{\theta}=\dot{\theta}\sqrt{L/g}$
0.2
0.15
0.10
0.05
0
0.1
0.2
0.3
0.4
0.5
0.6
0.7
0.8
0.9
1.0
1.1
TURNING RADIUS RATIO, L/R
SHIP SPEED IN THE STEADY TURNING (V_T), F_T = 0.1
M.58 - 0
M.58 - 7
SHIP SPEED IN THE STRAIGHT COURSE (VA)
F_A = 0.5
F_T = 0.1
HELM ANGLE
80°
45°
35°
25°
20°
0.1
0.2
0.3
0.4

Figure A-15

INTERACTION BETWEEN SHIP WAVES AND BOUNDARY LAYER

T. Yao-tsu Wu

Kármán Laboratory,
California Institute of Technology

INTERACTION BETWEEN SHIP WAVES AND BOUNDARY LAYER

1. Introduction

The well-known Froude scaling method of analyzing ship model resistance data presupposes that the total resistance experienced by a ship may be decomposed into two parts: the viscous component $D_v(Re)$ which depends on the Reynolds number, and the residual part $D_w(Fr)$ which depends on the Froude number. This was really an ingenious suggestion, considering the state-of-the-arts and technical information available at the time this scaling was introduced (more than 90 years ago). However, the actual difficulties encountered in practical applications of the scaling have revealed some ever-perplexing nature of this problem.

The purpose of the present note is to make a preliminary investigation on the interaction between ship waves and boundary layer by first evaluating, under some simplifying assumptions, the boundary layer in the presence of gravity waves at the free water surface. It seems that this approach to the problem is perhaps the only means of making estimates of this interaction phenomenon. In order to facilitate the analysis involved the approximate method of Kármán's momentum-integral equation is applied, together with making use of some recent developments in the boundary layer theory. With the boundary layer determined, one is enabled to deduce the skin friction on one hand, and to attain an equivalent ship form for the external potential flow on the other. For simplicity, several physical effects which may be pertinent to this problem have not been taken into consideration; they include (i) flow separation and eddy making, (ii) the change in wetted surface area and ability for model to trim, and (iii) the surface roughness.

The subject of the present study is stimulated by the activities connected with the "International Seminar on Theoretical Wave Resistance." The author regrets not being able to examine the results more fully and hence bring this study to a more complete form for presentation. Consequently, only very preliminary results are presented here.

2. General Formulation and Approach

A solid body moving through a real fluid, with or without a free surface, experiences a resistance. This resistance can be analyzed in several ways. First, by considering the local flow field near the body, the total resistance arises as the entire contribution of the surface forces exerted on the body by the fluid in contact with the body surface. The point of view may also be given to the total momentum of the flow "in the large" on the basis of the momentum theory. The principle of this approach is that the difference between the total momentum flux of fluid ahead and behind the body, including the momentum transmitted in the form of surface waves, is equal to the total resistance. Another quite different form of analysis is obtained by applying the principle of conservation of energy to the flow and by examining the way in which the work done by the resistance is dissipated and radiated. It may be remarked here that the problem is further complicated by the presence of free surfaces.

From the first approach the total force $\vec{R}$ acting on the body may therefore be evaluated from the surface integral

$$\vec{R} = \int_S (-p\vec{n} + \tau\vec{n})\, dS = \vec{R}_p + \vec{R}_f \qquad (1)$$

where p is the pressure, $\vec{n}$ the unit outward normal to the wetted body surface S, and τ is the viscous stress tensor so that τ operating on $\vec{n}$ yields the viscous stress at S. It can be shown that in the flow of an incompressible viscous fluid with no-slip boundary condition, with motion not necessarily steady, the viscous stress $\tau\vec{n}$ at the solid surface is perpendicular to both the vorticity vector and the surface normal $\vec{n}$ and hence is a shear force in nature (to be exact, $\vec{\tau n} = \mu$ (curl q) xn, μ being the viscosity coefficient). In this sense, the total resistance $\vec{R}$ may be said to consist of the skin friction $\vec{R}_f$ (the surface integral of the shear stress $\tau\vec{n}$) and the pressure resistance $\vec{R}_p$ (the surface integral of the normal stress $-p\vec{n}$). For flows of infinite extent, the pressure drag $\vec{R}_p$, which vanishes in inviscid flow, is due to the pressure distribution being modified from the potential flow by the presence of the boundary layer, and is usually called in this case the form drag. In the presence of a free surface, however, surface waves (such as gravity and capillary waves) may now exist to further modify the pressure distribution; in this case $\vec{R}_p$ includes therefore not only the form drag of the viscous origin but also the resistance which is intrinsically due to

wave-making. It may be said that the concept of wave resistance arises only when the far-field is brought into the picture; otherwise both the viscous form drag and wave resistance are contained in the surface integral of $(-p\vec{n})$. The interesting feature of the surface wave and boundary layer interaction is that it occurs as a whole entirety. The existence of the boundary layer affects the external potential flow and its wave system; the waves in turn influence the pressure distribution in the boundary layer and hence also the skin-friction. Therefore, the shape and structure of the boundary layer in the presence of waves must be determined with the interaction taken into account.

The problem is somewhat more precisely stated in terms of the dimensionless flow parameters. Introducing the nondimensional quantities

$$x_i^* = x_i/\ell, \quad q = q/U_o, \quad p^* = p/(\tfrac{1}{2}\rho U_o^2), \quad \tau^* = \tau/(\tfrac{1}{2}\rho U_o^2), \quad \vec{F}_x = \vec{F}/g \ , \tag{2}$$

where ℓ is a characteristic length and g is the gravitational constant, we find that with free surfaces, there naturally appear in the problem two flow parameters: the Froude number Fr and Reynolds number Re,

$$Fr = U_o/\sqrt{g\ell} \ , \qquad Re = U_o\ell/\nu \tag{3}$$

Writing (1) in the nondimensional form:

$$\vec{R}_* = \vec{R}/(\tfrac{1}{2}\rho U_o^2 S_o) = \int_{S_*} (-p_*\vec{n} + \frac{1}{Re}\tau_*\vec{n})\, dS_* \tag{4}$$

where $S_* = S/S_o$, S_o being some representative area of the body, we note that p_*, τ_* and hence also $\vec{R}_*$ will be functions of Fr and Re. When the flow is assumed inviscid, p_* is a function of Fr alone; and if the wave effect is insignificant, then τ_* depends on Re only. The interaction comes from those parts of p_* and τ_* that depend on Re and Fr both.

From the viewpoint of conservation of momentum and energy applied to a control surface enclosing the body, we note that the part of the resistance of the viscous origin (profile drag) will eventually appear in the form of a momentum defficiency as a result of viscous dissipation and diffusion, a process which is virtually confined in the boundary layer and the viscous wake. The asymptotic

cross section of the wake increases with downstream distance x like $x^{1/2}$ and $x^{2/3}$ respectively for the two- and three-dimensional case. Hence in accordance with the momentum consideration, the perturbation velocity must fall off like $x^{-1/2}$ and $x^{-2/3}$, respectively. This basic feature of the wake is expected not to be altered by the presence of free surface. On the other hand, the surface waves in steady motion are radiated to infinity in a wedge-like sector (for gravity waves in water, the included angle of the sector is about $2 \sin^{-1}(1/3)$. Since at a large distance r from the body the wave energy (proportional to amplitude squared) is propagated across a circular arc of length linear in r at the rate of the local group velocity, it follows that the wave amplitude, and hence also the perturbation velocity, falls off like $r^{-1/2}$ (except in a narrow parabolic ridge). It may be remarked here that if the wave resistance is determined from the waves in this sector but outside the wake, then it already contains a part (not the whole lot) of the interaction and is not free from the viscous effect.

The general approach by which the approximate method of solution is sought may be stated as follows. We consider as a qualitative category the class of surface piercing bodies which are sufficiently thin in the dimensions lateral to the free stream and sufficiently deep in draft, and the flow being further free from separation. Let the equation of the solid surface be given by

$$y = \pm \eta_o(x,z) \qquad \text{for} \qquad (x,z) \text{ in an area S,} \qquad (5)$$

in a Cartesian coordinate system with the x-axis directed along the free stream, the z-axis pointing vertically upward. The ship is said to be thin when $|\partial\eta/\partial x|$ and $|\partial\eta/\partial z|$ are everywhere small, the length-beam ratio large and the ratio of beam-to-draft moderately small. When the viscous effect is considered for a range of Re of interest, let the displacement thickness of the boundary layer over the solid surface S as well as in the wake region be denoted by $\delta_*(x,z)$, which is to be determined in the presence of the surface waves. On the basis of the classical boundary layer theory of Prandtl, we may assume that the flow exterior to the displacement thickness is inviscid and remains to possess a velocity potential. We use the displacement thickness since physically it is the distance by which the streamlines of external potential flow is displaced outwards as a consequence of the velocity reduction in the boundary layer. Thus the equivalent boundary for the external potential flow is now

$$y_e = \pm \eta(x,z) = \pm [\eta_o(x,z) + \delta_*(x,z)] \quad \text{for } (x,z) \text{ in S'} \quad (6)$$

where S' is the area in the x-z plane over which δ_* is appreciable (approximately the original area S and its extension into a part of the wake). The velocity potential of the external flow past this equivalent body y_o can be obtained by applying the thin ship theory of Michell (1898) or by using Havelock's analysis (1932) or by other methods, the solution may be denoted as $q = U_o + \text{grad}\varphi$,

$$\varphi(x,y,z) = [\delta_*(x,z)] \qquad (7)$$

the above form emphasizes φ being a "functional" of the unknown argument function δ_* over the entire surface S'. Such solution expressed in the Michell form or Havelock form is well known (e.g. see Wehausen 1960) and hence will not be reproduced here. From this solution one readily deduces the stream-wise velocity at the equivalent boundary of the potential flow, say $U(x,z)$ for (x,z) in S'. From the Bernoulli equation of the external flow, one thereby derives the pressure distribution

$$\frac{1}{\rho}\frac{\partial p}{\tau x} = - U \frac{\partial U}{\partial x} \quad , \qquad (8)$$

the value of which is needed for the calculation of the boundary layer. An alternative (and better) means of providing this information is by experimental measurements of the pressure distribution over the actual body surface; this latter method is applicable even when separation takes place.

In order to take into account in the boundary layer calculation the pressure distribution due to the body curvature and the surface waves, we apply the approximate method of Kármán-Pohlhausen momentum-integral equation which greatly simplifies the analysis. The accuracy of the result is expected to be adequate, though somewhat limited. Another advantage of using this method is that its adaptability to both the laminar and turbulent boundary layer and that the analyses in these two cases are closely analogous to each other. Since the velocity $U(x,z)$ determined from the external flow depends on the unknown thickness δ_* over the entire range S' and since calculation of this same quantity δ_* from the boundary layer solution depends on the local pressure distribution $U(x,z)$, we are led to a functional integral equation for δ_*. The integral equation, however, may be readily solved by iteration, starting with the wave-free solution as the zeroth order iteration. Consequently the skin-friction under the influence of the gravity waves can be computed.

Furthermore, with δ_* so determined, the external wave field, and hence the wave resistance, can be calculated by the classical inviscid theory with the new and equivalent body surface.

3. The Effect of Gravity Waves on Boundary Layer and Skin Friction

A complete calculation of the boundary layer for a given body which moves in or beneath a water surface and produces gravity waves is generally so complicated that it cannot be carried out in practice. However, the problem becomes more tractable by applying the approximate method of the momentum-integral equation of von Kármán. The accuracy of the approximate solutions so obtained have been found reasonable and adequate in previous cases and may be expected to hold valid in the presence of water waves. Since the boundary layer equation is of the parabolic type, the flow at a given station bears no upstream influence. Consequently we may treat first the boundary layer over the solid surface, leaving the viscous wake for a later stage.

Following the usual notation in boundary layer theory (e.g. Schlichting (1960)) the coordinates (x,y) are taken to lie in a horizontal plane and to be directed along the mean stream and normal to the solid boundary respectively, the z-axis still vertically upward; (u, v, w) are the corresponding velocities in the boundary layer. The velocity at the edge of the boundary layer will be denoted by $U(x,z)$, and at upstream infinity, by U_o. We shall restrict ourselves to the case of steady incompressible flow and to such a class of body shapes and wave profile that the boundary layer in the presence of the water waves may still be regarded as quasi-two-dimensional. More precisely, we mean that the rate of change of the boundary layer flow with the depth of submergence will be neglected, and hence, in this sense the vertical distance z appears only as a parameter. The shearing stress at the wall responsible for the friction drag will be denoted by τ_o for both laminar and turbulent boundary layers, and for the laminar case

$$\tau_o = \mu(\partial u/\partial y)_{y=0} \qquad (9)$$

In addition to τ_o, the other important physical quantities pertaining to the boundary layer theory are the displacement thickness δ_* and the momentum thickness θ, defined by

$$\delta_* = \int_o^{y_1} (1 - \frac{u}{U})dy, \qquad \theta = \int_o^{y_1} \frac{u}{U}(1 - \frac{u}{U})dy, \qquad (10)$$

where y_1 is taken to be greater than the boundary layer thickness $\delta(x,z)$ which is itself a rather fortuitous quantity. With this notation the momentum-integral equation for two-dimensional incompressible boundary layers may be written (see, e.g. Schlichting (1960))

$$\frac{\tau_o}{\rho U^2} = \frac{d\theta}{dx} + (2\theta + \delta_*)\frac{1}{U}\frac{dU}{dx} \tag{11}$$

which allows us to calculate δ_*, θ and τ_o for both the laminar and turbulent boundary layers. These two cases will be treated separately in the following.

3A. Laminar Boundary Layer

In order to take into account the no-slip condition at the wall, the continuity at the edge of boundary layer, the effect of pressure gradient, as well as the determination of separation, we assume, following K. Pohlhausen (1921), the velocity function in terms of the dimensionless distance from the wall $\eta = y/\delta(x,z)$ as

$$\frac{u}{U} = F(\eta) + \Lambda(x,z)\, G(\eta) \tag{12a}$$

where

$$F(\eta) = 1 - (1-\eta)^3(1+\eta), \quad G(\eta) = \frac{1}{6}\eta\,(1-\eta)^3, \tag{12b}$$

and Λ is a "shape factor" defined by

$$\Lambda = \frac{\delta^2}{\nu}\frac{dU}{dx}\left(= -\frac{\delta}{\mu U/\delta}\frac{dp}{dx}\right) \tag{12c}$$

which can be regarded as the ratio of the pressure to viscous shear stress.

Consequently the velocity profiles form a one-parameter family of approximate solutions which satisfy the boundary conditions

$$u = 0, \quad \nu\frac{\partial^2 u}{\partial y^2} = \frac{1}{\rho}\frac{\partial p}{\partial x} = -U\frac{dU}{dx} \quad \text{at} \quad y = 0,$$

$$u = U, \quad \frac{\partial u}{\partial y} = 0, \quad \frac{\partial^2 u}{\partial y^2} = 0 \quad \text{at} \quad y = \delta. \tag{13}$$

These conditions are of particular importance to include the physical effects encountered and are all satisfied by the exact solution. Substituting (12) in (9) - (10), we find that

$$\frac{\delta^*}{\delta} = \frac{3}{10} - \frac{\Lambda}{120}, \qquad \frac{\theta}{\delta} = \frac{37}{315} - \frac{\Lambda}{945} - \frac{\Lambda^2}{9072}, \qquad \frac{\tau_o \delta}{\mu U} = 2 + \frac{\Lambda}{6} \tag{14}$$

The profile at separation occurs at $(\partial u/\partial y)_o = \tau_o/\mu = 0$, or at $\Lambda = -12$. In order that u does not have a maximum value greater than U in the boundary layer, the range of Λ with physical significance is $-12 < \Lambda < 12$. The stagnation points corresponds to $\Lambda = 7.052$.*

Following Holstein and Bohlen (1951), it is convenient to introduce a second shape factor

$$K = Z \frac{dU}{dx}, \qquad Z = \frac{\theta^2}{\nu} \tag{15}$$

so the shape factors Λ and K are related by the universal function

$$\frac{K}{\Lambda} = \left(\frac{\theta}{\delta}\right)^2 = \left(\frac{37}{315} - \frac{\Lambda}{945} - \frac{\Lambda^2}{9072}\right)^2 . \tag{16}$$

By making use of (14) the momentum-integral equation (11) can be expressed in terms of Z, K, U in the highly condensed form

$$\frac{dz}{dx} = \frac{1}{U} F(K); \qquad K = Z \frac{dU}{dx}, \tag{17}$$

where F(K) is the following universal function

$$F(K) = 4\left(\frac{37}{315} - \frac{\Lambda}{945} - \frac{\Lambda^2}{9072}\right)\left[1 - \frac{58}{315}\Lambda + \left(\frac{1}{240} + \frac{1}{945}\right)\Lambda^2 + \frac{\Lambda^3}{9072}\right] \tag{18}$$

As pointed out by Walz (1941), the function F(K) can be approximated very closely by the linear function

$$F(K) = a - bK; \tag{19}$$

with a = 0.470 and b = 6 the approximation is particularly close between the stagnation point (K = 0.0770*) and the point of maximum velocity

*At stagnation point U = 0, hence from (17) $F(K_o) = 0$ at this point since dz/dx does not vanish at the same time. Now the zero of F(K) is K_o = 0.0770, corresponding to $\Lambda = 7.052$.

(K = 0). For simplicity the constants a, b will be formally retained until their numerical values are needed. With the approximation (19) the original equation (17) is reduced to a simple quadrature, giving

$$\frac{\Theta^2}{\nu} = aU^{-b}(x,z) \int_0^x [U(\xi,z)]^{b-1} \, d\xi \, . \qquad (20)$$

We have thus seen that by using the momentum-integral approximation and the assumption of replacing F(K) by a linear function of K we are able to curtail altogether the complicated computation of the boundary layer and finally obtain the momentum thickness Θ in a simple analytical form containing only the velocity U(x,z) at the outer edge of the boundary layer and the universal constants a and b.

In case the disturbance due to the solid body may be considered small, such as the conventional thin ships, we may write in general

$$U(x,z) = U_o[1 + u_1(x,z)], \quad |u_1| \ll 1, \qquad (21)$$

here $u_1(x,z)$ stands for the nondimensional perturbation velocity with respect to U_o. Substituting (21) in (20), we have

$$\frac{U_o\Theta^2}{\nu} = a \left\{x - bxu_1(x,z) + (b-1) \int_0^x u_1(\xi,z)d\xi + O(|u_1|^2)\right\} \qquad (22)$$

for a point (x,z) on the solid surface. From (15) and (22) we deduce the shape factor K as

$$K = \frac{U_o\Theta^2}{\nu} \frac{\partial u_1}{\partial x} = a \frac{\partial u_1}{\partial x} \left\{x - bxu\,(x,z) + (b-1) \int_0^x u_1(\xi,z)d\xi + O(u_1^2)\right\} \qquad (23)$$

Obviously K is a small quantity of first order in u_1. Expanding for the case of small disturbances, we obtain from (16) and (14) that

$$K = \left(\frac{37}{315}\right)^2 \Lambda \, [1 - 0.009\Lambda + O(\Lambda^2)] \, , \qquad (24)$$

$$\delta_*/\nu = 2.55 \, [1 - 0.0188\Lambda + O(\Lambda^2)] = 2.55 \, [1 - 1.36K + O(K^2)]. \qquad (25)$$

Combining (22) - (25), we readily obtain the displacement thickness as

$$\delta_* = 2.55\sqrt{\frac{\nu x}{U_o}}\left\{1 - (1.36)a\frac{\partial u_1}{\partial x} - \frac{b}{2}u_1 + \frac{b-1}{\partial x}\int_o^x u_1(\xi,z)d\xi + O(u_1^2)\right\} \tag{26}$$

where $U_o u_1$ is the perturbation x-velocity of the potential flow at the solid surface of the equivalent body of shape $y_e = \eta_o(x,z) + \delta_*(x,z)$. Since the solution u_1 depends on the body shape y_e, (26) gives the integral equation for the unknown displacement thickness δ_*. For the case of small disturbance, this integral equation can be solved by iteration. By taking $\delta_*^{(o)} = (2.55)\sqrt{\nu x/U_o}$, which is the flat plate solution, as the zeroth approximation for δ_* in the expression for u_1, (26) yields the first iteration $\delta_*^{(1)}$. This permits the process to be repeated iteratively for the solution of δ_*. In practical cases it is expected that the first iteration may be accepted without any appreciable loss of accuracy.

The local skin-friction coefficient C_f can be derived from the above result, giving

$$C_f(x,z) = \frac{\tau_o}{\frac{1}{2}\rho U_o^2} = \left(\frac{\tau_o\theta}{\mu U}\right)\left(\frac{U}{U_o}\right)\left(\frac{2\nu}{\theta U_o}\right) = \frac{0.47}{\sqrt{a}}\sqrt{\frac{\nu}{U_o x}}\left\{1 + \right.$$

$$\left. + (5.39)\,ax\frac{\partial u_1}{\partial x} + (1 + \frac{b}{2})u_1 - \frac{b-1}{2x}\int_o^x u_1(\xi,z)d\xi + O(u_1^2)\right\} \tag{27}$$

The total skin-friction drag, defined by

$$C_{D_f} = \frac{D_f}{\frac{1}{2}\rho U_o^2 S_o} = \frac{1}{S_o}\int_{-h}^{o} dz \int_o^{\ell(z)} C_f(x,z)dx \tag{28}$$

with D_f denoting the total skin-friction drag and S_o the total wetted surface area, can be obtained by integration of C_f, giving

$$C_{D_f} = \frac{0.94}{\sqrt{a}}\sqrt{\frac{\nu}{U_o}}\frac{1}{S_o}\int_{-h}^{o}\ell(z)\left\{1 + 2.70\,au_1(\ell,z)\right.$$

$$\left. + \frac{1 - 1.35a - 0.25b}{\sqrt{\ell(x)}}\int_o^{\ell}\frac{u_1}{\sqrt{\xi}}d\xi + \frac{b-1}{2\ell}\int_o^{\ell}u_1(\xi,z)d\xi\right\}dz. \tag{29}$$

This is the general result of the total skin-friction drag obtained from our small perturbation theory on the basis of no flow separation.

In order that in the limit as $u_1 \to 0$, the above solution C_{D_f} will reduce in the two-dimensional case to the exact solution of Blasius, namely,

$$C_{D_f} = 1.328 \frac{\nu}{U_o \ell} \qquad (30)$$

we shall take a = 0.50, b = 6 which give the corresponding displacement thickness δ_* 4.6% greater than the exact solutions.

It may be remarked here that if more accurate results are required for bodies not too thin, especially when separation is known to exist, the above method of approach can again be adopted in principle as the basic procedure for the numerical calculation.

3B. Turbulent Boundary Layer

Up to the present time the phenomena of turbulent boundary layers with pressure gradient and with possible occurrence of separation has been regarded as a very complicated subject and are still far from being completely understood. There are however several semi-empirical methods which can provide fairly satisfactory results. To begin with, some of the salient features of turbulent boundary layers are noteworthy. It has been observed experimentally that the shape of the velocity profile depends very strongly, much more so than the laminar case, on the pressure gradient. Furthermore, no general relationship between shear and dissipation in turbulent flow can be derived by purely theoretical considerations (the linear relationship between τ_o and the slope of mean velocity $\partial\tilde{u}/\partial y$, as analogous to (9), is no longer valid in turbulent flow), it is necessary to introduce an additional assumption which can be justified only by experimental observations. This partially explains that the integral forms of the momentum and energy equations are about the only means for calculating turbulent boundary layers. In the following we shall adopt the approximate method due to Buri (1931) which is analogous to Pohlhausen's method for laminar flow case and hence is of particular advantage to our consideration.

As no specific relation is given to the shearing stress τ_o in (11), this momentum-integral equation holds valid for laminar turbulent boundary layers alike. Same as in the laminar case, the momentum thickness θ and displacement thickness δ_*, defined by (10), are used as the

characteristic dimensions of the boundary layer. As to the shape factor for turbulent boundary layers, we may choose, following Buri, the dimensionless quantity

$$\Gamma = \frac{\theta}{U} \left(\frac{U\theta}{\nu}\right)^{1/n} \frac{dU}{dx}, \quad n = 4, \tag{31}$$

which is analogous to the factor K (with n = 1) of (12c) in the laminar case. Based on the measurements of Nikuradse, turbulent separation occurs when $\Gamma \sim -0.06$.

One essential difference between the laminar and turbulent momentum-integral equation is that in the latter case one must attain separate information of $\tau_o/\rho U^2$ and δ_*/θ. Following Buri, we assume that

$$\frac{\tau_o}{\rho U^2} = f_1(\Gamma) \left(\frac{U\theta}{\nu}\right)^{-1/n} \tag{32}$$

and

$$H = \frac{\delta_*}{\theta} = f_2(\Gamma) \tag{33}$$

where f_1 and f_2 are functions of the shape factor Γ only. Then the momentum-integral equation (11) reduces under these assumptions to

$$\frac{d}{dx}\left[\theta \left(\frac{U\theta}{\nu}\right)^{1/n}\right] = F(\Gamma), \tag{34a}$$

where

$$F(\Gamma) = \frac{n+1}{n} f_1(\Gamma) - \left[2 + \frac{1}{n} + \frac{n+1}{n} f_2(\Gamma)\right]\Gamma. \tag{34b}$$

Like the previous case of laminar boundary layers, the universal function $F(\Gamma)$ is also very nearly linear, or

$$F(\Gamma) = a' - b'\Gamma = a' - b' \frac{\theta}{U} \left(\frac{U\theta}{\nu}\right)^{1/n} \frac{dU}{dx} \tag{35}$$

The approximation enables (34) to be integrated in closed form:

$$\theta\left(\frac{U\theta}{\nu}\right)^{1/n} = U^{-b'}\left[A + a' \int_{x-x_t}^{x} U^{b'}(\xi, z)d\xi\right] \tag{36}$$

in which x_t is the point of transition from the laminar to turbulent flow, and A is a constant which can be determined from the value of θ of the laminar boundary layer at x_t.

In turbulent flow we have $4 < n < 6$ for $5 \times 10^2 < Re_\theta = U_o\theta/\nu < 10^5$, where $n = 4$ is valid for the lower end of this range of Re_θ and n gradually increases to 5, 6 for larger Re_θ. For a satisfactory over-all approximation we may take (see e.g. Schlichting (1960), p. 572)

$$\begin{aligned} &n = 4, \quad a' = 0.016, \quad b' = 4.0, \quad f_1(\Gamma) \sim 0.0128, \\ &n = 6, \quad a' = 0.0076, \quad b' = 3.67, \quad f_1(\Gamma) \sim 0.0065. \end{aligned} \tag{37}$$

The ratio $H = \delta_*/\theta$ can also be used as a shape factor (for its calculation see Schlichting (1960), ch. 22). With the flat plate, H ranges from 1.3 at low values of Re_θ to 1.4 at high end of Re_θ. Separation occurs at $H \sim 1.8$ to 2.4.

In the case when the boundary layer does not separate the momentum thickness $\theta(x,z)$ can be calculated from (36) with the above semi-empirical results; this essentially completes the calculation of the turbulent boundary layer provided $U(x,z)$ is already known. The local coefficient of skin friction can be obtained from (32) as a first approximation. A more accurate result is probably given by the empirical formula of Ludwieg and Tillman

$$\frac{\tau_o}{\rho U^2} = 0.123 \times 10^{-0.678H} \left(\frac{U\theta}{\nu}\right)^{0.268}, \tag{38}$$

after the factor H is determined. Finally, the total coefficient of skin friction is obtained by integration.

For the particular case of small disturbances, one may proceed in a similar manner as the laminar case to obtain θ. We also obtain an integral equation for δ_*, which can again be solved approximately by iteration. From this solution one further deduces the local skin friction and the total skin-friction. The details of this procedure and the formulas involved, however, will not be explicitly given here.

4. Flow in the Viscous Wave of the Obstacle

Investigation of the flow in the viscous wake of the wave-making body is also essential since without such knowledge the region of the external potential flow downstream of the body will be left undetermined, and consequently the problem of form drag and wave-making resistance will not be completely specified. It is known that the form drag is in general very difficult to compute or to make direct measurements, even in the absence of free surface. An indirect, but useful methods of determining profile drag (skin-friction and viscous form drag) is based on the relationship between the drag and the velocity distribution in the wake. In principle it can be used only in two-dimensional and axi-symmetric cases. However, we shall assume that the draft is so large that the effect of the free surface and the lower end of the body is relatively unimportant. We further assume that the flow may be considered quasi-two-dimensional in a distance of several body lengths downstream so that the coordinate z again plays the role of a parameter. Moreover, we re-iterate our assumption that the flow is not separated.

The problem of the viscous wake behind a solid body was first treated by S. Goldstein (1930) for the case of a flat plate. The calculation was made by the stepwise finite difference method, using Blasius' velocity profile at the trailing edge as the known initial condition.

Although the near wake field is very complicated, the asymptotic solution for large distances is easy to calculate and is known to be independent of the body shape, except for a scale factor. Since far away in the wake p recovers its free stream value and the nondimensional perturbation velocity $u_1 = (u/U_o - 1)$ is very small. Oseen's approximation is justified so that

$$U_o \frac{\partial u_1}{\partial x} = \nu \frac{\partial^2 u_1}{\partial y^2} \tag{39}$$

The boundary conditions are

$$\frac{\partial u_1(x,0)}{\partial y} = 0 \quad \text{and} \quad u_1(x,\infty) = 0 \tag{40}$$

The solution for the laminar wake is readily obtained and can be shown to be

$$u_1 = -\frac{C_D^*}{4}\left(\frac{U_o \ell}{\pi \nu x}\right)^{1/2} e^{-\frac{U_o y^2}{4\nu x}}, \qquad (41)$$

where C_D^* is the coefficient of profile drag (sum of skin friction and viscous form drag, based on U_o and ℓ). In the absence of free surface C_D^* is the total drag coefficient and, in particular for the flat plate, it is identical to C_{Df}. For arbitrary body shape, u_1 is therefore proportional to C_D^*, the only scale factor in (41) which cannot be obtained from the asymptotic considerations alone. From the above result we immediately deduce the asmyptotic property of the displacement and momentum thickness defined by (10) (note that they are referred to half side of the wake in this case)

$$\theta/\ell = \delta_*/\ell = C_D^*/4 \qquad (42)$$

which is valid for $\sqrt{\nu x/U_o}$ large compared with the body length ℓ. Therefore far downstream δ_* and θ become both equal to $C_D^*/4$, which is a known result.

In the region immediately downstream of the trailing edge of an arbitrary solid body, the effect of pressure gradient is of considerable importance. To take this effect into account it is convenient to apply again the momentum-integral equation (11) which is valid also for the wake flow provided τ_o is set to zero. We shall consider briefly this approximate method, taking into account some more recent results. The momentum-integral equation for the wake flow is thus

$$\frac{1}{\theta}\frac{d\theta}{dx} + (H + 2)\frac{1}{U}\frac{dU}{dx} = 0 \qquad (43)$$

where $H = \delta^*/\theta$, and the x-axis is now directed along the center-line of the wake. The previous calculation of the boundary layer over the solid surface enables one to evaluate the displacement thickness δ_{*1}, the momentum thickness θ_1 at the trailing edge $x - x_1$ and hence $H_1 = \delta_1^*/\theta_1$ in terms of given $U(x)$. Integrating (43) from the trailing edge $(x - x_1)$ to a station $x(>x_1)$,

$$\log \frac{\theta(x)}{\theta_1} + \log [U(x)]^{H+2} - \log [U_1]^{H_1+2} = \int_{H=H_1}^{H(x)} [\log U]\, dH, \qquad (44)$$

or

$$\frac{\theta(x)}{\theta_1} = \left[\frac{U_1}{U(x)}\right]^{H+2} \exp\left\{\int_{H_1}^{H} \log\left(\frac{U}{U_1}\right)\, dH\right\} \qquad (45a)$$

For x sufficiently large, $\theta = \theta_\infty$, $U = U_\infty$, $H_\infty = 1$, hence from (44) we also have

$$\frac{\theta_\infty}{\theta_1} = \left[\frac{U_1}{U_\infty}\right]^{(H_1+2)} \exp\left\{\int_{H_1}^{1} \log\left(\frac{U}{U_\infty}\right)\, dH\right\}. \qquad (45b)$$

Squire, based on experiments, introduced the following empirical relation

$$\frac{\log(U_\infty/U)}{H-1} = \frac{\log(U_\infty/U_1)}{H_1-1} = \text{const.} \qquad (46)$$

Consequently we obtain

$$\frac{\theta(x)}{\theta_1} = \left[\frac{U_1}{U(x)}\right]^{(H+2)} \left(\frac{U_1}{U_\infty}\right)^{\frac{1}{2}(H_1-H)^2/(H_1-1)}, \qquad (47)$$

and

$$\frac{\theta_\infty}{\theta_1} = \left(\frac{U_1}{U_\infty}\right)^{\frac{1}{2}(H_1+\zeta)} \qquad (48)$$

In the last result H_1 may be approximated by its round-off value $H_1 \sim 1.4$.

Summarizing, we note that (θ_1/ℓ) can be evaluated by the previous method (using the appropriate value of n). A practical method of determining (U_1/U_∞) is from a reading of the static pressure at the trailing edge. When the flow is free from separation, U_1/U_∞ in general does not differ appreciably from unity. The profile drag coefficient $C_D^* = C_{D_f} + C_D$ (form) is therefore given by (42) and (48), from which the form drag is deduced by further subtracting C_{D_f}.

Finally, it appears necessary to obtain an approximate estimate of the displacement thickness δ_* of the wake so that an equivalent boundary can be hopefully attained for the external flow. In the opinion of this author, this is perhaps the most difficult part of this problem. It should be remarked here that first, the wake at large distances is almost completely diffused and hence the concept of displacement thickness loses much of its original significance for the boundary layer over a solid surface. Even when the original significance remains valid for the wake, it is difficult to interpret the external potential flow as one past an infinite half body, as clearly suggested by (42). Whether the equivalent body should be open (semi-infinite) or closed has not been definitely settled. The issue is further perplexed by the finding that the wave drag is quite sensitive to the change of body shape of this kind (see, e.g. Weinblum (1938). Therefore the author is led to derive the contention that further systemic efforts are needed in order to clarify this point.

As an untested though the following suggestions may be mentioned. In the extension of the displacement thickness as the equivalent body surface from the trailing edge into the wake, it is thought to be important to have the streamline continuous in slope at the trailing edge. For simplicity let us consider the case the body has a pointed trailing edge with an included angle $2\alpha_1$. Then we assume that not only δ^* but also its slope are continuous at the trailing edge ($x = x_1$) in the actual flow. The latter condition requires that

$$\left(\frac{d\delta_1^*}{dx}\right)_+ = \left(\frac{d\delta_1^*}{dx}\right)_- - \alpha_1 \; (\equiv -m_1) \qquad (49)$$

where the subscript $\pm$ denotes $x = x_1 \pm 0$, the value δ_1^* and $(d\delta_1^*/dx)_-$ at $x = x_1$ being given by the boundary layer calculation over a solid surface. The continuity of δ_1^* and condition (49) may be incorporated into further consideration concerning the problem of the equivalent after body, whether it will be open or closed. For example, if m_1 of (49) is positive and if the aft-body is chosen to be closed, then a possible profile for verification would be

$$\delta^*(x) = \delta_1^* \, e^{-m_1(x-x_1)} \quad \text{for} \quad x > x_1 \, . \qquad (50)$$

5. The Boundary Layer Effect on Wave Profile and Wave Resistance

The classical theory of surface waves generated by a floating or submerged body is based on the assumption of potential flow of inviscid fluid. Following our earlier development we shall assume that the potential theory can be applied provided the equivalent body surface is used for the potential flow boundary. We note here a further impact of the problem of "a closed or open aft-body." As long as the viscous effect alone is concerned, perhaps this problem can be considered together with the viscous form drag. In the presence of also the gravity effect, and hence the wave field, one is further confronted by the problem of optimum approximation of the equivalent boundary in the wake so as to yield the best approximation of the wave field and hence also the wave resistance.

Suppose the equivalent body surface $y_e = \eta = \eta_o + \delta^*$ has been determined for $0 < x < \ell'(z)$, $-h < z < 0$, ($\ell' = \infty$ for the open aft-body) then the corresponding wave resistance, which is well known from the thin ship theory, is

$$R_w = \frac{4}{\pi}\rho U_o^2 \kappa^2 \int_1^\infty \{I^2(t) + J^2(t)\} \frac{t^2 dt}{\sqrt{t^2-1}} , \tag{51}$$

where $\kappa = g/U_o^2$,

$$\left.\begin{matrix} I(t) \\ J(t) \end{matrix}\right\} = \int_{-h}^{o} dz \int_o^{\ell'(z)} e^{\kappa z t^2} \left\{\begin{matrix} \cos(\kappa x t) \\ \sin(\kappa x t) \end{matrix}\right\} f(x,z)\, dx \tag{52}$$

and

$$f(x,z) = \frac{\partial \eta}{\partial x} = \frac{\partial \eta_o}{\partial x} + \frac{\partial \delta_*}{\partial x} = f_o + f_* . \tag{53}$$

Since the wave resistance is quadratic in f, therefore symbolically this result can be further expressed as

$$R_w = D_o + D_1 + D_2 , \tag{54}$$

$$D_o = \frac{4}{\pi}\rho U_o^2 \kappa^2 \int_1^\infty \{I_o^2(t) + J_o^2(t)\} \frac{t^2 dt}{\sqrt{t^2-1}} \tag{54a}$$

$$D_1 \quad \frac{8}{\pi}\rho U^2 \kappa^2 \int_1^\infty \{I_o(t)I_*(t) + J_o(t)J_*(t)\} \frac{t^2 dt}{\sqrt{t^2-1}} \tag{54b}$$

where $f(x) = f_o(x) + f_*(x) = d(\eta_o+\delta_*)/dx$, $x = \ell'$ is the terminating point of δ_* and

$$G(x,z) = \frac{2\kappa}{\pi}\left\{\int_0^1 e^{\kappa z t^2}\,\frac{\sin(\kappa x t)}{\sqrt{1-t^2}}\,dt - \int_1^\infty e^{\kappa z t^2}\,\frac{\cos(\kappa x t)}{\sqrt{t^2-1}}\,dt\right.$$

$$\left. - \frac{1}{\pi}\int_0^\infty t\sin(\kappa x t)\,dt\int_0^\infty \frac{t^2\cos(\kappa z\sigma) + \sigma\sin(\kappa z\sigma)}{(t^4+\sigma^2)\sqrt{t^2+\sigma^2}}\,\frac{d\sigma}{\sigma}\right. \qquad (57b)$$

The above solution is expressed in Michell's form. The function $G(x,z)$ can also be given in Havelock's form, the latter will however be omitted here.

6B. Displacement Thickness and Skin-Friction

By substituting (57) in (26), we obtain an integral equation for δ_* for the part of boundary layer over the strut surface, which can be solved by iteration. The problem of δ_* in the wake will not be pursued further here. The value of the skin-friction can now be calculation from (29).

6C. The Wave Resistance

The wave resistance of an infinitely deep strut is given by

$$R_w = \frac{4}{\pi}\rho U_o^2\int_1^\infty [A^2(\kappa t) + B^2(\kappa t)]\,\frac{dt}{t^2\sqrt{t^2-1}} \qquad (58a)$$

where

$$\left.\begin{matrix}A(k)\\ B(k)\end{matrix}\right\} = \int_0^{\ell'} f(x)\left\{\begin{matrix}\cos kx\\ \sin kx\end{matrix}\right\}dx \qquad (58b)$$

and $f(x) = f_o(x) + \delta_*(x)$. Now

$$A_o(k) = \int_0^\ell f_o(x)\cos kx\,dx = \frac{\epsilon}{k}\left\{-\sin k\ell + \frac{2}{k\ell}(1-\cos k\ell)\right\} \qquad (59a)$$

$$B_o(k) = \int_0^\ell f_o(x)\sin kx\,dx = \frac{\epsilon}{k}\left\{1+\cos k\ell - \frac{2}{k\ell}(\sin k\ell)\right\} \qquad (59b)$$

$$D_2 = \frac{4}{\pi}\rho U_o^2 \kappa^2 \int_1^\infty \{I_*^2(t) + J_*^2(t)\} \frac{t^2 dt}{\sqrt{t^2-1}} \qquad (54c)$$

in which I_o, I_* are defined in the same way as I of (52) except with f replaced by f_o and f_* respectively; and similarly for J_o and J_*. Here D_o is the classical Michell's ship resistance, D_1 is the drag due to the cross term of body-boundary-layer interaction, and D_2 is the contribution to the wave resistance from the boundary layer displacement alone. For vanishingly thin flat plate moving parallel to itself, D_2 is the sole contribution to wave resistance. For ordinary cases however, D_2 is in general insignificant compared with R_w. In order to give a rough picture of its effect, we list in the following the values of δ_* over a flat plate

(i) laminar case $\delta_*(x) = 1.72\sqrt{\nu x/U_o}$, (55a)

(ii) turbulent case $\delta_*(x) = 0.046\left(\frac{\nu}{U_o}\right)^{1/5} x^{4/5}$, $5\times10^5 < R_{e_x} < 10^7$ (55b)

6. Example - Lenticular Strut

As a simple example we consider a lenticular strut with profile

$$\eta_o(x) = \frac{\epsilon}{\ell} x(\ell - x) \quad \text{for} \quad 0 < x < \ell, \quad -h < z < 0 \qquad (56a)$$

so that

$$f_o(x) = \partial\eta_o/\partial x = \epsilon(1 - 2x/\ell) \qquad (56b)$$

where ϵ is taken to be small, the draft h is chosen to be deep enough to permit using the infinitely deep strut to approximate the wave resistance.

6A. External Potential Flow

Since only the longitudinal component of the potential flow velocity at the body surface is needed, we cite the result of the dimensionless perturbation velocity u_1, defined by (21), in the following:

$$u_1(x) = \int_0^\ell f(\xi)\, G(x-\xi, z)\, d\xi \qquad (57a)$$

$$A_*(k) = \int_0^{\ell} + \int_{\ell}^{\ell'} \delta_*(x) \cos kx dx = A_{*_1} + A_{*_2} \tag{60a}$$

$$B_*(k) = \int_0^{\ell} + \int_{\ell}^{\ell'} \delta_*(x) \sin kx dx = B_{*_1} + B_{*_2} \tag{60b}$$

Since the value of δ_* in the wake ($\ell < x < \ell'$) has not been definitely determined, the contribution of A_{*_2} and B_{*_2} to the wave resistance R_w will not be included in the following discussion. As a typical example we shall treat below the case of laminar boundary layer only.

Substituting (55a) in (60a, b), we obtain from (58) - (60) the following result:

$$R_w = D_o + D_1 + D_2 = \frac{2}{3} \rho U_o^2 \ell^2 \{\epsilon^2 I_o + \epsilon\delta_\ell I_1 + \delta_\ell^2 I_2\}, \tag{61a}$$

$$I_o = \frac{12}{\pi\beta^4} \int_1^{\infty} \{\beta^2 (1 + \cos \beta t) - \frac{4\beta}{t} \sin \beta t + 4 \frac{1 - \cos \beta t}{t}\} \frac{dt}{t^4 \sqrt{t^2-1}}, \tag{61b}$$

$$I_1 = \frac{6\sqrt{2}}{\pi\beta} \int_0^1 \frac{d\xi}{\sqrt{\xi}} \int_1^{\infty} \frac{\beta t \cos(\beta t/2) - \frac{1}{2} \sin(\beta t/2)}{\beta^2 t^4 \sqrt{t^2-1}} \sin[\beta t(\eta - \tfrac{1}{2})] dt \tag{61c}$$

$$I_2 = \frac{3}{2\pi} \int_1^{\infty} \frac{dt}{t^2 \sqrt{t^2-1}} \int_0^1 \int_0^1 \cos \beta t \, (x^2 - \xi^2) \, dx d\xi \tag{61d}$$

where $$\beta = k\ell = g\ell/U_o^2 = 1/Fr^2 \tag{61e}$$

$$\delta_\ell = 1.72 \sqrt{\frac{\nu}{U_o \ell}} = 1.72 \, Re_\ell^{-1/2} \tag{61f}$$

The integral in (61b) can be carried out completely in terms of Bessel functions as

$$I_o = \frac{8}{\pi\beta^2} (1 + \frac{16}{5\beta^2}) - \frac{32}{5\beta^2} (1 + \frac{3}{16} \beta^2 + \frac{1}{32} \beta^4) Y_o(\beta) + \frac{64}{5\beta^2} (1 + \frac{\beta^2}{16} + \frac{\beta^4}{64}) Y_1(\beta) - \frac{\pi}{2} (1 + \frac{1}{5} \beta^2)[Y_1(\beta) H_o(\beta) - Y_o(\beta) H_1(\beta)] \tag{62}$$

where $Y_n(\beta)$ denotes Weber's function and $_n(\beta)$, Struve's function, both being already tabulated. The integrals I_1 and I_2 can also be integrated further in terms of special functions; they are however less practical than the present form for computation. For large or small values of β, it is convenient to use the following asymptotic expansions:

(i) For β large:

$$I_o \sim \frac{8}{\pi\beta^2}\left\{1 + \frac{16}{5\beta^2} + \frac{3}{4}\sqrt{\frac{2\pi}{\beta}}\left[\cos\left(\beta + \frac{\pi}{4}\right) - \frac{15}{8\beta}\sin\left(\beta + \frac{\pi}{4}\right)\right]\right\} \quad (63a)$$

$$I_1 \sim \frac{6\sqrt{2}}{\beta^{3/2}}\left\{\frac{1}{5\sqrt{2}}\,\frac{\Gamma(7/4)}{\Gamma(5/4)} - \frac{1}{3\pi\sqrt{\beta}} + \frac{5}{14\sqrt{2\beta}}\,\frac{\Gamma(5/4)}{\Gamma(7/4)}\right.$$

$$\left. - \frac{1}{2\sqrt{2\beta}}\left[\sin\beta + \frac{1}{\sqrt{\pi\beta}}\cos\left(\beta + \frac{\pi}{4}\right) + \frac{1}{8\beta}\cos\beta + O\left(\frac{1}{\beta^{3/2}}\right)\right]\right. \quad (63b)$$

$$I_2 \sim \frac{3\pi}{32\beta}\left\{1 + \frac{8}{3\pi^2\beta}\left[1 + \frac{3\pi}{\sqrt{2}}\left(\sin\beta - \frac{19}{8\beta}\cos\beta\right) + O\left(\frac{1}{\beta^{3/2}}\right)\right]\right\} \quad (63c)$$

(ii) For β small:

$$I_o \sim \frac{\beta^2}{6\pi}\left\{\left(\log\frac{2}{C\beta}\right)\left(1 - \frac{\beta^2}{40}\right) + \frac{1}{4}\left[7 - \frac{73}{400}\beta^2 + O(\beta^4)\right]\right\} \quad (64a)$$

$$I_1 \sim \frac{\beta^2}{\pi\sqrt{2}}\left\{\frac{1}{3}\left(\log\frac{2}{C\beta}\right)\left(1 - \frac{\beta^2}{35}\right) + 0.559 - 0.0169\beta^2 + O(\beta^4 \log\beta)\right\} \quad (64b)$$

$$I_2 \sim \frac{3}{2\pi} - \frac{\beta^2}{4\pi}\left\{\left(\log\frac{2}{C\beta}\right)\left(\frac{8}{15} - \frac{16\beta^2}{1575}\right) + 1.813 - 1.068\log 2 - 0.044\beta^2\right\} \quad (64c)$$

In Equations (64a-c), C is the Euler constant $C = e^{\gamma} = 1.781$. The above result is plotted in Figure 1 with the results of the asymptotic formulas shown in light lines. The salient feature is that all I_o, I_1 and I_2 depend on the Froude number, $Fr = \beta^{-1/2}$, alone and their variations with β show differences, especially the dependence of I_2 on Fr for moderate and large values of Fr.

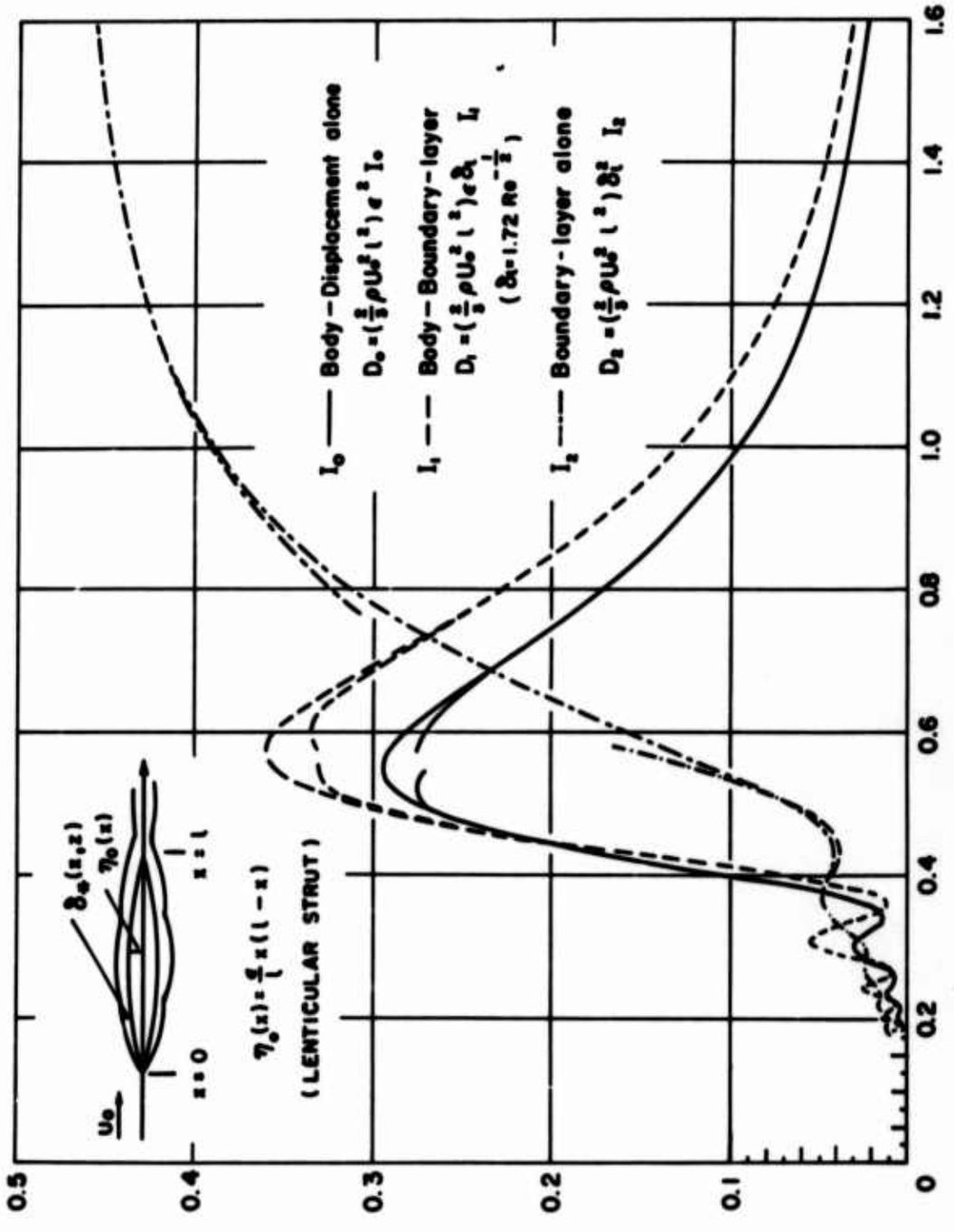

I_0 —— Body – Displacement alone
$D_0 = (\frac{8}{3}\rho U^2 (\frac{t}{l})^2) \sigma^2 I_0$
I_1 – – Body – Boundary – layer
$D_1 = (\frac{8}{3}\rho U^2 (\frac{t}{l})^2) \sigma \delta_1 I_1$
$(\delta_1 = 1.72\, Re^{-\frac{1}{2}})$
I_2 –·– Boundary – layer alone
$D_2 = (\frac{8}{3}\rho U^2 (\frac{t}{l})^2) \delta_1^2 I_2$
$\eta_0(x) = \frac{4}{l} x(l-x)$
(LENTICULAR STRUT)
$\delta_0(x,z)$
$\eta_0(x)$
U_0
x = 0
x = l
0
0.1
0.2
0.3
0.4
0.5
0.2
0.4
0.6
0.8
1.0
1.2
1.4
1.6
$F_r = \frac{1}{\sqrt{\beta}} = \frac{U}{\sqrt{gl}}$

FIGURE 1a.

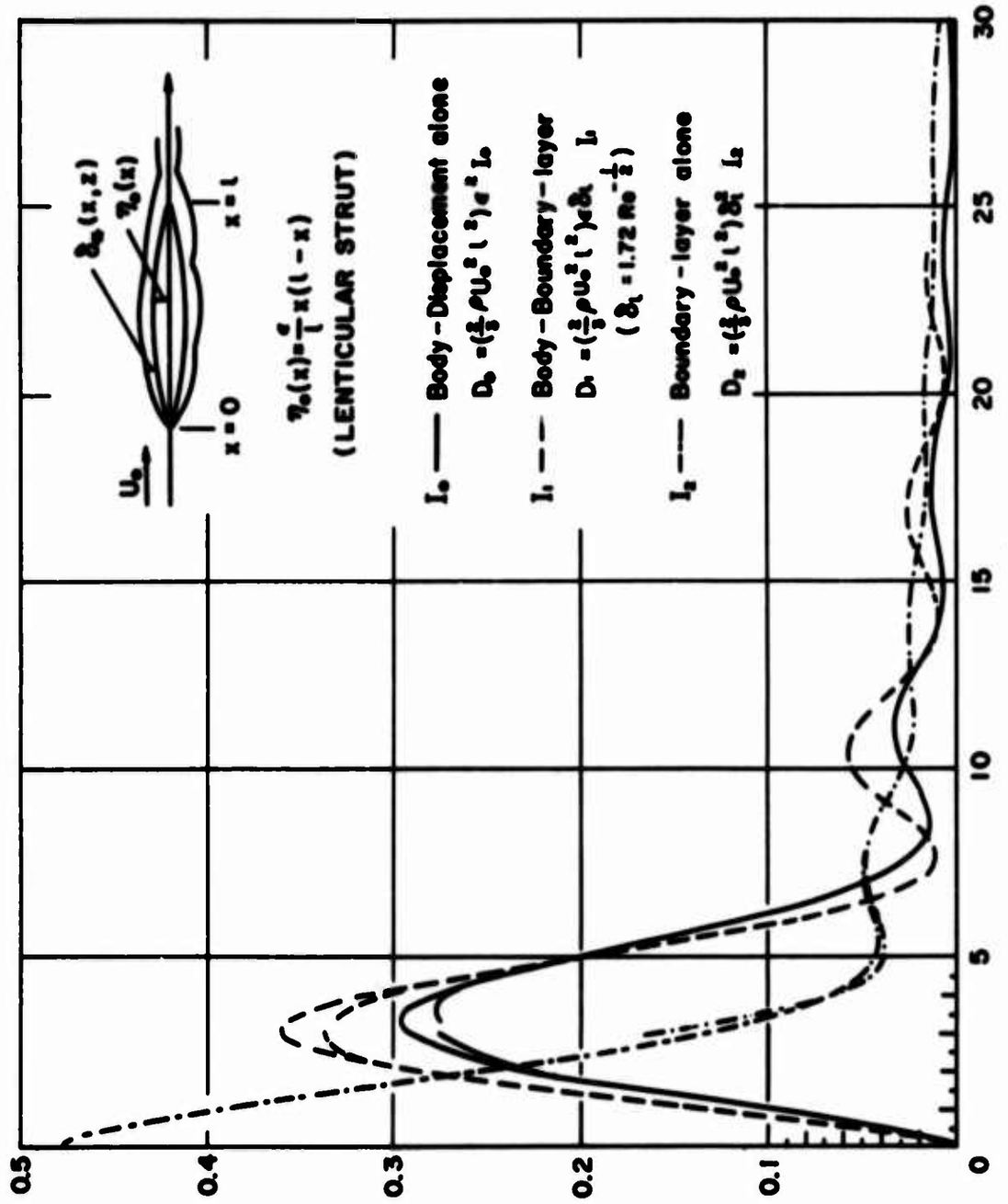

0.5
0.4
0.3
0.2
0.1
0
5
10
15
20
25
30
$\beta = \frac{gl}{U^2}$
I_0 —— Body-Displacement alone
$D_0 = (\frac{2}{3}\rho U_0^2 l^3)\alpha^2 I_0$
I_1 – – Body-Boundary-layer
$D_1 = (\frac{2}{3}\rho U_0^2 l^3)\alpha\delta_1 I_1$
$(\delta_1 = 1.72\, Re^{-\frac{1}{2}})$
I_2 —·— Boundary-layer alone
$D_2 = (\frac{4}{3}\rho U_0^2 l^3)\delta_1^2 I_2$
$\eta_0(x) = \frac{\alpha}{l} x(l-x)$
(LENTICULAR STRUT)
U_0
x = 0
x = l
$\delta_1(x,z)$
$\eta_0(x)$

FIGURE 1b.

REFERENCES

Buri, A. (1931) Thesis Zürich

Havelock, T. H. (1932) Proc. Roy. Soc., London 135, 136, 138.

Holstein, H., and Bohlen, T. (1940) Lilienthal - Bericht S 10.

Michell, T. (1898 Philos. Magazine.

Pohlhausen, K. (1921) ZAMM 1.

Schlichting, H. (1960) Boundary Layer Theory, 4th Ed. McGraw-Hill Company.

Walz, A. (1948) Ing. -Arch. 16 243.

Wehausen, J. V. and Laitone, E. V. (1960) Surface Waves, Encycl. Physics, Vol. 9, Springer-Verlag, Berlin.

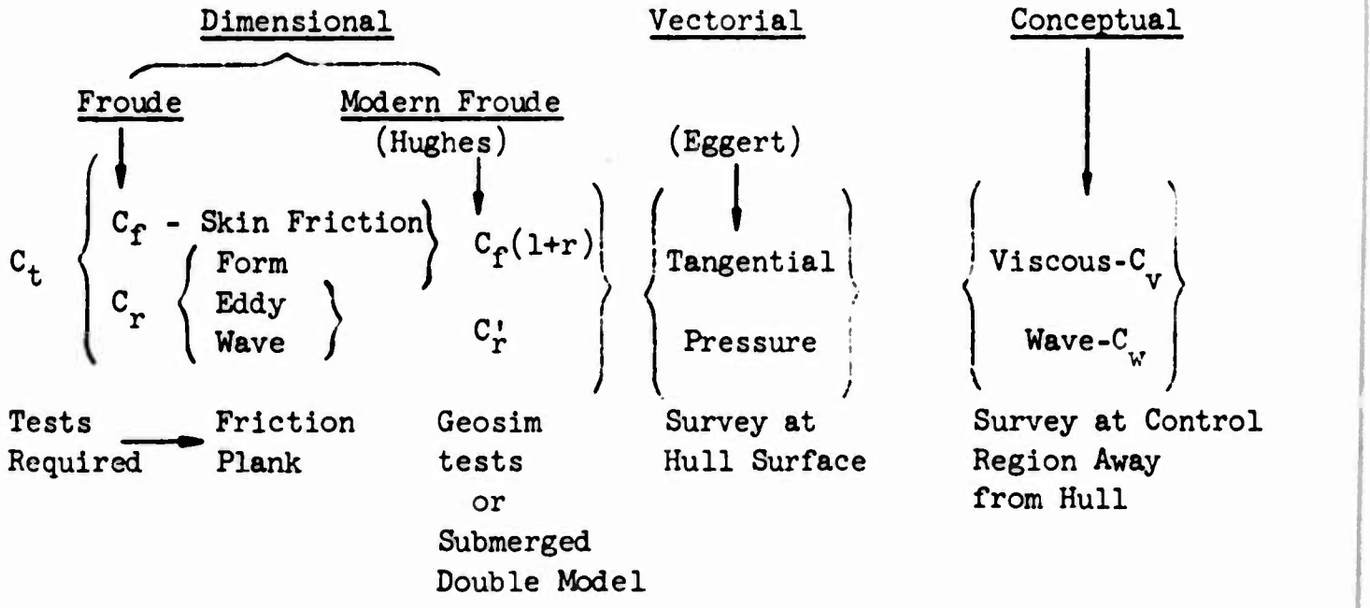
Weinblum, G. (1938) Schiffbau.

DISCUSSIONS

by Lawrence W. Ward

I have read Dr. Wu's paper with great interest as it bears on a question which I feel is important. Now that we have arrived at the last day I wonder if we are any closer to defining wave resistance in a real fluid. Perhaps the statement by the author on page 3 indicates the difficulty and wave resistance can only be defined in terms of behavior in the far-field. Even here there is no assurance that the wave resistance will not depend on the Reynolds number nor the viscous resistance on the Froude number, in fact we know there will be a noticable effect in each case. There are two main reasons for trying to break the total resistance into useful categories namely (1) scaling model test results and (2) understanding the phenomena involved, the latter being necessary for intelligent design. I think all that we can do now is to accept the fact that in a real fluid the two goals lead to different breakdowns which are related and hope in the future that these relationships can be established in a useful way. I append a table which I hope illustrates the present situation in regard to the above.

VARIOUS BREAKDOWNS OF SHIP RESISTANCE



by Dr. Gadd

I should like to make a few remarks on Professor Wu's paper.

Firstly he has assumed in his calculated example that the displacement thickness has values close to "flat plate" values right up to the stern. In a real case the boundary layer near the stern must be at least fairly close to the condition of separation. This is because sterns are usually wedge shaped, rather than cusped, so that if the boundary layer remained thin at the stern something approaching a stagnation point would occur. However no real boundary layer could withstand a pressure rising up to something close to stagnation pressure. Therefore, the boundary layer must smear out the corner at the stern, either by separating or at least by thickening rapidly in this region.

It follows that the wave-induced part of the pressure gradient may become very significant and introduce a highly non-two-dimensional effect near the stem, even to the boundary layer on a vertical strut of infinite draft, the case considered by Professor Wu. Thus if the wave alongside the body is such as to introduce an additional adverse pressure gradient near the stern, aggrarating the boundary-layer thickening effect already present due to the strut shape, it may well suffice near the surface to push the boundary layer over the cliff, as it were, into the condition of separation, whereas at moderate and great depths the boundary layer may only be approaching separation.

Once three-dimensional effects have been introduced, the two-dimensional momentum integral equation for the boundary layer becomes quite inapplicable. Thus for the careful experimental results of Klebanoff and Diehl, on supposedly two-dimensional turbulent separation, application of the momentum integral equation yields the ridiculous result that the skin friction increases towards separation. This is almost certainly to be attributed to the flow not being perfectly two-dimensional, even though the greatest pains were taken to try and make it so.

It seems to me, therefore, that the real problem that needs to be dealt with concerns the highly three-dimensional flow of a turbulent boundary layer near the condition of separation. Accordingly, much though I admire Professor Wu's skill in solving the two-dimensional problem of a boundary layer far from the condition of separation, I cannot see that it has a very close relevance to ship hydrodynamics.

by Dr. Timman

I greatly enjoyed Professor Wu's statements. It made me think about the things you do when you try to work out the boundary layer first which has its recourse in the potential flow; and of course the potential is more complicated here. I was also inclined to think about some of the boundary layer phenomena you meet when you consider a boundary layer along a wavy wall. Of course this is not a wavy wall, for the waves are in the fluid, but there you get quite peculiar phenomena. Now there are some calculations made by Gertler before the war, and now recently, I believe, by Professor Weinblum. These show that if you have a wavy wall then you have promoted pressure gradients and adverse pressure gradients. Thus you get earlier separation than if you just took the smooth flow. I am not quite sure that phenomena like this would not be met here so that even if conditions were favorable -- and I tend to agree with Mr. Gadd that they are not favorable here -- I think you will get local separation phenomena which will of course effect the wave motion. Now this is all too detailed to take account of in this first study. I expect that there will be boundary layer interaction between the outgoing waves and the boundary layer behavior itself. Once separation does occur you will get much stronger interaction. It is somewhat like the supersonic interaction which takes place between a shock wave and a boundary layer. These things become increasingly difficult as you try to include a greater number of effects. One of these that you must take into account is the three-dimensional phenomenon, though I am not sure that it will be so overall important, for this whole wave influence dies down if you go inside the fluid. I am inclined to think that these wave phenomena I spoke of would be of at least equal importance to the three-dimensionality for the surface waves we are concerned with. As far as I know this is the first time that anyone had the courage to undertake this problem.

I want to compliment Professor Wu on his courage and his initiative to undertake this problem.

AUTHOR'S REPLY

First, I should like to express my sincere appreciation for the comments and remarks made on my paper, and to the discussors for their interest in this work. Professor Timman's observations are particularly encouraging to me, and, I believe, to those who are interested in this problem; I hope we can devote a continued effort to an investigation of the viscous effects on ship waves so that some day we may further our knowledge on this subject to a state of being fully understood.

I wish to qualify the present work as a very preliminary effort since obviously there still exists an erronous gap between this very simple consideration and the eventual applications to real ships. In this respect I must say I fully appreciate Dr. Gadd's comment in point out some of the basic difficulties which are confronting us and which we must solve truthfully if we are to achieve a good understanding of the physical problem. I believe, however, that it would be fruitful to take sure steps first before we can attempt a leap to the final goal, to single out, as few a number as possible, the complicated effects, such as the thickening of the boundary layer near the stern, possible separation of the flow, turbulence, three-dimensional effects, etc., rather than tackle all these effects at once. It is my hope that under controlled environments we may be able to adopt for experimental purpose a sufficiently thin strut, to select a suitable range of the Reynolds number and the Froude number such that a laminar boundary layer can be realized over the entire strut and the flow can be kept from separation. It is for this idealized case that the much simplified assumptions introduced in this work are proposed to strive for a possible solution in order to establish a first base of our objectives and to test out the soundness of this approach. It is certainly true that if the flow is separated from the hull, then some sort of wake flow analysis must be incorporated; if the three-dimensional effect is dominating the boundary layer flow, then a strip theory, or some other method, must be introduced. This work would lose much of its original hope if it is proven that under no condition the flow can be kept free from separation and being influenced by the three-dimensional effect in the boundary layer flow.

I am indebted to Professor L. W. Ward for his proposed various break-down of ship resistance in the light of the present state of the art.

EFFECTS OF VISCOSITY ON WAVE RESISTANCE

C. Wigley

Office of Naval Research
Washington, D. C.

INTRODUCTION

In a perfect fluid there is no scale effect on the wave resistance. But, in a viscous fluid, the wave resistance depends, not only on the Froude Number, but also on the Reynolds' Number.

Since, in general, viscosity tends to decrease the wave resistance, this causes an increase in the wave resistance of the ship as compared with that of the model.

Hence the calculation of the wave resistance in a viscous fluid is of immediate practical importance.

In Reference 1 the writer has compared the wave resistance in a viscous fluid, calculated by Havelock's suggested approximation, (Reference 2) with actual discrepancies between calculated wave resistances and those estimated from model experiments, and in Reference 3 has given the approximate shape of the curve of correction to the calculated ship resistance in the case of a very long ship. This correction increases with the Froude Number up to a maximum at a Froude Number of about 0.27, and thereafter falls nearly to zero at a Froude Number of 0.45. There is some experimental support for such a curve, in particular may be quoted as diagram by Emerson (Reference 7). In the present paper Laurentieff's method (Reference 4) of calculating the resistance in a viscous fluid has been applied to a model, it is found that, as originally stated by Laurentieff, this gives changes due to viscosity which are much too small. The theoretical error here has been detected, and when a correction is applied the results are of the same type as found by Havelock's method.

GENERAL DISCUSSION OF LAURENTIEFF'S METHOD

His method of attacking the problem is to apply Michell's integral to the outer edge of the boundary layer and not to the form itself (see Figure on page 1285).

He assumes the thickness of the boundary layer to be independent of the depth, so that there is a discontinuity at the keel equivalent to a small flat bottom to which Michell's integral cannot be applied. This is not likely to affect wave resistance at low speeds, but may cause some difficulty at higher speeds.

The main objection to this procedure is the application of Michell's integral to a form which is open at the after end, whereas it should be applied only to a closed form. Laurentieff suggests that this is equivalent to assuming a very long wake behind the body of the same width as the boundary layer at the stern. But the objection to the use of Michell's integral in these circumstances still applies.

The motion is referred to Cartesian axes (X,Y,Z) parallel to those usually employed, but with the origin at the bow instead of amidships, and with the direction of the axis OX reversed, so that the relation between Laurentieff's coordinates and those generally used are

$$\begin{aligned} X &= L/2 - x \\ Y &= y \\ Z &= z \end{aligned} \qquad (6)^*$$

where L is the model length. Writing also B for the model beam, and T for its draught, and denoting the Reynolds' number by R_e, the thickness of the boundary layer at a distance X aft from the bow is assumed to be

$$t = 0.0924\ (L/2)(X/L)^{4/5}\ .R_e^{-1/5} \qquad (7)$$

---

* There are no Equations (1) to (5), the numbering starts with (6).

From this point we shall alter slightly the notation used by Laurentieff, both to simplify the reproduction, and to avoid confusion with the notation previously used. We shall introduce the symbol $k = g/v^2$, where v is the model speed. We shall also denote the Froude number $v/\sqrt{gL}$ by N, instead of using the symbol F as does Laurentieff.

His Equations (6) and (8) for the wave resistance of a model whose equation is $Y = F(X,Z)$, found by integrating along the outside of the boundary layer in order to allow for the viscosity then become

$$R = \frac{4\rho g^2}{\pi v^2}\left[\int_0^{\pi/2}(I^2 + J^2).\sec^3\theta d\theta + 2\int_0^{\pi/2}(I.I_1 + J.J_1).\sec^3\theta d\theta + \int_0^{\pi/2}(I_1^2 + J_1^2).\sec^3\theta d\theta\right] \qquad (8)$$

where

$$\left.\begin{aligned} I &= \iint (\delta F/\delta X).e^{kZ.\sec^2\theta}.\cos(kX\sec\theta).dX.dZ \\ J &= \iint (\delta F/\delta X).e^{kZ.\sec^2\theta}.\sin(kX.\sec\theta).dX.dZ \\ I_1 &= \iint (\delta t/\delta X).e^{kZ.\sec^2\theta}.\cos(kX.\sec\theta).dX.dZ \\ J_1 &= \iint (\delta t/\delta X).e^{kZ.\sec^2\theta}.\sin(kX.\sec\theta).dX.dZ \end{aligned}\right\} \qquad (9)$$

the double integrals being taken over the central plane of the model.

For a model with a rectangular central section, i.e. with bow and stern both vertical posts, the values of I_1 and J_1 become, as in Laurentieff's Equation (8b)

$$\left.\begin{aligned} I_1 &= \frac{-0.074L^{1/5}}{k.R_e^{1/5}}.(1 - e^{-kT.\sec^2\theta})\int_0^L X^{-1/5}.\cos(kX.\sec\theta).dX \\ J_1 &= \frac{-0.074L^{1/5}}{k.R_e^{1/5}}.(1 - e^{-kT.\sec^2\theta})\int_0^L X^{-1/5}.\sin(kX.\sec\theta).dX \end{aligned}\right\} \qquad (10)$$

These equations may be put into a more suitable form for calculations by the substitution $P = X/L$, $A = kL.\sec\theta$, $D = kT.\sec^2\theta$ when they become

$$I_1 = \frac{-0.074L}{k.R_e^{1/5}} \cdot (1 - e^{-D}) \int_0^1 P^{-1/5}.\cos(AP)\ .dP$$

$$J_1 = \frac{-0.074L}{k.R_e^{1/5}} \cdot (1 - e^{-D}) \int_0^1 P^{-1/5}.\sin(AP)\ .dP \qquad (11)$$

In Equation (8) the first integral represents the wave resistance in a perfect fluid. The other terms represent the effect of viscosity. From Equation (11) we see that, in it, the second integral contains a factor $R_e^{-1/5}$, while the third integral contains the factor $R_e^{-1/5}$. It follows that for all usual values of the Reynolds number R_e the third integral is negligible. The additional resistance due to viscosity is then given by

$$r = \frac{8\rho g^2}{\pi v^2} \int_0^{\pi/2} (I.I_1 + J.J_1).\sec^3\theta d\theta \qquad (12)$$

To calculate this additional resistance it is necessary to evaluate the integrand in this equation for a number of values of θ and then to find the value of r by approximate integration.

In order to calculate the integrand we have to know the values of the functions

$$K_1(A) = \int_0^1 P^{-1/5}.\cos\,(AP).dP$$

and (13)

$$K_2(A) - \int_0^1 P^{-1/5}.\sin\,(AP).dP$$

which are factors in I_1 and J_1 respectively.

These have been calculated by use of a digital computer for values of A less than 25.0, at intervals of 0.2, and to five significant figures.

For values of A greater than 25 use has been made of the relation

$$A.^{4/5}K_1(A) = (A - \pi)^{4/5}.K_1(A - \pi) + \int_{(A-\pi)}^{A} X^{-1/5}.\cos(X).dX \qquad (14)$$

and the corresponding relation for $K_2(A)$ to calculate for a number of higher values of A. The remaining integral in Equation (14) was calculated by approximate integration.

The accuracy of this calculation was checked by using it to give calculated values of the functions already computed, and at values of A about 25 the error was never as much as one per cent, and generally much less. The values of $K_1(A)$ and $K_2(A)$ thus found are tabulated in the Appendix.

Numerical Calculations Already Made

These equations have been applied to Model 829 whose equation, in the usual co-ordinates, is

$$\begin{aligned} y &= b(1 - x^2/a^2)(1 - 0.2x^2/a^2)(1 - z^2/d^2) \\ &= b(1 - z^2/d^2).\cos(\pi x/2a). \quad \text{to a sufficient approximation} \end{aligned} \qquad (15)$$

Using the quantities A and D from Equation (11), for this form

$$\begin{aligned} I &= -\pi(B/2).F(D).A.\sin(A)/(\pi^2 - A^2).D \\ J &= +\pi(B/2).F(D).A[1 + \cos(A)]/(\pi^2 - A^2).D \\ I_1 &= 0.037.R_e^{-1/5}.L(1 - e^{-D}).K_1(A)/D \\ J_1 &= 0.037.R_e^{-1/5}.L(1 - e^{-D}).K_2(A)/D \end{aligned} \qquad (16)$$

when, from Equation (12)

$$r = \frac{-0.148\ \rho.g^2}{v^2}.R_e^{-1/5}(L/D).(1 - e^{-D})BA[(K_1(A).(1 + \cos.A) - K_2(A).\sin.(A)]/(\pi^2 - A^2) \qquad (17)$$

Results of Preliminary Numerical Calculations

Using Equation (17) the value of the change in wave-resistance due to viscosity (r) has been worked out for three Froude numbers, and all three results show a very small decrease in wave resistance.

With R_w written for the wave resistance in a perfect fluid we find that

N	-r/R
0.284	0.004
0.303	0.010
0.360	0.006

From other calculations, and alsc from the experimental results with reversed unsymmetrical models, it seems that the effect of viscosity is much underestimated by the use of Laurentieff's equations without some correction.

It was suspected that this discrepancy was connected with the objection to his methods mentioned on page 20 above, i.e. his application of Michell's integral to a form which is not a closed body.

Therefore the effect was investigated of closing the boundary layer at the stern by the addition of a vertical parabolic cylinder (see Figure 1). The draught of this was the same as that of the model, and its thickness at the model stern equal to that of the boundary layer. Since the slope of the boundary layer at the stern varies with the depth, owing to the three-dimensional shape of the model, this cylinder cannot meet the boundary layer at the model stern without some discontinuity in the slope there.

The equation of this parabolic cylinder, referred to the usual axes of x, y, and z with the origin amidships and Ox reckoned positive in the direction of motion was

$$(x + L/2 + p)^2 = qy \qquad (18)$$

where the constants p and q are chosen so as to satisfy the conditions that, at the stern, when $x + L/2 = 0$, the value of y is the same as that of the boundary layer, and the slope dy/dx is the same as that of the boundary layer at a depth equal to 1/4 of the draught of

MODEL-829

Waterlines of Form and Boundary Layer, with Suggested Extension to Boundary Layer.

Froude Number N = 0.285, Reynolds' Number $R_e = 8.35 \times 10^6$

Beam scale exaggerated four times.

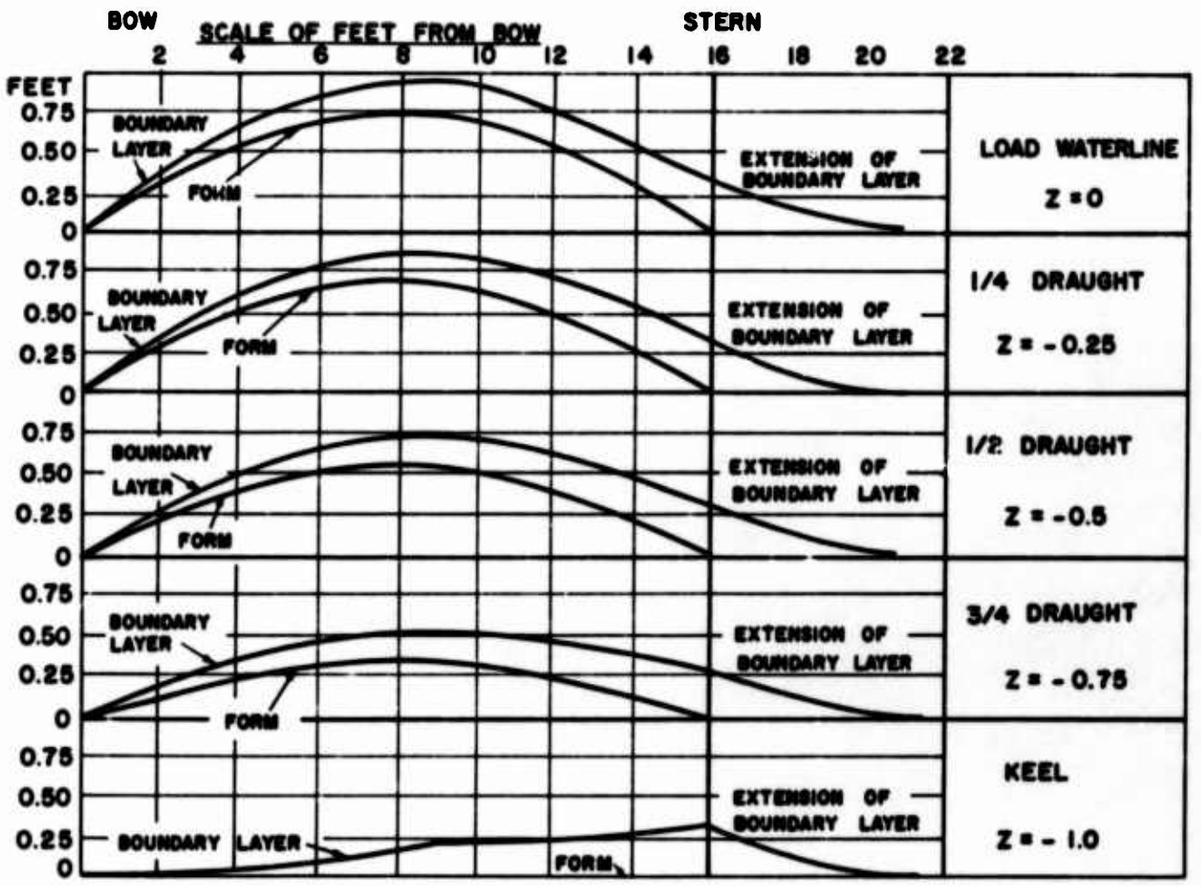


Figure 1.

the model. For the reasons stated above the slope cannot be made continuous at the stern for all depths with this form of ending, but this approximation will cause the discontinuity to be very small near the water surface, which is very much the most important region for the wave resistance.

For N = 0.285 the actual discontinuities are

Draft (feet)	Angle of Discontinuity (degrees)	
0	+0.5	
0.25	0	+ is convex to axis
0.50	-1.7	- is concave to axis
0.75	-4.3	
1.00	-8.0	

This discontinuity is hardly to be seen on the small scale figure of the figure, except near the keel. These considerations give the values of p and q as

$$p = 14.8.R_e^{-1/5} [0.138 - 0.37R_e^{-1/5}] \qquad (19)$$

$$q = 29.6.R_e^{-1/5} [0.138 - 0.37R_e^{-1/5}]^2$$

When terms involving the factor $R_e^{-2/5}$ are neglected as previously, this gives us an extra term in the viscous wave resistance

$$= r_1 = \frac{8\rho g^2}{v^2} \int_0^{\pi/2} J.J_c \sec^3\theta d\theta \qquad (20)$$

where

$$J = \int\int (\delta F/\delta x).e^{gx.\sec^2\theta/v^2}.\sin(gx.\sec\theta).dx.dz,$$

the double integral being taken over the central plane of the model.

Hence

$$J = \pi B.F(D).A.\cos(A/2)./(\pi^2 - A^2).D \qquad (21)$$

Also

$$J_c = \int\int 2(x + L/2 + p).e^{gz.\sec^2\theta/v^2}.\sin(gx.\sec\theta/v^2).dx.dz.$$

taken over the central plane of the parabolic extension.

Hence

$$J_c = -(1 - e^{-D}) \left[L^2.\sin(Ap/L + A/2) - L.^2\sin(A/2) - ALp.\cos(A/2)\right] /DA^2 \qquad (22)$$

whence

$$r_1 = \frac{\rho g^2.BL}{v^2} \int_0^{\pi/2} \frac{(1-e^{-D})}{DA^2} .F(\ ).\cos(A/2). \left[L.\sin(Ap/l. + A/2) - L.\sin.(A/2) - Ap.\cos(A/2)\right].d\theta \qquad (23)$$

In these A and D are the quantities defined in Equation (11). Also for Model 829, L = 16, B = 1.5, and T = 1. In order to simplify the equations the value of 1.0 has already been substituted for T.

Preliminary calculations have been made from these formulae for two Froude numbers of 0.284 and 0.303. The former was selected because previous work showed that the greatest effect of viscosity on wave resistance was to be expected at about that speed, and the latter was chosen to confirm that the effect decreases as the speed is increased beyond about a Froude number of about 0.29.

The value of $(r + r_1)/R_w$, the proportionate decrease in wave resistance due to viscosity was found to be 0.39 at N = 0.284, and 0.07 at N = 0.303.

These extensions of the form by the addition of parabolic cylinders derived as described above had lengths respectively of 5 feet and 4.8 feet, that is about 0.3 of the actual length of the form itself. It is deduced from the comparison of the calculated

and measured resistance curves that the effect of viscosity is actually to increase the effective length of the form by about 8 per cent, or 1.3 feet for this model.

This suggests that the suggested extensions are too long, and for this reason a calculation was made for a parabolic cylinder whose length was only 1.3 feet. This implied the neglect of the condition of continuity of angle at the stern, and angles of discontinuity there were then from 12 to 20 degrees.

At N = 0.284 the viscosity effect was reduced from 0.39 to 0.15, but this change must be largely due to the extra resistance of the comparatively large angles of discontinuity at the stern. In order to avoid these discontinuities an ending has been devised without them, but the numerical complexity was so great that no result has yet been obtained.

Comparison Between Ship and Model

The calculated effects of viscosity on wave resistance would cause the resistance of a ship, derived from that of a model, to be underestimated. Using the above preliminary results the resistance of a ship derived from experiments with a model of 16 feet length would be underestimated by the following percentages:

Froude Number	Ship Length 400 ft.	576 ft.	784 ft.	1024 ft.
0.284	5.4	5.8	6.1	6.3
0.303	1.1	1.2	1.2	1.3

Comparison with a similar calculation made by a different method, and for a different model (Reference 5) confirms the drop in the effect between the two Froude numbers. Attention should also be drawn to a recent paper by Emerson (Reference 6) who gives in Figure 1 of that paper a comparison between the wavemaking resistance for a model, and that of the corresponding ship (the Lucy Ashton). Assuming that any allowance for roughness does not depend on the Froude number, this shows a maximum difference between the two curves at a value of N = 0.27, which agrees well both with the curve of Reference 5, and with the above calculation.

General Conclusions and Proposed Further Progress

Although the numerical work has not advanced enough to enable general conclusions to be finally drawn, yet it appears at the present stage that Laurentieff's application of Michell's integral to a form which is not a closed body underestimates very greatly the effect of viscosity on the wave resistance.

The calculations made by an amended method give a result of the same order as found in other ways, which is also confirmed by model experiments with reversed unsymmetrical models, and, in one case, by an actual comparison of ship wave resistance with that of a model. Hence it is proposed to make further detailed calculations, both for the form already used, and also for a second form, in order to confirm the results. This second form will be unsymmetrical fore and aft, and its measured resistance is known in either direction of motion. The difference in resistance thus found on reversal can be compared directly with the difference in wave resistance in a viscous fluid, and should prove a good check on the accuracy of the various assumptions.

A P P E N D I X

VALUES OF $K_2 = \int_0^1 P^{-1/5}.\mathrm{SIN}(AP).dP$

BY COMPUTER

Calculated by Method of Pg. 23

A	K_2	A	K_2	A	K_2	A	K_2
0.2	+0.110761	8.6	+0.274751	17.0	+0.131618	24.61	0.05017
0.4	+0.219430	8.8	+0.284822	17.2	+0.118955	25.13	0.04411
0.6	+0.323971	9.0	+0.290889	17.4	+0.106374	25.66	0.04857
0.8	+0.422454	9.2	+0.292761	17.6	+0.097325	26.18	0.06225
1.0	+0.513108	9.4	+0.290418	17.8	+0.083228	26.71	0.07971
1.2	+0.594363	9.6	+0.284003	18.0	+0.073457	27.23	0.09982
1.4	+0.664892	9.8	+0.273810	18.2	+0.065327	27.75	0.10855
1.6	+0.723642	10.0	+0.260267	18.4	+0.059084	28.27	0.11175
1.8	+0.769857	10.2	+0.243917	18.6	+0.054895	28.80	0.10539
2.0	+0.803095	10.4	+0.225391	18.8	+0.052843	29.32	0.09178
2.2	+0.823233	10.6	+0.205381	19.0	+0.052927	29.85	0.07340
2.4	+0.830468	10.8	+0.184614	19.2	+0.055065	30.37	0.05852
2.6	+0.825297	11.0	+0.163822	19.4	+0.059096	30.89	0.04327
2.8	+0.808507	11.2	+0.143716	19.6	+0.064788	31.42	0.03835
3.0	+0.781139	11.4	+0.124956	19.8	+0.071850	31.94	0.04024
3.2	+0.744456	11.6	+0.108134	20.0	+0.079945	32.46	0.04809
3.4	+0.699904	11.8	+0.093749	20.2	+0.088702	32.99	0.06810
3.6	+0.649064	12.0	+0.082194	20.4	+0.097732	33.51	0.08377
3.8	+0.593607	12.2	+0.073742	20.6	+0.106644	34.03	0.09129
4.0	+0.535242	12.4	+0.068543	20.8	+0.115058	34.56	0.09395
4.2	+0.475667	12.6	+0.066617	21.0	+0.122624	35.08	0.08735
4.4	+0.416526	12.8	+0.067864	21.2	+0.129030	35.62	0.07336
4.6	+0.359357	13.0	+0.072064	21.4	+0.134017	36.13	0.06345
4.8	+0.305558	13.2	+0.078895	21.6	+0.137388	36.65	0.05089
5.0	+0.256347	13.4	+0.087943	21.8	+0.139010	37.18	0.03819
5.2	+0.212739	13.6	+0.098724	22.0	+0.138826	37.70	0.03415
5.4	+0.175520	13.8	+0.110705	22.2	+0.136846	38.75	0.04229
5.6	+0.145237	14.0	+0.123320	22.4	+0.133156	39.27	0.05961
5.8	+0.122189	14.2	+0.136000	22.6	+0.127905	39.79	0.07280
6.0	+0.106432	14.4	+0.148188	22.8	+0.121301	40.32	0.07914
6.2	+0.097788	14.6	+0.159365	23.0	+0.113603		
6.4	+0.095858	14.8	+0.169066	23.2	+0.105108		
6.6	+0.100052	15.0	+0.176896	23.4	+0.096140		
6.8	+0.109611	15.2	+0.182545	23.6	+0.087037		
7.0	+0.123643	15.4	+0.185797	23.8	+0.078134		
7.2	+0.141158	15.6	+0.186535	24.0	+0.069758		
7.4	+0.161106	15.8	+0.184745	24.2	+0.062205		
7.6	+0.182413	16.0	+0.180511	24.4	+0.055738		
7.8	+0.204022	16.2	+0.174012	24.6	+0.050572		
8.0	+0.224926	16.4	+0.165510	24.8	+0.046866		
8.2	+0.244202	16.6	+0.155341	25.0	+0.044722		
8.4	+0.261036	16.8	+0.143899				

A P P E N D I X

VALUES OF $K_1 = \int_0^1 P^{-1/5} . \cos(AP) . dP$

BY COMPUTER

Calculated by Method of Pg. 23

A	K_1	A	K_1	A	K_1	A	K_1
0.2	+1.242871	8.6	+0.151249	17.0	-0.019022	24.61	+0.00707
0.4	+1.221650	8.8	+0.131469	17.2	-0.020912	25.13	+0.02692
0.6	+1.186830	9.0	+0.109884	17.4	-0.020476	25.66	+0.04620
0.8	+1.139217	9.2	+0.087356	17.6	-0.017798	26.18	+0.06010
1.0	+1.079908	9.4	+0.064745	17.8	-0.013046	26.71	+0.06374
1.2	+1.010259	9.6	+0.042880	18.0	-0.006467	27.23	+0.05777
1.4	+0.931850	9.8	+0.022530	18.2	+0.001629	27.75	+0.04275
1.6	+0.846438	10.0	+0.004378	18.4	+0.010879	28.27	+0.02504
1.8	+0.755908	10.2	-0.011001	18.6	+0.020881	28.80	+0.00812
2.0	+0.662227	10.4	-0.023159	18.8	+0.031217	29.32	-0.00162
2.2	+0.567385	10.6	-0.031785	19.0	+0.041460	29.85	-0.00947
2.4	+0.473342	10.8	-.0036709	19.2	+0.051200	30.37	-0.00453
2.6	+0.381983	11.0	-0.037911	19.4	+0.060052	30.89	+0.00612
2.8	+0.295059	11.2	-0.035508	19.6	+0.067677	31.42	+0.02251
3.0	+0.214153	11.4	-0.029750	19.8	+0.073789	31.94	+0.03860
3.2	+0.140635	11.6	-0.021007	20.0	+0.078167	32.46	+0.05036
3.4	+0.075636	11.8	-0.009746	20.2	+0.080663	32.99	+0.05273
3.6	+0.020017	12.0	+0.003485	20.4	+0.081206	33.51	+0.04809
3.8	-0.025637	12.2	+0.018082	20.6	+0.079803	34.03	+0.03563
4.0	-0.061033	12.4	+0.033407	20.8	+0.076537	34.56	+0.02118
4.2	-0.086163	12.6	+0.048819	21.0	+0.071562	35.08	+0.00723
4.4	-0.101294	12.8	+0.063692	21.2	+0.065096	35.60	-0.00220
4.6	-0.106951	13.0	+0.077442	21.4	+0.057413	36.13	-0.00709
4.8	-0.103895	13.2	+0.089545	21.6	+0.048829	36.65	-0.00301
5.0	-0.093084	13.4	+0.099559	21.8	+0.039689	37.18	+0.00575
5.2	-0.075643	13.6	+0.107134	22.0	+0.030354	37.70	+0.01939
5.4	-0.052822	13.8	+0.112025	22.2	+0.021186	38.22	+0.03291
5.6	-0.025951	14.0	+0.114099	22.4	+0.012535	38.75	+0.04320
5.8	+0.003601	14.2	+0.113336	22.6	+0.004723	39.27	+0.04475
6.0	+0.034472	14.4	+0.109824	22.8	-0.001964	39.79	+0.03902
6.2	+0.065348	14.6	+0.103759	23.0	-0.007291	40.32	+0.01989
6.4	+0.095001	14.8	+0.095428	23.2	-0.011080		
6.6	+0.122326	15.0	+0.085199	23.4	-0.013216		
6.8	+0.146370	15.2	+0.073505	23.6	-0.013650		
7.0	+0.166351	15.4	+0.060824	23.8	-0.012403		
7.2	+0.181682	15.6	+0.047660	24.0	-0.009559		
7.4	+0.191979	15.8	+0.034524	24.2	-0.005264		
7.6	+0.197060	16.0	+0.021913	24.4	+0.000280		
7.8	+0.196945	16.2	+0.010292	24.6	+0.006829		
8.0	+0.191848	16.4	+0.000076	24.8	+0.014100		
8.2	+0.182152	16.6	-0.008384	25.0	+0.021787		
8.4	+0.168398	16.8	-0.014813				

LIST OF SYMBOLS

(Foot-pound-second units used throughout)

Symbol	Meaning
a	1/2 length of form
A	$kL.\sec\theta$
b	1/2 beam of form
B	Beam of form (=2b)
d	draught of form
D	$kT.\sec^2\theta$
e	exponential constant (2.718)
g	gravitational constant (32.2)
I	integrals defined in Equation (9)
I_1	
j	integral defined in Equation (21)
J_c	integral defined in Equation (22)
k	g/v^2
$K_1(A)$	$\int_0^1 P^{-1/5}.\cos(AP).dP$
$K_2(A)$	$\int_0^1 P^{-1/5}.\sin(AP).dP$
L	Length of form (2a)
N	Froude Number ($= v/\sqrt{gL}$
p	constant in Equation (18)
P	X/L
q	constant in Equation (18)
r	wave resistance correction for viscosity from Laurentieff
R_e	Reynolds' Number = vL/ν
R_L	calculated wave resistance in viscous fluid from Laurentieff ($= R_w + r$)
R_w	calculated wave resistance in a perfect fluid
t	thickness of boundary layer
t_s	thickness of boundary layer at stern
T	draught of form (=d)
v	speed of advance
x	distance forward of amidships
X	distance aft from bow ($= L/2 - x$)
y	distance from center line
Y	do do do do
z	distance above water surface
Z	do do do do

Symbol	Meaning
θ	independent variable of integ. ion
ν	kinematic coefficient of viscosity, taken as 1.236×10^{-5} for water
π	ratio of circumference to radius of circle = 3.1416
ρ	density of water (= 1.938)

LIST OF REFERENCES

1. Third Report to O.N.R. on Calculation of Wave Resistance at Low and Moderate Speeds, by C. Wigley, March, 1961.

2. Calculations Illustrating the Effect of Boundary Layer on Wave Resistance by T. H. Havelock, T.I.N.A. Vol. 90, p. 92 (1948).

3. Schiffsbautechnik Bd. 9, 1962, Heft 46, p. 69.

4. The Influence of the Boundary Layer on the Wave Resistance of a Ship, V.M. Laurentieff (Translation No. 245 of D.T.M.B. dated April 1952 by Ralph D. Cooper).
   Original Russian Reports of the Academy of Science, U.S.S.R., 1951, Vol. LXXX, No. 6.

5. The Effect of Viscosity on Wave Resistance by C. Wigley, Schiffsbautechnik, Heft 46, Band 9, April 1962, p. 69.

6. A Note on Froude's Law by A. Emerson, paper read at meeting of April, 1963 of R.I.N.A., will appear in Trans. I.N.A., Vol. 105.

NOTE: Trans. I.N.A. stands for Transactions of Royal Institution of Naval Architects, London.

ON THE DETERMINATION OF THE WAVE RESISTANCE OF A SHIP MODEL BY AN ANALYSIS OF ITS WAVE SYSTEM

PART II

K. Eggers

Institut Fur Schiffbau
University of Hamburg

Translated from paper published in Schiffstechnik Bd. 10 - Heft 52, June 1963.

ON THE DETERMINATION OF THE WAVE RESISTANCE OF A SHIP MODEL BY AN ANALYSIS OF ITS WAVE SYSTEM

In a previous paper (Schiffstechnik, Vol. 9, 1962) it was shown that the energy transport in the wave system of a ship, - and thereby its wave resistance, - can be determined from the velocity distribution in a control plane perpendicular to the direction of travel. If in some domain validity of a linearized theory is assumed and if the flow is supposed to be represented there by a series of 'free waves' - i.e. of single waves which appear stationary when reviewed from the ship and which separately satisfy all boundary conditions of the problem if the ship were not present - , then the resistance can already be determined from the measurement of the wave profile in the control plane and its derivative in the direction of travel. All information necessary is provided by the 'spectrum', i.e. the amplitude distribution, of the free wave system. It was shown that formal expressions for these amplitudes could be obtained from measurement of two wave profiles perpendicular to the direction of travel or from profiles parallel to this direction for motion along a canal of finite width.

In the following, a justification of the assumptions underlying above statements is presented. We show that in general the velocity distribution in two control surfaces is necessary must be known to determine the wave pattern in the region between them, but that in some interior region, far enough from both of them, we will essentially have a pattern of free waves which always can be determined from the flow distribution in <u>one</u> vertical plane therein and this again is determined for free waves by the configuration of the wave profile induced in this plane and its derivative normal to this plane.

Experimentally, it has already been shown by Sarma by evaluation of a series of stereographic photographs that the portion of free waves dominates even in a region as close as a fourth of the model length behind the stern for medium Froude numbers. In particular he found that even in the domain afront of the bow wave system's reflection at the tank walls the free wave system can adequately be represented by waves compatible with the finite tank width restriction. This might be considered in contradiction to the argument that influence of tank width on wave pattern should be felt only after wave reflection has happened. But it appeared that ahead of reflection domain dustribution of amplitudes is not essentially influenced by choice of some hypothetical tank width by making the

continuous spectrum a discrete one, provided b is sufficiently large. Behind the region of reflection, however, consistence of free wave concept will not result if we let a wrong tank width underly our evaluations.

Application of the formulas derived for determination of amplitude components from profiles along longitudinal cuts, as derived earlier, assumes first of all uniform convergence of the series expression for the free wave system in a region extending to infinity behind the ship. We show that for any truncation of the profile to a finite length the strong accumulation of admitted compatible wave numbers will permit uniform approximation of any arbitrary continuous wave profile even if the amplitudes of any finite number of wave components selected from the set admitted is arbitrarily fixed in advance! And thus the wave profile does not produce sufficient information even for an upper estimate of the amplitudes. This obviously reflects the fact that the flow distribution on a vertical plane of infinite extent, but still not a closed boundary, does not yield pertinent information to the elliptical boundary problem present here.

If we proceed from the premise that a finite number of non-zero components can represent the free wave system adequately, then the amplitudes of these are determined uniquely as linear combinations of the Fourier coefficients of profiles from sections oblique to the ship's path or parallel and truncated at finite distance. However, this leads to systems of linear equations, as only for perpendicular the orthogonality relations of trigonometric functions - resp. the inversion formula for Fourier integrals in case of unrestricted water - can be utilized.

The expressions derived earlier for very long profiles along longitudinal cuts are based on orthogonality relations of the bases of almost-periodic functions and thus avoid inversion of linear equations. Some numerical examples, however, based on a theoretical amplitude distribution, showed that even under assumption of a finite number of components contributing to the profile the profile must be taken of tremendous length in order to yield reasonable approximation for the wave resistance to be determined.

The following investigations are based on the construction of the velocity potential due to a source singularity which proceeds with uniform velocity beyond the free surface of water in a canal of width b and depth h . This potential surves as a Green's function of our boundary value problem. Although the present paper in its structure

and notation was devised as a second part to previous work, the derivations should possibly be followed independently. All notations and some references to the first part are listed at the end of this work.

4. Stepwise Approach to the Wave Field of a Source Moving Stationary in a Canal

The velocity potential $G(x,y,z)$ of a source with output -4π in a point $\{\xi,\eta,\zeta\}$ with $-b/2 \leq \eta \leq b/2$, $-h \leq \zeta \leq 0$, moving stationary with speed c in x direction, is determined by the conditions:

$$\Delta\,(G-1/r) = 0 \quad \text{in the domain} \quad \{-b/2 \leq y \leq b/2,\ -h \leq z \leq 0\}\ . \tag{4.01}$$

where $r = \sqrt{(x-\xi)^2 + (y-\eta)^2 + (z-\zeta)^2} \geq 0$ is

$$G_y = 0 \text{ for } y = b/2 \quad \text{(tank wall)} \tag{4.02}$$

$$G_y = 0 \text{ for } y = -b/2 \quad \text{(tank wall)} \tag{4.03}$$

$$G_x = 0 \text{ for } z = -h \quad \text{(tank bottom)} \tag{4.04}$$

$$G_{xx} + K_o G_z = 0 \quad \text{for} \quad z = 0 \tag{4.05}$$

(Linearized boundary condition for the free surface)

$$\lim_{x \to \infty} G_x = 0 \tag{4.06}$$

(Radiation of waves in aft direction only).

First we restrict our analysis to determination of the function G_x representing the flow component in x direction, subject to the same boundary conditions (4.01) - (4.06) as G ; this makes sure convergence of some series and the legitimacy of some limiting processes we have to perform in intermediary steps. The components G_y and G_z are uniquely determined by G_x . If two different integral functions to G_x satisfy all conditions (4.01)- (4.05), then their difference as a potential function depending on y and z only can only be a constant, as its normal derivatives at the boundaries of the domain $\{-b/2 \leq y \leq b/2,\ -h \leq z \leq 0\}$ are identically zero due to (4.02) - (4.05).

Introducing polar coordinates by relations

$$x - \xi = \varrho \cos\alpha ; \quad y - \eta = \varrho \sin\alpha \tag{4.07}$$

we have[10] for $z - \zeta \neq 0$, $\sigma = \frac{z-\zeta}{|z-\zeta|}$:

$$G_1 \doteq (\varrho^2 + (z-\zeta)^2)^{-1/2} = \int_0^\infty J_0(k\varrho)\, e^{-\sigma k (z-\zeta)}\, dk \tag{4.08}$$

(J_0 = Bessel Function) and as we have[9]

$$J_0(k\varrho) = {}^1/_{2\pi} \int_0^{2\pi} e^{ik\varrho\cos\Theta}\, d\Theta = {}^1/_{2\pi} \int_0^{2\pi} e^{ik\varrho\cos(\Theta-\alpha)}\, d\Theta \tag{4.09}$$

we finally get

$$G_1 = {}^1/_{2\pi} \int_0^{2\pi}\int_0^\infty e^{-\sigma k(z-\zeta) + ik\varrho\cos(\Theta-\alpha)}\, dk\, d\Theta \tag{4.10a}$$

and for the derivative regarding x :

$$G_{1x} = {}^1/_{2\pi} \int_0^{2\pi}\int_0^\infty ik\cos\Theta\, e^{-\sigma k(z-\zeta) + ik\varrho\cos(\Theta-\alpha)}\, dk\, d\Theta. \tag{4.10b}$$

The substitution of variables

$$u \doteq k\sin\Theta \qquad\qquad w \doteq k\cos\Theta \tag{4.11}$$

with Jacobian

$$\frac{\delta(u,w)}{\delta(k,\Theta)} = k \geq 0 \tag{4.12}$$

results to the Fourier integral representation

$$G_{1x} = {}^1/_{8\pi} \int_0^\infty\int_0^\infty iw\, k^{-1}\, e^{-\sigma k(z-\zeta) + iu(y-\eta) + iw(x-\xi)}\, du\, dw, \tag{4.13}$$

where we kept the symbol k with the meaning

$$k \doteq \sqrt{u^2 + w^2} \geq 0 . \tag{4.14}$$

We now construct the function $G_x(x,y,z)$ starting with G_{1x} by addition of complementary terms which successively provide for satisfaction of conditions (4.02) - (4.06).

A function G_{2x} which meets condition (4.02), can be found by reflection on the wall $y = b/2$ in a form as

$$G_{2x} \doteqdot G_{1x}(x, y, z) + G_{1x}(x, b - y, z) . \tag{4.15}$$

The further boundary condition (4.03) is met by the expression

$$G_{3x} \doteqdot \sum_{\gamma=-\infty}^{\infty} G_{2x}(x, y + 2\gamma b, z) \tag{4.16}$$

which develops by continued reflection on the planes $y = 2b\gamma$ ($\gamma = \pm 1, 2, \ldots$).

In detail from (4.13), (4.15), and (4.16) we get the convergent expression

$$G_{3x} = {}^{1}/_{8\pi} \int_{-0}^{\infty} \int_{-0}^{\infty} iw/k^{-1}\, e^{-k(z-\zeta)+iw(x-\xi)} \cdot dw \cdot (e^{-iuy} + e^{iu(b-y)})\, e^{-iu\eta} \lim_{N\to\infty} \sum_{\gamma=-N}^{N} e^{2b\gamma iu}\, du . \tag{4.17}$$

Application of the identities

$$\sum_{-N}^{N} e^{i2b\gamma u} \equiv \frac{\sin(2N+1)bu}{\sin bu} \tag{4.18}$$

and[15]

$$F(u_\nu) = \lim_{N\to\infty} \frac{1}{\pi} \int_{u_\nu - \frac{\pi}{2b}}^{u_\nu + \frac{\pi}{2b}} F(u) \frac{\sin Nbu}{\sin bu}\, b\, du \tag{4.19}$$

for continuous function $F(u)$ and

$$u_\nu \doteqdot \frac{\nu\pi}{b} \quad (\nu = 0, \pm 1, \pm 2, \ldots) \tag{4.20}$$

gives

$$G_{3x} = \frac{1}{2b} \int_{w=-\infty}^{\infty} e^{iw(x-\xi)} \sum_{\nu=-\infty}^{\infty} e^{ek_\nu(z-\zeta)} \frac{iw}{k_\nu}\, dw \left(e^{iu_\nu(y-\eta)} + e^{iu_\nu(b-y-\eta)} \right) \tag{4.21}$$

with

$$k_\nu \doteqdot \sqrt{w^2 + u_\nu^2} \geq 0 \tag{4.22}$$

i.e.

$$G_{3x} = \frac{1}{b} \int_{-\infty}^{\infty} \sin w(x - \xi) \sum_{\nu=-\infty}^{\infty} e^{-ek_\nu(z-\zeta)} \frac{w}{k_\nu}\, dw \cdot \cos u_\nu(b/2 - y) \cos u_\nu(b/2 - \eta) . \tag{4.23}$$

The formula (4.23) shows that the effect of infinite number of reflections is equivalent to summation of the integral (4.13) regarding the variable u by trapezoidal rule as quadrature formula, selecting a stepwidth of $\Delta u = \pi/b$; the limiting process $b \to \infty$ then reduces (4.23) to (4.13).

The term $\nu = 0$ of (4.23) by the way corresponds to the x-component of the flow due to a source of output $-4\pi/b$ in plane two dimensional flow with potential

$$\varphi(q) = \frac{-1}{b} \ln \{(x-\xi)^2 + (z-\zeta)^2\} \tag{4.24}$$

as we have[11]

$$\varphi_x(q) = -\frac{2(x-\xi)}{b((x-\xi)^2 + (z-\zeta)^2)} = \frac{-2}{b} \int_0^\infty e^{-w(z-\zeta)} w \sin w(x-\xi)\, dw . \tag{4.25}$$

To meet the boundary condition (4.04) on the bottom we complete G_{3x} by a reflection on the bottom, i.e. we put

$$G_{4x}(x,y,z) = G_{3x}(x,y,z) + G_{3x}(x,y-2h-z) . \tag{4.26}$$

For the domain of physical interest, i.e. for $z \geq -h$, in the second part of (4.26) corresponding to (4.23) we have to insert $\sigma = -1$, and thus get in detail

$$G_{4x} = -\frac{1}{b} \int_{-\infty}^{\infty} w \sin w(x-\xi) \sum_{\nu=-\infty}^{\infty} \frac{1}{k_\nu} \{(1+\sigma) e^{-k_\nu(\zeta+h)} \mathfrak{Cof}\, k_\nu(z+h) + (1-\sigma) e^{-k_\nu(\zeta+h)} \mathfrak{Cof}\, k_\nu(z+h)\}\, dw \cos u_\nu \left(\frac{b}{2} - y\right) \cos u_\nu \left(\frac{b}{2} - \eta\right) \tag{4.27}$$

Convergence and summability of the integrand for $z - \zeta \neq 0$ can be derived from the estimate

$$\sum_{\nu=-\infty}^{\infty} \left[\frac{w}{k_\nu} (1+\sigma) \mathfrak{Cof}\, k_\nu(\zeta+h) e^{-k_\nu(z+h)} + \frac{w}{k_\nu} (1-\sigma) \mathfrak{Cof}\, k_\nu(z+h) e^{-k_\nu(\zeta+h)} \right]$$

$$\leq \sum_{\nu=-\infty}^{\infty} 2 \frac{w}{k^\nu} e^{\sigma k_\nu |z-\zeta|} \leq 2 \sum_{\nu=-\infty}^{\infty} e^{-\left|\frac{u_\nu}{2}(z-\zeta)\right|} \cdot e^{-\left|\frac{w}{2}(z-\zeta)\right|} ; \tag{4.28}$$

and as the integrand of (4.27) is holomorphic on the real w-axis and thereby differentiable, we have by partial integration

$$G_{4x} = 0\{(x-\xi)^{-1}\}. \tag{4.29}$$

If we determine an integral function G_4 to G_{4x} by replacing the factor $\sin(w_\nu x)$ by the term $-1/w$, $\cos(w_\nu x)$ in the summands of (4.27) with $\nu \neq 0$, and if for the term $\nu = 0$ we make use of relations (4.24), (4.25) we find this function as

$$G_4 = \frac{2}{b}\int_{-\infty}^{\infty} \cos w(x-\xi) \sum_{\nu=1}^{\infty} \frac{1}{k_\nu}\Big((1+\sigma)\, e^{-k_\nu(z+h)} \operatorname{Cof} k_\nu(\zeta+h) + (1-\sigma)\, e^{-k_\nu(\zeta+h)} \operatorname{Cof} k_\nu(z+h)\Big) dw \cdot \cos u_\nu(b/2-y) \cos u_\nu(b/2-\eta) - \frac{1}{b}\ln\{(x-\xi)^2+(z-\zeta)^2\} \tag{4.30}$$

and by an estimate similar to (4.28)

$$G_4 = -\frac{1}{b}\ln\{(x-\xi)^2+(z-\zeta)^2\} + 0\{(x-\xi)^{-1}\} \tag{4.31}$$

The fact that the estimates (4.29) and (4.31) - corresponding to (4.08) - can be derived only for $z \neq \zeta$ is of no concern for our derivations to follow, as we will have to find estimates only for integrals regarding ζ, the integrands of which are products of G or G_x with bonded functions. Essentially we have

$$\begin{aligned}
&\int_a^e \{(1+\sigma)\, e^{-k_\nu(z+h)} \operatorname{Cof} k_\nu(\zeta+h) + (1-\sigma)\, e^{-k_\nu(\zeta+h)} \operatorname{Cof} k_\nu(z+h)\}\, d\zeta \\
&= 2\int_{-h}^{e} e^{-k_\nu(z+h)} \operatorname{Cof} k_\nu(\zeta+h)\, d\zeta + 2\int_{z}^{e} e^{-k_\nu(\zeta+h)} \operatorname{Cof} k_\nu(z+h)\, d\zeta \\
&= -\frac{2}{k} e^{-k_\nu(z+h)}\{\operatorname{Sin} k_\nu(z+h) - \operatorname{Cof} k_\nu(z+h)\} + e^{-k_\nu h} \operatorname{Cof} k_\nu(z+h) = \\
&= -\frac{2}{k}\{e^{-k_\nu h} \operatorname{Cof} k_\nu(z+h) - e^{-2k_\nu(z+h)}\}
\end{aligned} \tag{4.32}$$

and with increasing k_ν this has exponential decay. It follows that for estimates of the integrals ((6.13), (6.14) ff) the relations (4.29), (4.31) may be used as well for $z = \zeta$, provided $z < 0$.

To satisfy the boundary condition for the free surface (4.05) as well, we complete G_{4x} by a term which, similar to (4.27) in case $\sigma = -1$, corresponds to a distribution of sources beyond the free surface in the plane $\zeta = h$. We set $G_{5x}(x,y,z) \doteqdot G_{4x}(x,y,z) +$

$$+ \sum_{\nu=-\infty}^{\infty} \frac{1}{b} \int_{-\infty}^{\infty} L_\nu(w) \operatorname{Cof}(k_\nu(z+h)) \sin(w(x-\xi))\, dw \cdot \cos u_\nu\left(\frac{b}{2} - y\right) \cos u_\nu\left(\frac{b}{2} - \eta\right) \tag{4.33}$$

and determine the functions $L_\nu(w)$, by postulating the condition equivalent to (4.05)

$$G_{5xxx} + K_0 G_{5xz} = 0 \qquad \text{for } z = 0 \tag{4.34}$$

for the single terms of the Fourier representation (4.27) regarding y. We derive the relations

$$2(w^2 + k_\nu K_0) e^{-k_\nu h} \operatorname{Cof}(k_\nu(\zeta+h)) + (K_0 k_\nu \operatorname{Tg}(k_\nu h) - w^2) \operatorname{Cof}(k_\nu h) \cdot L_\nu(w) = 0 \qquad (\nu = 0, 1, 2, \ldots) \tag{4.35}$$

i.e.

$$G_{5x} = G_{4x} - \sum_{\nu=-\infty}^{\infty} \frac{2}{b} \int_{-\infty}^{\infty} \frac{J_\nu(w)}{H_\nu(w)} \sin w(x-\xi)\, dw \cos u_\nu\left(\frac{b}{2} - y\right) \cos u_\nu\left(\frac{b}{2} - \eta\right) \tag{4.36}$$

with

$$J_\nu(w) \doteqdot \frac{w(w^2 + k_\nu K_0) \operatorname{Cof}(k_\nu(z+h)) \operatorname{Cof}(k_\nu(\zeta+h)) e^{-k_\nu h}}{k_\nu \operatorname{Cof} k_\nu h} \tag{4.37}$$

and

$$H_\nu(w) \doteqdot K_0 k_\nu \operatorname{Tg} k_\nu h - w^2. \tag{4.38}$$

5. The Accomplishment of the Asymptotic Boundary Conditions

After a determination of the zeros of the functions $H_\nu(w)$ in the complex w-plane we have the possibility to develop the integrals regarding w in (4.33) in series due to the corresponding residual contributions, which provide a complete set of eigenfunctions to represent any solution of (4.02) - (4.05). However, for our present investigation we are interested only in the behavior of G_{5x} for large values of $|x - \xi|$. We shall se that in this domain only the contribution of the single positive real zeros w_ν of the functions $H_\nu(w)$ are essential.

We have

$$H_\nu(0) = u_\nu K_0 \operatorname{Tg} u_\nu h \geq 0 \tag{5.01}$$

whereas for large values of w the term $-w^2$ is dominant. We further have

$$\frac{dk_\nu}{dw} = \frac{w}{k_\nu} \tag{5.02}$$

and thereby

$$\frac{dH_\nu}{dw} = \frac{K_0}{k_\nu} w \operatorname{Tg} k_\nu h + w K_0 h \operatorname{Cof}^{-2} k_\nu h - 2w \tag{5.03}$$

and for a real zero w_ν of H_ν we especially have

$$\frac{dH_\nu}{dw} = -w_\nu \operatorname{Cof}^{-2} \varkappa_\nu h \left\{ \operatorname{Cof}^2 \varkappa_\nu h \cdot \left(1 + \frac{u_\nu^2}{\varkappa_\nu^2} \right) - K_0 h \right\} \tag{5.04}$$

with

$$\varkappa_\nu = \sqrt{u_\nu^2 + w_\nu^2} > 0 . \tag{5.05}$$

The value (5.04) is always smaller than zero, as from a relation

$$\operatorname{Cof}^2 \varkappa_\nu h \cdot (1 + u_\nu^2/\varkappa_\nu^2) \leq K_0 h \tag{5.06}$$

there would follow

$$\operatorname{Cof}^2 \varkappa_\nu h \left(1 + \frac{u_\nu^2}{w_\nu^2} \right) \leq \frac{w_\nu^2 h}{\varkappa_\nu} \operatorname{Ctg} \varkappa_\nu h \tag{5.07}$$

and thereby

$$\mathfrak{Sin}\, 2\varkappa_\nu h \frac{1+\frac{u_\nu^2}{w_\nu^2}}{1-\frac{u_\nu^2}{w_\nu^2}} \leq 2\varkappa_\nu h \tag{5.08}$$

which is possible only for $u_\nu = w_\nu = 0$. However, if the continuous and bounded function $H_\nu(w)$ has a negative derivative for all its zeros, it can have one zero only!

We further have

$$w_{\nu+1} > w_\nu \qquad (\nu = 1, 2, \ldots) \tag{5.09}$$

and if $u_\nu > K_0\sqrt{2}$, we have

$$u_\nu \geq w_\nu \tag{5.10}$$

as the inequality

$$u_\nu^2 < w_\nu^2 = K_0\sqrt{u_\nu^2 + w_\nu^2}\ \mathfrak{Tg}\,(\sqrt{u_\nu^2 + w_\nu^2}\cdot h) \leq K_0\sqrt{2}\,u_\nu \tag{5.11}$$

leads to a contradiction of (5.10).

From (4.37) we find

$$J_\nu(w) \leq (K_0 + w)\, w\, e^{k_\nu(z+\zeta)} \tag{5.12}$$

we further have

$$\frac{dJ_\nu}{dw} = \frac{wJ_\nu}{k_\nu}\left\{\frac{2k_\nu + k_0}{w^2 + k_\nu K_0} - \frac{1}{k_\nu} + (z+h)\,\mathfrak{Tg}\,k_\nu(z+h) + \right.$$
$$\left. + (\zeta+h)\,\mathfrak{Tg}\,k_\nu(\zeta+h) - h\,\mathfrak{Tg}\,k_\nu h\right\}. \tag{5.13}$$

If for the density of the values w_ν we take as a measure the number of values $\mu < \nu$, for which $|w_\mu| < |w_\nu|$ holds, divided by the absolute value of w_ν then the limit of this ratio, the asymptotic density, becomes infinite, as we have

$$\lim_{\nu\to\infty}\frac{\nu}{w_\nu}=\frac{b}{\pi}\lim_{\nu\to\infty}\frac{u_\nu}{\sqrt{K_0 x_\nu \operatorname{tg} x_\nu h}}\geq\frac{b}{\pi}\lim_{\nu\to\infty}\sqrt{\frac{u_\nu}{K_0\sqrt{2}}}=\infty\,! \tag{5.14}$$

From (5.03) and (5.13) it follows that to any value $K_0h>0$ and to any constant Δ with $0<\Delta<2$ there exists a value ν_0 such that for any $\nu\geq\nu_0$ we have

$$-w\Delta\geq\frac{dH_\nu}{dw}\geq-2w \tag{5.15}$$

$$-\Delta\geq\frac{d^2H_\nu}{dw^2}\geq-2 \tag{5.16}$$

$$0<\frac{dJ_\nu}{dw}<J_\nu w\Delta \tag{5.17}$$

for all $w\geq 0$ and finally

$$|u_\nu|\geq K_0\sqrt{2} \tag{5.18}$$

to guarantee (5.10).

For $\nu=0$ we have $k_\nu=w$; $H_0(w)$ has a twofold zero at $w=0$, another one, which is simple, at w_0 , which is the positive root of

$$K_0 \operatorname{tg} wh - w = 0 \tag{5.19}$$

which exists under $k_0h>0$ only, as only then (5.03) will become negative for $w=0$. We split up

$$\frac{1}{H_0}=\delta_0\frac{1}{H_0}+(1-\delta_0)\frac{1}{H_0} \tag{5.20}$$

with

$$\delta_0\doteq w/w_0 \quad \text{for } K_0h>1 \tag{5.21}$$

$$\delta_0\doteq 0 \qquad \text{for } K_0h>1 \tag{5.22}$$

and thus have from (4.36)

$$G_{5x} = G_{4x} - \frac{4}{b} \sum_{\nu=-\infty}^{\infty} \int_0^{\infty} \delta_\nu \frac{J_\nu(w)}{H_\nu(w)} \sin w_\nu (x-\xi)\, dw$$

$$\cdot \cos u_\nu (b/2-y) \cos u_\nu (b/2-\eta) - \frac{-4}{b} \int_0^{\infty} (1-\delta_0) \frac{J_0(w)}{H_0(w)} \sin w (x-\xi)\, dw \qquad (5.23)$$

with

$$\delta_\nu \doteqdot 1 \qquad \text{for } \nu \neq 0. \qquad (5.24)$$

The improper integrals on the right side of (5.23) shall be defined in the sense of Cauchy principal values; we th achieve that G_{5x} - same as G_{4x} - becomes an odd function of $x - \xi$. To meet the asymptotic boundary condition (4.06) we then require an even complementary term, which cancels G_{5x} for large positive x. This term might be interpreted as a modification of the path of integration in the complex w-plane with tendency to bypass the poles on the real axis in the lower half plane. We shall see that only the value of the integrand function in the vicinity of these poles contributes to the asymptotic expressions, i.e. only the ratios $J_\nu(w_\nu)/H_\nu(w_\nu)$.

After selection of a suitable number ε with $0 < \varepsilon < w_{\nu_0}$ we therefore perform splitting up as

$$\frac{J_r(w)}{H_r(w)} = F_r^{(1)}(w) + F_r^{(2)}(w) + F_r^{(3)}(w) + F_r^{(4)}(w) \qquad (5.25)$$

$$F_r^{(1)} \doteqdot 0 \text{ for } |w-w_r| \leq \varepsilon; \quad F_r^{(1)} \doteqdot \frac{J_r(w)}{H_r(w)} \text{ for } |w-w_r| > \varepsilon \qquad (5.26)$$

$$F_r^{(2)} \doteqdot \frac{J_r(w) - J_r(w)}{H_r(w)} \text{ for } |w-w_r| \leq \varepsilon; \; F_r^{(2)} \doteqdot 0 \text{ for } |w-w_r| > \varepsilon \qquad (5.27)$$

$$F_r^{(3)} \doteqdot \frac{J_r(w_r)}{H_r(w_r)} - \frac{J_r(w_r)}{H_r'(w_r)} \cdot \frac{1}{w-w_r} \text{ for } |w-w_r| \leq \varepsilon;$$

$$F_r^{(3)} \; 0 \text{ for } |w-w_r| > \varepsilon \qquad (5.28)$$

$$F_r^{(4)} \doteqdot \frac{J_r(w_r)}{H_r'(w_r)} \cdot \frac{1}{w-w_r} \text{ for } |w-w_r| \leq \varepsilon;$$

$$F_r^{(4)} \doteqdot 0 \text{ for } |w-w_r| > \varepsilon \quad . \qquad (5.29)$$

Of all functions thus defined only the functions $F_4(w)$ are not bounded at the points $w = w_\nu$, they have single poles. To obtain some estimates we shall now assume that $z + \zeta < 0$; i.e. that location of source and of flow are not in the undisturbed free surface simultaneously. For the present, let us further assume $\nu > \nu_0$. Then the mean value theorem of differential calculus gives

$$|H_\nu(w)| = |w - w_\nu| \, |H_\nu'(\hat{w}_\nu)| \tag{5.30}$$

with

$$w_\nu \leq \hat{w}_\nu \leq w \text{ for } w \geq w_\nu ; \; w \leq \hat{w}_\nu \leq w_\nu \text{ for } w \geq w_\nu \tag{5.31}$$

But due to (5.15) this means

$$|H_\nu(w)| \geq |w - w_\nu| \, \Delta \cdot w_\nu \qquad \text{for } w \geq w_\nu \tag{5.32}$$

$$|H_\nu(w)| \geq |w - w_\nu| \, \Delta \cdot w \qquad \text{for } \varepsilon \leq w \leq w_\nu \tag{5.33}$$

(i.e. for almost all ν for fixed w)

$$|H_\nu(w)| \geq H_{\nu_0}(\varepsilon) \qquad \text{for } 0 \leq w \leq \varepsilon \tag{5.34}$$

and therefore there exist a positive bond

$$S = \text{Min} \{\varepsilon^2 \Delta, H_{\nu_0}(\varepsilon)\} \tag{5.35}$$

such that if $|w - w_\nu| > \varepsilon$ we have, uniformly in w and for all $\nu > \nu_0$

$$|H_\nu(w)| \geq S . \tag{5.36}$$

and due to (5.12) we then have

$$|F_\nu^{(1)}(w)| \leq \frac{(K_0 + w)}{S} \, w \, e^{k_\nu (z+\zeta)} . \tag{5.37}$$

The derivatives of the functions $F_\nu^{(i)}$ - $(i = 1,2,3,4)$ - are not uniquely defined at the points $|w - w_\nu| = \varepsilon$; if we fix their value to zero then, we have

$$\left|\frac{dF_\nu^{(1)}}{dw}\right| \leq \left|\frac{J_\nu'}{H_\nu}\right| + \left|\frac{J_\nu H_\nu'}{H^2}\right| \leq J_\nu \left\{\frac{w\Delta}{S} + \frac{2w}{S^2}\right\} \leq 2w^2 (w + K_0) \cdot \left\{\frac{w\Delta}{S} + \frac{2w}{S^2}\right\} e^{w(z+\zeta)} \tag{5.38}$$

due to (5.12) and (5.22), i.e. $\dfrac{dF_\nu^{(1)}}{dw}$ is integrable regarding w.

And as we have

$$\frac{u_\nu}{2} + \frac{w_\nu}{2} \leq \sqrt{u_\nu^2 + w_\nu^2} = k_\nu \tag{5.39}$$

it follows from (5.12) that

$$\sum_{\nu=\nu_0}^{\infty} F_\nu^{(1)}(w) \leq \frac{w(w+K_0)}{S} e^{w(z+\zeta)/2} \sum_{\nu=\nu_0}^{\infty} e^{\nu\pi(z+\zeta)/2b} \tag{5.40}$$

and this means that the sum is convergent and integrable in the interval $0 \leq w < \infty$. As the functions $F_\nu^{(1)}(w)$ with $\nu \leq \nu_0$ are integrable as well, we find:

The integral $\int_0^\infty \sum_{\nu=1}^{\infty} F_\nu^{(1)}(w) \sin w\,(x-\xi)\,dw$ exists.

Consider now the function

$$F_\nu^{(2)}(w) = \frac{J_\nu(w_\nu) - J_\nu(w)}{H_\nu(w)} \text{ for } |w - w_\nu| \leq \varepsilon . \tag{5.41}$$

Application of the mean value theorem to the function J_ν and H_ν gives

$$F_\nu^{(2)}(w) = -\frac{J_\nu'(\tilde{w}_\nu)(w - w_\nu)}{H_\nu'(\hat{w}_\nu)(w - w_\nu)} \tag{5.42}$$

where the derivatives J_ν' and H_ν' are taken in general at two different points $\tilde{w}_\nu$ and $\hat{w}_\nu$. Due to (5.10), (5.12), (5.15) we then get the estimate

$$|F_\nu^2(w)| \leq \frac{(w_\nu + \varepsilon)\,\Lambda \cdot J_\nu(w)}{(w_\nu - \varepsilon)\,\Delta} \leq \frac{(u_\nu + \varepsilon)(u_\nu + K_0 + \varepsilon)}{w_{\nu_0} - \varepsilon} e^{(u_\nu + \varepsilon)(z+\zeta)} . \tag{5.43}$$

As we have $H_\nu(w_\nu) = 0$, we may write the expression (5.28) for $F_\nu^{(3)}(w)$ as follows:

$$F_\nu^{(3)}(w) = J_\nu(w_\nu) \frac{H_\nu(w) - [H_\nu(w_\nu) + (w - w_\nu) H_\nu'(w_\nu)]}{H'(w_\nu)(w - w_\nu) H_\nu(w)} . \tag{5.44}$$

The mean value theorem, applied on the numerator and on the function $H_\nu(w)$ in the denominator then gives

$$F_\nu^{(3)}(w) = J_\nu(w_\nu) \frac{(w - w_\nu)^2/2!\; H_\nu''(\hat{\hat{w}}_\nu)}{H_\nu'(\hat{w}_\nu)(w - w_\nu)^2 H_\nu'(w_\nu)} \tag{5.45}$$

where $\hat{w}_\nu$ and $\hat{w}_\nu$ will be different point within the range $[w_\nu - \varepsilon, w_\nu + \varepsilon]$. We thus get the estimate

$$|F_\nu^{(3)}(w)| \leq J_\nu(w_\nu) \frac{2}{2 \cdot \Delta^2 (w_\nu - \varepsilon)^2}$$
$$\leq \frac{(u_\nu + \varepsilon)(u_\nu + K_0 + \varepsilon)}{\Delta^2 (w_{\nu_0} - \varepsilon)^2} e^{(u_\nu - \varepsilon)(x+\zeta)} \tag{5.46}$$

from which results

$$\left| \int_0^\infty \{F_\nu^{(2)} + F_\nu^{(3)}\} dw \right|$$
$$\leq 2\varepsilon \frac{u_\nu + \varepsilon}{w_{\nu_0} - \varepsilon} (u_\nu + K_0 + \varepsilon) \left(1 + \frac{1}{\Delta^2 (w_{\nu_0} - \varepsilon)}\right) e^{(u_\nu - \varepsilon)(x+\zeta)} \tag{5.47}$$

But this means that $\sum_{\nu=1}^{\infty} (F_\nu^{(2)} + F_\nu^{(3)}$ is convergent and integrable, and due to (5.40) we can state:

The integral

$$\int_0^\infty \sum_{\nu=1}^{\infty} \{F_\nu^{(1)} + F_\nu^{(2)} + F_\nu^{(3)}\} \sin w(x - \xi) dw$$

exists.

A formal partial integration now gives

$$\sum_{\nu=1}^{\infty} \int_0^\infty \{F_\nu^{(1)} + F_\nu^{(2)} + F_\nu^{(3)}\} \sin w(x - \zeta) dw =$$
$$= \frac{1}{x - \xi} \sum_{\nu=1}^{\infty} \int_0^\infty \frac{d}{dw} \{F_\nu^{(1)} + F_\nu^{(2)} + F_\nu^{(3)}\} \cos w_\nu (x - \xi) dw$$
$$+ \frac{1}{x - \xi} \frac{1}{\varepsilon} \sum_{\nu=1}^{\infty} \frac{J_\nu(w_\nu)}{H_\nu'(w_\nu)} \left[\cos[(w_\nu + \varepsilon)(x - \xi)] + \cos[(w_\nu - \varepsilon)(x - \xi)]\right]. \tag{5.48}$$

With (5.38) we had shown that $\frac{dF_\nu^{(1)}}{dw}$ is integrable. The functions $\frac{dF_\nu^{(2)}}{dw}$ and $\frac{dF_\nu^{(3)}}{dw}$ are bounded and nonzero only in a finite range, that means that all integrals appearing in (5.48) do exist. The second sum on the right side is absolutely convergent, as for $\nu \geq \nu_0$ we have

$$\left| \frac{J_\nu(w_\nu)}{H_\nu'(w_\nu)} \right| \leq \frac{(K_0 + u_\nu)}{w_{\nu_0} \cdot \Delta} u_\nu e^{u_\nu(z+\zeta)} \tag{5.49}$$

as the summations with $\nu < \nu_0$ are bounded.

The convergence of the series on the left side of (5.48) is absolute as well. Thus the first sum of the right side, being the difference of two converging series, must converge. We thereby get the asymptotic estimate

$$\sum_{\nu=1}^{\infty} \int_0^{\infty} \{F_\nu^{(1)} + F_\nu^{(2)} + F_\nu^{(3)}\} \sin w(x-\xi)\, dw = 0\{(x-\xi)^{-1}\} \tag{5.50}$$

and thus

$$\sum_{\nu=1}^{\infty} \int_0^{\infty} \{F_\nu^{(1)} + F_\nu^{(2)} + F_\nu^{(3)}\} \sin w(x-\xi)\, dw \cdot \cdot \cos u_\nu\left(\frac{b}{2} - y\right) \cos u_\nu\left(\frac{b}{2} - \eta\right) = 0\{(x-\xi)^{-1}\}. \tag{5.51}$$

Consider now the term

$$\sum_{\nu=1}^{\infty} \int_0^{\infty} F_\nu^{(4)} \sin w(x-\xi)\, dw = \sum_{\nu=1}^{\infty} \frac{J_\nu(w_\nu)}{H_\nu'(w_\nu)} \cdot \int_{w_\nu - \varepsilon}^{w_\nu + \varepsilon} \frac{\sin w(x-\xi)}{w - w_\nu}\, dw \tag{5.52}$$

Making the substitution

$$t = (w - w_\nu)(x - \xi) \tag{5.53}$$

we find

$$\sum_{\nu=1}^{\infty}{}' \int_0^{\infty} F_\nu^{(4)} \sin w\,(x-\xi)\,dw = \sum_{\nu=1}^{\infty} \frac{J_\nu(w_\nu)}{H_\nu'(w_\nu)} \cdot \int_{t=-s(x-\xi)}^{s(x-\xi)} \frac{\sin(w(x-\xi)+t)}{t}\,dt =$$

$$= \int_{-s(x-\xi)}^{s(x-\xi)} \frac{\sin t}{t}\,dt \sum_{\nu=1}^{\infty} \frac{J_\nu(w_\nu)}{H_\nu'(w_\nu)} \cos w_\nu (x-\xi)\,. \tag{5.54}$$

But we have[14]

$$\int_{-s(x-\xi)}^{s(x-\xi)} \frac{\sin t}{t}\,dt = \pi \operatorname{sign}(x-\xi) + 0\{(x-\xi)^{-1}\}\,. \tag{5.55}$$

The sum (5.54) converges absolutely due to (5.49); due to (5.51), (5.54), (5.55) we therefore have:

$$\sum_{\nu=1}^{\infty} \int_0^{\infty} \{F_\nu^{(1)} + F_\nu^{(2)} + F_\nu^{(3)} + F_\nu^{(4)}\} \sin w\,(x-\xi)\,dw$$

$$\cdot \cos u_\nu\left(\frac{b}{2}-y\right) \cdot \cos u_\nu\left(\frac{b}{2}-\eta\right)$$

$$= \sum_{\nu=1}^{\infty} \int_0^{\infty} \frac{J_\nu(w)}{H_\nu(w)} \sin w\,(x-\xi)\,dw \cdot \cos u_\nu\left(\frac{b}{2}-y\right) \cdot \cos u_\nu\left(\frac{b}{2}-\eta\right)$$

$$= \sum_{\nu=1}^{\infty} \frac{J_\nu(w_\nu)}{H_\nu'(w_\nu)} \pi \cos w_\nu (x-\xi) \cdot \cos u_\nu\left(\frac{b}{2}-y\right)$$

$$\cdot \cos u_\nu\left(\frac{b}{2}-\eta\right) \cdot \operatorname{sign}(x-\xi) + 0\{(x-\xi)^{-1}\}\,. \tag{5.56}$$

The sum of terms with $\nu < 0$ is identical memberwise with that of terms $\nu > 0$, we therefore only are left with an estimate of the terms with $\nu = 0$ in (5.23).

For $K_0 h > 1$ we find in analog manner as for terms with $\nu > 0$

$$\int_0^\infty \delta_0 \frac{J_0(w)}{H_0(w)} \sin w(x-\xi)\, dw =$$

$$= \frac{J_0(w_0)}{H_0'(w_0)} \pi \cos w_0(x-\xi)\, \operatorname{sign}(x-\xi) + 0\{(x-\xi)^{-1}\}. \qquad (5.57)$$

For $K_0 h < 1$, due to the fact that $\delta_0 = 0$, there is no corresponding contribution.

The last term of (5.23) is explicitely given as, - compare (4.37) and (4.38) with $k_\nu = w$ -

$$\frac{4}{b} \int_0^\infty (1-\delta_0) \frac{w(w^2 + w K_0)}{K_0 w \operatorname{Tg} wh - w^2} \cdot \frac{\operatorname{Cof} w(z+h) \operatorname{Cof} w(\zeta+h) e^{-wh}}{w \operatorname{Cof} wh} \sin w(x-\xi)\, dw$$

$$= \frac{4}{b} \int_0^\infty \begin{Bmatrix} w_0 - w \\ w_0 \end{Bmatrix} \frac{1}{w_0} \frac{w}{K_0 \operatorname{Tg} wh - w} \qquad (5.58)$$

$$\cdot \frac{(w + K_0) \operatorname{Cof} w(z+h) \operatorname{Cof} w(\zeta+h) e^{-wh}}{\operatorname{Cof} wh} \cdot \frac{\sin w(x-\xi)\, dw}{w} \qquad \text{for } K_0 h \begin{Bmatrix} > 1 \\ < 1 \end{Bmatrix}$$

The integrand is bounced and continuous at $w = 0$. Especially we have

$$\lim_{w \to 0} \frac{K_0 w}{K_0 \operatorname{Tg} wh - w} = K_0 \left[\frac{d}{dw}(K_0 \operatorname{Tg} wh - w)\right]^{-1} = \qquad (5.59)$$

$$= \frac{K_0}{K_0 h - 1}.$$

This suggests splitting up the last term of (5.23) as follows:

$$-\frac{4}{b}\int_0^\infty (1-\delta_0)\frac{J_0(w)}{H_0(w)}\sin w(x-\xi)\,dw =$$

$$=-\frac{4K_0h}{b(K_0h-1)}\int_0^\infty \frac{\sin w(x-\xi)}{w}\,dw +$$

$$+\frac{4}{b}\int_0^\infty\left\{\frac{K_0}{w(K_0h-1)}-(1-\delta_0)\frac{J_0(w)}{H_0(w)}\right\}\sin w(x-\xi)\,dw\,. \qquad (5.60)$$

The expression in long brackets is a holomorphis function of w on all points of the w axis and thus differentiable. Partial integration yields;

$$\frac{4}{b}\int_0^\infty\left\{\frac{K_0}{w(K_0h-1)}-(1-\delta_0)\frac{J_0(w)}{H_0(w)}\right\}\sin w(x-\xi)dw$$

$$=\frac{4}{b}\int_0^\infty\left[\frac{-K_0}{w^2(K_0h-1)}-\right.$$

$$\left.-\frac{d}{dw}\left\{(1-\delta_0)\frac{J_0(w)}{H_0(w)}\right\}\right]\cos w(x-\xi)\,dw\,\frac{1}{x-\xi} \qquad (5.61)$$

The integral on the right side exists, as $J_0(w)$ has an exponential decay; the first integral corresponds to the function Integral-sinus for argument zero and therefore is equal to $\pi/2 \cdot \text{sign}\,(x-\xi)$ [14]. We thus have

$$\frac{-4}{b}\int_0^\infty (1-\delta_0)\frac{J_0(w)}{H_0(w)}\sin w(x-\xi)\,dw =$$

$$=\frac{-2\pi K_0}{b(K_0h-1)}\,\text{sign}\,(x-\xi)+0\{(x-\xi)^{-1}\}\,. \qquad (5.62)$$

From (4.29), (5.23), (5.55), (5.60) we may now conclude that

$$G_{5x} = \frac{-4\pi}{b}\,\mathrm{sign}\,(x-\xi)\left[\frac{K_0}{2(K_0 h-1)} + \right.$$
$$+ \sum_{\nu=-\infty}^{\infty}{}' \frac{J_\nu(w_\nu)}{H_\nu'(w_\nu)} \cos w_\nu (x-\xi) \cos u_\nu \left(\frac{b}{2}-y\right)$$
$$\left. \cdot \cos u_\nu \left(\frac{b}{2}-\eta\right)\right] + 0\,\{(x-\xi)^{-1}\} \qquad (5.63)$$

where the asteric at the summation sign should indicate that for $K_0 h < 1$ only the indices $\nu \neq 0$ should be considered. - We further may conclude that the function

$$G_x = G_{5x} + \frac{4\pi}{b}\left[\frac{K_0}{2(K_0 h-1)}\right.$$
$$\left. + \sum_{\nu=-\infty}^{\infty}{}' \frac{J_\nu(w_\nu)}{H_\nu'(w_\nu)} \cos w_\nu (x-\xi) \cos u_\nu \left(\frac{b}{2}-y\right) \cos u_\nu \left(\frac{b}{2}-\eta\right)\right] \qquad (5.64)$$

meets all conditions resulting from (4.01)-(4.06), i.e. that its indefinite integral regarding x is the function $G(x,y,z)$ to be determined. In particular for $x \to +\infty$ we have

$$G_x = 0\,\{(0-\xi)^{-1}\} \qquad (5.65)$$

and for $x \to -\infty$, taking account of (4.33) and (5.04),

$$G_x = \frac{4\pi K_0}{b(K_0 h-1)} + \frac{8\pi}{b} \sum_{\nu=-\infty}^{\infty}{}' \frac{w_\nu^2 + K_0 \varkappa_\nu}{\varkappa_\nu} \cdot$$
$$\cdot \frac{\mathfrak{Cof}\,\varkappa_\nu (z+h)\,\mathfrak{Cof}\,\varkappa_\nu (\zeta+h)\,\mathfrak{Cof}\,\varkappa_\nu h \cdot e^{-\varkappa_\nu h}}{\mathfrak{Cof}^2 \varkappa_\nu h \cdot (1+(u_\nu/\varkappa_\nu)^2) - K_0 h} \cos w_\nu (x-\xi) \cdot \qquad (5.66)$$
$$\cdot \cos u_\nu (b/2-y) \cos u_\nu (b/2-\eta) + 0\,\{(x-\xi)^{-1}\}.$$

Due to $H_\nu(w_\nu) = 0$ we have

$$w_\nu^2 = K_0 \varkappa_\nu \mathfrak{Tg}\,\varkappa_\nu h. \qquad (5.67)$$

By repeated substitution of this relation we finally get from (5.66)

$$G_x = 4\pi\left[\frac{K_0}{b(K_0 h-1)} + \sum_{\nu=-\infty}^{\infty} w_\nu \gamma_\nu \{\varphi_\nu^c(x,y,z)\,\varphi_\nu^c(\xi,\eta,\zeta)\right.$$
$$\left. + \varphi_\nu^s(x,y,z)\,\varphi_\nu^s(\xi,\eta,\zeta)\}\right] + 0\,\{(x-\xi)^{-1}\}. \qquad (5.68)$$

with

$$\gamma_\nu \doteqdot \frac{-4\,w_\nu \varkappa_\nu \mathfrak{Cof}^2 \varkappa_\nu h}{b\,[(\varkappa_\nu^2 + u_\nu^2)\,\mathfrak{Sin}\,2\varkappa_\nu h - 2\,w_\nu^2 \varkappa_\nu h]}$$

$$(\nu = \pm 1, 2, \ldots \text{ and } \nu = 0 \text{ for } K_0 h > 1)$$

$$\gamma_\nu \doteqdot 0 \qquad \text{for } \nu = 0,\ K_0 h < 1 \tag{5.69}$$

$$\varphi_\nu^c(x,y,z) + i\,\varphi_\nu^s(x,y,z) \doteqdot$$

$$\doteqdot \frac{\mathfrak{Cof}\,\varkappa_\nu (z+h)}{\mathfrak{Cof}\,\varkappa_\nu h}\, e^{i w_\nu x} \cos u_\nu \left(\frac{b}{2} - y\right) \doteqdot \varphi_{-\nu}^c + i\,\varphi_{-\nu}^s . \tag{5.70}$$

In the limiting case $h \to \infty$ we have in particular

$$\gamma_\nu = \frac{-2\,w_\nu \varkappa_\nu}{b\,(\varkappa_\nu^2 + u_\nu^2)} \tag{5.71}$$

$$\varphi_\nu^c(x,y,z) + i\,\varphi_\nu^s(\xi,\eta,\zeta) = e^{\varkappa_\nu z + i w_\nu x} \cos u_\nu \left(\frac{b}{2} - y\right) \tag{5.72}$$

with

$$w_\nu^2 = K_0 \varkappa_\nu \tag{5.73}$$

due to (5.67).

If we now construct an integral function G to G_x by, starting with (4.30), also in (4.32) in the term $G_{5x} - G_{4x}$, inserting $-\cos w_\nu(x-\xi)/w$ for $\sin w(x-\xi)$ and in (5.60) $\sin \frac{w_\nu(x-\xi)}{w_\nu}$ for $\cos w_\nu(x-\xi)$ and finally

$$\frac{4\pi K_0 (x-\xi)}{b\,(K_0 h - 1)} \text{ for } \frac{4\pi K_0}{b\,(K_0 h - 1)},$$

then it may be shown that all estimates we derived for the series expansion of $G_x - G_{4x}$ are valid a' fortiori for the function $G - G_4$, as for w sufficiently large the estimates (5.12), (5.17), for the functions J_ν, $\frac{dJ_\nu}{dw}$ will hold if we insert in place of J_ν the function $J_\nu^* = \frac{J_\nu}{w}$. There is only the last term in the expression (5.23) for which this step needs special consideration, as the contribution

$$g_0^* = \int_0^\infty \frac{4}{b}\,(1-\delta_0)\,\frac{J_0(w)}{H_0(w)}\,\frac{\cos w\,(x-\xi)}{w}\,dw \tag{5.74}$$

represents a divergent integral. Alternatively we put

$$g_o = \int_{-\infty}^{\infty} f(w) \frac{\mathfrak{Cof}\, w(z+h)\, \mathfrak{Cof}\, w(\zeta+h) \cos w(x-\xi) - 1}{w^2} \tag{5.75}$$

with

$$f(w) \doteq \frac{2}{b} \begin{Bmatrix} 1 \\ 1 - |w|/w_o \end{Bmatrix} (|w| + K_o) \cdot \frac{w}{K_o\, \mathfrak{Tg}\, wh - w} \cdot \frac{e^{-|w|h}}{\mathfrak{Cof}\, wh} \cdot \begin{Bmatrix} K_o h < 1 \\ K_o h > 1 \end{Bmatrix}. \tag{5.76}$$

The expression g_o is equivalent to g_o^* save the additional term -1 in the numerator not contributing to the derivatives to coordinates, but providing convergence. Now we have the partition:

$$\frac{1 - \mathfrak{Cof}\, w(z+h)\, \mathfrak{Cof}\, w(\zeta+h) \cos w(x-\xi)}{w^2} = \tag{5.77}$$
$$= h(w) - s(w) \cos w(x-\xi)$$

with

$$h(w) \doteq \frac{1 - \cos w(x-\xi)}{w^2} \tag{5.78}$$

$$s(w) \doteq \frac{2\, \mathfrak{Sin} \frac{w}{2} (z+h) + 2\, \mathfrak{Sin} \frac{w}{2} (\zeta+h)}{w^2} + \frac{4\, \mathfrak{Sin} \frac{w}{2} (z+h)\, \mathfrak{Sin} \frac{w}{2} (\zeta+h)}{w^2} \tag{5.79}$$

and thereby

$$g_o = \int_{-\infty}^{\infty} f(w)\, h(w)\, dw - \int_{-\infty}^{\infty} f(w)\, s(w) \cos w(x-\xi)\, dw. \tag{5.80}$$

The function $f(w)$ is an even function of w and has monotonic exponential decay for w large. In particular it is square-integrable. For $w = 0$ it approaches continuously o the value $f(0) = 2K_o/b(K_o h - 1)$. The product $f(w) \cdot s(w)$ approaches zero exponentially for large w as long as we have $z + \zeta < 0$; this gives

$$\int_{-\infty}^{\infty} f(w)\, s(w) \cos w(x-\xi) dw = 0\, \{(x-\xi)^{-1}\}. \tag{5.81}$$

The function $h(w)$ has a Fourier transform[10]

$$H(u) \doteq \frac{1}{\sqrt{2\pi}} \int_{-\infty}^{\infty} h(w)\, e^{iuw}\, dw = \begin{cases} \pi\{|x-\xi| - |u|\} & \text{for } |u| \leq |x-\xi| \\ 0 & \text{for } |u| \geq |x-\xi| \end{cases} \tag{5.82}$$

Now let

$$F(u) \doteq \int_{-\infty}^{\infty} f(w)\, e^{iuw}\, dw \tag{5.83}$$

be the even Fourier transform of $f(w)$.

The convolution of the functions $f(w)$ and $h(w)$

$$g(w) \doteq \int_{-\infty}^{\infty} f(w')\, h(w+w')\, dw' \equiv \int_{-\infty}^{\infty} f(w-w')\, h(w')\, dw \tag{5.84}$$

is continuous and square-integrable as well and has the transform

$$G(u) = F(u)\, H(u)\,. \tag{5.85}$$

Especially we have the inversion formula

$$g(w) = \frac{1}{\sqrt{2\pi}} \int_{-\infty}^{\infty} F(u)\, H(u)\, e^{-iuw}\, du\,. \tag{5.86}$$

But then we have

$$g(0) = \frac{1}{2\pi} \int_{u=-|x-\xi|}^{|x-\xi|} \int_{w=-\infty}^{\infty} f(w)\, e^{iuw}\, dw\, \pi\,(|x-\xi| - |u|)\, du =$$

$$= \pi|x-\xi|\, f(0) - \sqrt{2\pi} \int_{0}^{\infty} u\, F(u)\, du - \sqrt{2\pi} \int_{|x-\xi|}^{\infty} (|x-\xi| - u)\, F(u)\, du\,. \tag{5.87}$$

The function $f(w)$ is holomorphic on the real w axis except at $w = 0$, i.e. differentiable. The derivatives have exponential decay as well for large w , that means that the Fourier transform $F(u)$ will have sufficient decay for large u to let the first integral in (5.87) exist and let the last integral vanish like $O\{(x-\xi)^{-1}\}$. Summing up, we get

$$g_0 = g(0) - \int_{-\infty}^{\infty} f(w)\, s(w) \cos w(x-\xi)\, dw =$$

$$= (x-\xi)\frac{2K_0}{b(K_0h-1)} + C + 0\{(x-\xi)^{-1}\} \tag{5.88}$$

where the quantity C, defined by

$$C = \int_0^{\infty} u \int_{-\infty}^{\infty} f(w)\, e^{juw}\, dw\, du, \tag{5.89}$$

depends on K_0h and b only. Adding the potential of some parallel flow similar to (5.60) we finally, taking account of (4.31), have for $x \to +\infty$

$$G = -\frac{1}{b}\ln\{(x-\xi)^2 + (z-\zeta)^2\} + C + 0\{(x-\xi)^{-1}\} \tag{5.90}$$

and for $x \to -\infty$

$$G = -\frac{1}{b}\ln\{(x-\xi)^2 + (z-\zeta)^2\} + C + 4\pi\frac{K_0(x-\xi)}{b(K_0h-1)}$$

$$+ \sum_{\nu=-\infty}^{\infty} \gamma_\nu \{\varphi_\nu^s(x,y,z)\,\varphi_\nu^c(\xi,\eta,\zeta) - \varphi_\nu^c(x,y,z)\,\varphi_\nu^s(\xi,\eta,\zeta)\} + 0\{(x-\xi)^{-1}\} \tag{5.91}$$

6. <u>Considerations on flow through control surfaces and amount of information necessary for unique determination of free wave systems</u>.

Let us consider the quantity

$$\Phi(a,\xi,\eta,\zeta) = \int_{-h}^{0}\int_{-b/2}^{b/2} G_x\, dy\, dz \Big|_{x=-a;\, a>0} \tag{6.01}$$

which might be regarded as the transport of the flow G_x through the control surface $\{x = -a,\ -h \le z \le 0,\ -b/2 \le y \le b/2\}$. If we take mean values regarding x, only the terms with $\nu = 0$ of G_x will contribute. If we assume a sufficiently large, then the mean value of Φ regarding choice of a, which we symbolize as $\bar{\Phi}$, will depend on the first term of (5.66) only; we have

$$\bar{\Phi} - 0\{(a-\xi)^{-1}\} = bh\frac{4\pi K_0}{b(K_0h-1)} = 4\pi\frac{K_0h}{K_0h-1}\begin{cases}<0 \text{ for } K_0h<1\\ >0 \text{ for } K_0h>1\end{cases} \tag{6.02}$$

As however G becomes singular in $\{x = \xi, y = \eta, z = \zeta\}$ like an inverse distance, we should expect $\bar{\Phi} = 4\pi$ instead. The apparent violation of the continuity equation expressed by (6.02) might now be explained by some diffusion of the flow through the undisturbed free surface $z = 0$; the vertical flow between two cuts $x = a$ and $x = -a$ comes out as

$$\int_{-b/2}^{b/2}\int_{-a}^{a} G_z\,dxdy = -\frac{1}{K_0}\int_{-b/2}^{b/2}\int_{-a}^{a} G_{xx}\,dxdy =$$

$$= -\frac{1}{K_0}\int_{-b/2}^{b/2}\{G_x(a) - G_x(-a)\}\,dy = +\frac{4\pi K_0}{K_0h-1} \tag{6.03}$$

But just this amount is the deviation of (6.02) against 4π . If we consider the linearized condition for the elevation $\bar{\zeta}$ of the free surface above its undisturbed position,

$$\tilde{\zeta} = \frac{c}{g}G_x \tag{6.04}$$

then we find that behind a source of emission rate 4π, moving with velocity c in x-direction, an asymptotic wave elevation

$$\tilde{\zeta} = \frac{4\pi c^{-1}}{b(K_0h-1)} \tag{6.05}$$

is developed, i.e. a negative elevation in the supercritical case $K_0h < 1$ within a linearized theory, i.e. for $G_x \ll c$, the horizontal flow between the plane $z = 0$ and the free surface may be neglected. Then the vertical flow (6.03) corresponds to the local increase of the stationary asymptotic wave elevation.

The parallel flow represented by the first term of (5.66) was obviously overlooked in a derivation of the asymptotic potential due to a two dimensional source by Haskind,[18] therefore the development of a nonoscillatory wave elevation has - to author's knowledge - never been mentioned yet.

Having derived asymptotic estimates of the functions G and G_x, we now are able to showthat very arbitraty wave fields at a sufficient distance behind their orgin may be represented in terms of the functions $\varphi_\nu^c(x,y,z)$, $\varphi_\nu^s(x,y,z)$ and a parallel flow c_o. It is merely necessary to express this wave field, i.e. its potential φ by means of Green's theorem, in terms of this Green's function G and the flow characteristics at boundary surfaces.

We shall prove:
If within a certain domain B, determined by relations $x' - a \leq x \leq x' + a$, $|y| \leq b/2$, $-h \leq z \leq 0$, the function $\varphi(x,y,z)$ is harmonic and subject to boundary conditions

$$\varphi_{xy} = 0 \qquad \text{for} \quad y = \pm b/2 \tag{6.06}$$
$$\varphi_{xz} = 0 \qquad \text{for} \quad z = -h \tag{6.07}$$
$$\varphi_{xxx} + K_o\varphi_{xz} = 0 \qquad \text{for} \quad z = 0 \tag{6.08}$$

then in the vicinity of some plane $x = x'$ we have for $z < 0$ an absolutely convergent representation

$$\varphi_x(x,y,z) = \frac{g}{c}\sum_{\nu=-\infty}^{\infty}\{\beta_\nu\varphi_\nu^c(x,y,z) - \alpha_\nu\varphi_\nu^s(x,y,z)\} + c_o + 0\{a^{-1}\}. \tag{6.09}$$

The series shown here is uniformly convergent for any fixed $z < 0$ in x and y over the entire x,y plane. This means in particular, that the approach (2.01) on which we based calculation of wave resistance in our previous paper, can deviate from the most general expression admitted for φ_x by our boundary conditions only by a parallel flow and by a term vanishing with a^{-1}.

Green's formula implies:

$$\varphi_x(x,y,z) = \frac{1}{4\pi}\int\left\{\varphi_x(\xi,\eta,\zeta)\frac{\partial}{\partial n}G(x,y,z,\xi,\eta,\zeta) - G(x,y,z,\xi,\eta,\zeta)\frac{\partial}{\partial n}\varphi_x(\xi,\eta,\zeta)\right\}dS \tag{6.10}$$

if the point $\{x,y,z\}$ is situated in the interior of the domain B, whereby the integral has to be extended over the boundary surface S of B and the operation $\frac{\partial}{\partial n}$ should mean a differentiation regarding ξ,η,ζ in the direction of the outer normal. Due to conditions (4.02), (4.03), (4.04), (6.06) and (6.07) the contributions of the boundaries $y = \pm b/2$ and $z = -h$ may be dropped. The integration over the plane $z = 0$ can, due to (4.05) and (6.06) be reduced to a line integration as in (6.03), as we have

$$\int_{x'-a}^{x'+a}\int_{-b/2}^{b/2}\{\varphi_x G_\zeta - G\,\varphi_{x\zeta}\}\,d\eta d\zeta = \frac{1}{K_0}\int_{x'-a}^{x'+a}\int_{-b/2}^{b/2}\{\varphi_x G_{\xi\xi} - G\,\varphi_{x\xi\xi}\}\,d\eta d\zeta =$$

$$= \frac{1}{K_0}\int_{-b/2}^{b/2}\{\varphi_x G_\xi - G\,\varphi_{x\xi}\}\,d\eta \Bigg|_{\xi = x'-a}^{\xi = x'+a} \qquad (6.11)$$

and thus (6.10) may be written as

$$\varphi_x(x,y,z) = \Bigg| \frac{1}{4\pi}\int_{-b/2}^{b/2}\Bigg[\int_{-h}^{0}\{\varphi_x G_\zeta - G\,\varphi_{x\zeta}\}\,d\zeta -$$

$$- \frac{1}{K_0}\{\varphi_x G_\xi - G\,\varphi_{x\xi}\}_{\zeta=0}\Bigg]d\eta \Bigg|_{\xi = x'-a}^{\xi = x'+a} \qquad (6.12)$$

For $x \approx x'$ and for large values of a - especially for $a \gg b$, $a \gg h$ - we now have due to (5.65) and (5.90)

$$G(x,y,z,x'-a,\eta,\zeta) = -\frac{1}{b}\ln a + C + 0\{a^{-1}\} \qquad (6.13)$$

$$G_x(x,y,z,x'-a,\eta,\zeta) = 0\{a^{-1}\}. \qquad (6.14)$$

For $\xi = x' + a$, due to (5.91) and (5.66), we have however

$$G(x,y,z,x'+a,\eta,\zeta) = \frac{-1}{b}\ln a + C + 4\pi\,\frac{K_0(x-x'-a)}{b(K_0 h - 1)}$$

$$+ 4\pi\sum_{\nu=-\infty}^{\infty}\gamma_\nu\{\varphi_\nu^s(x,y,z)\,\varphi_\nu^c(x'+a,\eta,\zeta)$$

$$- \varphi_\nu^c(x,y,z)\,\varphi_\nu^s(x'+a,\eta,\zeta)\} + 0\{a^{-1}\} \qquad (6.15)$$

$$G_x(x,y,z,x'+a,\eta,\zeta) =$$

$$= \frac{4\pi K_0}{b(K_0 h - 1)} + 4\pi\sum_{\nu=-\infty}^{\infty} w_\nu\gamma_\nu\{\varphi_\nu^c(x,y,z)\,\varphi_\nu^c(x'+a,\eta,\zeta) +$$

$$+ \varphi_\nu^s(x,y,z)\,\varphi_\nu^s(x'+a,\eta,\zeta)\} + 0\{a^{-1}\}.$$

(6.16)

If we replace the function G on the left side of (6.10) by a constant, then the right side will vanish. We therefore are authorized to increase G by a term $1/b \ln a - C$. This essentially means that only the values of φ_x and φ_{xx} in the plane $x = x' + a$ determine the value of φ_x at the point $\{x,y,z\}$; by substitution of (6.13), (6.14), (6.15) and (6.16) in (6.10) we get

$$\varphi_x(x,y,z) = \frac{K_0}{b(K_0 h - 1)} \int_{-b/2}^{b/2} \left\{ \int_{-h}^{0} \varphi_x(x'+a,\eta,\zeta)\, d\zeta - \frac{1}{K_0} \varphi_x(x'+a,\eta,0) \right\} d\eta$$

$$+ \frac{K_0(x'+a-x)}{b(K_0 h - 1)} \int_{-b/2}^{b/2} \left\{ \int_{-h}^{0} \varphi_{x\xi}(x'+a,\eta,\zeta)\, d\zeta - \frac{1}{K_0} \varphi_{x\xi}(x'+a,\eta,0) \right\} d\eta$$

$$+ \sum_{\nu=-\infty}^{\infty} \gamma_\nu \varphi_\nu^{\,c}(x,y,z) \int_{-b/2}^{b/2} \left\{ \int_{-h}^{0} (w_\nu \varphi_\nu^{\,c} \varphi_x - \varphi_\nu^{\,s} \varphi_{x\xi})\, d\zeta - \frac{1}{K_0} (w_\nu \varphi_\nu^{\,c} \varphi_x - \varphi_\nu^{\,s} \varphi_{x\xi}) \right\} d\eta$$

$$+ \sum_{\nu=-\infty}^{\infty} \gamma_\nu \varphi_\nu^{\,s}(x,y,z) \int_{-b/2}^{b/2} \left\{ \int_{-h}^{0} (w_\nu \varphi_\nu^{\,s} \varphi_x + \varphi_\nu^{\,c} \varphi_{x\xi})\, d\zeta - \right.$$

$$\left. - \frac{1}{K_0} (w_\nu \varphi_\nu^{\,s} \varphi_x + \varphi_\nu^{\,c} \varphi_{x\xi}) \right\} d\eta + 0\{a^{-1}\}. \qquad (6.17)$$

Within the integrals of formula (6.14) the functions and have to be taken at $\xi = x' + a$; besides, in the integrals with factor $1/K_0$ we have to insert for ζ the value of zero.

The expansions (5.66) and (5.75) are for $z < 0$ absolutely convergent, uniform in x and y; if φ_x and φ_{xx} is bounded on $x = x' + a$, (6.14) will as well for $z < 0$ represent a convergent expansion in terms of functions $\varphi_\nu^{\,c}$ and $\varphi_\nu^{\,s}$ and the asymptotic parallel flow, - the second summand of (6.14) disappears for incompressible flow and shall no longer be considered. If we apply Green's formula on function φ_{xx} instead of φ_x, we may conclude that for a harmonic function φ_{xx} for $z < 0$ there is a development regarding these components as well, in the Fourier partition regarding y the terms in φ_x and φ_{xx} must correspond, i.e. the expansion (6.07) may be differentiated term by term. Substitution of (6.07) into (6.14) and comparison of coefficients then yield the relations:

$$\gamma_\nu \int_{\zeta=-h}^{0} \left[\int_{\eta=-b/2}^{b/2} \left(\varphi_\nu^{\,i} \frac{\delta}{\delta\xi} \varphi_\lambda^{\,j} - \varphi_\lambda^{\,j} \frac{\delta}{\delta\xi} \varphi_\nu^{\,i} \right) d\zeta - \right.$$

$$\left. - \frac{1}{K_0} \left(\varphi_\nu^{\,i} \frac{\delta}{\delta\xi} \varphi_\lambda^{\,j} - \varphi_\lambda^{\,j} \frac{\delta}{\delta\xi} \varphi_\nu^{\,i} \right) \right] d\eta = \delta_{\nu\lambda} (1 - \delta_{ij}) \varepsilon_j$$

$$(j, i = c, s;\ \nu, \lambda = 0, 1, 2, \ldots) \qquad (6.18)$$

where $\delta_{\nu\lambda}$ and δ_{ij} represent Kronnecker symbols, with especially

$$\delta_{ss} = \delta_{cc} = 1, \quad \delta_{sc} = \delta_{cs} = 0 \tag{6.19}$$

Further we have used the definitions

$$\sigma_j = 1 \text{ for } j = s, \qquad \sigma_j = -1 \text{ for } j = c \tag{6.20}$$

These generalized orthogonality relations of the eigenfunctions $\varphi_\nu{}^c$, $\varphi_\nu{}^s$ may be confirmed by substitution of the expressions (5.70).

We have:

$$\int_{-h}^{0}\left(\varphi_\nu{}^i \frac{\partial}{\partial\xi}\varphi_\nu{}^j - \varphi_\nu{}^j \frac{\partial}{\partial\xi}\varphi_\nu{}^i\right)d\zeta = \frac{\operatorname{Sin} 2\varkappa_\nu h + 2\varkappa_\nu h}{4\varkappa_\nu \operatorname{Cof}^2 \varkappa_\nu h}\left(\varphi_\nu{}^i(\xi,\eta,0)\frac{\partial}{\partial\xi}\varphi_\nu{}^j(\xi,\eta,0) - \varphi_\nu{}^j(\xi,\eta,0)\frac{\partial}{\partial\xi}\varphi_\nu{}^i(\xi,\eta,0)\right) \tag{6.21}$$

furthermore

$$\int_{-h}^{0}\left(\varphi_\nu{}^i \frac{\partial}{\partial\xi}\varphi_\nu{}^j - \varphi_\nu{}^j \frac{\partial}{\partial\xi}\varphi_\nu{}^i\right)d\xi = \frac{\operatorname{Sin} 2\varkappa_\nu h + 2\varkappa_\nu h}{4\varkappa_\nu \operatorname{Cof}^2 \varkappa_\nu h}\left(\varphi_\nu{}^i(\xi,\eta,0)\frac{\partial}{\partial\xi}\varphi_\nu{}^j(\xi,\eta,0) - \varphi_\nu{}^j(\xi,\eta,0)\frac{\partial}{\partial\xi}\varphi_\nu{}^i(\xi,\eta,0)\right) \tag{6.22}$$

i.e. integration over the surface $-h \le \zeta \le 0$, $-b/2 \le \eta \le b/2$ may be reduced to a simple integration regarding η . We further find

$$\gamma_\nu\left\{\frac{\operatorname{Sin} 2\varkappa_\nu h + 2\varkappa_\nu h}{4\varkappa_\nu \operatorname{Cof}^2 \varkappa_\nu h} - \frac{1}{K_0}\right\} = \frac{1}{w_\nu b} \tag{6.23}$$

and thereby can simplify (6.17) to

$$\varphi_x(x,y,z) = \frac{1}{b}\int_{-b/2}^{b/2}\sum_{-\infty}^{\infty}\left\{\varphi_x(x_s,\eta,0)\cos w_\nu(x_s - x) - \varphi_{xz}(x_s,\eta,0)\sin w_\nu(x_s - x)\right\} \frac{\operatorname{Cof}\varkappa_\nu(z+h)}{\operatorname{Cof}\varkappa_\nu h}\cos u_\nu\left(\frac{b}{2} - \eta\right)d\eta \cos u_\nu\left(\frac{b}{2} - y\right)$$
$$+ \frac{1}{b}\int_{-b/2}^{b/2}\left[\int_{-h}^{0}\varphi_x(x_s,\eta,\zeta)\,d\zeta - \frac{1}{K_0}\varphi_x(x_s,\eta,0)\right]d\eta\,\frac{K_0}{K_0 h - 1} + 0\{a^{-1}\} \tag{6.24}$$

But this means that, - save some parallel flow, - the asyptotic flow φ_x for $z < 0$ behind a stationary moving disturbance and thereby the wave elevation

$$\tilde{\zeta} = \lim_{z \to 0} -\frac{c}{g} \varphi_x(x, y, z) \tag{6.25}$$

is uniquely determined by the elevation in a transverse cut $x = x_s$ and its derivative in x-direction on this cut!

Even if the series (6.09) will in general for $z = 0$ only have a formal significance and a general method of summation cannot be provided here, its uniform convergence and thereby the representation of the wave elevation

$$\tilde{\zeta} = -\frac{c}{g} \varphi_{x\,z=0} \tag{6.26}$$

as a uniformly convergent series is justified, if within the range of integration $\{x = x' + a,\ z = 0\}$ the functions φ_x and φ_{xx} are twice continuously differentiable regarding y. This follows by partial integration, if we take account of $\varphi_y = \varphi_{y_x} = \varphi_{y_{xx}} = 0$ for $y = \pm b/2$ (No flow through canal walls.)

7. Formulae for determination of φ from wave profiles

For application of Green's formula in (6.17) we selected a control surface within the fluid orthogonal to the bottom as well as to the tank walls. This not only rendered possible reduction of the domain of integrations to the line $z = 0$ for the components of G and G_x, but as well permitted direct determination of the coefficients α_ν, β_ν by use of the orthogonality relations (6.18) and thereby to find the straightforward expression for the flow through (6.24). Under choice of a more general surface we could as well represent the flow in term of its values at this surface, but we would have no direct access to the coefficients α_ν, β_ν and thereby to the wave resistance

$$R = \frac{\varrho g b}{2} \sum_{\nu=-\infty}^{\infty} A_\nu^{*2} (1 - c_x^\nu / c). \tag{7.01}$$

with

$$A_\nu^{*2} = \frac{1}{4}(\alpha_\nu^2 + \beta_\nu^2) = A_{-\nu}^{*2}. \tag{7.02}$$

and

$$c_x^\nu = c\cos^2\Theta_\nu \frac{\mathfrak{Sin}\, 2\varkappa_\nu h + 2\varkappa_\nu h}{2\,\mathfrak{Sin}\, 2\varkappa_\nu h} \qquad (7.03)$$

as the component of the velocity of transport of energy of an oblique wave in the x-direction. (These formulae were derived as (2.28), (2.29) and (2.27) in the previous paper under assumption of a flow (6.09) with the parallel flow component and the 0-term neglected).

For a pair of two parallel cuts perpendicular to the tank walls in distance Δ with respective wave profiles ζ^+ and ζ^- we derived

$$4A_\nu^{*2} = \beta_\nu^2 + \alpha_\nu^2 = \frac{1}{b^2\cos^2 w_\nu \Delta}\left(\int_{-b/2}^{b/2}(\zeta^+ + \zeta^-)\cos u_\nu (b/2 - y)\,dy\right)^2$$
$$+ \frac{1}{b^2\sin^2 w_\nu \Delta}\left(\int_{-b/2}^{b/2}(\zeta^+ - \zeta^-)\cos u_\nu (b/2 - y)\,dy\right)^2. \qquad (7.04)$$

as Equation (3.06).

A wave profile of finite length parallel to the walls, say in a plane $y = y_s$, does not provide sufficient information for application of Green's formula and determination of the flow field. This reflected in some properties of the set of functions $\{\cos w_\nu x, \sin w_\nu x\}$. We showed in (5.14) that the quotient ν/w_ν tends to infinity with increasing ν, i.e. the qunatities w_ν have no finite asymptotic density on the real axis. But a theorem of Müntz[16] states that the system of functions $\{\cos w_\nu x, \sin w_\nu x\}$ is complete on any finite x-interval, that means that any continuous function may in any interval be approximated by linear combinations of functions out of this set in a manner that the deviation uniformly becomes arbitrary small. It follows that coefficients of such approximations cannot be determined unique, as the set of w_ν after diminuation of at least a finite number of its members still is of infinite asymptotic density. We therefore have no possibility even to derive upper bounds for the values of the coefficients from the information of such a finite profile.*

*To elucidate this situation, it could be mentioned that the set of functions $[\sin \nu x, \cos \nu x]$ $(\nu = 0,1,2\ldots)$ has a finite asymptotic density equal to one. This system is complete for uniform approximation only on intervals of length equal or smaller than 2π. In the latter case coefficients are nonunique as well and there cannot be given an upper bound for their absolute value.

Only in the limiting case of infinite length of the profile there is a unique determination of the flow in the vicinity of the profile; a uniformly convergent series

$$\zeta_\mu(x) = \sum_{\nu=-\infty}^{\infty} \{\beta_\nu \cos w_\nu x - \alpha_\nu \sin w_\nu x\} \cos u_\nu \left(\frac{b}{2} - y_\mu\right) \tag{7.05}$$

$$\alpha_\nu = \alpha_{-\nu}, \quad \beta_\nu = \beta_{-\nu} \tag{7.06}$$

represents a so called almost-periodic function, whose expansion coefficients can[17] be determined (3.13), (3.14) by

$$\beta_\nu = \lim_{T\to\infty} \frac{1}{T} \int_{x_0}^{x_0+T} \zeta_\mu(x) \cos w_\nu x \, dx \; \frac{1}{\cos u_\nu (b/2 - y_\mu)} \tag{7.07}$$

$$\alpha_\nu = \lim_{T\to\infty} \frac{1}{T} \int_{x_0}^{x_0+T} \zeta_\mu(x) \sin w_\nu x \, dx \; \frac{1}{\cos u_\nu (b/2 - y_\mu)} \tag{7.08}$$

independent of x_0 . For such values of ν with $\cos u_\nu (b/2-y_s) \neq 0$ we may express α_ν , β_ν through the function $\delta\zeta/\zeta y$ on the same longitudional cut. - But only a restricted subset of the set of all almost-periodic functions on the real axis may be represented by a series (7.05) with uniform convergence for all x .

An approximate determination of the flow from the information of such a cut may, however, have sense if we know at which term we may safely truncate a series (7.05). For this, the example to follow should provide an estimate.

8. Wave spectrum of a parabola ship

In the theory of wave resistance as well as in model experiments very often reference is made to the wave pattern created by a continuous distribution of sources of output $q \, d\xi \, d\zeta$ on a vertical rectangular plane

$$\{-L/2 \leq \xi \leq L/2, \; -D \leq \zeta \leq 0, \; \eta = 0\}$$

$$\text{with} \quad q = \frac{-8Bc\,\xi}{L^2} . \tag{8.01}$$

In Havelock's theory such a distribution is considered representative for a ship of parabolic waterlines and rectangular sections of length L , breadth B and draught D . According to Inui it is pertinent to regard this distribution as representative for the Rankine-body which it generates in the half-space $z < 0$ under a flow c in

-x-direction.

If we remember that (5.68) represents the asymptotic flow of a source of output -4π at the point $\{\xi,\eta,\zeta\}$ and if we now insert $-q\,d\xi\,d\zeta$ instead of the factor 4π after integration over the rectangular plane we get for the asymptotic flow in x-direction

$$\varphi_x = \frac{-1}{b}\int_{-D}^{0}\int_{-L/2}^{L/2}\frac{8Bc}{L^2}\sum_{\nu=-\infty}^{\infty}{}'\xi\, e^{\varkappa_\nu(z+\zeta)}\cos w_\nu(x-\xi)\cos u_\nu\left(\frac{b}{2}-y\right)d\xi\,d\zeta\,\frac{2w_\nu^2\varkappa_\nu}{\varkappa_\nu^2+u_\nu^2}\cos\left(u_\nu\frac{b}{2}\right)$$

$$= \frac{-32Bc}{bL^2}\sum_{\nu=-\infty}^{\infty}\int_{-L/2}^{L/2}\xi\sin w_\nu\xi\,d\xi\int_{-D}^{0}e^{\varkappa_\nu\zeta}\,d\zeta\,e^{\varkappa_\nu z}\sin w_\nu x\cos u_\nu y\,\frac{w_\nu^2\varkappa_\nu}{\varkappa_\nu^2+u_\nu^2} \qquad (8.02)$$

and thereby for the wave elevation

$$\tilde{\zeta} = \frac{c}{g}\varphi_{x_{z=0}} = \frac{16B}{bK_0L^2}\sum_{\nu=-\infty}^{\infty}\frac{\sin\left(w_\nu\frac{L}{2}\right)-\left(w_\nu\frac{L}{2}\right)\cos\left(w_\nu\frac{L}{2}\right)}{\varkappa_\nu^2+u_\nu^2}$$

$$(1-e^{-\varkappa_\nu D})\sin w_\nu x\cos u_\nu\left(\frac{b}{2}-y\right)\cos\left(u_\nu\frac{b}{2}\right). \qquad (8.04)$$

Comparing this with (6.09) we find

$$\beta_\nu = 0,\quad \alpha_\nu = \frac{32B}{bK_0L^2}\,\frac{\sin\left(w_\nu\frac{L}{2}\right)-\left(w_\nu\frac{L}{2}\right)\cos\left(w_\nu\frac{L}{2}\right)}{\varkappa_\nu^2+u_\nu^2}\,(1-e^{-\varkappa_\nu D}) \qquad (8.05)$$

i.e.

$$\alpha_\nu = \{\nu^{-3/2}\} \qquad (8.06)$$

(compare (8.17)); this provides uniform convergence of the series (8.04). If we now insert (8.) into the expression (7.01) for the wave resistance, we have

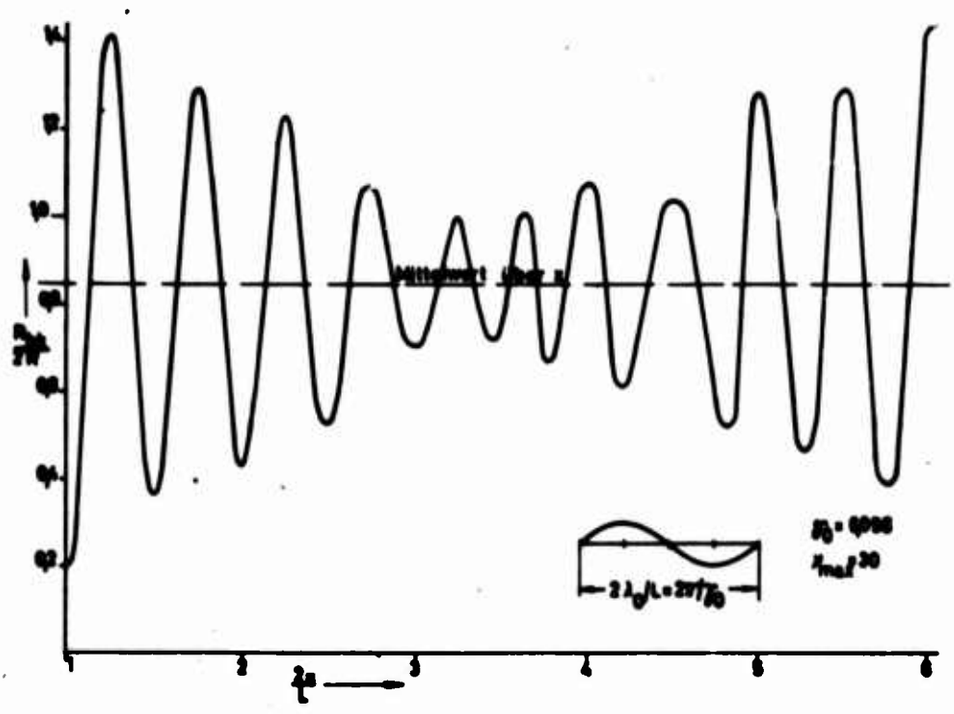
$$R = \frac{32\varrho g B^2}{\pi\gamma_0^2L^2}\sum_{\nu=-\infty}^{\infty}{}'\frac{(1-e^{-\varkappa_\nu D})^2}{\varkappa_\nu^2(\varkappa_\nu^2+u_\nu^2)}\left[\sin\left(w_\nu\frac{L}{2}\right)-w_\nu\frac{L}{2}\cos\left(w_\nu\frac{L}{2}\right)\right]^2\frac{2\pi}{b} \qquad (8.07)$$

with

$$\gamma_0 = K_0\frac{L}{2} \qquad (8.08)$$

and thereby in the limiting case $b\to\infty$

$$R = \frac{32\varrho g B^2}{\pi\gamma_0^2L^2}\int_{-\infty}^{\infty}\frac{(1-e^{-\varkappa D})^2}{\varkappa^2(\varkappa^2+u^2)}\left\{\sin\left(w\frac{L}{2}\right)-w\frac{L}{2}\cos\left(w\frac{L}{2}\right)\right\}^2du \qquad (8.09)$$



Contribution of the flow of potential energy (= 1/2 R_{kk} of (8.13)) to the total theoretical wave resistance R for parabolic ship in dependence of distance x from midship section.

where , w and u are interrelated through

$$w^2 = x^2 - u^2 \tag{8.10}$$

$$\left(\frac{w}{x}\right)^2 = \frac{K_0}{2u}\left(\sqrt{1+4(u/K_0)^2}-1\right) \tag{8.11}$$

$$w = \frac{K_0}{\sqrt{w/x}} \qquad \sqrt{\frac{K_0}{2}\left(K_0+\sqrt{K_0^2+4u^2}\right)} = u\sqrt{\frac{2K_0}{\sqrt{K_0^2+4u^2}-K_0}} \tag{8.12}$$

If we approximate wave resistance by the approach of Korvin-Kroukovsky from the wave elevation in a cut $x = x_s$, then we have to evaluate

$$R_{kk}(x_s) = \varrho g \int_{-b/2}^{b/2} \zeta^2\, dy = \frac{32\,\varrho g B^2}{\pi \gamma_0^2 L^2} \sum_{\nu=-\infty}^{\infty} \frac{(1-e^{-x_\nu D})^2 \left\{\sin\left(w_\nu \frac{L}{2}\right) - \left(w_\nu \frac{L}{2}\right)\cos\left(w_\nu \frac{L}{2}\right)\right\}^2}{x_\nu^2 (u_\nu^2 + x_\nu^2)} \frac{4x_\nu^2 \sin^2(w_\nu x_s)}{u_\nu^2 + x_\nu^2} \tag{8.13}$$

The terms of (8.13) deviate from those of (8.07) by factors

$$\frac{4\varkappa_\nu^2 \sin^2 w_\nu x_s}{\varkappa_\nu^2 + u_\nu^2} = \frac{4u_\nu^2 + 4w_\nu^2}{2u_\nu^2 + w_\nu^2} \sin^2 w_\nu x_s . \tag{8.14}$$

If we average these term over a large domain of possible x_s, we have to replace $\sin^2 w_\nu x$ by $1/2$ and these factors will in general turn out to be larger than one. For $\nu = 0$ we have

$$\frac{2\varkappa_0^2}{\varkappa_0^2 + u_0^2} = 2, \tag{8.15}$$

for $u_\nu/K_0 \to \infty$ we have $w_\nu/u_\nu \to 0$, as from (8.10), (8.11), (8.12) it follows that

$$w_\nu = \frac{\sqrt{2}\, u_\nu}{\sqrt{\sqrt{1 + 4(u_\nu/K_0)^2} - 1}} = \sqrt{K_0 u_\nu}\left\{1 + 0\left(\frac{u_\nu}{K_0}\right)^{-1}\right\} \tag{8.16}$$

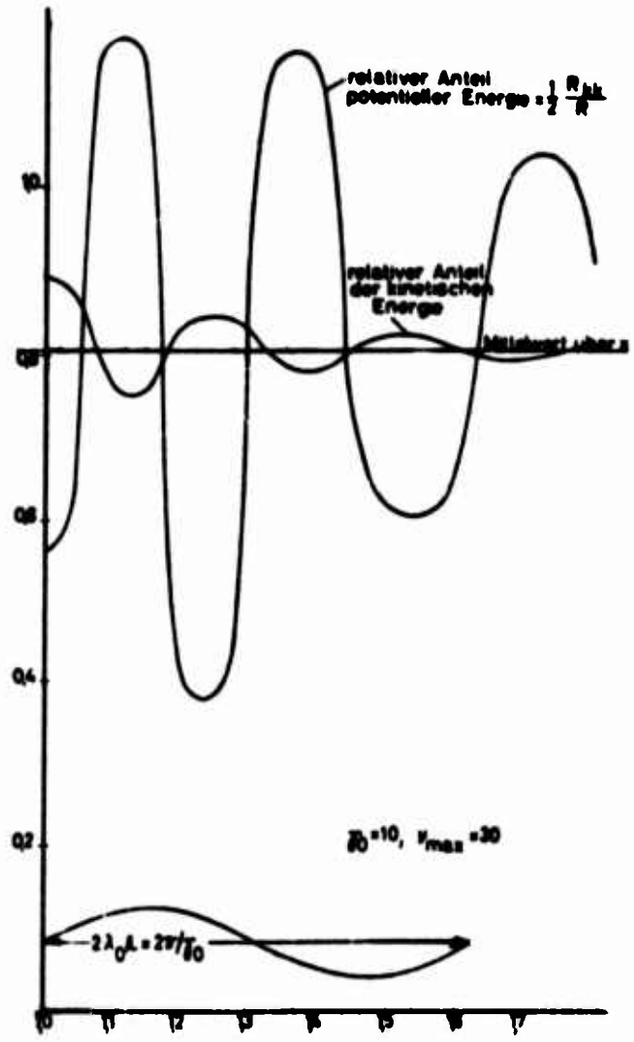
We therefore have

$$\frac{2\varkappa_\nu^2}{\varkappa_\nu^2 + u_\nu^2} \to 1 \qquad \text{for } u_\nu/K_0 = \frac{2\pi\nu}{K_0 b} \to \infty . \tag{8.17}$$

We therefore may conclude that an average value according to (8.33) will the less extend above (8.07) the smaller is $K_0 b$, i.e. the larger the speed of the stationary wave field. This is true particularly due to the fact that the relative contribution to (8.07) of terms with high ν, i.e. of the waves traveling more or less divergent, increases with decreasing $K_0 b$, as the factor decreases more slowly then with ν.

In the range of high velocities, where harmonic analysis of wave profiles across the tank is increasingly complicated by the divergent wake region behind the model, the method of Korvin-Kroukovsky might find application after introduction of a suitable method of averaging.

For the method proposed by the author, however, it is considered a faborable fact that for low speeds, where measurements are rendered more difficult due to smaller wave elevations, the relative importance of the first terms in the wave pattern expansion increases.



Contribution of flow of potential energy and of flow of kinetic energy through vertical control surface to theoretical wave resistance of the parabolic ship in dependence of this surface's distance from midship section.

NOMENCLATURE

$\doteq$	defining sign of equality, quantity left is defined
B,D,L	breadth, draught, length of a ship according (8.01)
C	constant according (5.89)
G	velocity potential of a source of output -4π
G_1,G_2,G_3,G_4,G_5	successive approximations to G
$F_\nu^{(i)},J_\nu,H_\nu,L_\nu$	intermediary functions according (5.25), (4.37), (4.38), (4.33)
$K_0 = g/c^2$	characteristic wave number
T	interval length
F(u),G(u),H(u)	fourier transforms according (5.83), (5.85), (5.82)
a	distance of control surface
b	canal width
c	speed of the ship
c_o	speed of some uniform flow
c_E^ν	component of velocity of energy transport along x direction
g	acceleration of gravity
h	height of undisturbed free surface over bottom
k,u,w	variables of integration with meaning of wave numbers, u, w in y, x directions
k_ν	special wave number according (4.22)
u_ν	special wave number, according (4.20)
w_ν	special wave number, positive zero of (4.38)
q	source density (8.01)
x,y,z	coordinates, originating at undisturbed free surface, x in direction of ship's advance, z upwards

$h(w), g(w), h(w), s(w)$ auxiliary functions (5.76), (5.84), (5.87), (5.79)

α_ν, β_ν expansion coefficients (6.09)

γ_ν coefficients (5.69) resp. (5.71)

γ_o velocity parameter (8.08)

δ_ν coefficients (5.21), (5.22), (5.24)

Δ La'place operator: a constant according (5.15), half distance of cuts (7.04)

ζ wave elevation

ξ, η, ζ coordinates of source analogous to x,y,z

Θ angle of wave propagation

$\varkappa$ wave number (8.10)

$\varkappa_\nu$ special wave number according (5.05)

ν, γ density

σ signum of $z - \zeta$ according (4.08)

φ velocity potential of wave field (flow = positive gradient!)

$\varphi_\nu^s, \varphi_\nu^c$ expansion functions (5.70), (5.72)

Φ flow integral (6.01)

REFERENCES

1. HAVELOCK: Calculation of wave resistance, Proc. Roy. Soc. A 144, Jan. 34, S, 514-521.

2. HOGNER: Contribution to the Theory of Ship Waves. Ark. Math. Astr. og Fysik 17, No. 12, 1923.

3. URSELL: On Kelvin's Ship-Wave Pattern. Journ. Fluid Mech. 6, 1960, S. 418-431.

4. INUI: Asympt. Expansions applied to Problems of Ship-Waves and Wavemaking Resistance. Proc. 5th Jap. Nat. Congr. for Appl. Mech. 1955.

5. EGGERS: Über die Ermittlung hydrodynamischer Kräfte aus Impuls- und Energieansätzen. Schiffstechnik Heft 21, 1957.

6. LAMB: Hydrodynamics. 6th edition 1952, S. 383. Cambridge University Press.

7. KORVIN-KROUKOVSKY: Contribution to Meeting of H5 panel of Society of Naval Architects and Marine Engineers, New York 28, July, 1960 (unpublished)

8. WEHAUSEN: Surface Waves. Handbuch d. Physik, S. 484-486, Bd. IX 1960, Springer, Berlin.

9. ERDELYI: Higher Transcendental Functions. Bd. 2, S. 81, McGraw Hill 1953.

10. ERDELYI: Tables of Integral Transforms. Bd. 1, S. 182, S. 20, McGraw Hill 1953.

11. RYSHIK-GRADSTEIN: Summem, Produkte, Integrale. S. 234, S. 180, Berlin 1957.

12. ERDELYI: Asymptotic Expansions. Dover Publ. 1956.

13. BOCHNER: Vorlesungen über Fourier'sche Integrale. Chelsea Publ. New York 1948.

14. JAHNKE-EMDE-LÖSCH: Tafeln höherer Funktionen. S. 18, Teubner, Stuttgart 1960.

15. MANGOLD-KNOOP: Einf. Höhere Mathematik. Bd. 3, S. 513.

16. SCHWARTZ: Theorie generale des fonctions moyenne-periodiques, Annals of Mathematics, Bd. 48, S.880, 881.

17. MAAK: Fastperiodische Funktionen. S. 28 und 113 ff. Springer 1951.

18. HASKIND: On the Progressive Motion of a Body in the Vicinity of the free Surface of a heavy Fluid of Finite Depth (Russian) Prikladnaja mathematika i mechanika IX 1945, (2.13) p. 67-78.

19. KELDISH, M. W., and SEDOW, L. I.: Theory of Wave Resistance in a Canal of Finite Depth. Proceedings of the Conference on Surface Waves, Moskow 136, p. 143-152 (Russian).